NUREG/CR-0927
TREE-1272
for the U.S. Nuclear Regulatory Commission

EXPERIMENT DATA REPORT FOR PBF/LOFT LEAD ROD TEST SERIES (TESTS LLR-S0, -3, -4, -4A, and -5)

RUSSELL J. BUCKLAND DAVID H. SCHWIEDER

October 1979

EG&G Idaho, Inc.

IDAHO NATIONAL ENGINEERING LABORATORY

DEPARTMENT OF ENERGY

IDAHO OPERATIONS OFFICE UNDER CONTRACT DE-AC07-76IDO1570

1405 001

7911280414

1405 002

Available from
National Technical Information Service
Springfield, Virginia 22161
Price: Printed Copy A17 Microfiche $3.00

The price of this document for requesters
outside the North American continent can
be obtained from the National Technical
Information Service.

NUREG/CR-0927
TREE-1272
R3

EXPERIMENT DATA REPORT FOR PBF/LOFT LEAD ROD TEST SERIES (TESTS LLR-S0, -3, -4, -4A, and -5)

Russell J. Buckland
David H. Schwieder

EG&G IDAHO, INC,
IDAHO FALLS, IDAHO 83401

October 1979

PREPARED FOR THE
U.S. NUCLEAR REGULATORY COMMISSION
AND THE U.S. DEPARTMENT OF ENERGY
IDAHO OPERATIONS OFFICE
UNDER CONTRACT NO. DE-AC07-76IDO1570
NRC FIN NO. A6038

ABSTRACT

Recorded test data are presented for Tests LLR-S0, LLR-3, LLR-4, LLR-4A, and LLR-5 of the Thermal Fuels Behavior Program PBF/LOFT Lead Rod (LLR) Test Series. This test series, conducted in the Power Burst Facility, was designed to provide a parametric evaluation of the expected mechanical response of the LOFT fuel rods to a loss of coolant event. The data, presented in the form of graphs in engineering units, have been analyzed only to the extent necessary to ensure they are reasonable and consistent. These uninterpreted data from the LLR tests are presented in advance of detailed analysis and interpretation.

SUMMARY

The Loss-of-Fluid Test (LOFT) Lead Rod (LLR) Test Series was conducted in the Power Burst Facility (PBF) as part of the Thermal Fuels Behavior Program which is conducted by EG&G Idaho, Inc., for the U.S. Nuclear Regulatory Commission (NRC). The PBF/LOFT lead rod tests were performed to provide a parametric evaluation of the expected mechanical response of the LOFT fuel rods to loss-of-coolant over a wide range of initial power levels. The LOFT facility is the major NRC sponsored testing facility which simulates the response of a light water reactor over a wide range of loss-of-coolant accident (LOCA) conditions. The LOFT facility is to be used for sequential loss-of-coolant experiments, provided extensive fuel rod failures do not occur.

The PBF/LOFT Lead Rod Test Series comprised five tests, Tests LLR-S0, -3, -4, -4A, and -5. These tests were designed to simulate the test conditions for the planned LOFT loss-of-coolant experiments. However, Test LLR-S0 was a preliminary systems checkout test and did not correspond to a particular planned LOFT test.

The PBF/LOFT lead rod tests had the following objectives: (a) to experimentally evaluate the extent of cladding collapse and waisting that would be expected to occur during the LOFT loss-of-coolant accident transients; (b) to evaluate the effects of collapsed cladding and pellet-cladding interaction on the mechanical response of the fuel rods subjected to subsequent power increases, long-term preconditioning, and loss-of-coolant conditions; and (c) to provide experimental data to bench mark the Fuel Rod Analysis Program (FRAP) analytical model that will be used for requalification of the LOFT core.

The PBF was designed to provide the neutron and coolant environment required to simulate conditions in a light-water reactor during postulated accident events. The test facility components for the LLR tests include:

(1) A reactor vessel and driver core region to provide the neutron environment

(2) An in-pile tube in the center of the driver core to contain the test rods

(3) A pressurized water flow loop to provide the coolant environment in the in-pile tube

(4) A blowdown system to simulate a loss-of-coolant accident

(5) A reflood and quench system to provide cooling and long-term quenching of the fuel after a test is completed.

Each LLR test utilized four symmetrically positioned and separately shrouded LOFT design, PWR-type fuel rods. A total of seven fuel rods were tested during the five LLR tests. Each fuel rod consisted of a 0.914 m-long fuel stack of unirradiated, 93% theoretical density, 9.5 wt% UO_2 fuel, and was backfilled with helium at atmospheric pressure.

The test procedure for each test included: (a) a nonnuclear heatup to establish initial test coolant conditions; (b) a period of nuclear operation to accomplish fuel preconditioning, power calibration, and decay heat buildup; and (c) a blowdown transient with subsequent test fuel reflood and quench. The rods were subjected to a blowdown similar to one expected in LOFT during a 200% double-ended cold leg break.

Maximum test fuel rod cladding temperatures attained during the blowdown transient of each test were as follows:

1405 005

	Temperature (K)					
Test Rod:	312-1	312-2	312-3	312-4	345-1	399-2
Test LLR-S0	650	615	675	640		
Test LLR-3	950	925	1005	870		
Test LLR-4	1130	1170			1060	
Test LLR-4A		1150			1075	1260
Test LLR-5	995	1015			1005	

Test Rod 345-2, used in Tests LLR-4, LLR-4A, and LLR-5, was not instrumented with cladding thermocouples.

The system instrumentation was designed to measure and record the important events that occurred prior to and during the test blowdowns. Each test rod and its shroud cooling environment were fully instrumented. The blowdown piping coolant variables were further characterized through use of instrumented spool pieces which provided temperature, pressure, velocity, and density information during the blowdown transients.

The data obtained from this test have been subjected to a thorough review and subsequently categorized as qualified, restrained, trend, or failed data. The blowdown data of each test are presented in the main body of this report and the power calibration and preconditioning data are included on the microfiche attached to the back cover.

CONTENTS

FIGURES

TEST LLR-S0

TEST LLR-3

1405 017

TEST LLR-5

TEST LLR-4

TEST LLR-4A

TABLES

1405 037

EXPERIMENT DATA REPORT FOR PBF/LOFT LEAD ROD TEST SERIES (TESTS LLR-S0, -3, -4, -4A, and -5)

I. INTRODUCTION

The Thermal Fuels Behavior Program (TFBP) is one of several programs being conducted by the Water Reactor Research Directorate of EG&G Idaho, Inc., for the U.S. Nuclear Regulatory Commission (NRC). The TFBP performs an integral analytical and experimental study of the behavior of nuclear fuel rods under normal, off-normal, and accident conditions in light water reactors (LWR). Data from the TFBP experimental effort are used to determine the completeness and accuracy of analytical models developed to predict fuel rod behavior for a wide range of postulated reactor operating conditions.

The Loss-of-Fluid Test (LOFT) facility[1] is the major NRC sponsored testing facility which simulates the response of a light-water reactor over a wide range of loss-of-coolant accident (LOCA) conditions. The LOFT facility is intended to be used for sequential loss-of-coolant experiments (LOCEs), provided extensive fuel rod failures do not occur. The LOFT Lead Rod Test Series, conducted in the Power Burst Facility (PBF), was performed to provide a parametric evaluation of the expected mechanical response of the LOFT fuel rods to loss-of-coolant over a wide range of initial power levels.

The specific objectives of the PBF/LLR Tests were to:

(1) Experimentally evaluate the extent of cladding collapse and waisting that would be expected to occur during the LOFT LOCA transients

(2) Evaluate the effects of collapsed cladding and pellet-cladding interaction on the mechanical response of the fuel rods subjected to subsequent power increases, long-term preconditioning, and loss-of-coolant conditions

(3) Provide experimental data to bench mark the Fuel Rod Analysis Program (FRAP) analytical model that will be used for requalification of the LOFT core.

The LLR tests were conducted within the in-pile tube (IPT), the test space located vertically in the center of the PBF reactor core. The PBF loop coolant and blowdown systems allowed simulation of LWR coolant conditions in the IPT and provided the subsequent blowdown capability. The test train, an experimental support apparatus, positioned the test fuel rods in the core region of the IPT and provided support for the test instrumentation. Each of the LLR tests was performed with four identical, separately shrouded, LOFT design fuel rods with an active length of 0.914 m.

The LLR Test Series consisted of five individual tests, Tests LLR-S0, -3, -4, -4A, and -5. The first test, Test LLR-S0, was a low power system operational test which provided a check of total system performance. The next three tests, Tests LLR-3, 5, and -4, corresponded to the planned LOFT Tests L2-3, L2-5, and L2-4, respectively. The final test, Test LLR-4A, was included to complete the test series objective of performing one test using deformed test fuel rods.

Each test sequence consisted of (a) a nonnuclear system heatup to establish test coolant conditions; (b) a preblowdown nuclear operating period to calibrate the test fuel rods with the reactor core power, precondition the test fuel rods, and establish the required test fuel rod decay heat; and (c) a blowdown transient which included a reflood simulation and was terminated by quench cooling of the test fuel. Blowdown was initiated by opening the cold leg high-speed valves, which simulated a 200% double-ended cold leg break.

This report presents the data from all nuclear and blowdown portions of the LLR tests in a form readily usable by the nuclear community in advance of detailed analysis and interpretation. The data have been subjected to a thorough review and categorized as qualified, restrained, trend, or failed data. The blowdown transient data for each test are presented in Section IV and power calibration and preconditioning data plots are included on microfiche attached to the back cover of this report.

Section II of this report presents the system configuration, procedures, initial test conditions, and events that are specific to the LLR tests; Section III provides brief descriptions of test instrumentation; and Section IV presents information necessary for data interpretation. Appendix A describes the methods used in applying posttest corrective adjustments to the data and subsequent qualification; and Appendix B presents a guide to the uncertainty associated with the data.

1405 039

II. SYSTEM AND EVENTS FOR PBF/LOFT LEAD ROD TESTS

The following system configuration, procedures, and events are specific to PBF/LOFT Lead Rod Tests -S0, -3, -4, -4A, and -5.

1. SYSTEM CONFIGURATION

The Power Burst Facility reactor, shown in Figure 1, consists of a uranium oxide driver core and a central flux trap contained in an open tank reactor vessel. A pressurized water coolant flow loop provides a wide range of coolant conditions within the flux trap test space.

1.1 PBF Core

The PBF core is a right-circular annulus 1.3 m in diameter and 0.91 m in length, enclosing the vertical flux trap which is 0.21 m in diameter. This core has been designed for steady-state and power burst operation. The core contains eight control rods for reactivity control during steady-state operation and four transient rods for dynamic control during transient conditions. Each of the control and transient rods consists of a stainless steel canister which contains a cylindrical annulus of boron carbide and is operated in an air-filled shroud. A cutaway view of the PBF core is shown in Figure 2.

1.2 In-Pile Tube

An in-pile tube (IPT) fits in the central flux trap region and contains the test train assembly. The IPT is a thick-walled, Inconel 718, high strength pressure tube designed to contain the steady-state operating pressure and pressure surges from any test fuel rod failures. Any conceivable failure of the test fuel during the test (such as cladding failure, gross fuel melting, fuel-coolant interactions, fuel failure propagation, fission product release, or metal-water reactions) can be safely contained by the PBF IPT without damage to the driver core.

A radial cross section of the IPT in the reactor core area is shown in Figure 3. A flow tube is positioned inside the IPT to direct the coolant flow. Coolant flow enters the top of the IPT above the reactor core and flows down the annulus between the IPT wall and the flow tube. The flow reverses at the bottom, passes up through the test train assembly, and exits above the reactor core at the IPT outlet. The flow tube consists of an upper stainless steel section, a center zircaloy-2 section for neutron economy in the test fuel, and a lower catch basket section for a heat sink and collection of fuel fragments. A nitrogen gas annulus is provided between the IPT wall and aluminum core filler piece because of the temperature gradient between the two.

1.3 Loop Coolant System

The loop coolant system provides cooling water to the IPT at controllable pressures, temperatures, and flow rates which simulates the planned test conditions for the LOFT loss-of-coolant experiments. The system includes a pressurizer, a pump, heat exchangers for removing the energy transferred to the coolant by the test fuel, a flow control valve, acoustic filters and thermal swell accumulators to attenuate any pressure surges from fuel failure, and electrical heaters to control the inlet temperature. A measurement spool in the IPT inlet line provides measurements of preblowdown initial conditions.

1.4 PBF LOCA System

Simulation of a loss-of-coolant accident is provided by the PBF-LOCA system. A schematic of the pressurized water loop and LOCA system is shown in Figure 4. The isolation and bypass valves are actuated immediately prior to blowdown initiation to allow continued loop operation at normal conditions through the bypass valve. Blowdown capability is provided by two blowdown lines tied into the IPT inlet

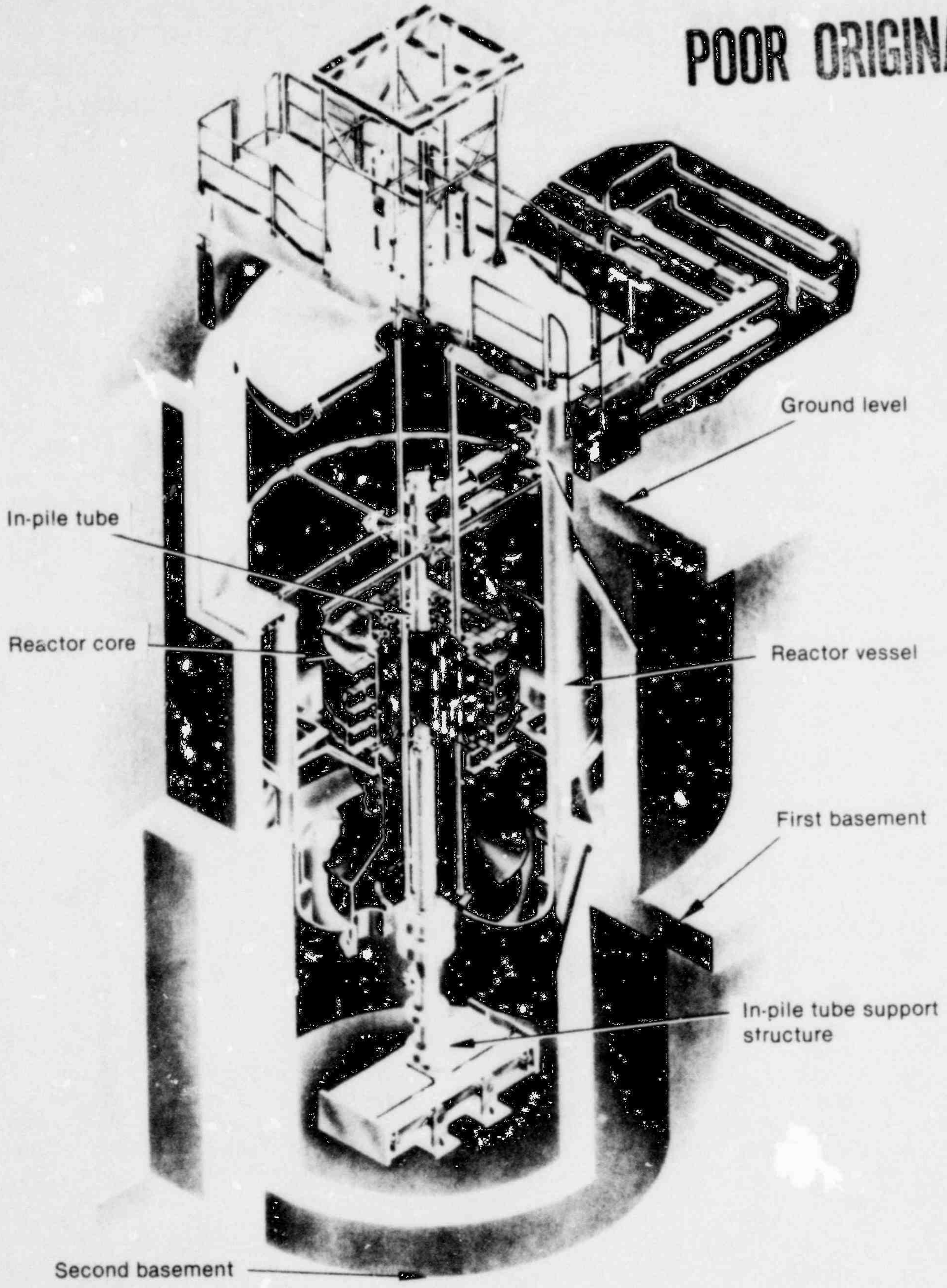

Fig. 1 Power Burst Facility reactor - cutaway view.

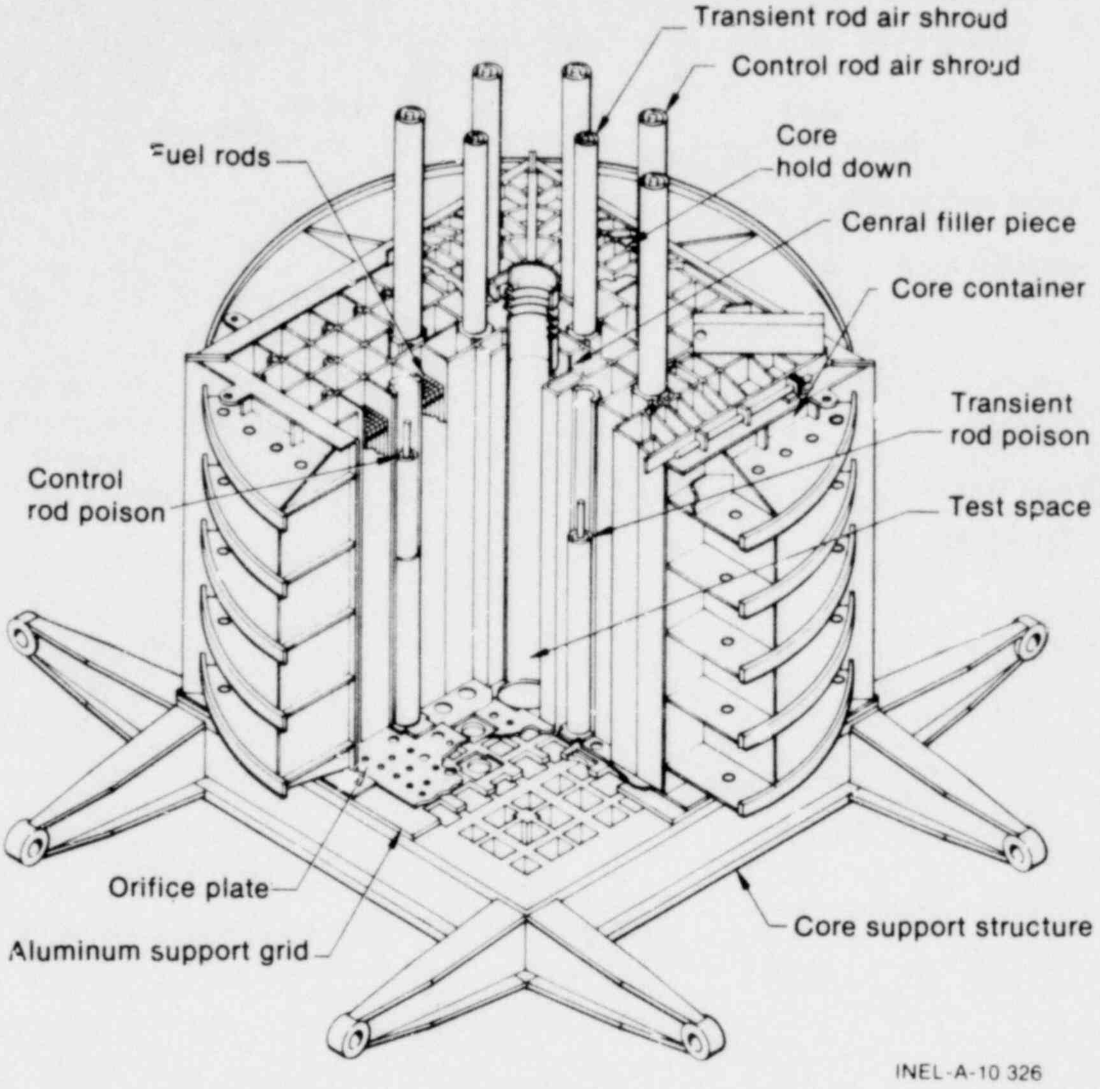

Fig. 2 Power Burst Facility core - cutaway view.

and outlet lines (cold leg-IPT inlet and hot leg-IPT outlet). Each line contains a measurement spool, two quick opening and closing (>100 ms) blowdown valves, and two Henry nozzles which provide the break plane and control the break flow rate and depressurization rate. The Henry nozzles, used in the LOFT lead rod tests, were venturi type restrictors with throat diameters as tabulated in Table I.

A small line connects the hot and cold blowdown piping legs with a controllable valve which maintains sufficient flow to keep the legs at a constant temperature prior to blowdown initiation. The sequencing of valve operation during blowdown is controlled by a time sequential programmer in the PBF programming and monitoring system. The PBF LLR test hardware includes a direct injection reflood capability at a constant flow rate which simulates the LOFT LOCA transients. The reflood line utilizes water from the quench system and injects it through the IPT top head, down the center of the test train hardware and into the lower plenum of the IPT. Following reflood injection, posttest quench cooling is accomplished by opening the quench valve, GB-LM-11-8, and closing valve GB-LM-11-18 and the cold leg blowdown valves to permit coolant from the quench tank to enter the IPT. The quench tank is pressurized to 1.37 MPa by a nitrogen gas system and heated to approximately 366 K. After the quench tank is emptied (about 60 s) coolant is pumped from the storage tank for up to four hours to maintain test rod cooling. The blowdown header and tank collect and contain the coolant ejected from the IPT and piping during blowdown, reflood, and quench cooling. Figure 5 presents an isometric of the PBF LOCA system showing relative locations of major system components.

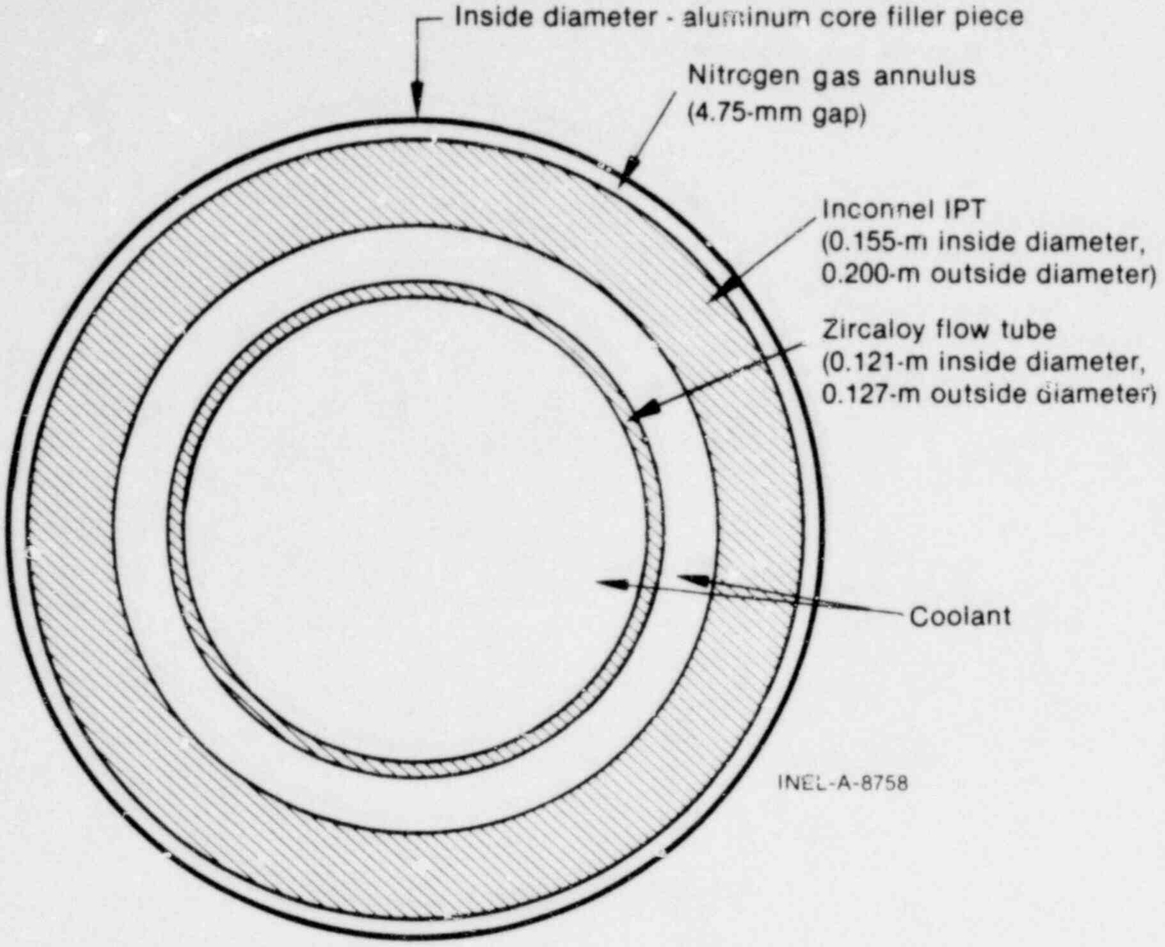

Fig. 3 **Radial cross section of the PBF in-pile tube.**

1.5 Test Fuel Rods

The test assembly used in the LOFT lead rod tests consisted of four identical, separately shrouded PWR-type unirradiated fuel rods positioned and supported in the IPT by the LLR test train hardware. Some of the test rods were replaced between tests with a total of seven rods being used in the five LLR tests. The geometry of the active length of the fuel rods is identical with the LOFT fuel and LOFT cladding was utilized in their fabrication. The plenum pressure selected corresponds to the backfill pressure utilized for the LOFT Experiment Series L2[2] fuel rods. The fuel rod designations and the specific tests for which each rod was used are described in Table II.

Table III lists the design characteristics of the test fuel rods used in the LLR tests.

Each test fuel rod was encased within a circular flow shroud and attached as a unit to the test train hardware. The test rods were rigidly secured at their top end and were free to expand axially downward. For Tests LLR-S0 and -3, Rods 312-1 and 312-2 were encased in zircaloy-4 flow shrouds, and Rods 312-3 and 312-4 were encased in stainless steel shrouds which simulated the LOFT peripheral, low power rods. The power ratio between the zircaloy-4 shrouded (high power) and the stainless steel shrouded (low power) rods was 1.0 to 0.87. Rod 312-3, a low power, stainless steel shrouded rod failed during Test LLR-3 due to a leak in the cladding. Both stainless steel shrouded rods were removed from the test train following Test LLR-3 because one low power rod in the test train does not accurately simulate the power ratio between the LOFT center and peripheral rods. All subsequent tests used zircaloy-4 shrouded test rods exclusively. A cross section of the IPT and test train providing test rod and shroud geometry is shown in Figure 6.

1405 043

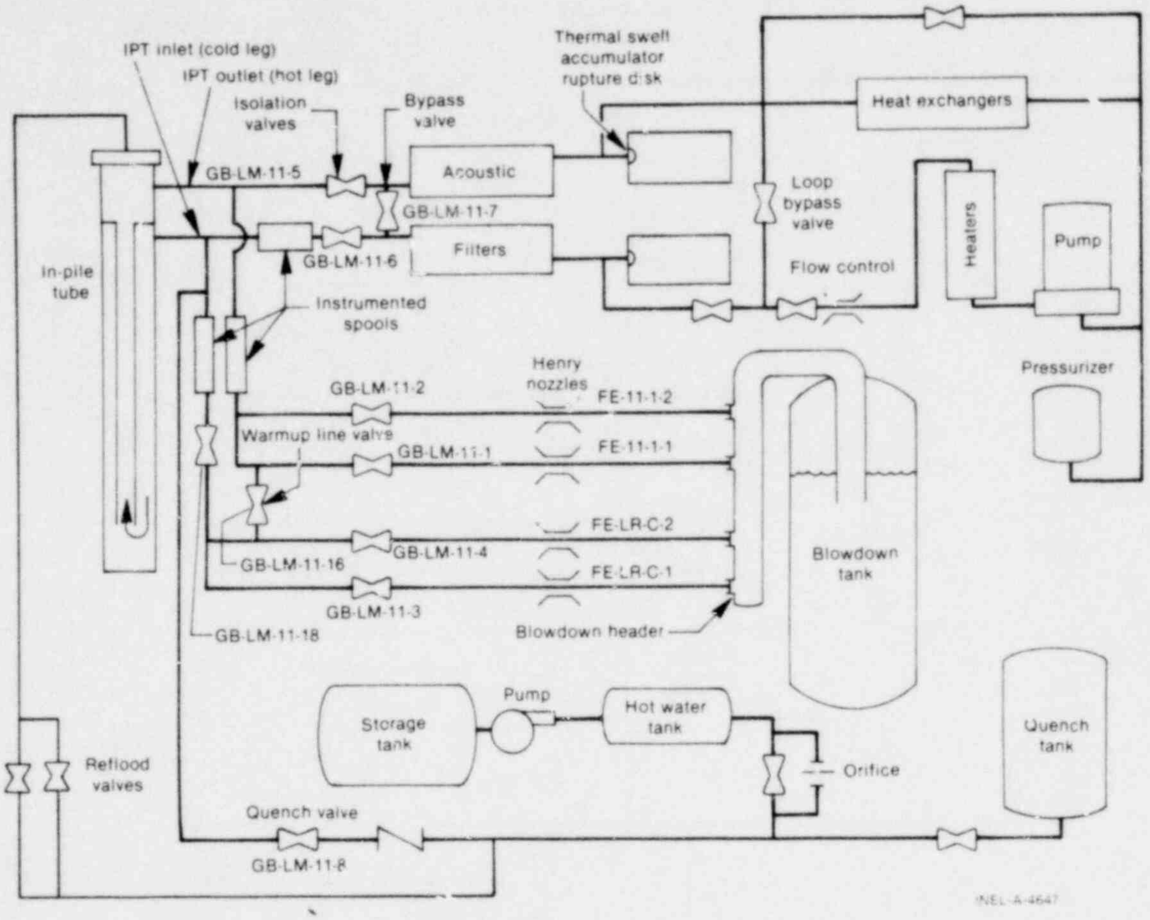

Fig. 4 PBF loop and LOCA system - schematic.

TABLE I

NOZZLE LOCATIONS AND DIAMETERS FOR LLR TESTS

Location	Nozzle Designation	Throat Diameter (mm)
Hot leg	FE-11-1-1	14.22
Hot leg	FE-11-1-2	13.56
Cold leg	FE-LR-C-1	12.47
Cold leg	FE-LR-C-2	23.90

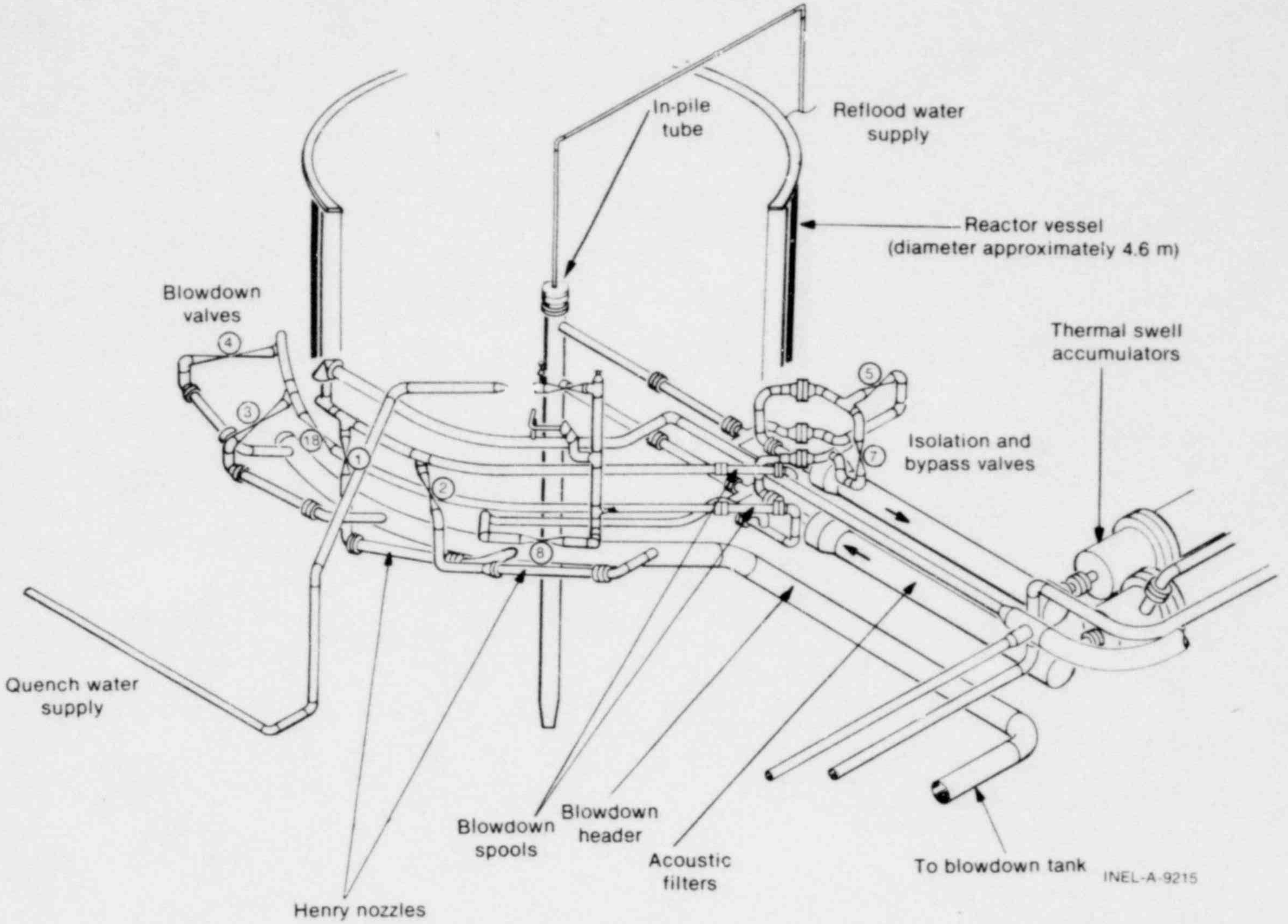

Fig. 5 PBF LOCA system - isometric.

1405 045

TABLE II

LOFT LEAD ROD TEST FUEL RODS

Rod	Designation	LLR Tests
1	312-1	LLR-SO, -3, -5, -4
2	312-2	LLR-SO, -3, -5, -4, -4A
3	312-3	LLR-SO, -3
4	312-4	LLR-SO, -3
5	345-1	LLR-5, -4, -4A
6	345-2	LLR-5, -4, -4A
8[a]	399-2	LLR-4A

---

[a] Rod 7, designated 399-1, was a spare and was not used.

1.6 LLR Test Train

The LLR test train symmetrically positioned the test fuel rods in the driver core test space. An axial cross section illustration of the LLR test train within the IPT is shown in Figure 7. During preblowdown steady-state conditions, the coolant entered the IPT inlet where approximately 75% flowed upwards through a controlled bypass to the upper plenum and out the IPT outlet. The remaining 25% of the coolant passed downward outside the IPT flow tube to the lower plenum and then upward through the lower particle screen to the inlets of the four test rod flow shrouds. The lower support plate was designed to minimize bypass flow outside the fuel rod shrouds to less than 2% of the total test rod shroud flow. The coolant then passed inside each circular flow shroud, past each test fuel rod, and out through a check valve (to prevent reverse fluid flow during blowdown events) to the common upper plenum region. This total experiment flow then passed through the upper particle screen, mixed with the controlled bypass flow, and exited the IPT.

To provide relative hydraulic volumes characteristic of the LOFT system, filler pieces were inserted in the IPT exit volume, the upper plenum, and the downcomer region. The central hanger tube, which is zircaloy in the active core region, provided support for the test train components and an injection path for reflood water into the lower plenum.

1405 046

TABLE III

PBF/LOFT LEAD ROD TEST FUEL ROD DESIGN CHARACTERISTICS

Characteristic	Nominal Value
Fuel	
Material	UO_2
Pellet outside diameter (mm)	9.294 ± 0.0127
Pellet length (mm)	15.24 ± 0.635
Pellet enrichment (wt%)	9.5 ± 0.5
Density (% theoretical density)	93.0 ± 1.5
Fuel stack length (m)	0.9144 ± 0.0008
End configuration	Dished
Burnup (MWd/t)	0
Center hole diameter (mm)	1.85 ± 0.05
Insulator Pellet	
Material	Al_2O_3
Length (mm)	5.08 ± 0.254
Diameter (mm)	8.89 ± 0.05
Cladding	
Material	Zircaloy-4
Tube outside diameter (mm)	10.7 ± 0.038
Tube inside diameter (mm)	9.48 ± 0.038
Thickness (mm)	0.61
Overall length (m)	0.9906
Fuel Rod	
Plenum void volume (cm^3)	2.95 ± 5%
Filler gas	Helium
Filler gas purity	94.9% He, 5% Ar, 0.1% impurities
Initial gas pressure (MPa)	0.1034
Diametral gap (mm)	0.191
Overall length (m)	0.9986

1405 047

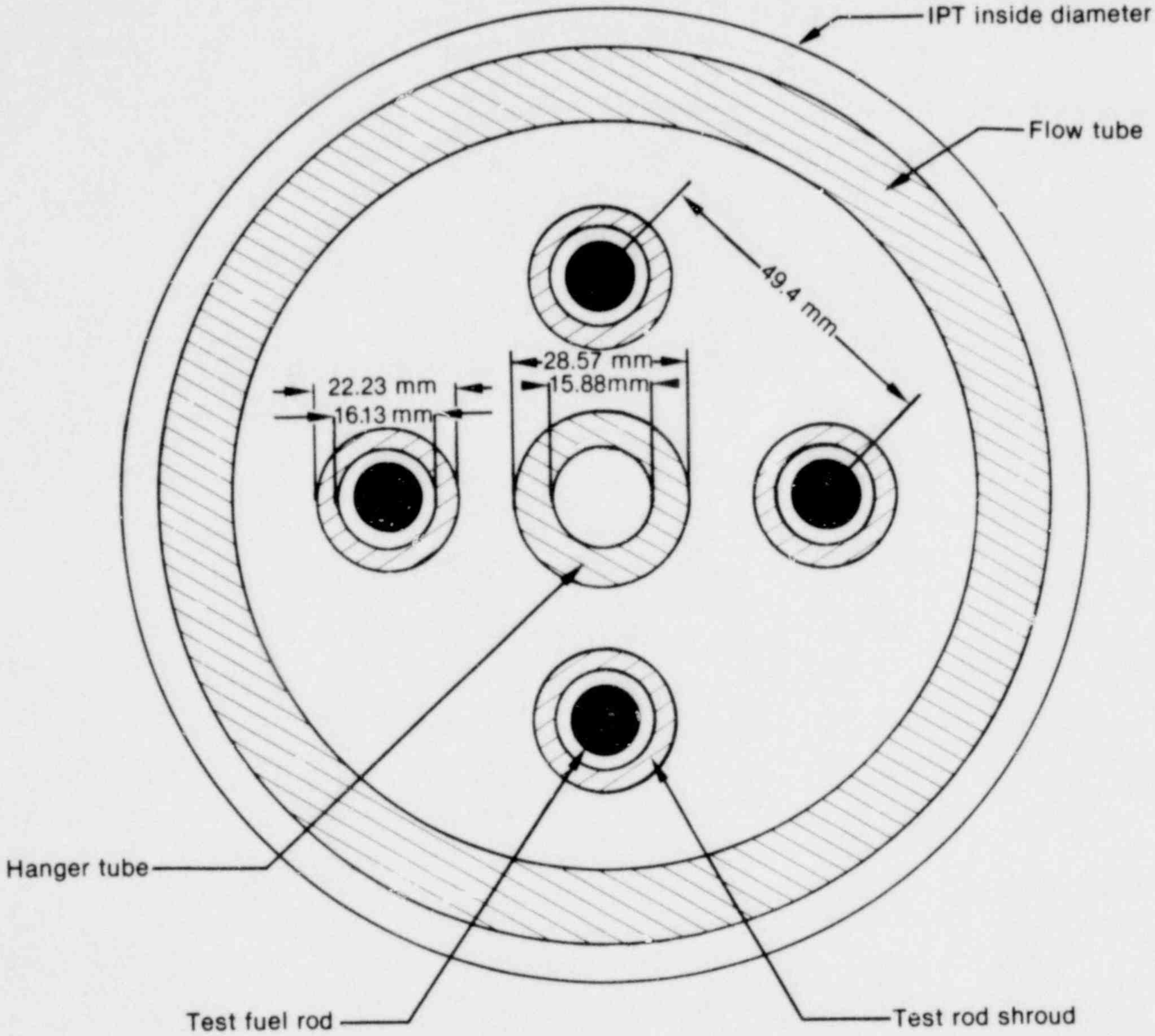

INEL-A-12 962

Fig. 6 LOFT lead rod test rod and shroud geometry.

1405 048

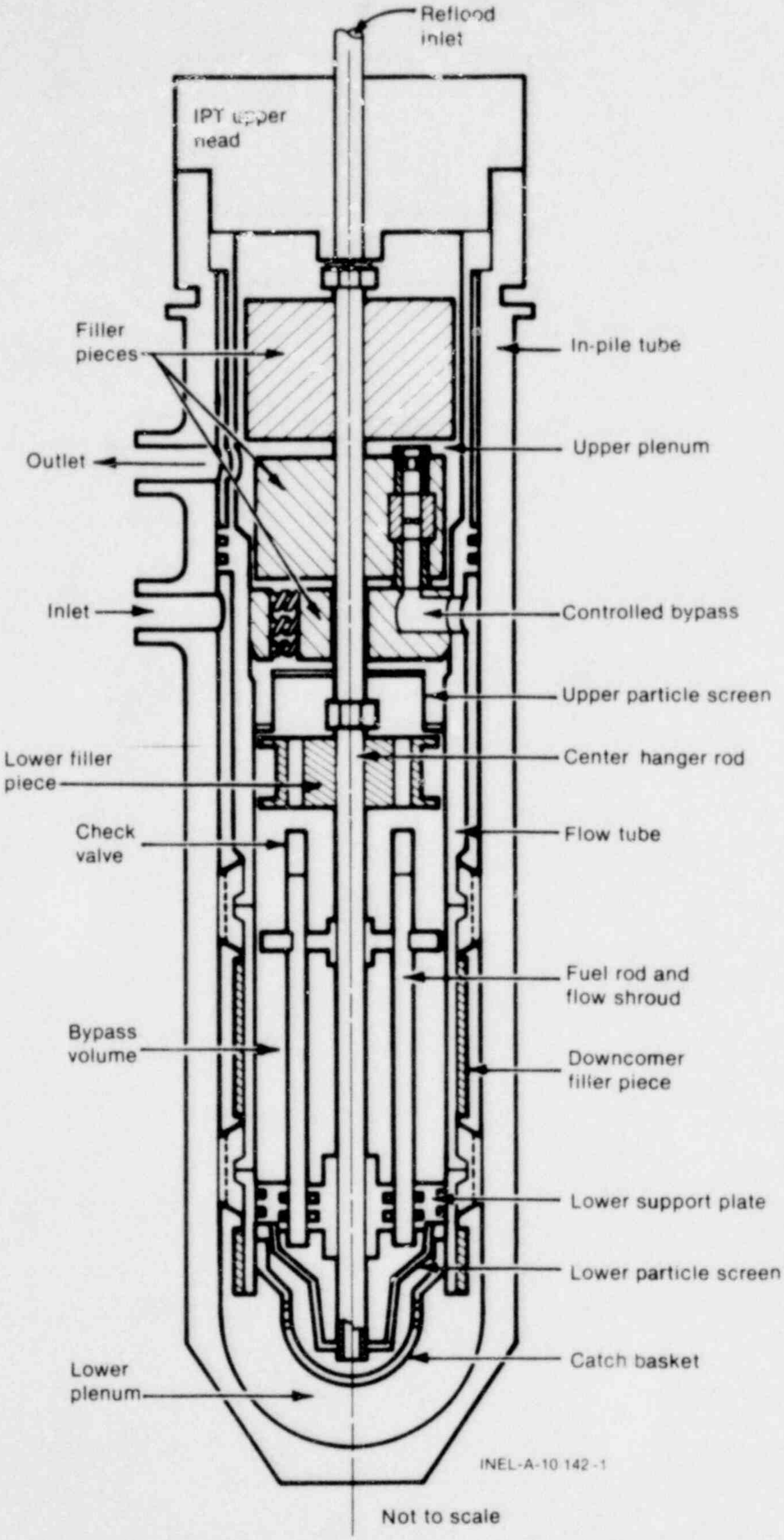

Fig. 7 LOFT lead rod test train illustration.

2. EXPERIMENT CONDUCT

The LOFT Lead Rod Test Series consisted of five separate, four-rod tests designated as Tests LLR-S0, LLR-3, LLR-4, LLR-4A, and LLR-5. Each test comprised three major phases: (a) heatup; (b) fuel preconditioning, power calibration, and decay heat buildup; and (c) blowdown, reflood, and quench.

2.1 Heatup Phases

Prior to nuclear operation, each of the five tests began with heatup of the IPT loop system and establishing the coolant conditions of temperature, pressure, and flow necessary to perform the test. During each heatup of the pressurized water coolant flow loop, the coolant chemistry requirements were adjusted and established within the following limits:

pH range	5.7 to 10.2
Specific conductivity	1.4 to 48 μS/cm
Dissolved oxygen	< 0.1 ppm
Chlorides	< 0.15 ppm
Total suspended solids	< 1.0 ppm

Instrumentation calibrations and status checks were also performed throughout the heatup phases. In order to quantify flow leakages, and the controlled bypass and shroud bypass flows, the warmup line valve was closed and the volumetric flow through the inlet spool was compared with the sum of the flow rates through the four fuel rod shrouds in the test train. The controlled bypass flow was determined to be approximately 270% of the total steady-state shroud flow; very close to the intended 300%. Coolant leakage paths in the test train (which included the lower support plate, controlled bypass, and flow tube seals) were calculated to be less than 10% of the total steady state shroud flow.

2.2 Fuel Preconditioning, Power Calibration, and Decay Heat Buildup Phases

Each of the five test blowdowns was preceded by several hours of nuclear operation with the experiment at test conditions. Test fuel rod preconditioning was accomplished by several slow reactor power ramp cycles which promoted fuel pellet cracking and relocation, and allowed the initiation of pellet-cladding mechanical interaction to stabilize. During the slow power ramps, and at specific steady state power levels, the individual test rod powers were calculated from a thermal balance using measurements of the coolant pressure, inlet temperature, temperature increase across each test rod shroud, and the flow rate inside each shroud. An axial peaking factor of 1.34 was used in the calculations of rod peak powers. This power calibration portion served to calibrate the thermal-hydraulically determined test rod power with the reactor neutron detector chambers and the self-powered neutron detectors (SPNDs) mounted on the test train. The ramp rates used during this phase were similar to those that LOFT uses during Power Ascension Experiment Series L2.

An uninterrupted period of nuclear operation at the approximate desired test rod power for blowdown was performed immediately prior to the time of each blowdown initiation. This 2- to 3-hour period of constant power operation was necessary to build up the decay heat in the rods to approximately 79 to 82% of the maximum possible.

2.3 Blowdown, Reflood, and Quench Phases

Driver core power at the time of blowdown initiation for the LLR tests was controlled by the servo-controlled transient rods. Shutdown of the driver core, termed reactor scram, was accomplished by rapid insertion (approximately 100 ms) of the control rods to their seat, or in-core position. The warmup line valve was manually closed just prior to blowdown initiation for all tests. Reflood was programmed to be initiated well into the blowdown transients followed by quench cooling which terminated each test.

Table IV provides the reactor power reduction and valve sequencing times during the blowdown, reflood, and quench phases of each test.

The following paragraphs describe the events particular to each of the five LLR tests:

Test LLR-S0

The LOFT lead rod test program was initiated with a low-power, nuclear blowdown system operating test, Test LLR-S0. The blowdown was initiated on February 14, 1979. This test provided the opportunity to check system instrumentation, valve sequencing, system performance, and driver core controllability during the transient. The preblowdown driver core power of 1.5 MW was maintained 2 seconds into the transient at which time it was decreased to 1.0 MW using a 0.2-second ramp. Power was then maintained at 1.0 MW until the reactor was scrammed 20 seconds after blowdown initiation.

Test LLR-3

Test LLR-3 used the same test rods that were used in Test LLR-S0. The blowdown for Test LLR-3 was initiated on February 28, 1979. Reflood was initiated 35 seconds into the transient and quench cooling at 166 seconds; this sequence was identical to that of Test LLR-S0. No abnormalities were noted with the valve sequencing.

Test LLR-5

Two new unirradiated fuel rods were used in Test LLR-5. Blowdown was initiated on March 24, 1979. A two-second delayed reactor scram was used to attain higher cladding temperatures than those in Test LLR-3. Reflood was initiated as programmed at 120 seconds; however, quench cooling failed to initiate at 173 seconds. Test fuel quench was eventually accomplished by opening the loop isolation valves 300 seconds after initiation of blowdown.

Test LLR-4

On March 30, 1979, blowdown was initiated for Test LLR-4. A delayed reactor scram of 2.6 seconds was used to attain cladding temperatures that would result in uniform circumferential cladding collapse and waisting of the cladding. At approximately 15 seconds into the transient the loop isolation valves cycled open and shut, and the cold leg blowdown valves cycled shut and then opened. This abnormal behavior continued intermittently for the remainder of the transient and invalidated test results beyond 15 seconds. Since the maximum mechanical deformation of the test fuel was expected to have occurred during the first 12 seconds of the transient, the anomalous actuation of the isolation and blowdown valves did not affect the primary test objectives.

Test LLR-4A

Test LLR-4A was performed to investigate the effect of power ramping and an additional blowdown on three of the deformed test rods from Test LLR-4. The fourth test rod had been unirradiated prior to the test. Blowdown was initiated on May 18, 1979. A delayed scram of 2.85 seconds was used to attain cladding temperatures comparable to those attained in Test LLR-4. Reflood was initiated at 120 seconds into the transient and quench cooling at 239 seconds. The system performed as programmed.

TABLE IV

BLOWDOWN EVENT SEQUENCE FOR LOFT LEAD ROD TESTS

Time after initiation of blowdown (s)	Test LLR-S0	Test LLR-3	Test LLR-5	Test LLR-4	Test LLR-4A
-0.1	Loop bypass valve (GB-LM-11-7) opened and loop isolation valves (GB-LM-11-5,-6) closed[a].	Loop bypass valve (GB-LM-11-7) opened and loop isolation valves (GB-LM-11-5,-6) closed.	Loop bypass valve (GB-LM-11-7) opened and loop isolation valves (GB-LM-11-5,-6) closed.	Loop bypass valve (GP-LM-11-7) opened and loop isolation valves (GB-LM-11-5,-6) closed.	Loop bypass valve (GB-LM-11-7) opened and loop isolation valves (GB-LM-11-5, -6) closed.
Blowdown initiation	Cold leg blowdown valves (GB-LM-11-3, -4) opened. Reactor power maintained.	Cold leg blowdown valves (GB-LM-11-3, -4) opened. Reactor scrammed.	Cold leg blowdown valves (GB-LM-11-3, -4) opened. Reactor power maintained.	Cold leg blowdown valves (GB-LM-11-3, -4) opened. Reactor power maintained.	Cold leg blowdown valves (GB-LM-11-3, -4) opened. Reactor power maintained
2.0	Reactor power reduction ramp to 1 MW initiated.		Reactor scrammed.		
2.2	Reactor power at 1 MW.				
2.6				Reactor scrammed.	
2.85					Reactor scrammed.
3.65	Cold leg blowdown valve (GB-LM-11-4) closed.	Cold leg blowdown valve (GB-LM-11-4) closed.	Cold leg blowdown valve (GB-LM-11-4) closed.	Cold leg blowdown valve (GB-LM-11-4) closed.	Cold leg blowdown valve (GB-LM-11-4) closed.
15				Loop isolation valves and cold leg blowdown valves began abnormal cycling which continued for the remainder of the transient.	
20	Reactor scrammed.				
22	Cold leg blowdown valve (GB-LM-11-4) opened.	Cold leg blowdown valve (GB-LM-11-4) and hot leg blowdown valve (GB-LM-11-2) opened.	Cold leg blowdown valve (GB-LM-11-4) opened.		Cold leg blowdown valve (GB-LM-11-4) opened.
25	Cold leg blowdown valve (GB-LM-11-4) closed.	Cold leg blowdown valve (GB-LM-11-4) closed.			
35	Reflood initiated.	Reflood initiated.			
120			Reflood initiated.		Reflood initiated.

TABLE IV (continued)

Time after initiation of blowdown (s)	Test LLR-S0	Test LLR-3	Test LLR-5	Test LLR-4	Test LLR-4A
166	Hot leg blowdown valves and quench valve opened; cold leg blowdown valve (GB-LM-11-3) and cold leg shut off valve (GB-LM-11-18) closed.	Hot leg blowdown valve (GB-LM-11-1) and quench valve opened; cold leg blowdown valve (GB-LM-11-3) and cold leg shut off valve (GB-LM-11-18) closed.			
173			Hot leg blowdown valves opened; cold leg blowdown valves (GB-LM-11-3, -4) and cold leg shut off valve (GB-LM-11-18) closed. Quench flow was not initiated as programmed.		
239					Hot leg blowdown valves and quench valve opened; cold leg blowdown valves (GB-LM-11-3, -4) and cold leg shut off valve (GB-LM-11-18) closed.
300			Loop isolation valves (GB-LM-11-5, -6) opened to provide fuel quench.		

---

a. The time required for the blowdown system valves to change states is ≈100 ms.

III. INSTRUMENTATION AND MEASUREMENTS

Instrumentation for the LLR tests was designed to measure and record the important events that occur prior to and during a LOCA test. The measurements presented in this report have been divided into four instrumentation sections: (a) fuel rod, (b) test train, (c) spool piece, and (d) plant.

1. FUEL ROD INSTRUMENTATION

The test fuel rods were instrumented for measurements of internal gas pressure, cladding surface temperature, fuel centerline temperature, plenum temperature, and cladding elongation. This instrumentation is specified in the following description and the geometric orientation is shown in Figures 8, 9, and 10 for Tests LLR-S0 and -3, LLR-5 and -4, and LLR-4A, respectively.

The measurement identifiers are included in parentheses and consist of 18 characters. The first eight characters indicate the type of measurement and are followed by two blank spaces. Characters 11 through 18 uniquely identify the measurement by specifying its orientation, location, manufacturer, or range.

(1) One molybdenum-rhenium sheathed, tungsten-rhenium thermocouple was located within each test fuel rod to measure the fuel centerline temperature. The following thermocouples were positioned axially at the center of the active fuel of Rods 312-2, 312-4, and 345-2.

(TFCL3122 +.00TC02)
(TFCL3124 +.00TC04)
(TFCL3452 +.00TC06)

Thermocouples positioned 0.076 m above the center of the active fuel of Rods 312-1, 312-3, 345-1, and 399-2 were as follows.

(TFCL3121 +.08TC01)
(TFCL3123 +.08TC03)
(TFCL3451 +.08TC05)
(TFCL3992 +.08TC08)

(2) One stainless steel sheathed, magnesia insulated, Type K thermocouple was located at the midplane of the upper plenum of each test fuel rod to measure the plenum gas temperature. The measurement identifiers are as follows.

(PLNMTEMP 312-1R01)
(PLNMTEMP 312-2R02)
(PLNMTEMP 312-3R03)
(PLNMTEMP 312-4R04)
(PLNMTEMP 345-1R05)
(PLNMTEMP 345-2R06)
(PLNMTEMP 399-2R08)

(3) Two titanium sheathed, magnesia insulated, Type K cladding surface thermocouples with spaded junctions were installed on each of the test fuel rods except for Rod 345-2. A thermocouple was located 0.076 m above the active fuel center at 180-degree azimuthal orientation (zero degrees is toward the test train center for all rods) on Rods 312-1, 312-2, 312-3, 312-4, and 345-1. The following indicates the measurement identifiers used.

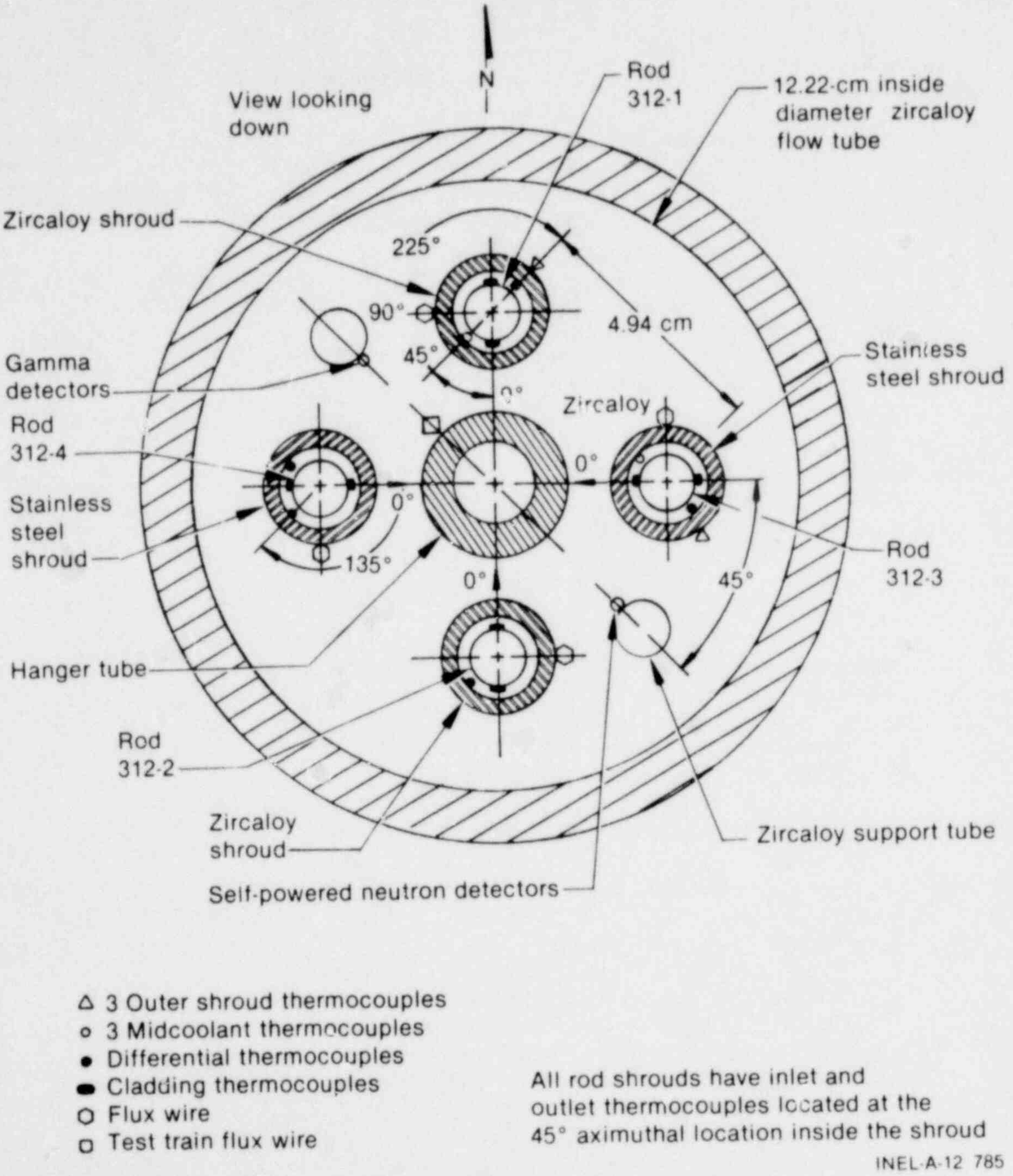

All rod shrouds have inlet and outlet thermocouples located at the 45° aximuthal location inside the shroud

INEL-A-12 785

Fig. 8 Test fuel rod instrumentation orientation schematic - Tests LLR-S0 and -3.

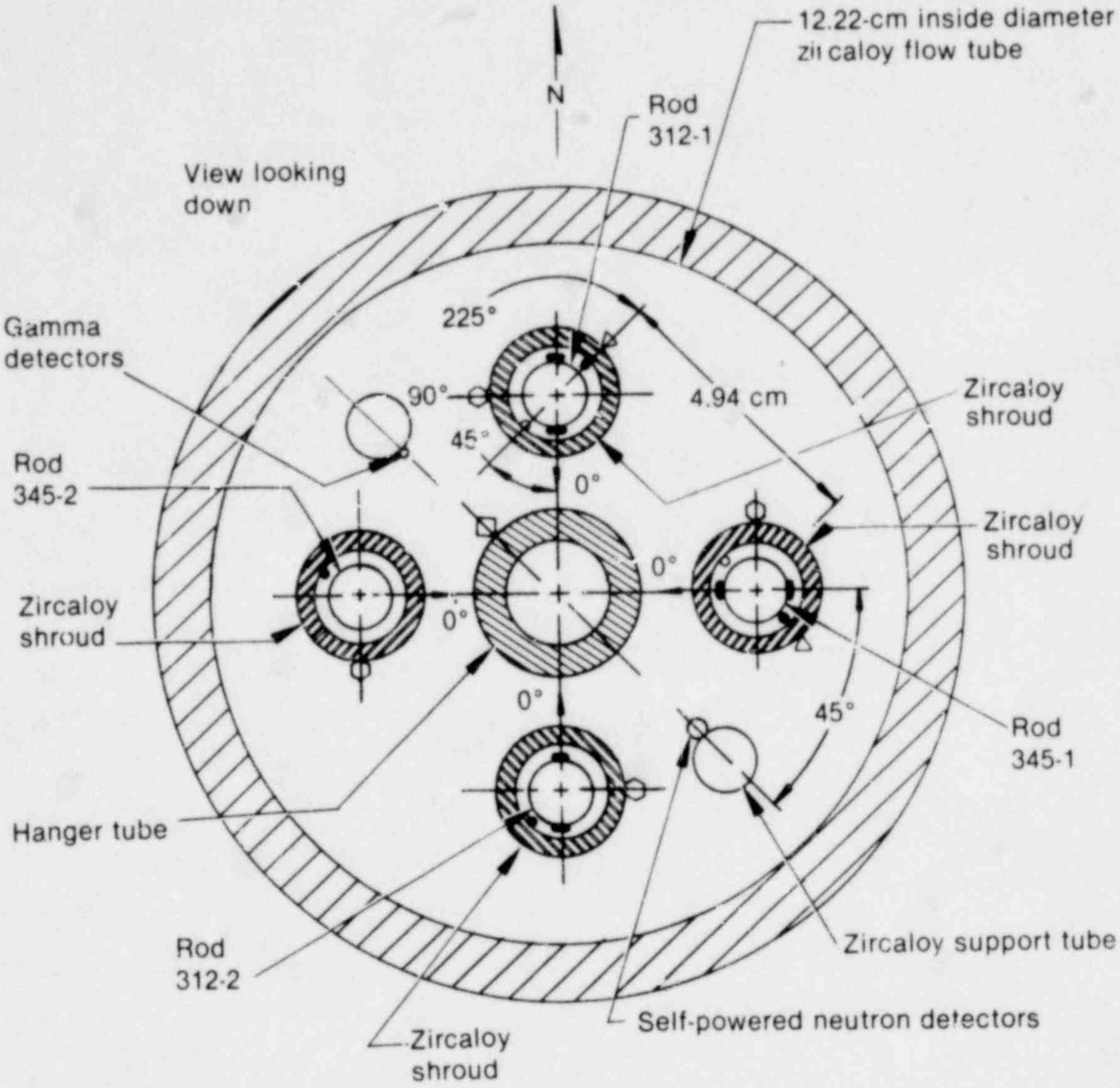

- △ 3 Outer shroud thermocouples
- ○ 3 Midcoolant thermocouples
- ● Differential thermocouples
- ⬬ Cladding thermocouples
- ○ Flux wire
- □ Test train flux wire

All rod shrouds have inlet and outlet thermocouples located at the 45° aximuthal location inside the shroud.

INEL-A-12 786-1

Fig. 9 Test fuel rod instrumentation orientation schematic - Tests LLR-5 and -4.

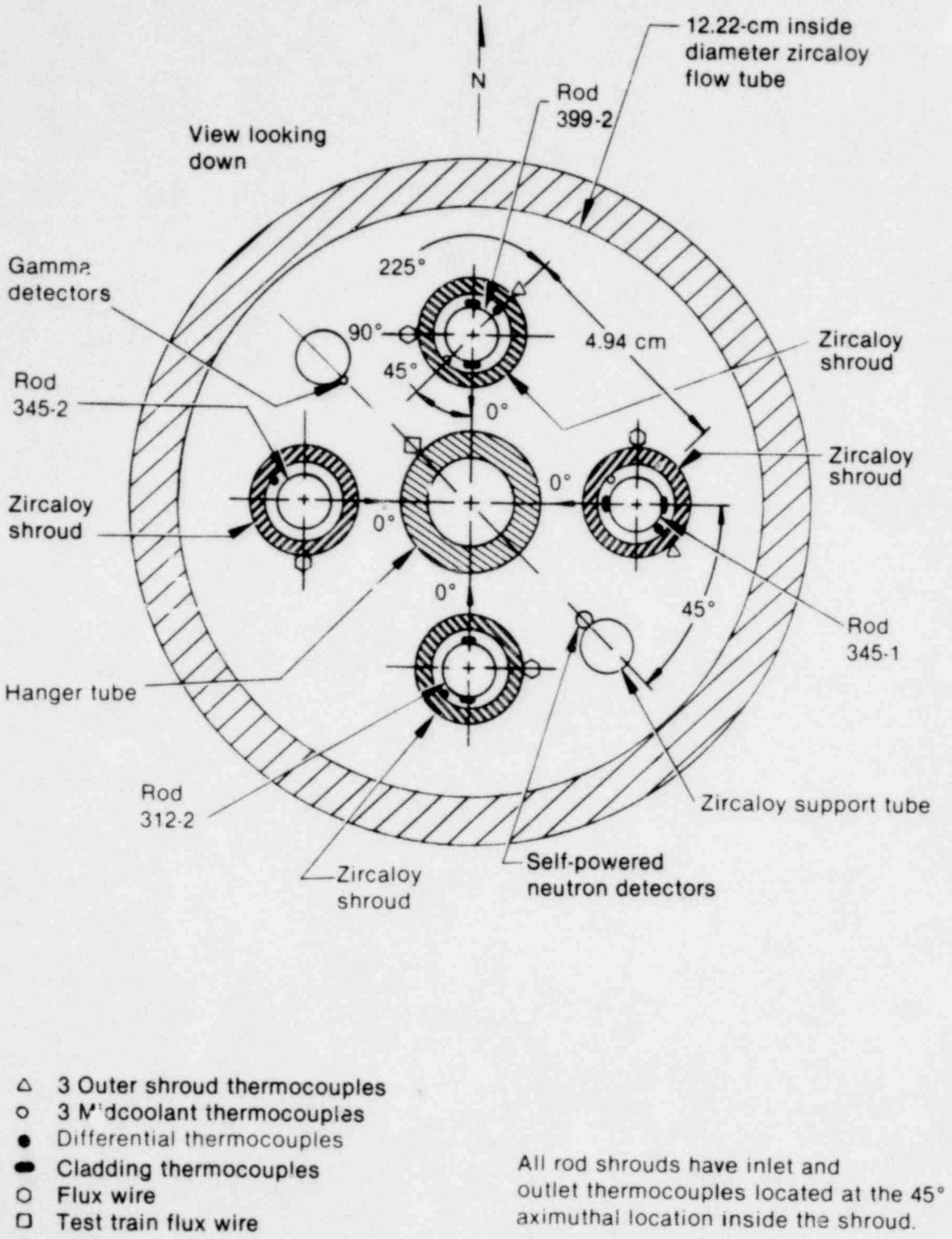

All rod shrouds have inlet and outlet thermocouples located at the 45° aximuthal location inside the shroud.

INEL-A-12 770

Fig. 10 Test fuel rod instrumentation orientation schematic - Test LLR-4A.

(CLAD3121 +0818001)
(CLAD3122 +0818002)
(CLAD3123 +0818003)
(CLAD3124 +0818004)
(CLAD3451 +0818005)

The second thermocouple was located 0.076 m above the active fuel center at zero-degree azimuthal orientation on Rods 312-1, 312-3, 312-4, and 345-1 except for Rod 312-2 where it was positioned at the active fuel center. The following list indicates the measurement identifiers used.

(CLAD3121 +0800001)
(CLAD3122 +0000002)
(CLAD3123 +0800003)
(CLAD3124 +0800004)
(CLAD3451 +0800005)

Test Rod 399-2 had a thermocouple mounted at the active fuel center and 180-degree azimuthal orientation (CLAD3992 +0018008).

and a second located 0.143 m below the active fuel center and zero degree-azimuthal orientation (CLAD3992 -1400008).

(4) One 3.45 MPa Kaman Sciences Corporation pressure transducer was mounted just above each test fuel rod outside the shroud within a thermal shield to minimize temperature effects. The transducers were attached to the fuel rod end caps with a 1.6-mm outside diameter tube to measure the test fuel rod plenum pressure. The following indicates the measurement indentifiers used.

(RODPRESS 312-1R01)
(RODPRESS 312-2R02)
(RODPRESS 312-3R03)
(RODPRESS 312-4R04)
(RODPRESS 345-1R05)
(RODPRESS 345-2R06)
(RODPRESS 399-2R08)

(5) One EG&G Idaho, Inc. linear variable differential (LVDT) transformer was mounted below each of the four test fuel rod positions in the test train to measure the cladding axial elongation of the test fuel rods. The following identifies the measurement identifiers that were used.

(LVDT ROD 312-1 01)
(LVDT ROD 312-2 02)
(LVDT ROD 312-3 03)
(LVDT ROD 312-4 04)
(LVDT ROD 345-1 03)
(LVDT ROD 345-2 04)
(LVDT ROD 399-2 01)

2. TEST TRAIN INSTRUMENTATION

The test train hardware provided support for a variety of devices which measured the temperature, pressure, and volumetric flow rates of the coolant within the IPT; the material temperature of the test rod shrouds; and the local neutron and gamma flux. The test train instrumentation is shown in Figure 11 and specified in the following description. Figures 8, 9, and 10 provide radial orientation of the thermocouples associated with the test rod shrouds.

(1) A Chromel-Alumel, Type K thermocouple with stainless steel sheath and magnesia insulation measured the coolant temperature at the inlet of each test rod shroud. The thermocouple tip was located at the bottom of the active fuel stack, pointing downward, with the tip centerline standing away from the inside shroud surface 1.3 mm. The measurement identifiers used are as follows.

(INLTTEMP 312-1R01)
(INLTTEMP 312-2R02)
(INLTTEMP 312-3R03)
(INLTTEMP 312-4R04)
(INLTTEMP 345-1R05)
(INLTTEMP 345-2R06)
(INLTTEMP 399-2R08)

(2) A Chromel-Alumel, Type K thermocouple with stainless steel sheath and magnesia insulation measured the coolant temperature at the outlet of each test rod shroud. The thermocouple tip was located at the top of the active fuel stack, pointing downward, with the tip centerline standing away from the inside shroud surface 1.3 mm. The following indicates the measurement identifiers that were used.

(OUT TEMP 312-1R01)
(OUT TEMP 312-2R02)
(OUT TEMP 312-3R03)
(OUT TEMP 312-4R04)
(OUT TEMP 345-1R05)
(OUT TEMP 345-2R06)
(OUT TEMP 399-2R08)

(3) Three Chromel-Alumel, Type K thermocouples with stainless steel sheath and magnesia insulation measured the coolant temperature near the active fuel midpoints of Rods 312-1, 312-3, 345-1, and 399-2 only. The thermocouple tip centerlines were mounted 1.3 mm away from the inside shroud surface pointing downward into the coolant flow. One thermocouple was located at the center of the active fuel of each rod. The measurement identifiers are as follows.

(MIDT3121 +.000R01)
(MIDT3123 +.000R03)
(MIDT3451 +.000R05)
(MIDT3992 +.000R08)

A second thermocouple was 0.152 m below the center of the active fuel of each rod. The following indicates the measurement identifiers.

(MIDT3121 -.152R01)
(MIDT3123 -.152R03)
(MIDT3451 -.152R05)
(MIDT3992 -.152R08)

A third thermocouple was located 0.152 m above the center of the active fuel of each rod. The following indicates the measurement identifiers used.

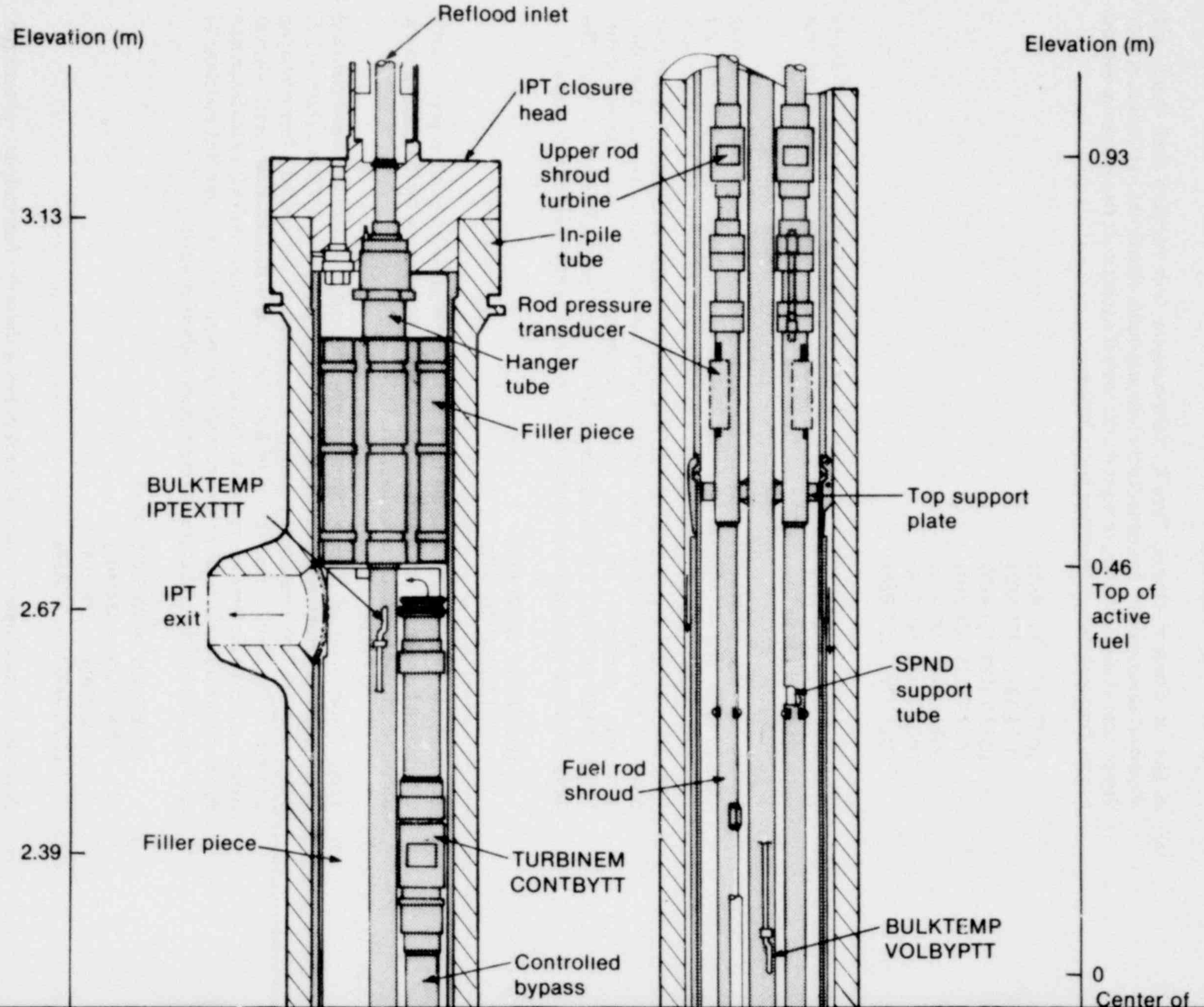
Reflood inlet
Elevation (m)
IPT closure head
Upper rod shroud turbine
3.13
In-pile tube
Rod pressure transducer
Hanger tube
Filler piece
BULKTEMP IPTEXTTT
IPT exit
2.67
Filler piece
2.39
TURBINEM CONTBYTT
Controlled bypass
Elevation (m)
0.93
Top support plate
0.46
Top of active fuel
SPND support tube
Fuel rod shroud
BULKTEMP VOLBYPTT
0
Center of

1405 060

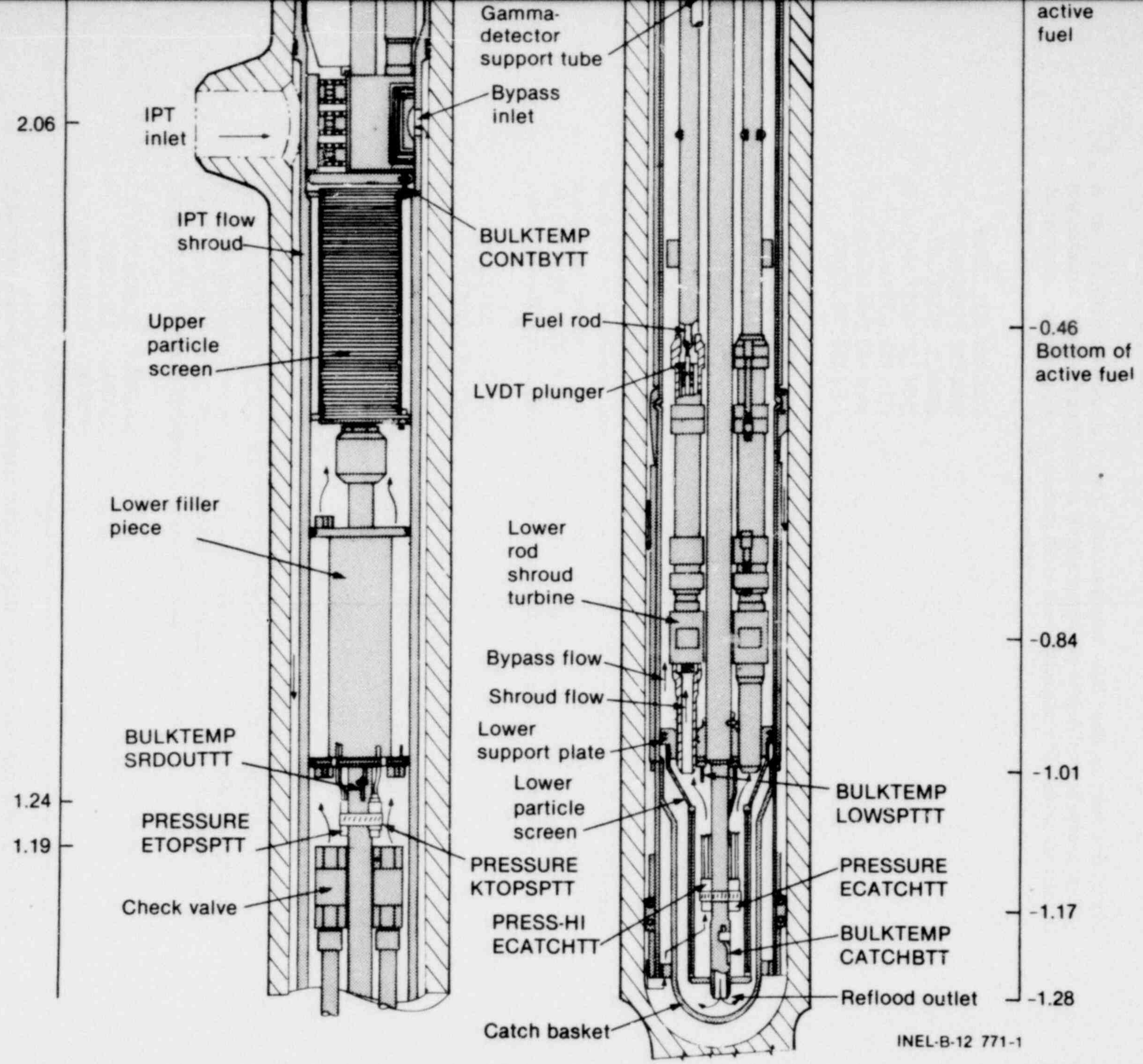

Fig. 11 Axial cross section of test train assembly.

(MIDT3121 +.152R01)
(MIDT3123 +.152R03)
(MIDT3451 +.152R05)
(MIDT3992 +.152R08)

(4) A pair of Chromel-Alumel, Type K thermocouples with stainless steel sheath and magnesia insulation were positioned in the inlet and outlet of each test rod shroud, at 225-degree azimuthal orientation, to measure the coolant temperature rise across the test rod length. The measurement identifiers are as follows.

(DELT3121 225 R01)
(DELT3122 225 R02)
(DELT3123 225 R03)
(DELT3124 225 R04)
(DELT3451 225 R05)
(DELT3452 225 R06)
(DELT3992 225 R08)

An additional thermocouple pair mounted on test Rod 312-4 shroud at 135-degree azimuthal orientation provided a second differential temperature measurement for that rod (DELT3124 135 RO4).

Failure of the differential temperature measurement for Rod 312-1 following Tests LLR-S0 and -3 required the installation of additional thermocouples for Tests LLR-5 and -4. A new thermocouple was installed in the outlet check valves of both Rods 312-1 and 312-2. A new differential temperature measurement for each rod was then produced by combining these new thermocouples with a common, existing inlet thermocouple mounted on the lower support plate (this measurement, BULKTEMP LOWSPTTT, was consequently lost for Tests LLR-5 and -4 only). The new differential temperature measurements for Rods 312-1 and 312-2 were designated.

(DELT3121 CVSP R01)
(DELT3122 CVSP R02)

The duplicate measurement installed for Rod 312-2 was provided to allow performance comparison between the new differential temperature measurement on Rod 312-1 and the original configuration of the other test rods.

(5) Three Chromel-Alumel, Type K thermocouples with magnesia insulation and flattened spade junctions were attached directly to the outside of each shroud of Rods 312-1, 312-3, 345-1, and 399-2 to measure the material temperature of the shroud. Thermocouples attached to the stainless steel shroud of Rod 312-3 used a stainless steel sheath whereas those attached to the three zirconium shrouds used a titanium sheath with a tantalum barrier at the weld junction. One thermocouple was located at the active fuel midplane of each rod. The following indicates the measurement identifiers used.

(TSRD3121 +.000R01)
(TSRD3123 +.000R03)
(TSRD3451 +.000R05)
(TSRD3992 +.000R08)

A second thermocouple was located 0.152 m below the active fuel midplane of each rod. The measurement identifiers are as follows.

(TSRD3121 -.152R01)
(TSRD3123 -.152R03)
(TSRD3451 -.152R05)
(TSRD3992 -.152R08)

A third thermocouple was located 0.152 m above the active fuel midplane of each rod. The following indicates the measurement identifiers used.

(TSRD3121 +.152R01)
(TSRD3123 +.152R03)
(TSRD3451 +.152R05)
(TSRD3992 +.152R08)

(6) Six Chromel-Alumel, Type K thermocouples were mounted adjacent to the test train hanger rod and center tie rod to measure bulk coolant temperature throughout the IPT. These thermocouples were mounted with the tip 10 thermocouple diameters from the nearest sheath attachment, the tip centerline standing away from the hanger rod 3.2 mm, and the tip pointing downward. The lowest of the six thermocouples was located within the catch basket in the lower plenum (BULKTEMP CATCHBTT).

A second thermocouple extended a short distance below the lower support plate in the lower plenum (BULKTEMP LOWSPTTT).

The third thermocouple was positioned at the midplane of the active fuel in the bypass volume outside the test rod shrouds (BULKTEMP VOLBYPTT).

The fourth thermocouple was positioned 51 mm above the test fuel rod shroud outlets (BULKTEMP SRDOUTTT).

The fifth thermocouple measured the coolant temperature in the area of the controlled bypass inlet and was located about 60 mm below this inlet (BULKTEMP CONTBYTT).

The uppermost thermocouple was positioned opposite the outlet of the IPT (BULKTEMP IPTEXTTT).

(7) A 17.2-MPa EG&G Idaho, Inc. strain post pressure transducer was mounted within the catch basket to measure the coolant inlet pressure of the lower plenum (PRESSURE ECATCHTT).

(8) A 17.2-MPa EG&G Idaho, Inc. strain post pressure transducer and a 17.2-MPa Kaman Sciences Corp. eddy current pressure transducer were mounted side by side just above the test fuel rod shroud outlet check valves to measure coolant outlet pressure above the top support plate. The measurement identifiers used are as follows.

(PRESSURE ETOPSPTT)
(PRESSURE KTOPSPTT)

(9) A 69-MPa EG&G Idaho, Inc. strain post pressure transducer was mounted within the catch basket to measure the maximum overpressure in the lower plenum (PRESS-HI ECATCHTT).

(10) A Flow Technology, Inc. bi-directional turbine flowmeter was mounted above and below each test fuel rod within the flow shroud to measure the inlet and outlet volumetric flow

rates of each test fuel rod shroud. The identifiers provide azimuthal orientation within the test train with the north position corresponding to zero degrees. The following indicates the measurement identifiers used.

(TURB3121 UP000N01)
(TURB3121 LO000N01)
(TURB3122 UP180N02)
(TURB3122 LO180N02)
(TURB3123 UP090N03)
(TURB3123 LO090N03)
(TURB3124 UP270N04)
(TURB3124 LO270N04)
(TURB3451 UP090N03)
(TURB3451 LO090N03)
(TURB3452 UP270N04)
(TURB3452 LO270N04)
(TURB3992 UP000N01)
(TURB3992 LO000N01)

(11) One Flow Technology, Inc. turbine flowmeter measured the volumetric flow rate within the controlled bypass piping (TURBINEM CONTBYTT).

(12) Seven Reuter-Stokes cobalt, self-powered neutron detectors (SPNDs) were installed in a vertical column 3.49 cm radially from the test train center and at 135-degree test train azimuthal orientation, to measure the relative neutron flux. The centers of the active portion of each SPND were axially located at 0.343, 0.228, and 0.142 m above the active fuel midplane; at the active fuel midplane; and 0.114, 0.228, and 0.343 m below the active fuel midplane. The following measurement identifiers were used.

(NEUTFLUX +.343 TT)
(NEUTFLUX +.228 TT)
(NEUTFLUX +.142 TT)
(NEUTFLUX +.000 TT)
(NEUTFLUX -.114 TT)
(NEUTFLUX -.228 TT)
(NEUTFLUX -.343 TT)

(13) Three Reuter-Stokes platinum gamma flux detectors were installed in a vertical column 3.49 cm radially from the test train center and at 315-degree test train azimuthal orientation, to measure the relative gamma flux. The detectors were axially located 0.228 m above the active fuel midplane, at the active fuel midplane, and 0.228 m below the active fuel midplane. The measurement identifiers used are as follows.

(GAMMAFLX +.228 TT)
(GAMMAFLX +.000 TT)
(GAMMAFLX -.228 TT)

3. MEASUREMENT SPOOL INSTRUMENTATION

The three measurement spools provided additional initial conditions and blowdown instrumentation which further characterized the blowdown coolant variables of pressure, temperature, velocity, and density in the lines leading to the Henry nozzle break planes. Schematics of the measurement spools showing associated instrumentation positions are provided in Figures 12 and 13. Instrumentation for the measurement spools is described as follows:

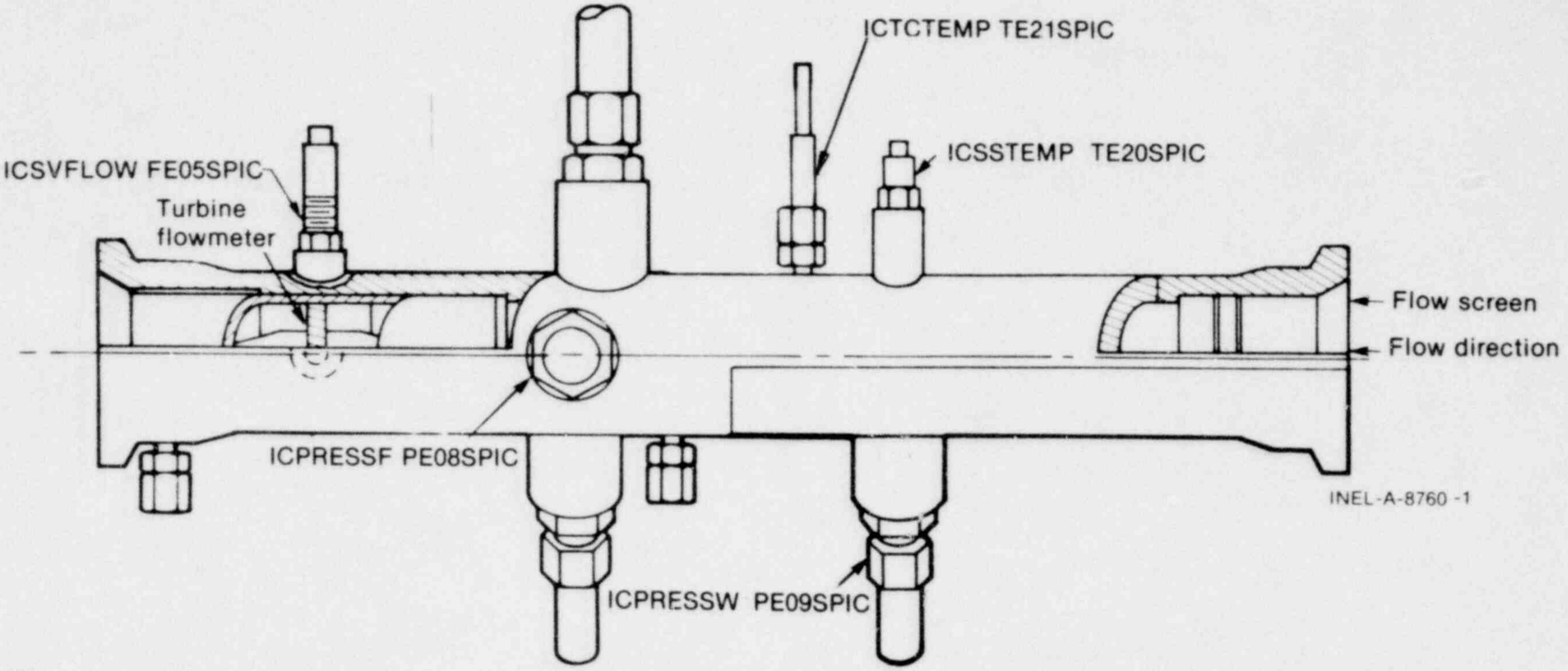

Fig. 12 Initial condition spool for LOFT lead rod tests.

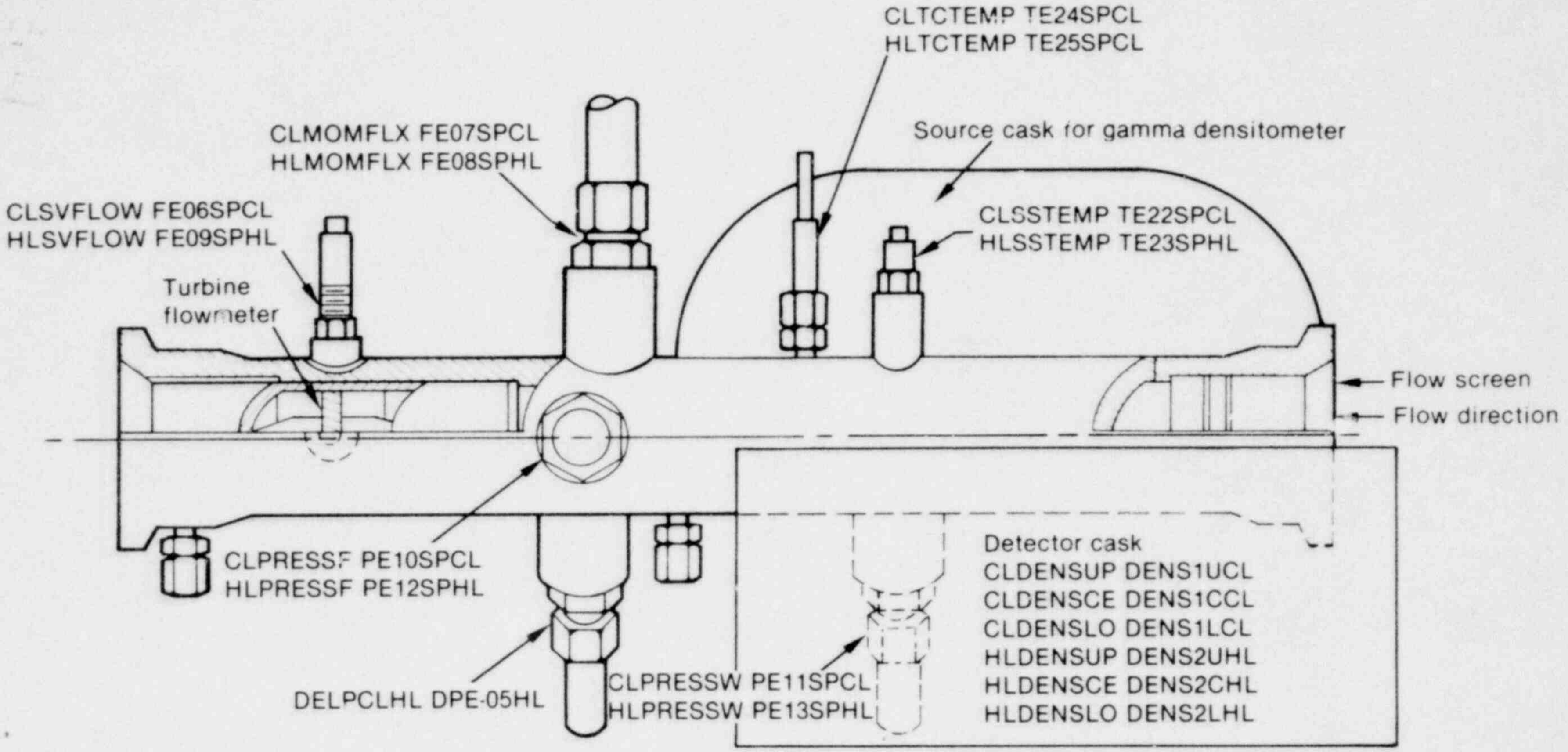

INEL-A-8332-3

Fig. 13 Blowdown spool for LOFT lead rod tests.

1405 066

(1) A Rosemount Company resistance temperature detector was installed in each spool piece to measure the steady state preblowdown temperature of the coolant in each spool. The following measurement identifiers were used.

(ICSSTEMP TE20SPIC)
(CLSSTEMP TE22SPCL)
(HLSSTEMP TE23SPHL)

(2) A Nanmac Corporation Type K ribbon thermocouple was installed in each spool piece to measure the coolant temperature during the blowdown transient. The measurement identifiers used are as follows.

(ICTCTEMP TE21SPIC)
(CLTCTEMP TE24SPCL)
(HLTCTEMP TE25SPHL)

(3) A Precise Sensors flush mounted pressure transducer was installed on each spool piece to measure the subcooled decompression transients. The following measurement identifiers were used.

(ICPRESSF PE08SPIC)
(CLPRESSF PE10SPCL)
(HLPRESSF PE12SPHL)

(4) A Precise Sensors water-cooled, stand-off mounted pressure transducer was installed on each spool piece to measure the preblowdown and saturated decompression coolant pressures. The measurement identifiers used are as follows.

(ICPRESSW PE09SPIC)
(CLPRESSW PE11SPCL)
(HLPRESSW PE13SPHL)

(5) A BLH Electronics pressure difference transducer was connected to both blowdown spools to measure the coolant pressure differential from the hot leg to the cold leg blowdown piping (DELPCLHL DPE-05HL).

(6) A Flow Technology, Inc. unidirectional, full flow turbine flowmeter was installed in each spool piece to measure preblowdown coolant velocity within the inlet spool, and blowdown velocities from the IPT in the hot and cold leg spools. The following measurement identifiers were used.

(ICSVFLOW FE05SPIC)
(CLSVFLOW FE06SPCL)
(HLSVFLOW FE09SPHL)

(7) A Ramapo Instrument Co., Inc. drag disk installed in each blowdown spool measures the coolant momentum flux during the transient. It was positioned in the center of the flow area and intercepted approximately 12% of the flow area. The measurement identifiers used are as follows.

(CLMOMFLX FE07SPCL)
(HLMOMFLX FE08SPHL)

(8) An EG&G Idaho, Inc. three-beam gamma densitometer measured the coolant density within both the cold and hot leg spool pieces. The densitometers use the attenuation of

gamma rays from a Cesium-137 source to sense the density of fluid within the blowdown spool. The three beams traverse the upper, center, and lower parts of the horizontal spool pieces as shown in Figures 14 and 15. The following indicates the measurement identifiers used.

(CLDENSUP DENS1UCL)
(CLDENSCE DENS1CCL)
(CLDENSLO DENS1LCL)
(HLDENSUP DENS2UHL)
(HLDENSCE DENS2CHL)
(HLDENSLO DENS2LHL)

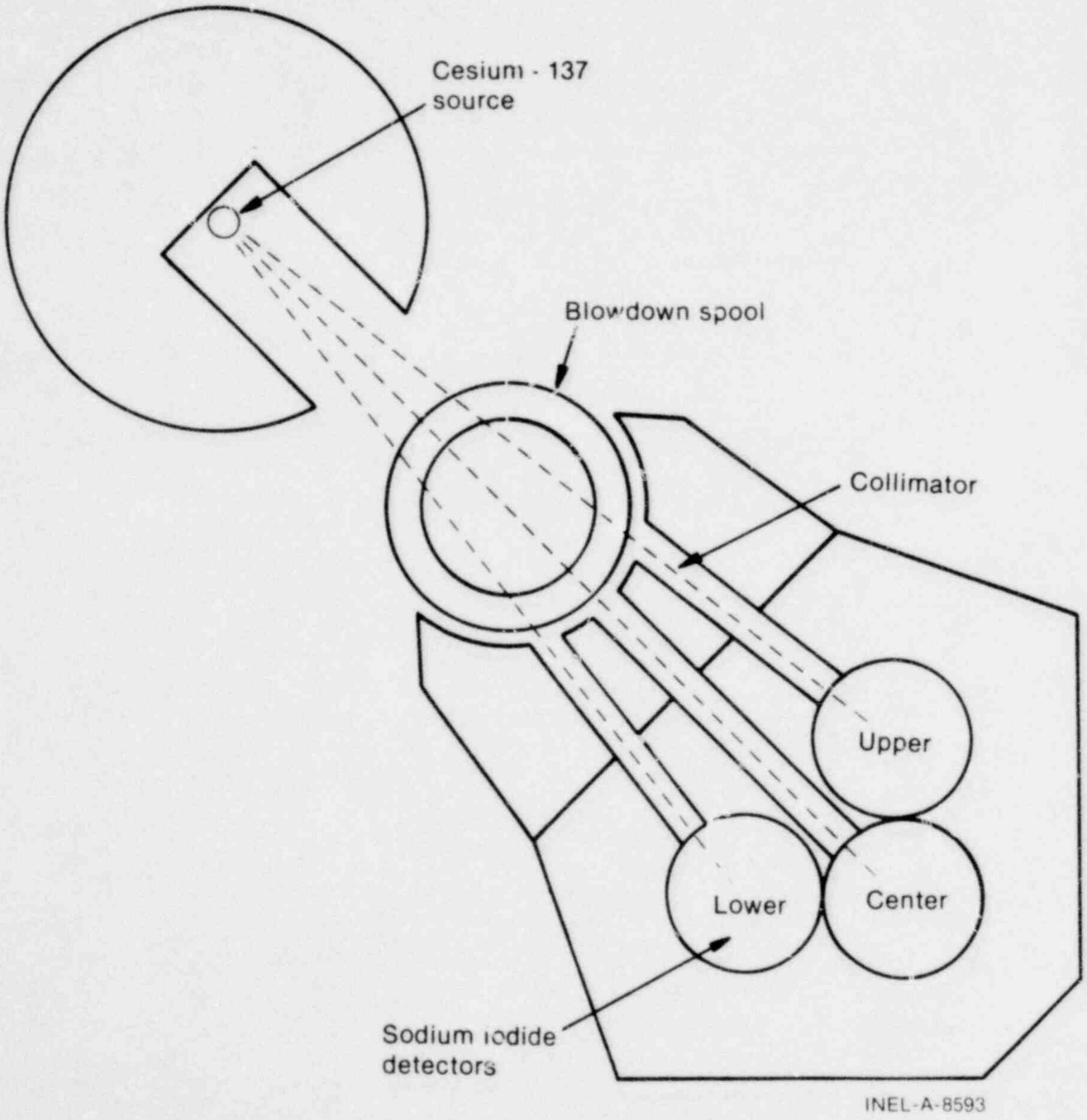

Fig. 14 Gamma beam densitometer.

1405 068

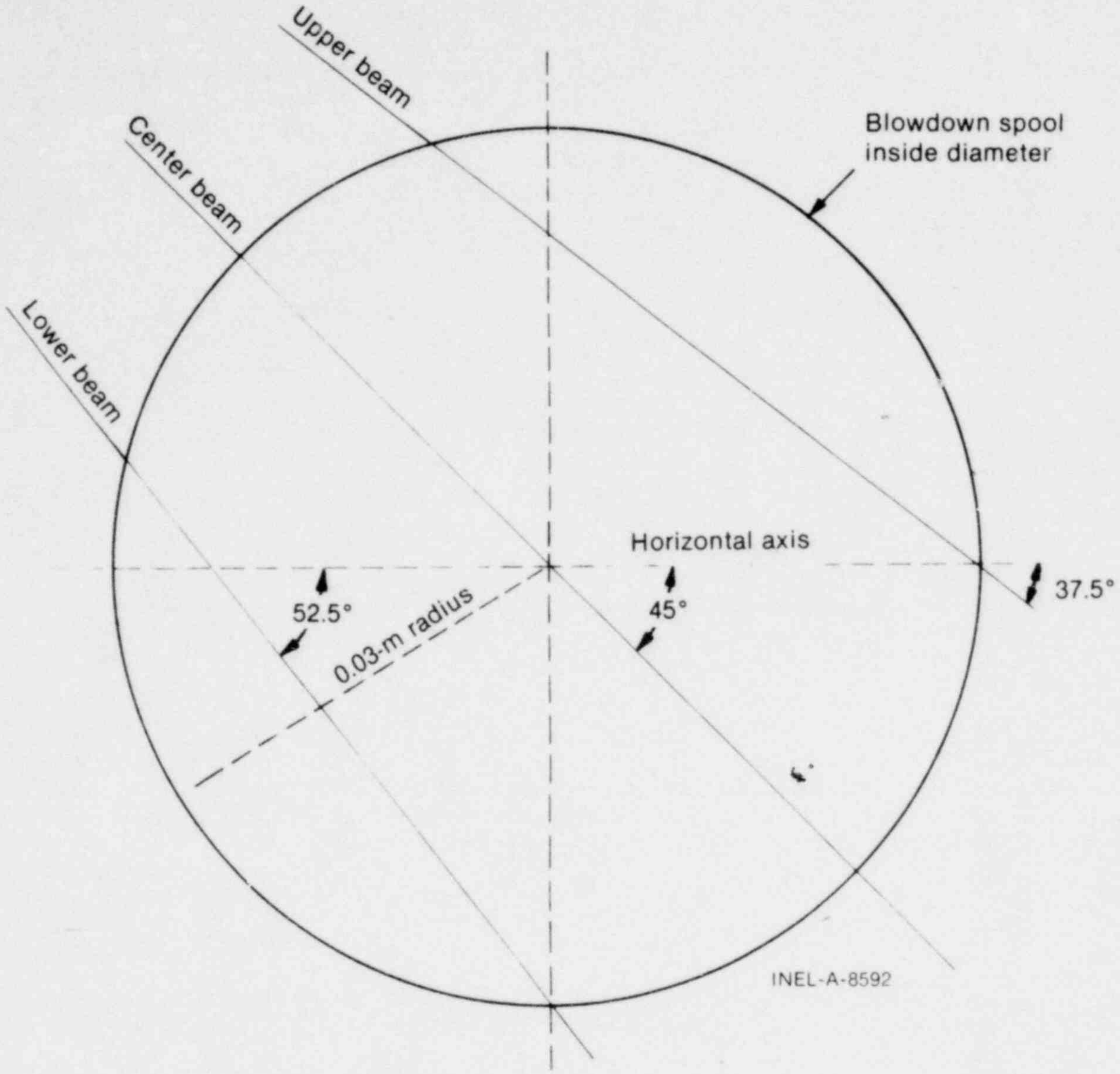

Fig. 15 Gamma beam densitometer paths through the blowdown spools.

To calculate the total average density, the vertical density gradient was assumed to be linear; then the chordal densities were fit to the model and integrated over the spool piece cross section. The measurement identifiers used are as follows.

(CLDENAVE DENS1 CL)
(HLDENAVE DENS2 HL)

In the two blowdown spools the flow regime can be considered homogeneous in most cases. The fluid is made homogeneous by flow dispersing screens located in the inlet section of the spool pieces. These screens are designed to remove fluid swirl caused by upstream piping and then disperse and homogenize the fluid. At low velocities and high void fractions, the flow will degenerate into a stratified state which introduces significant flow regime errors in the data presented.

1405 069

4. PLANT INSTRUMENTATION

The plant instrumentation included measurement of the PBF driver core power, fission products in the experimental loop, and the reflood volumetric flow rate. Ionization chambers sensitive to gamma and neutron radiation provided reactor power, and their locations are shown in the driver core cross section, Figure 16. The fission product detection system withdrew a continuous sample stream from the coolant loop near the IPT outlet and monitored the sample for fission products which would indicate test rod failure. The coolant transit time from the IPT to the detector locations was approximately 2 minutes. The plant instrumentation is specified in the following description.

(1) One 2.5- by 3.8-cm NaI crystal gamma ray detector was used to determine the gross gamma count rate in the sample line before, during, and after fission product release. The output from this detector was fed into two single channel analyzers. One analyzer measured the gamma-ray intensity in the 150- to 3400-kev energy range (FPDSGAMA NUM 01FP)

and the other in the 3400- to 6300-kev energy range (FPDSGAMA NUM 03FP).

(2) One 7.6- by 7.6-cm NaI crystal gamma ray detector did not view the sample stream but measured the effectiveness of the detector enclosure shielding against direct reactor radiation. This detector measured the gamma-ray intensity in the 150- to 6300-kev energy range (FPDSGAMA NUM 02FP).

(3) One BF_3 delayed neutron detector was used to detect delayed neutrons in the sample stream (FPDSNEUT NEUTRNFP).

(4) Two Flow Technology, Inc. turbine flowmeters were installed in the parallel portion of the reflood line to measure the volumetric reflood flow rate through the two control valves. The following indicates the measurement identifiers used.

(REFLDSYS FLO 01PT)
(REFLDSYS FLO 02PT)

(5) Two Westinghouse Electric Corporation, WX-31994, ionization chambers installed in the west and east corners of the PBF driver core measured the steady-state reactor power. The measurement identifiers used are as follows.

(REACTPOW PPS-01PT)
(REACTPOW PPS-02PT)

1405 070

POOR ORIGINAL

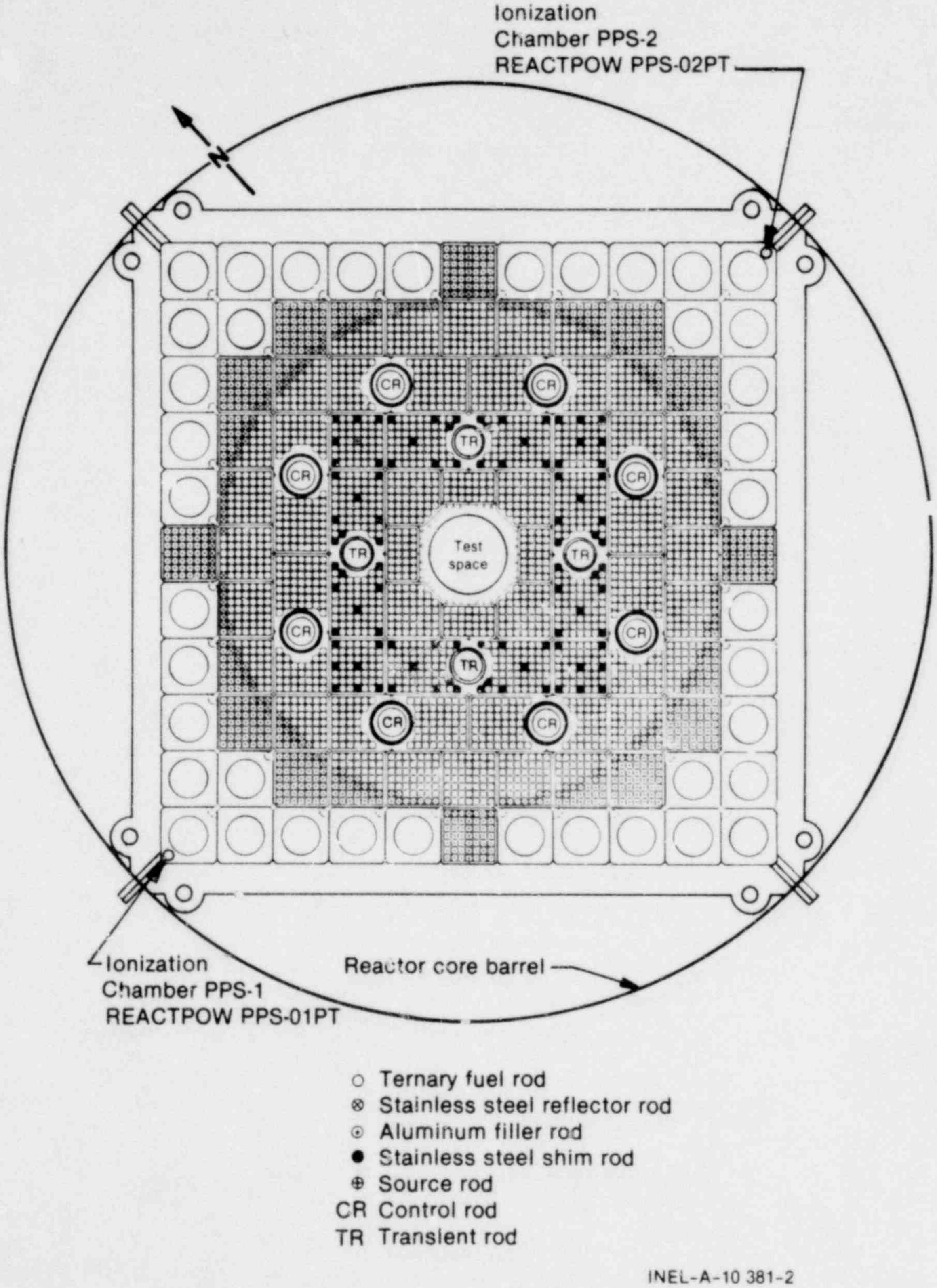

Fig. 16 Radial cross section of the PBF reactor core with ionization chamber locations.

1405 071

IV. DATA PRESENTATION

The data from the LLR Tests are presented with brief comment. The processing analysis has been performed only to the extent necessary to obtain appropriate engineering units and to ensure that the data are reasonable and consistent. All the data in this report were subjected to a thorough review by comparing instrument channel outputs with duplicate measurements, calculated variable values, initial conditions, and pre- and postcalibration results. Appendix A describes the methods used to determine the adjustments that have been applied to the presented data and provides the basis for categorizing the data as follows:

(1) Qualified engineering unit data (QEUD) - qualified to represent the variable being measured within specified uncertainty limits

(2) Restrained data - appear reasonable but are not within uncertainty limits, or data are not available from an independent channel for comparison

(3) Trend data - are suitable for illustrative purposes but probably not for numerical analysis

(4) Failed data - are irretrievable due to a transducer, signal conditioning, or data channel failure or inadequate rejection of extraneous noise, transients, or frequencies.

All detector analog output was digitized and recorded by the PBF data acquisition and reduction system (PBF/DARS). The PBF/DARS tape recording system was configured to record at four different bandwidths:

(1) dc to 10 Hz

(2) dc to 100 Hz

(3) dc to 5 kHz

(4) dc to 20 kHz.

Table V lists all the measurements included in this report and specifies the measurement location, the type of detector, the detector range and frequency response, and the PBF/DARS recording range and bandwidth. Table VI lists the qualification category of the data and references the measurement to the corresponding figure for each test.

The data graphs, Figures 17 through 533, for the blowdown portions of the five tests are presented on the subsequent pages of this report. Time zero for the blowdown data is the time of blowdown initiation (that is, the time when the cold leg blowdown valves first begin to open). The power calibration and preconditioning data are included on microfiche which is attached to the back cover of this report. The time of blowdown on these plots varies for each test as follows:

	Blowdown Initiation (hours after start of power calibration)
Test LLR-S0	31.5
Test LLR-3	26.5
Test LLR-5	16.7
Test LLR-4	12.3
Test LLR-4A	13.3

The scales selected for the graphs do not reflect the obtainable resolution of the data.

Appendix B discusses the analysis of the data which provides a guide to the uncertainty associated with measurements in the PBF system.

TABLE V

TEST LLR INSTRUMENTATION

Measurement		Detector Location and Comments[a]	Range[a]		Frequency Response[a]	
			Detector	Data Acquisition System	Detector	Data Acquisition System
Fuel Rod						
TFCL3121	+.08TC01	Tungsten-rhenium thermocouple within Rod 312-1, 0.076 m above active fuel center to measure fuel centerline temperature.	346 to 2920 K	280 to 2500 K	350 Hz	10 Hz
TFCL3122	+.00TC02	Rod 312-2, at the active fuel center.	349 to 2893 K			
TFCL3123	+.08TC03	Rod 312-3, 0.076 m above the active fuel center.	352 to 2895 K			
TFCL3124	+.00TC04	Rod 312-4, at the active fuel center.	344 to 2873 K			
TFCL3451	+.08TC05	Rod 345-1, 0.076 m above the active fuel center.	340 to 2902 K			
TFCL3452	+.00TC06	Rod 345-2, at the active fuel center.	348 to 2905 K			
TFCL3992	+.08TC08	Rod 399-2, 0.076 m above the active fuel center.	346 to 2920 K			
PLNMTEMP	312-1R01	Type K thermocouple at the midplane of the upper plenum of Rod 312-1 to measure the plenum gas temperature.	273 to 1309 K	280 to 1530 K	>8 Hz	10 Hz
PLNMTEMP	312-2R02	Rod 312-2.				
PLNMTEMP	312-3R03	Rod 312-3.				
PLNMTEMP	312-4R04	Rod 312-4.				
PLNMTEMP	345-1R05	Rod 345-1.				
PLNMTEMP	345-2R06	Rod 345-2.				
PLNMTEMP	399-2R08	Rod 399-2.				
CLAD3121	+0818001	Type K thermocouple on Rod 312-1 cladding surface, 0.076 m above the active fuel center and 180° orientation, to measure cladding temperature.	273 to 1309 K	280 to 1530 K	350 Hz	10 Hz
CLAD3121	+0800001	Rod 312-1, 0.076 m and 0° orientation.				
CLAD3122	+0818002	Rod 312-2, 0.076 m and 180° orientation.				
CLAD3122	+0000002	Rod 312-2, at the active fuel center and 0° orientation.				
CLAD3123	+0818003	Rod 312-3, 0.076 m and 180° orientation.				
CLAD3123	+0800003	Rod 312-3, 0.076 m and 0° orientation.				
CLAD3124	+0818004	Rod 312-4, 0.076 m and 180° orientation.				
CLAD3124	+0800004	Rod 312-4, 0.076 m and 0° orientation.				
CLAD3451	+0818005	Rod 345-1, 0.076 m and 180° orientation.				
CLAD3451	+0800005	Rod 345-1, 0.076 m and 0° orientation.				
CLAD3992	+0018008	Rod 399-2, at the active fuel center and 180° orientation.				
CLAD3992	-1400008	Rod 399-2, 0.143 m below the active fuel center and 0° orientation.				

1405 073

TABLE V (continued)

Measurement	Detector Location and Comments[a]	Range[a]		Frequency Response[a]	
		Detector	Data Acquisition System	Detector	Data Acquisition System
RODPRESS 312-1R01	Pressure transducer connected to Rod 312-1 endcap to measure plenum pressure.	0 to 3.4 MPa	0 to 1.34 MPa	58 kHz	10 Hz
RODPRESS 312-2R02	Rod 312-2.				
RODPRESS 312-3R03	Rod 312-3.				
RODPRESS 312-4R04	Rod 312-4.				
RODPRESS 345-1R05	Rod 345-1.				
RODPRESS 345-2R06	Rod 345-2.				
RODPRESS 399-2R08	Rod 399-2.				
LVDT ROD 312-1 01	Linear variable differential transformer mounted under Rod 312-1 in the north Number 1 position to measure the cladding axial elongation.	-12.7 to 12.7 mm	-12.7 to 12.7 mm	3.5 kHz	10 Hz
LVDT ROD 312-2 02	Rod 312-2 in the south Number 2 position.				
LVDT ROD 312-3 03	Rod 312-3 in the east Number 3 position.				
LVDT ROD 312-4 04	Rod 312-4 in the west Number 4 position.				
LVDT ROD 345-1 03	Rod 345-1 in the east Number 3 position.				
LVDT ROD 345-2 04	Rod 345-2 in the west Number 4 position.				
LVDT ROD 399-2 01	Rod 399-2 in the north Number 1 position.				
Test Train					
INLTTEMP 312-1R01	Type K thermocouple in shroud inlet of Rod 312-1 at the bottom of the active fuel stack to measure the shroud coolant inlet temperature.	273 to 1309 K	280 to 1530 K	>8 Hz	10 Hz
INLTTEMP 312-2R02	Rod 312-2.				
INLTTEMP 312-3R03	Rod 312-3.				
INLTTEMP 312-4R04	Rod 312-4.				
INLTTEMP 345-1R05	Rod 345-1.				
INLTTEMP 345-2R06	Rod 345-2.				
INLTTEMP 399-2R08	Rod 399-2.				
OUT TEMP 312-1R01	Type K thermocouple in shroud outlet of Rod 312-1 at the top of the active fuel stack to measure the shroud coolant outlet temperature.	273 to 1309 K	280 to 1530 K	>8 Hz	10 Hz
OUT TEMP 312-2R02	Rod 312-2.				
OUT TEMP 312-3R03	Rod 312-3.				
OUT TEMP 312-4R04	Rod 312-4.				
OUT TEMP 345-1R05	Rod 345-1.				
OUT TEMP 345-2R06	Rod 345-2.				
OUT TEMP 399-2R08	Rod 399-2.				

TABLE V (continued)

Measurement	Detector Location and Comments[a]	Range[a]		Frequency Response[a]	
		Detector	Data Acquisition System	Detector	Data Acquisition System
MIDT3121 +.000R01	Type K thermocouple in the shroud coolant of Rod 312-1 at the active fuel center to measure the shroud coolant middle temperature.	273 to 1309 K	280 to 1530 K	>8 Hz	10 Hz
MIDT3121 -.152R01	Rod 312-1, 0.152 m below the active fuel center.				
MIDT3121 +.152R01	Rod 312-1, 0.152 m above the active fuel center.				
MIDT3123 +.000R03	Rod 312-3, at the active fuel center.				
MIDT3123 -.152R03	Rod 312-3, 0.152 m below the active fuel center.				
MIDT3123 +.152R03	Rod 312-3, 0.152 m above the active fuel center.				
MIDT3451 +.000R05	Rod 345-1, at the active fuel center.				
MIDT3451 -.152R05	Rod 345-1, 0.152 m below the active fuel center.				
MIDT3451 +.152R05	Rod 345-1, 0.152 m above the active fuel center.				
MIDT3992 +.000R08	Rod 399-2, at the active fuel center.				
MIDT3992 -.152R08	Rod 399-2, 0.152 m below the active fuel center.				
MIDT3992 +.152R08	Rod 399-2, 0.152 m above the active fuel center.				
DELT3121 225 R01	A pair of Type K thermocouples in the inlet and outlet of Rod 312-1 shroud, at 225° orientation, to measure the coolant temperature differential.	-23 to 23 K	-30 to 30 K	>8 Hz	100 Hz
DELT3122 225 R02	Rod 312-2 at 225° orientation.				
DELT3123 225 R03	Rod 312-3 at 225° orientation.				
DELT3124 225 R04	Rod 312-4 at 225° orientation.				
DELT3124 135 R04	Rod 312-4 at 135° orientation.				
DELT3451 225 R05	Rod 345-1 at 225° orientation.				
DELT3452 225 R06	Rod 345-2 at 225° orientation.				
DELT3992 225 R08	Rod 399-2 at 225° orientation.				
DELT3121 CVSP R01	A pair of Type K thermocouples, one in the check valve of Rod 312-1 shroud and one near the test train lower support plate to measure the coolant temperature differential.				
DELT3122 CVSP R02	Rod 312-2.				
TSRD3121 +.000R01	Type K thermocouple attached to the outside of Rod 312-1 shroud at the active fuel center to measure the shroud material temperature.	273 to 1309 K	280 to 1530 K	350 Hz	10 Hz
TSRD3121 -.152R01	Rod 312-1, 0.152 m below the active fuel center.				
TSRD3121 +.152R01	Rod 312-1, 0.152 m above the active fuel center.				
TSRD3123 +.000R03	Rod 312-3, at the active fuel center.				
TSRD3123 -.152R03	Rod 312-3, 0.152 m below the active fuel center.				
TSRD3123 +.152R03	Rod 312-3, 0.152 m above the active fuel center.				
TSRD3451 +.000R05	Rod 345-1, at the active fuel center.				

TABLE V (continued)

Measurement	Detector Location and Comments[a]	Range[a]		Frequency Response[a]	
		Detector	Data Acquisition System	Detector	Data Acquisition System
TSRD3451 -.152R05	Rod 345-1, 0.152 m below the active fuel center.	273 to 1309 K	280 to 1530 K	350 Hz	10 Hz
TSRD3451 +.152R05	Rod 345-1, 0.152 m above the active fuel center.				
TSRD3992 +.000R08	Rod 399-2, at the active fuel center.				
TSRD3992 -.152R08	Rod 399-2, 0.152 m below the active fuel center.				
TSRD3992 +.152R08	Rod 399-2, 0.152 m above the active fuel center.				
BULKTEMP CATCHBTT	Type K thermocouple in the test train coolant in the catch basket to measure bulk coolant temperature.	273 to 1309 K	280 to 1530 K	>8 Hz	10 Hz
BULKTEMP LOWSPTTT	Below the lower support plate.				
BULKTEMP VOLBYPTT	At the active fuel center in the shroud bypass volume.				
BULKTEMP SRDOUTTT	Above the test rod shroud outlets.				
BULKTEMP CONTBYTT	Adjacent to the controlled bypass inlet.				
BULKTEMP IPTEXTTT	Opposite the outlet of the in-pile tube.				
PRESSURE ECATCHTT	EG&G Idaho, Inc. strain post pressure transducer mounted within the catch basket to measure test train coolant pressure.	0 to 17.2 MPa	0 to 17.2 MPa	>350 Hz	10 Hz
PRESSURE ETOPSPTT	EG&G Idaho, Inc. strain post pressure transducer mounted above the shroud outlets to measure coolant pressure above the top support plate.				
PRESSURE KTOPSPTT	Kaman Sciences Corp. eddy current pressure transducer mounted above the shroud outlets to measure coolant pressure above the top support plate.	0 to 17.2 MPa	0 to 17.2 MPa	58 kHz	100 Hz
PRESS-HI ECATCHTT	High-range, EG&G Idaho, Inc. strain post pressure transducer mounted within the catch basket to measure test train coolant over pressure.	0 to 41.4 MPa	0 to 68.9 MPa	>350 Hz	10 Hz
TURB3121 UP000N01	Bi-directional turbine flowmeter mounted above Rod 312-1 in the 0°, Number 1 test train position to measure the shroud volumetric outlet flow rate.	-0.9 to 0.9 l/s	-2.5 to 2.5 l/s	117 Hz	5 kHz
TURB3121 L000N01	Below Rod 312-1 in the 0°, Number 1 position inlet.				
TURB3122 UP180N02	Above Rod 312-2 in the 180°, Number 2 position outlet.				
TURB3122 L0180N02	Below Rod 312-2 in the 180°, Number 2 position inlet.				
TURB3123 UP090N03	Above Rod 312-3 in the 90°, Number 3 position outlet.				
TURB3123 L0090N03	Below Rod 312-3 in the 90°, Number 3 position inlet.				
TURB3124 UP270N04	Above Rod 312-4 in the 270°, Number 4 position outlet.				
TURB3124 L0270N04	Below Rod 312-4 in the 270°, Number 4 position inlet.				
TURB3451 UP090N03	Above Rod 345-1 in the 90°, Number 3 position outlet.				

TABLE V (continued)

Measurement	Detector Location and Comments[a]	Range[a] Detector	Range[a] Data Acquisition System	Frequency Response[a] Detector	Frequency Response[a] Data Acquisition System
TURB3451 LO090N03	Below Rod 345-1 in the 90°, Number 3 position inlet.	-0.9 to 0.9 l/s	-2.5 to 2.5 l/s	117 Hz	5 kHz
TURB3452 UP270N04	Above Rod 345-2 in the 270°, Number 4 position outlet.				
TURB3452 LO270N04	Below Rod 345-2 in the 270°, Number 4 position inlet.				
TURB3992 UP000N01	Above Rod 399-2 in the 0°, Number 1 position outlet.				
TURB3992 LO000N01	Below Rod 399-2 in the 0°, Number 1 position inlet.				
TURBINEM CONTBYTT	Bi-directional turbine flowmeter mounted inside the controlled bypass piping to measure volumetric flow rate.	-12 to 12 l/s	-12 to 12 l/s	117 Hz	20 kHz
NEUTFLUX +.343 TT	SPND mounted on test train 0.343 m above the active fuel center to measure relative neutron flux.	10^{-11} to 10^{-3} A	10^{-11} to 10^{-3} A	>7 Hz	10 Hz
NEUTFLUX +.288 TT	0.228 m above the active fuel center.				
NEUTFLUX +.142 TT	0.142 m above the active fuel center.				
NEUTFLUX +.000 TT	At the active fuel center.				
NEUTFLUX -.114 TT	0.114 m below the active fuel center.				
NEUTFLUX -.228 TT	0.228 m below the active fuel center.				
NEUTFLUX -.343 TT	0.343 m below the active fuel center.				
GAMMAFLX +.228 TT	Gamma flux detector mounted on test train 0.228 m above the active fuel center to measure relative gamma flux.	10^{-11} to 10^{-3} A	10^{-11} to 10^{-3} A	>7 Hz	10 Hz
GAMMAFLX +.000 TT	At the active fuel center.				
GAMMAFLX -.228 TT	0.228 m below the active fuel center.				
Measurement Spool					
ICSSTEMP TE20SPIC	Resistance temperature detector in the initial condition spool to measure steady state preblowdown coolant temperature.	273 to 968 K	280 to 766 K	>1.75 Hz	10 Hz
CLSSTEMP TE22SPCL	In the cold leg spool				
HLSSTEMP TE23SPHL	In the hot leg spool.				
ICTCTEMP TE21SPIC	Type K ribbon thermocouple in the initial condition spool to measure transient coolant temperature.	280 to 1530 K	280 to 1530 K	>8 Hz	100 Hz
CLTCTEMP TE24SPCL	In the cold leg spool.				
HLTCTEMP TE25SPHL	In the hot leg spool.				
ICPRESSF PE08SPIC	Flush mounted pressure transducer in the initial condition spool to measure the subcooled decompression transients.	0 to 34.5 MPa	0 to 20.7 MPa	23.3 kHz	10 Hz

TABLE V (continued)

Measurement		Detector Location and Comments[a]	Range[a] Detector	Range[a] Data Acquisition System	Frequency Response[a] Detector	Frequency Response[a] Data Acquisition System
CLPRESSF	PE10SPCL	In the cold leg spool.	0 to 20.7 MPa			
HLPRESSF	PE12SPHL	In the hot leg spool.				
ICPRESSW	PE09SPIC	Water-cooled, stand off mounted pressure transducer in the initial condition spool to measure the preblowdown and saturated coolant pressures.	0 to 20.7 MPa	0 to 20.7 MPa	23.3 kHz	100 Hz
CLPRESSW	PE11SPCL	In the cold leg spool.				
HLPRESSW	PE13SPHL	In the hot leg spool.				
DELPCLHL	DPE-05HL	Pressure difference transducer to measure the delta pressure between the hot leg and cold leg spool pieces.	0 to 0.35 MPa	0 to 0.7 MPa	350 Hz	100 Hz
ICSVFLOW	FE05SPIC	Unidirectional turbine flowmeter in the initial condition spool to measure volumetric flow rate.	0.04 to 6.5 l/s	0 to 10 l/s	>3.5 Hz	5 kHz
CLSVFLOW	FE06SPCL	In the cold leg spool.	0.02 to 48.5 l/s			
HLSVFLOW	FE09SPHL	In the hot leg spool.	0.02 to 49.1 l/s			
CLMOMFLX	FE07SPCL	Drag disk in the cold leg spool to measure coolant momentum flux.	0 to 1.6×10^4 $kg/m \cdot s^2$	0 to 1.6×10^4 $kg/m \cdot s^2$	87.5 Hz	5 kHz
HLMOMFLX	FE08SPHL	In the hot leg spool.				
CLDENSUP	DENS1UCL	Gamma detector in the Number 1 densitometer to measure the coolant density along the upper beam in the cold leg spool.	0 to 1000 kg/m^3	0 to 800 kg/m^3	>2 Hz	100 Hz
CLDENSCE	DENS1CCL	Center beam.				
CLDENSLO	DENS1LCL	Lower beam.				
CLDENAVE	DENS1 CL	Calculated parameter providing total average density over the cold leg spool piece cross section.				
HLDENSUP	DENS2UHL	Gamma detector in the Number 2 densitometer to measure the coolant density along the upper beam in the hot leg spool.	0 to 1000 kg/m^3	0 to 800 kg/m^3	>2 Hz	100 Hz
HLDENSCE	DENS2CHL	Center beam.				
HLDENSLO	DENS2LHL	Lower beam.				
HLDENAVE	DENS2 HL	Calculated parameter providing total average density over the hot leg spool piece cross section.				

TABLE V (continued)

		Range[a]		Frequency Response[a]	
Measurement	Detector Location and Comments[a]	Detector	Data Acquisition System	Detector	Data Acquisition System
Plant					
REFLDSYS FLO 01PT	Turbine flowmeter in the Number 1 reflood supply line to measure the volumetric reflood flow rate.	0 to 0.2 l/s	0 to 0.2 l/s	>3.5 Hz	100 Hz
REFLDSYS FLO 02PT	In the parallel Number 2 reflood supply line.	0 to 1.6 l/s	0 to 1.6 l/s		
REACTPOW PPS-01PT	Ionization chamber installed in the west corner of the PBF driver core to measure reactor power.	0 to 28 MW	0 to 28 MW	Not Available	10 Hz
REACTPOW PPS-02PT	In the east corner.				
FPDSGAMA NUM 01FP	NaI crystal gamma ray detector in the fission product detection system to measure gamma-ray intensity of the loop coolant in the 150- to 3400-keV energy range.	10 to 10^6 cts	10 to 10^6 cts	Sample stream delay 2 minutes	5 Hz
FPDSGAMA NUM 03FP	In the 3400- to 6300-keV energy range.				
FPDSGAMA NUM 02FP	Measured direct reactor radiation in the 150- to 6300-keV energy range for background purposes.				
FPDSNEUT NEUTRNFP	BF_3 delayed neutron detector to detect delayed neutrons in the loop coolant.				

---

[a] Statements at the beginning of a measurement category regarding location and comments, range, and frequency response apply to all subsequent measurements unless specified otherwise.

TABLE VI

TEST LLR DATA PRESENTATION AN

	Test LLR-S0				Test LLR-3				Test LLR-	
	Preblowdown[a]		Blowdown		Preblowdown		Blowdown		Preblowdown	
Measurement	Microfiche Address	Qualification	Figure	Qualification	Microfiche Address	Qualification	Figure	Qualification	Microfiche Address	Qualification
Fuel Rod										
TFCL3121 +.08TC01	B1	Trend[b]	17,18	Trend[b]	B4	Trend[b]	135,136	Trend[b]	E7	Trend[b]
TFCL3122 +.00TC02	C1	Trend[b]	19,20	Trend[b]	C4	Trend[b]	137,138	Trend[b]	F7	Trend[b]
TFCL3123 +.08TC03		Failed		Failed		Failed		Failed		--
TFCL3124 +.00TC04	D1	Qualified	21,22	Trend[b]	D4	Trend[c]		Failed[d]		--
TFCL3451 +.08TC05		--		--		--		--	G7	Qualified
TFCL3452 +.00TC06		--		--		--		--	H7	Qualified
TFCL3992 +.08TC08		--		--		--		--		--
PLNMTEMP 312-1R01	E1	Qualified	23	Qualified	E4	Qualified	139	Qualified	I7	Qualified
PLNMTEMP 312-2R02	F1	Qualified	24	Qualified	F4	Qualified	140	Qualified	J7	Qualified
PLNMTEMP 312-3R03	G1	Qualified	25	Qualified	G4	Qualified	141	Qualified		--
PLNMTEMP 312-4R04	H1	Qualified	26	Qualified	H4	Qualified	142	Qualified		--
PLNMTEMP 345-1R05		--		--		--		--	K7	Qualified
PLNMTEMP 345-2R06		--		--		--		--	L7	Qualified
PLNMTEMP 399-2R08		--		--		--		--		--
CLAD3121 +0818001	I1	Qualified	27,28	Qualified	I4	Qualified	143,144	Qualified	M7	Qualified
CLAD3121 +0800001	J1	Qualified	29,30	Qualified	J4	Qualified	145,146	Qualified	N7	Qualified
CLAD3122 +0818002	K1	Qualified	31,32	Qualified	K4	Qualified	147,148	Qualified	O7	Qualified
CLAD3122 +0000002	L1	Qualified	33,34	Qualified	L4	Qualified	149,150	Qualified	P7	Qualified
CLAD3123 +0818003	M1	Qualified	35,36	Qualified	M4	Qualified	151,152	Qualified		--
CLAD3123 +0800003	N1	Qualified	37,38	Qualified	N4	Qualified	153,154	Qualified		--
CLAD3124 +0818004	O1	Qualified	39,40	Qualified	O4	Qualified	155,156	Qualified		--
CLAD3124 +0800004	P1	Qualified	41,42	Qualified	P4	Qualified	157,158	Qualified		--
CLAD3451 +0818005		--		--		--		--	B8	Qualified
CLAD3451 +0800005		--		--		--		--	C8	Qualified
CLAD3992 +0018008		--		--		--		--		--
CLAD3992 -1400008		--		--		--		--		--
RODPRESS 312-1R01	B2	Trend[f]	43	Trend[f]	B5	Restrained[f]		Failed	D8	Trend[f]
RODPRESS 312-2R02	C2	Trend[f]	44	Trend[f]	C5	Restrained[f]		Failed	E8	Trend[f]
RODPRESS 312-3R03		Failed		Failed	D5	Trend[g]		Failed		--
RODPRESS 312-4R04	D2	Trend[f]	45	Trend[f]	E5	Restrained[f]		Failed		--
RODPRESS 345-1R05		--		--		--		--	F8	Trend[f]
RODPRESS 345-2R06		--		--		--		--	G8	Trend[f]
RODPRESS 399-2R08		--		--		--		--		--
LVDT ROD 312-1 01[i]	E2	Qualified	46,47	Trend[j]	F5	Restrained[j]	159,160	Trend[j]	H8	Restrained[j]
LVDT ROD 312-2 02	F2	Qualified	48,49	Trend[j]	G5	Restrained[j]	161,162	Trend[j]	I8	Restrained[j]
LVDT ROD 312-3 03	G2	Qualified	50,51	Trend[j]	H5	Restrained[j]	163,164	Trend[j]		--
LVDT ROD 312-4 04	H2	Qualified	52,53	Trend[j]	I5	Restrained[j]	165,166	Trend[j]		--
LVDT ROD 345-1 03		--		--		--		--	J8	Restrained[j]
LVDT ROD 345-2 04		--		--		--		--	K8	Restrained[j]
LVDT ROD 399-2 01		--		--		--		--		--
Test Train										
INLTTEMP 312-1R01		Not presented	54	Qualified		Not presented	167	Qualified		Not recorded
INLTTEMP 312-2R02		Not presented	55	Qualified		Not presented	168	Qualified		Not presented
INLTTEMP 312-3R03		Not presented	56	Qualified		Not presented	169	Qualified		--
INLTTEMP 312-4R04		Not presented	57	Qualified		Not presented	170	Qualified		--
INLTTEMP 345-1R05		--		--		--		--		Not presented
INLTTEMP 345-2R06		--		--		--		--		Not presented
INLTTEMP 399-2R08		--		--		--		--		--
OUT TEMP 312-1R01		Not presented	58	Qualified		Not presented	171	Qualified		Not recorded
OUT TEMP 312-2R02		Not presented	59	Qualified		Not presented	172	Qualified		Not presented
OUT TEMP 312-3R03		Not presented	60	Qualified		Not presented	173	Qualified		--
OUT TEMP 312-4R04		Not presented	61	Qualified		Not presented	174	Qualified		--
OUT TEMP 345-1R05		--		--		--		--		Not presented
OUT TEMP 345-2R06		--		--		--		--		Not presented
OUT TEMP 399-2R08		--		--		--		--		--
MIDT3121 +.000R01		Not presented	62,63	Qualified		Not presented	175,176	Qualified		Not recorded
MIDT3121 -.152R01		Not presented	64	Qualified		Not presented	177	Qualified		Not recorded
MIDT3121 +.152R01		Not presented	65	Qualified		Not presented	178	Qualified		Not recorded
MIDT3123 +.000R03		Not presented	66,67	Qualified		Not presented	179,180	Qualified[o]		--
MIDT3123 -.152R03		Not presented	68	Qualified		Not presented	181	Qualified[o]		--

1405 080

QUALIFICATION

5		Test LLR-4				Test LLR-4A			
Blowdown		Preblowdown		Blowdown		Preblowdown		Blowdown	
Figure	Qualification	Microfiche Address	Qualification	Figure	Qualification	Microfiche Address	Qualification	Figure	Qualification
249,250	Trend[b]	J10	Trend[b]	361	Trend[b]		--		--
251,252	Trend[b]	K10	Trend[b]	362	Trend[b]	M13	Trend[b]	439, 440	Trend[b]
	--		--		--		--		--
	--		--		--		--		--
253,254	Qualified	L10	Qualified	363	Qualified	N13	Qualified	441,442	Qualified
255,256	Qualified	M10	Qualified	364	Qualified	O13	Qualified	443,444	Qualified
	--		--		--	L13	Qualified		Failed[e]
257	Qualified	N10	Qualified	365	Qualified		--		--
258	Qualified	O10	Qualified	366	Qualified	B14	Qualified	446	Qualified
	--		--		--		--		--
	--		--		--		--		--
259	Qualified	P10	Qualified	367	Qualified	C14	Qualified	447	Qualified
260	Qualified	B11	Qualified	368	Qualified	D14	Qualified	448	Qualified
	--		--		--	P13	Qualified	445	Qualified
261,262	Qualified	C11	Qualified	369	Qualified		--		--
263,264	Qualified	D11	Qualified	370	Qualified		--		--
265,266	Qualified	E11	Qualified	371	Qualified	G14	Qualified	453,454	Qualified
267,268	Qualified	F11	Qualified	372	Qualified	H14	Qualified	455,456	Qualified
	--		--		-		--		--
	--		--		--		--		--
	--		--		--		--		--
	--		--		--		--		--
269,270	Qualified	G11	Qualified	373	Qualified	I14	Qualified	457,458	Qualified
271,272	Qualified	H11	Qualified	374	Qualified	J14	Qualified	459,460	Qualified
	--		--		--	E14	Qualified	449,450	Qualified
	--		--		--	F14	Qualified	451,452	Qualified
	Failed	I11	Trend[j]		Failed		--		--
	Failed	J11	Trend[j]		Failed	L14	Trend[h]		Failed
	--		--		--		--		--
	--		--		--		--		--
	Failed	K11	Trend[j]		Failed	M14	Trend[h]		Failed
	Failed	L11	Trend[j]		Failed	N14	Trend[h]		Failed
	--		--		--	K14	Qualified		Failed
273,274	Trend[j]	M11	Restrained[j]	375	Trend[j]		--		--
275,276	Trend[j]		Failed		Failed	P14	Restrained[j]	463,464	Trend[j]
	--		--		--		--		--
	--		--		--		--		--
277,278	Trend[j]	N11	Restrained[j]	376	Trend[j]		Failed	465,466	Trend[j]
279,280	Trend[j]	O11	Restrained[j]	377	Trend[j]		Failed		Failed
	--		--		--	O14	Trend[j]	461,462	Trend[j]
	Not recorded		Not recorded		Not recorded		--		--
281	Qualified[k]		Not presented	378	Qualified		Not presented	468	Qualified[k]
	--		--		--		--		--
	--		--		--		--		--
282	Qualified[k]		Not presented	379	Qualified		Not presented	469	Qualified[k]
283	Qualified[k]		Not presented	380	Qualified		Not presented	470	Qualified[k]
	--		--		--		Not presented	467	Qualified[k]
	Not recorded		Not recorded		Not recorded		--		--
284	Qualified[l]		Not presented	381	Qualified		Not presented	472	Qualified[m]
	--		--		--		--		--
	--		--		--		--		--
285	Qualified[l]		Not presented	382	Qualified		Not presented	473	Qualified[m]
286	Qualified[l]		Not presented	383	Qualified		Not presented	474	Qualified[m]
	--		--		--		Not presented	471	Qualified[m]
	Not recorded		Not recorded		Not recorded		--		--
	Not recorded		Not recorded		Not recorded		--		--
	Not recorded		Not recorded		Not recorded		--		--
	--		--		--		--		--
	--		--		--		--		--

POOR ORIGINAL

Measurement	Test LLR-S0				Test LLR-3			
	Preblowdown[a]		Blowdown		Preblowdown		Blowdown	
	Microfiche Address	Qualification	Figure	Qualification	Microfiche Address	Qualification	Figure	Qualification
MIDT3123 +.152R03		Not presented	69	Trend[n]		Not presented	182	Qualified[o]
MIDT3451 +.000R05		--		--		--		--
MIDT3451 -.152R05		--		--		--		--
MIDT3451 +.152R05		--		--		--		--
MIDT3992 +.000R08		--		--		--		--
MIDT3992 -.152R08		--		--		--		--
MIDT3992 +.152R08		--		--		--		--
DELT3121 225 R01	I2	Qualified	70	Qualified	J5	Qualified	183	Trend[p]
DELT3122 225 R02	J2	Qualified	71	Qualified	K5	Qualified	184	Trend[p]
DELT3123 225 R03	K2	Qualified	72	Qualified	L5	Qualified	185	Trend[p]
DELT3124 225 R04	L2	Qualified	73	Qualified	M5	Qualified	186	Trend[p]
DELT3124 135 R04	M2	Qualified	74	Qualified	N5	Qualified	187	Trend[p]
DELT3451 225 R05		--		--		--		--
DELT3452 225 R06		--		--		--		--
DELT3992 225 R08		--		--		--		--
DELT3121 CVSP R01		--		--		--		--
DELT3122 CVSP R02		--		--		--		--
TSRD3121 +.000R01		Not presented	75	Qualified		Not presented	188	Qualified
TSRD3121 -.152R01		Not presented	76	Qualified		Not presented	189	Qualified
TSRD3121 +.152R01		Not presented	77	Trend[n]		Not presented	190	Trend[n]
TSRD3123 +.000R03		Not presented	78	Qualified		Not presented	191	Trend[n]
TSRD3123 -.152R03		Not presented	79	Qualified		Not presented	192	Qualified
TSRD3123 +.152R03		Not presented	80	Qualified		Not presented	193	Qualified
TSRD3451 +.000R05		--		--		--		--
TSRD3451 -.152R05		--		--		--		--
TSRD3451 +.152R05		--		--		--		--
TSRD3992 +.000R08		--		--		--		--
TSRD3992 -.152R08		--		--		--		--
TSRD3992 +.152R08		--		--		--		--
BULKTEMP CATCHBTT		Not presented	81	Qualified		Not presented	194	Qualified
BULKTEMP LOWSPTTT		Not presented	82	Qualified		Not presented	195	Qualified
BULKTEMP VOLBYPTT		Not presented	83	Qualified		Not presented	196	Qualified
BULKTEMP SRDOUTTT		Not presented	84	Qualified		Not presented	197	Qualified
BULKTEMP CONTBYTT		Not presented	85	Qualified		Not presented	198	Qualified
BULKTEMP IPTEXTTT		Not presented	86	Qualified		Not presented	199	Qualified
PRESSURE ECATCHTT		Not presented	87	Qualified		Not presented	200	Qualified
PRESSURE ETOPSPTT	N2	Qualified	88	Qualified	O5	Qualified	201	Qualified
PRESSURE KTCPSPTT		Not presented	89	Trend[t]		Not presented	202	Restrained[u]
PRESS-HI ECATCHTT		Not presented	90	Trend[v]		Not presented	203	Restrained[v]
TURB3121 UP000N01[w]	O2	Qualified	91	Qualified	P5	Qualified	204	Restrained[x]
TURB3121 LO000N01	P2	Qualified	92,93	Qualified	B6	Qualified	205,206	Restrained[x]
TURB3122 UP180N02	B3	Qualified	94	Qualified	C6	Qualified	207	Restrained[x]
TURB3122 LO180N02	C3	Qualified	95,96	Qualified	D6	Qualified	208,209	Restrained[x]
TURB3123 UP090N03	D3	Qualified	97	Qualified	E6	Qualified	210	Restrained[x]
TURB3123 LO090N03	E3	Qualified	98,99	Qualified	F6	Qualified	211,212	Restrained[x]
TURB3124 UP270N04	F3	Qualified	100	Qualified	G6	Qualified	213	Restrained[x]
TURB3124 LO270N04	G3	Qualified	101,102	Qualified	H6	Qualified	214,215	Restrained[x]
TURB3451 UP090N03		--		--		--		--
TURB3451 LO090N03		--		--		--		--
TURB3452 UP270N04		--		--		--		--
TURB3452 LO270N04		--		--		--		--
TURB3992 UP000N01		--		--		--		--
TURB3992 LO000N01		--		--		--		--
TURBINEM CONTBYTT		Not presented	103,104	Qualified		Not presented	216,217	Trend[aa]
NEUTFLUX +.343 TT[cc]		Not recorded		Failed		Failed		Failed
NEUTFLUX +.228 TT	H3	Qualified	105	Qualified	I6	Qualified	218	Qualified
NEUTFLUX +.142 TT		Not recorded	106	Qualified		Not recorded	219	Qualified
NEUTFLUX +.000 TT		Not recorded	107	Qualified	J6	Qualified	220	Qualified
NEUTFLUX -.114 TT	I3	Qualified	108	Qualified	K6	Qualified	221	Qualified
NEUTFLUX -.228 TT	J3	Qualified	109	Qualified	L6	Qualified	222	Qualified
NEUTFLUX -.343 TT		Not recorded	110	Qualified		Not recorded	223	Qualified
GAMMAFLX +.228 TT		Not recorded	111	Qualified	M6	Qualified	224	Qualified
GAMMAFLX +.000 TT	K3	Qualified	112	Qualified	N6	Qualified	225	Qualified
GAMMAFLX -.228 TT		Not recorded	113	Qualified		Not recorded	226	Qualified

1405 082

POOR ORIGINAL

E VI (continued)

Test LLR-5				Test LLR-6				Test LLR-4A			
Preblowdown		Blowdown		Preblowdown		Blowdown		Preblowdown		Blowdown	
fiche ess	Qualification	Figure	Qualification	Microfiche Address	Qualification	Figure	Qualification	Microfiche Address	Qualification	Figure	Qualification
	--		--		--		--		--		--
	Not presented	287,288	Qualified[o]		Not presented	384	Qualified		Not presented	479,480	Qualified[o]
	Not presented	289	Qualified[o]		Not presented	385	Qualified		Not presented	481	Qualified[o]
	Not presented	290	Qualified[o]		Not presented	386	Qualified		Not presented	482	Qualified[o]
	--		--		--		--		Not presented	475,476	Qualified[o]
	--		--		--		--		Not presented	477	Qualified[o]
	--		--		--		--		Not presented	478	Qualified[o]
	--		--		--		--		--		--
8	Qualified	291	Trend[p]	B12	Qualified	388	Trend[p]	C15	Qualified		Failed
	--		--		--		--		--		--
	--		--		--		--		--		--
	--		--		--		--		--		--
8	Qualified	293	Trend[p]	D12	Qualified	390	Trend[p]	D15	Qualified		Failed
8	Qualified	294	Trend[p]	E12	Qualified	391	Trend[p]		Failed		Failed
	--		--		--		--	B15	Qualified		Failed
8	Restrained[q]		Failed	P11	Qualified	387	Trend[p]		--		--
8	Restrained[q]	292	Trend[p,q]	C12	Qualified	389	Trend[p,q]		--		--
	Not presented	295	Qualified		Not presented	392	Qualified		--		--
	Not presented	296	Qualified		Not presented	393	Qualified		--		--
	Not presented	297	Qualified		Not presented	394	Qualified		--		--
	--		--		--		--		--		--
	--		--		--		--		--		--
	--		--		--		--		--		--
	Not presented	298	Qualified		Not presented	395	Qualified		Not presented	486	Qualified
	Not presented	299	Qualified		Not presented	396	Qualified		Not presented	487	Qualified
	Not presented	300	Qualified		Not presented	397	Qualified		Not presented	488	Qualified
	--		--		--		--		Not presented	483	Qualified
	--		--		--		--		Not presented	484	Qualified
	--		--		--		--		Not presented	485	Qualified
	Not presented	301	Qualified[r]		Not presented	398	Qualified		Not presented	489	Qualified[r]
	--		--		--		--		Not presented	490	Qualified[r]
	Not presented	302	Qualified[r]		Not presented	399	Qualified		Not presented	491	Qualified[r]
	Not presented	303	Qualified[r]		Not presented	400	Qualified		Not presented	492	Qualified[r]
	Not presented	304	Qualified[r]		Not presented	401	Qualified		Not presented	493	Qualified[r]
	Not presented	305	Qualified[r]		Not presented	402	Qualified		Not presented	494	Qualified[r]
	Not presented	306	Trend[s]		Not presented	403	Trend[s]		Not presented	495	Qualified
B9	Trend[s]	307	Trend[s]	F12	Qualified	404	Trend[s]	E15	Qualified	496	Qualified
	Not presented	308	Qualified		Not presented	405	Trend[s]		Not presented	497	Trend[s]
	Not presented	309	Trend[s]		Not presented		Failed		Not presented	498	Trend[s]
C9	Qualified	310	Restrained[y]	G12	Qualified	406	Restrained[y]		--		--
D9	Qualified	311,312	Restrained[y]	H12	Qualified	407	Restrained[y]		--		--
E9	Qualified	313	Restrained[y]	I12	Qualified	408	Restrained[y]	H15	Qualified	502	Restrained[y]
F9	Qualified	314,315	Restrained[y]	J12	Qualified	409	Restrained[y]	I15	Qualified	503,504	Restrained[y]
	--		--		--		--		--		--
	--		--		--		--		--		--
	--		--		--		--		--		--
	--		--		--		--		--		--
G9	Qualified	316	Restrained[y]	K12	Qualified	410	Restrained[y]	J15	Qualified	505	Restrained[y]
H9	Qualified	317,318	Restrained[y]	L12	Qualified	411	Restrained[y]	K15	Qualified	506,507	Restrained[y]
I9	Qualified	319	Restrained[y]	M12	Qualified	412	Restrained[y]	L15	Qualified	508	Restrained[y]
J9	Trend[z]		Failed		Failed		Failed	M15	Qualified	509,510	Restrained[y]
	--		--		--		--	F15	Qualified	499	Restrained[y]
	--		--		--		--	G15	Qualified	500,501	Restrained[y]
	Not presented	320,321	Trend[bb]		Not presented	413	Trend[bb]		Not presented		Failed
	Failed		Failed		Failed		Failed		Failed		Failed
K9	Qualified	322	Qualified	N12	Qualified	414	Qualified	N15	Qualified	511	Qualified
L9	Qualified	323	Qualified	O12	Qualified	415	Qualified	O15	Qualified	51[illegible]	Qualified
M9	Qualified	324	Qualified	P12	Qualified	416	Qualified	P15	Qualified	513	Qualified
N9	Qualified	325	Qualified	B13	Restrained[aa]	417	Qualified		Failed		Failed
O9	Qualified	326	Qualified		Failed		Failed	B16	Restrained[aa]	514	Qualified
P9	Qualified	327	Qualified	C13	Qualified	418	Qualified	C16	Qualified	515	Qualified
B10	Qualified	328	Qualified	D13	Qualified	419	Qualified	D16	Qualified	516	Qualified
C10	Qualified	329	Qualified	E13	Qualified	420	Qualified	E16	Qualified	517	Qualified
D10	Qualified	330	Qualified	F13	Qualified	421	Qualified	F16	Qualified	518	Qualified

POOR ORIGINAL

TABLE VI (contin

Measurement		Test LLR-SO				Test LLR-3				Test LL	
		Preblowdown[a]		Blowdown		Preblowdown		Blowdown		Preblowdown	
Measurement		Microfiche Address	Qualification	Figure	Qualification	Microfiche Address	Qualification	Figure	Qualification	Microfiche Address	Qualification
Measurement Spool											
ICSSTEMP	TE20SPIC	L3	Qualified	114	Qualified[l]	O6	Qualified	227	Qualified[l]	E10	Qualified
CLSSTEMP	TE22SPCL	M3	Qualified	115	Qualified[l]	P6	Qualified	228	Qualified[l]	F10	Qualified
HLSSTEMP	TE23SPHL	N3	Qualified	116	Qualified[l]	B7	Qualified	229	Qualified[l]	G10	Qualified
ICTCTEMP	TE21SPIC		Not presented		Failed		Not presented		Failed		Not presented
CLTCTEMP	TE24SPCL		Not presented	117	Qualified[l]		Not presented	230	Qualified[l]		Not presented
HLTCTEMP	TE25SPHL		Not presented	118	Qualified[l]		Not presented	231	Qualified[l]		Not presented
ICPRESSF	PE08SPIC		Not presented		Failed		Not presented	232	Qualified		Not presented
CLPRESSF	PE10SPCL		Not presented	119	Qualified		Not presented	233	Qualified		Not presented
HLPRESSF	PE12SPHL		Not presented	120	Qualified		Not presented	234	Qualified		Not presented
ICPRESSW	PE09SPIC		Not presented	121	Qualified		Not presented	235	Qualified		Not presented
CLPRESSW	PE11SPCL		Not presented	122,123	Qualified		Not presented	236,237	Qualified		Not presented
HLPRESSW	PE13SPHL		Not presented	124	Qualified		Not presented	238	Qualified		Not presented
DELPCLHL	DPE-05HL		Not presented	125,126	Restrained[gg]		Not presented	239,240	Restrained[gg]		Not presented
ICSVFLOW	FE05SPIC		Not presented	127	Qualified		Not presented	241	Trend[hh]		Not presented
CLSVFLOW	FE06SPCL		Not presented	128,129	Qualified		Not presented	242,243	Trend[hh]		Not presented
HLSVFLOW	FE09SPHL		Not presented	130	Qualified		Not presented	244	Qualified		Not presented
CLMOMFLX	FE07SPCL		Not presented		Failed		Not presented		Failed		Not presented
HLMOMFLX	FE08SPHL		Not presented		Failed		Not presented		Failed		Not presented
CLDENSUP	DENS1UCL		Not presented		Failed		Not presented		Failed		Not presented
CLDENSCE	DENS1CCL		Not presented		Failed		Not presented	245	Restrained[gg]		Not presented
CLDENSLO	DENS1LCL		Not presented		Failed		Not presented		Failed		Not presented
CLDENAVE	DENS1 CL		Not presented		Failed		Not presented		--		Not presented
HLDENSUP	DENS2UHL		Not presented		Failed		Not presented		Failed		Not presented
HLDENSCE	DENS2CHL		Not presented		Failed		Not presented		Failed		Not presented
HLDENSLO	DENS2LHL		Not presented		Failed		Not presented		Failed		Not presented
HLDENAVE	DENS2 HL		Not presented		Failed		Not presented		Failed		Not presented
Plant											
REFLDSYS	FLO 01PT		Not presented	131	Qualified		Not presented		Failed		Not presented
REFLDSYS	FLO 02PT		Not presented	132	Qualified		Not presented	246	Qualified		Not presented
REACTPOW	PPS-01PT	O3	Qualified	133	Qualified	C7	Qualified	247	Qualified	H10	Qualified
REACTPOW	PPS-02PT	P3	Qualified	134	Qualified	D7	Qualified	248	Qualified	I10	Qualified
FPDSGAMA	NUM 01FP[kk]		Not recorded		Not presented		Not recorded		Not presented		Not recorded
FPDSGAMA	NUM 02FP		Not recorded		Not presented		Not recorded		Not presented		Not recorded
FPDSGAMA	NUM 03FP		Not recorded		Not presented		Not recorded		Not presented		Not recorded
FPDSNEUT	NEUTRNFP		Not recorded		Not presented		Not recorded		Not presented		Not recorded

---

a. For all Test LLR-SO preblowdown plots, data were not recorded from 19 to 23.5 hours.

b. A large uncertainty in the absolute value of this data was the result of lead reversal and subsequent correction.

c. Thermocouple indicates intermittent failure.

d. Rod cladding failed and resulted in thermocouple failure.

e. Temperature exceeded thermocouple limits.

f. Incorrect temperature compensation resulted in large uncertainty.

g. Rod 312-3 cladding failed resulting in saturated transducer prior to blowdown depressurization.

h. Data display a large time dependent drift.

i. The LVDTs were adjusted to zero at ambient coolant conditions prior to nuclear operation.

j. Significant uncertainty in data due to temperature corrections.

k. Probable thermocouple dry-out occurs at about 5 s and data may reflect pipe wall radiation effects until rewetting by reflood and quench.

POOR ORIGINAL

ed)

-5		Test LLR-4				Test LLR-4A			
Blowdown		Preblowdown		Blowdown		Preblowdown		Blowdown	
Figure	Qualification	Microfiche Address	Qualification	Figure	Qualification	Microfiche Address	Qualification	Figure	Qualification
331	Qualified[l]	G13	Qualified	422	Qualified	G16	Qualified	519	Qualified[dd]
332	Qualified[l]	H13	Qualified	423	Qualified[l]	H16	Qualified	520	Qualified[dd]
333	Qualified[l]	I13	Qualified	424	Qualified	I16	Qualified	521	Qualified[dd]
	Failed		Not presented		Failed		Not presented	522	Qualified[dd]
334	Qualified[r]		Not presented	425	Qualified		Not presented	523	Qualified[dd]
335	Qualified[r]		Not presented	426	Qualified		Not presented	524	Qualified[dd]
336	Restrained[ee]		Not presented	427	Qualified		Not presented	525	Qualified
337	Restrained[ee]		Not presented	428	Qualified		Not presented		Failed
338	Qualified		Not presented		Failed		Not presented		Failed
339	Restrained[ee]		Not presented	429	Qualified		Not presented		Failed[ff]
340,341	Restrained[ee]		Not presented	430	Qualified		Not presented		Failed[ff]
342	Restrained[ee]		Not presented	431	Qualified		Not presented		Failed[ff]
343,344	Restrained[gg]		Not presented		Failed		Not presented		Failed
345	Trend[hh]		Not presented		Failed		Not presented		Failed
346,347	Trend[hh]		Not presented	432	Trend[hh]		Not presented		Failed
348	Trend[hh]		Not presented		Failed		Not presented		Failed
	Failed		Not presented		Failed		Not presented		Failed
	Failed		Not presented		Failed		Not presented		Failed
349	Restrained[gg]		Not presented		Failed		Not presented	526	Restrained[gg]
350	Restrained[gg]		Not presented		Failed		Not presented	527	Restrained[gg]
351	Restrained[gg]		Not presented		Failed		Not presented	528	Restrained[gg]
352	Restrained[gg]		Not presented		Failed		Not presented	529	Restrained[gg]
353	Restrained[gg]		Not presented	433	Trend[ii]		Not presented		Failed
354	Restrained[gg]		Not presented	434	Trend[ii]		Not presented		Failed
355	Restrained[gg]		Not presented	435	Trend[ii]		Not presented		Failed
356	Restrained[gg]		Not presented	436	Trend[ii]		Not presented		Failed
357	Qualified		Not presented		Not presented[jj]		Not presented	530	Qualified
358	Qualified		Not presented		Not presented[jj]		Not presented	531	Qualified
359	Qualified	J13	Qualified	437	Qualified	J16	Qualified	532	Qualified
360	Qualified	K13	Qualified	438	Qualified	K16	Qualified	533	Qualified
	Not presented		Not recorded		Not presented		Not recorded		Not presented
	Not presented		Not recorded		Not presented		Not recorded		Not presented
	Not presented		Not recorded		Not presented		Not recorded		Not presented
	Not presented		Not recorded		Not presented		Not recorded		Not presented

1405 085

TA

	Test LLR-S0				Test LLR-3			
	Preblowdown[a]		Blowdown		Preblowdown		Blowdown	
Measurement	Microfiche Address	Qualification	Figure	Qualification	Microfiche Address	Qualification	Figure	Qualification

l. Probable thermocouple dry-out occurs from approximately 30 to 175 s and data may reflect pipe wall radiation effects.

m. Probable thermocouple dry-out occurs from approximately 25 to 140 s and data may reflect pipe wall radiation effects.

n. Trend because of large offset and inconsistent output.

o. Probable thermocouple dry-out occurs at approximately 5 s into the blowdown and data may reflect pipe wall radiation eff

p. The delta temperature measurements during blowdown are subject to steam environment, wall radiation effects, and amplifi

q. Measurement somewhat suspect because of remote location of thermocouples.

r. Probable thermocouple dry-out occurs at approximately 30 s into the blowdown and data may reflect pipe wall radiation ef

s. Large offset applied to data.

t. Large offset and drift in data due to temperature effects.

u. Significant uncertainty due to temperature effects.

v. System electronics problem resulted in large offset.

w. Turbine qualification applies only to values in excess of 0.05 l/s. For absolute values less than 0.05 l/s data are qua

x. Debris from rod failure during blowdown results in trend qualification for all rod turbine data >12 s after blowdown ini

y. Debris from the Test LLR-3 rod failure caused turbine bearing problems. Data with absolute values <0.4 l/s are qualifie

z. Turbine operation intermittent, majority of data are Failed.

aa. Data are extremely noicy.

bb. Turbine not calibrated because of fuel rod failure debris in bearings.

cc. SPNDs are qualified trend for all values <5 nA.

dd. Probable thermocouple dry-out occurs from approximately 30 to 240 s and data may reflect pipe wall radiation effects.

ee. Restrained because of large offset applied to data.

ff. Transducer coolant water supply failed.

gg. No duplicate measurement for comparison.

hh. A large uncertainty in the accuracy of the transducer exists because of severe overranging on previous tests.

ii. No pretest calibration performed.

jj. Abnormal cycling of the loop isolation valves at 15 s invalidated the remaining portion of the Test LLR-4 blowdown inclu

kk. The sample line from the experimental loop to the FPDS is isolated from the IPT-blowdown piping after blowdown initiatio

POOR ORIGINAL

BLE VI (continued)

Test LLR-5				Test LLR-4				Test LLR-4A			
Preblowdown		Blowdown		Preblowdown		Blowdown		Preblowdown		Blowdown	
rofiche dress	Qualification	Figure	Qualification	Microfiche Address	Qualification	Figure	Qualification	Microfiche Address	Qualification	Figure	Qualification

cts until rewetting by reflood and quench.

r saturation at _50 K resulting in Trend qualification.

ects until rewetting by reflood and quench.

ified trend.

iation.

trend.

ing reflood.

and therefore will not indicate fuel rod failure until flow from the loop to the IPT is reestablished.

1405 087

TEST LLR-S0

1405 088

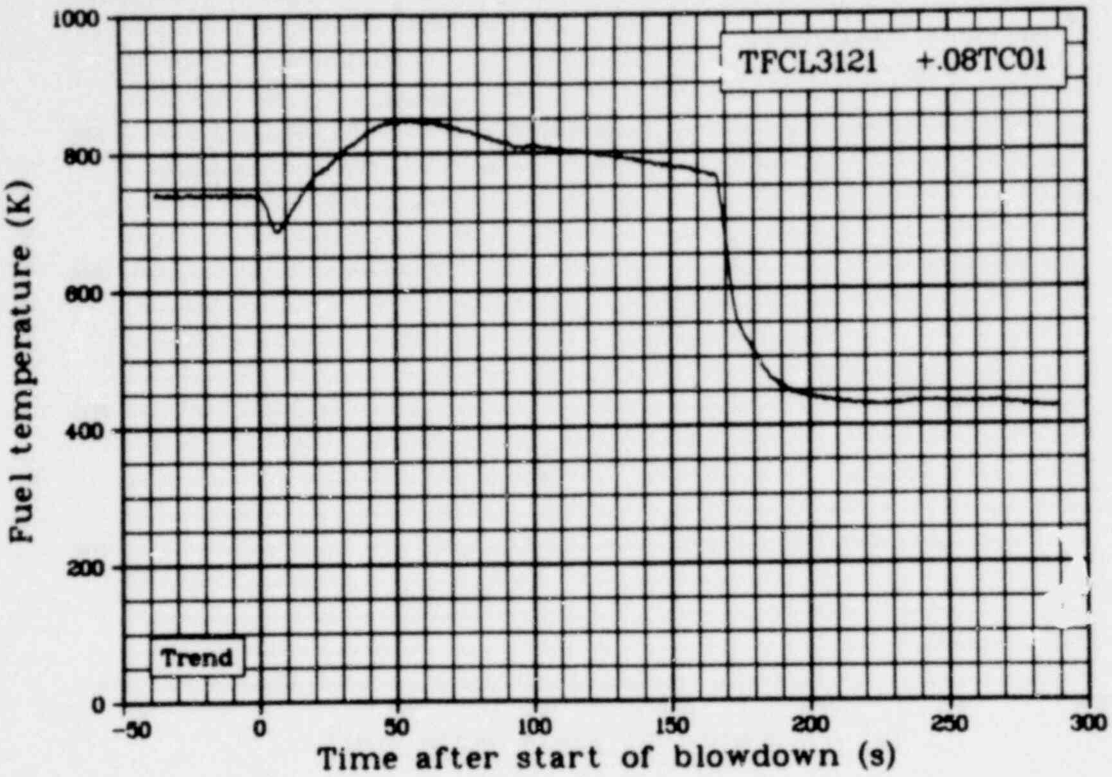

Fig. 17 Fuel temperature in Rod 312-1, 0.08 m above the fuel stack midplane (TFCL3121 +.08TC01), from -50 to 300 s.

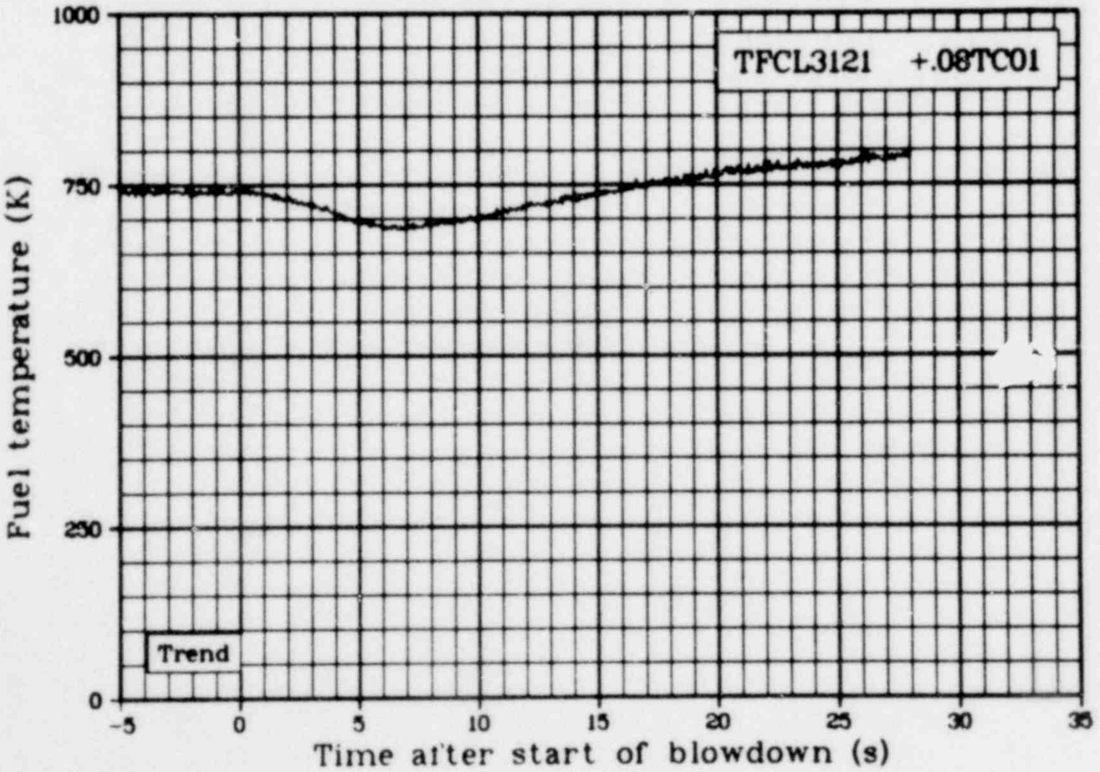

Fig. 18 Fuel temperature in Rod 312-1, 0.08 m above the fuel stack midplane (TFCL3121 +.08TC01), from -5 to 35 s.

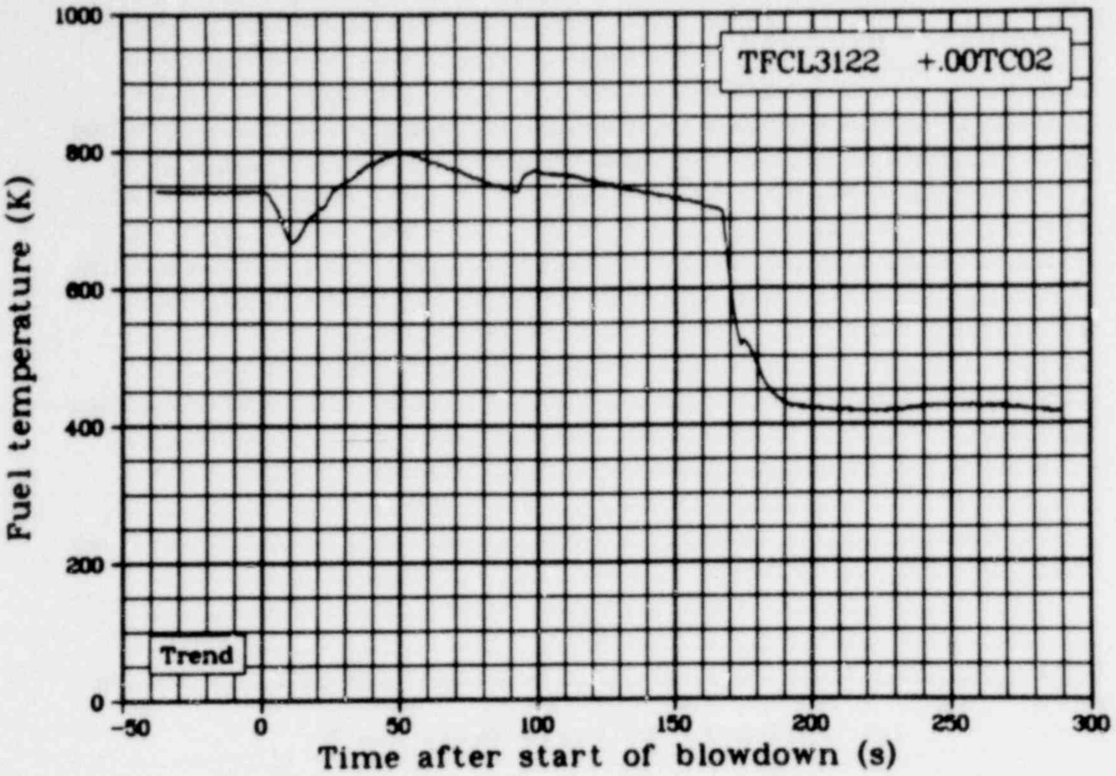

Fig. 19 Fuel temperature in Rod 312-2, at fuel stack midplane (TFCL3122 + .00TC02), from -50 to 300 s.

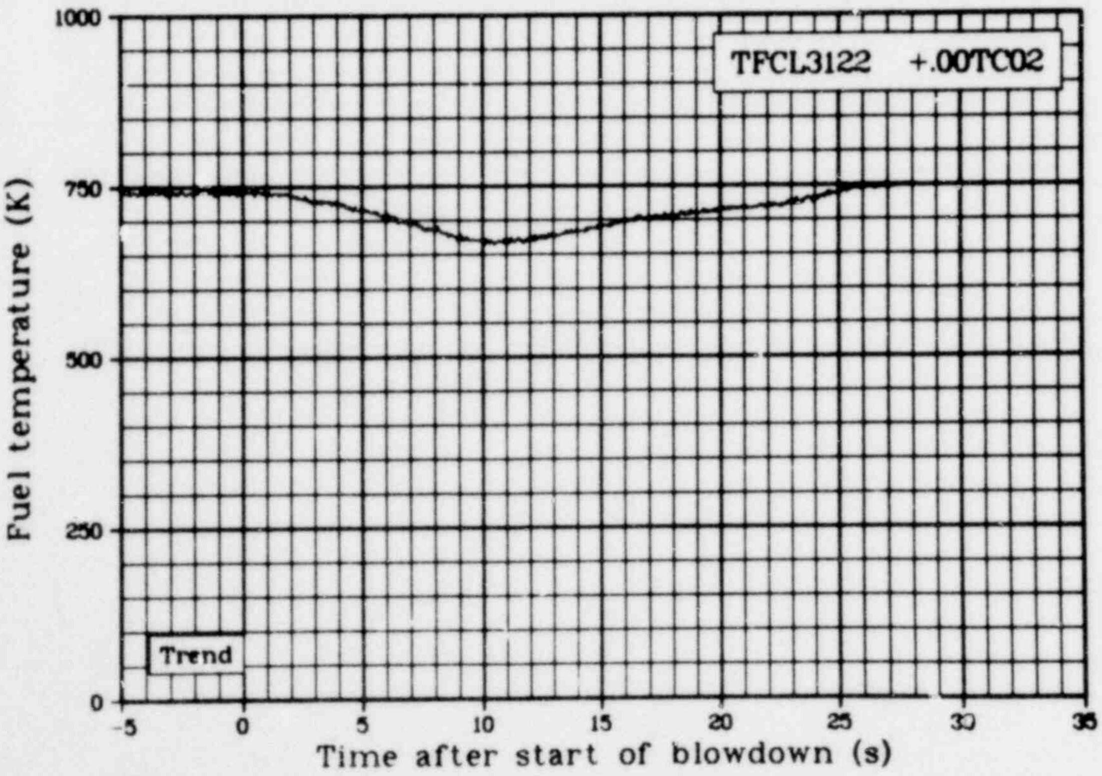

Fig. 20 Fuel temperature in Rod 312-2, at fuel stack midplane (TFCL3122 + .00TC02), from -5 to 35 s.

1405 090

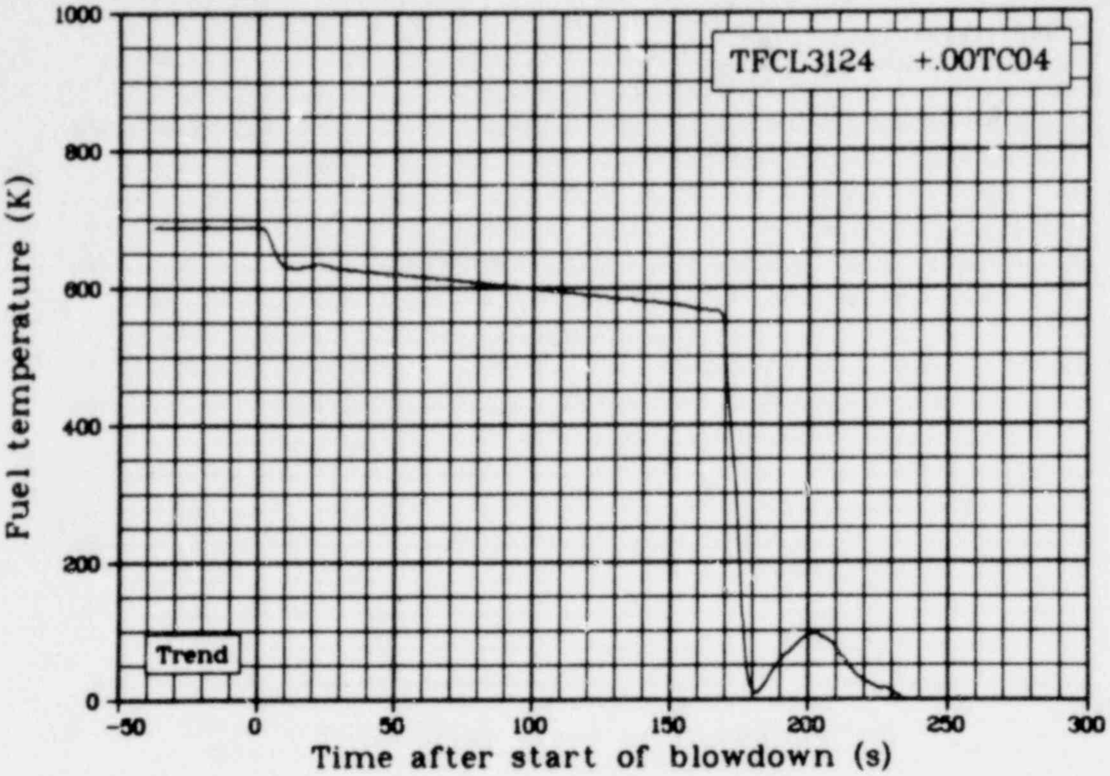

Fig. 21 Fuel temperature in Rod 312-4, at fuel stack midplane (TFCL3124 + .00TC04), from -50 to 300 s.

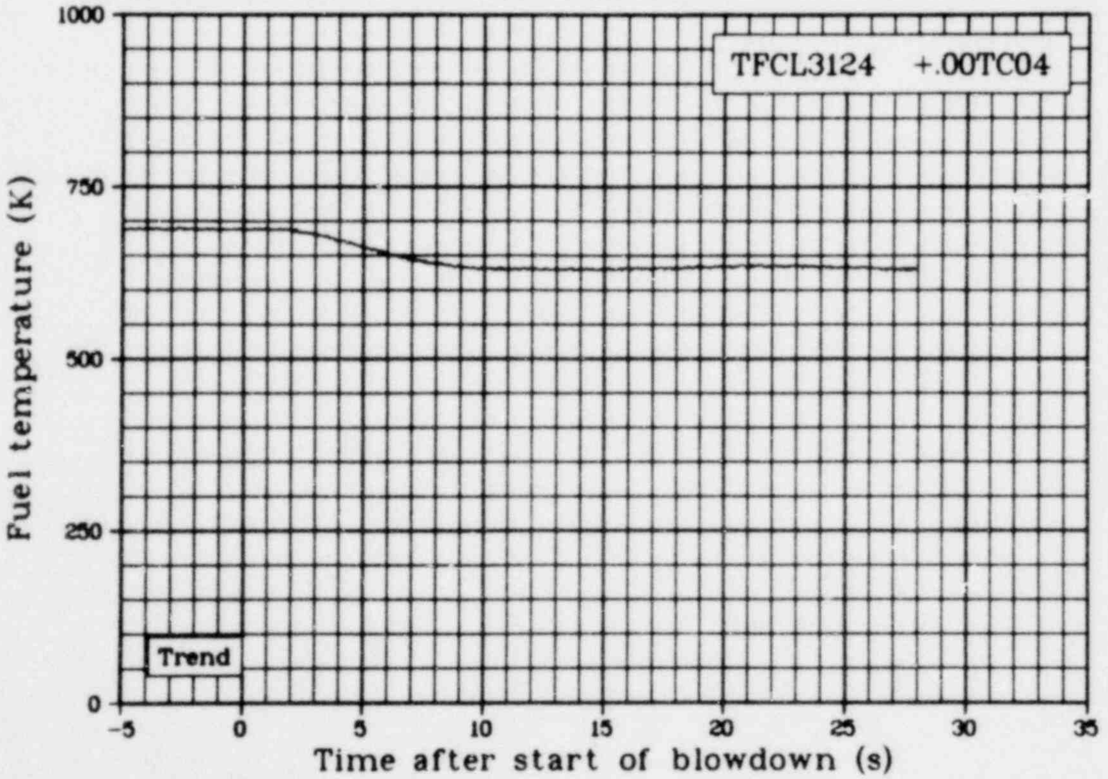

Fig. 22 Fuel temperature in Rod 312-4, at fuel stack midplane (TFCL3124 + .00TC04), from -5 to 35 s.

1405 091

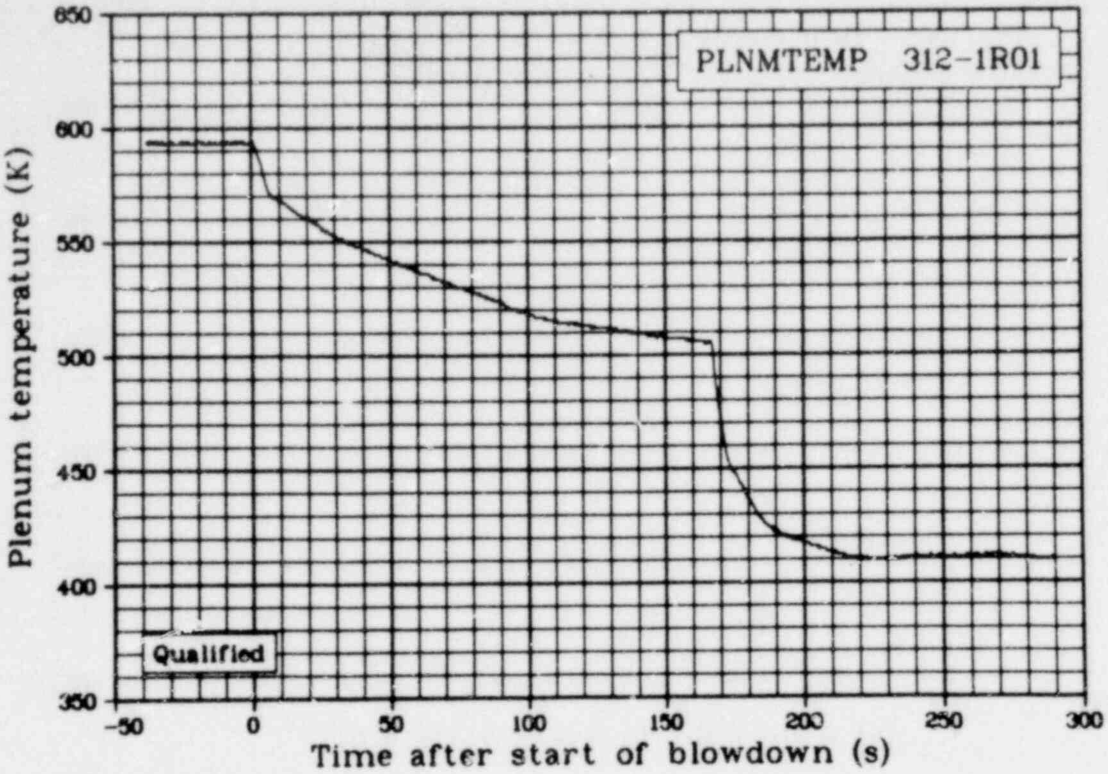

Fig. 23 Plenum temperature in Rod 312-1, (PLNMTEMP 312-1R01), from -50 to 300 s.

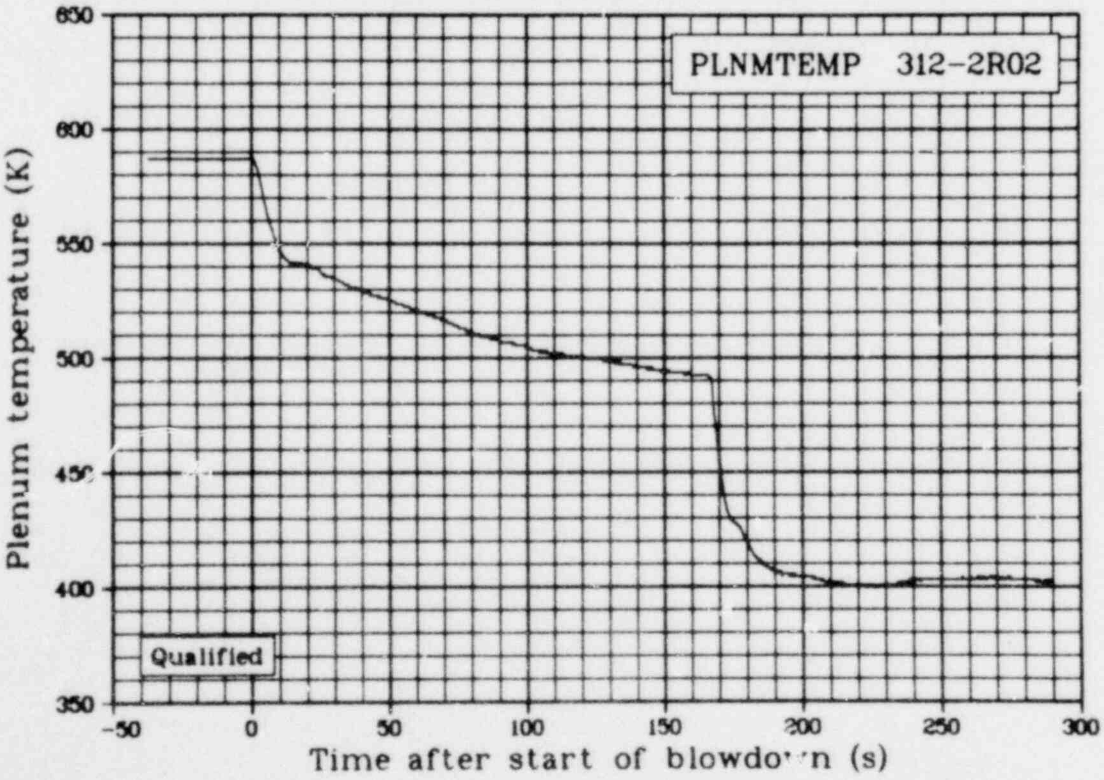

Fig. 24 Plenum temperature in Rod 312-2, (PLNMTEMP 312-2R02), from -50 to 300 s.

1405 092

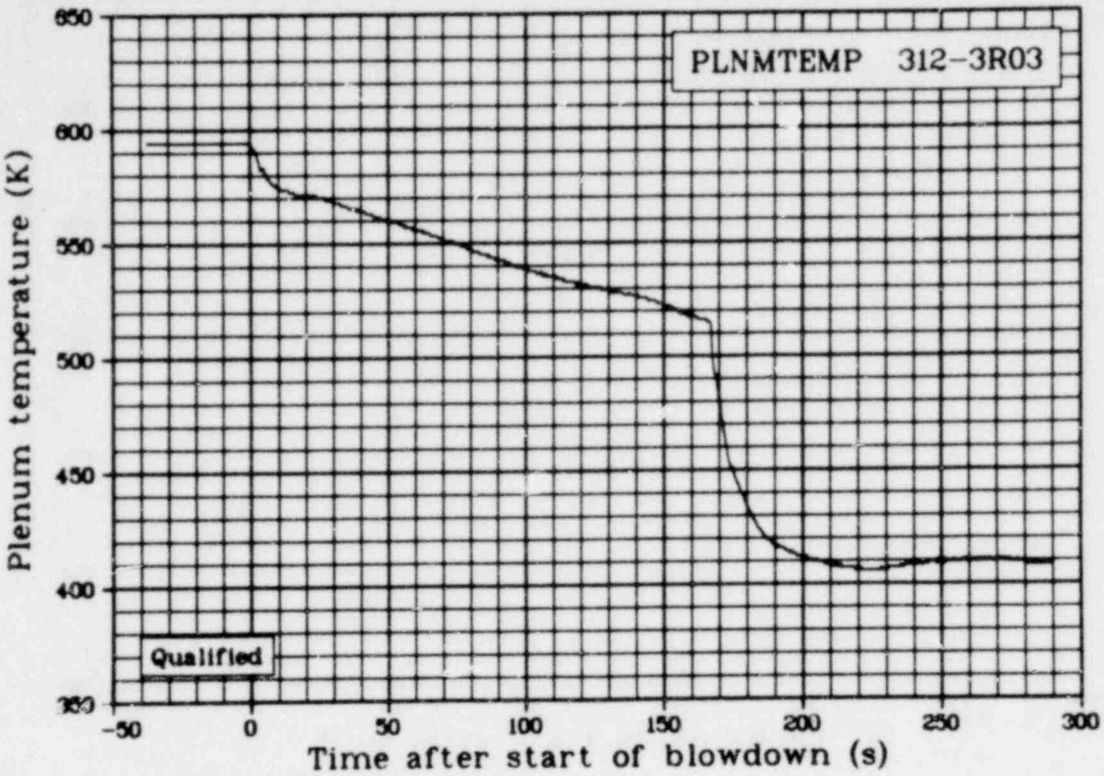

Fig. 25 Plenum temperature in Rod 312-3, (PLNMTEMP 312-3R03), from -50 to 300 s.

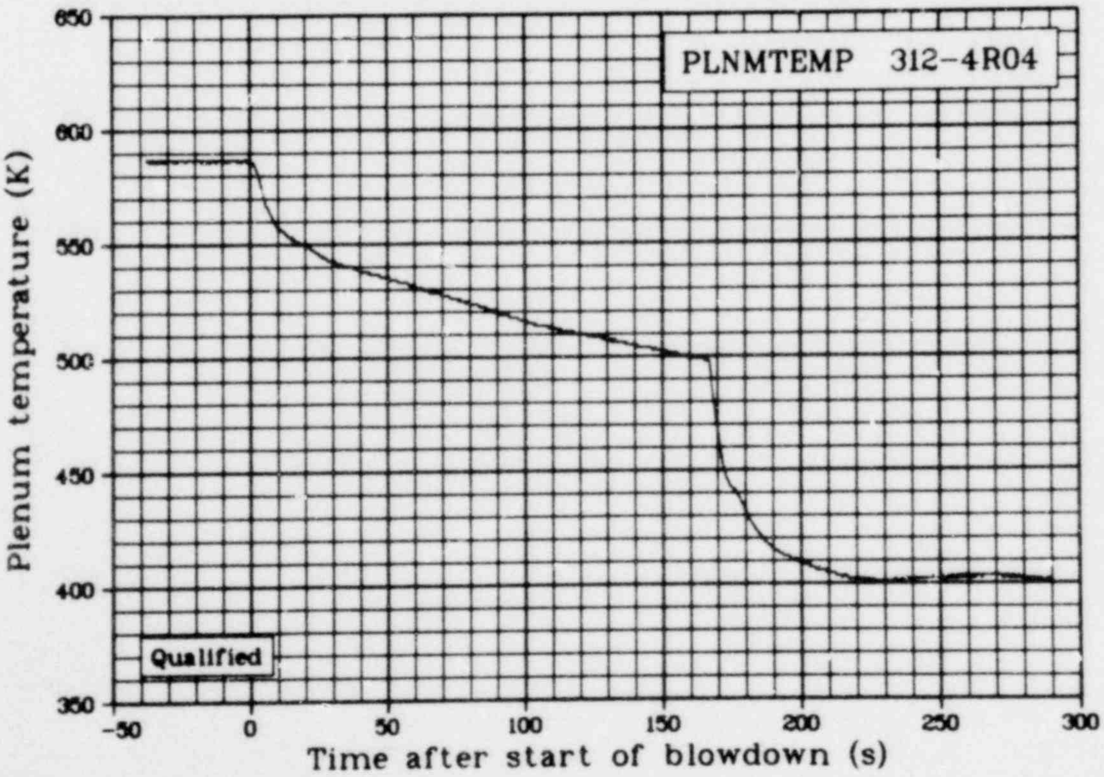

Fig. 26 Plenum temperature in Rod 312-4, (PLNMTEMP 312-4R04), from -50 to 300 s.

1405 093

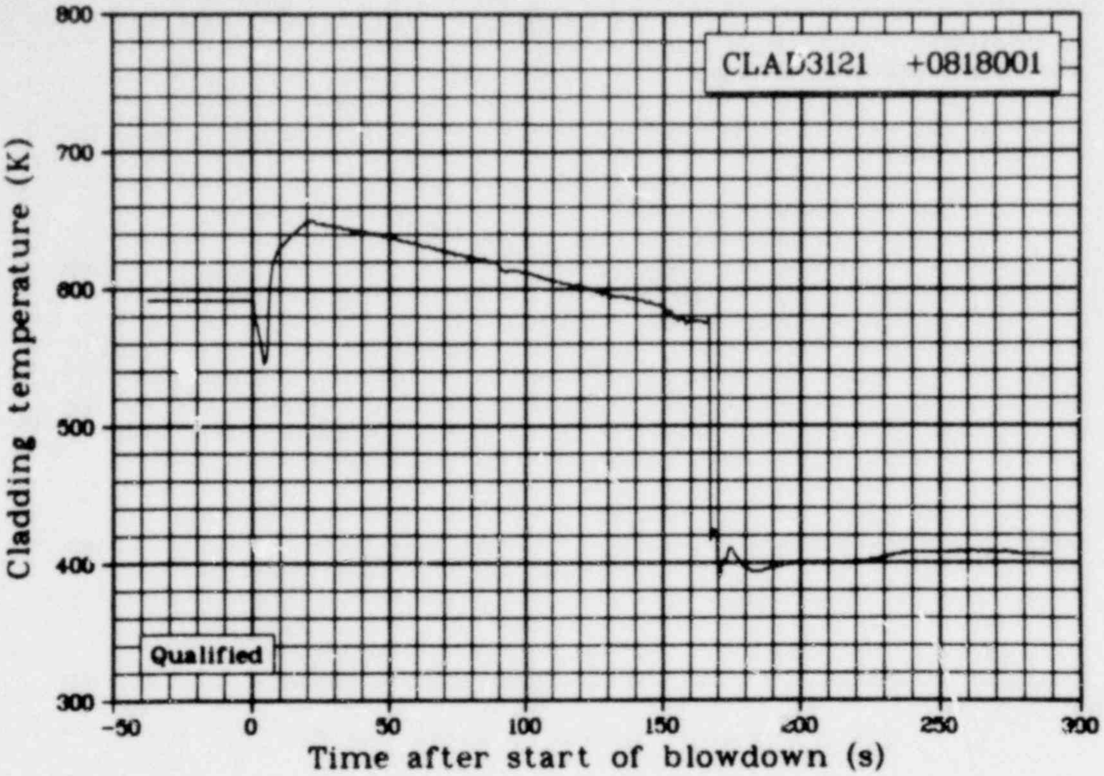

Fig. 27 Cladding temperature, Rod 312-1, at 180 degrees and 0.08 m above fuel stack midplane (CLAD3121 +0818001), from -50 to 300 s.

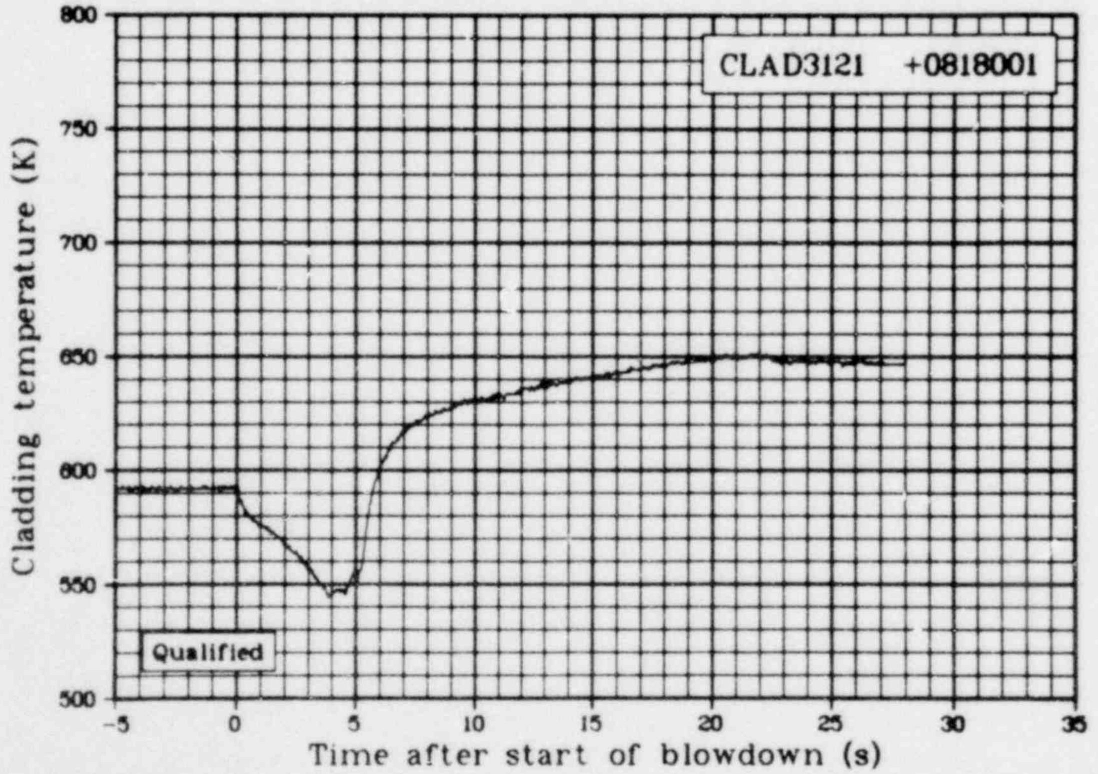

ig. 28 Cladding temperature, Rod 312-1, at 180 degrees and 0.08 m above fuel stack midplane (CLAD3121 +0818001), rom -5 to 35 s.

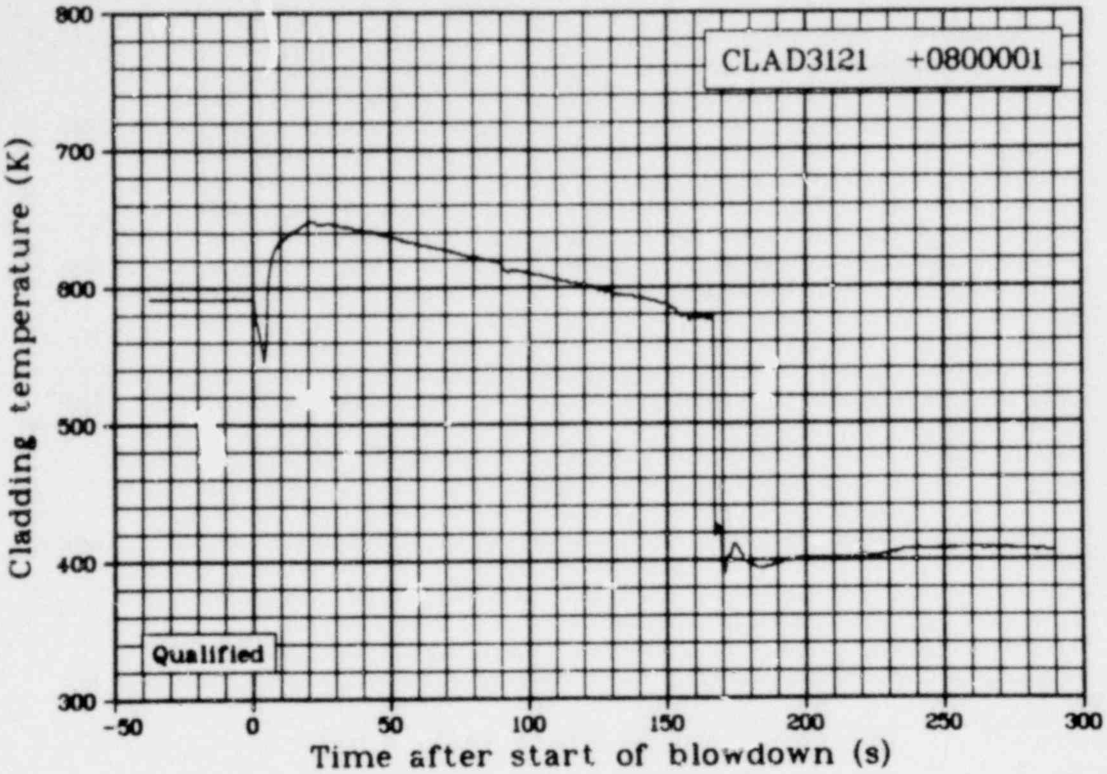

Fig. 29 Cladding temperature, Rod 312-1, at 0 degrees and 0.08 m above fuel stack midplane (CLAD3121 + 0800001), from -50 to 300 s.

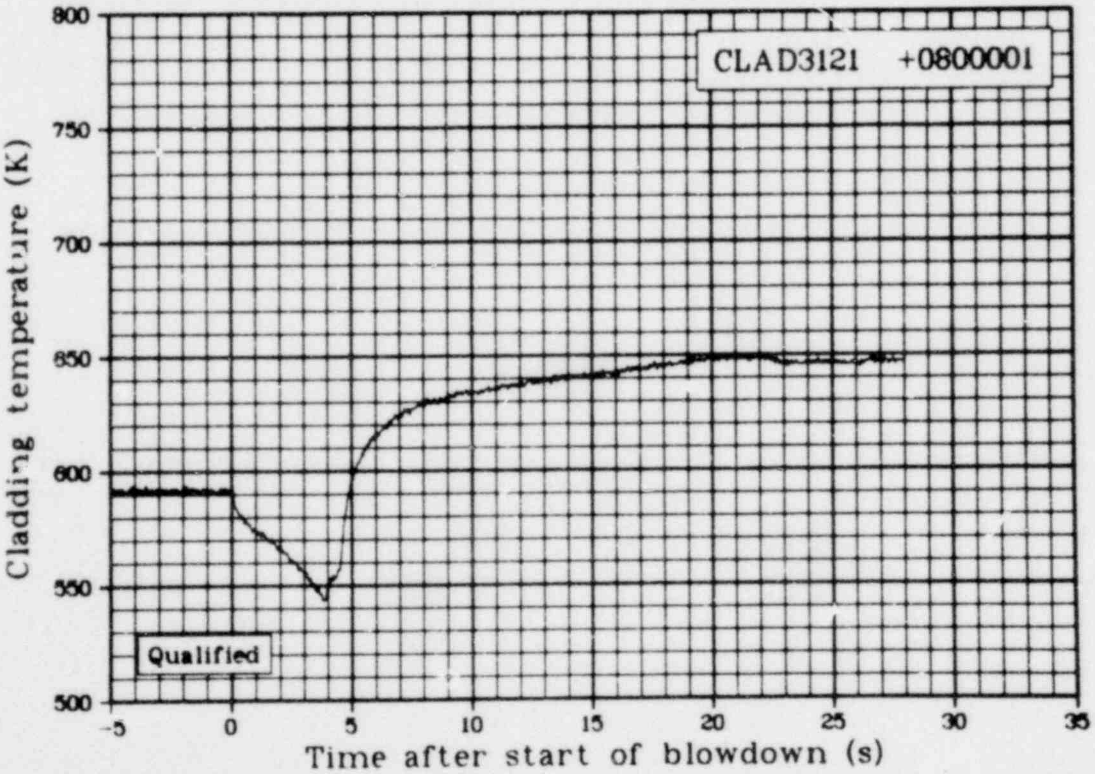

Fig. 30 Cladding temperature, Rod 312-1, at 0 degrees and 0.08 m above fuel stack midplane (CLAD3121 + 0800001), from -5 to 35 s.

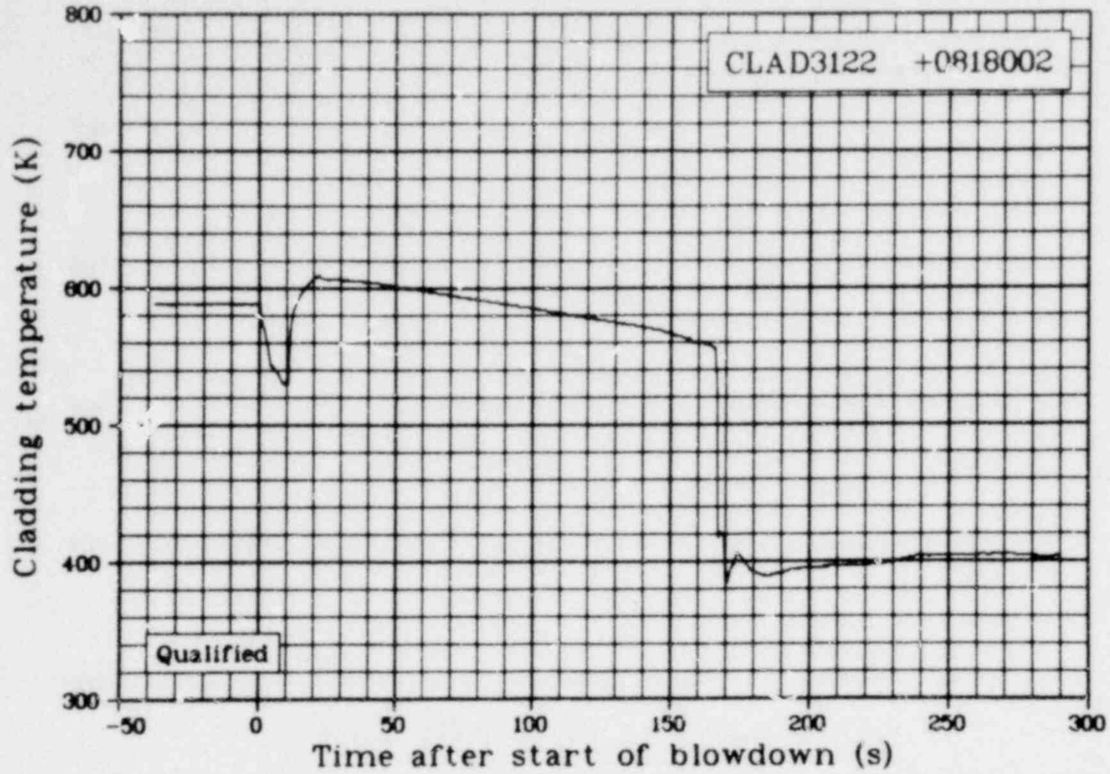

Fig. 31 Cladding temperature, Rod 312-2, at 180 degrees and 0.08 m above fuel stack midplane (CLAD3122 +0818002), from -50 to 300 s.

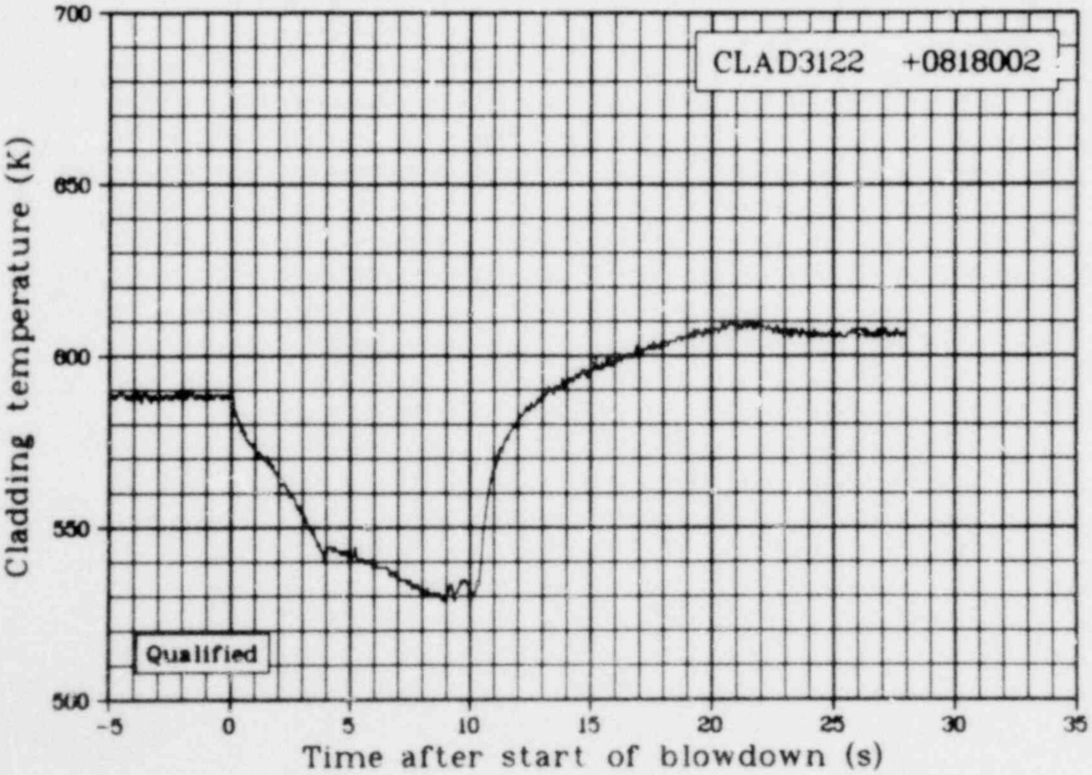

Fig. 32 Cladding temperature, Rod 312-2, at 180 degrees and 0.08 m above fuel stack midplane (CLAD3122 +0818002), from -5 to 35 s.

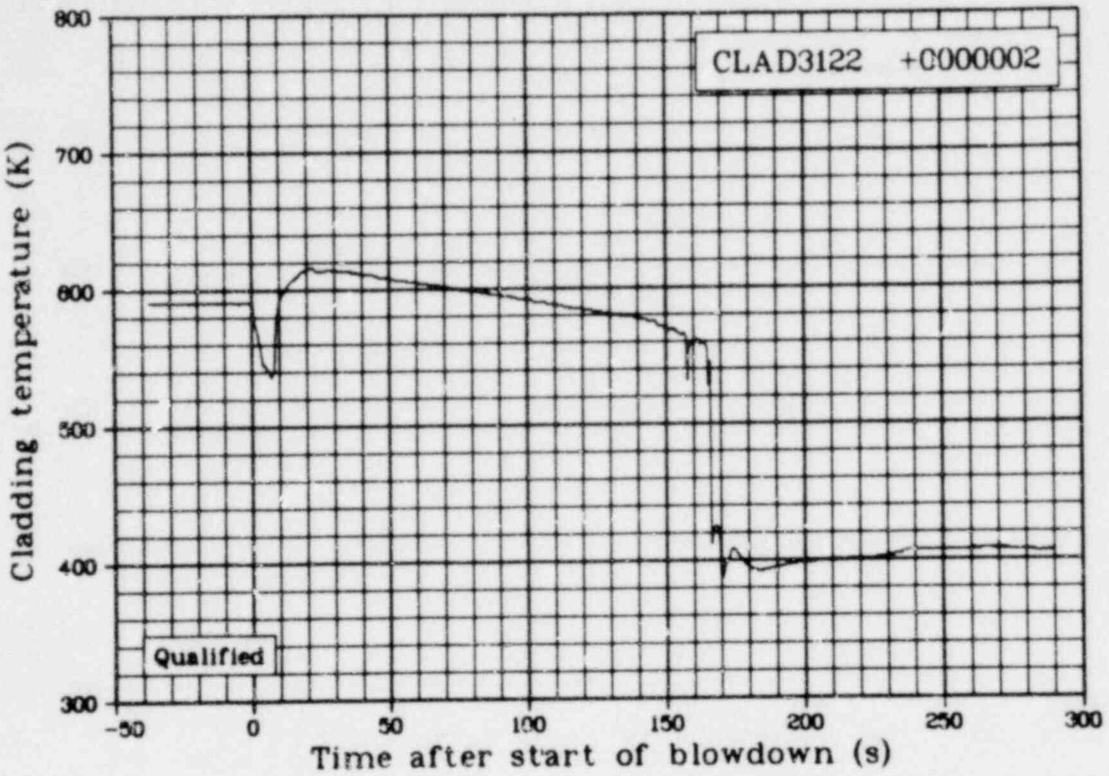

Fig. 33 Cladding temperature, Rod 312-2, at 0 degrees and fuel stack midplane (CLAD3122 + 0000002), from -50 to 300 s.

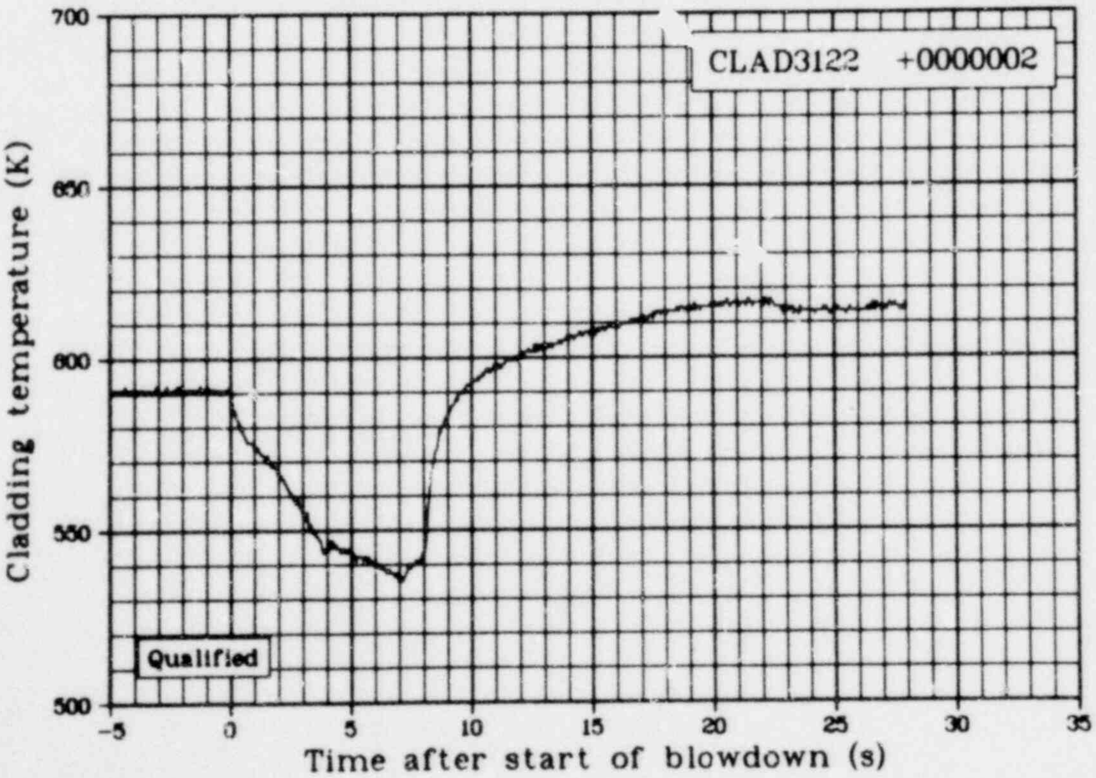

Fig. 34 Cladding temperature, Rod 312-2, at 0 degrees and fuel stack midplane (CLAD3122 + 0000002), from -5 to 35 s.

1405 097

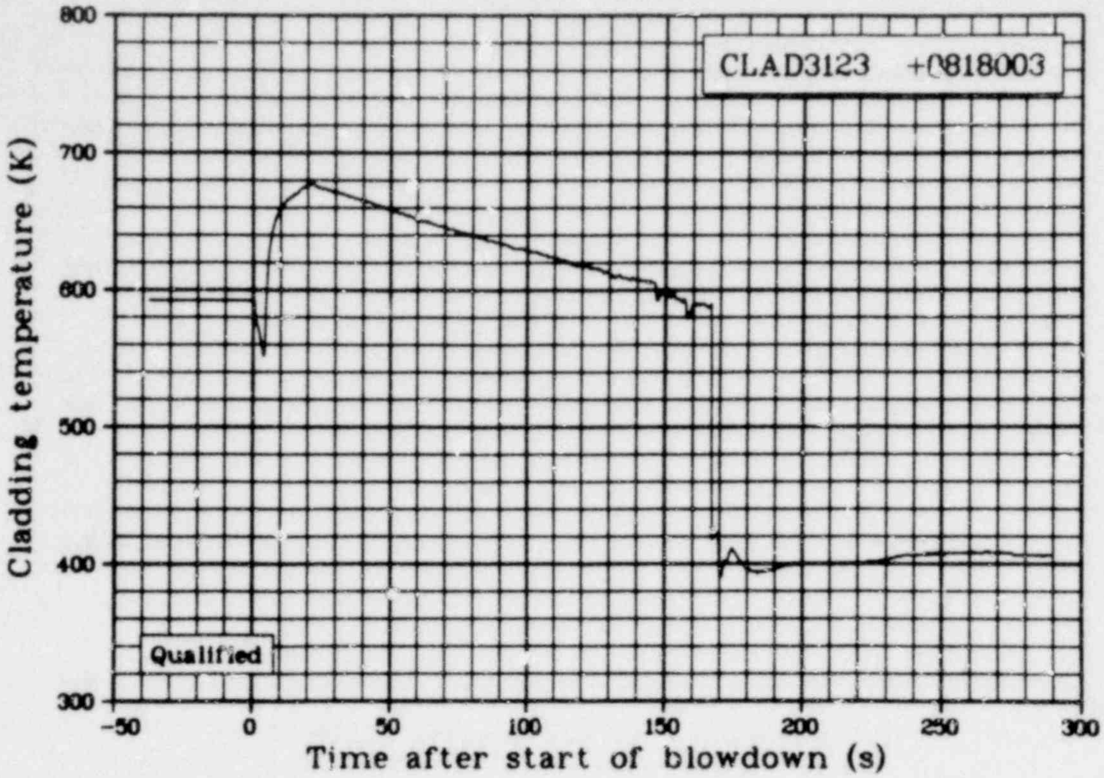

Fig. 35 Cladding temperature, Rod 3 2-3, at 180 degrees and 0.08 m above fuel stack midplane (CLAD3123 + 0818003), from -50 to 300 s.

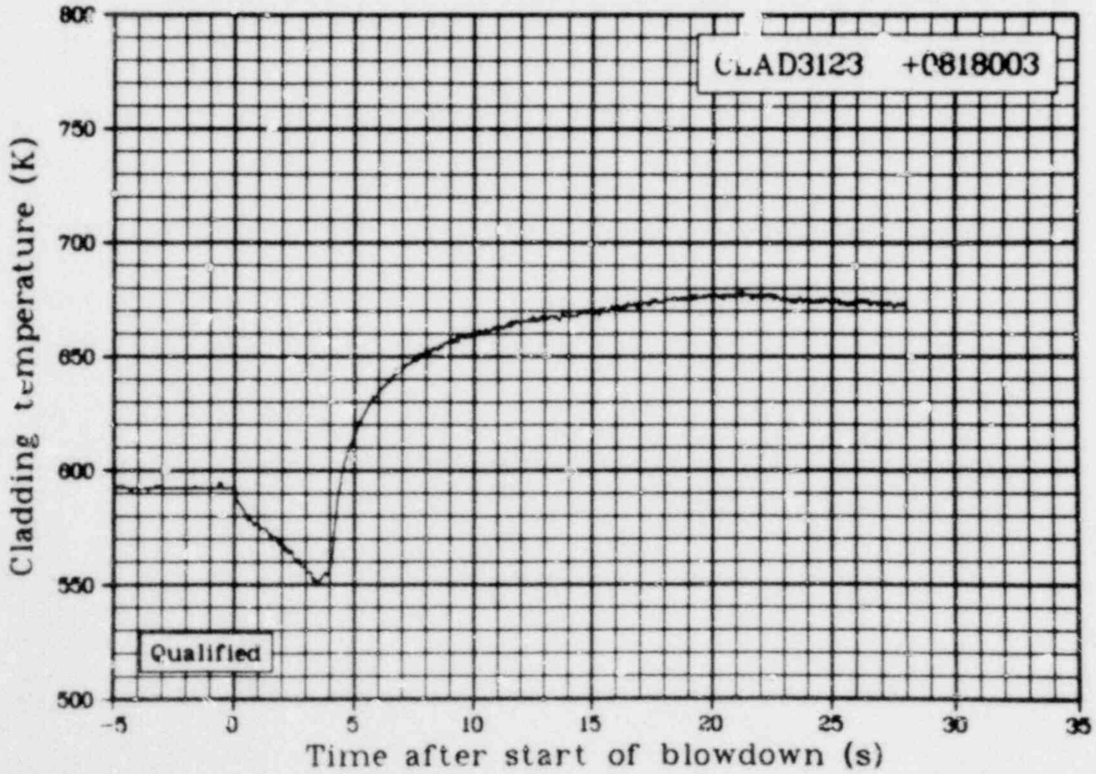

Fig. 36 Cladding temperature, Rod 312-3, at 180 degrees and 0.08 m above fuel stack midplane (CLAD3123 + 0818003), from -5 to 35 s.

1405 098

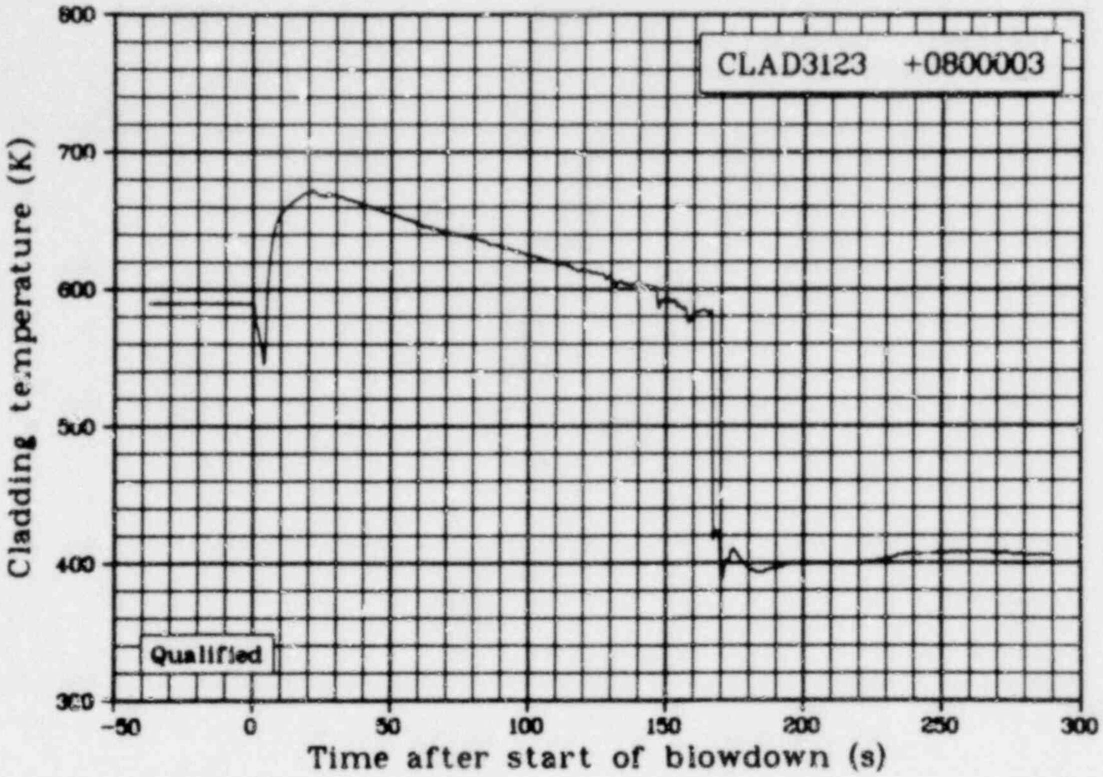

Fig. 37 Cladding temperature, Rod 312-3, at 0 degrees and 0.08 m above fuel stack midplane (CLAD3123 +0800003), from -50 to 300 s.

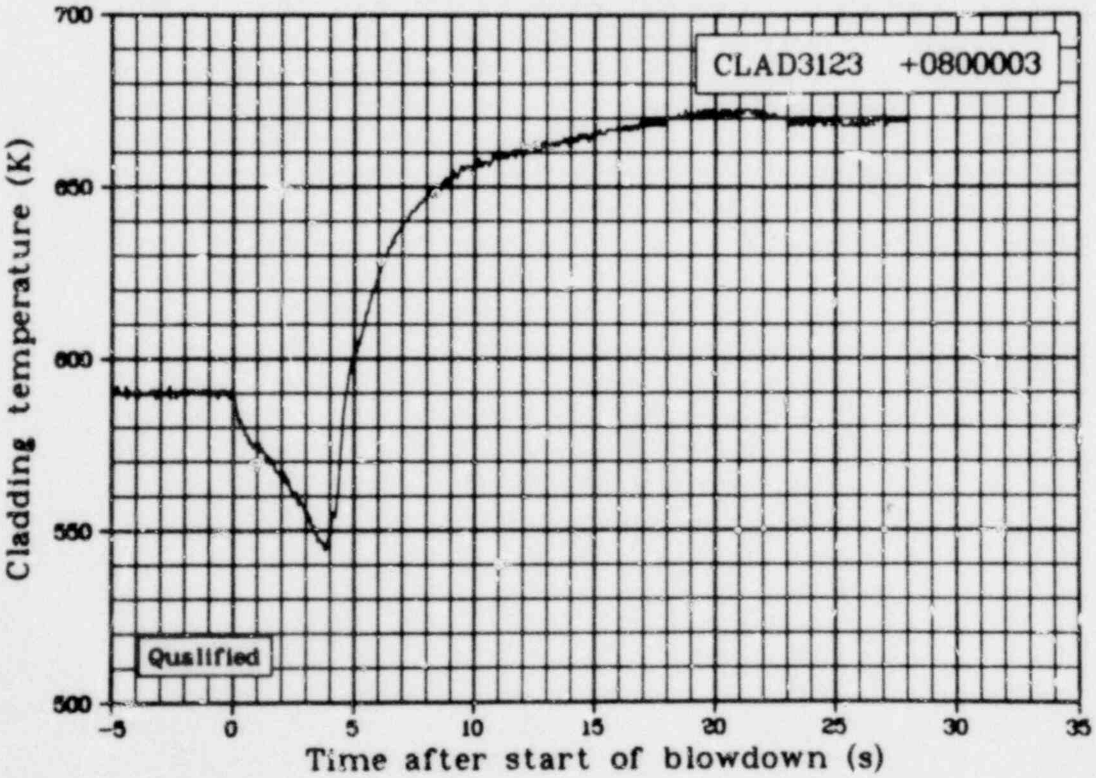

Fig. 38 Cladding temperature, Rod 312-3, at 0 degrees and 0.08 m above fuel stack midplane (CLAD3123 +0800003), from -5 to 35 s.

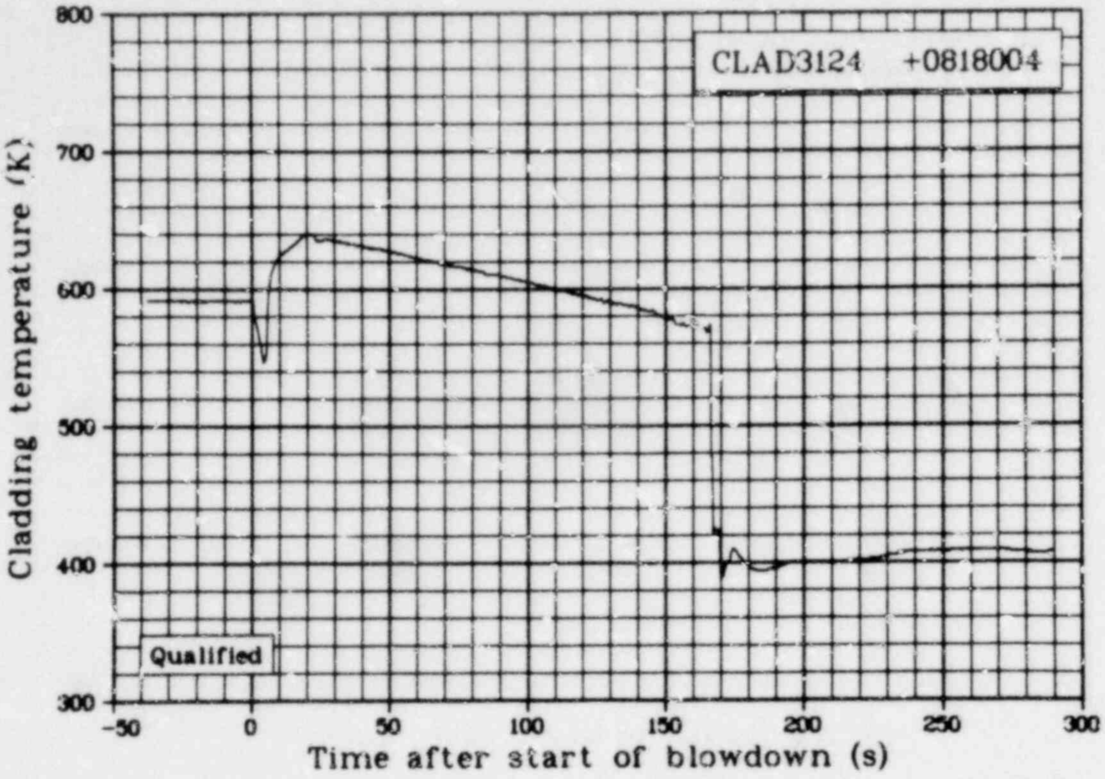

Fig. 39 Cladding temperature, Rod 312-4, at 180 degrees and 0.08 m above fuel stack midplane (CLAD3124 +0818004), from -50 to 300 s.

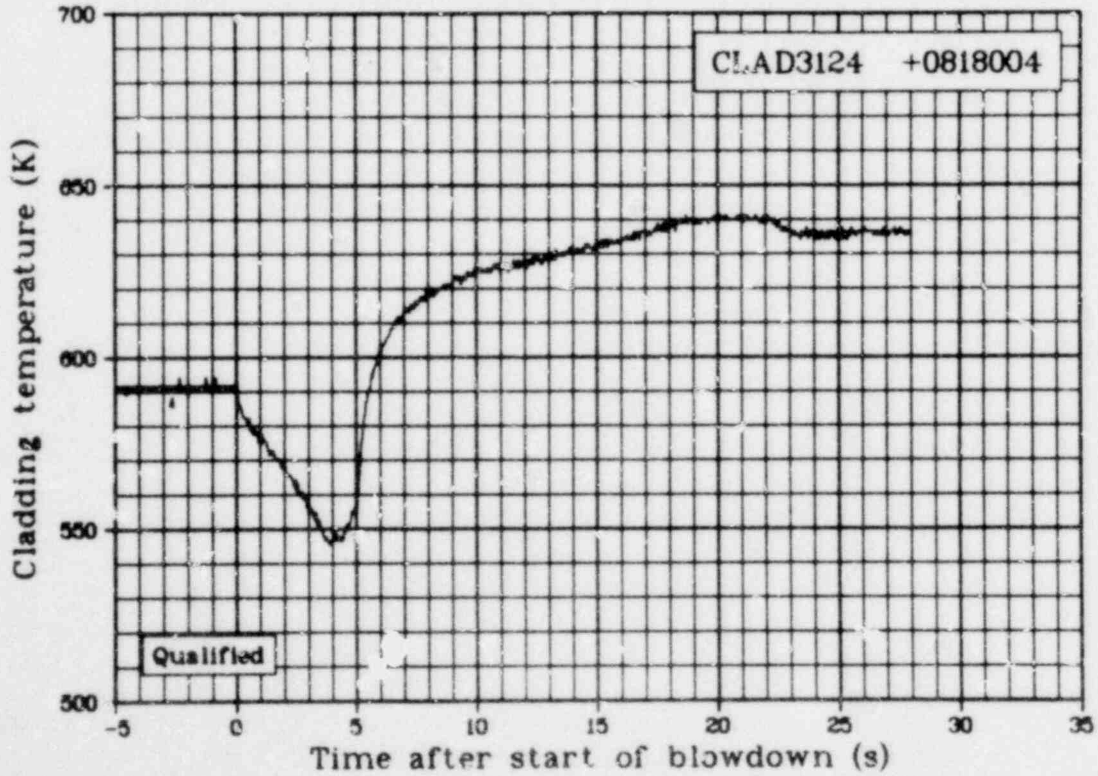

Fig. 40 Cladding temperature, Rod 312-4, at 180 degrees and 0.08 m above fuel stack midplane (CLAD3124 +0818004), from -5 to 35 s.

1405 100

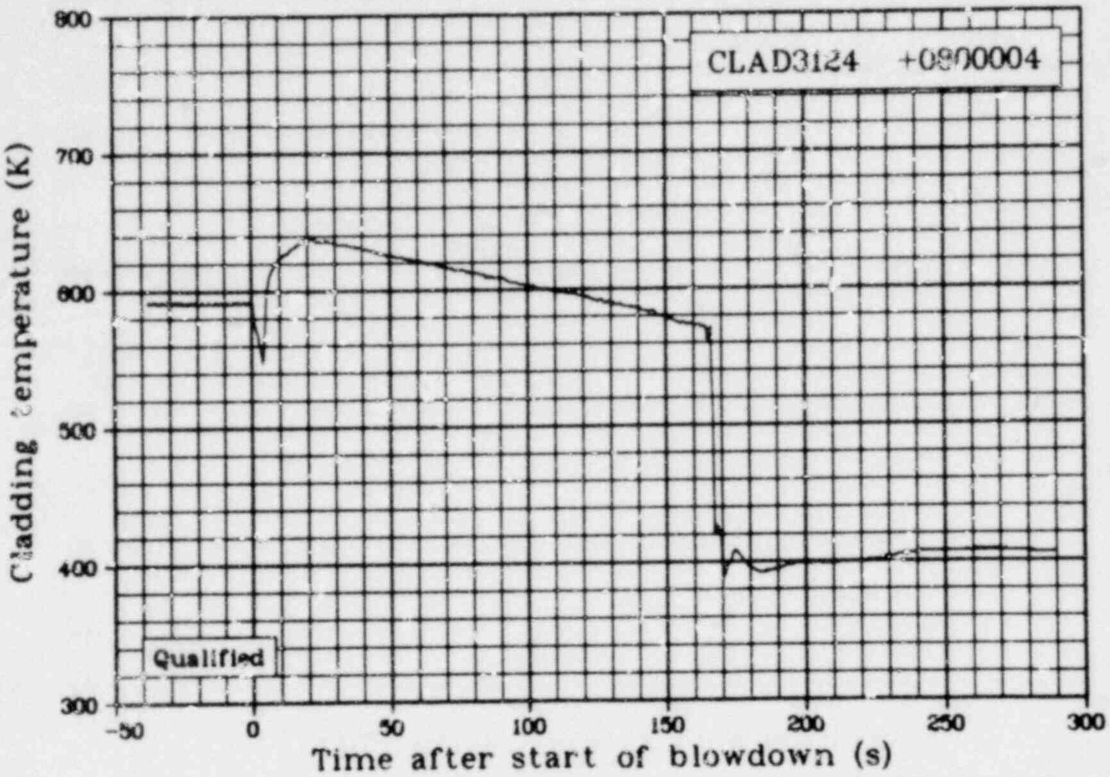

Fig. 41 Cladding temperature, Rod 312-4, at 0 degrees and 0.08 m above fuel stack midplane (CLAD3124 +0800004), from -50 to 300 s.

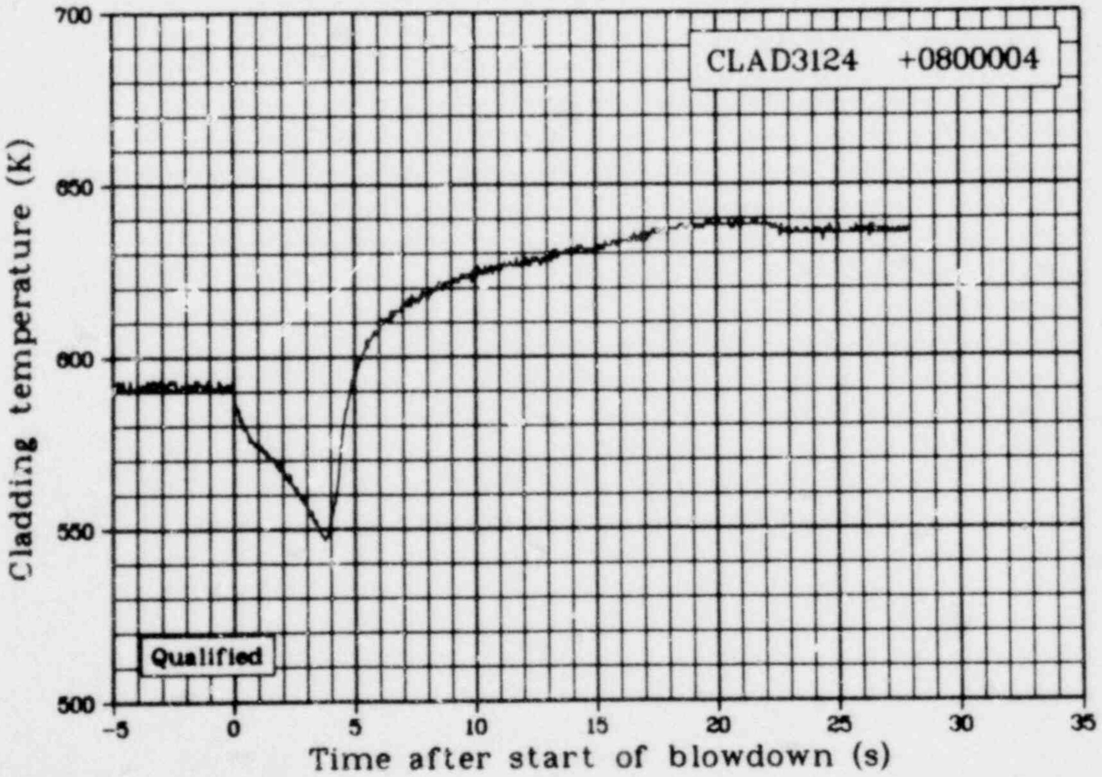

Fig. 42 Cladding temperature, Rod 312-4, at 0 degrees and 0.08 m above fuel stack midplane (CLAD3124 +0800004), from -5 to 35 s.

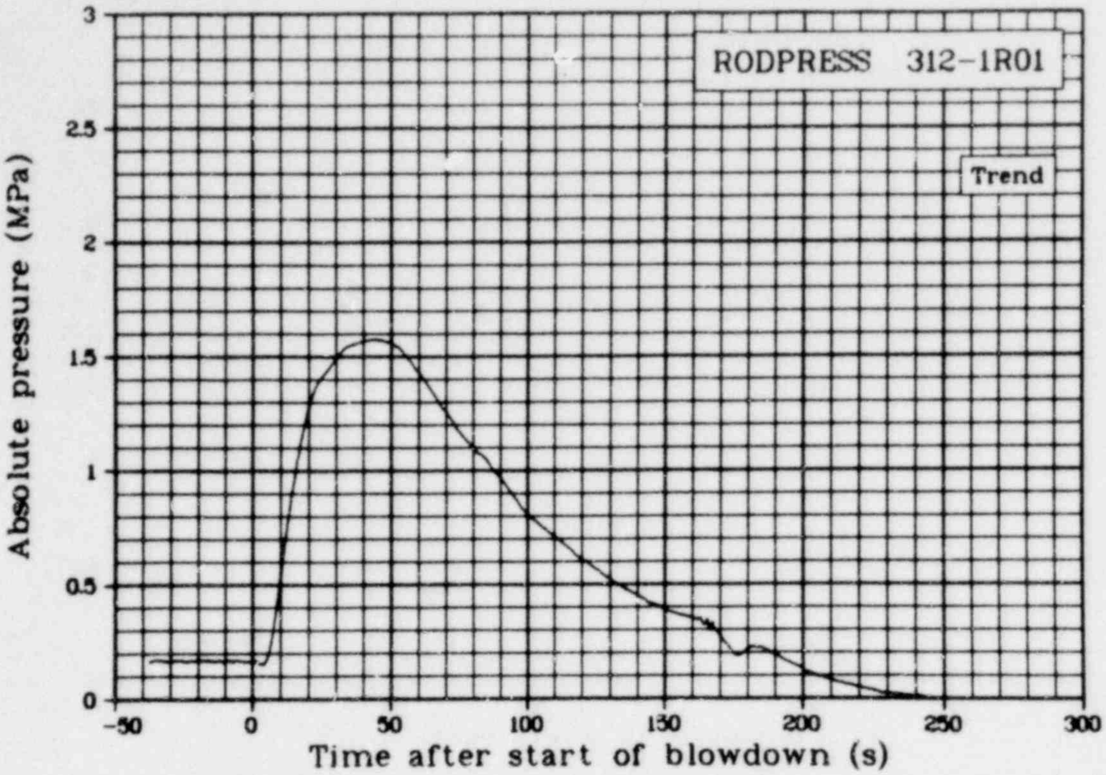

Fig. 43 Absolute pressure in Fuel Rod 312-1 plenum (RODPRESS 312-1R01), from -50 to 300 s.

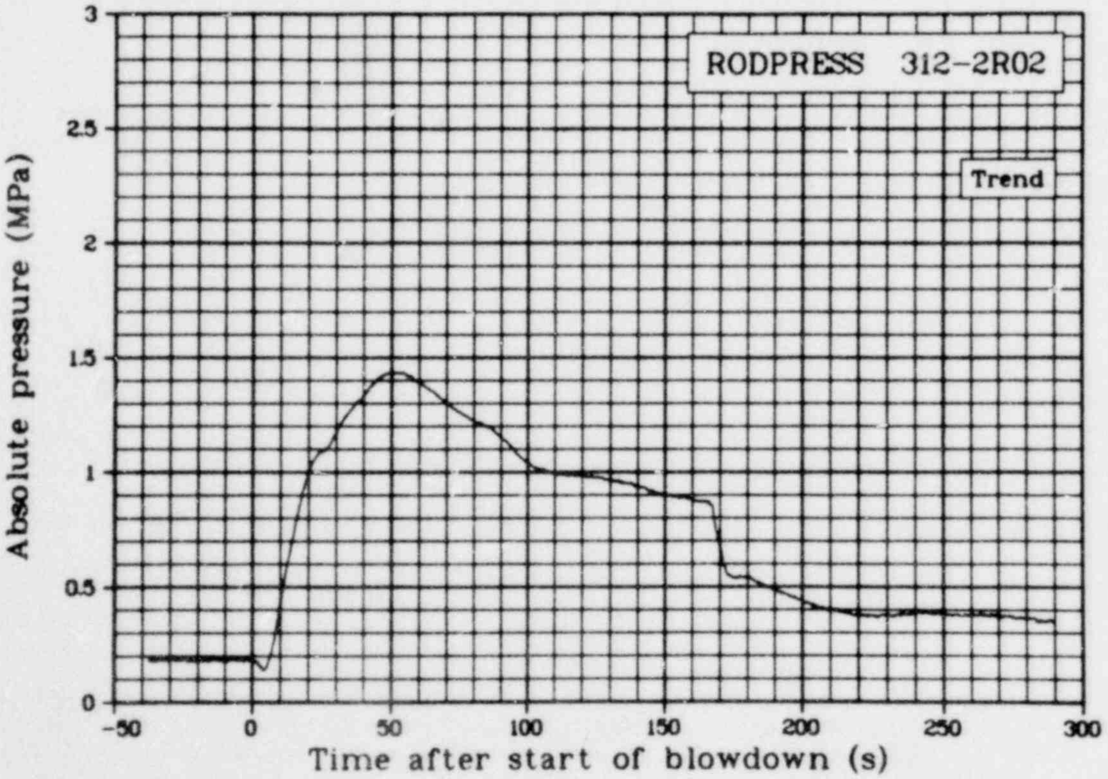

Fig. 44 Absolute pressure in Fuel Rod 312-2 plenum (RODPRESS 312-2R02), from -50 to 300 s.

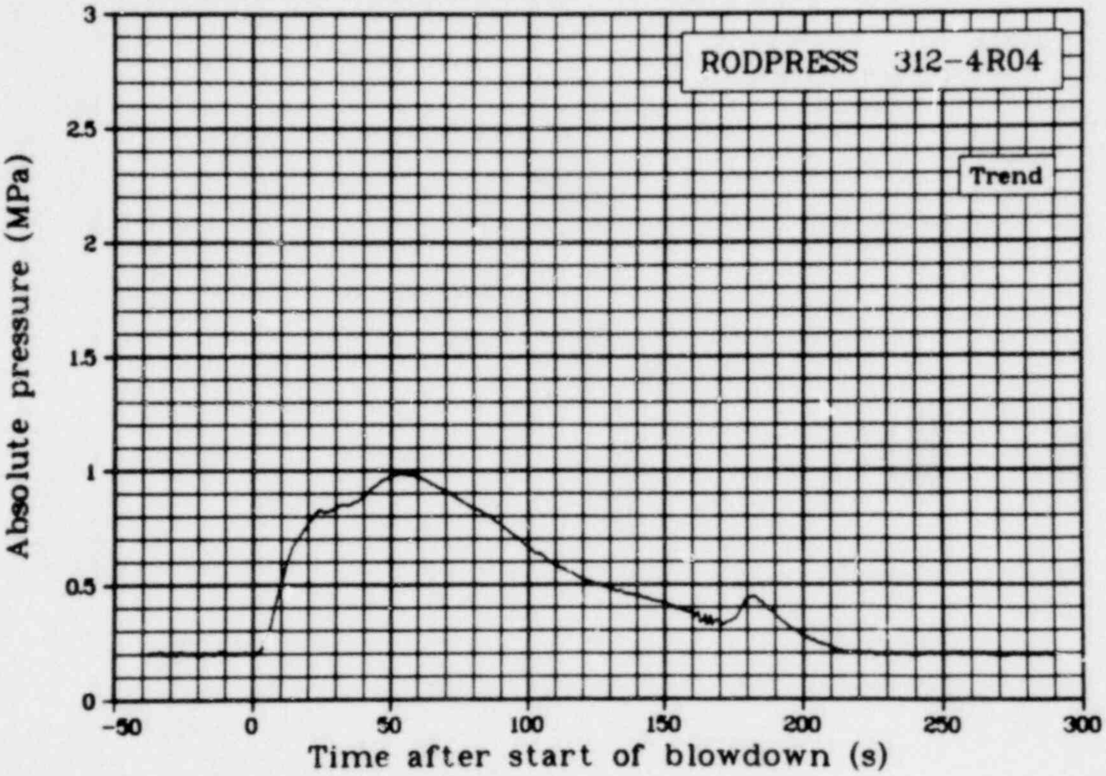

Fig. 45 Absolute pressure in Fuel Rod 312-4 plenum (RODPRESS 312-4R04), from -50 to 300 s.

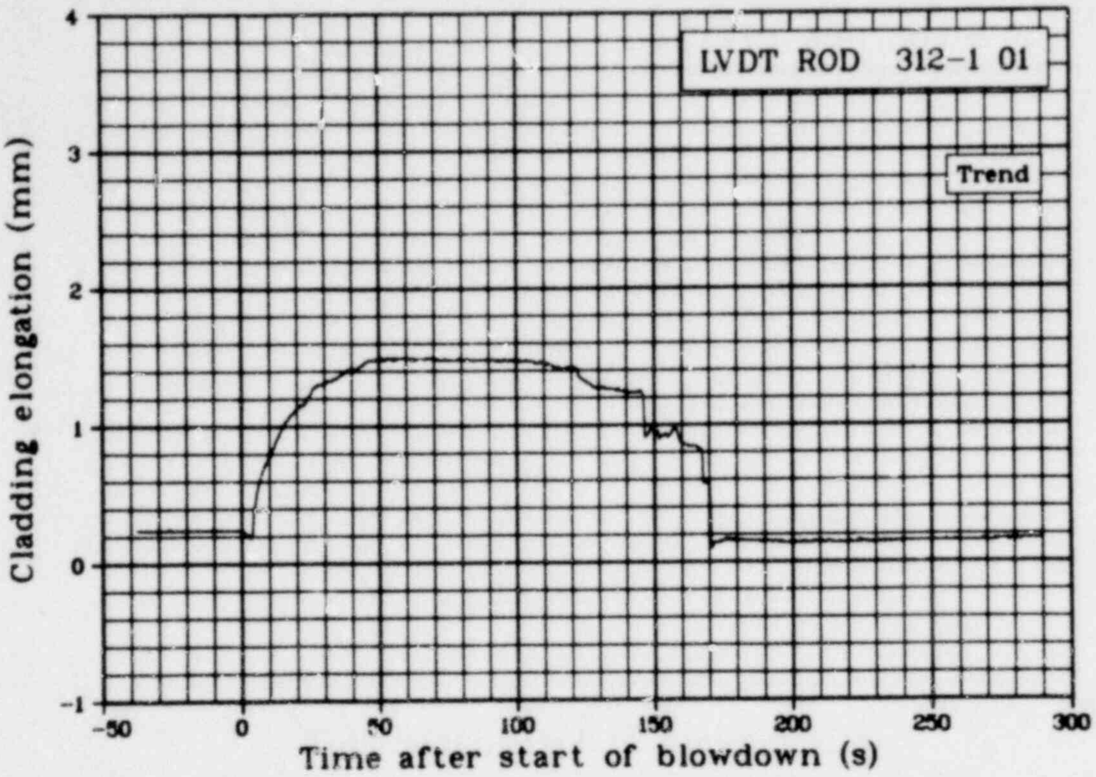

Fig. 46 Cladding elongation of Fuel Rod 312-1 (LVDT ROD 312-1 01), from -50 to 300 s.

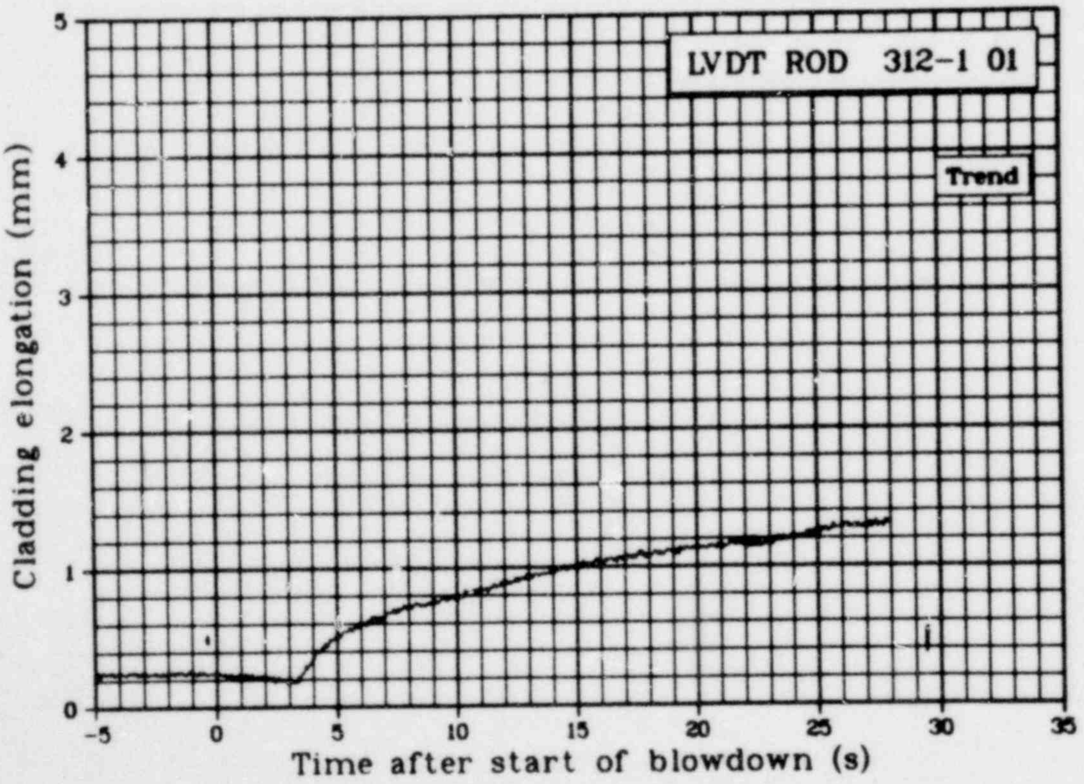

Fig. 47 Cladding elongation of Fuel Rod 312-1 (LVDT ROD 312-1 01), from -5 to 35 s.

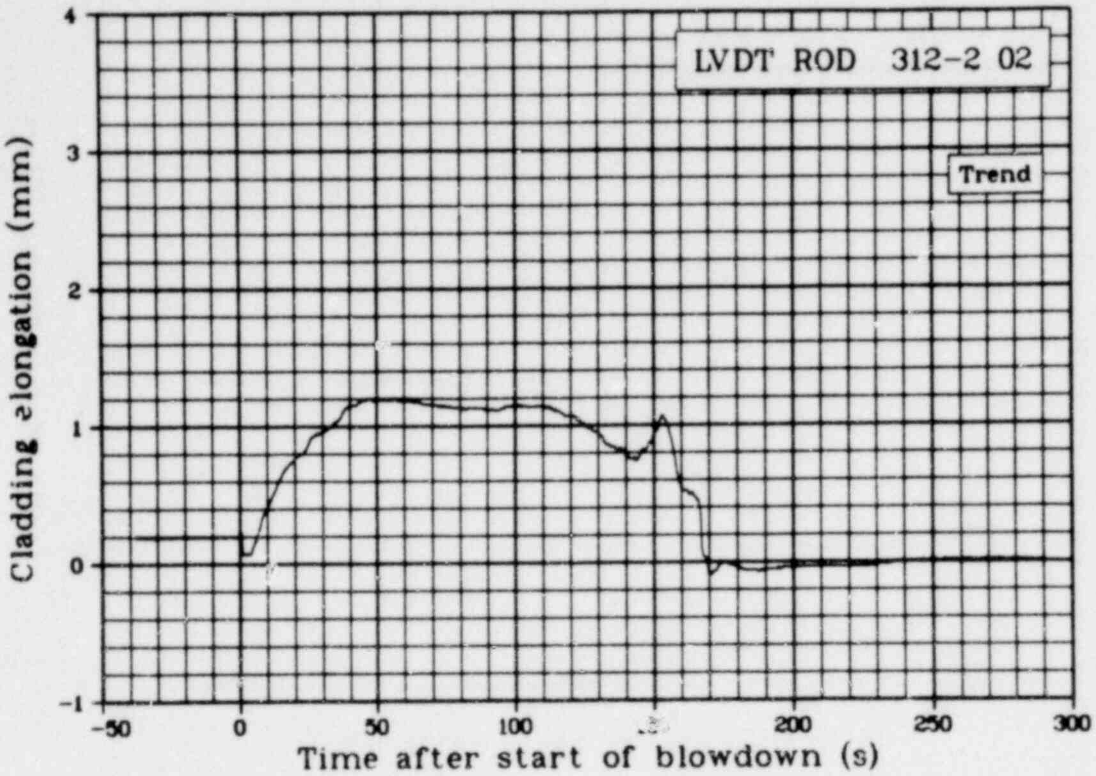

Fig. 48 Cladding elongation of Fuel Rod 312-2 (LVDT ROD 312-2 02), from -50 to 300 s.

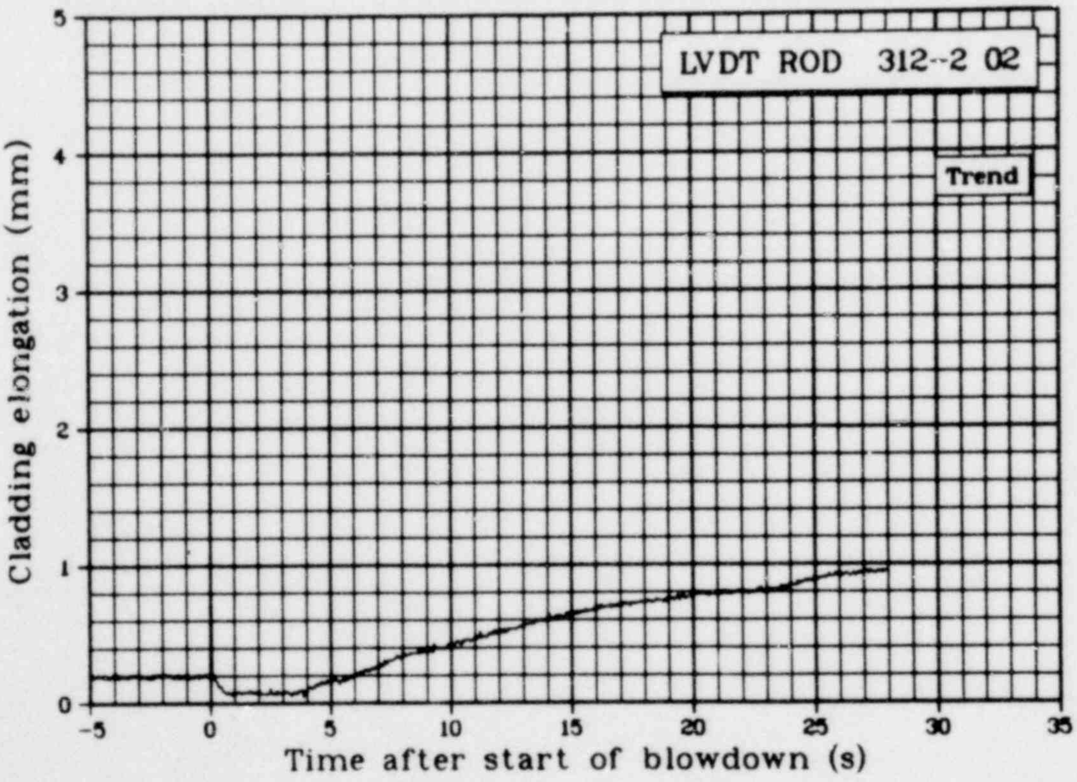

Fig. 49 Cladding elongation of Fuel Rod 312-2 (LVDT ROD 312-2 02), from -5 to 35 s.

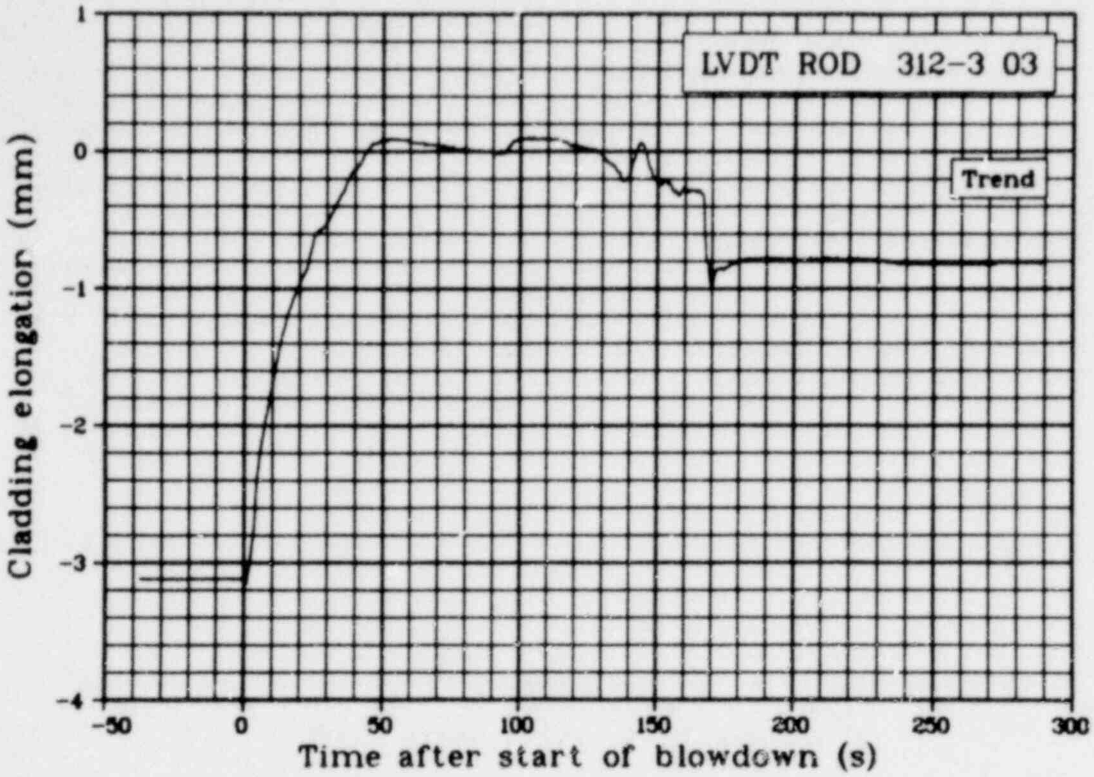

Fig. 50 Cladding elongation of Fuel Rod 312-3 (LVDT ROD 312-3 03), from -50 to 300 s.

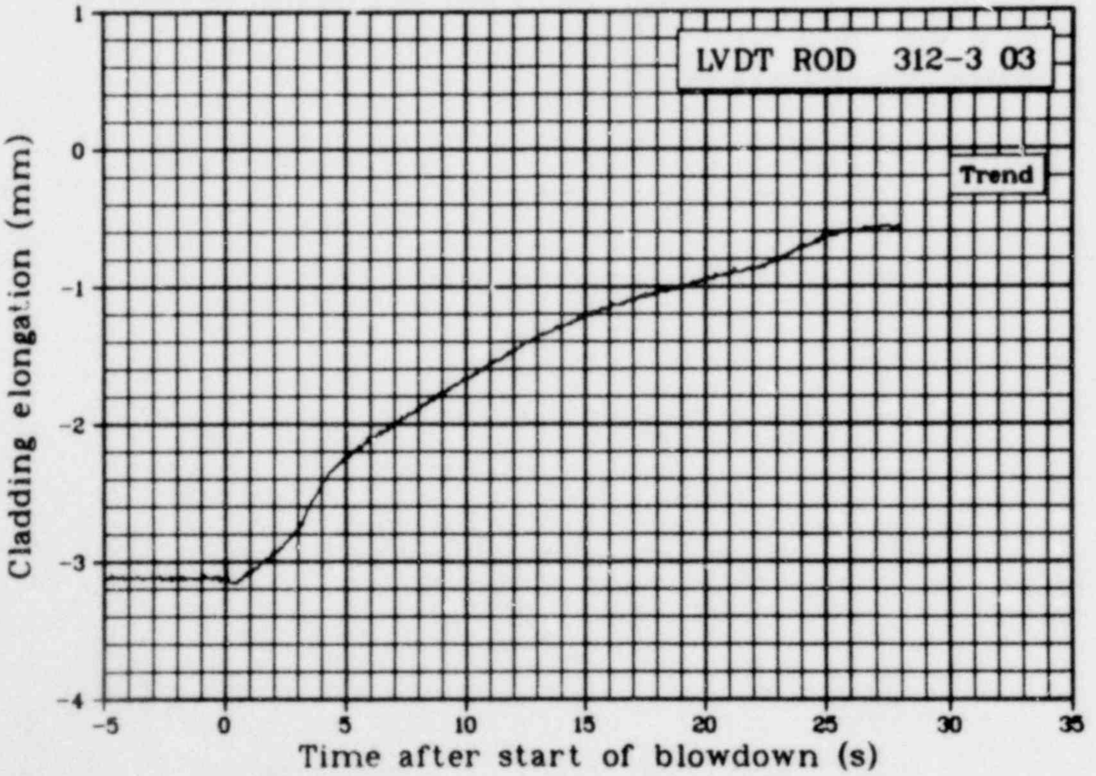

Fig. 51 Cladding elongation of Fuel Rod 312-3 (LVDT ROD 312-3 03), from -5 to 35 s.

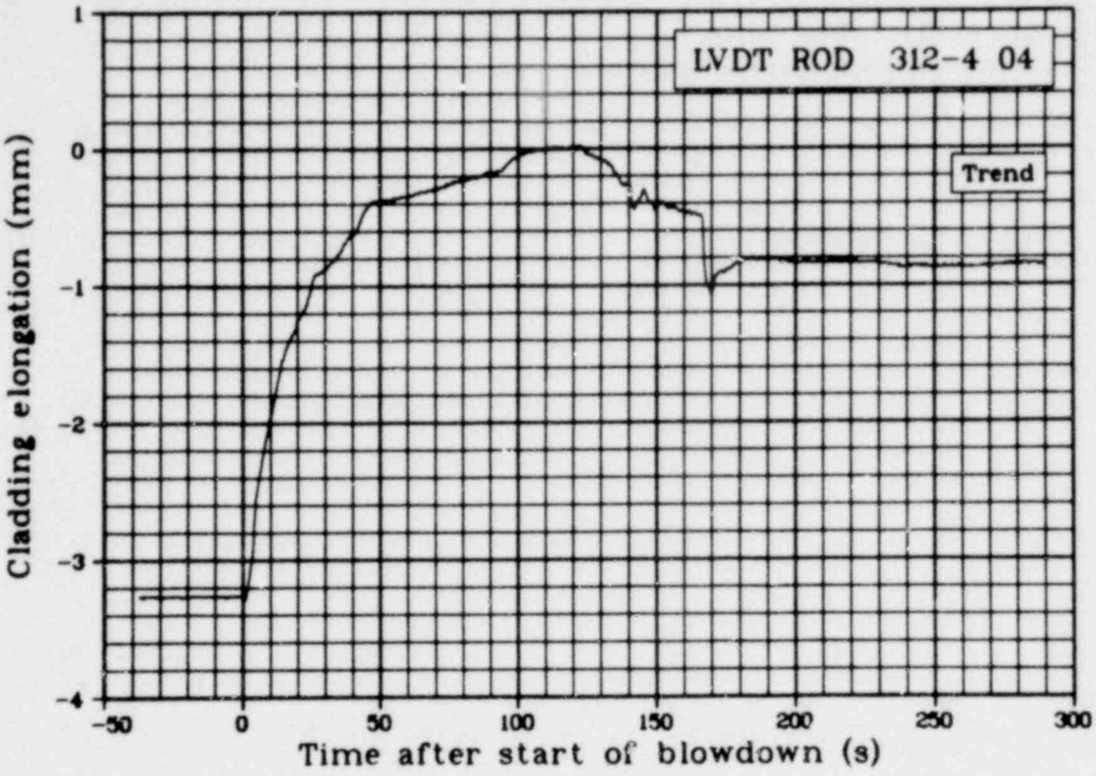

Fig. 52 Cladding elongation of Fuel Rod 312-4 (LVDT ROD 312-4 04), from -50 to 300 s.

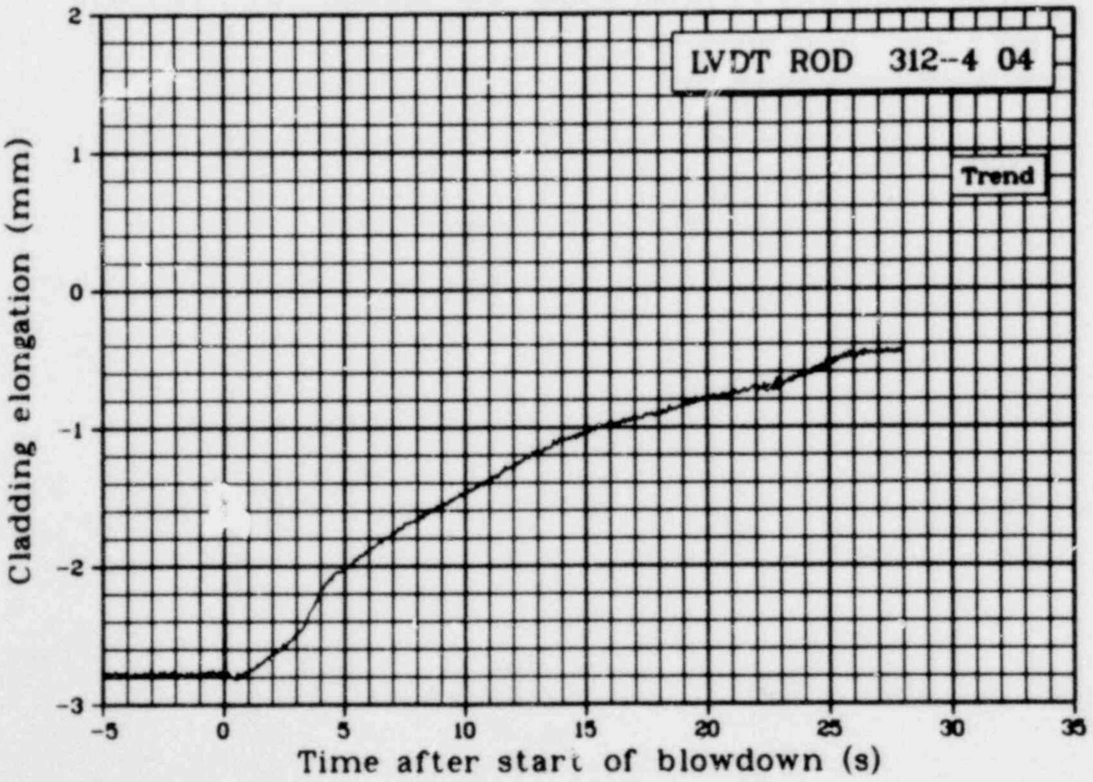

Fig. 53 Cladding elongation of Fuel Rod 312-4 (LVDT ROD 312-4 04), from -5 to 35 s.

1405 107

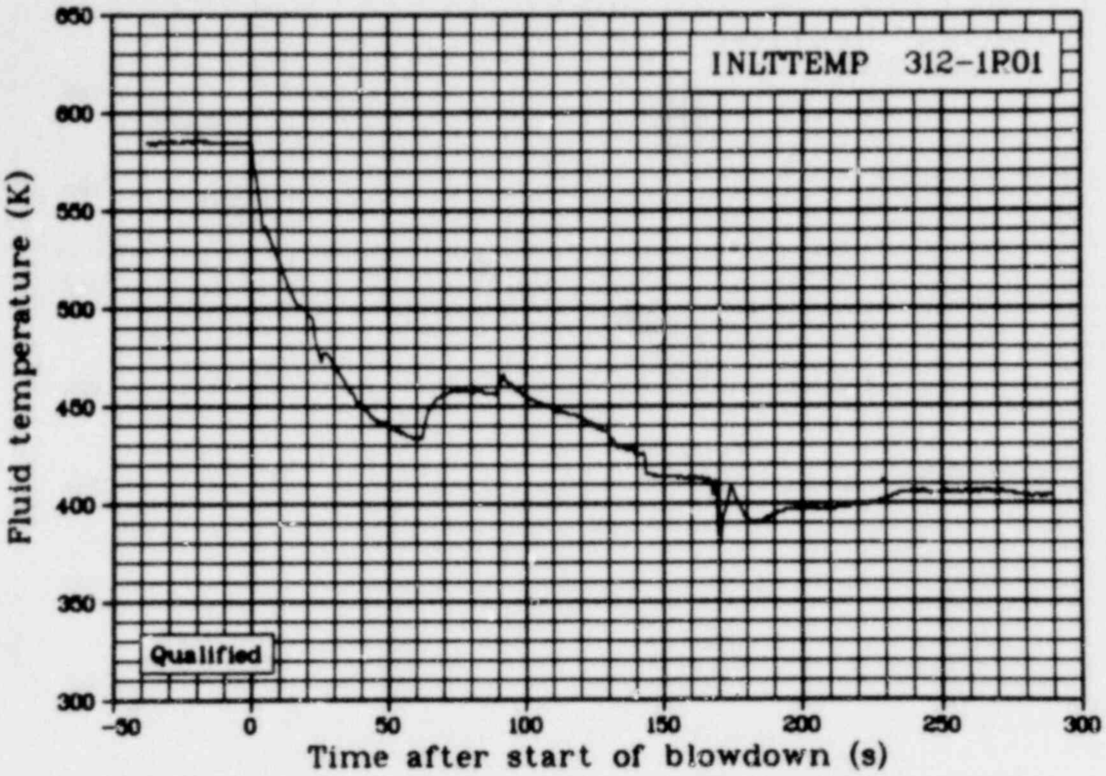

Fig. 54 Fluid temperature of Fuel Rod 312-1 coolant inlet (INLTTEMP 312-1R01), from -50 to 300 s.

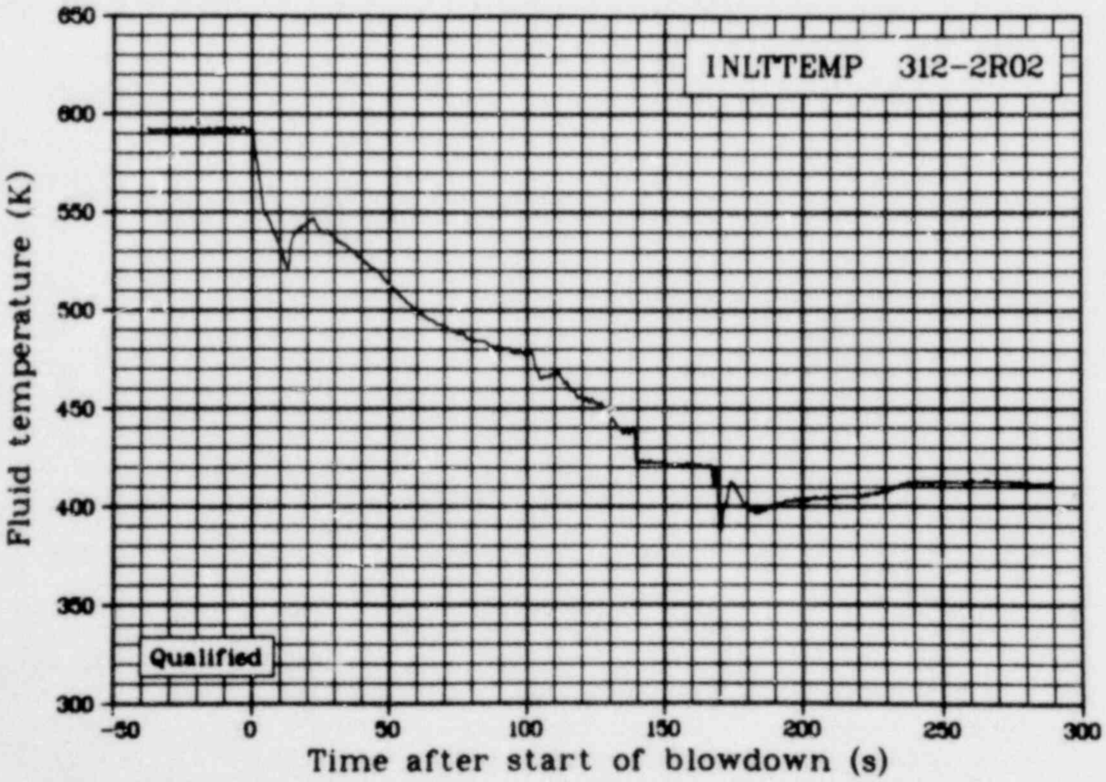

Fig. 55 Fluid temperature of Fuel Rod 312-2 coolant inlet (INLTTEMP 312-2R02), from -50 to 300 s.

1405 108

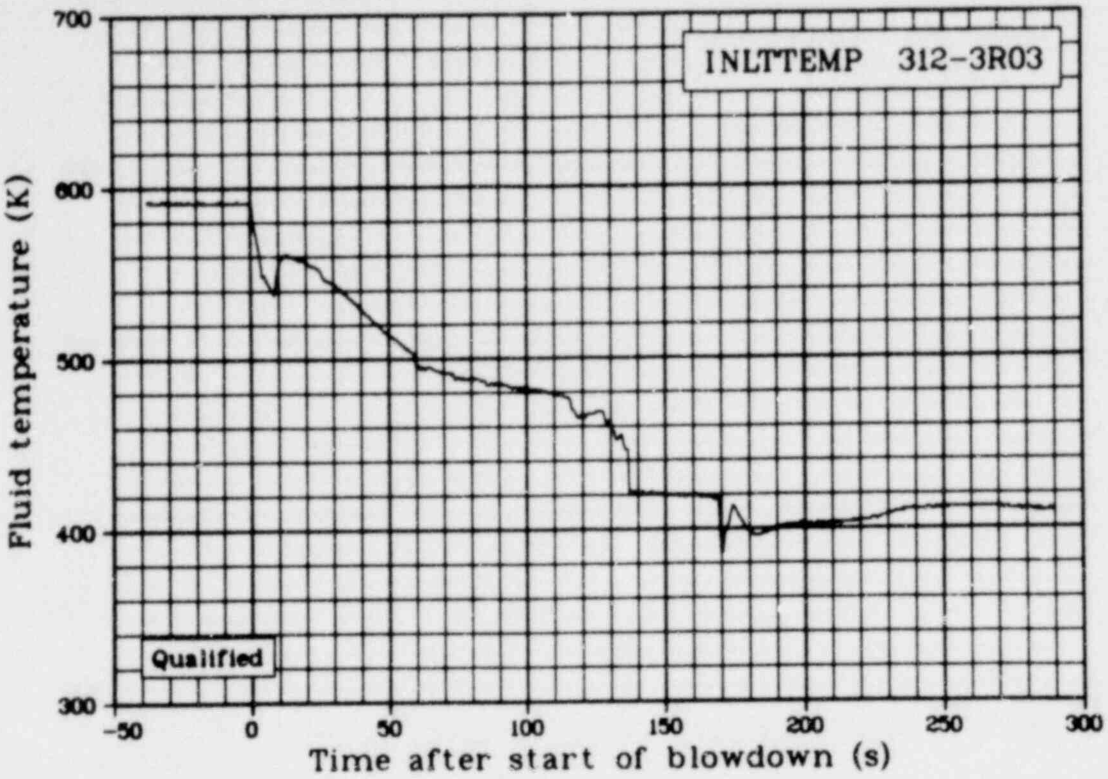

Fig. 56 Fluid temperature of Fuel Rod 312-3 coolant inlet (INLTTEMP 312-3R03), from -50 to 300 s.

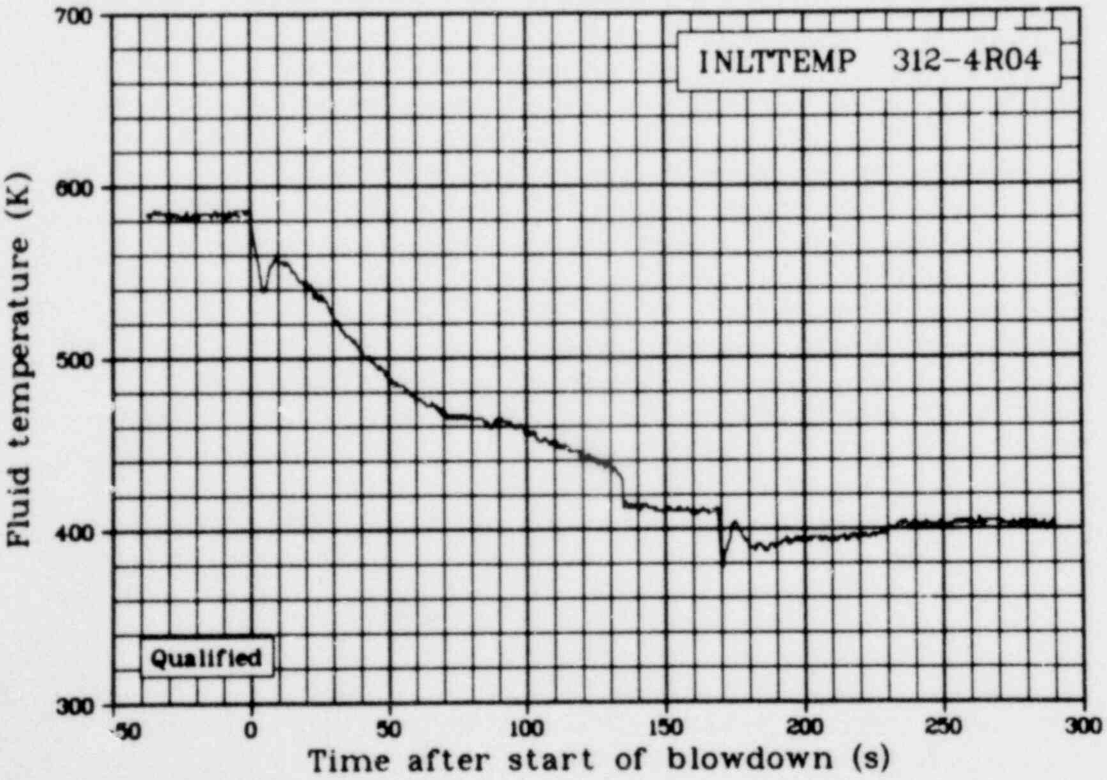

Fig. 57 Fluid temperature of Fuel Rod 312-4 coolant inlet (INLTTEMP 312-4R04), from -50 to 300 s.

1405 109

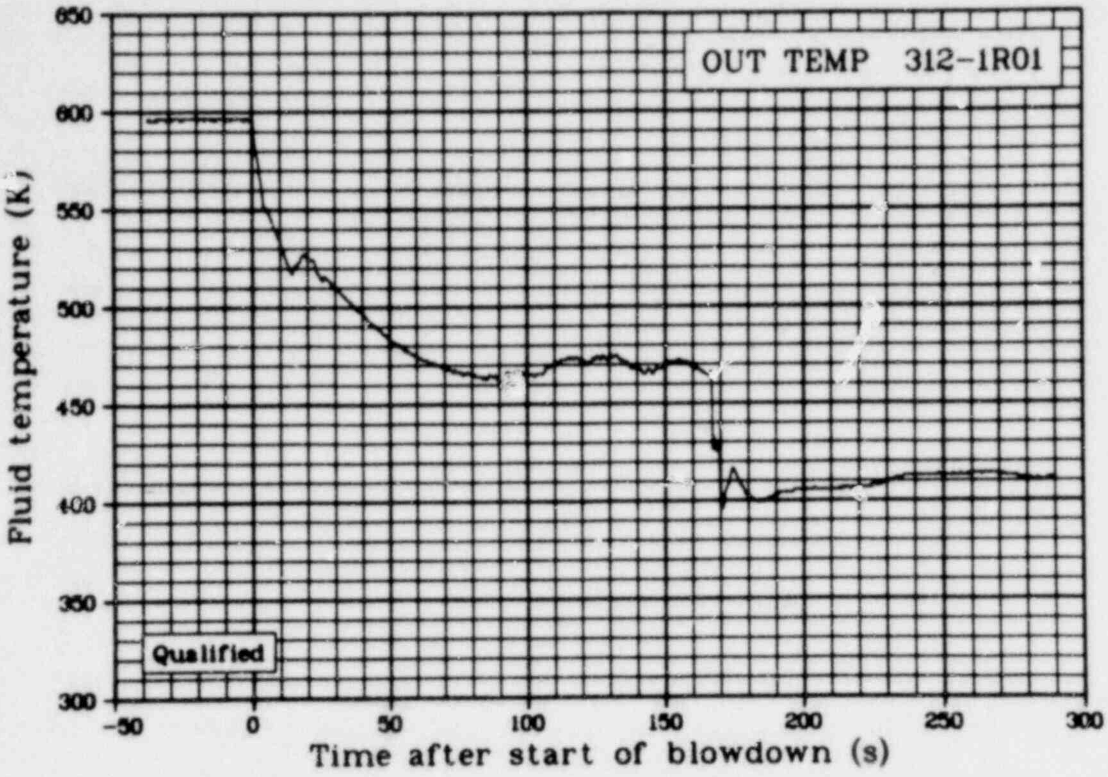

Fig. 58 Fluid temperature of Fuel Rod 312-1 coolant outlet (OUT TEMP 312-1R01), from -50 to 300 s.

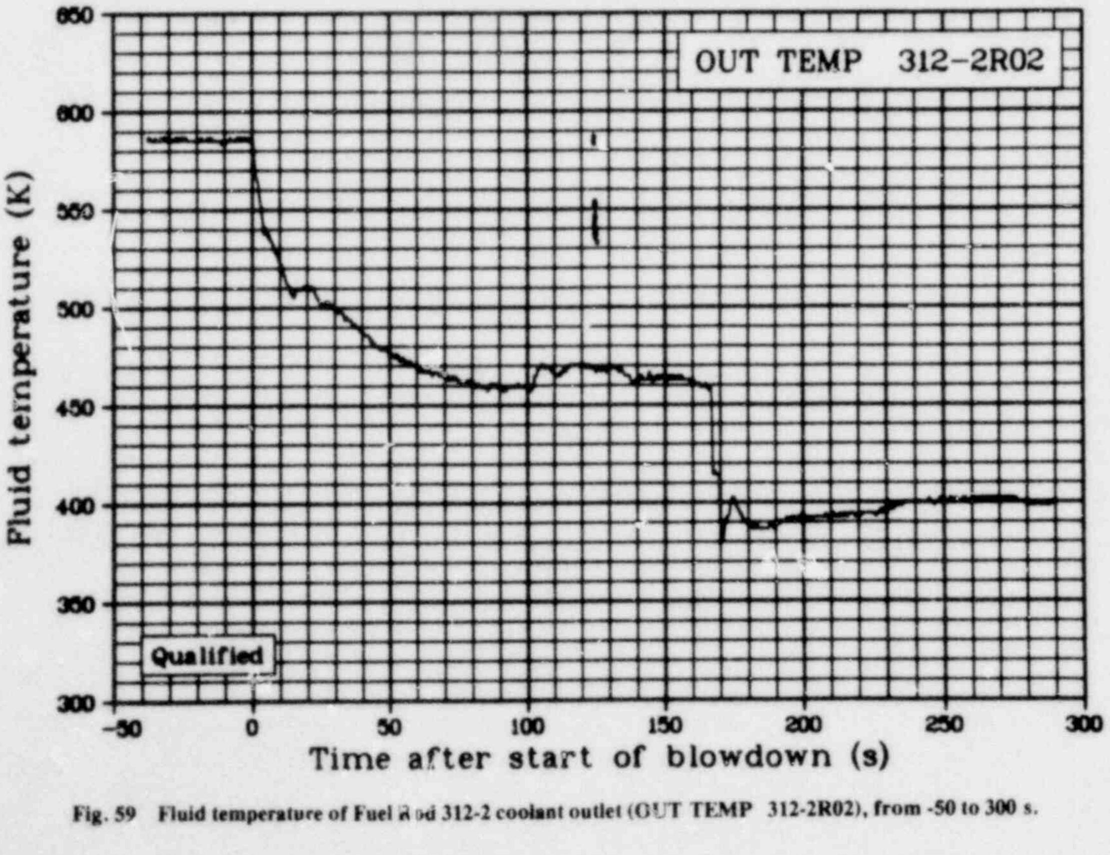

Fig. 59 Fluid temperature of Fuel Rod 312-2 coolant outlet (OUT TEMP 312-2R02), from -50 to 300 s.

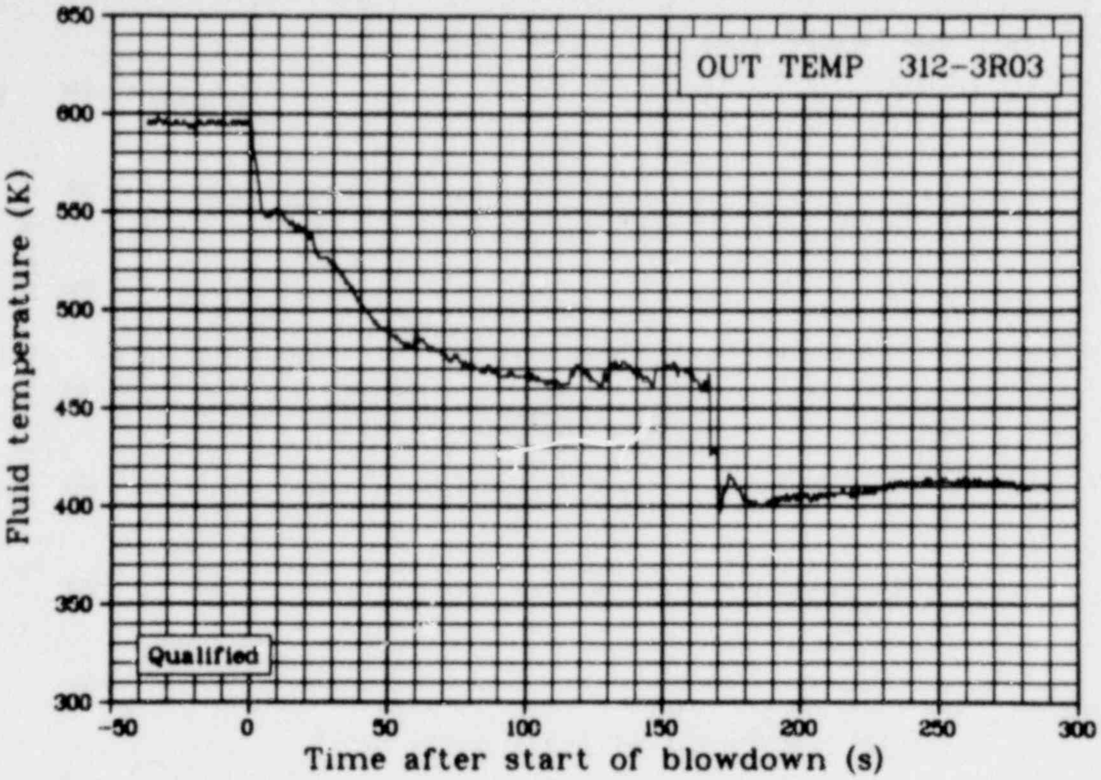

Fig. 60 Fluid temperature of Fuel Rod 312-3 coolant outlet (OUT TEMP 312-3R03), from -50 to 300 s.

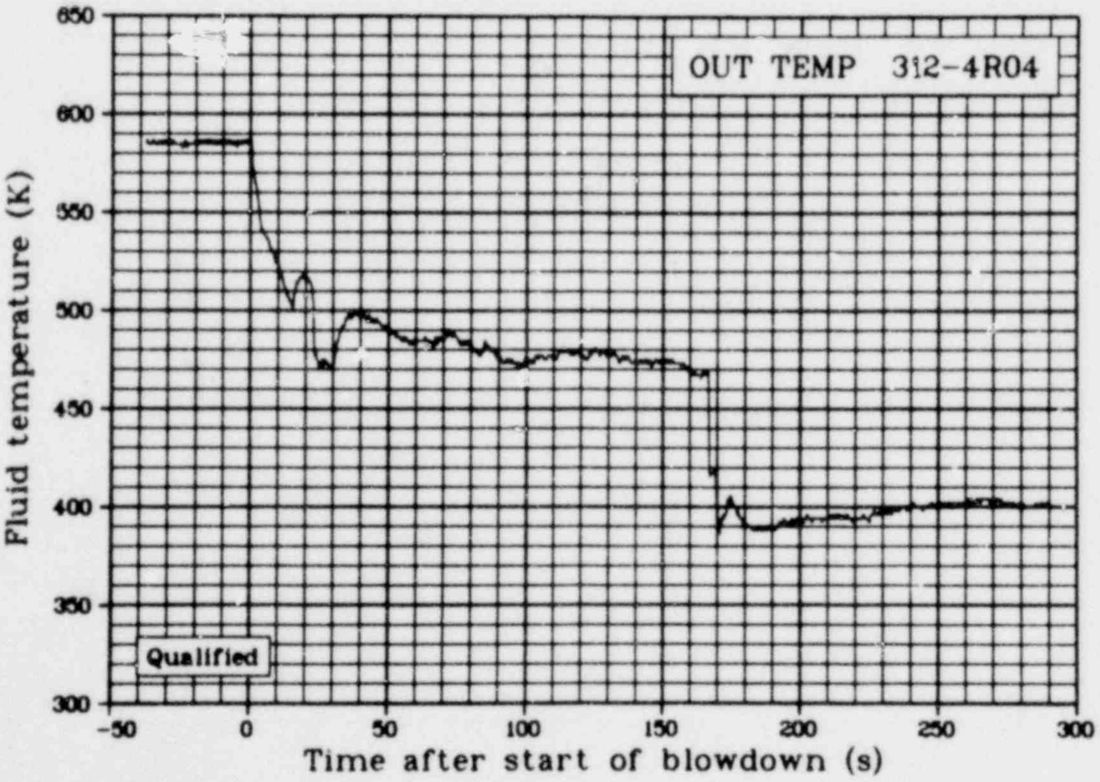

Fig. 61 Fluid temperature of Fuel Rod 312-4 coolant outlet (OUT TEMP 312-4R04), from -50 to 300 s.

1405 111

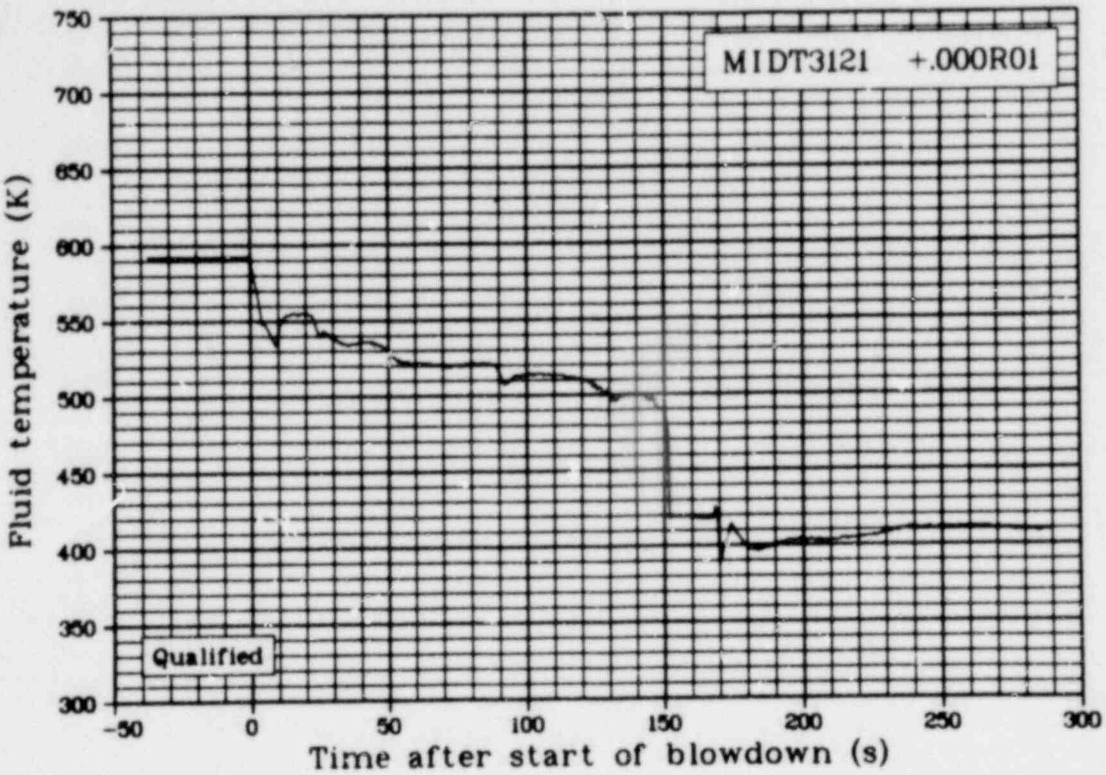

Fig. 62 Fluid temperature of Fuel Rod 312-1, at fuel stack midplane (MIDT3121 + .000R01), from -50 to 300 s.

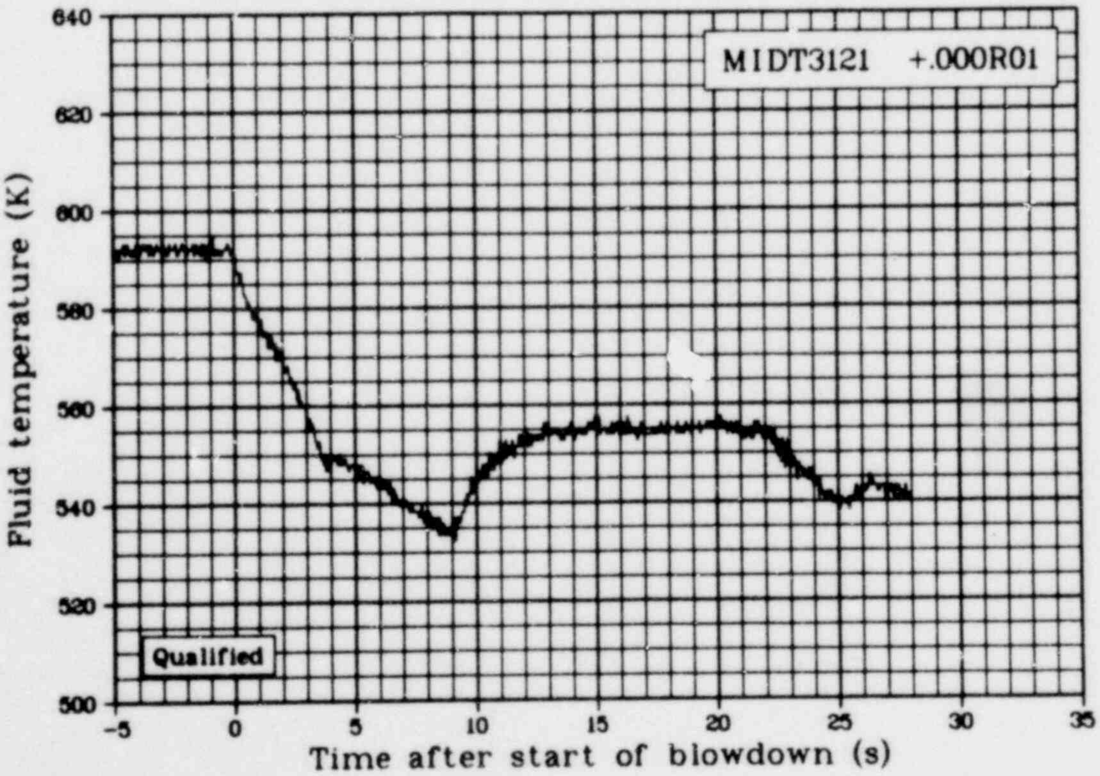

Fig. 63 Fluid temperature of Fuel Rod 312-1, at fuel stack midplane (MIDT3121 + .000R01), from -5 to 35 s.

1405 112

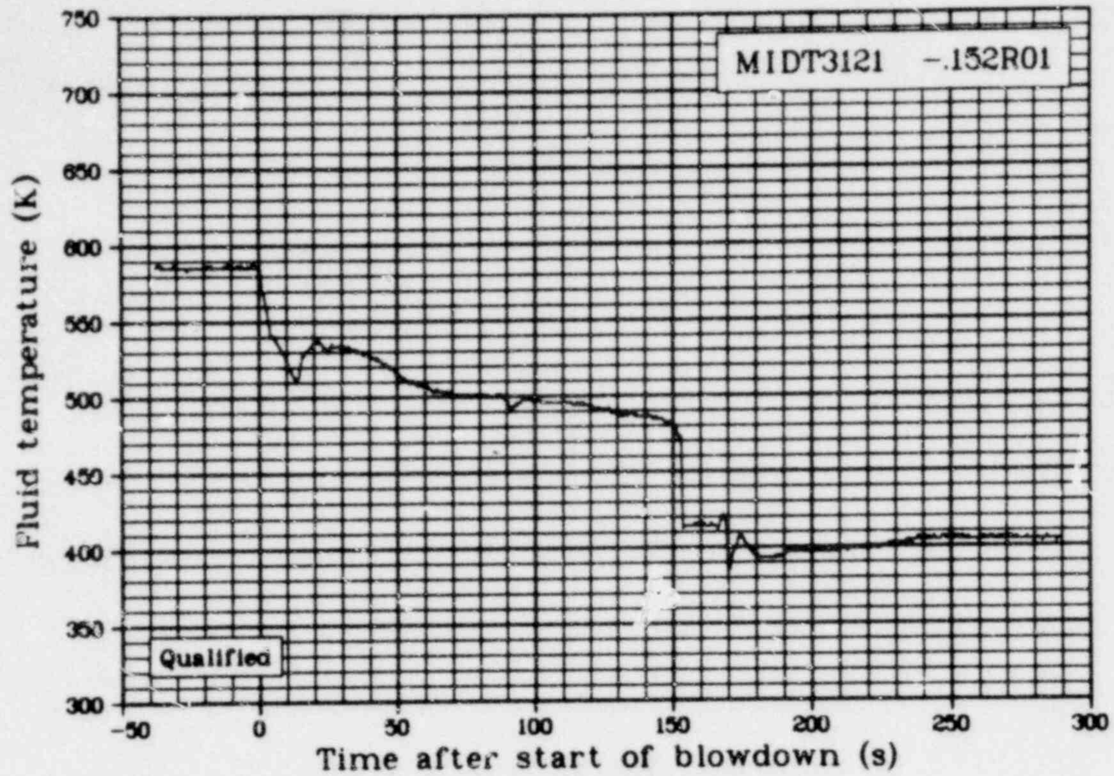

Fig. 64 Fluid temperature of Fuel Rod 312-1, 0.152 m below fuel stack midplane (MIDT3121 -.152R01), from -50 to 300 s.

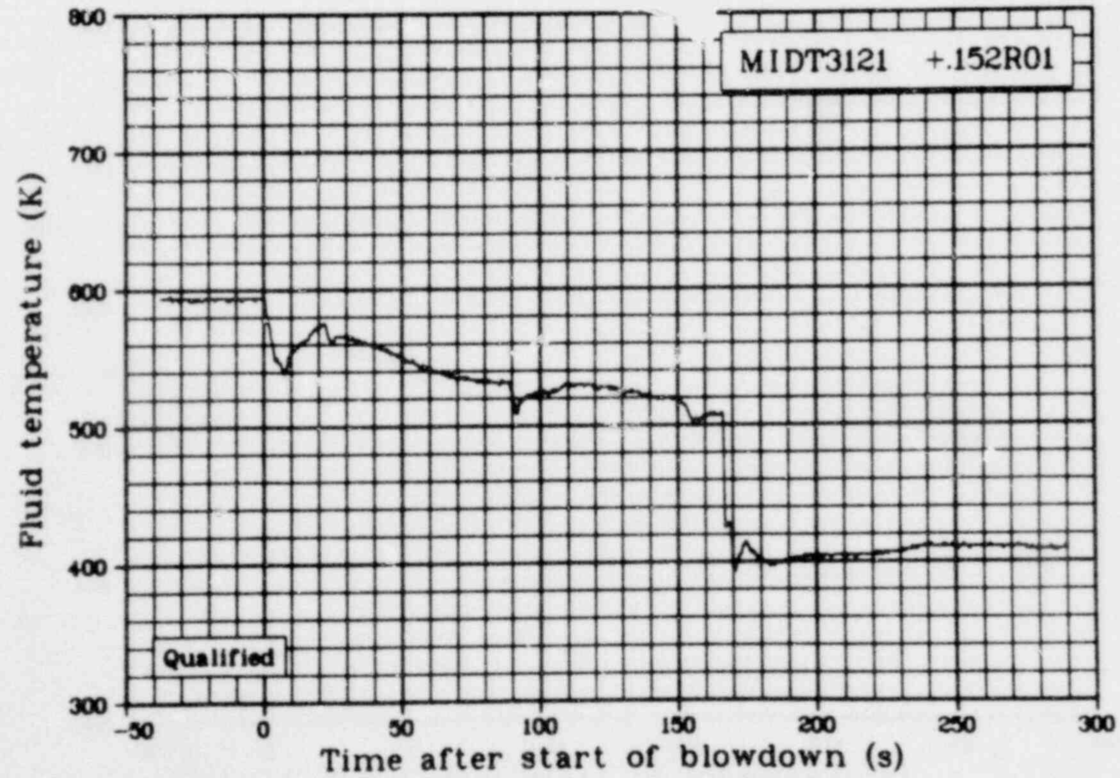

Fig. 65 Fluid temperature of Fuel Rod 312-1, 0.152 m above fuel stack midplane (MIDT3121 +.152R01), from -50 to 300 s.

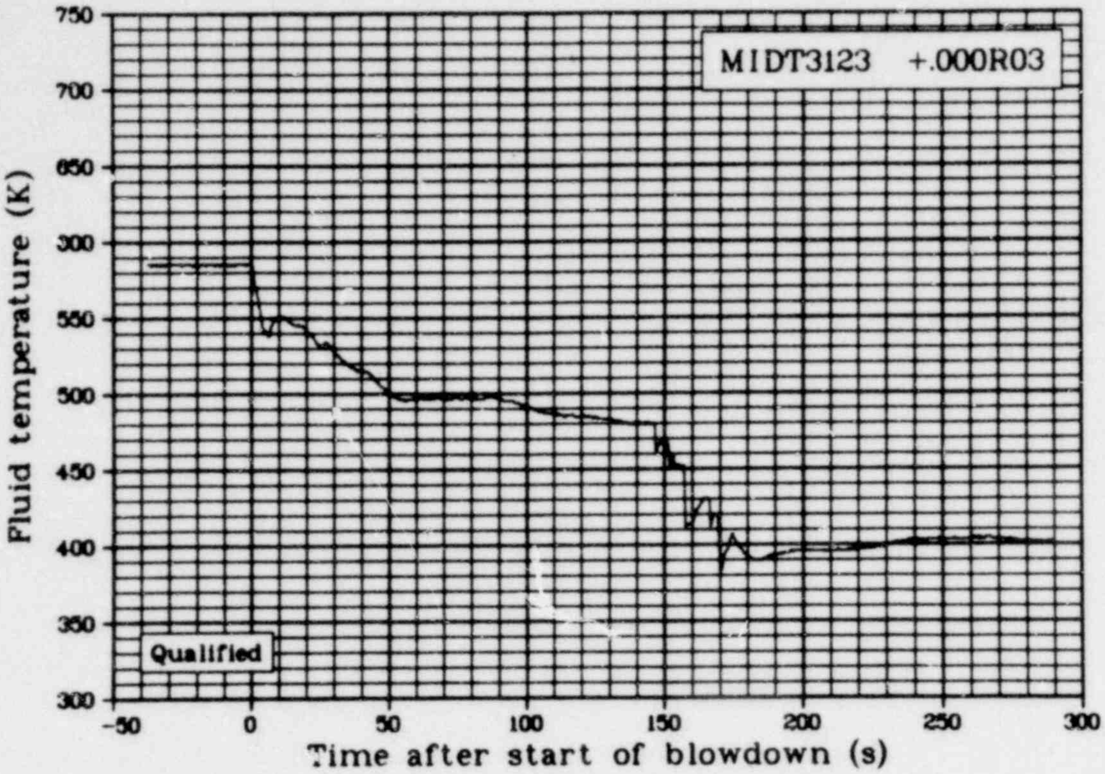

Fig. 66 Fluid temperature of Fuel Rod 312-3, at fuel stack midplane (MIDT3123 +.000R03), from -50 to 300 s.

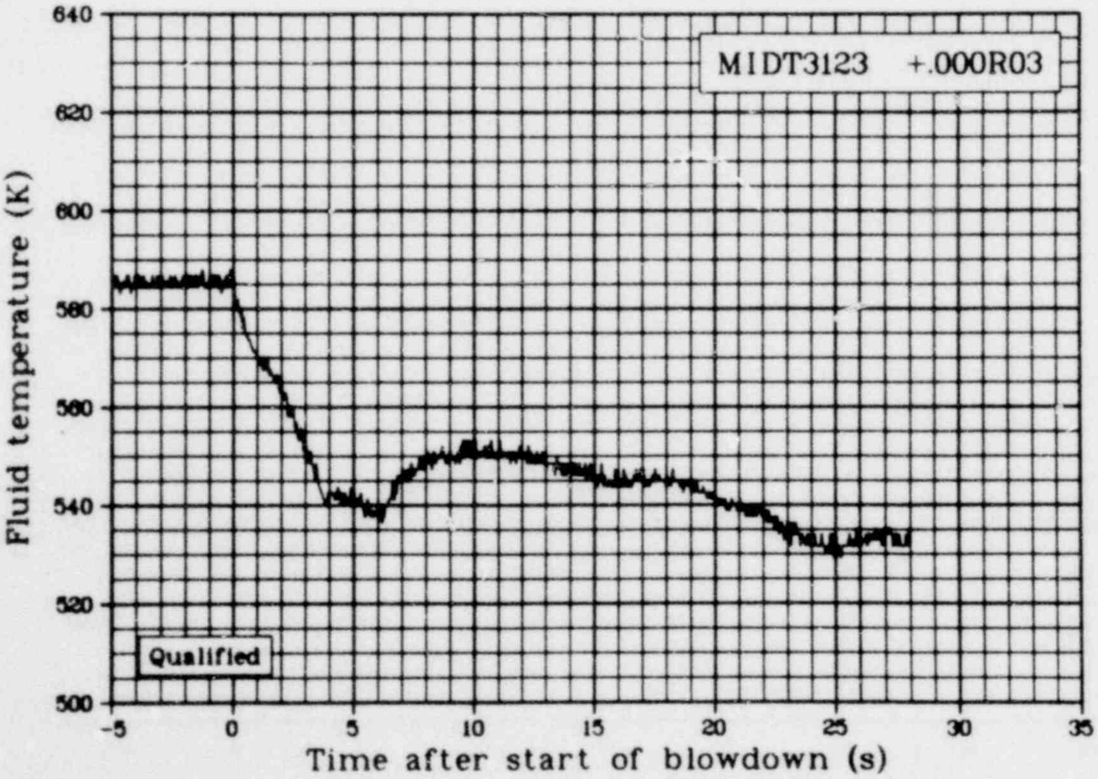

Fig. 67 Fluid temperature of Fuel Rod 312-3, at fuel stack midplane (MIDT3123 +.000R03), from -5 to 35 s.

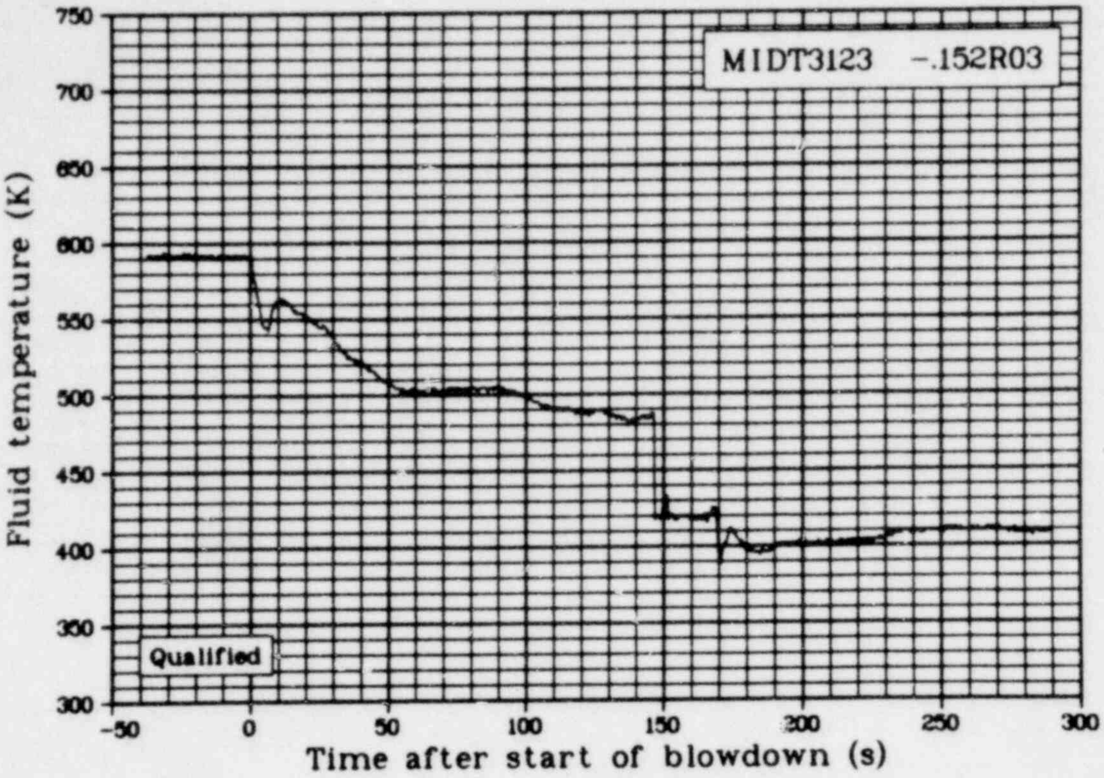

Fig. 68 Fluid temperature of Fuel Rod 312-3, 0.152 m below fuel stack midplane (MIDT3123 .-152R03), from -50 to 300 s.

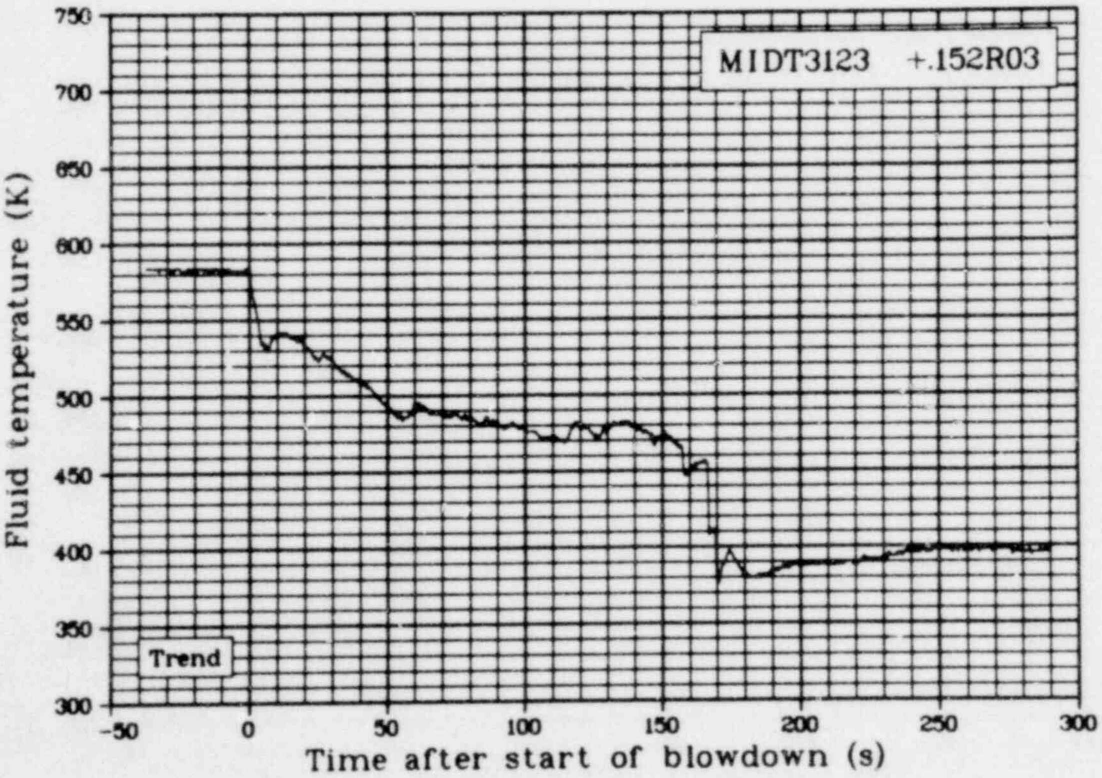

Fig. 69 Fluid temperature of Fuel Rod 312-3, 0.152 m above fuel stack midplane (MIDT3123 .152R03), from -50 to 300 s.

1405 115

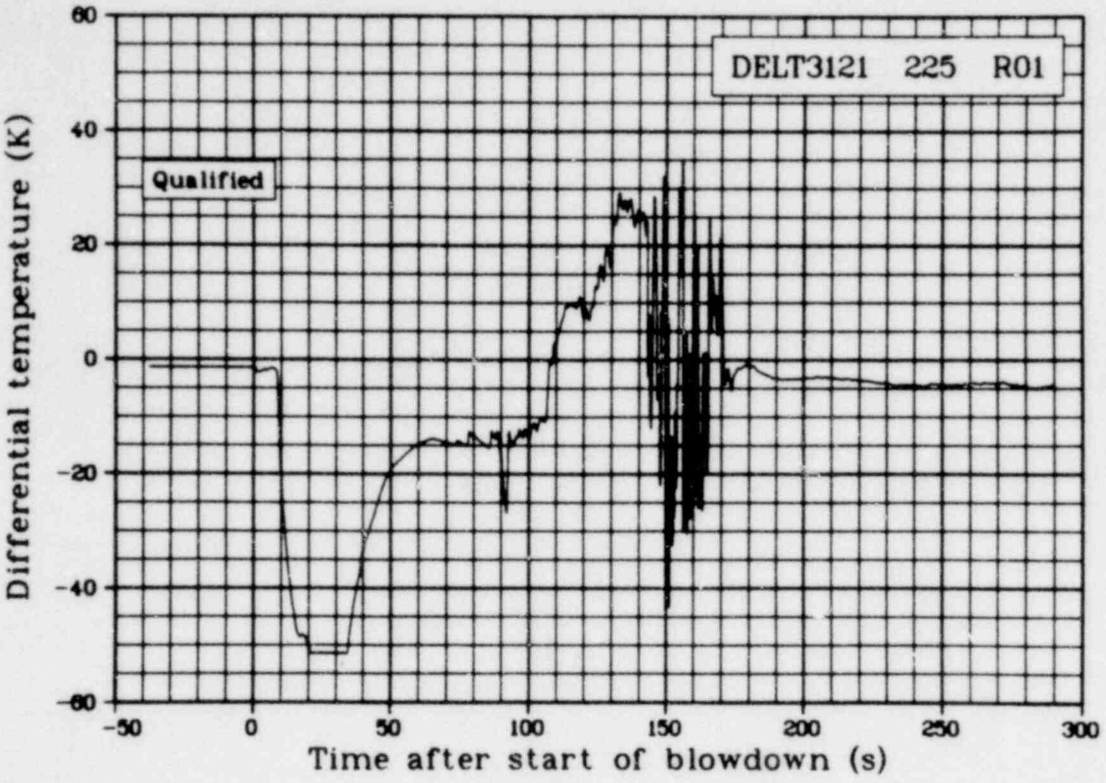

Fig. 70 Differential temperature of Rod 312-1 coolant inlet and outlet (DELT3121 225 R01), from -50 to 300 s.

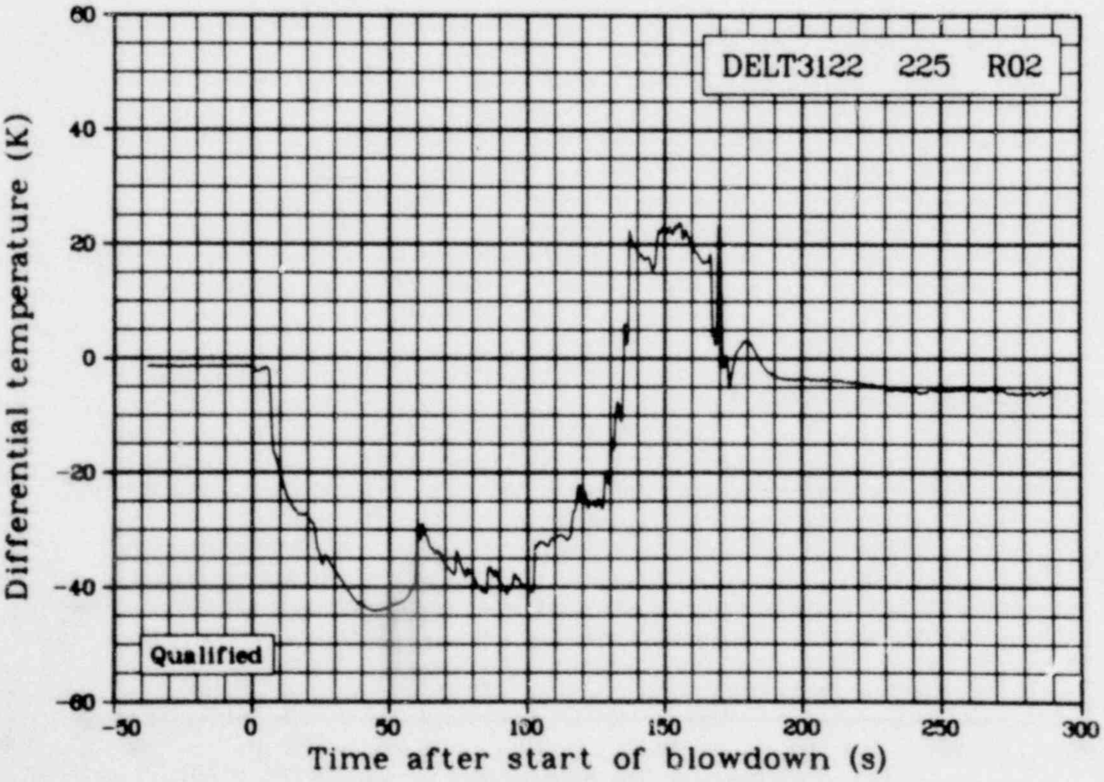

Fig. 71 Differential temperature of Rod 312-2 coolant inlet and outlet (DELT3122 225 R02), from -50 to 300 s.

1405 116

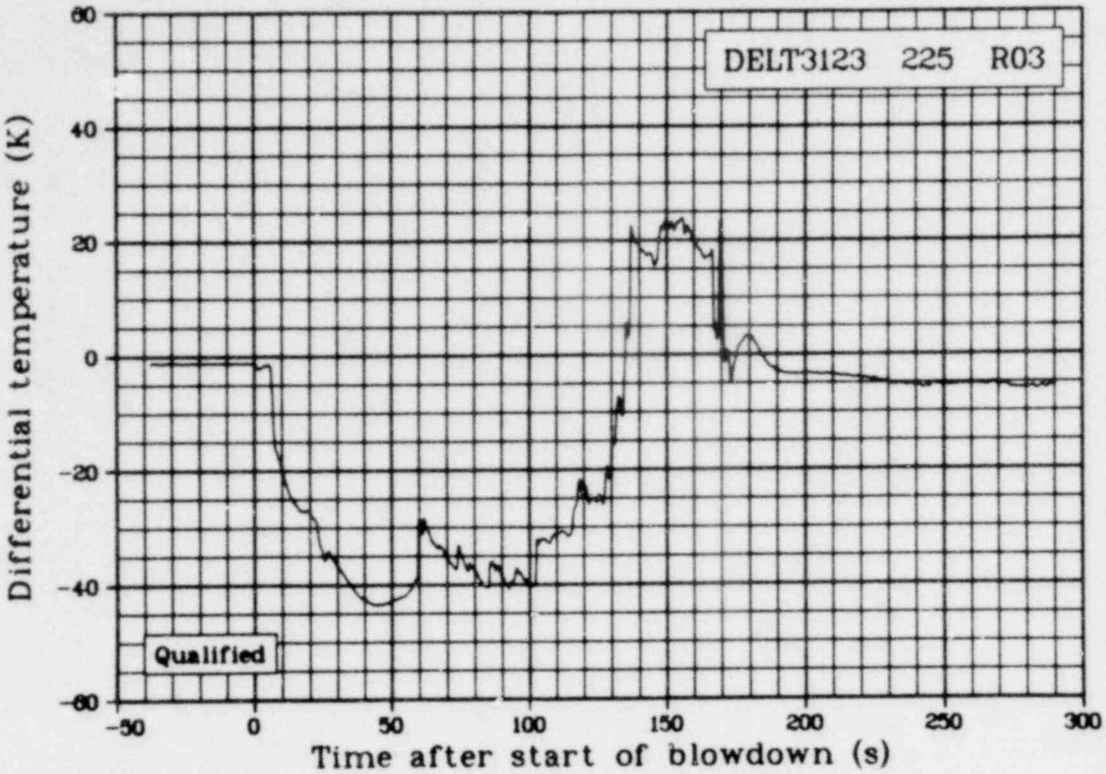

Fig. 72 Differential temperature of Rod 312-3 coolant inlet and outlet (DELT3123 225 R03), from -50 to 300 s.

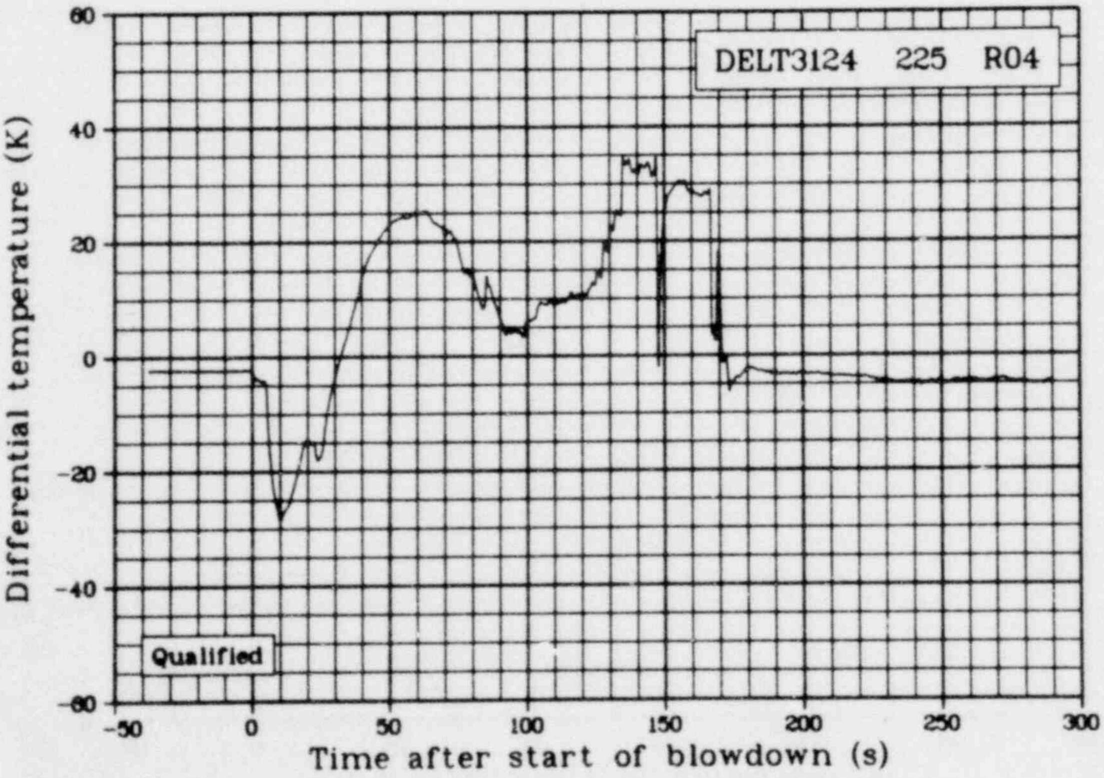

Fig. 73 Differential temperature of Rod 312-4 coolant inlet and outlet (DELT3124 225 R04), from -50 to 300 s.

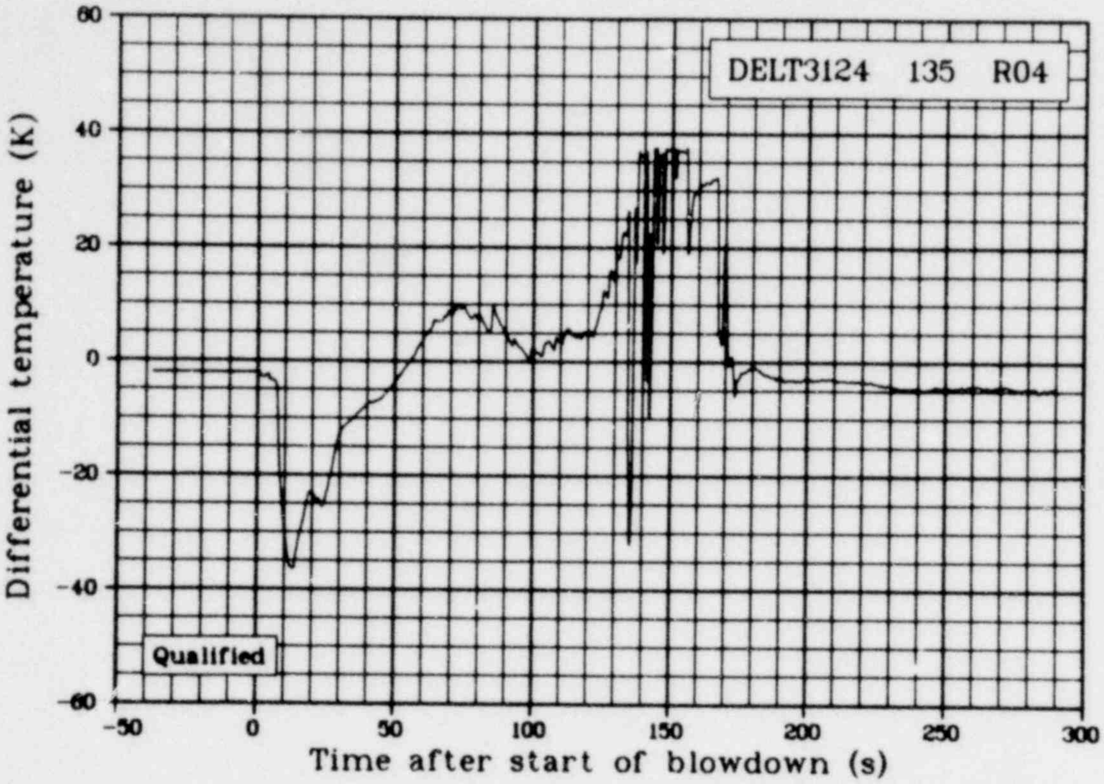

Fig. 74 Differential temperature of Rod 312-4, at 135 degrees, coolant inlet and outlet (DELT3124 135 R04), from -50 to 300 s.

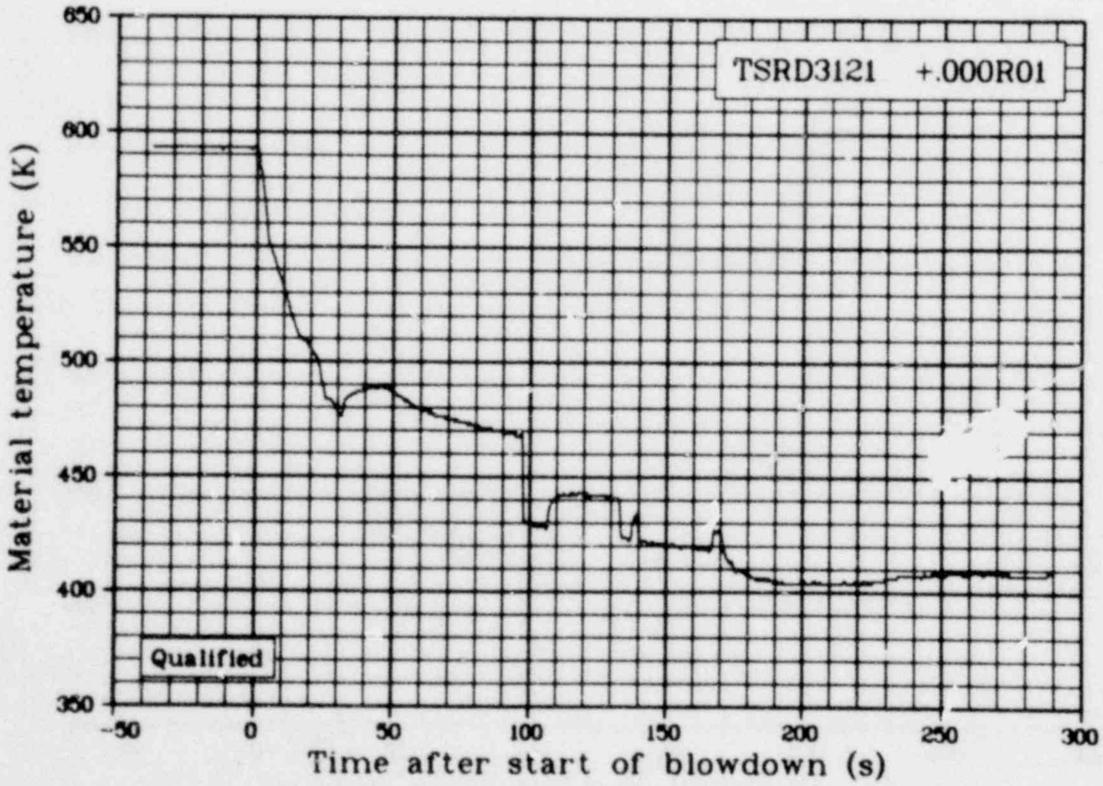

Fig. 75 Material temperature Rod 312-1 shroud, at fuel stack midplane (TSRD3121 + .000R01), from -50 to 300 s.

1405 118

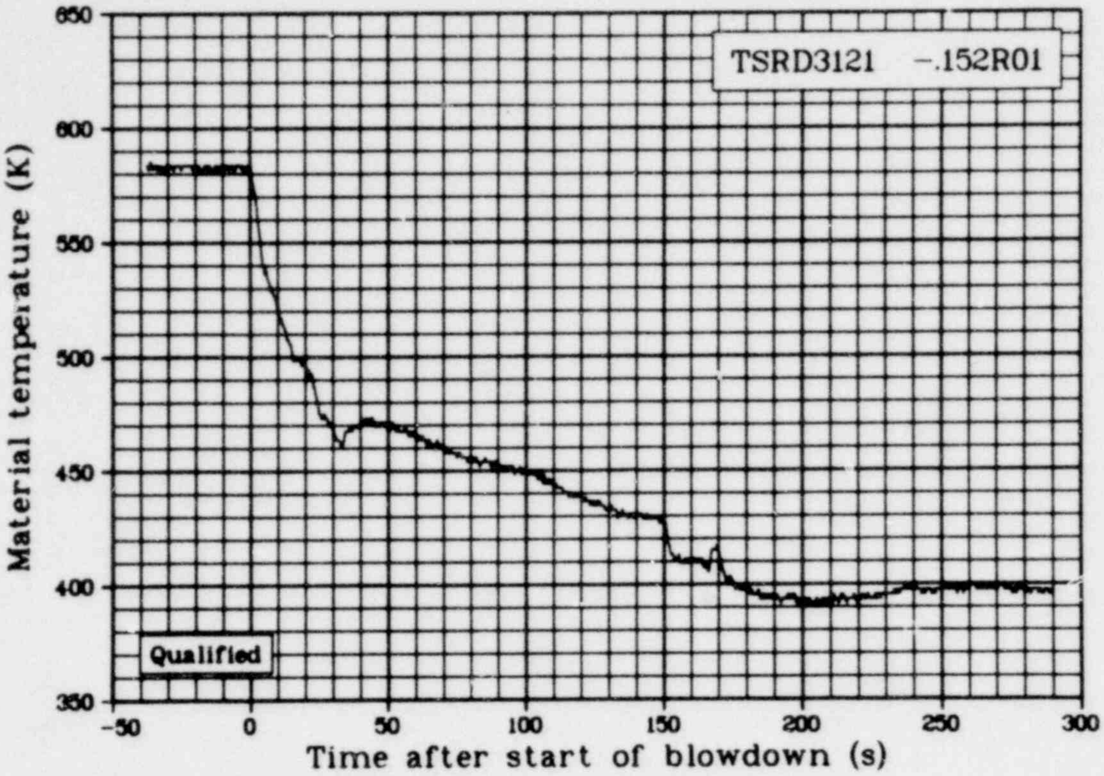

Fig. 76 Material temperature Rod 312-1 shroud, 0.152 m below fuel stack midplane (TSRD3121 -.152R01), from -50 to 300 s.

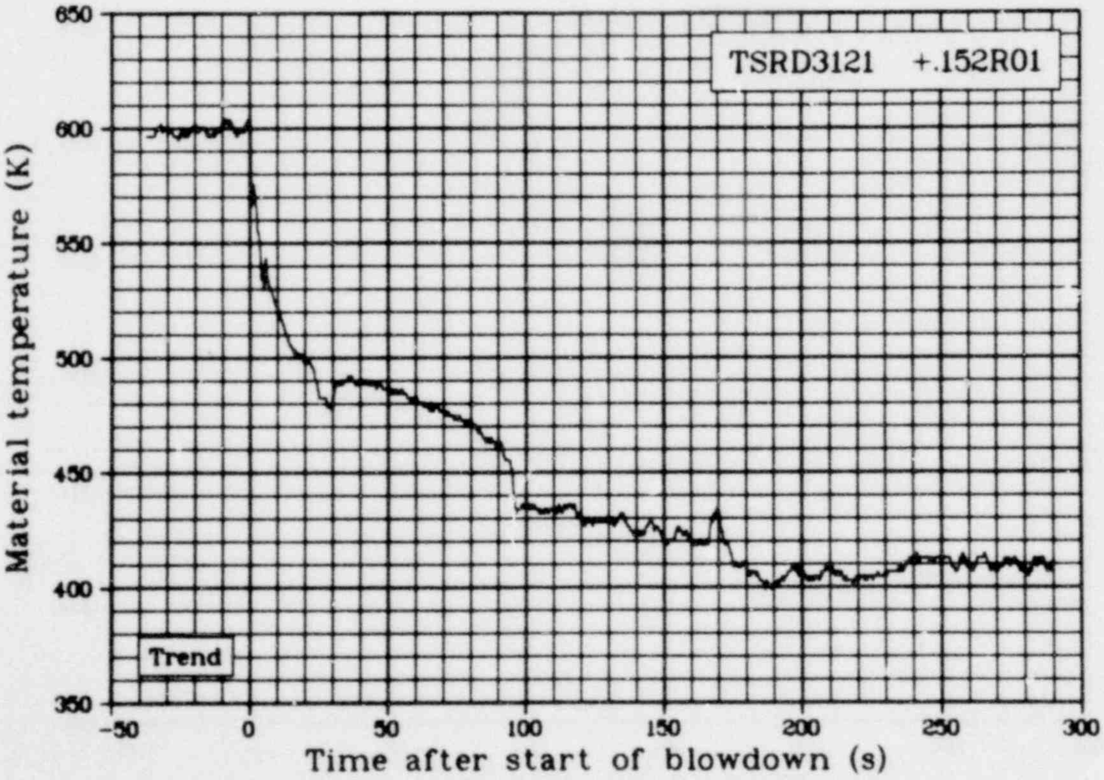

Fig. 77 Material temperature Rod 312-1 shroud, 0.152 m above fuel stack midplane (TSRD3121 +.152R01), from -50 to 300 s.

1405 119

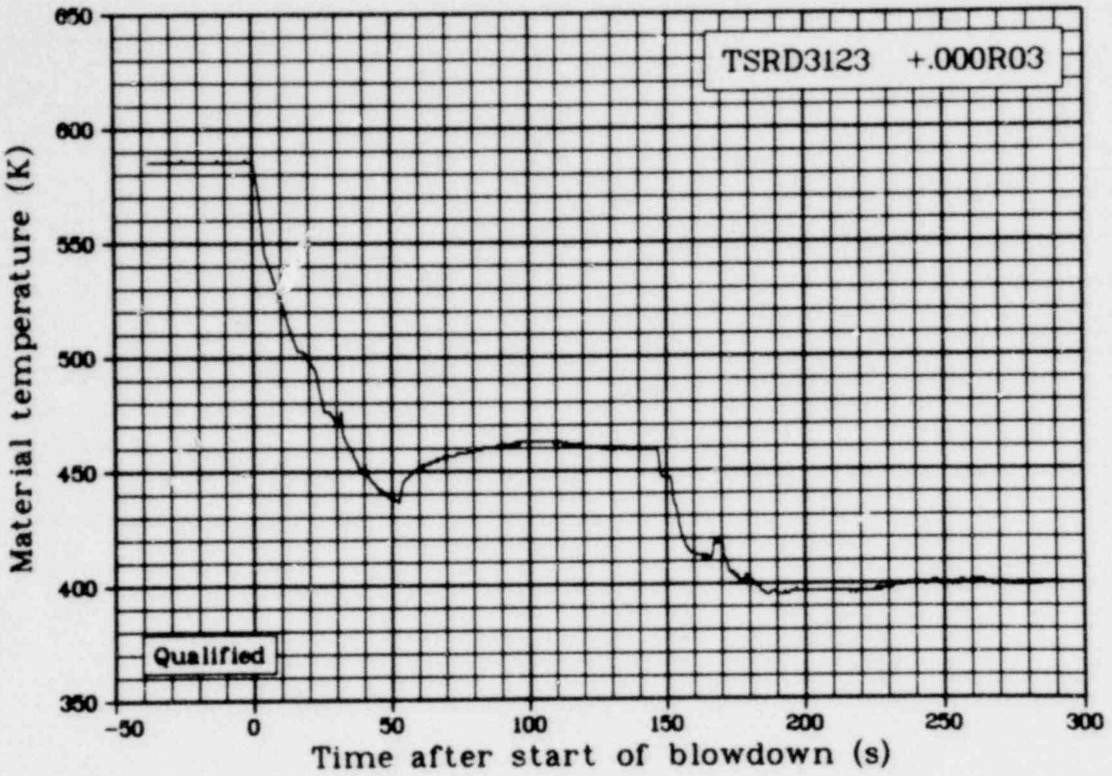

Fig. 78 Material temperature Rod 312-3 shroud, at fuel stack midplane (TSRD3123 + .000R03), from -50 to 300 s.

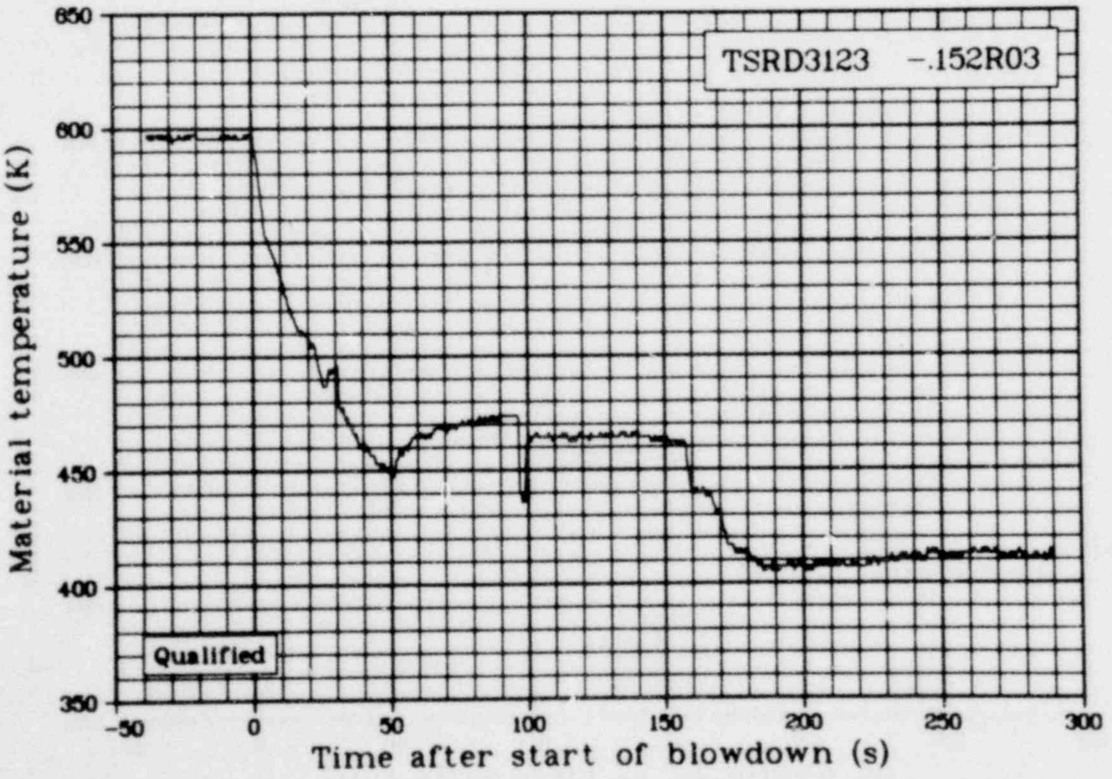

Fig. 79 Material temperature Rod 312-3 shroud, 0.152 m below fuel stack midplane (TSRD3123 -.152R03), from -50 to 300 s.

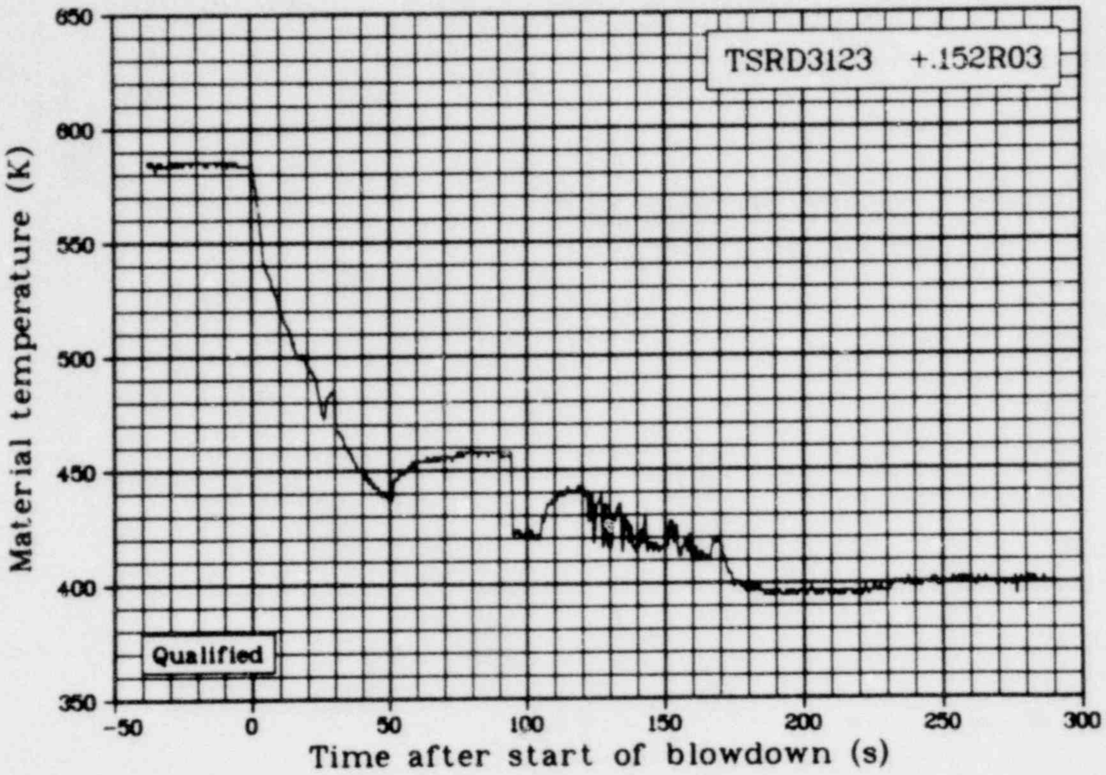

Fig. 80 Material temperature Rod 312-3 shroud, 0.152 m above fuel stack midplane (TSRD3123 +.152R03), from -50 to 300 s.

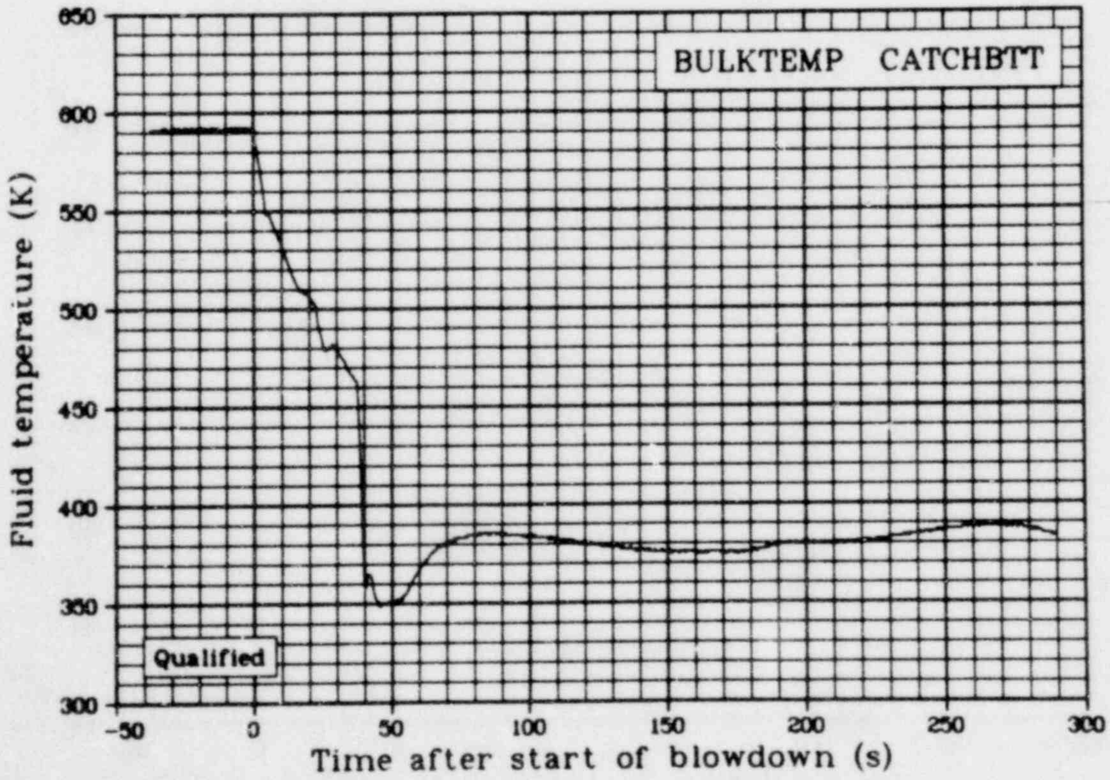

Fig. 81 Fluid temperature in test train catch basket (BULKTEMP CATCHBTT), from -50 to 300 s.

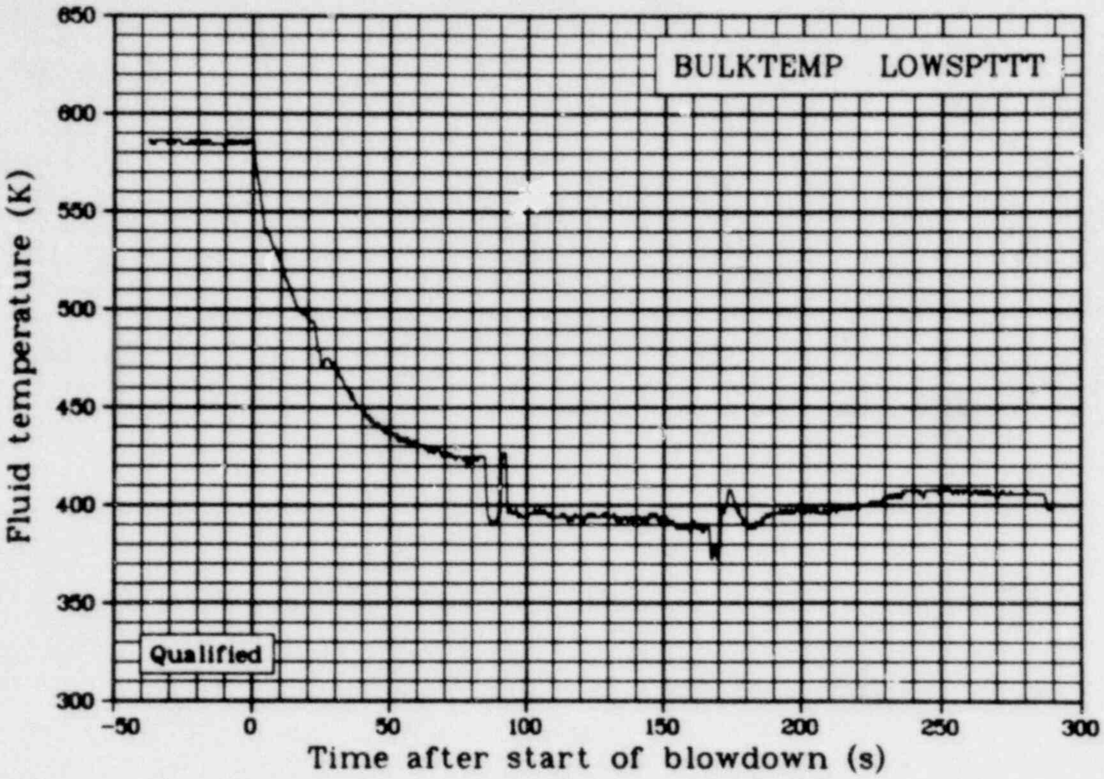

Fig. 82 Fluid temperature below test train lower support plate (BULKTEMP LOWSPTTT), from -50 to 300 s.

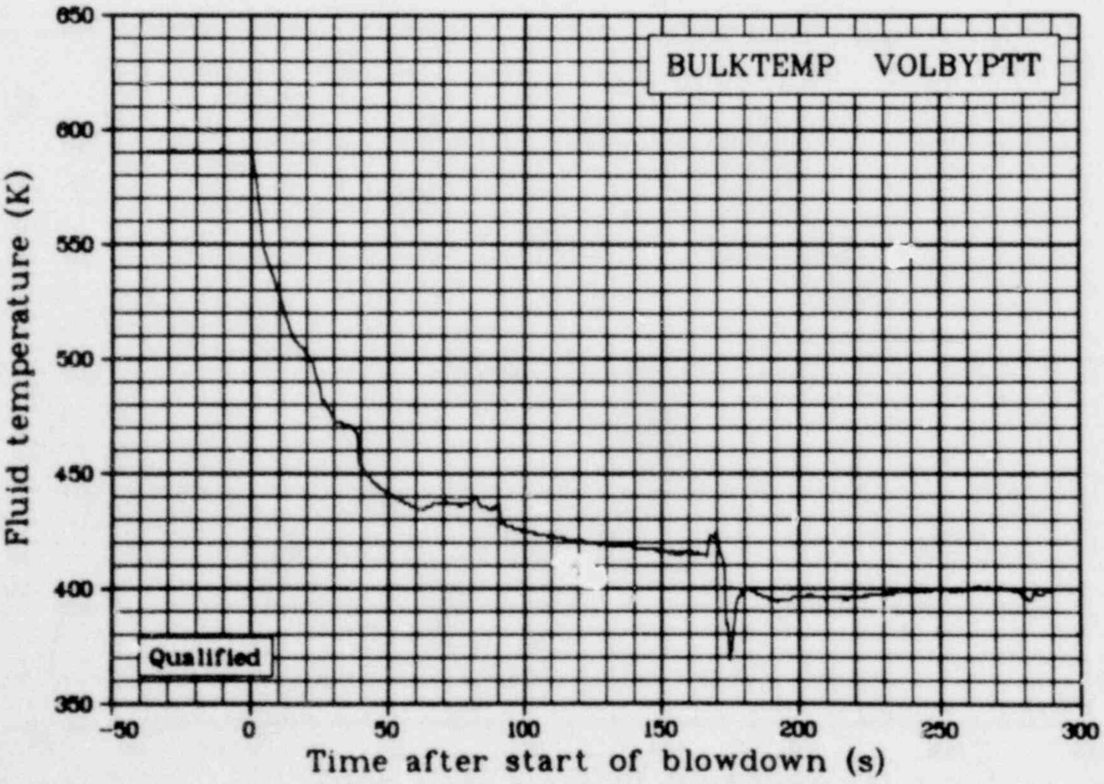

Fig. 83 Fluid temperature in bypass volume at fuel stack midplane (BULKTEMP VOLBYPTT), from -50 to 300 s.

1405 122

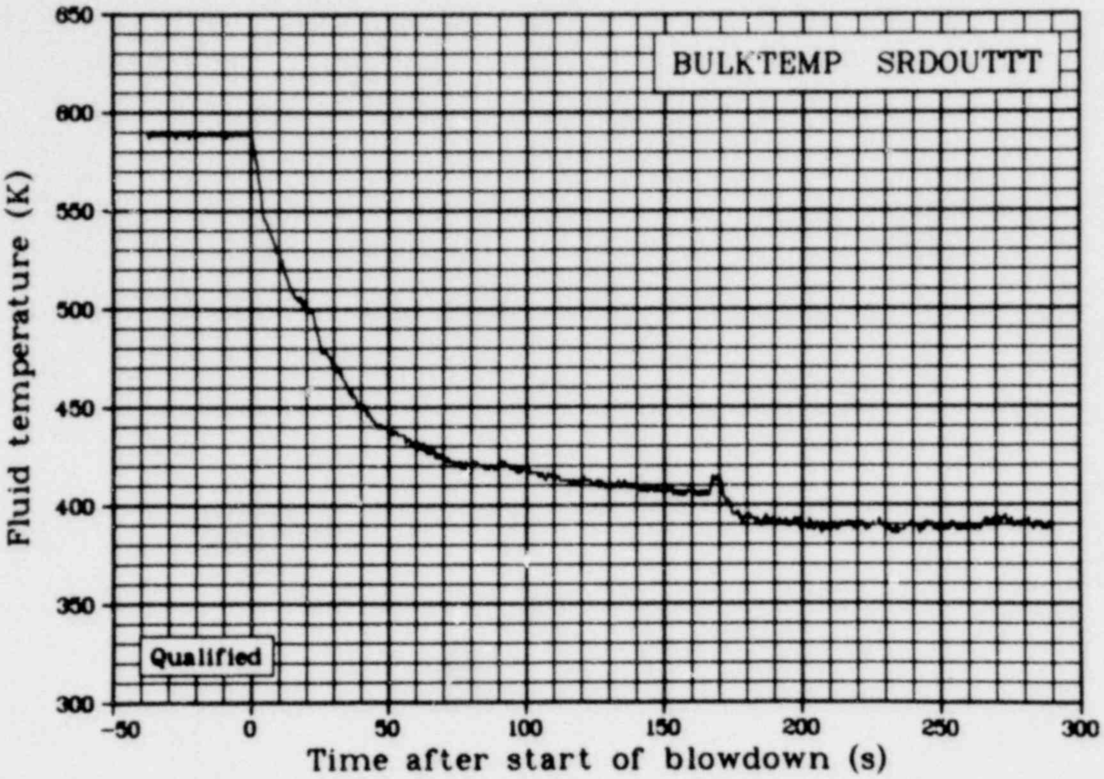

Fig. 84 Fluid temperature 0.05 m above flow shroud outlets (BULKTEMP SRDOUTTT), from -50 to 300 s.

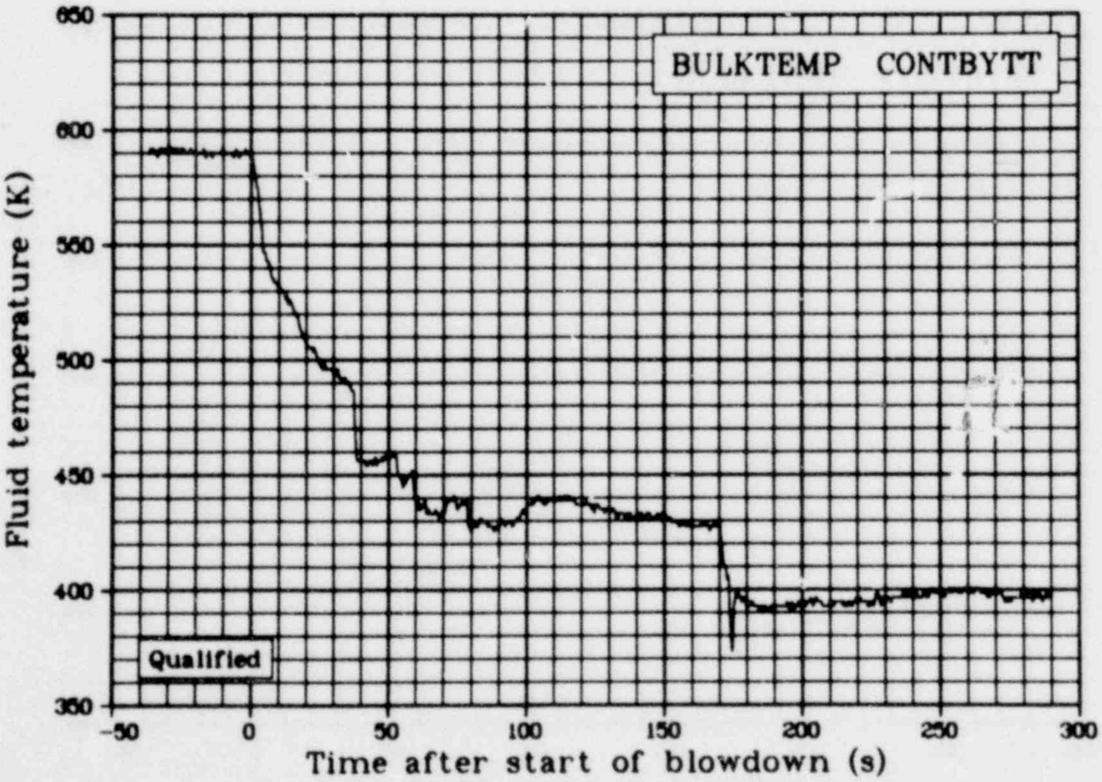

Fig. 85 Fluid temperature at test train controlled bypass inlet (BULKTEMP CONTBYTT), from -50 to 300 s.

1405 123

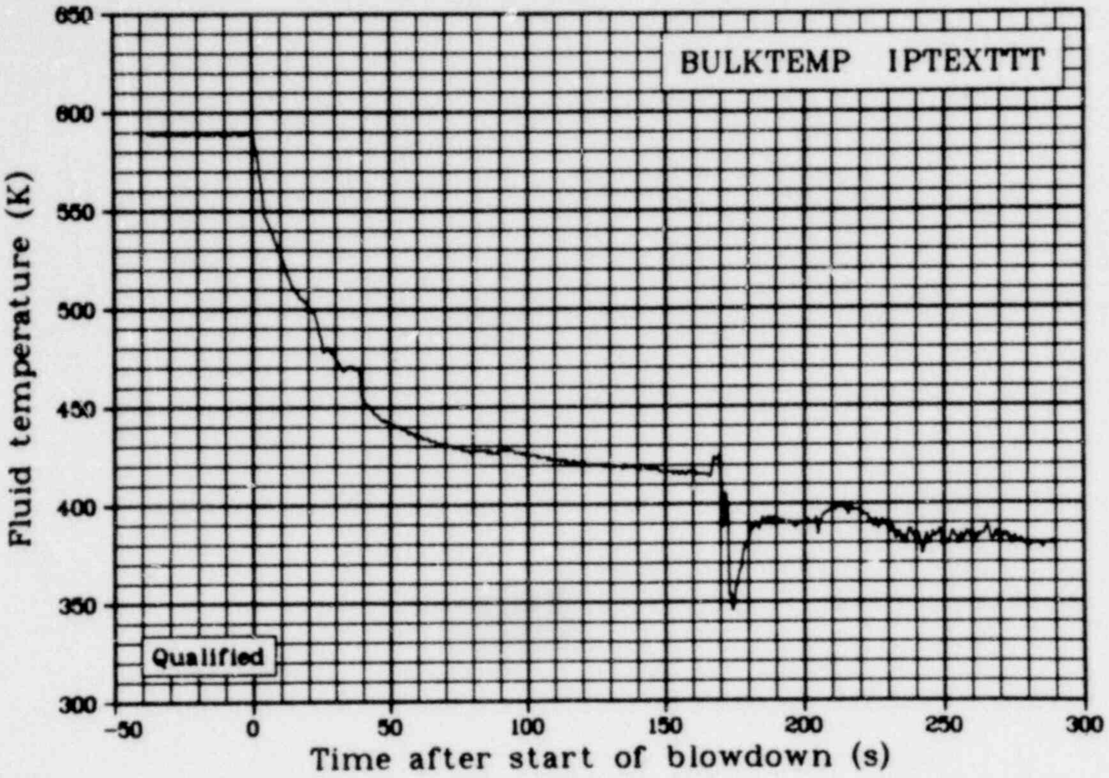

Fig. 86 Fluid temperature at IPT exit (BULKTEMP IPTEXTTT), from -50 to 300 s.

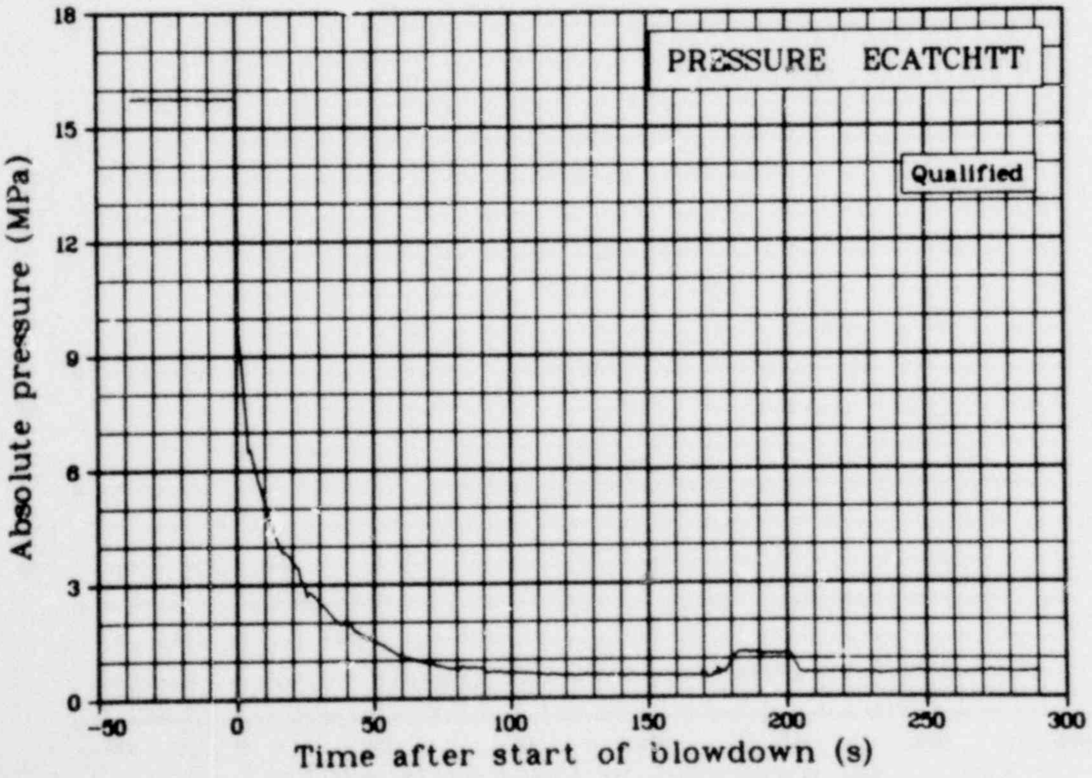

Fig. 87 Absolute pressure in test train catch basket (BULKTEMP ECATCHTT), from -50 to 300 s.

1405 124

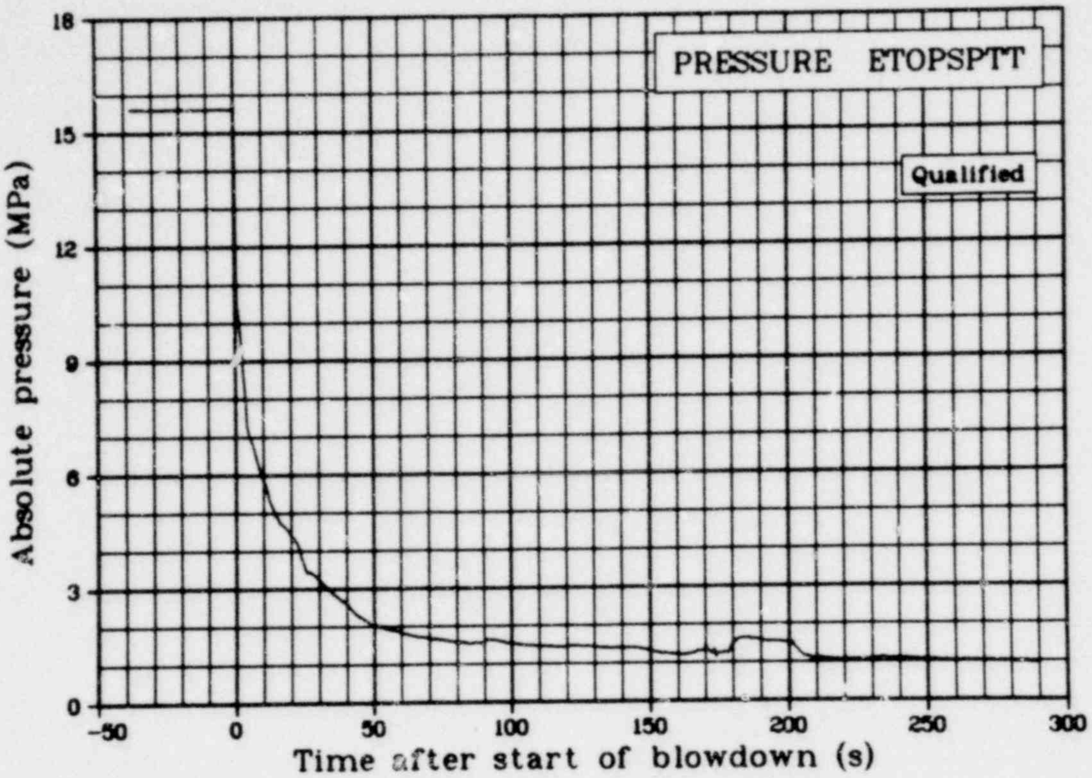

Fig. 88 Absolute pressure above test train top support plate (PRESSURE ETOPSPTT), from -50 to 300 s.

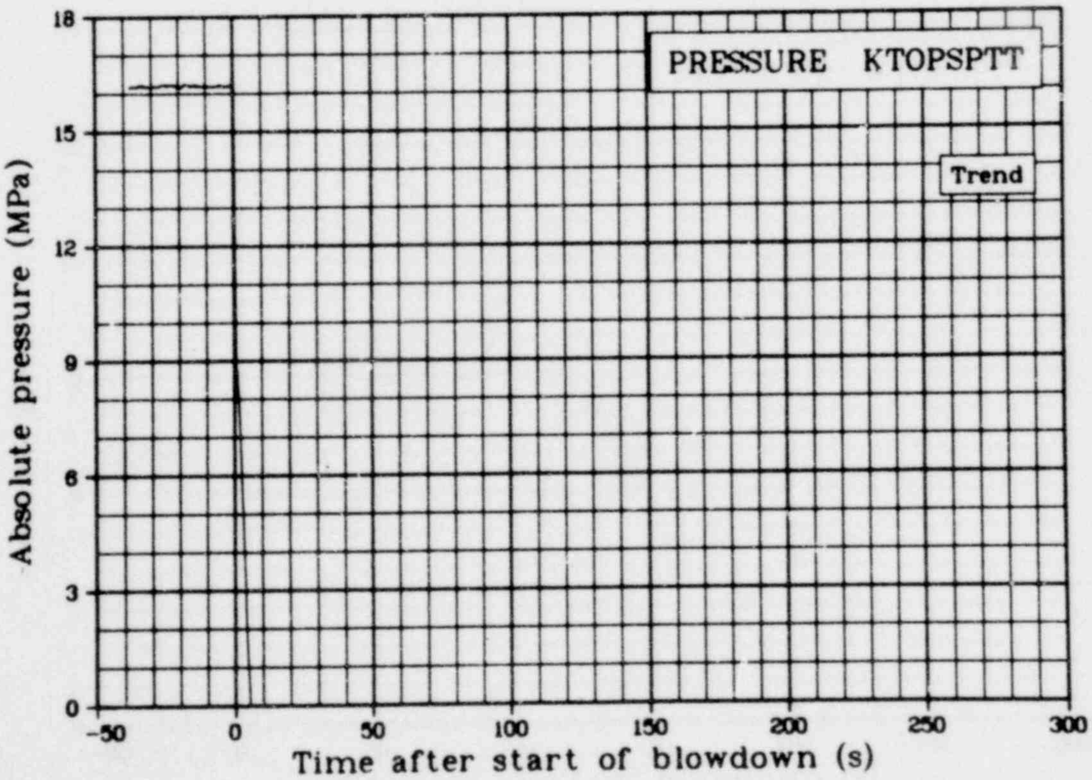

Fig. 89 Absolute pressure above test train top support plate (PRESSURE KTOPSPTT), from -50 to 300 s.

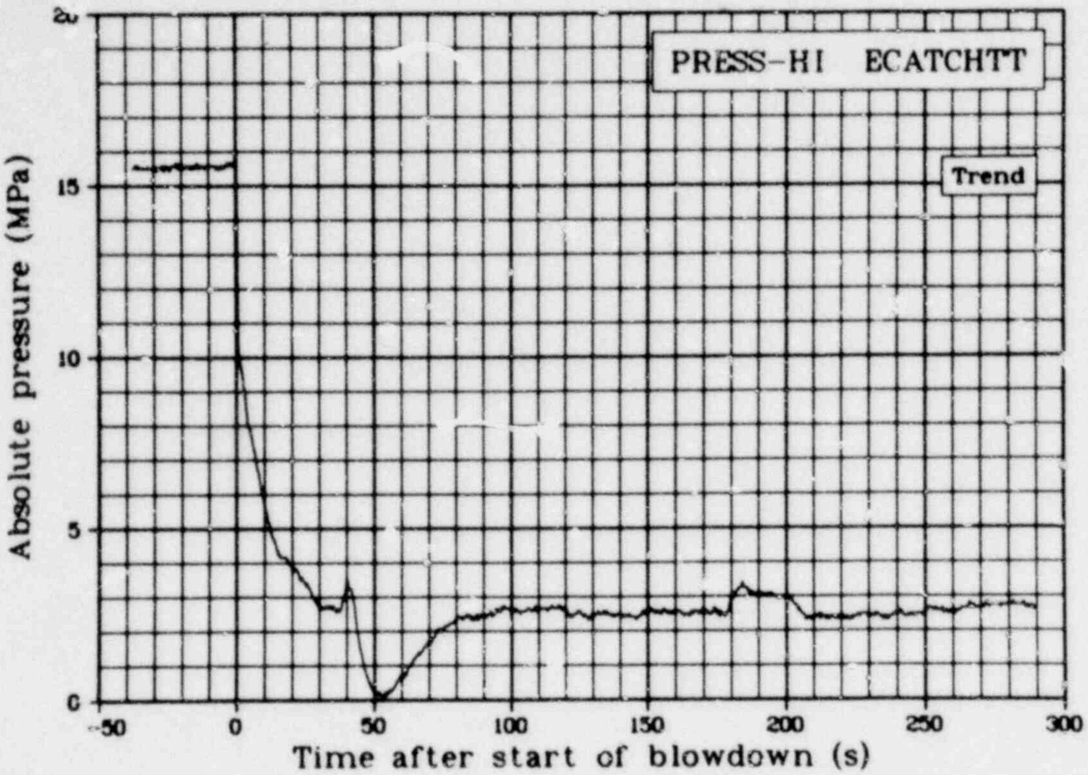

Fig. 90 Absolute pressure in test train catch baske. (PRESS-HI ECATCHTT), from -50 to 300 s.

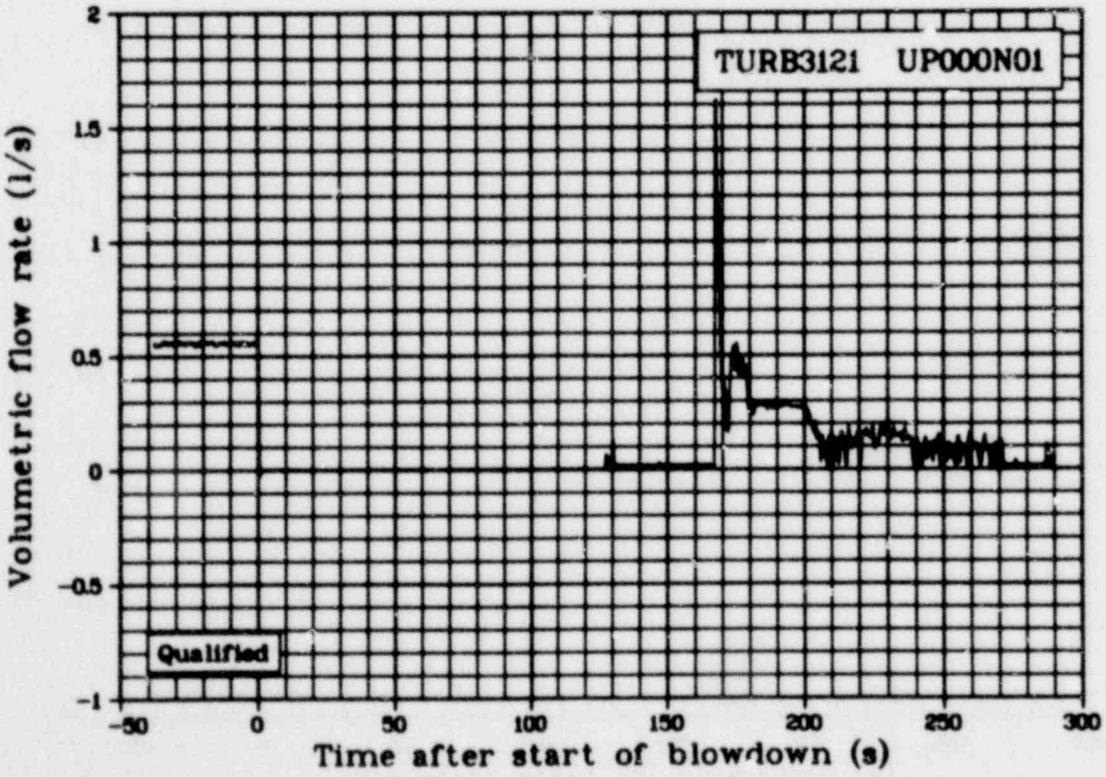

Fig. 91 Volumetric flow rate in Fuel Rod 312-1 upper shroud (TURB3121 UP000N01), from -50 to 300 s.

1405 126

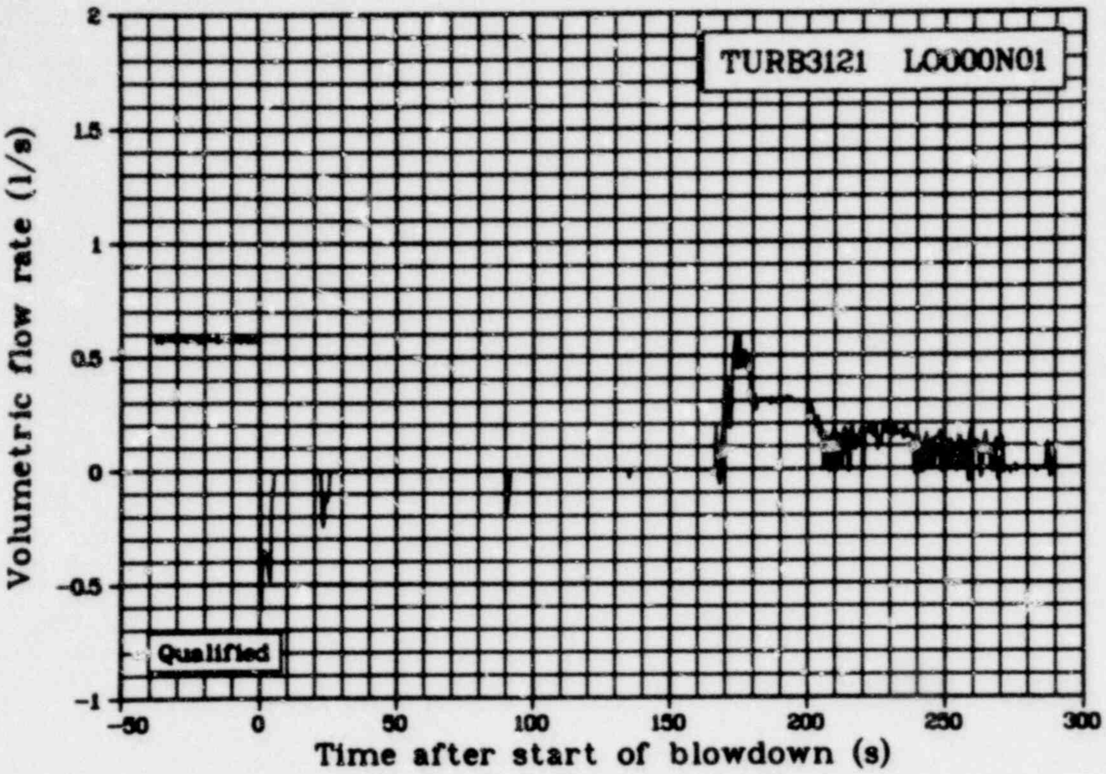

Fig. 92 Volumetric flow rate in Fuel Rod 312-1 lower shroud (TURB3121 L0000N01), from -50 to 300 s.

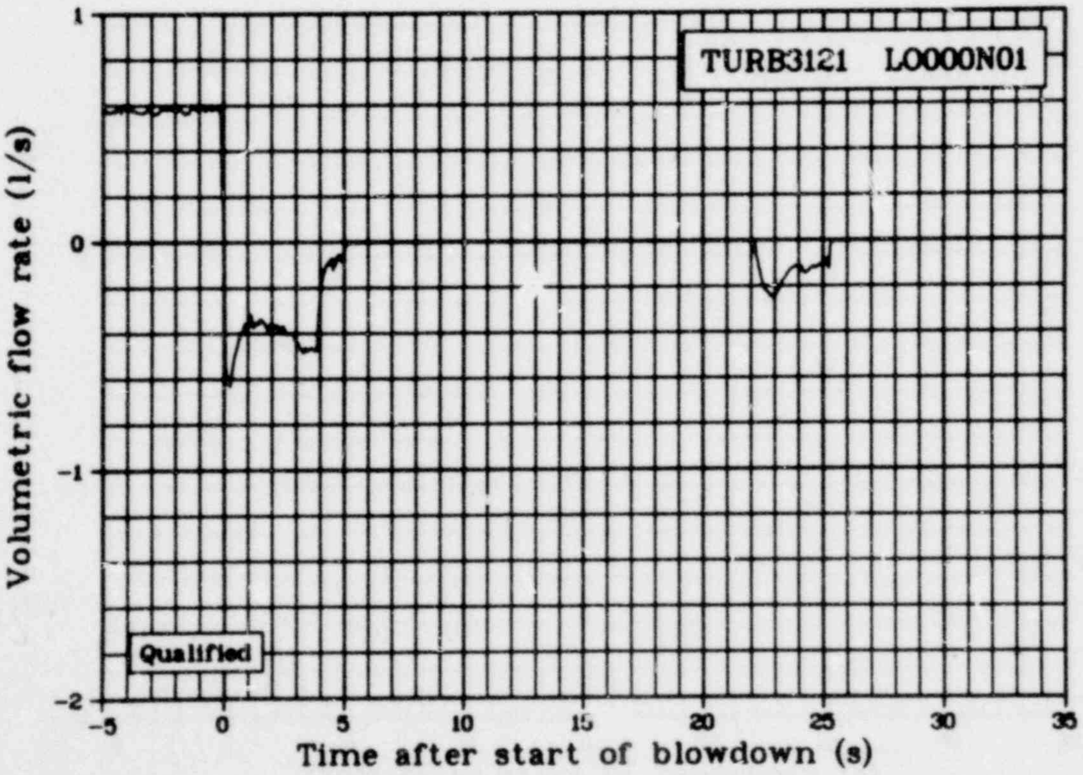

Fig. 93 Volumetric flow rate in Fuel Rod 312-1 lower shroud (TURB3121 L0000N01), from -5 to 35 s.

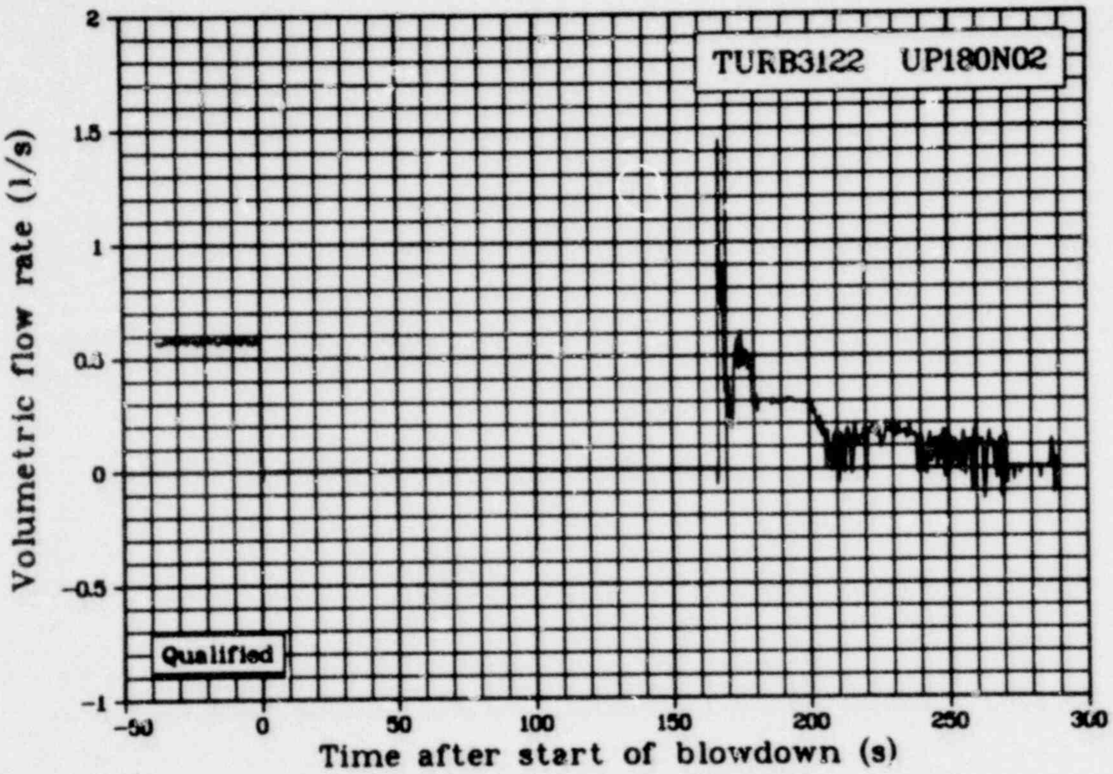

Fig. 94 Volumetric flow rate in Fuel Rod 312-2 upper shroud (TURB3122 UP180N02), from -50 to 300 s.

1405 128

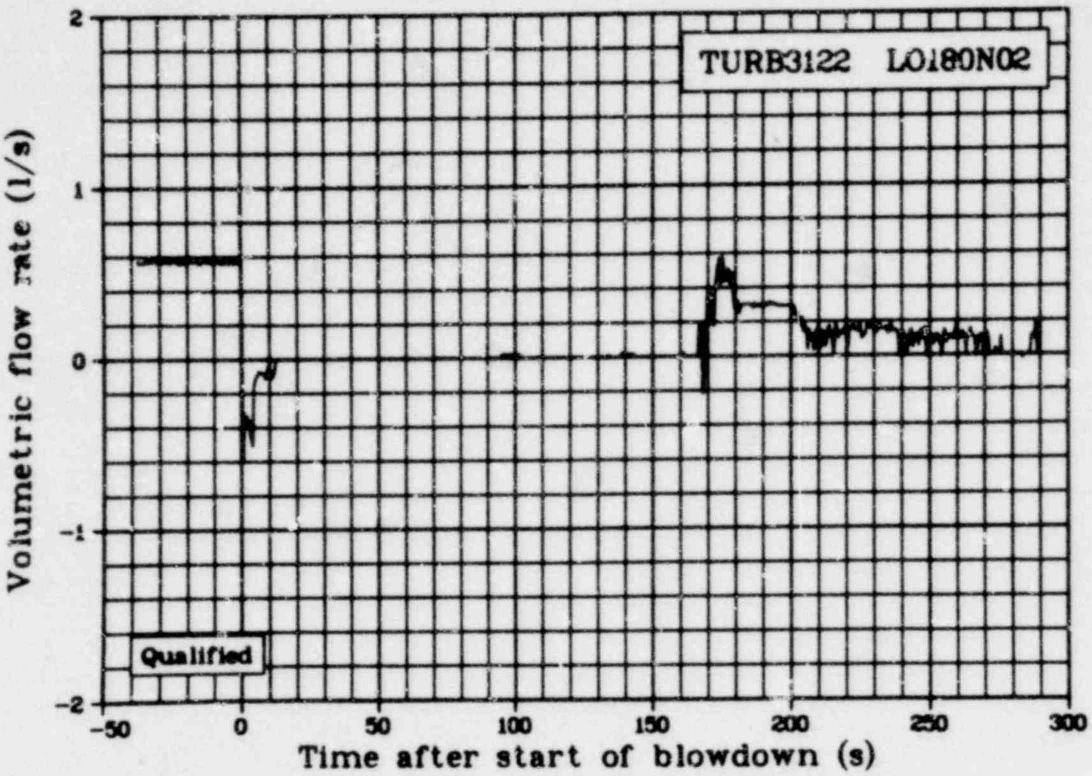

Fig. 95 Volumetric flow rate in Fuel Rod 312-2 lower shroud (TURB3122 L0180N02), from -50 to 300 s.

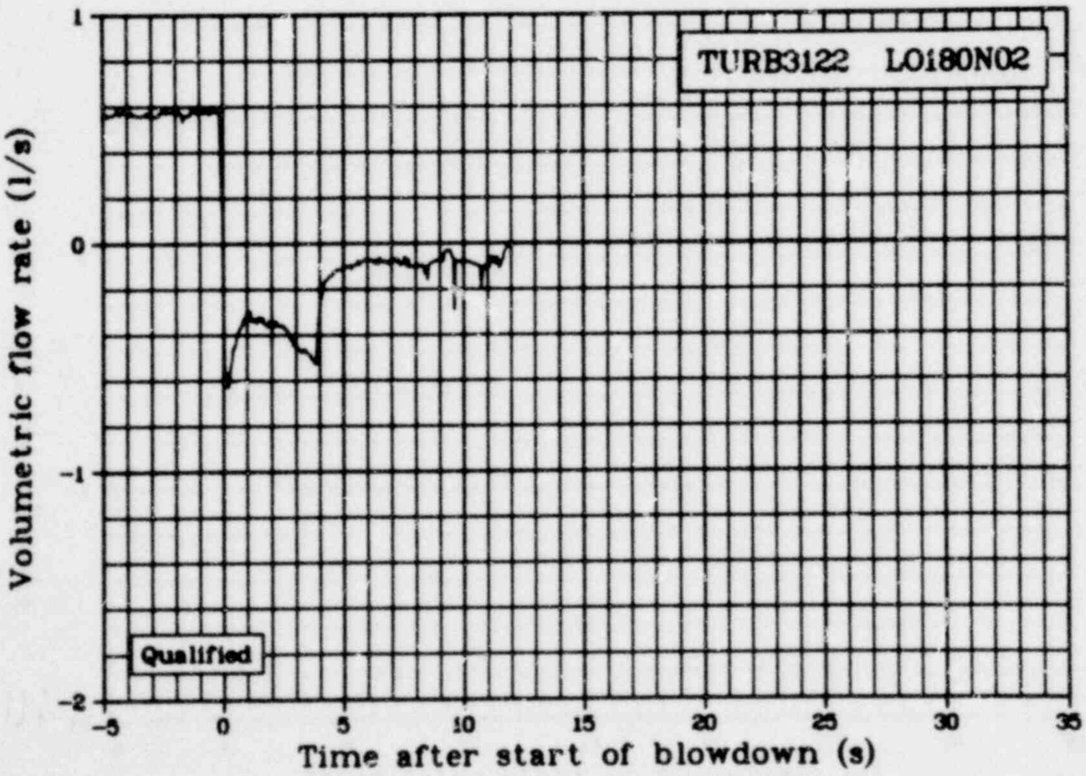

Fig. 96 Volumetric flow rate in Fuel Rod 312-2 lower shroud (TURB3122 L0180N02), from -5 to 35 s.

1405 129

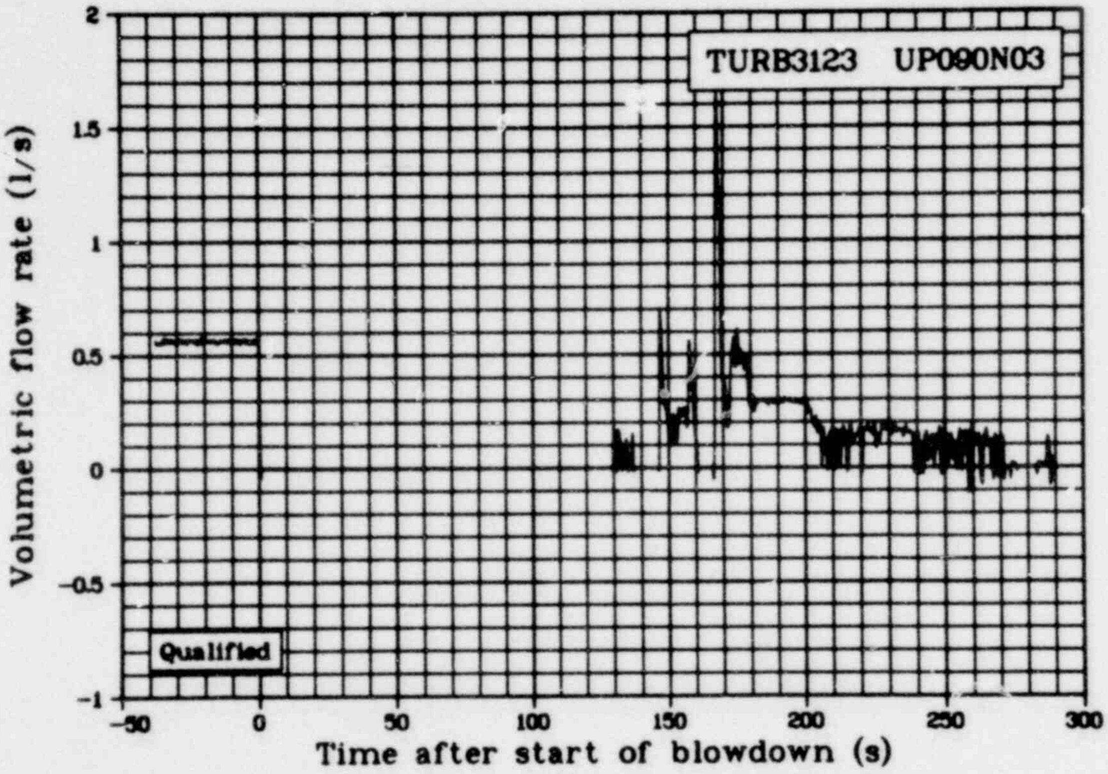

Fig. 97 Volumetric flow rate in Fuel Rod 312-3 upper shroud (TURB3123 UP090N03), from -50 to 300 s.

1405 130

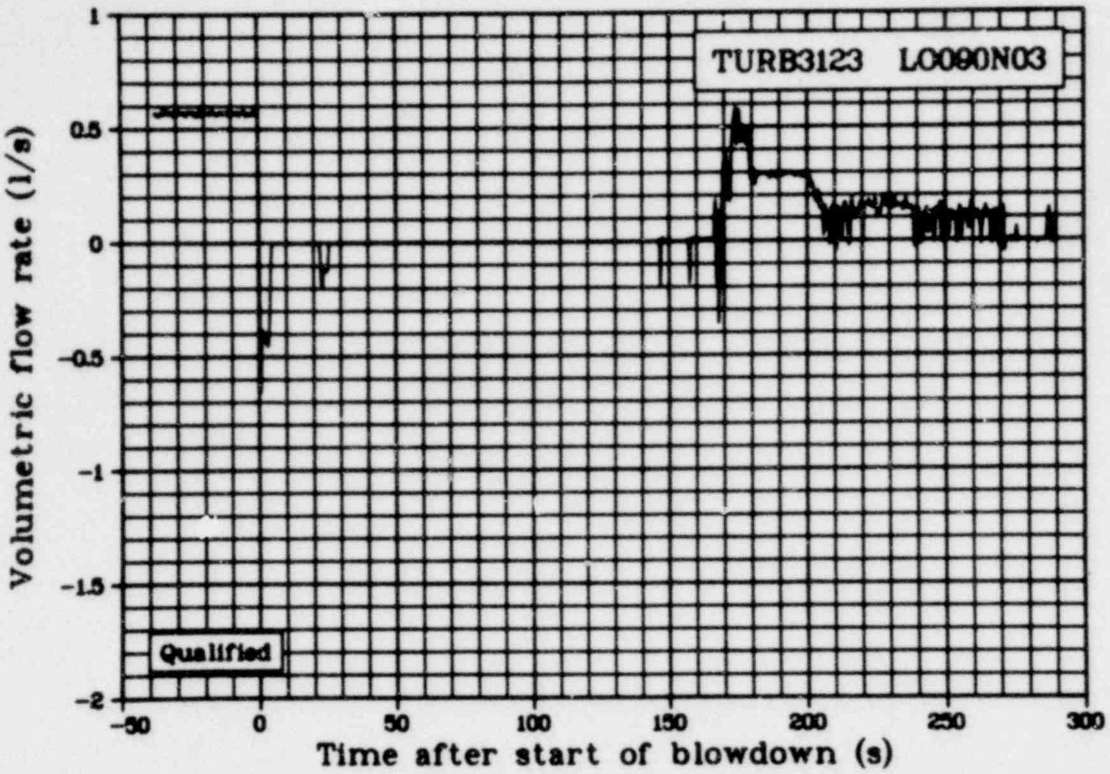

Fig. 98 Volumetric flow rate in Fuel Rod 312-3 lower shroud (TURB3123 L0090N03), from -50 to 300 s.

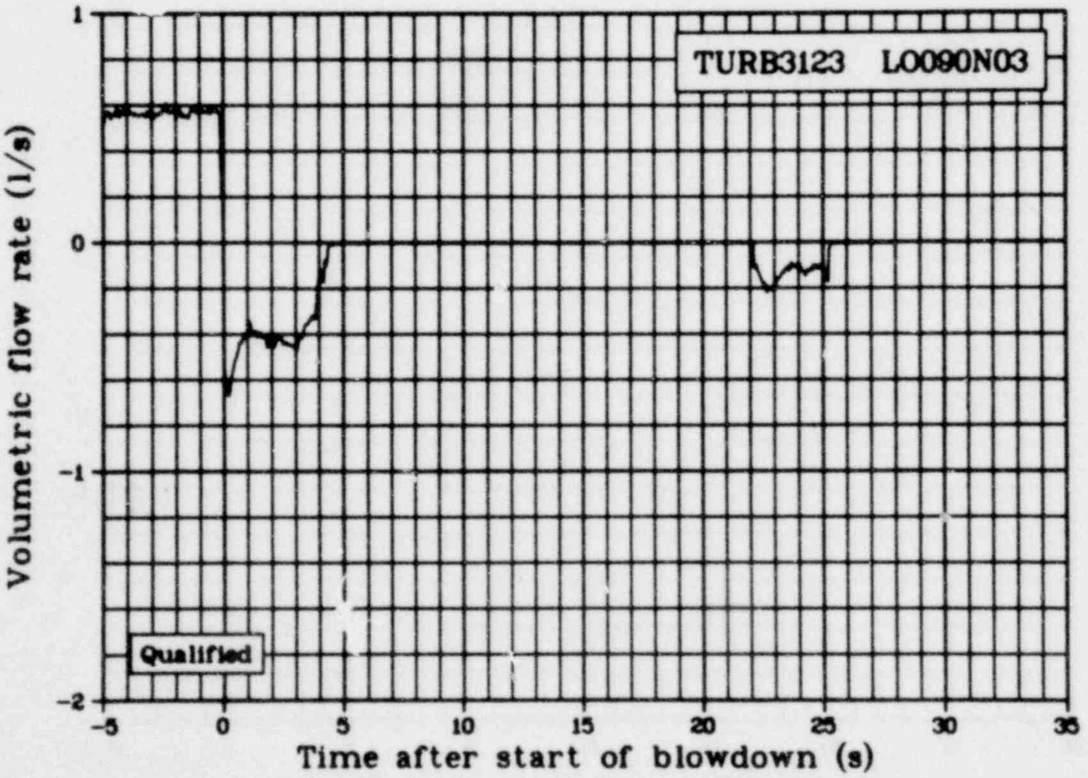

Fig. 99 Volumetric flow rate in Fuel Rod 312-3 lower shroud (TURB3123 L0090N03), from -5 to 35 s.

1405 131

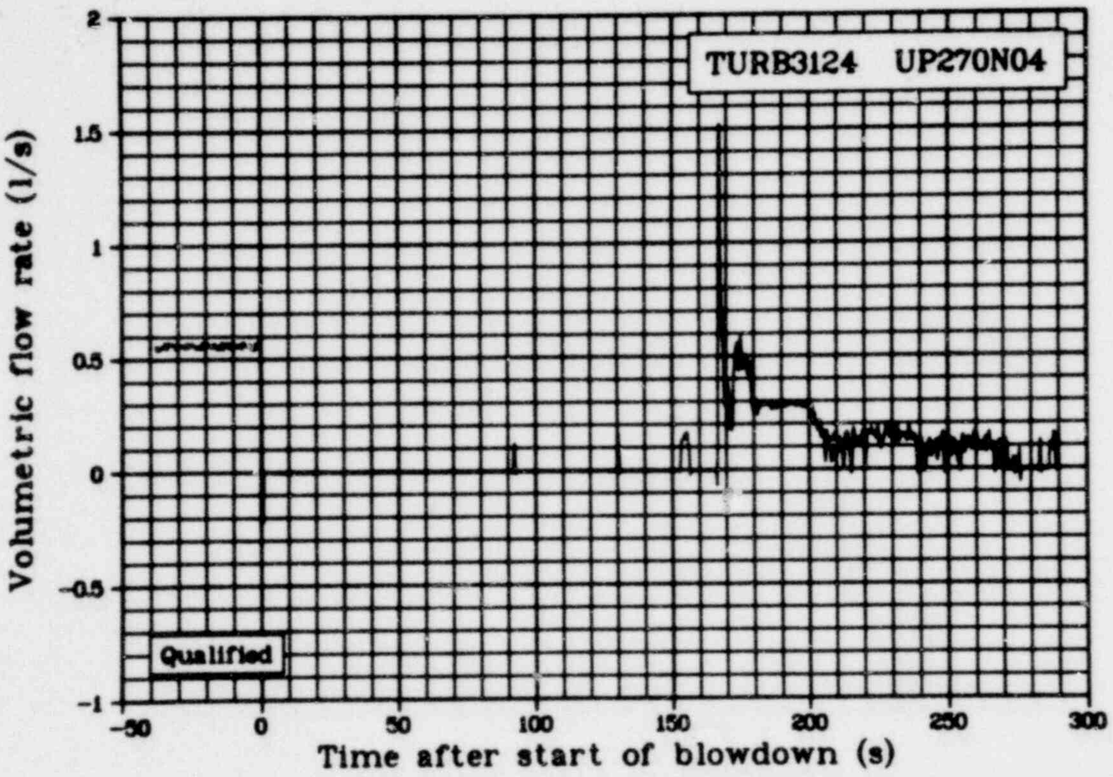

Fig. 100 Volumetric flow rate in Fuel Rod 312-4 upper shroud (TURB3124 UP270N04), from -50 to 300 s.

1405 132

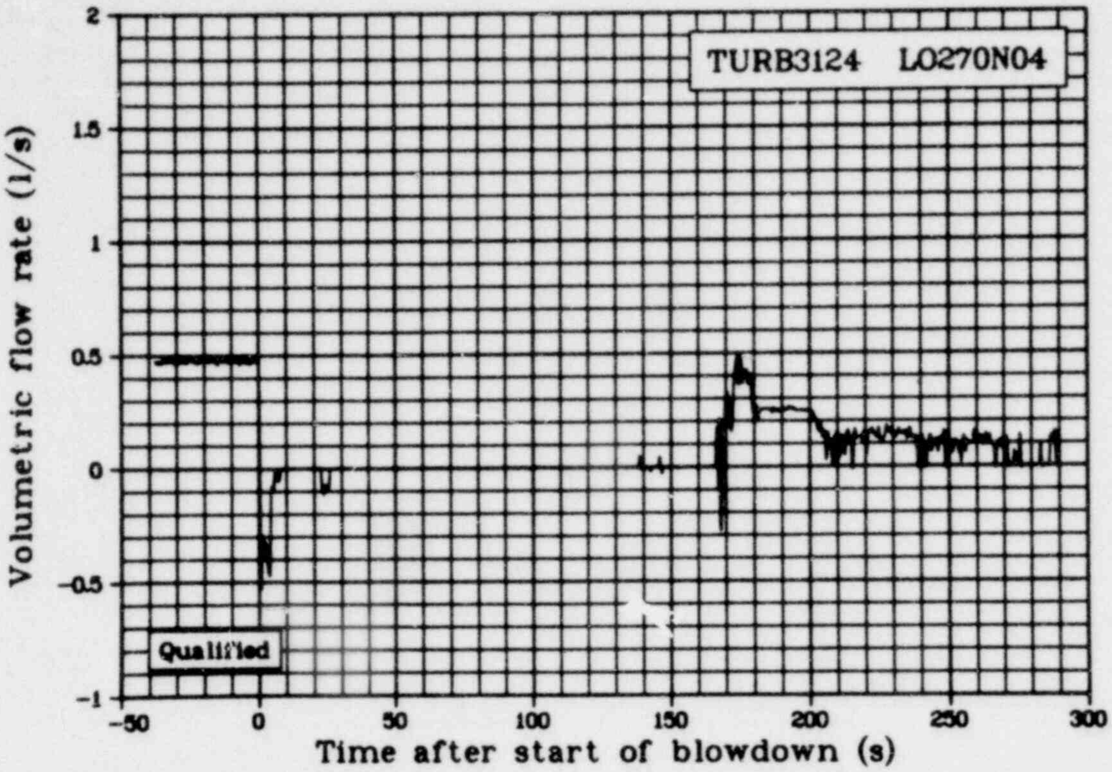

Fig. 101 Volumetric flow rate in Fuel Rod 312-4 lower shroud (TURB3124 L0270N04), from -50 to 300 s.

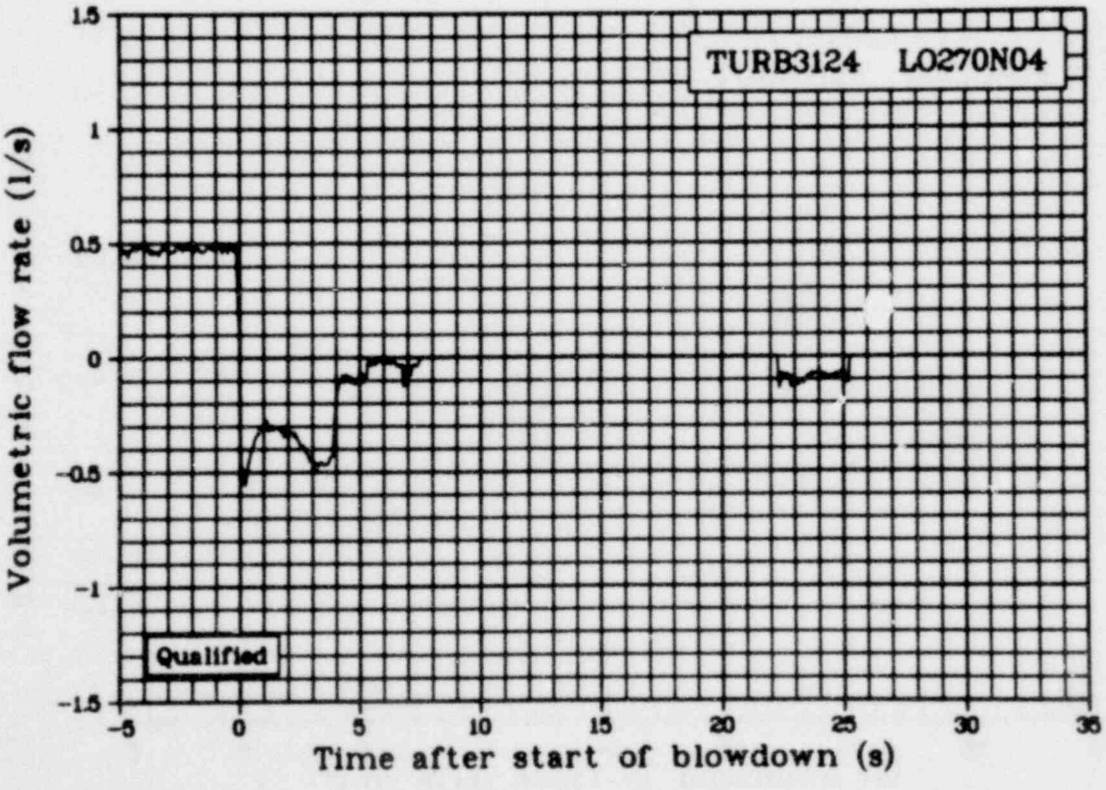

Fig. 102 Volumetric flow rate in Fuel Rod 312-4 lower shroud (TURB3124 L0270N04), from -5 to 35 s.

1405 133

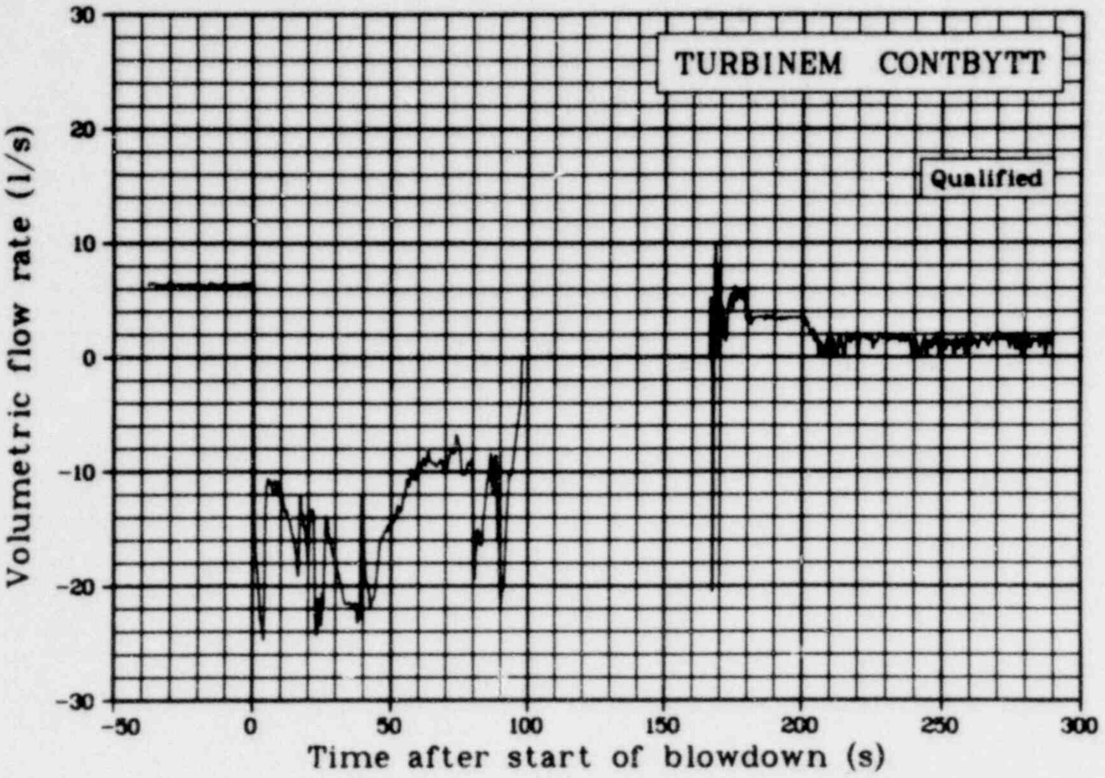

Fig. 103 Volumetric flow rate in test train controlled bypass (TURBINEM CONTBYTT), from -50 to 300 s.

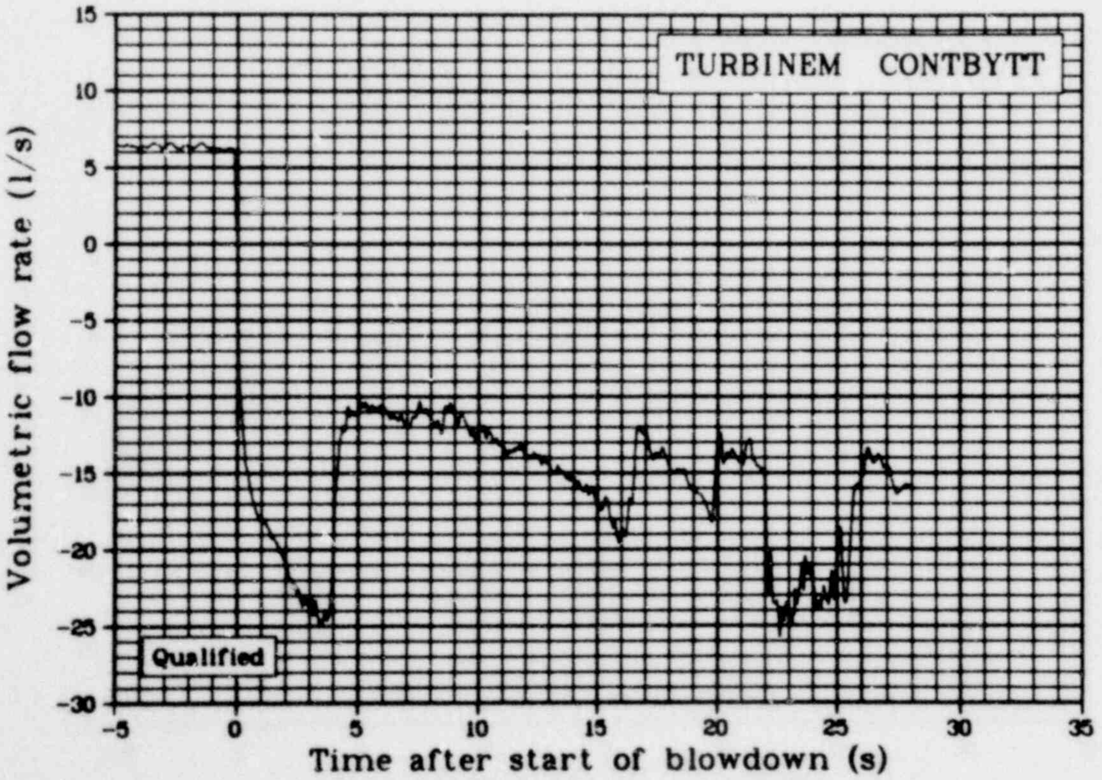

Fig. 104 Volumetric flow rate in test train controlled bypass (TURBINEM CONTBYTT), from -5 to 35 s.

1405 134

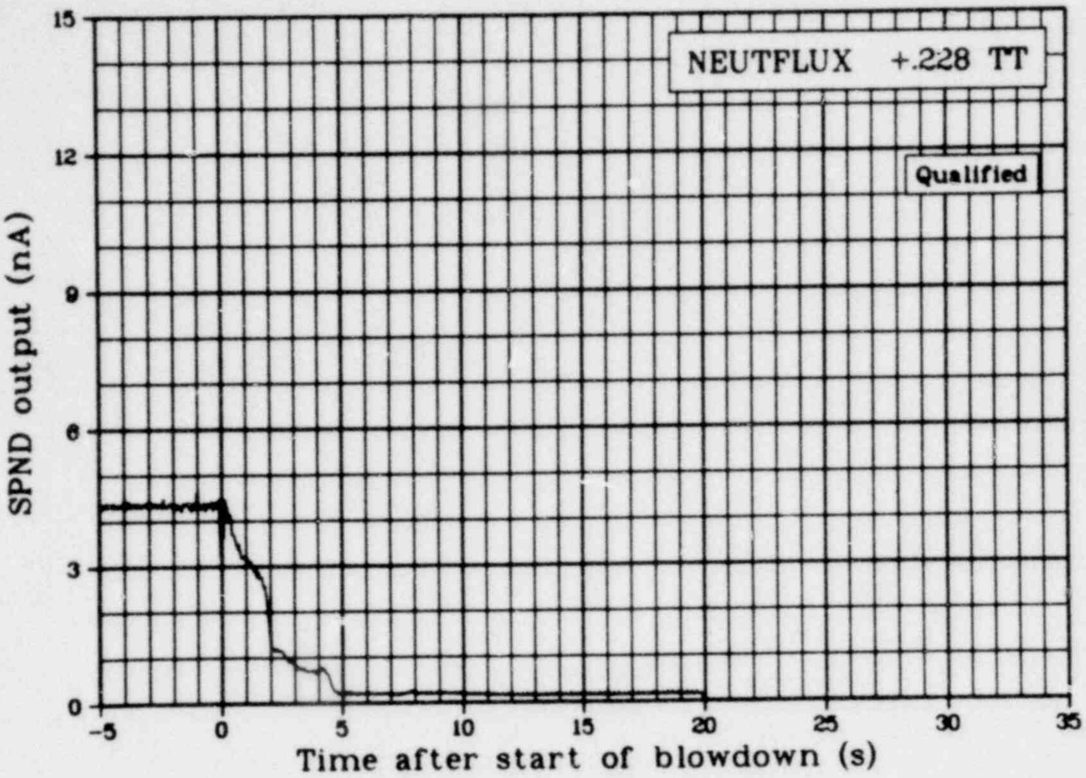

Fig. 105 Neutron flux 0.228 m above fuel stack midplane (NEUTFLUX +.228 TT), from -5 to 35 s.

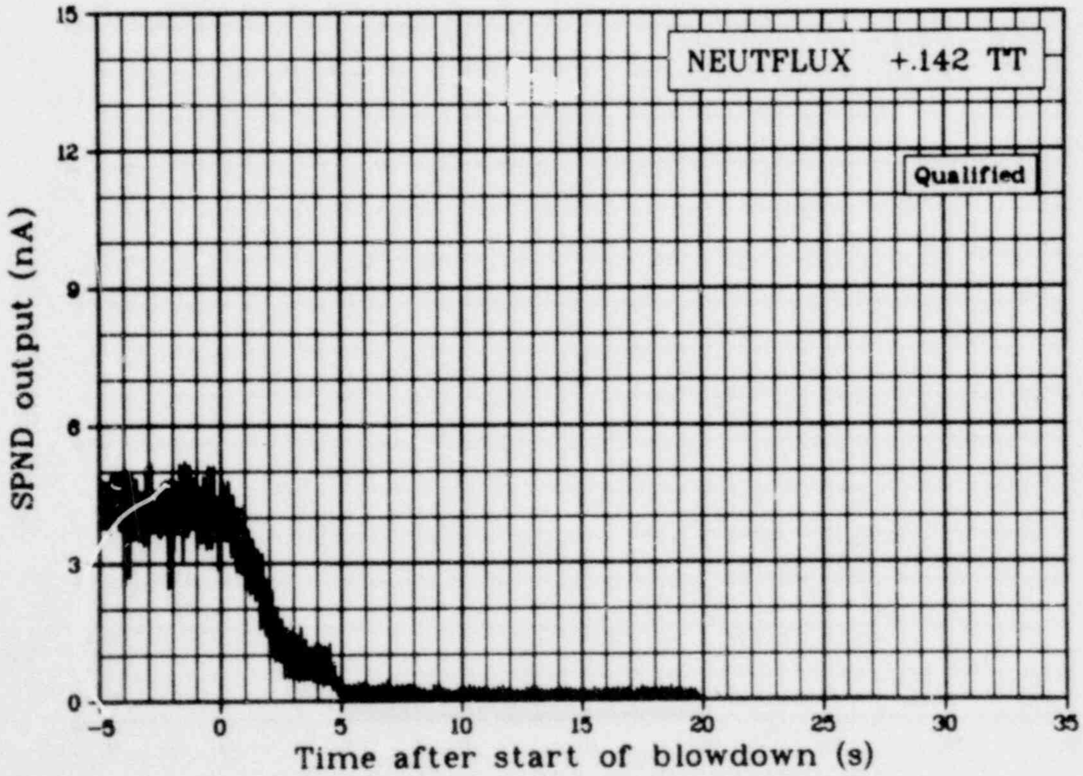

Fig. 106 Neutron flux 0.142 m above fuel stack midplane (NEUTFLUX +.142 TT), from -5 to 35 s.

1405 135

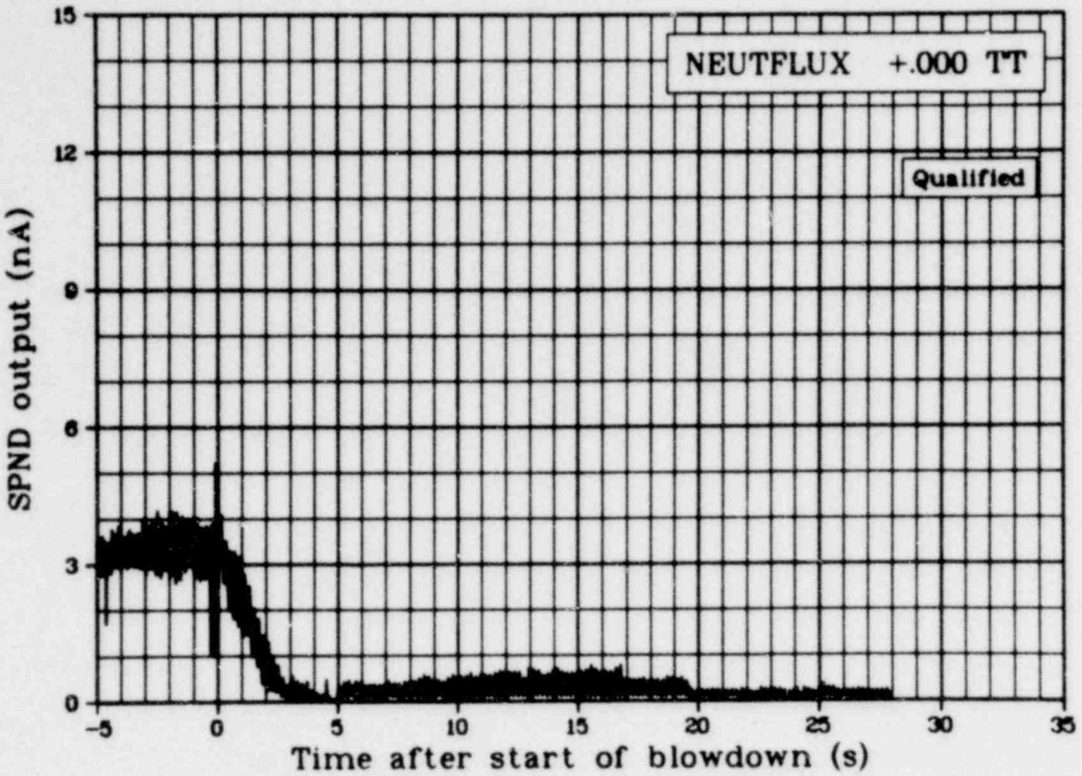

Fig. 107 Neutron flux at fuel stack midplane (NEUTFLUX +.000 TT), from -5 to 35 s.

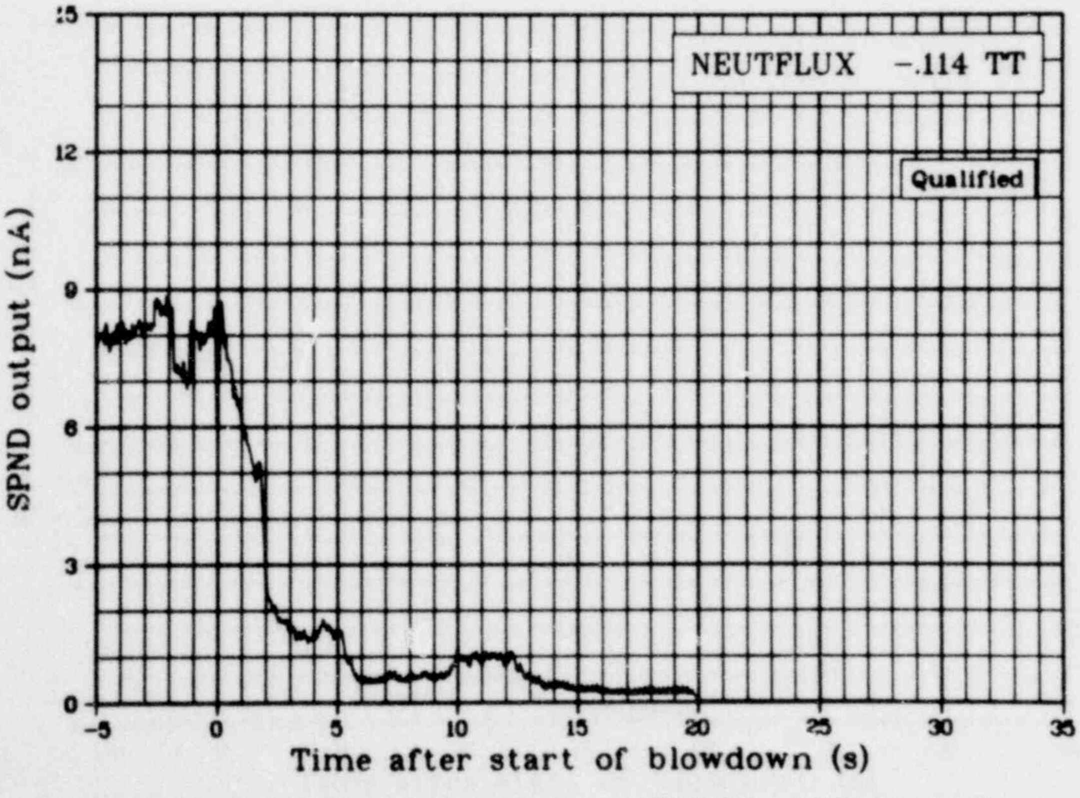

Fig. 108 Neutron flux 0.114 m below fuel stack midplane (NEUTFLUX -.114 TT), from -5 to 35 s.

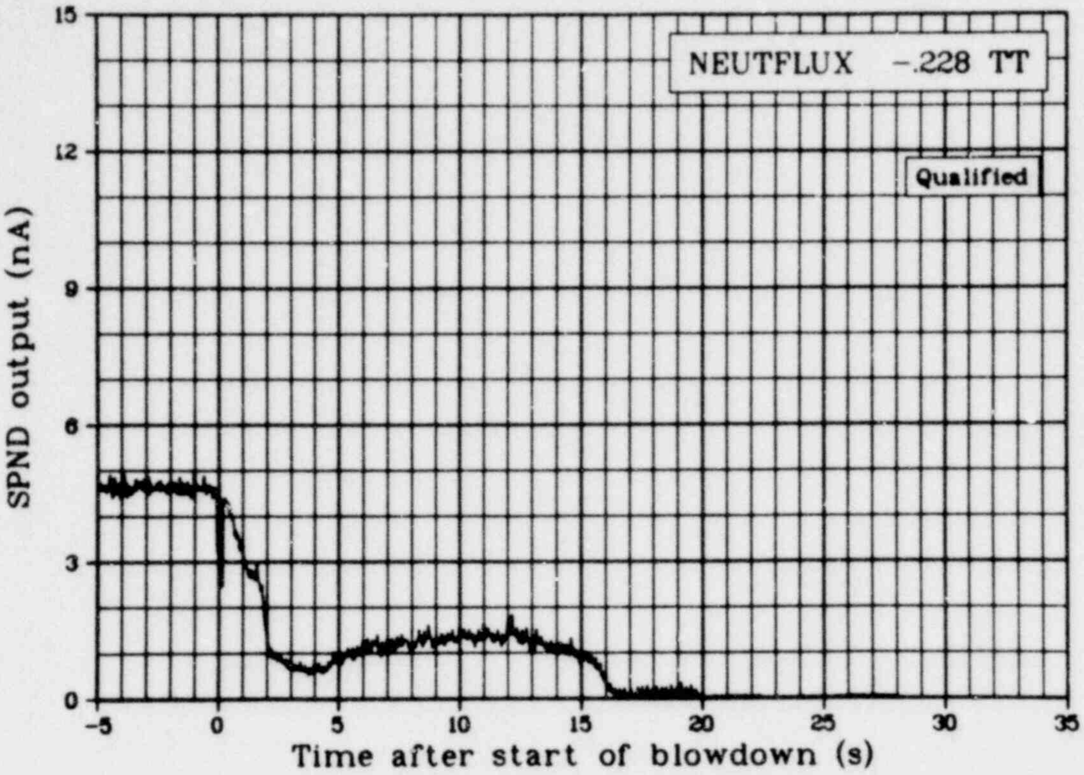

Fig. 109 Neutron flux 0.228 m below fuel stack midplane (NEUTFLUX -.228 TT), from -5 to 35 s.

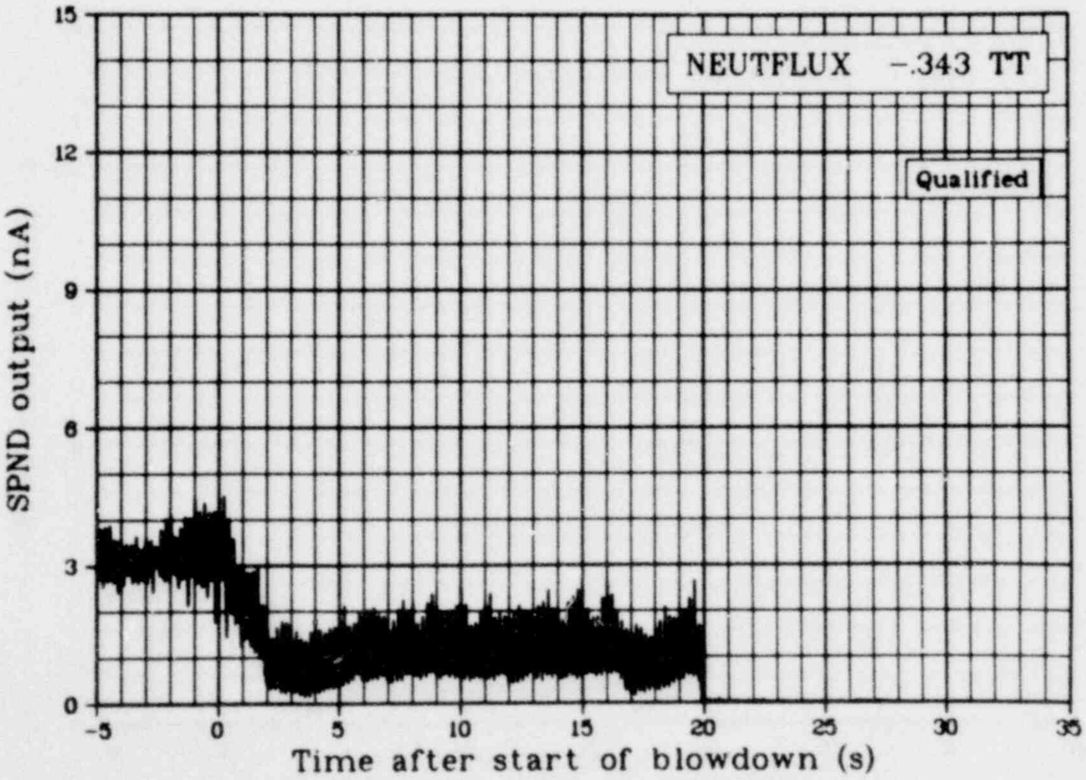

Fig. 110 Neutron flux 0.343 m below fuel stack midplane (NEUTFLUX -.343 TT), from -5 to 35 s.

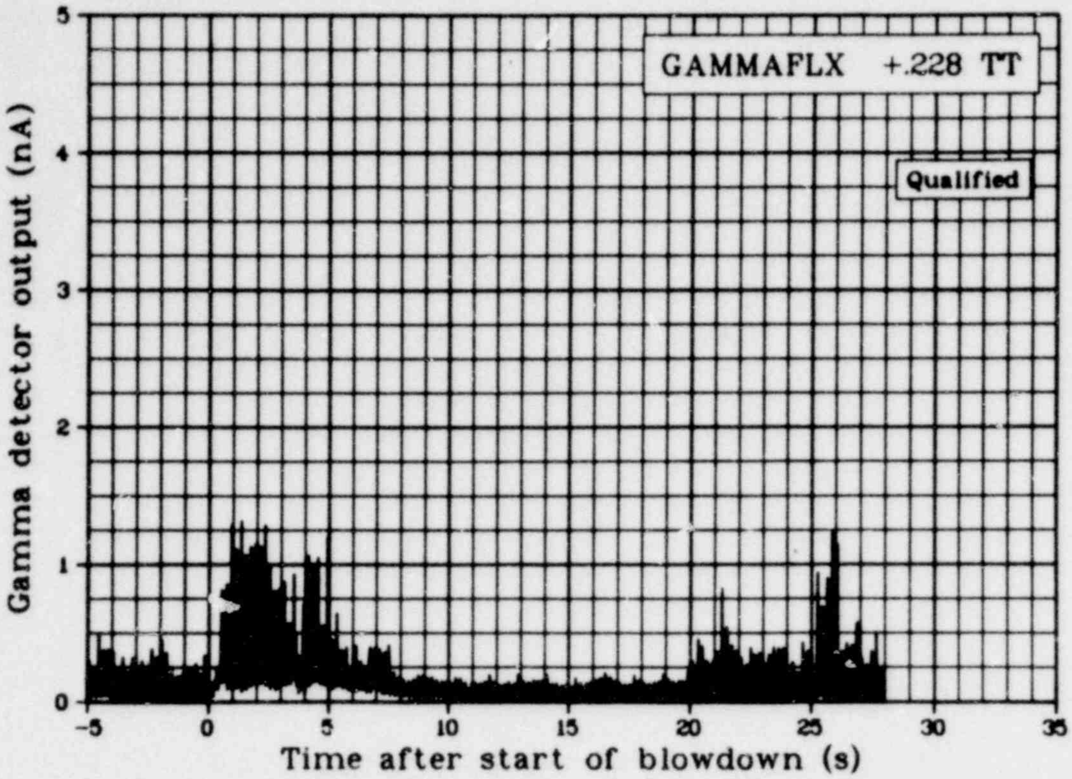

Fig. 111 Gamma flux 0.228 m above fuel stack midplane (GAMMAFLX +.228 TT), from -5 to 35 s.

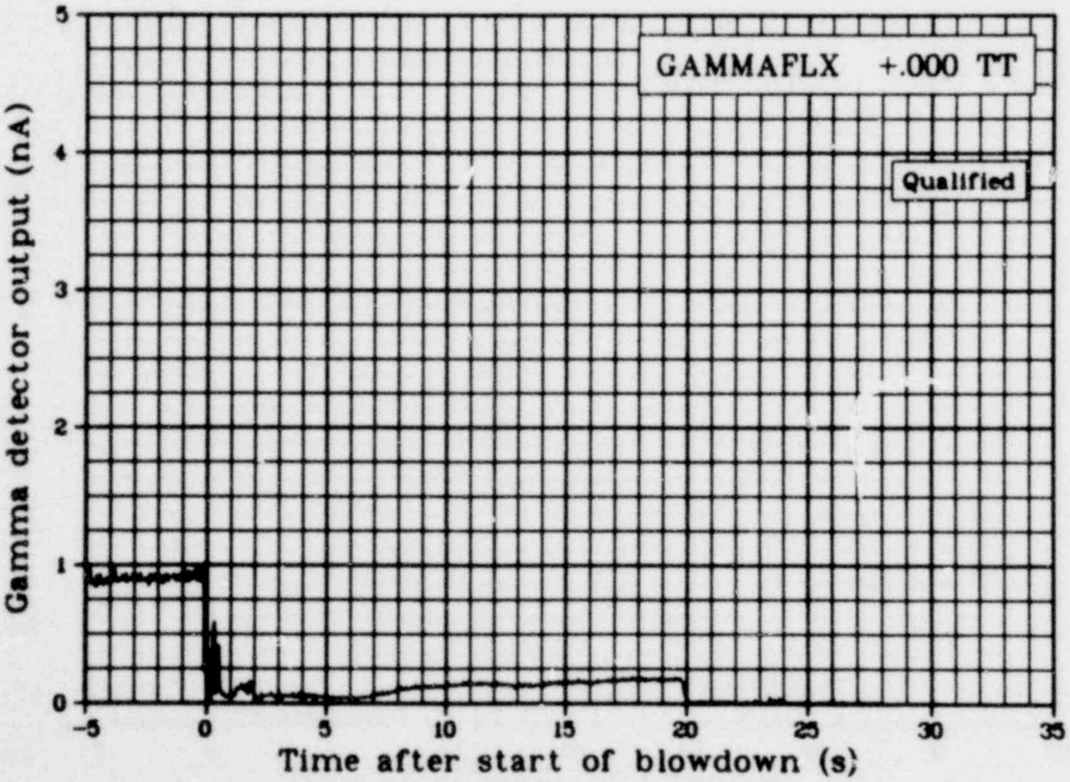

Fig. 112 Gamma flux at fuel stack midplane (GAMMAFLX +.000 TT), from -5 to 25 s.

1405 138

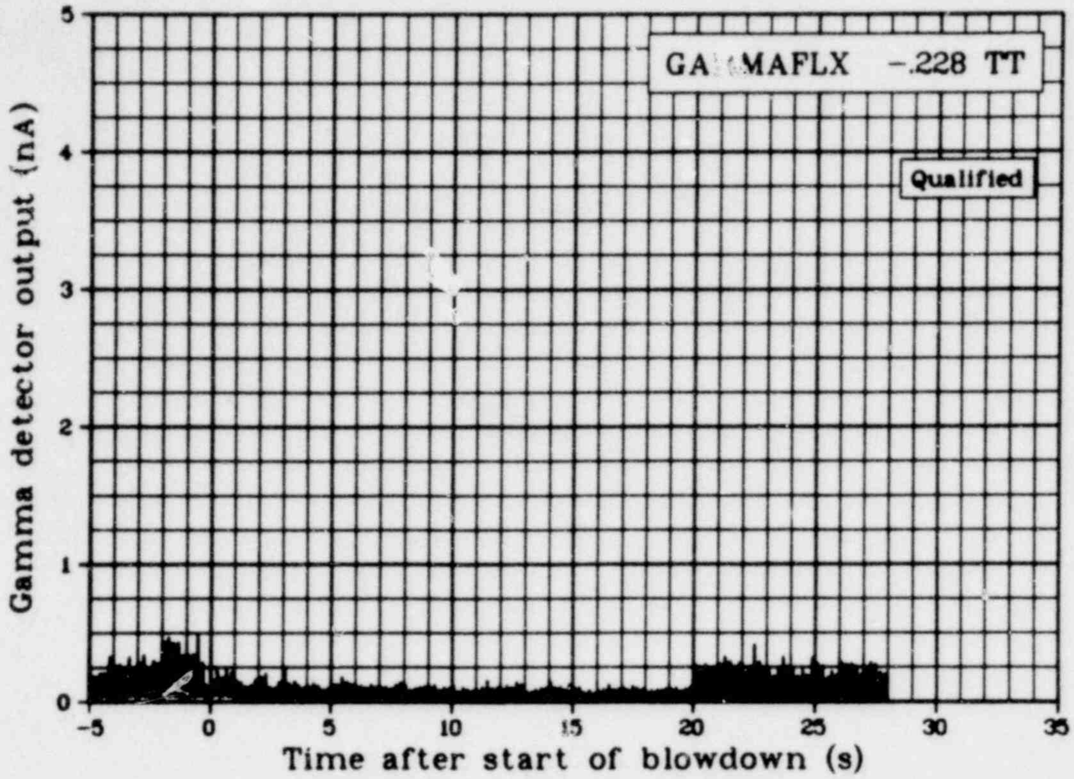

Fig. 113 Gamma flux 0.228 m below fuel stack midplane (GAMMAFLX -.228 TT), from -5 to 35 s.

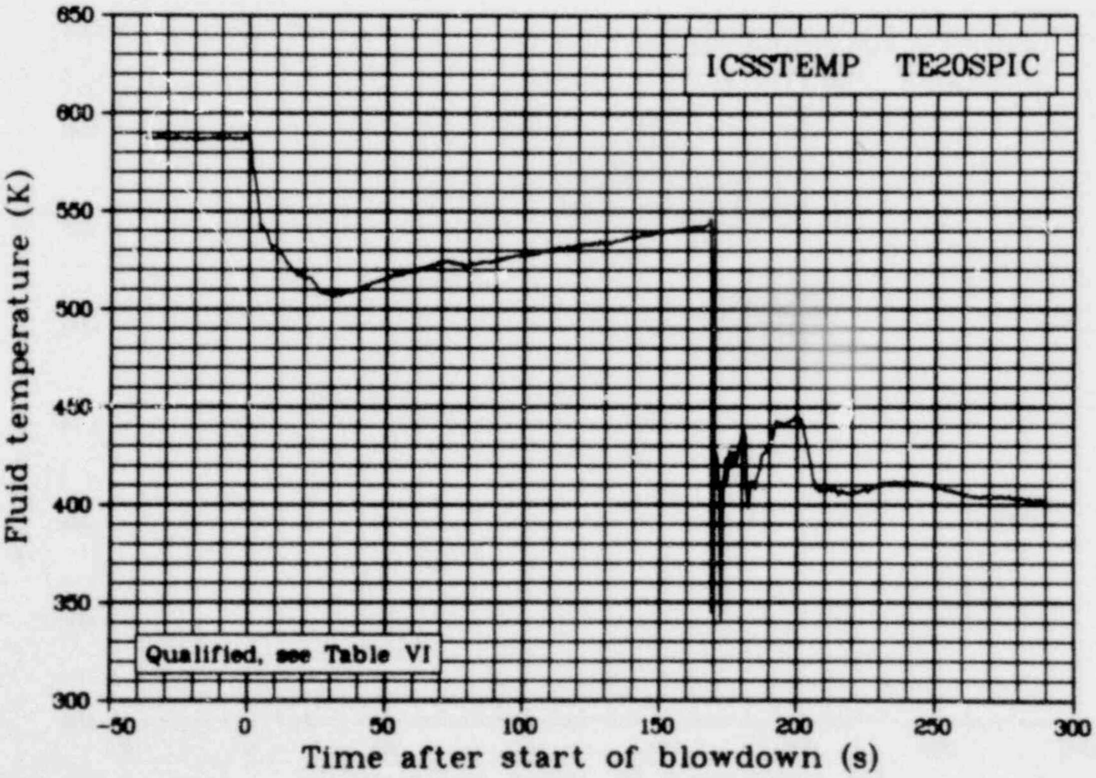

Fig. 114 Fluid temperature in initial condition spool (ICSSTEMP TE20SPIC), from -50 to 300 s.

1405 139

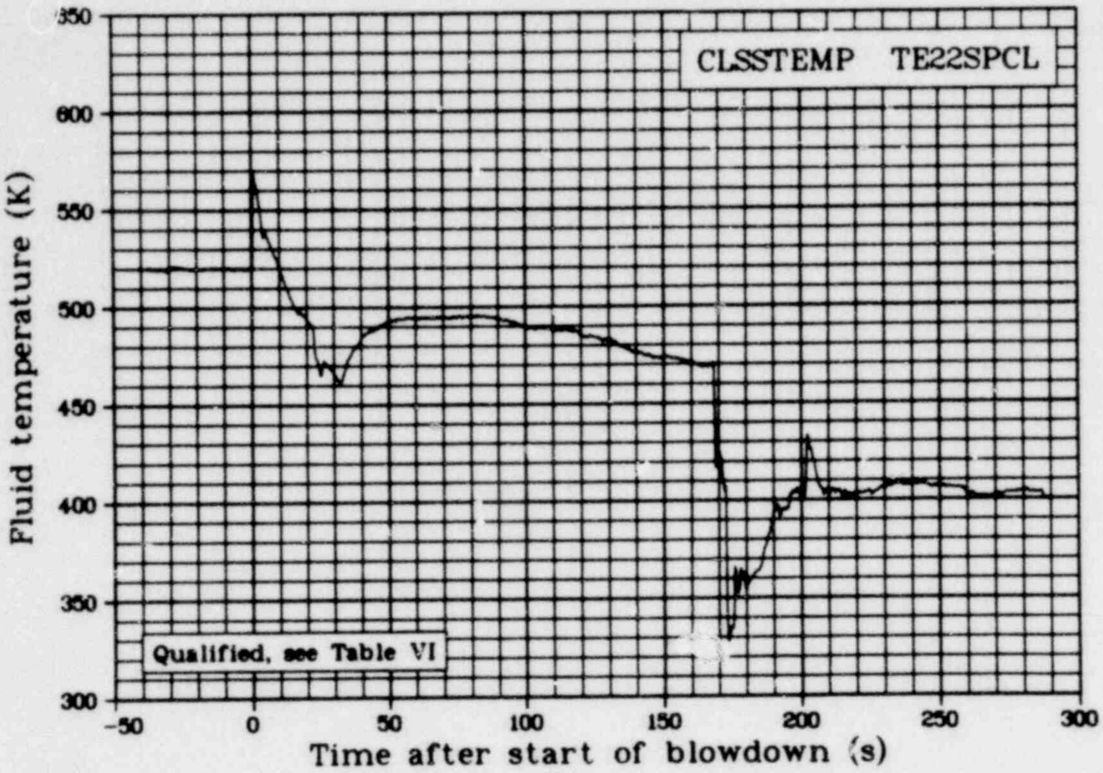

Fig. 115 Fluid temperature in cold leg blowdown spool (CLSSTEMP TE22SPCL), from -50 to 300 s.

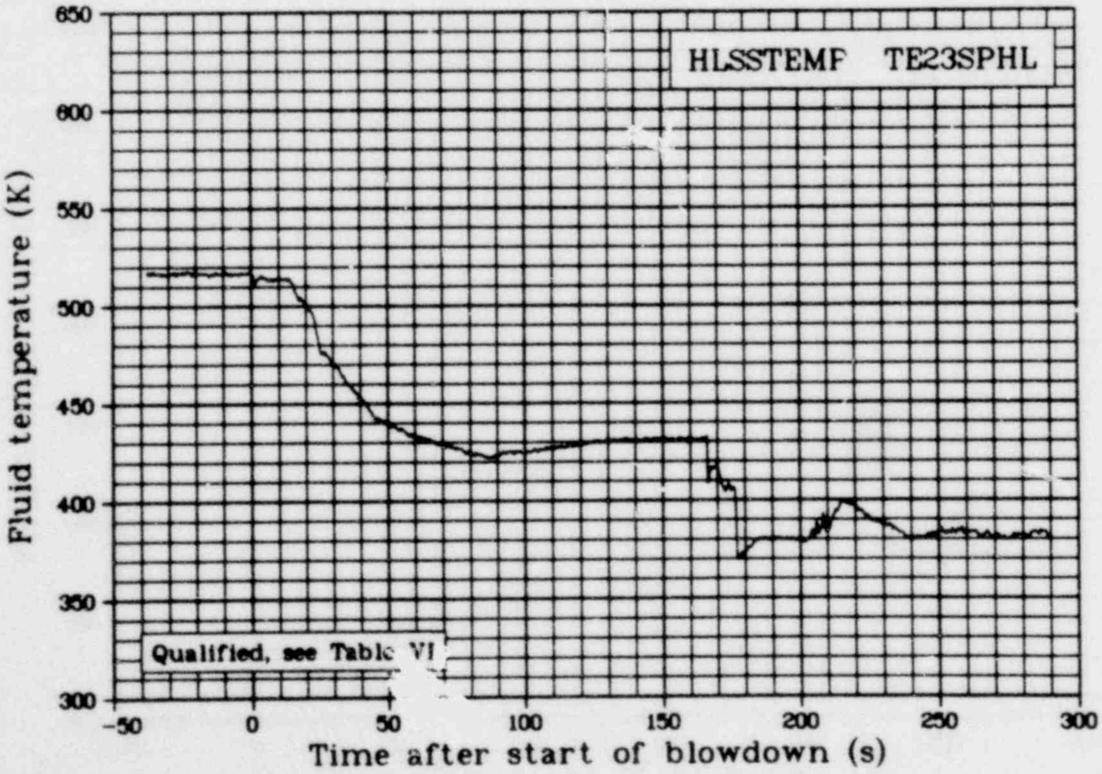

Fig. 116 Fluid temperature in hot leg blowdown spool (HLSSTEMP TE23SPHL), from -50 to 300 s.

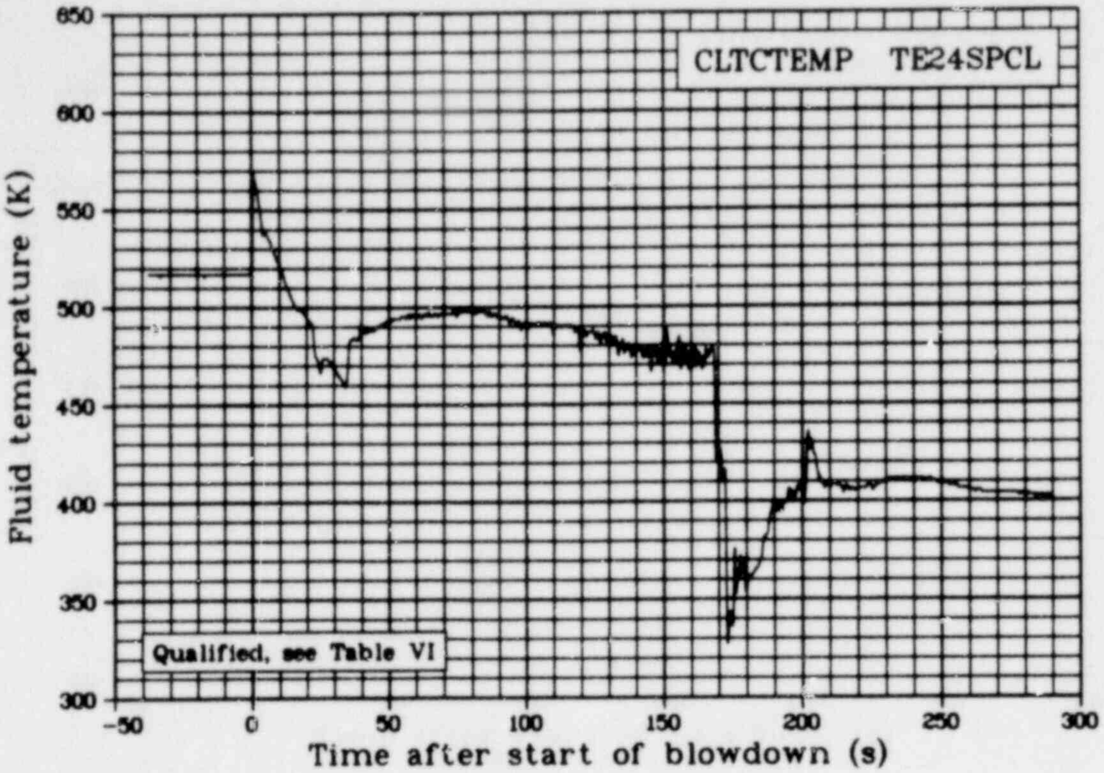

Fig. 117 Fluid temperature in cold leg blowdown spool (CLTCTEMP TE24SPCL), from -50 to 300 s.

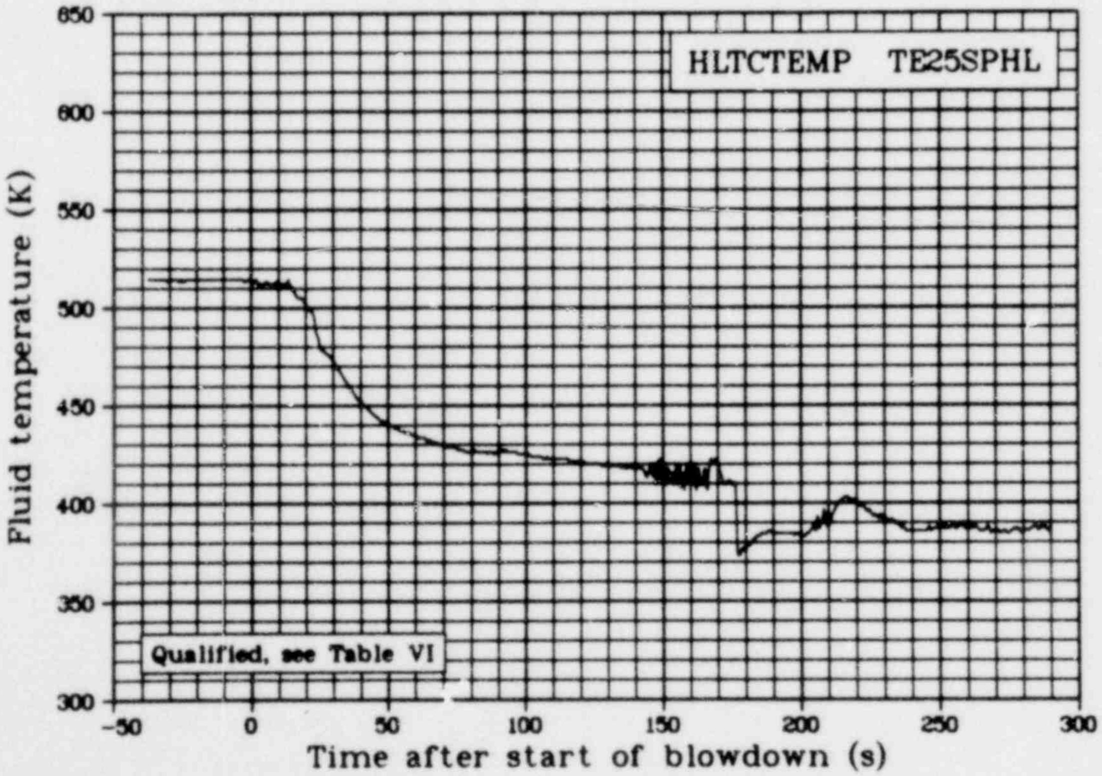

Fig. 118 Fluid temperature in hot leg blowdown spool (HLTCTEMP TE25SPHL), from -50 to 300 s.

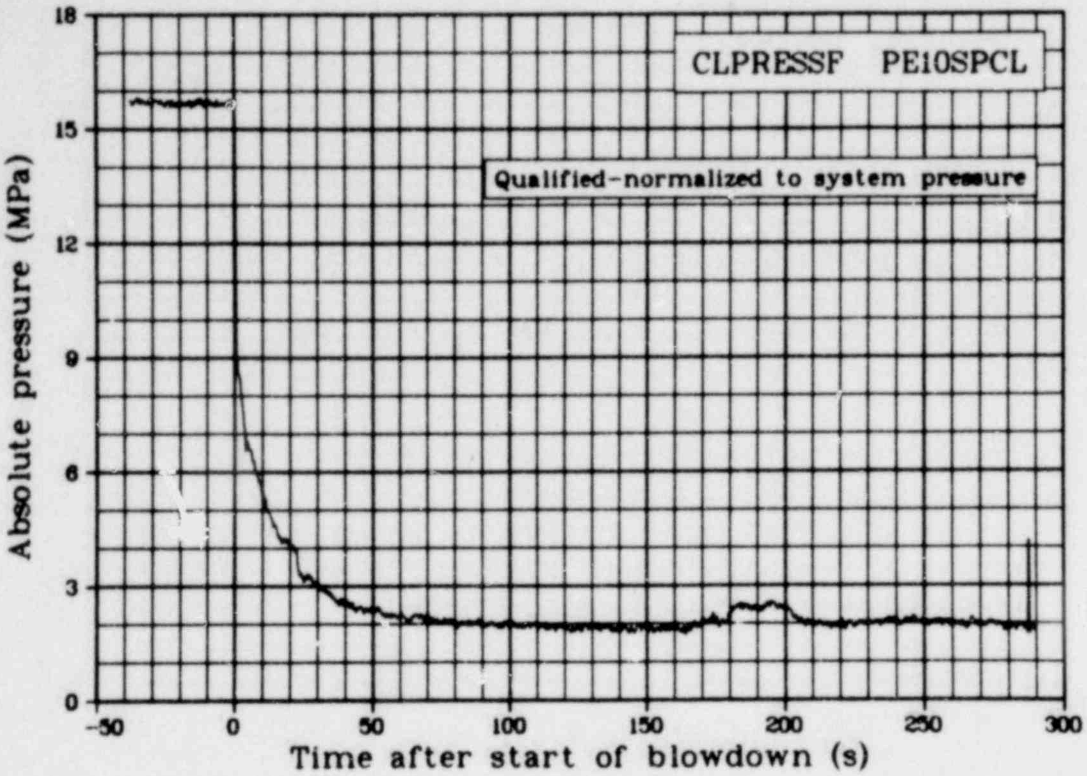

Fig. 119 Absolute pressure in cold leg blowdown spool (CLPRESSF PE10SPCL), from -50 to 300 s.

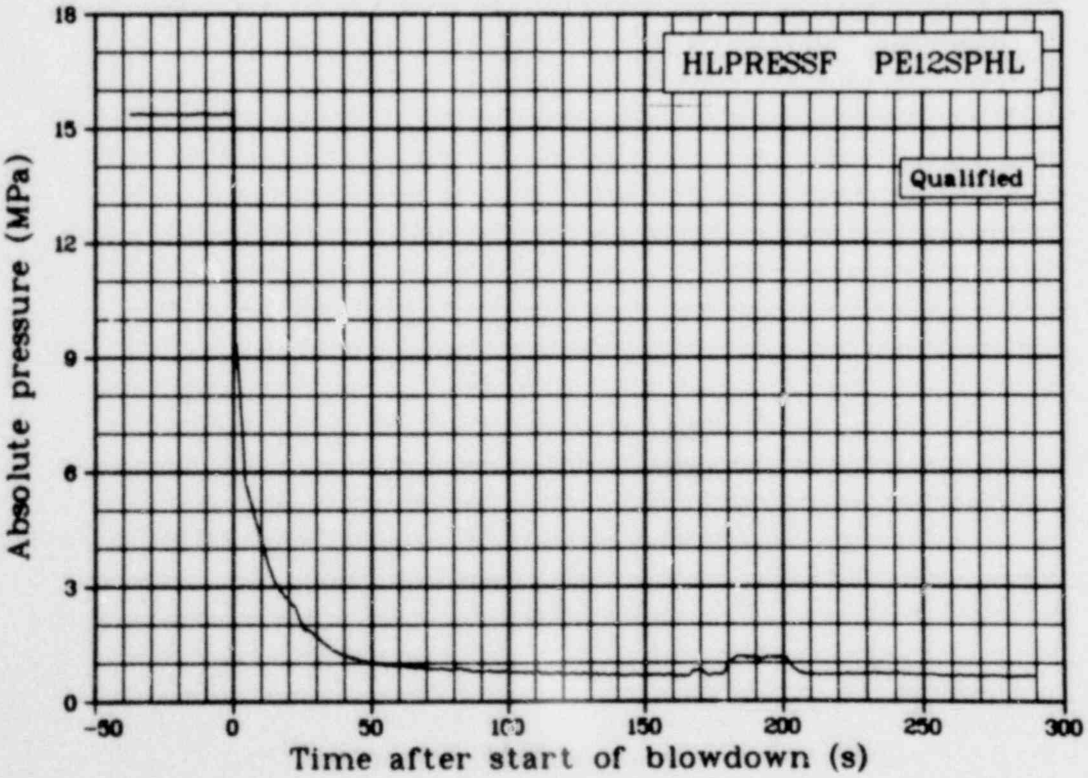

Fig. 120 Absolute pressure in hot leg blowdown spool (HLPRESSF PE12SPHL), from -50 to 300 s.

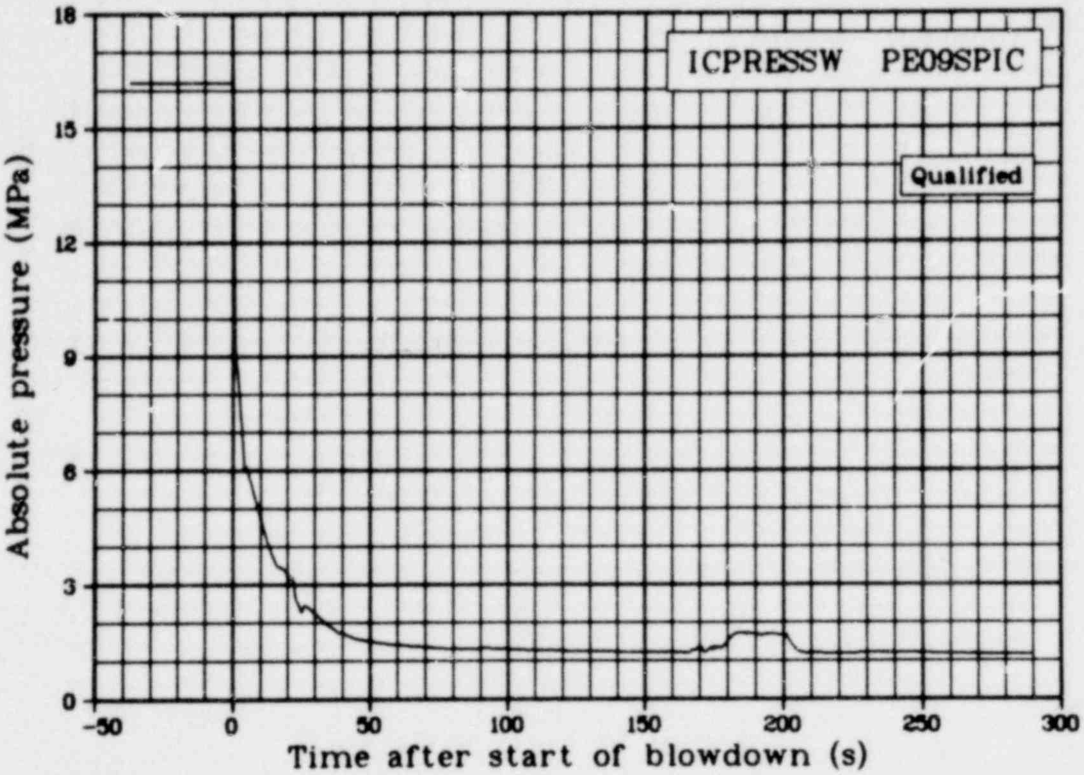

Fig. 121 Absolute pressure in initial condition spool (ICPRESSW PE09SPIC), from -50 to 300 s.

1405 143

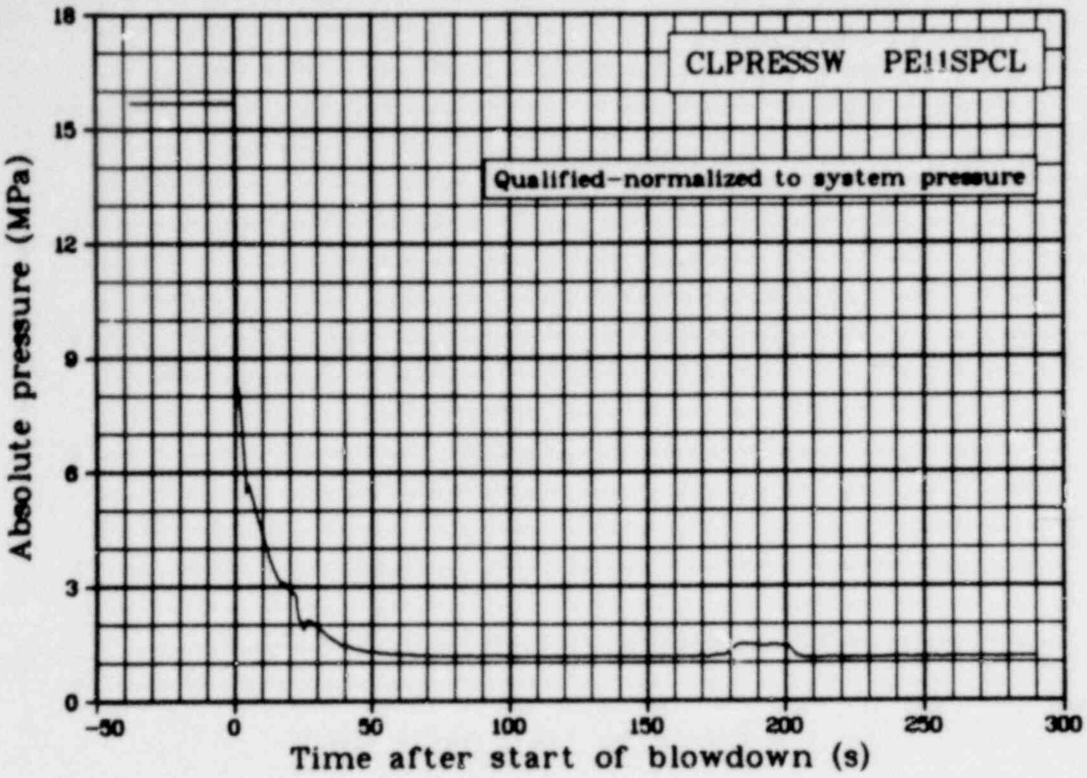

Fig. 122 Absolute pressure in cold leg blowdown spool (CLPRESSW PE11SPCL), from -50 to 300 s.

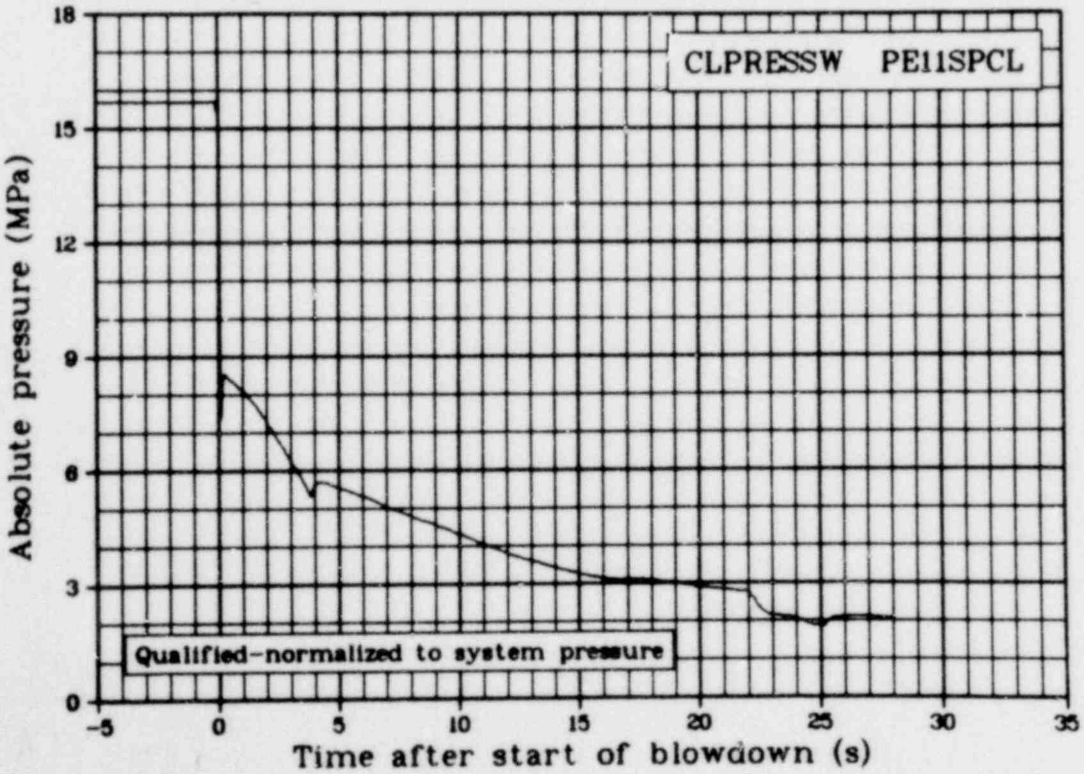

Fig. 123 Absolute pressure in cold leg blowdown spool (CLPRESSW PE11SPCL), from -5 to 35 s.

1405 144

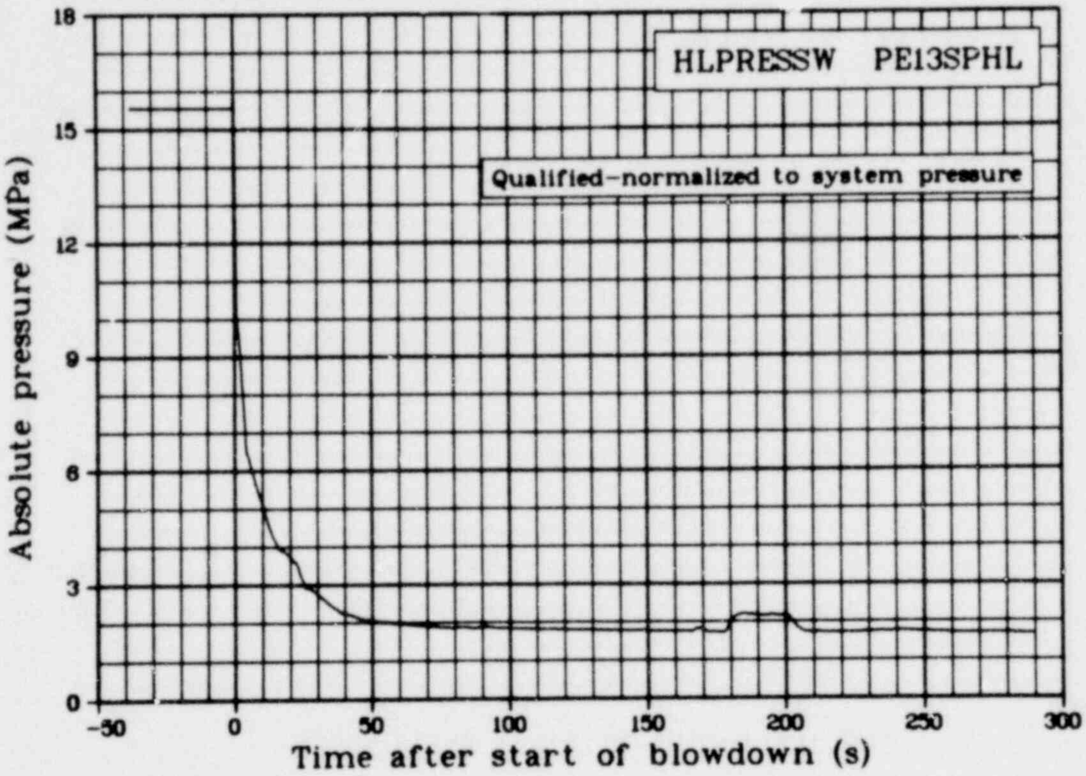

Fig. 124 Absolute pressure in hot leg blowdown spool (HLPRESSW PE13SPHL), from -50 to 300 s.

1405 145

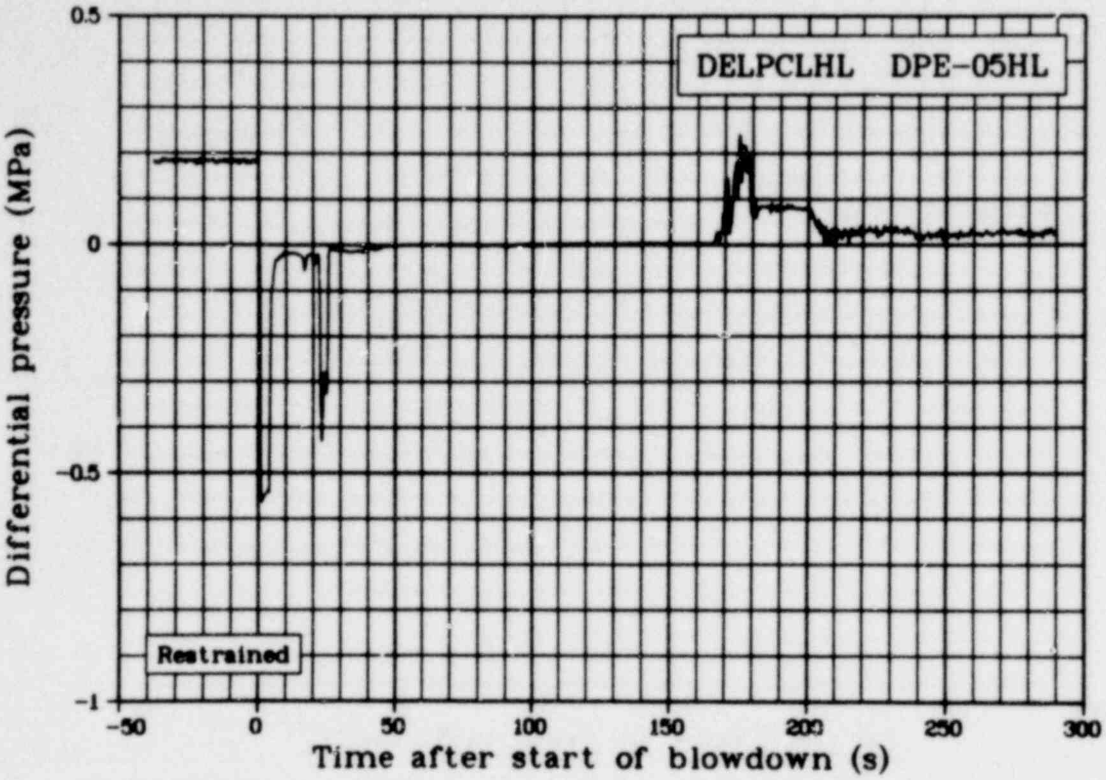

Fig. 125 Differential pressure between blowdown spools (DELPCLHL DPE-05HL), from -50 to 300 s.

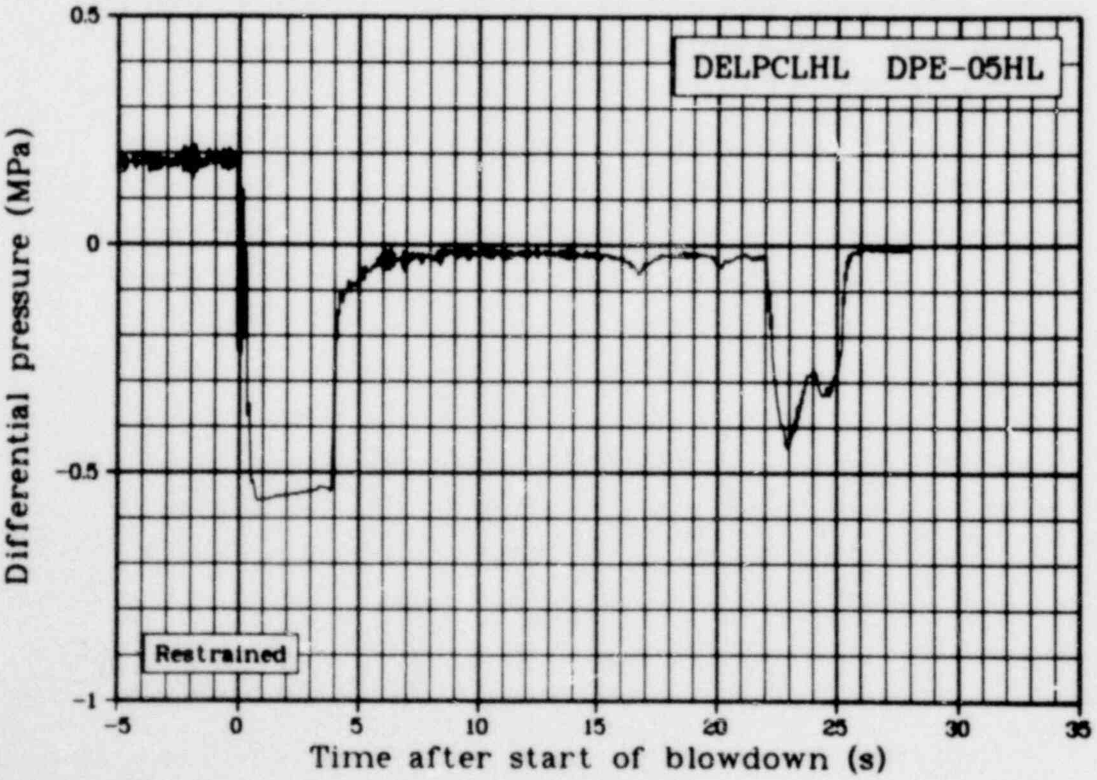

Fig. 126 Differential pressure between blowdown spools (DELPCLHL DPE-05HL), from -5 to 35 s.

1405 146

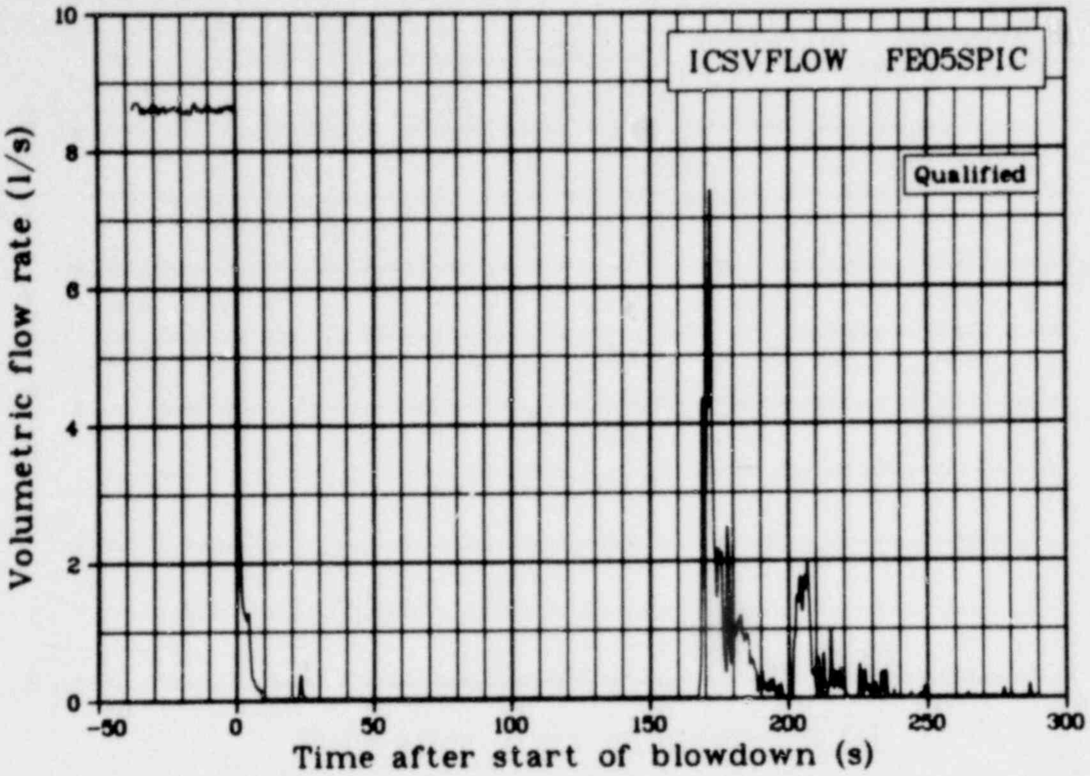

Fig. 127 Volumetric flow rate in initial condition spool (ICSVFLOW FEO5SPIC), from -50 to 300 s.

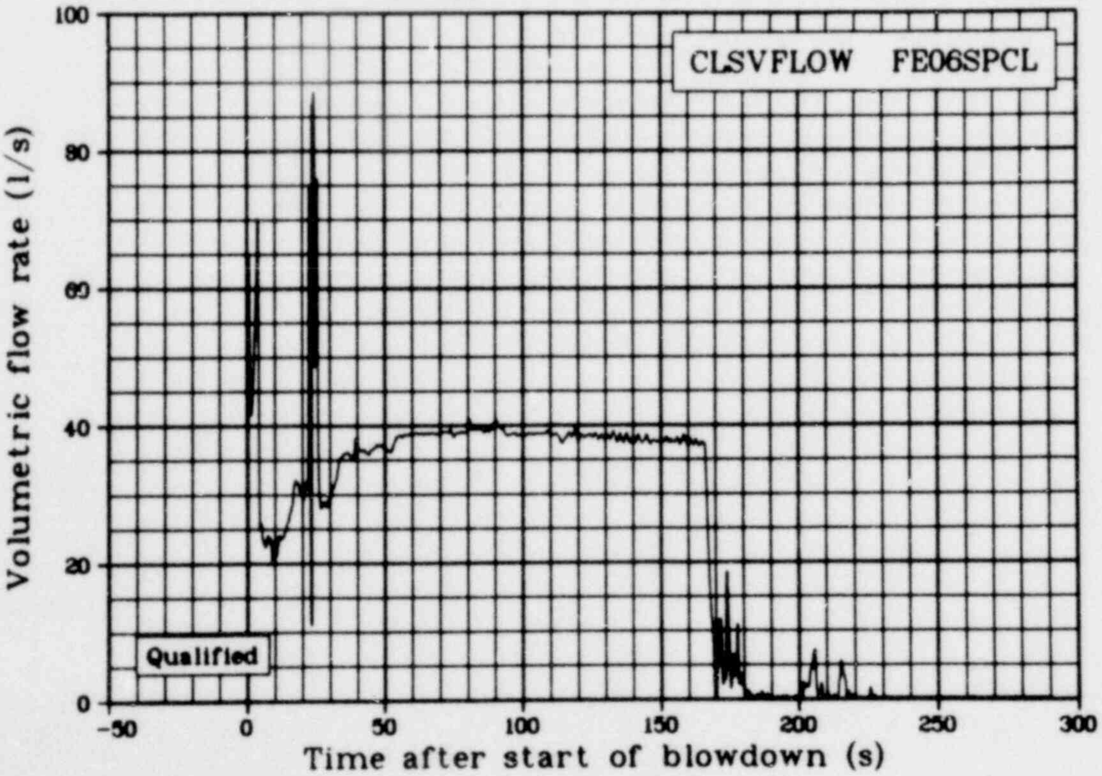

Fig. 128 Volumetric flow rate in cold leg blowdown spool (CLSVFLOW FE06SPCL), from -50 to 300 s.

1405 147

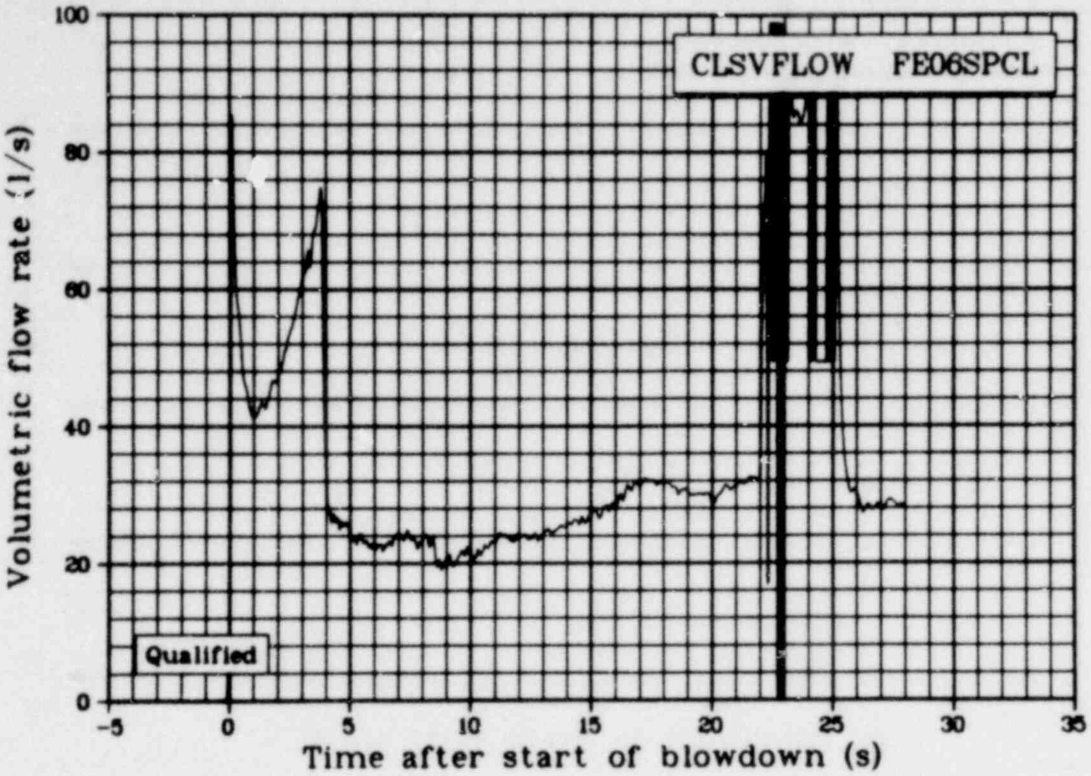

Fig. 129 Volumetric flow rate in cold leg blowdown spool (CLSVFLOW FE06SPCL), from -5 to 35 s.

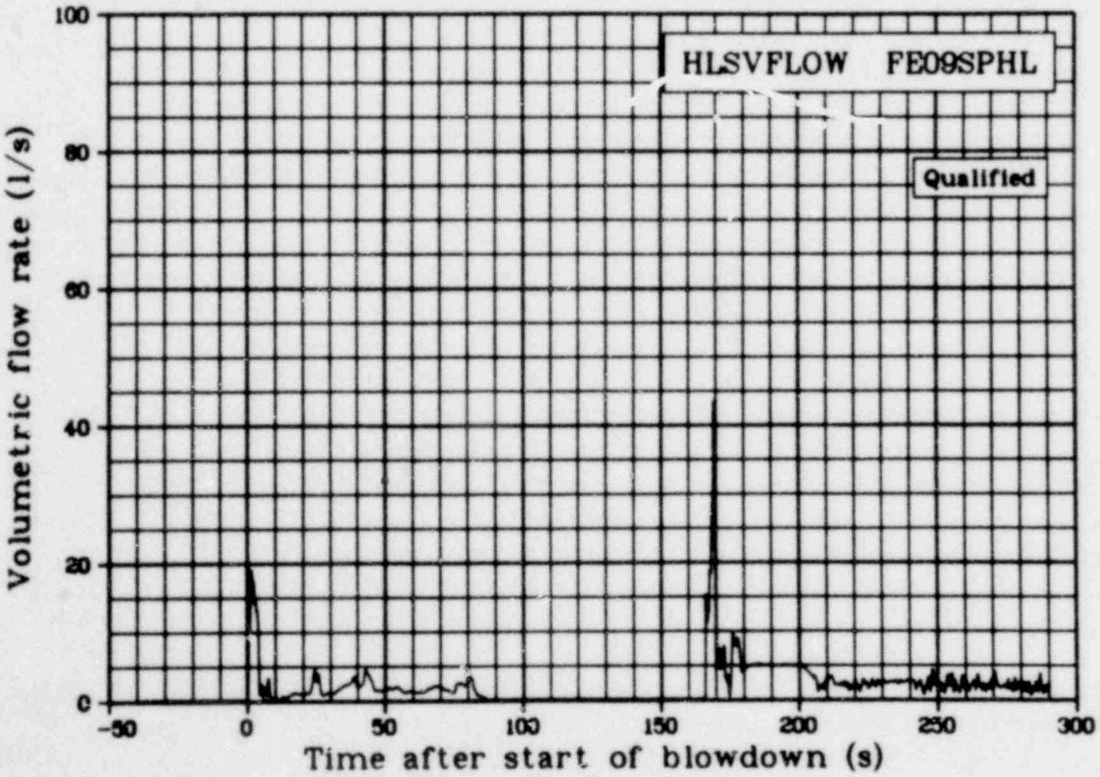

Fig. 130 Volumetric flow rate in hot leg blowdown spool (HLSVFLOW FE09SPHL), from -50 to 300 s.

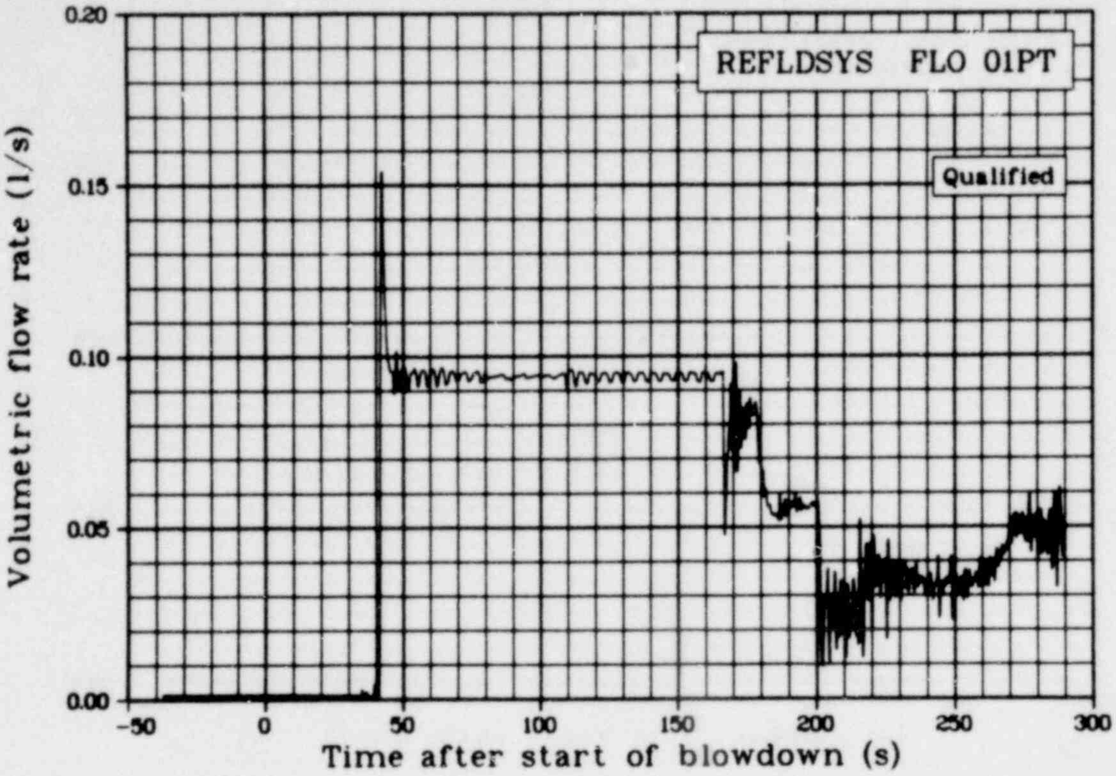

Fig. 131 Volumetric flow rate in reflood line No. 1 (REFLDSYS FL0 01PT), from -50 to 300 s.

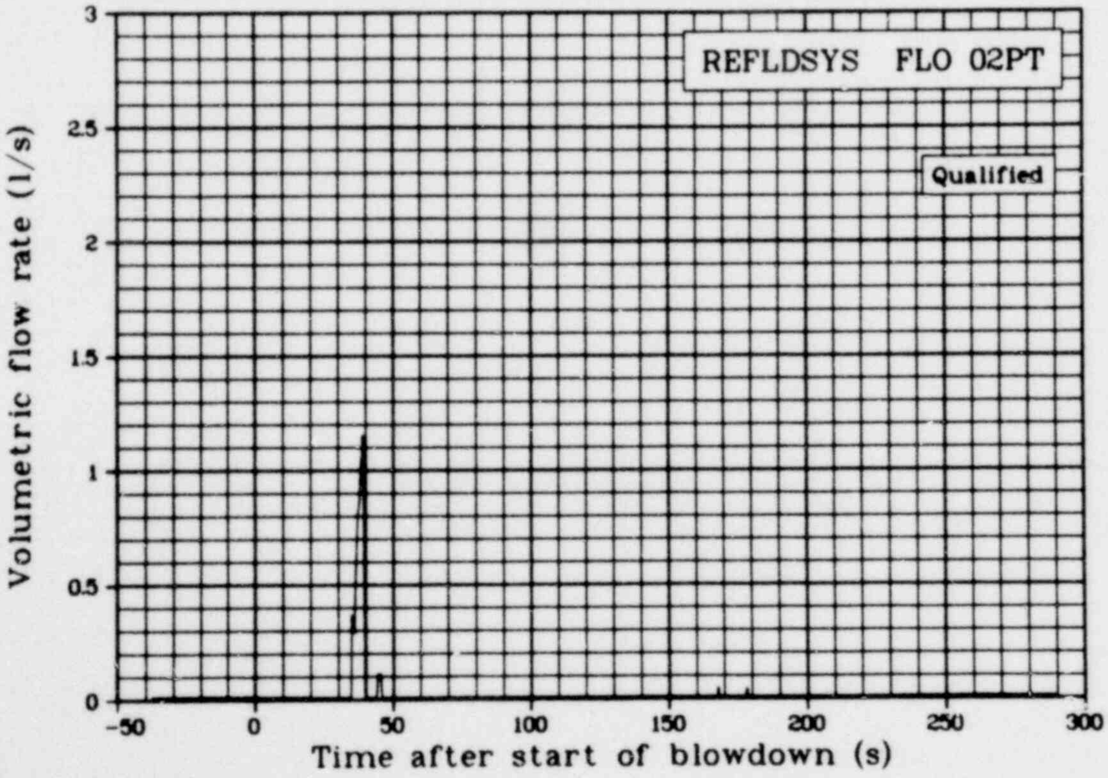

Fig. 132 Volumetric flow rate in reflood line No. 2 (REFLDSYS FL0 02PT), from -50 to 300 s.

1405 149

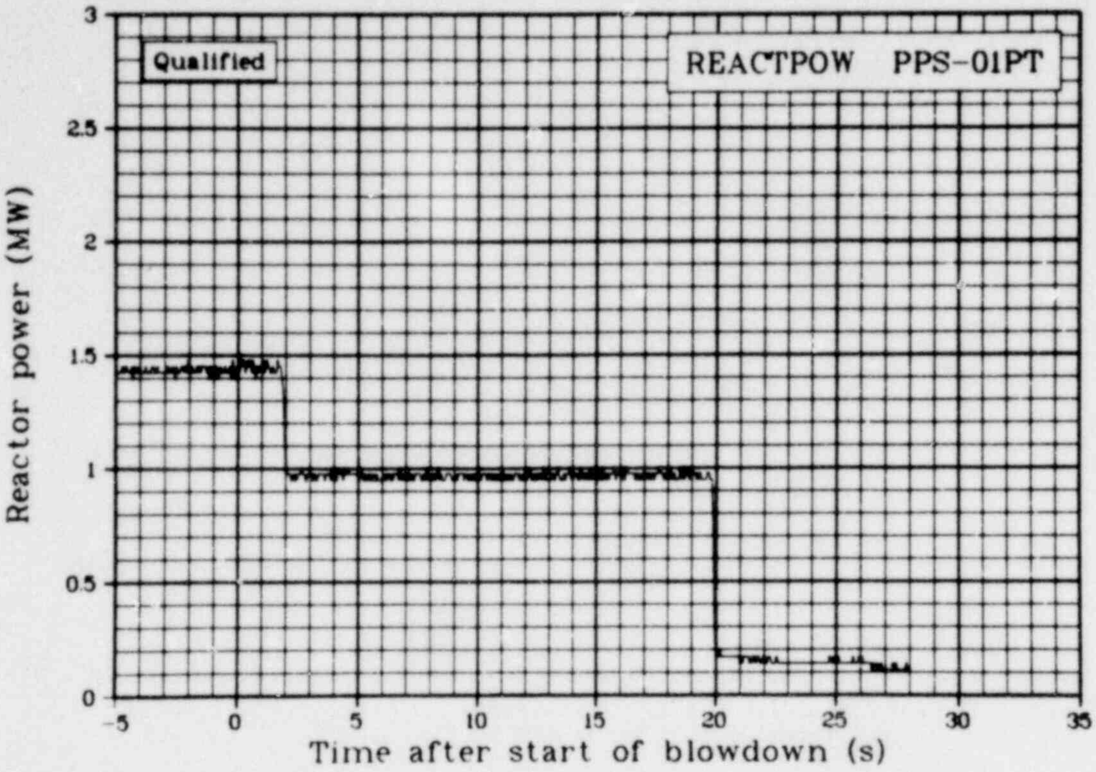

Fig. 133 Reactor power from Core Ionization Chamber PPS-1 (REACTPOW PPS-01PT), from -5 to 35 s.

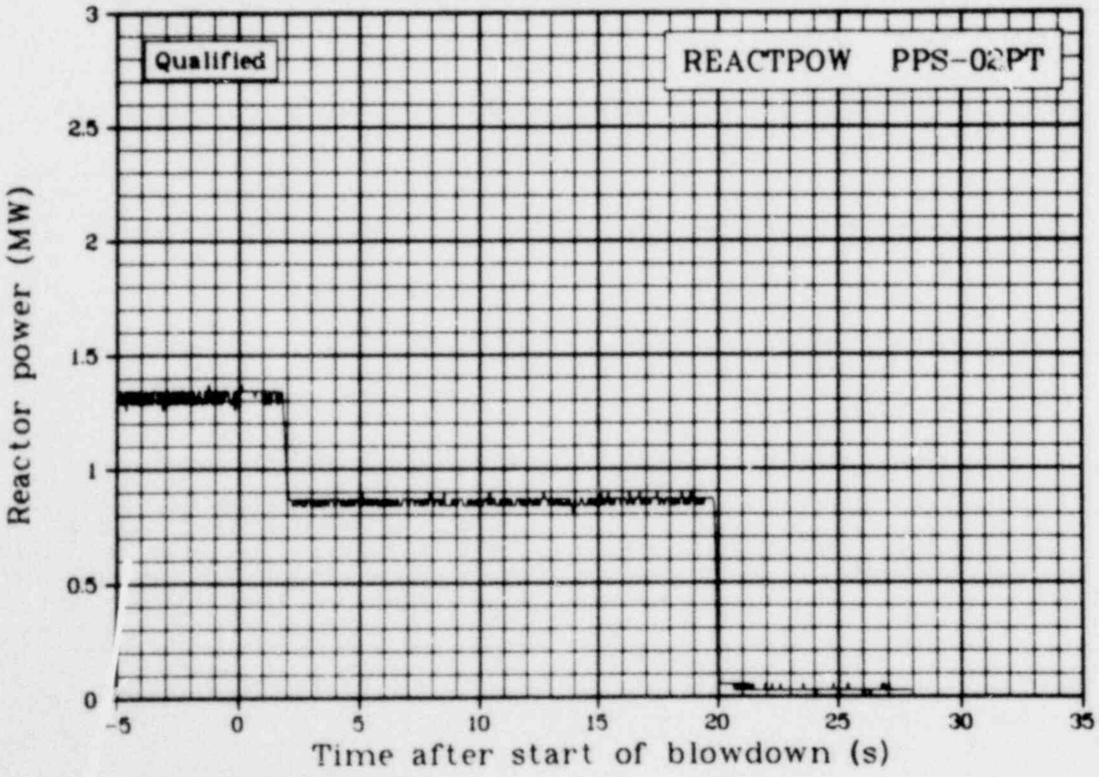

Fig. 134 Reactor power from Core Ionization Chamber PPS-2 (REACTPOW PPS-02PT), from -5 to 35 s.

TEST LLR-3

1405 151

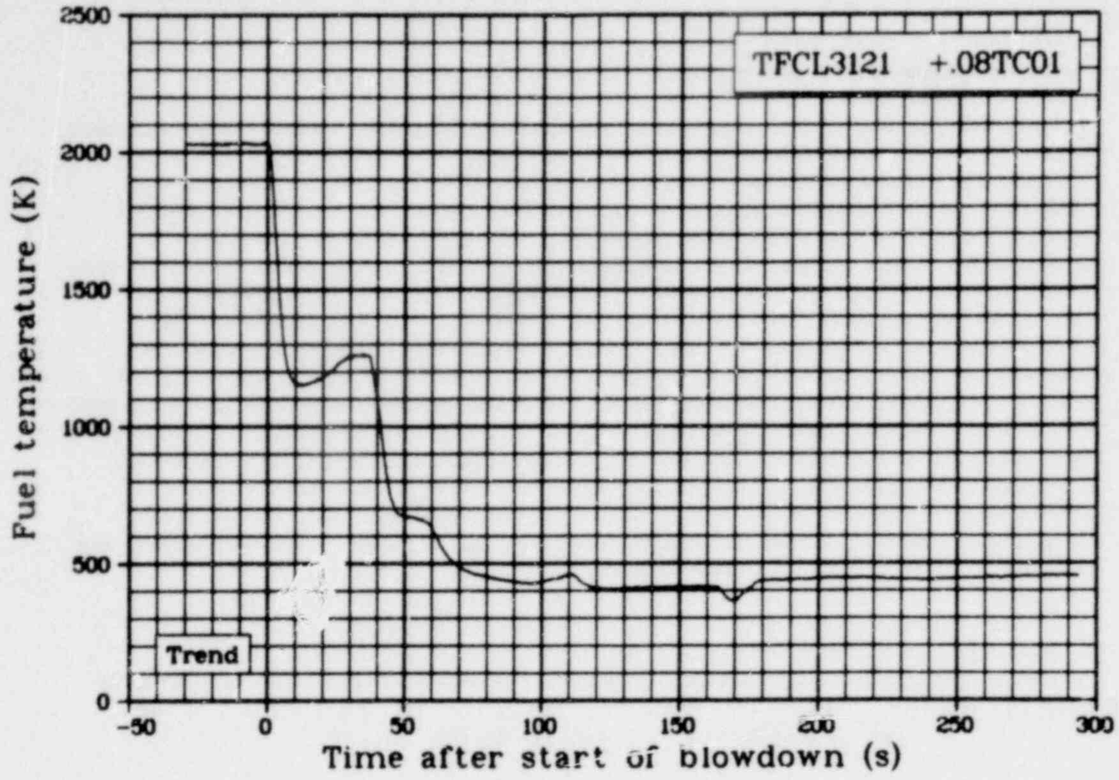

Fig. 135 Fuel temperature in Rod 312-1, 0.08 m above the fuel stack midplane (TFCL3121 + .08TC01), from -50 to 300 s.

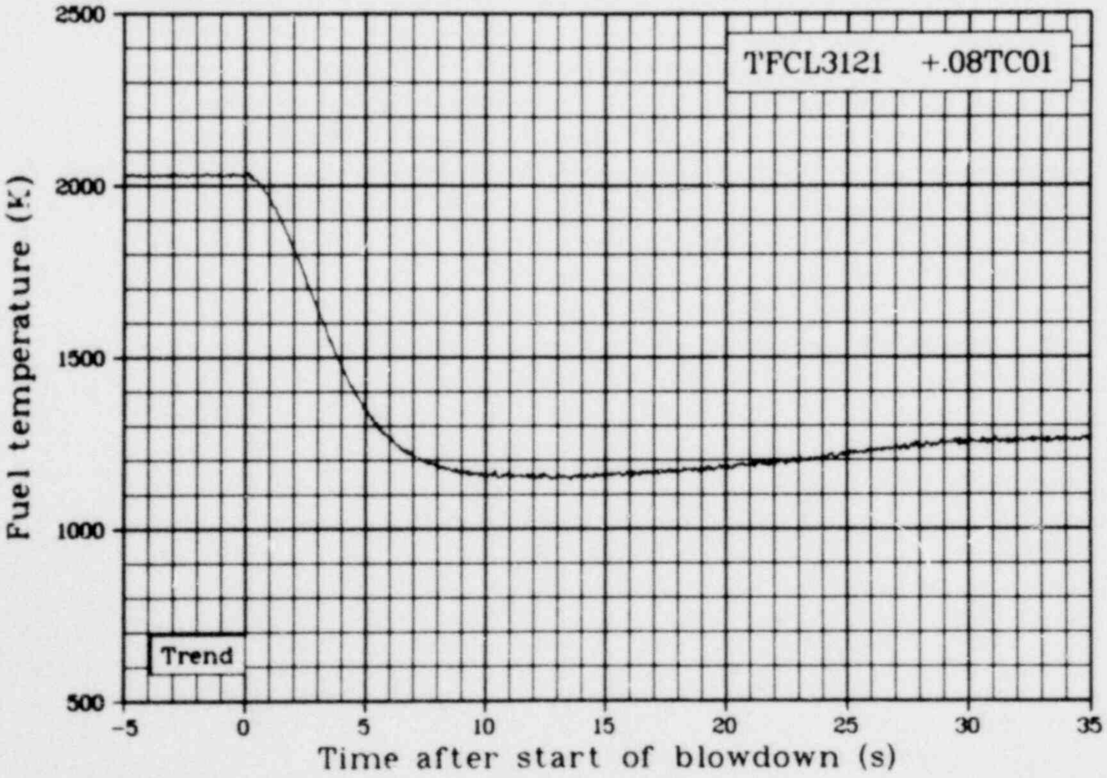

Fig. 136 Fuel temperature in Rod 312-1, 0.08 m above the fuel stack midplane (TFCL3121 + .08TC01), from -5 to 35 s.

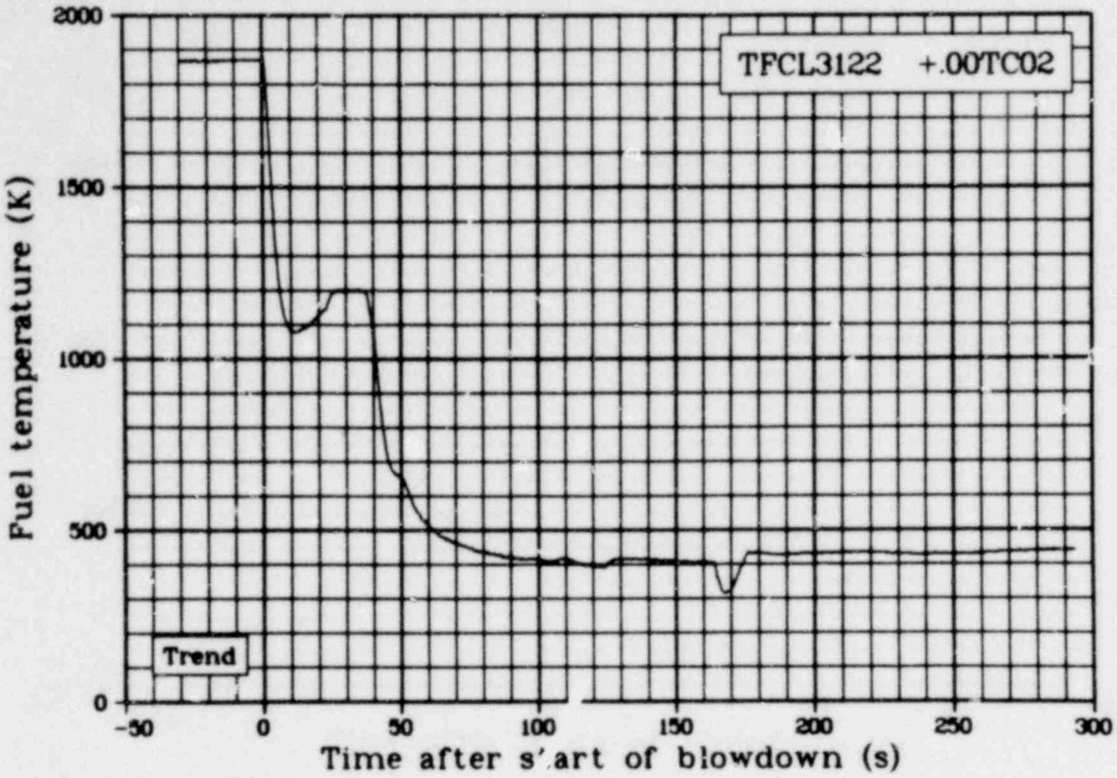

Fig. 137 Fuel temperature in Rod 312-2, at fu.l stack midplane (TFCL3122 +.00TC02), from -50 to 300 s.

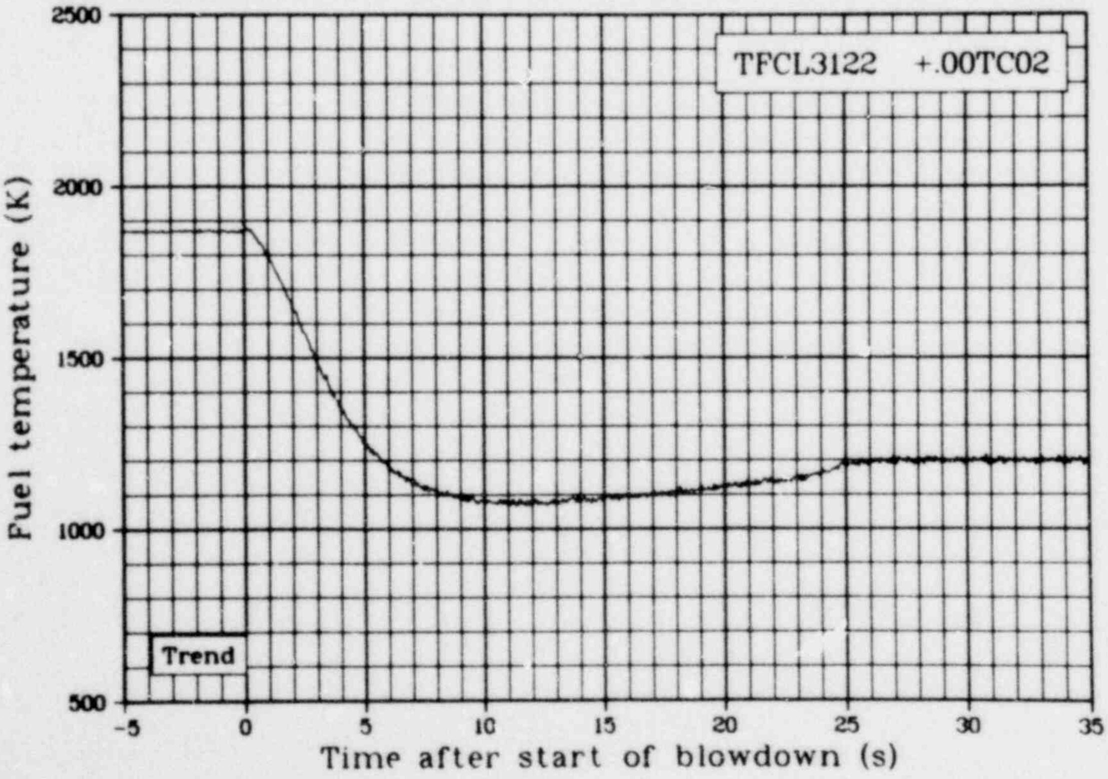

Fig. 138 Fuel temperature in Rod 312-2, at fuel stack midplane (TFCL3122 +.00TC02), from -5 to 35 s.

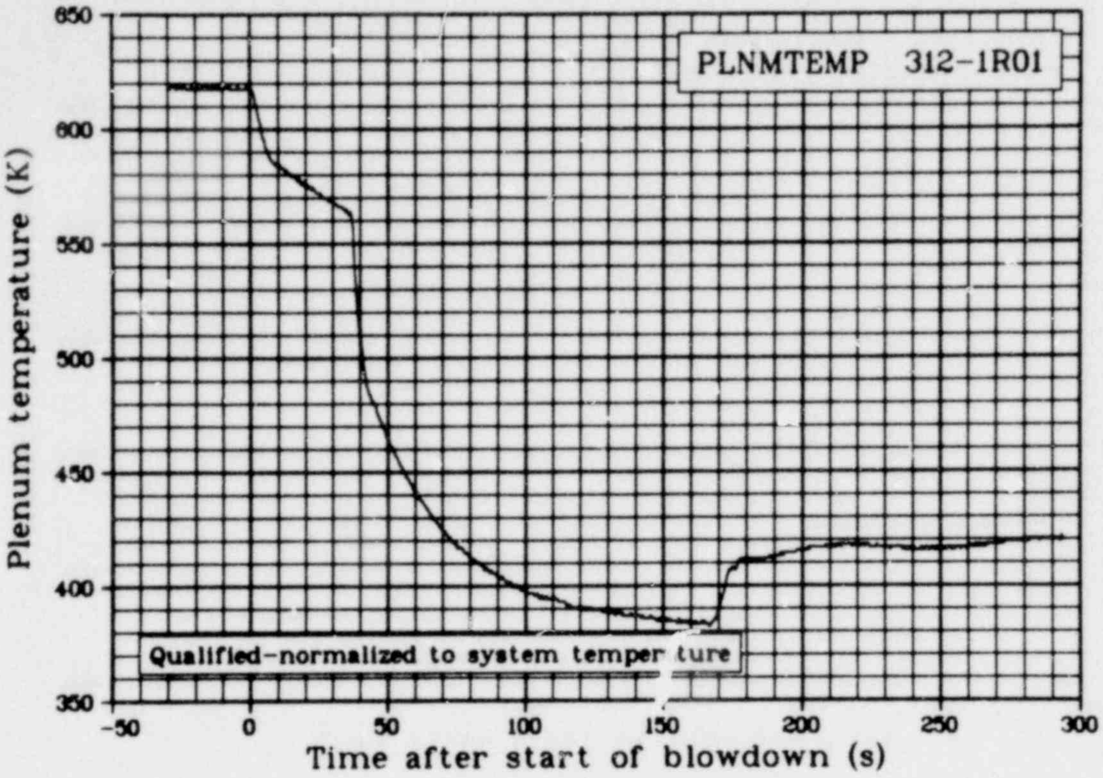

Fig. 139 Plenum temperature in Fuel Rod 312-1, (PLNMTEMP 312-1R01), from -50 to 300 s.

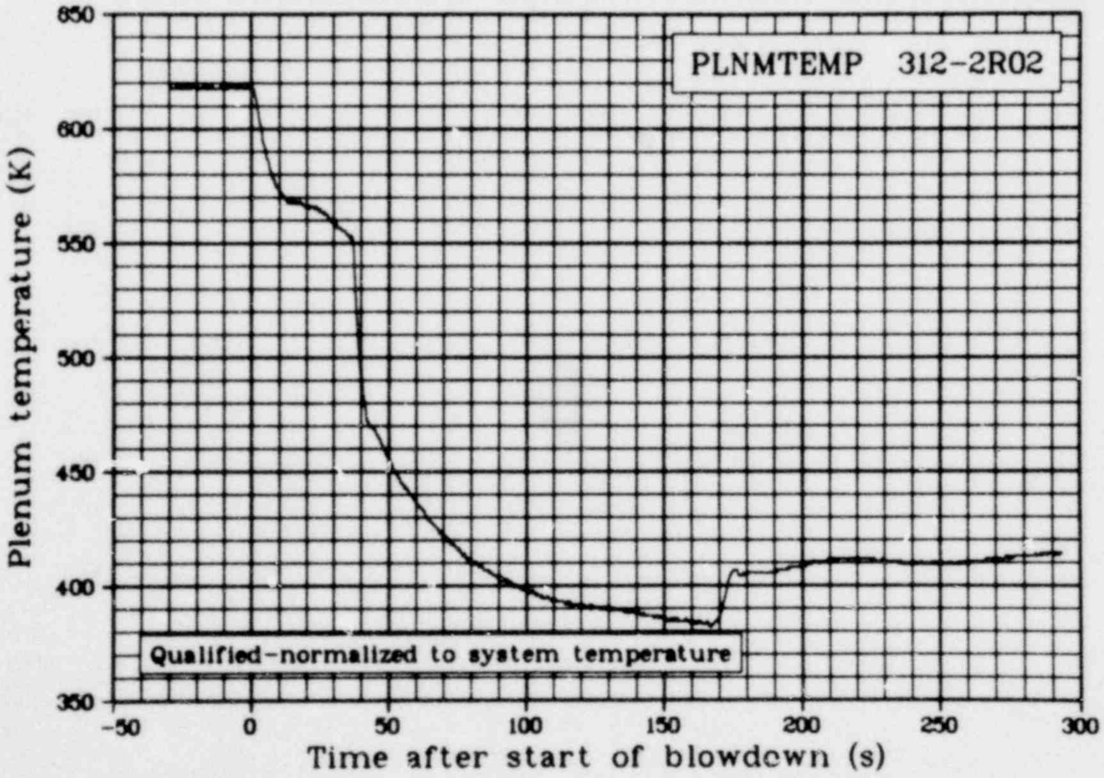

Fig. 140 Plenum temperature in Fuel Rod 312-2, (PLNMTEMP 312-2R02), from -50 to 300 s.

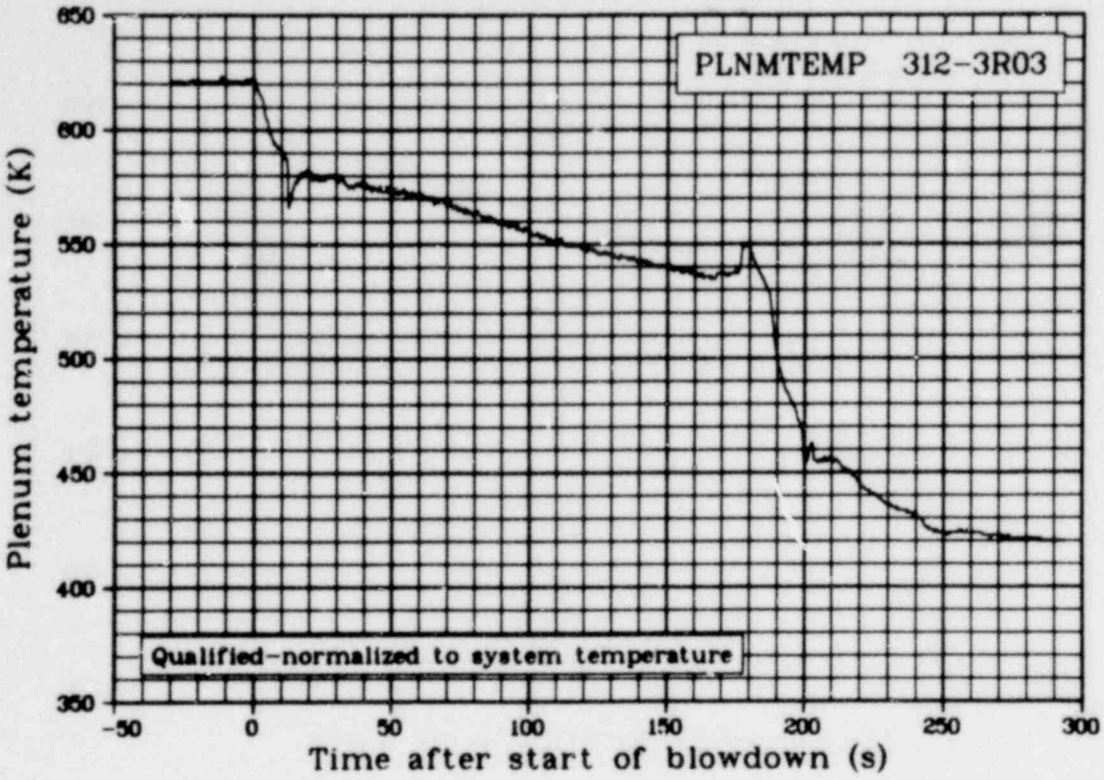

Fig. 141 Plenum temperature in Fuel Rod 312-3, (PLNMTEMP 312-3R03), from -50 to 300 s.

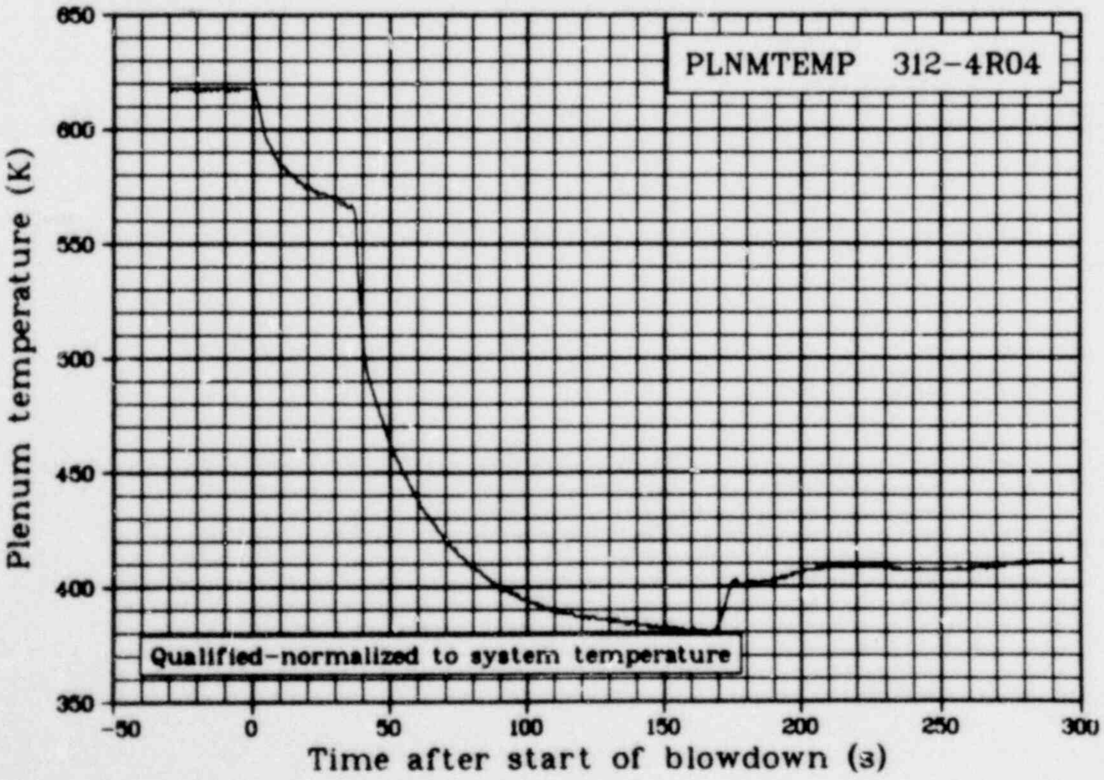

Fig. 142 Plenum temperature in Fuel Rod 312-4, (PLNMTEMP 312-4R04), from -50 to 300 s.

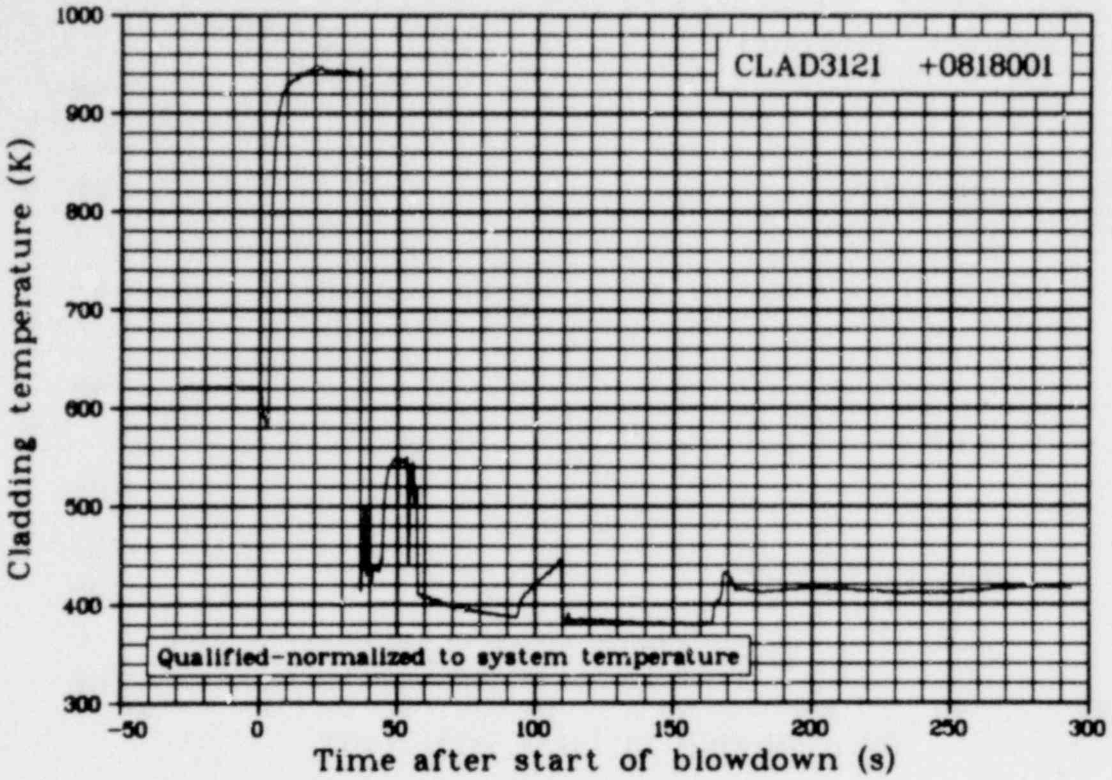

Fig. 143 Cladding temperature, Rod 312-1, at 180 degrees and 0.08 m above fuel stack midplane (CLAD3121 +0818001), from -50 to 300 s.

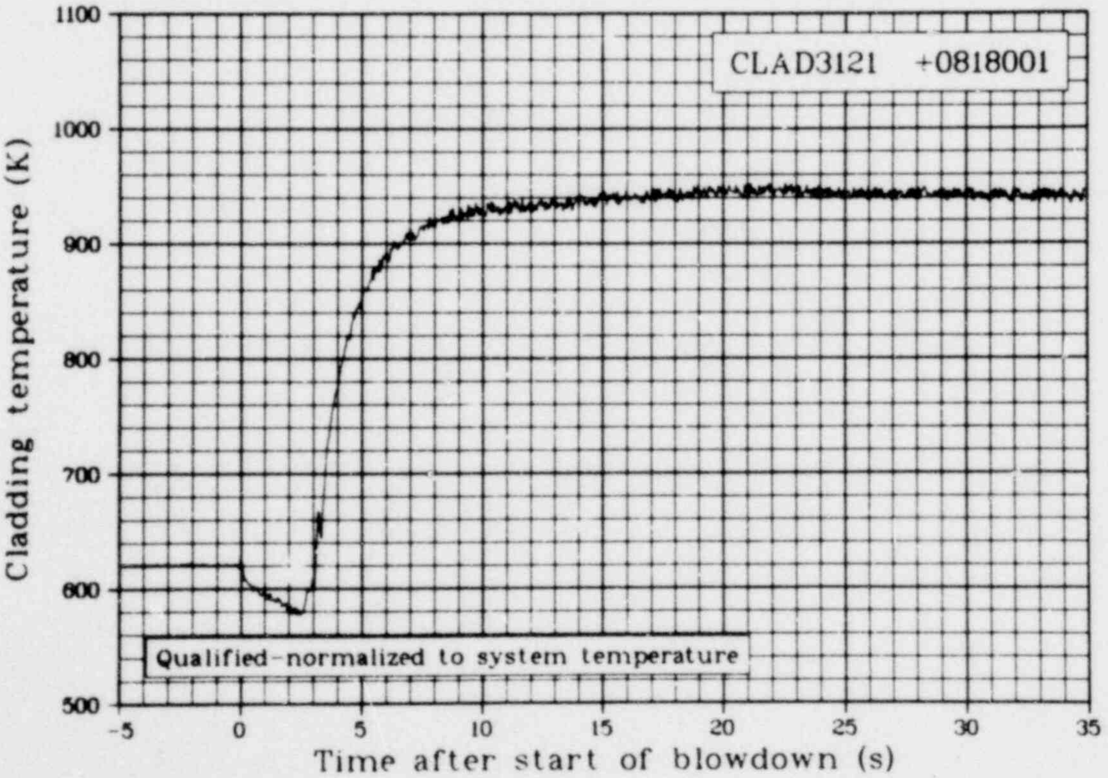

Fig. 144 Cladding temperature, Rod 312-1, at 180 degrees and 0.08 m above fuel stack midplane (CLAD3121 +0818001), from -5 to 35 s.

1405 156

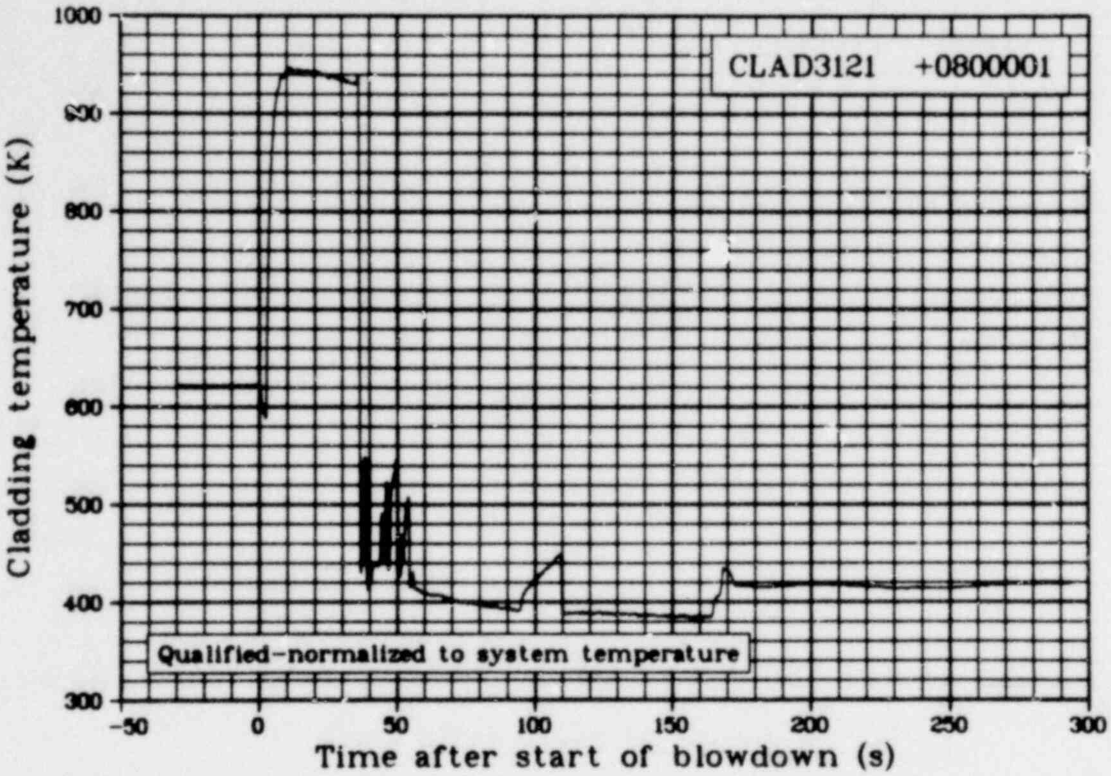

Fig. 145 Cladding temperature, Rod 312-1, at 0 degrees and 0.08 m above fuel stack midplane (CLAD3121 +0800001), from -50 to 300 s.

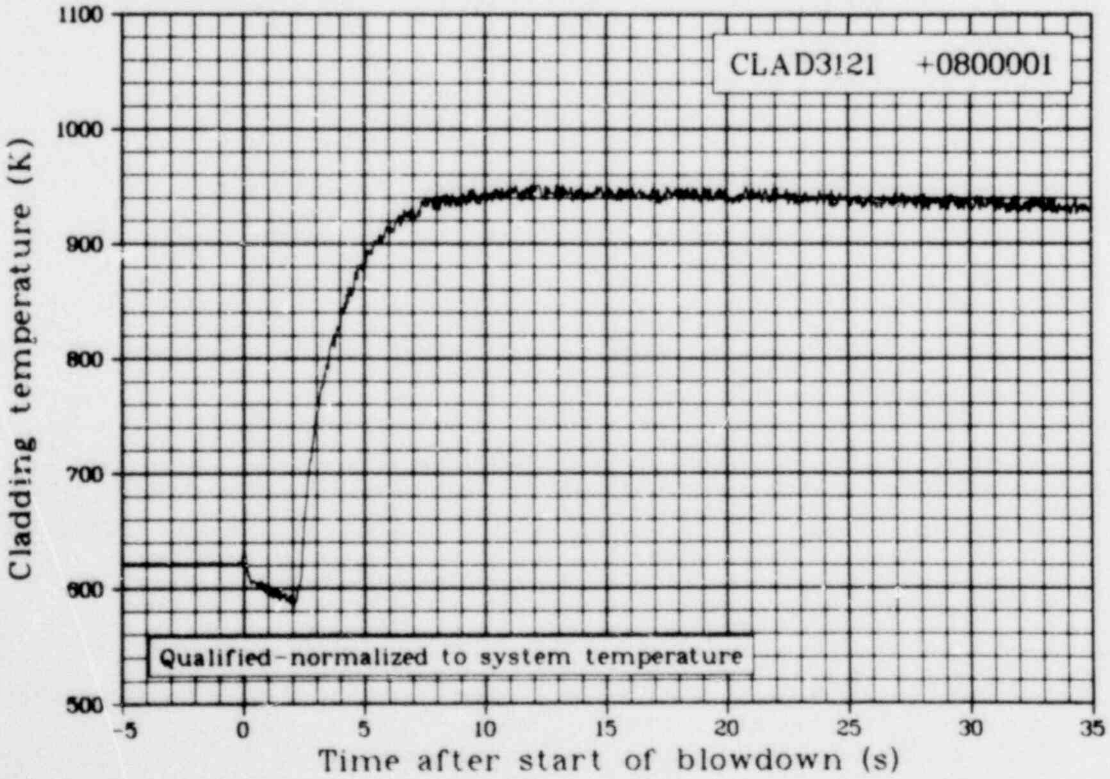

Fig. 146 Cladding temperature, Rod 312-1, at 0 degrees and 0.08 m above fuel stack midplane (CLAD3121 +0800001), from -5 to 35 s.

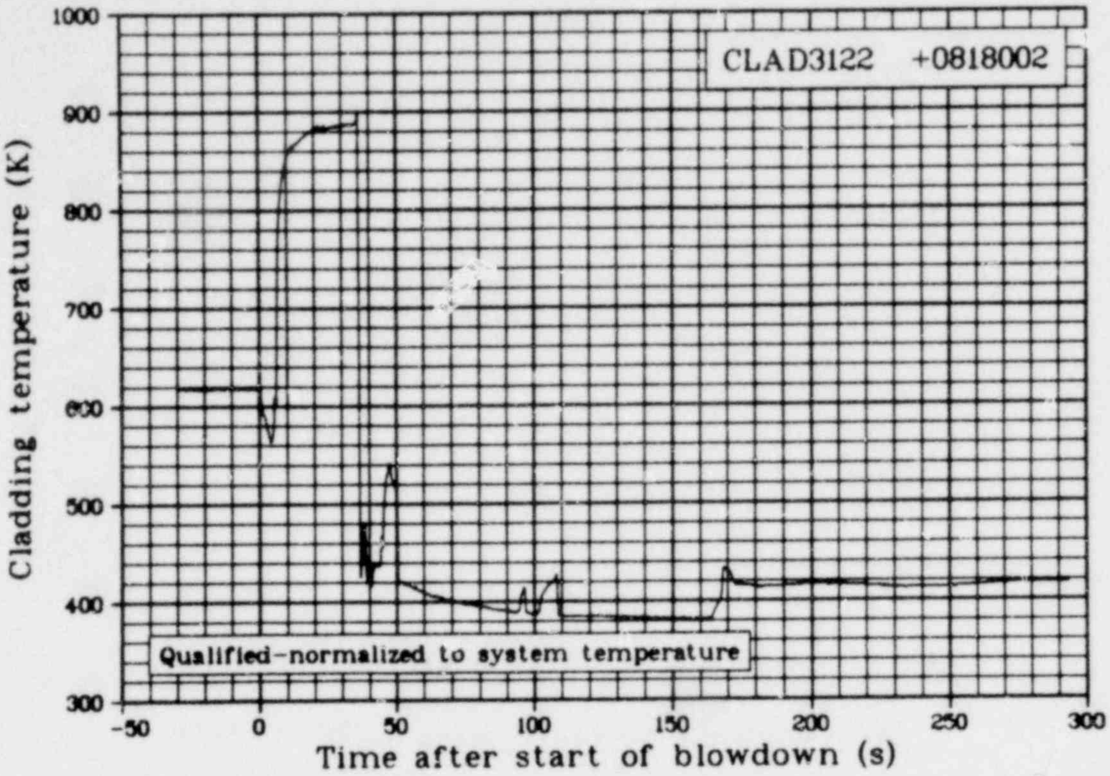

Fig. 147 Cladding temperature, Rod 312-2, at 180 degrees and 0.08 m above fuel stack midplane (CLAD3122 +0818002), from -50 to 300 s.

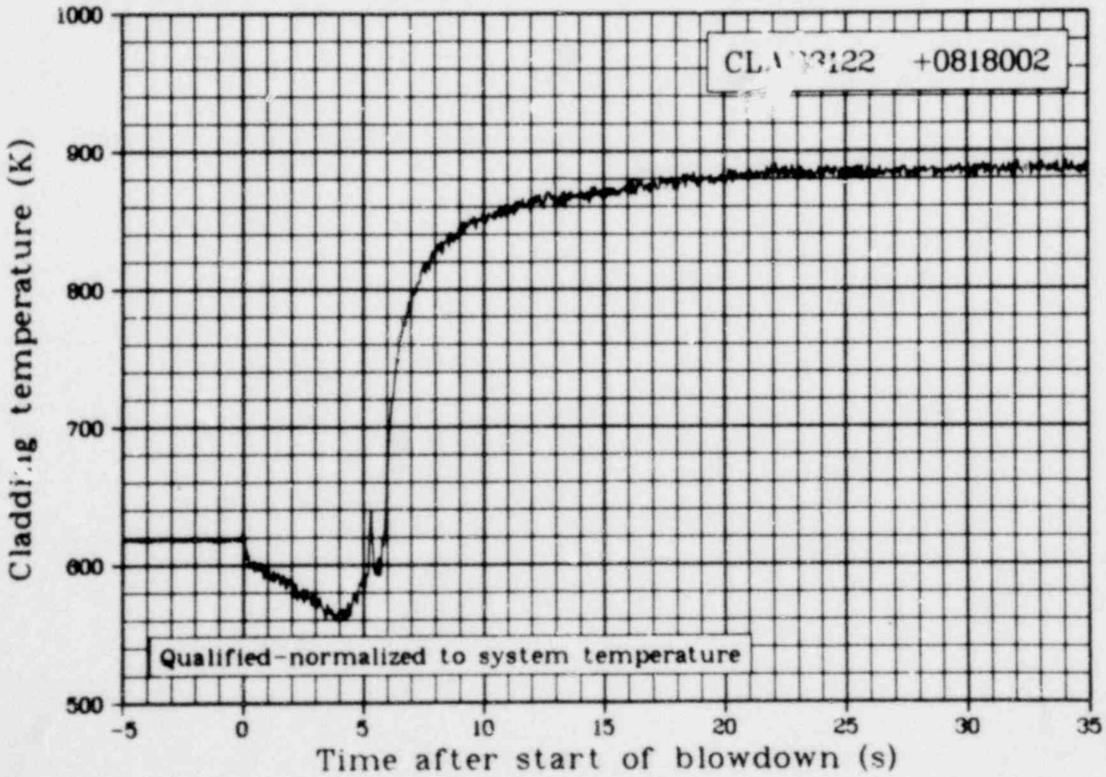

Fig. 148 Cladding temperature, Rod 312-2, at 180 degrees and 0.08 m above fuel stack midplane (CLAD3122 +0818002), from -5 to 35 s.

1405 158

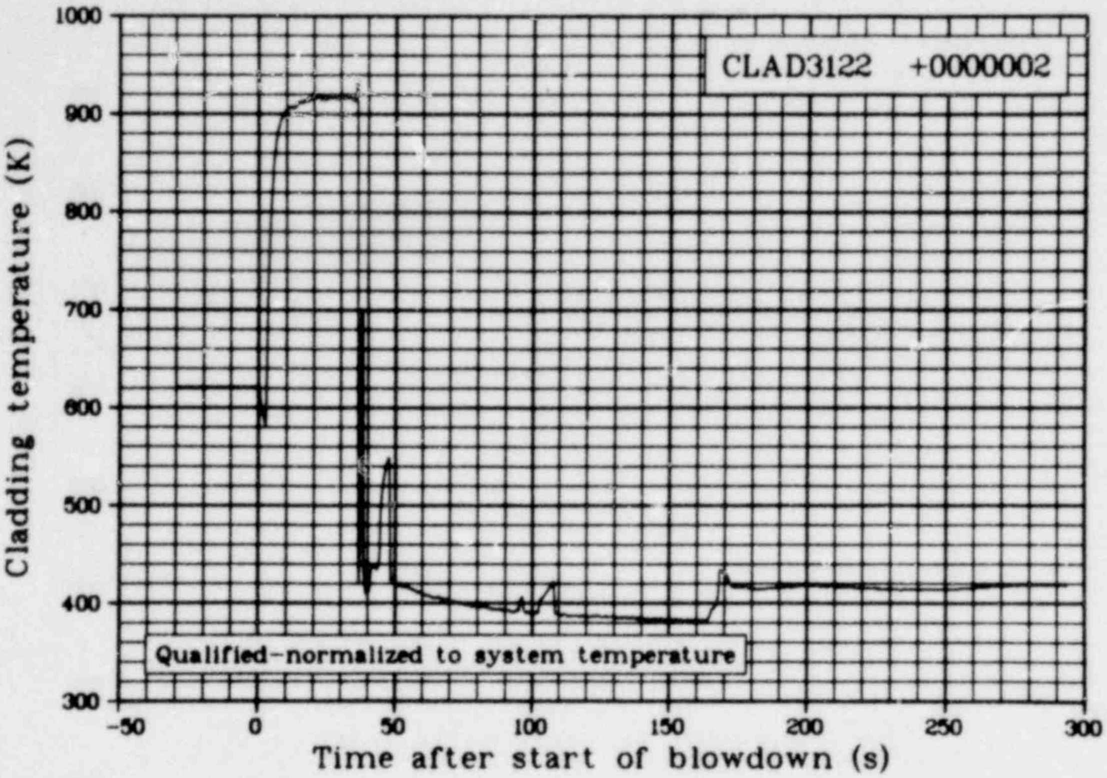

Fig. 149 Cladding temperature, Rod 312-2, at 0 degrees and fuel stack midplane (CLAD3122 + 0000002), from -50 to 300 s.

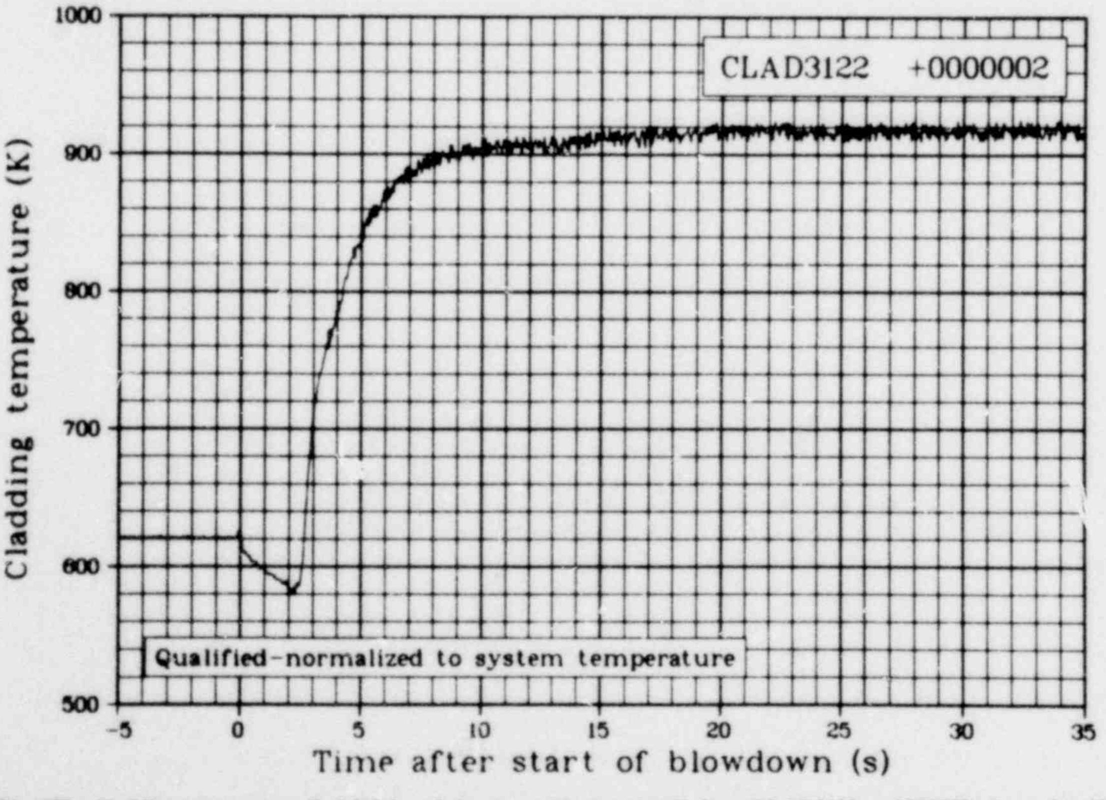

Fig. 150 Cladding temperature, Rod 312-2, at 0 degrees and fuel stack midplane (CLAD3122 + 0000002), from -5 to 35 s.

1405 159

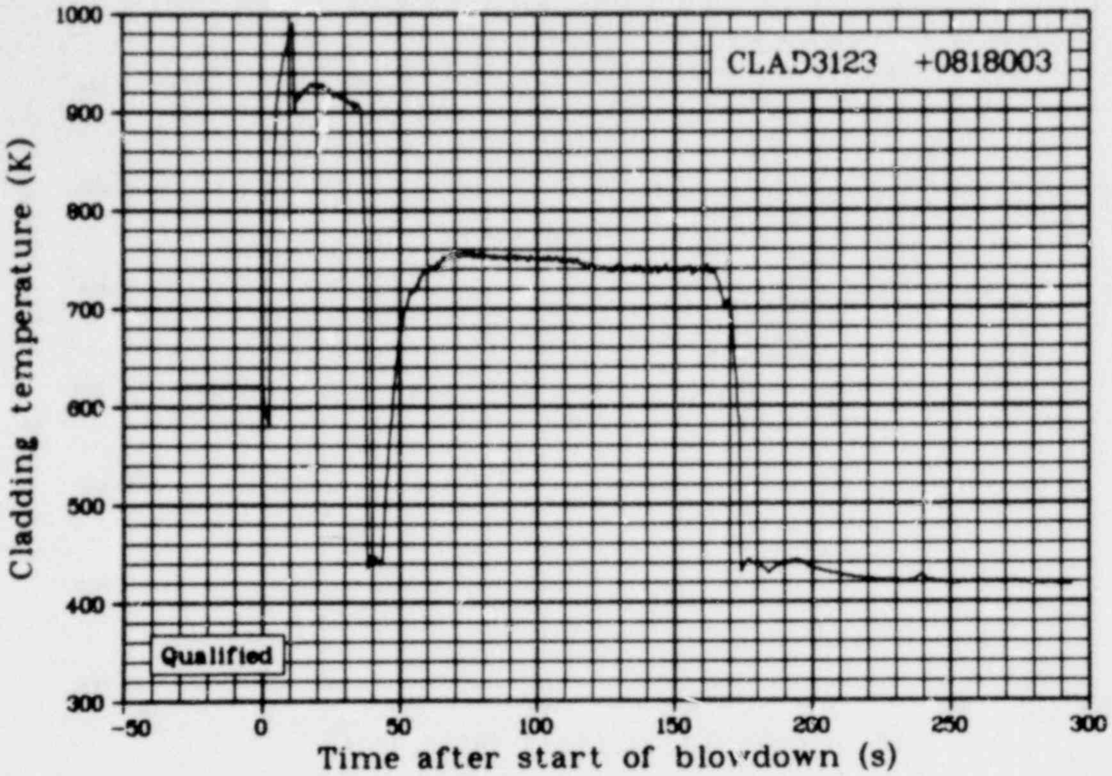

Fig. 151 Cladding temperature, Rod 312-3, at 180 degrees and 0.08 m above fuel stack midplane (CLAD3123 +0818003), from -50 to 300 s.

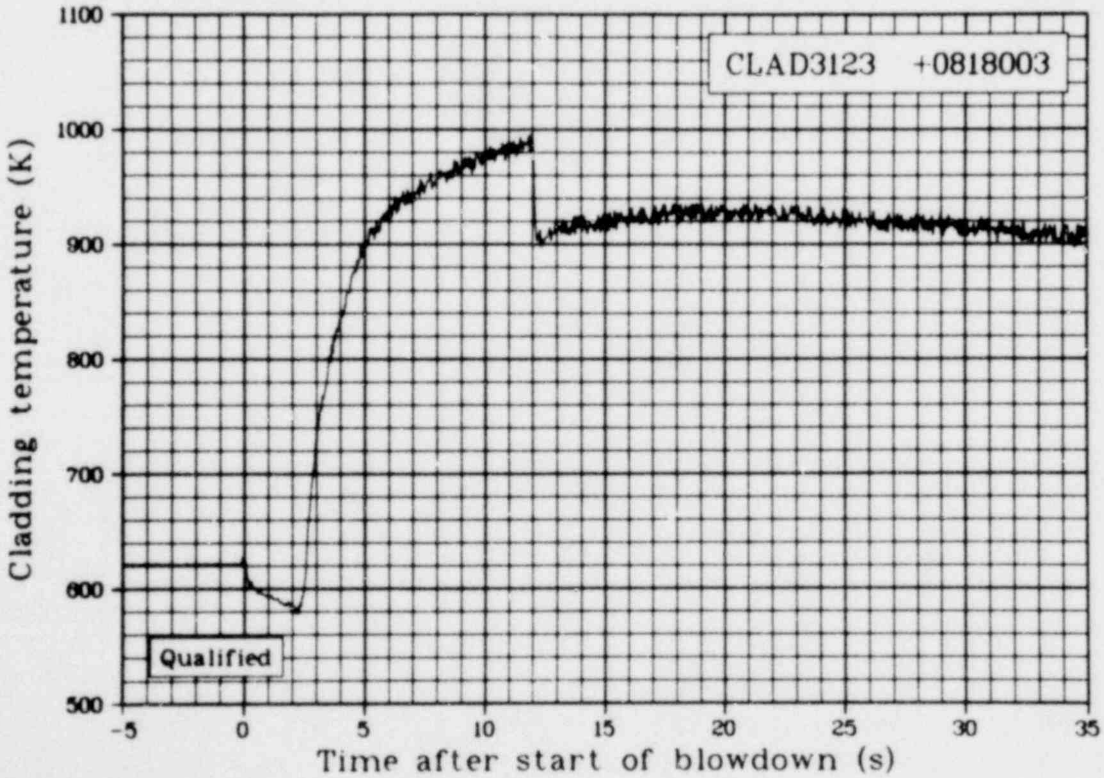

Fig. 152 Cladding temperature, Rod 312-3, at 180 degrees and 0.08 m above fuel stack midplane (CLAD3123 +0818003), from -5 to 35 s.

1405 160

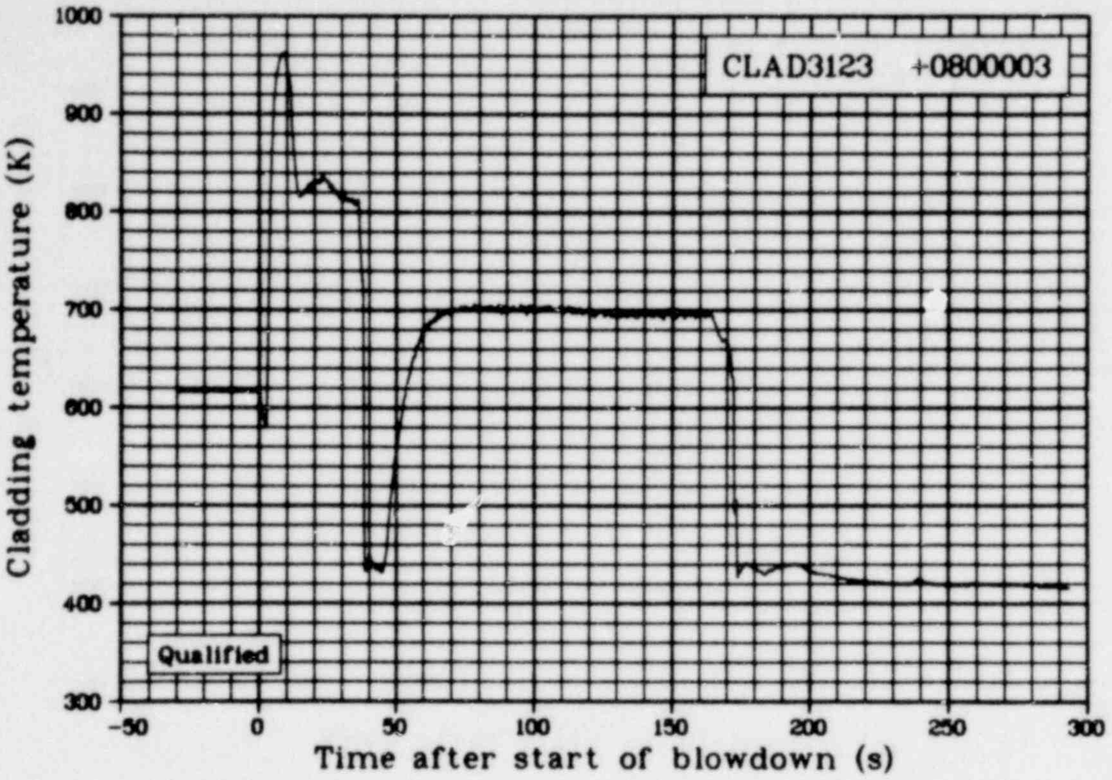

Fig. 153 Cladding temperature, Rod 312-3, at 0 degrees and 0.08 m above fuel stack midplane (CLAD3123 +0800003), from -50 to 300 s.

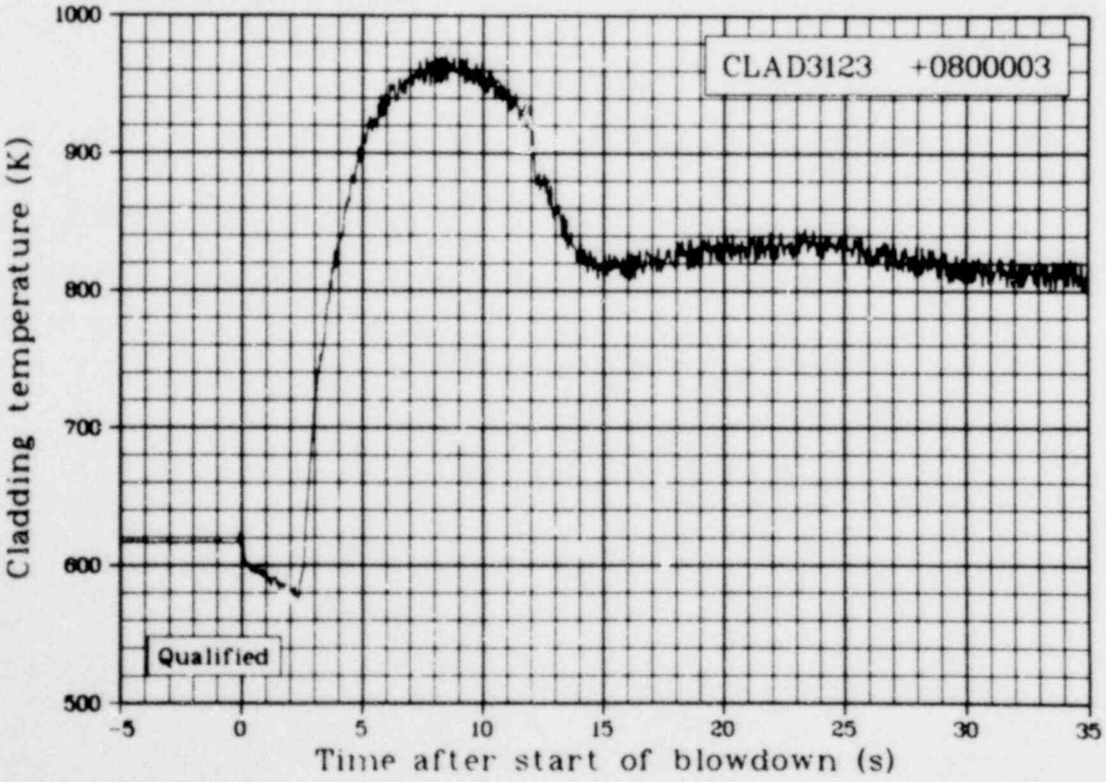

Fig. 154 Cladding temperature, Rod 312-3, at 0 degrees and 0.08 m above fuel stack midplane (CLAD3123 +0800003), from -5 to 35 s.

1405 161

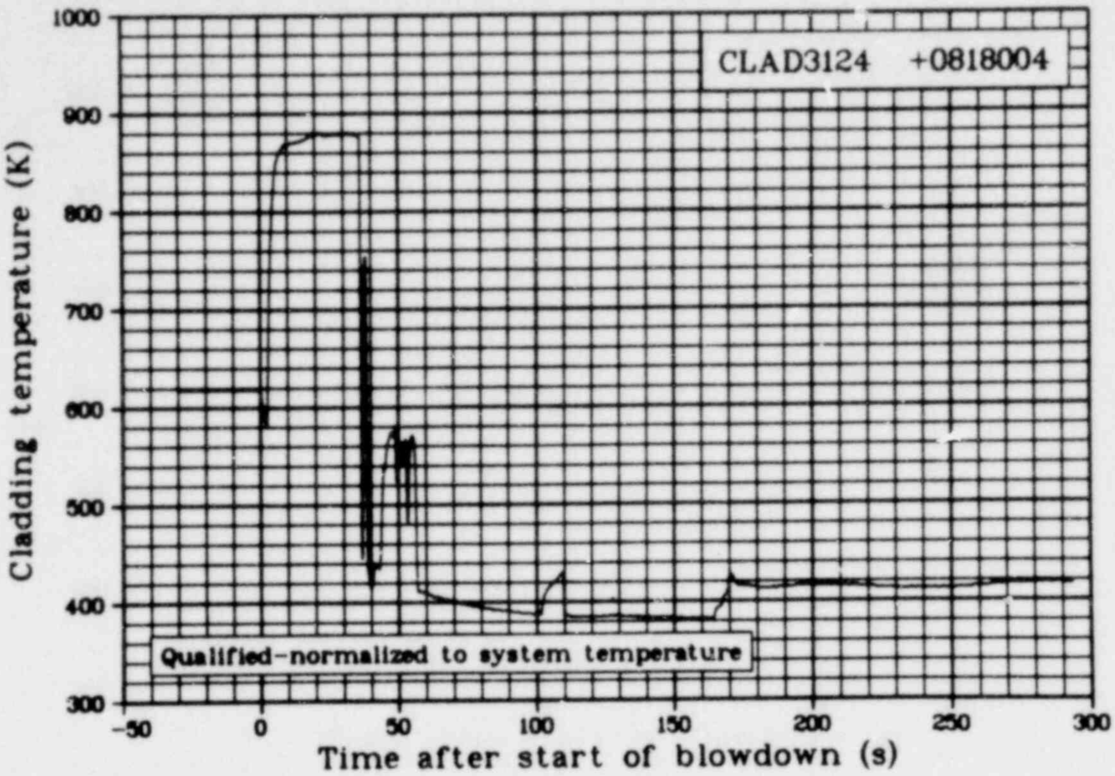

Fig. 155 Cladding temperature, Rod 312-4, at 180 degrees and 0.08 m above fuel stack midplane (CLAD3124 +0818004), from -50 to 300 s.

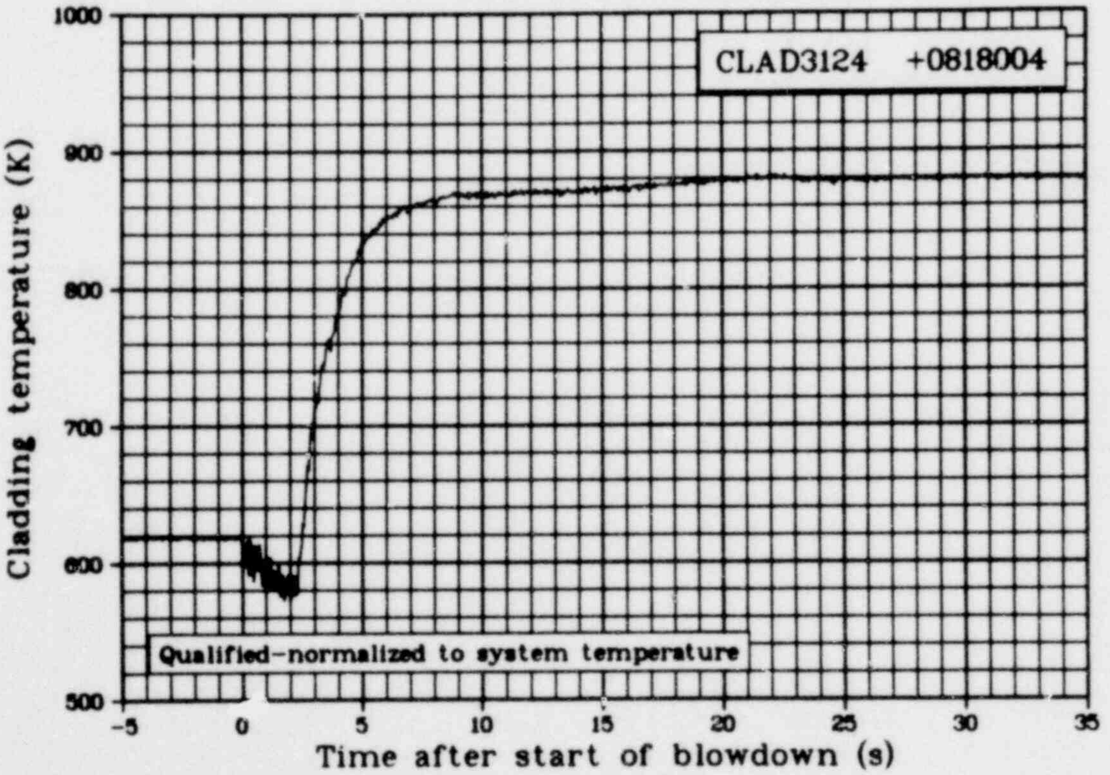

Fig. 156 Cladding temperature, Rod 312-4, at 180 degrees and 0.08 m above fuel stack midplane (CLAD3124 +0818004), from -5 to 35 s.

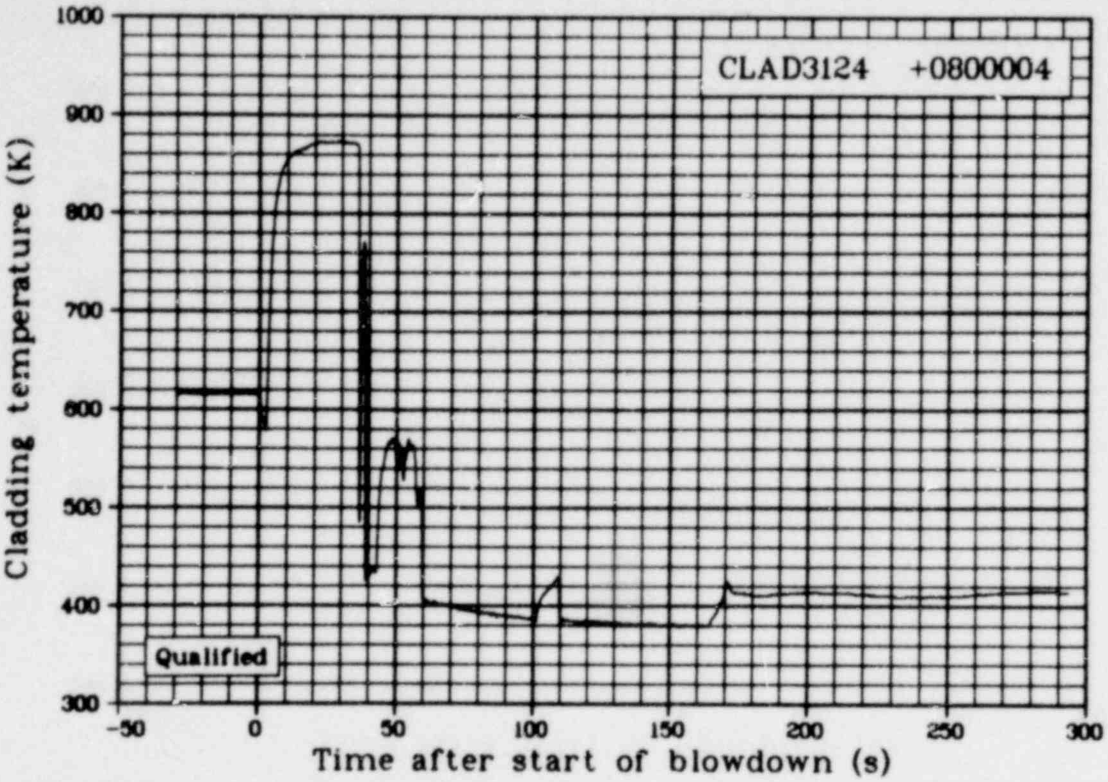

Fig. 157 Cladding temperature, Rod 312-4, at 0 degrees and 0.08 m above fuel stack midplane (CLAD3124 +0800004), from -50 to 300 s.

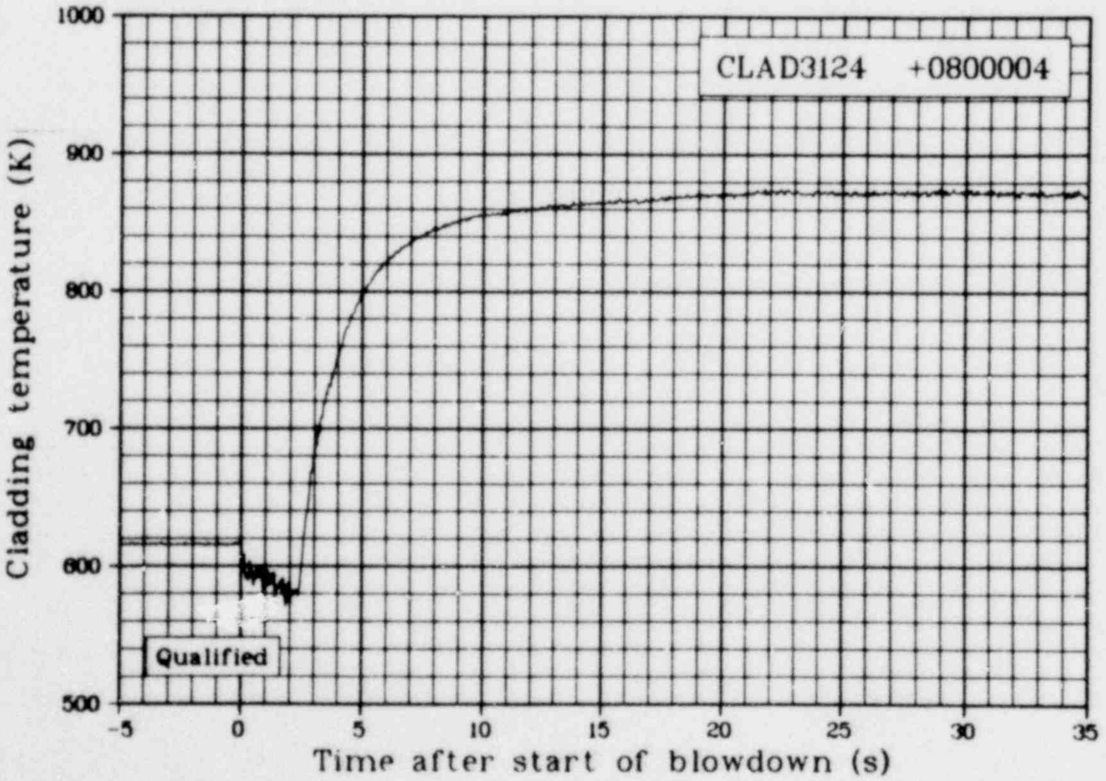

Fig. 158 Cladding temperature, Rod 312-4, at 0 degrees and 0.08 m above fuel stack midplane (CLAD3124 +0800004), from -5 to 35 s.

1405 163

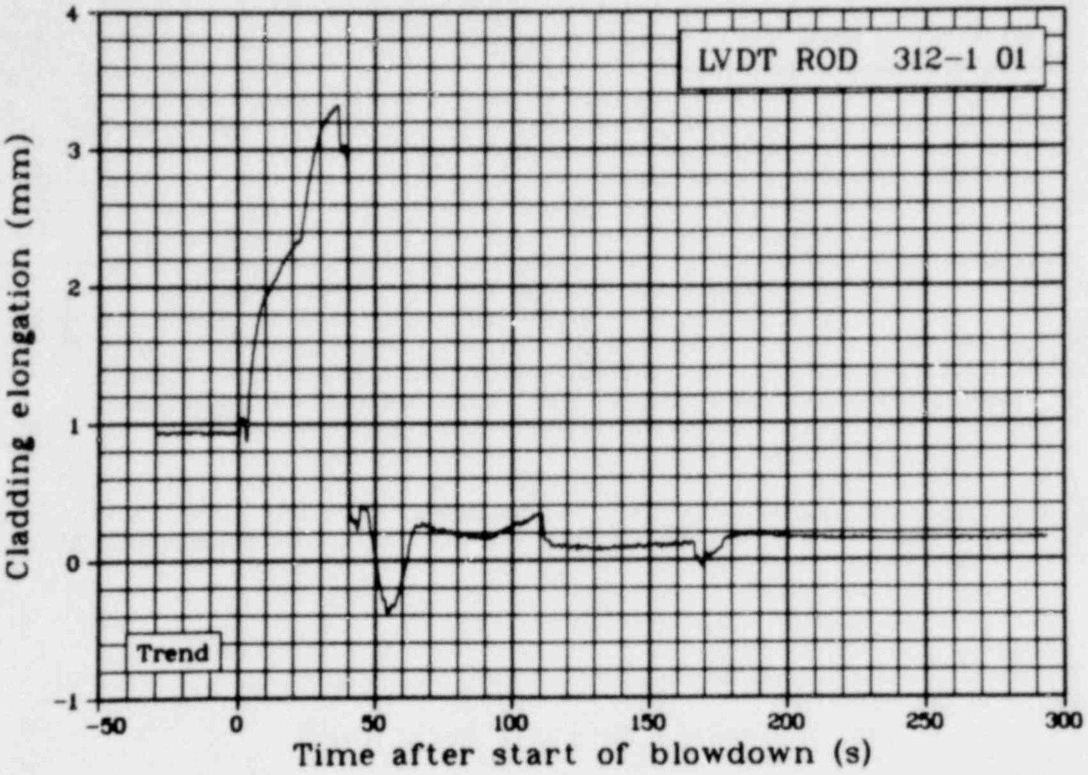

Fig. 159 Cladding elongation of Fuel Rod 312-1 (LVDT ROD 312-1 01), from -50 to 300 s.

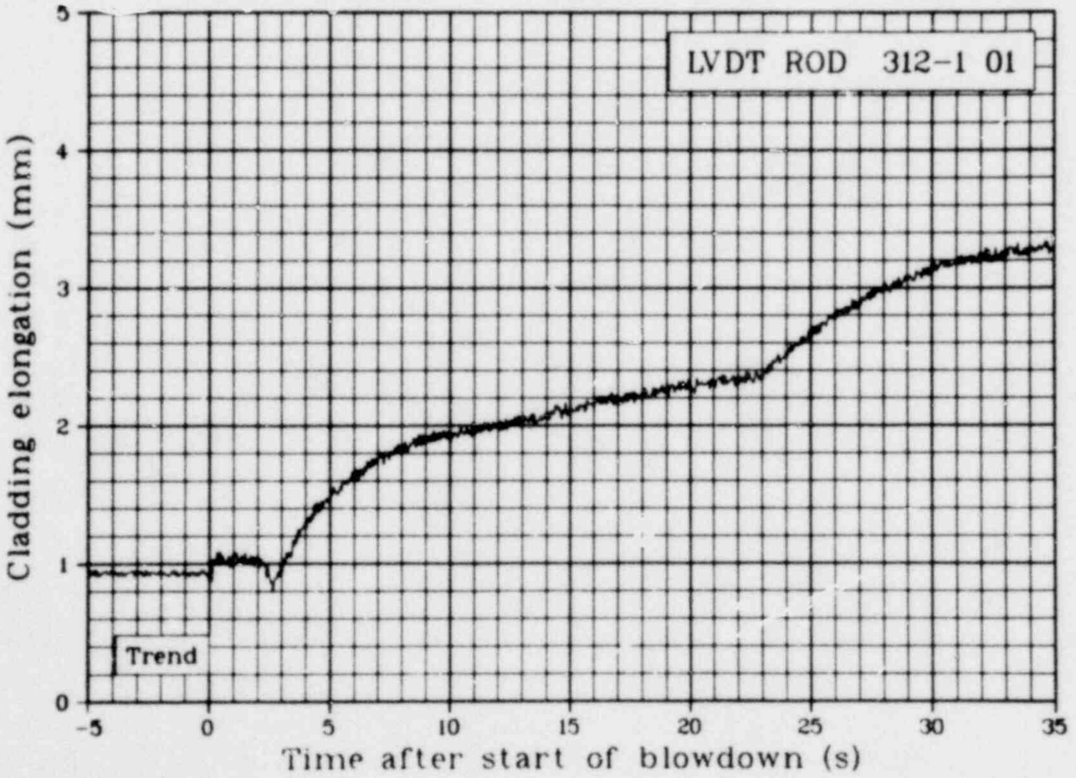

Fig. 160 Cladding elongation of Fuel Rod 312-1 (LVDT ROD 312-1 01), from -5 to 35 s.

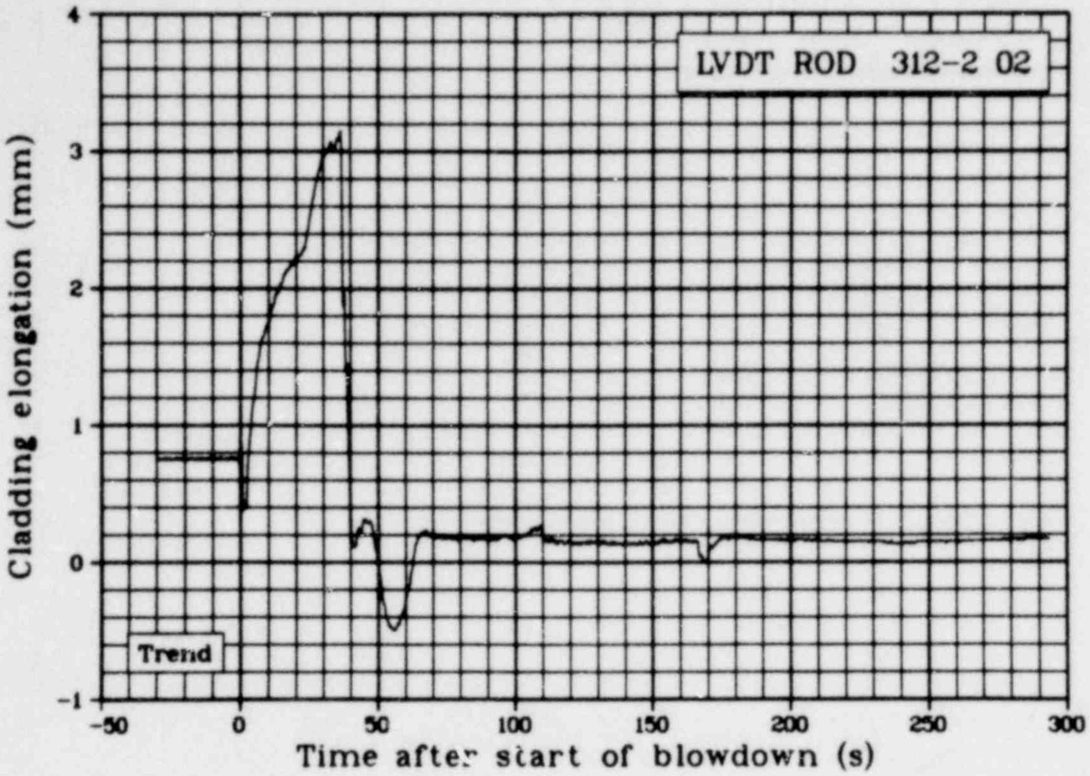

Fig. 161 Cladding elongation of Fuel Rod 312-2 (LVDT ROD 312-2 02), from -50 to 300 s.

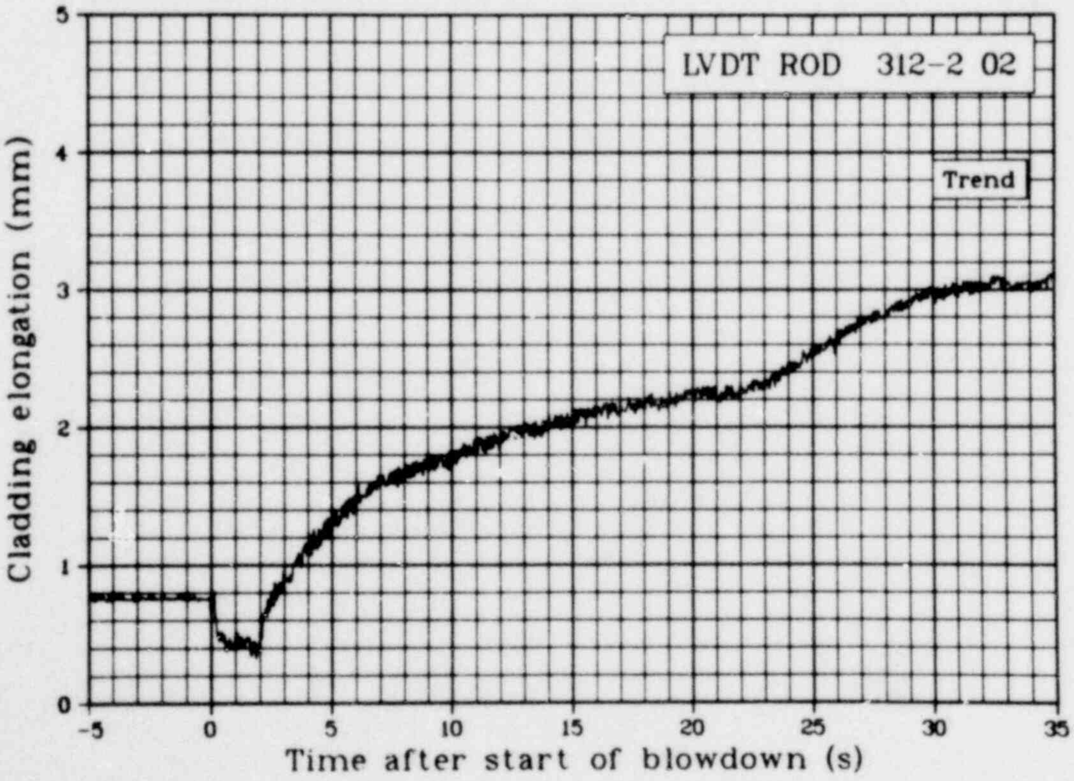

Fig. 162 Cladding elongation of Fuel Rod 312-2 (LVDT ROD 312-2 02), from -5 to 35 s.

1405 165

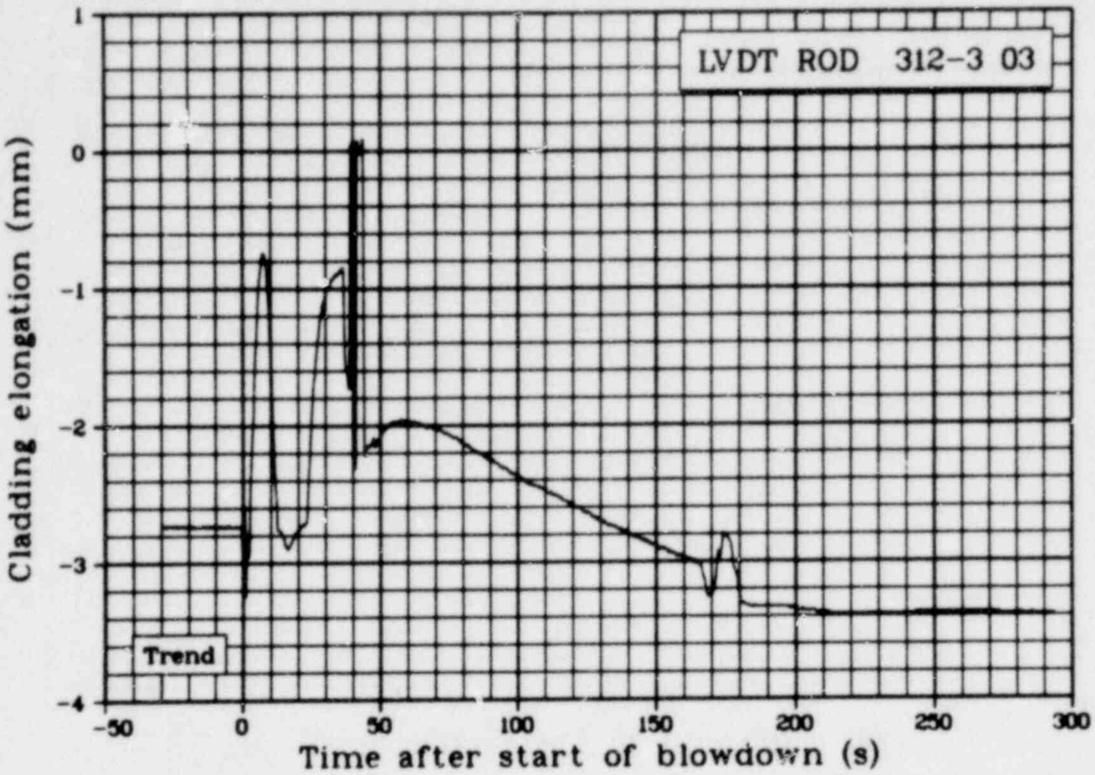

Fig. 163 Cladding elongation of Fuel Rod 312-3 (LVDT ROD 312-3 03), from -50 to 300 s.

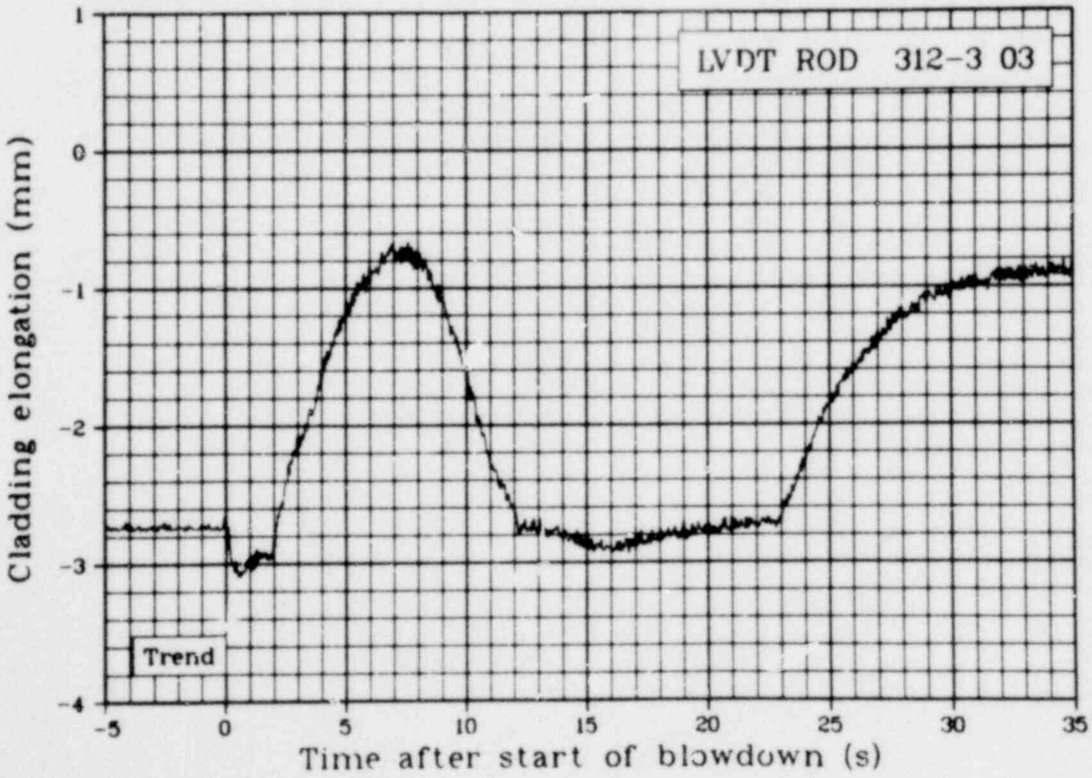

Fig. 164 Cladding elongation of Fuel Rod 312-3 (LVDT ROD 312-3 03), from -5 to 35 s.

1405 166

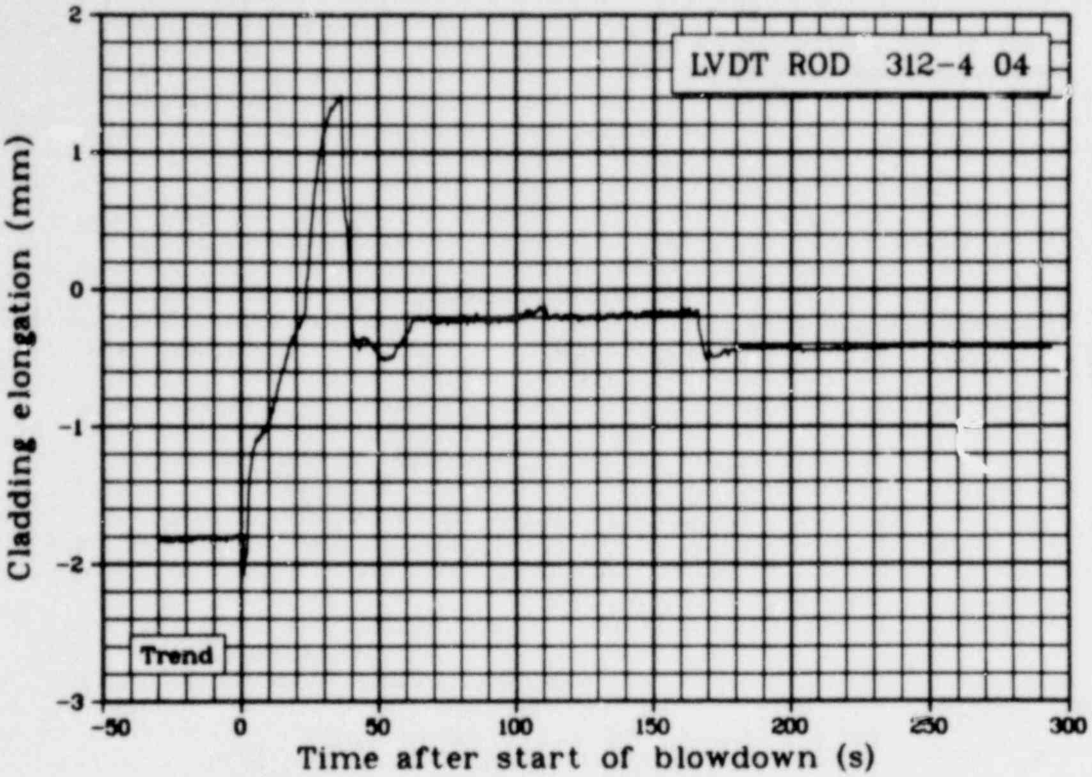

Fig. 165 Cladding elongation of Fuel Rod 312-4 (LVDT ROD 312-4 04), from -50 to 300 s.

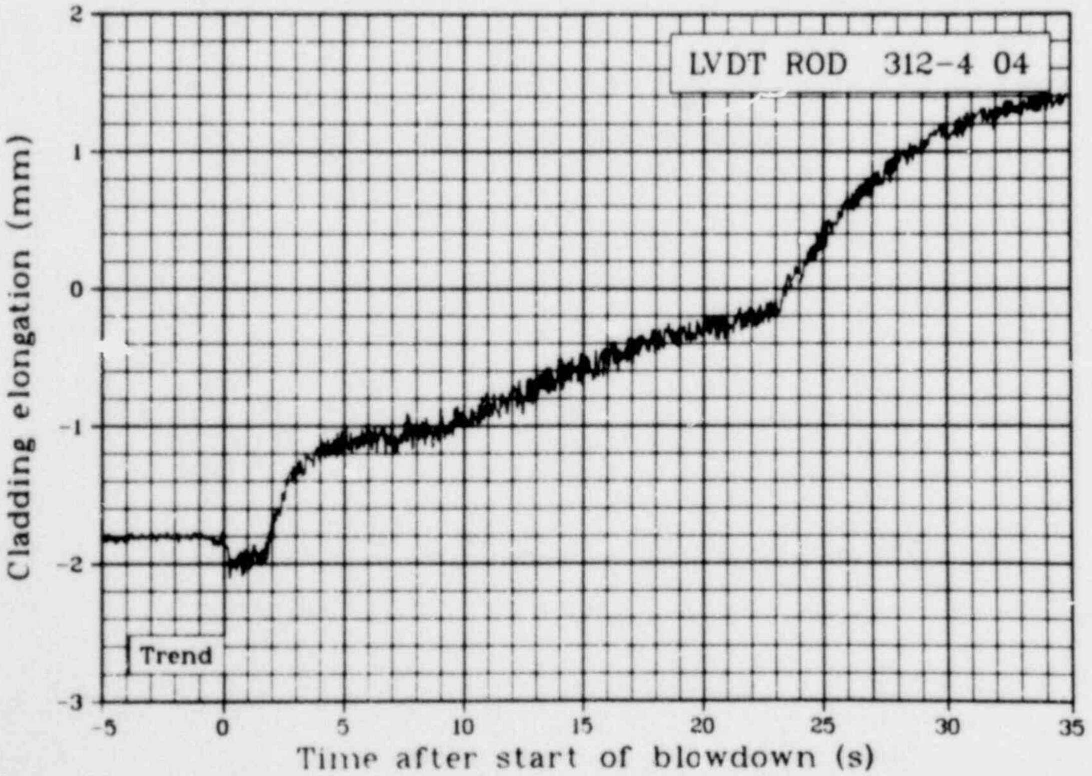

Fig. 166 Cladding elongation of Fuel Rod 312-4 (LVDT R(.D 312-4 04), from -5 to 35 s.

1405 167

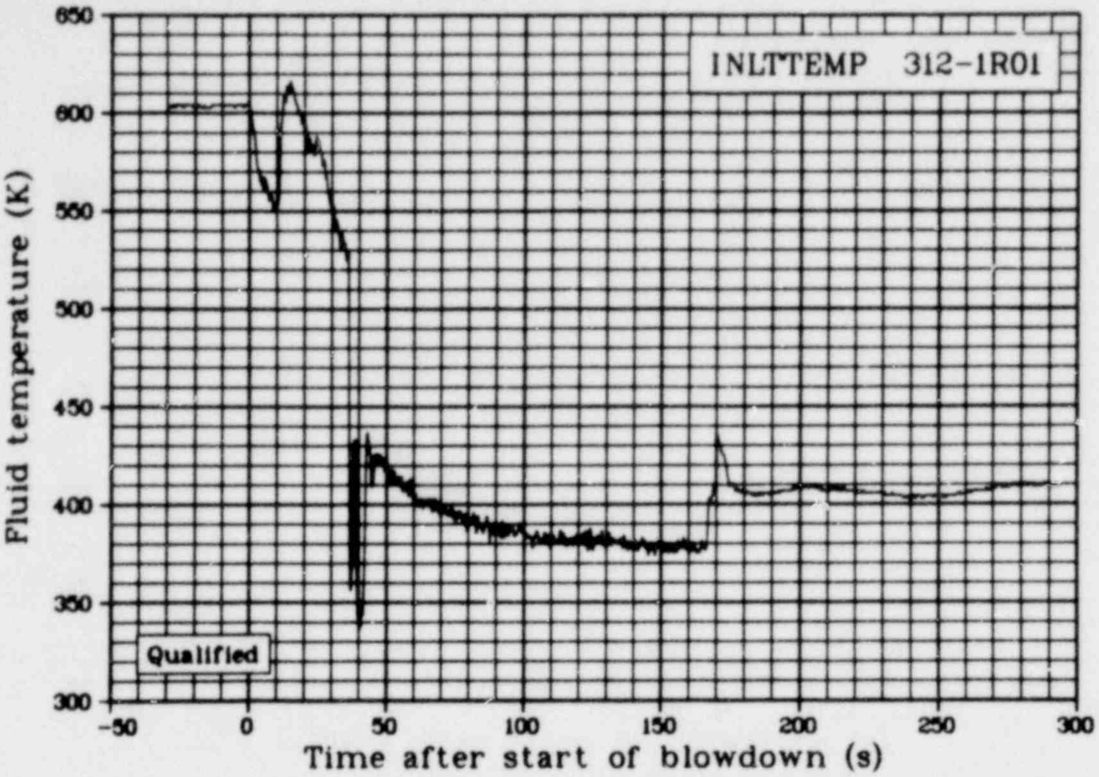

Fig. 167 Fluid temperature of Fuel Rod 312-1 coolant inlet (INLTTEMP 312-1R01), from -50 to 300 s.

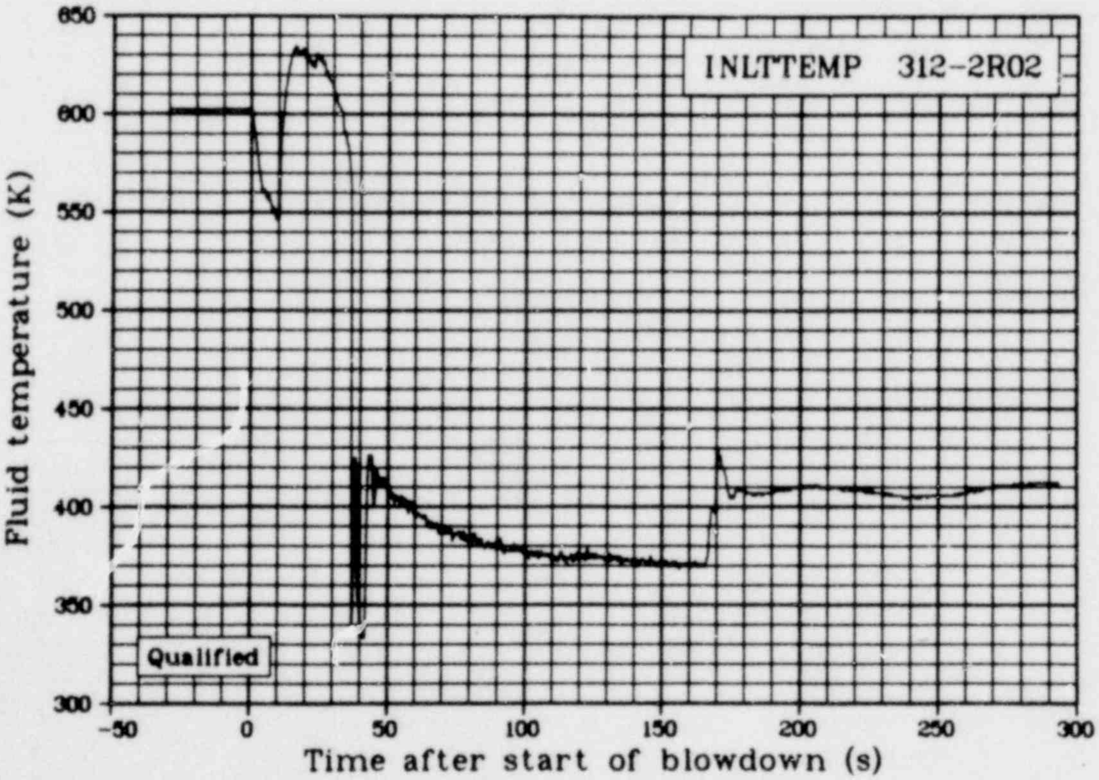

Fig. 168 Fluid temperature of Fuel Rod 312-2 coolant inlet (INLTTEMP 312-2R02), from -50 to 300 s.

1405 168

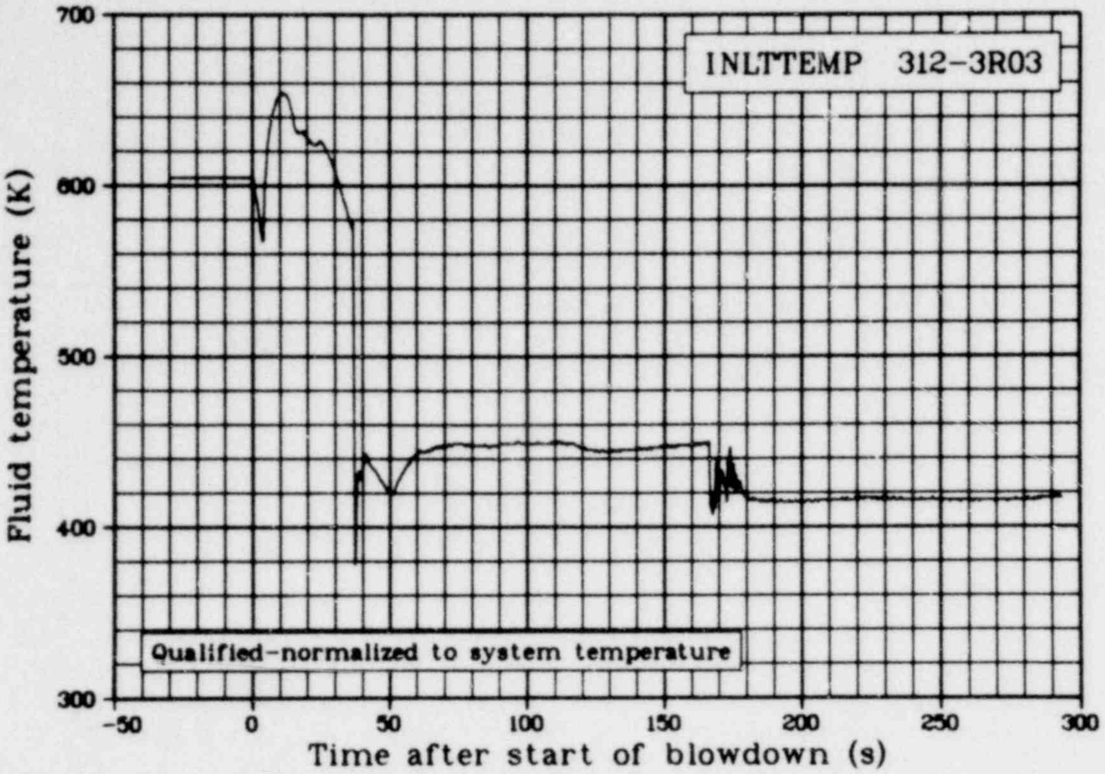

Fig. 169 Fluid temperature of Fuel Rod 312-3 coolant inlet (INLTTEMP 312-3R03), from -50 to 300 s.

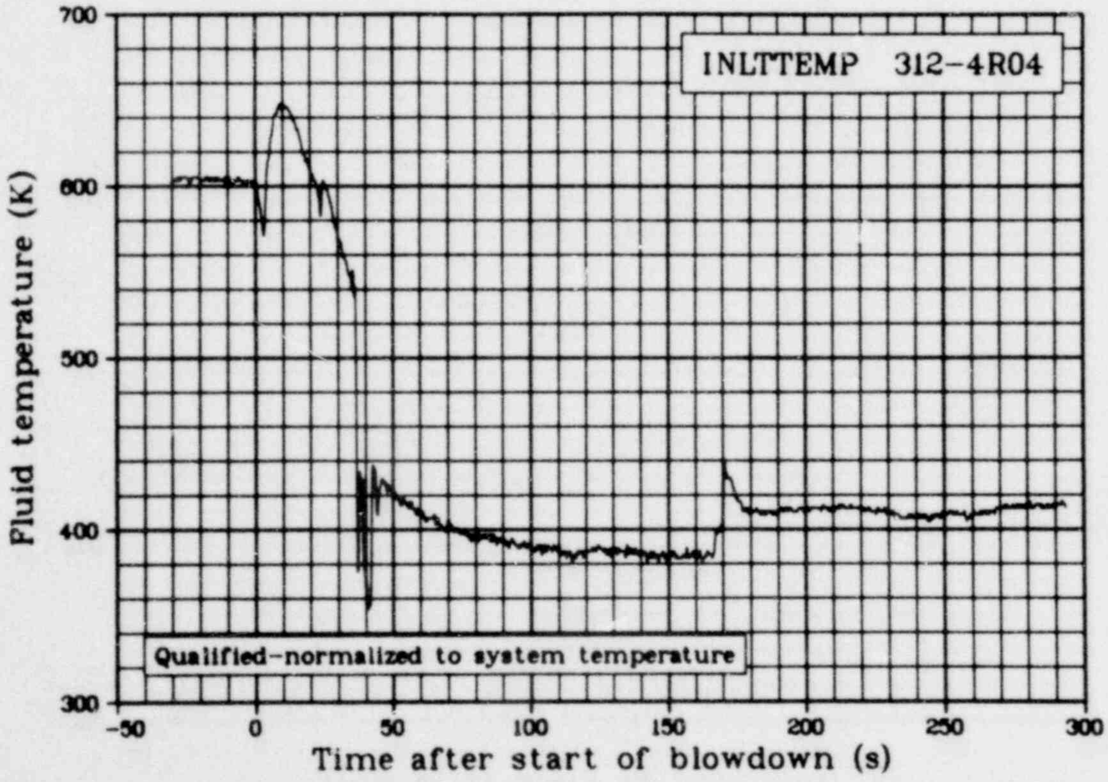

Fig. 170 Fluid temperature of Fuel Rod 312-4 coolant inlet (INLTTEMP 312-4R04), from -50 to 300 s.

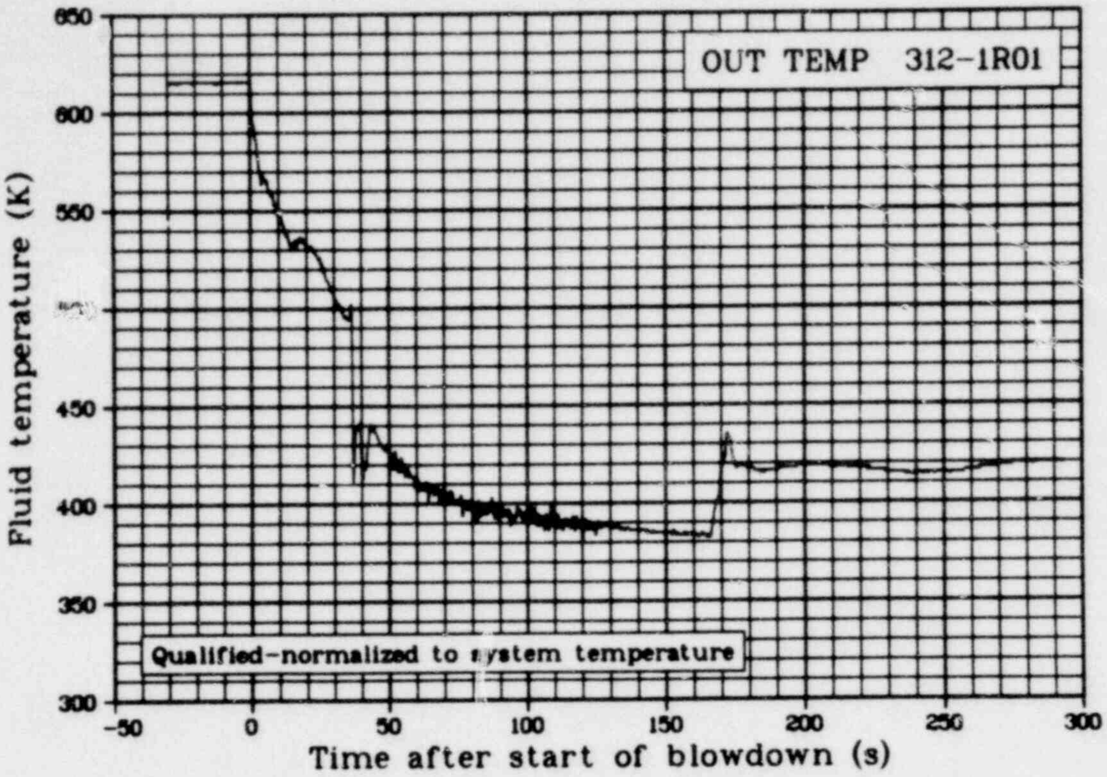

Fig. 171 Fluid temperature of Fuel Rod 312-1 coolant outlet (OUT TEMP 312-1R01), from -50 to 300 s.

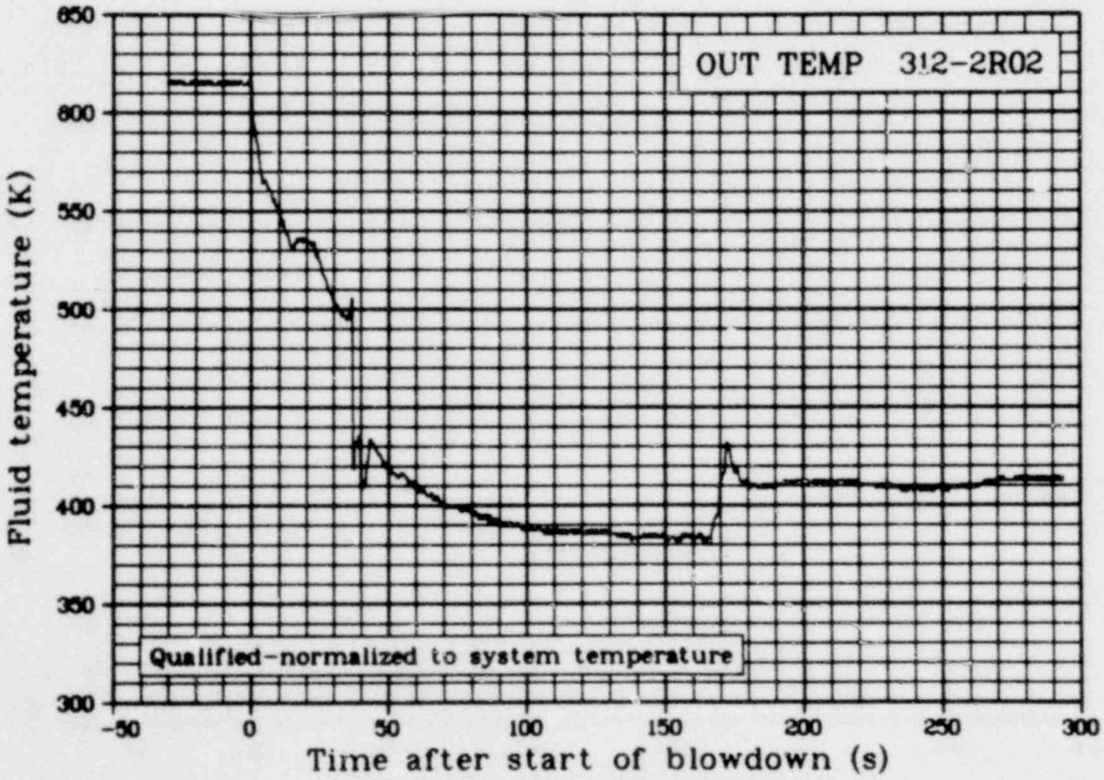

Fig. 172 Fluid temperature of Fuel Rod 312-2 coolant outlet (OUT TEMP 312-2R02), from -50 to 300 s.

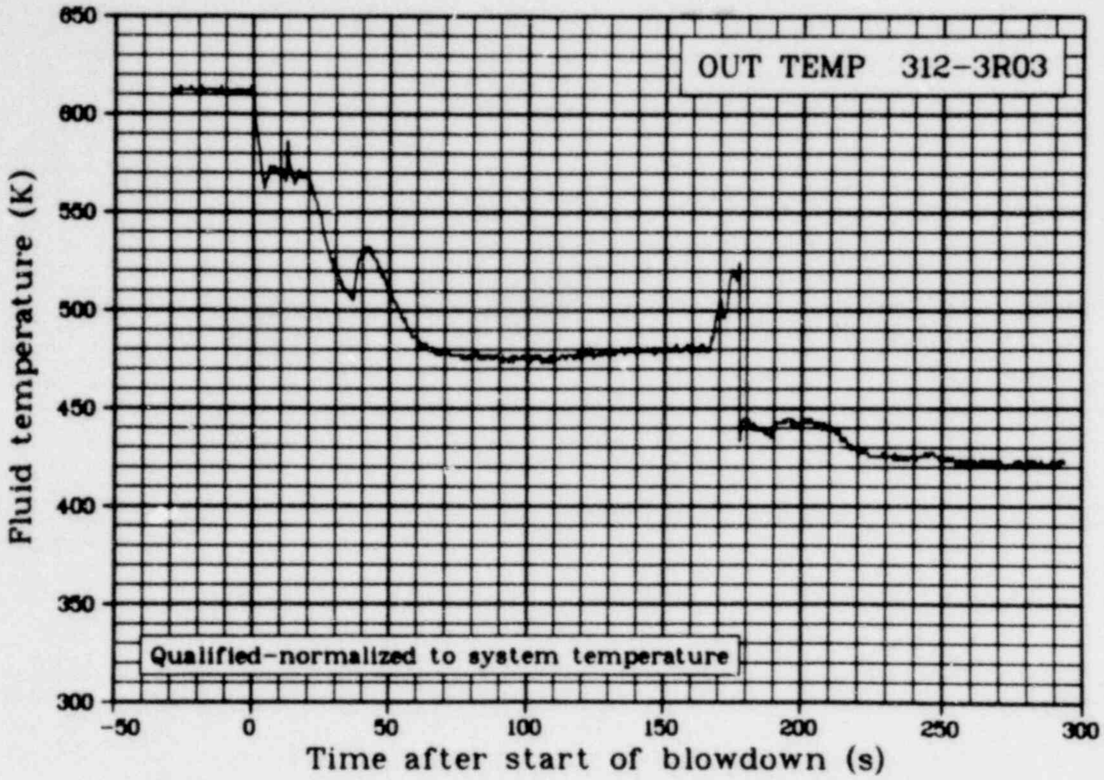

Fig. 173 Fluid temperature of Fuel Rod 312-3 coolant outlet (OUT TEMP 312-3R03), from -50 to 300 s.

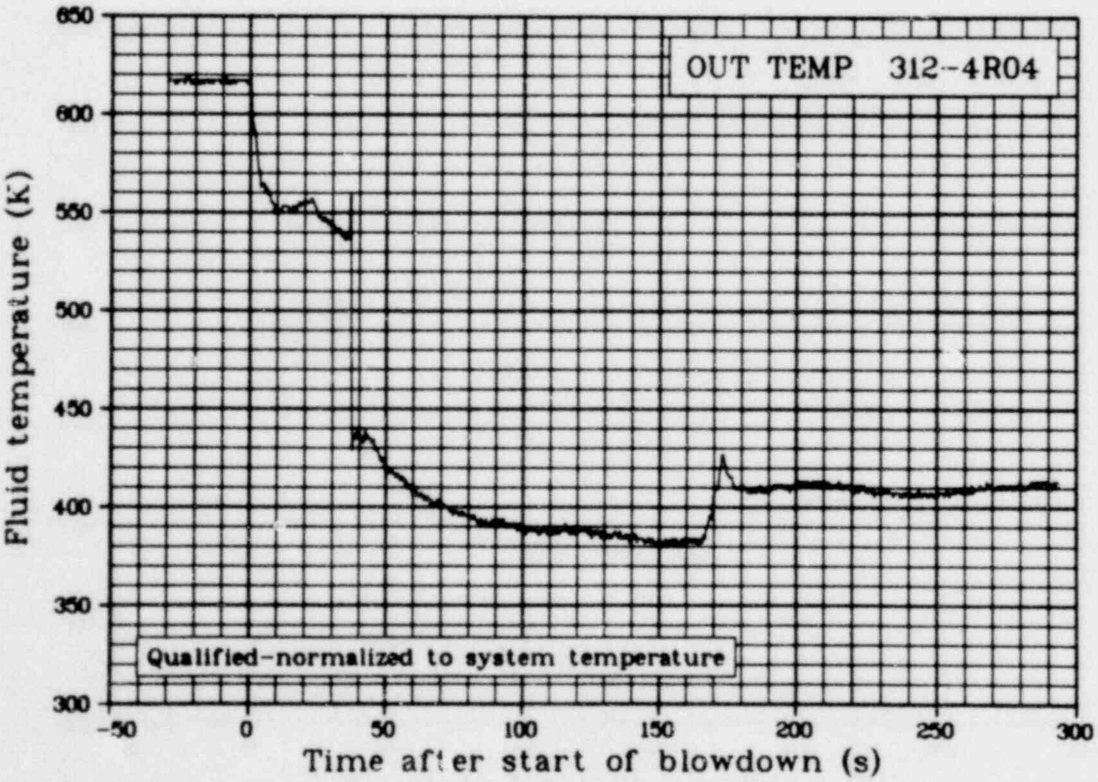

Fig. 174 Fluid temperature of Fuel Rod 312-4 coolant outlet (OUT TEMP 312-4R04), from -50 to 300 s.

1405 171

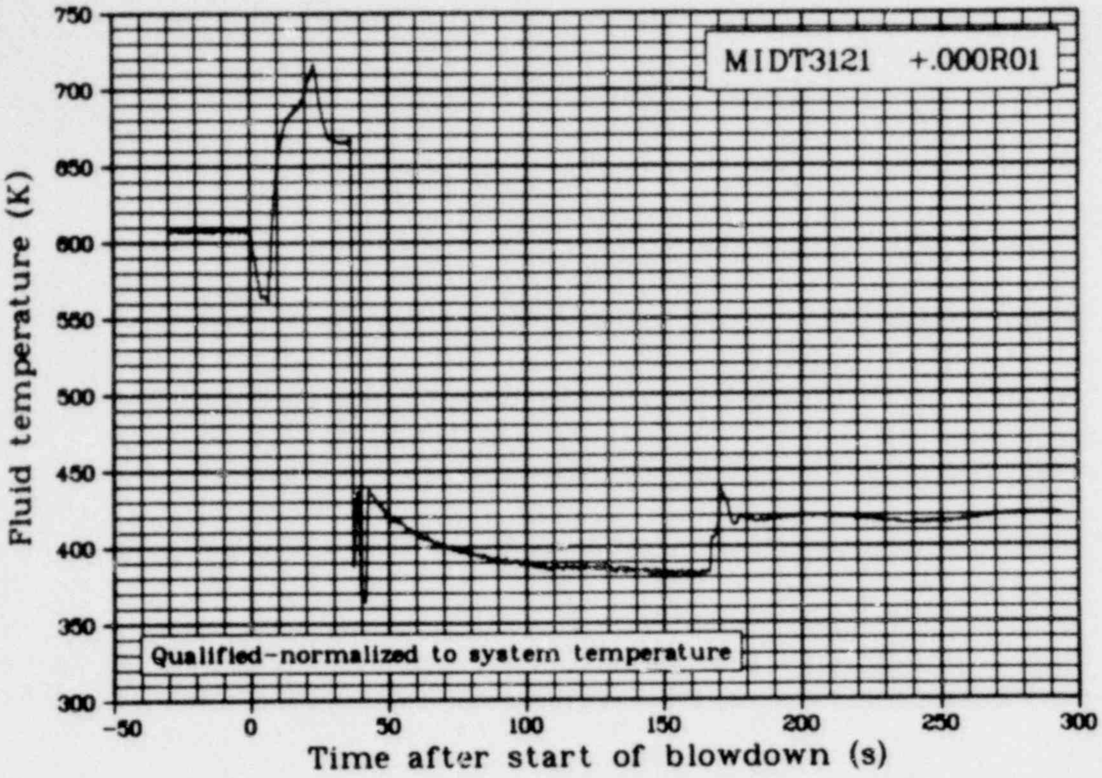

Fig. 175 Fluid temperature of Fuel Rod 312-1, at fuel stack midplane (MIDT3121 + .000R01), from -50 to 300 s.

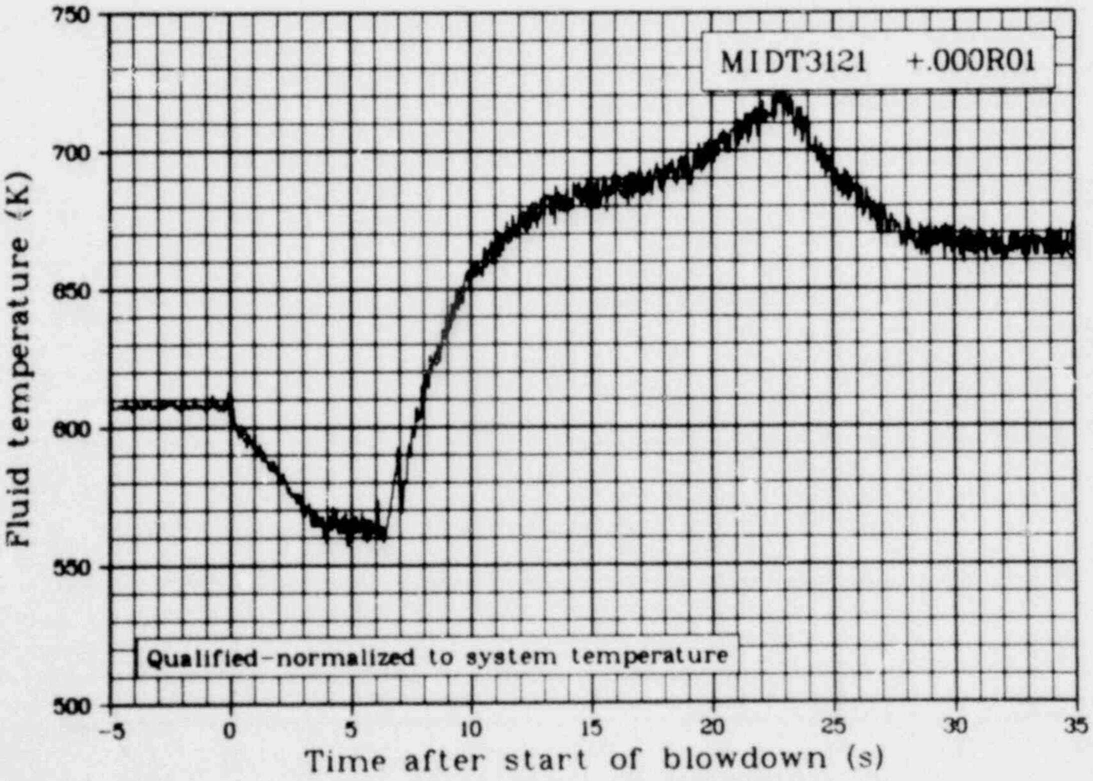

Fig. 176 Fluid temperature of Fuel Rod 312-1, at fuel stack midplane (MIDT3121 + .000R01), from -5 to 35 s.

1405 172

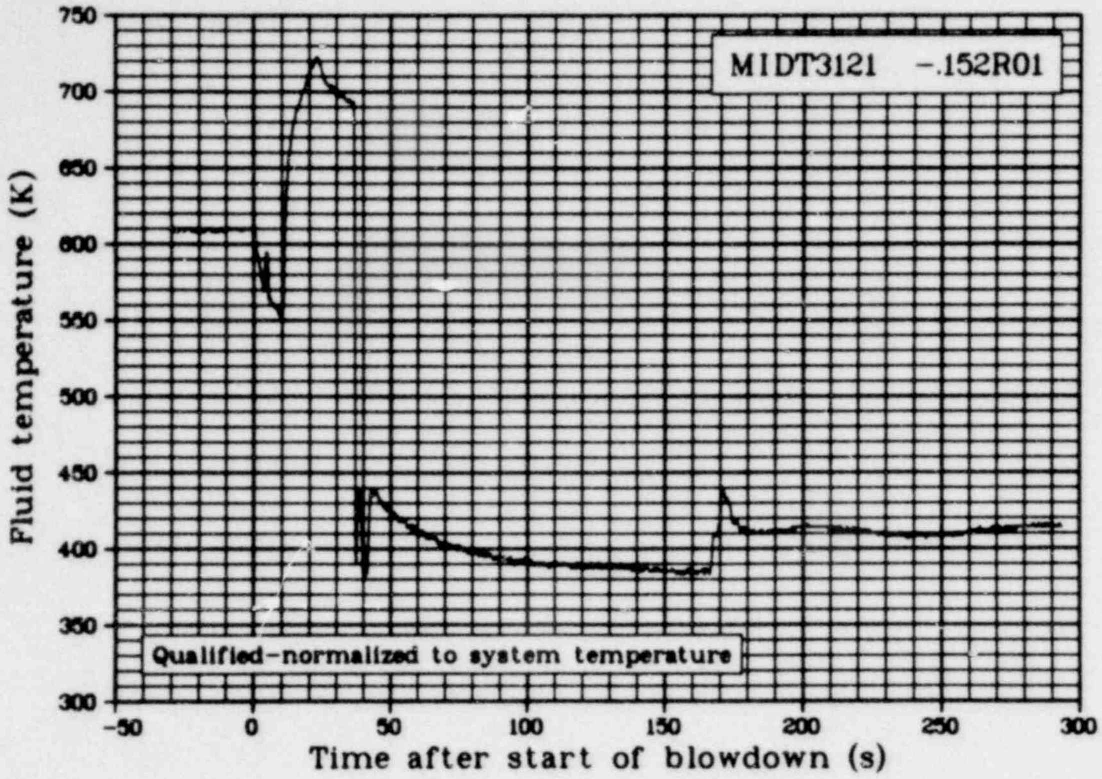

Fig. 177 Fluid temperature of Fuel Rod 312-1, 0.152 m below fuel stack midplane (MIDT3121 -.152R01), from -50 to 300 s.

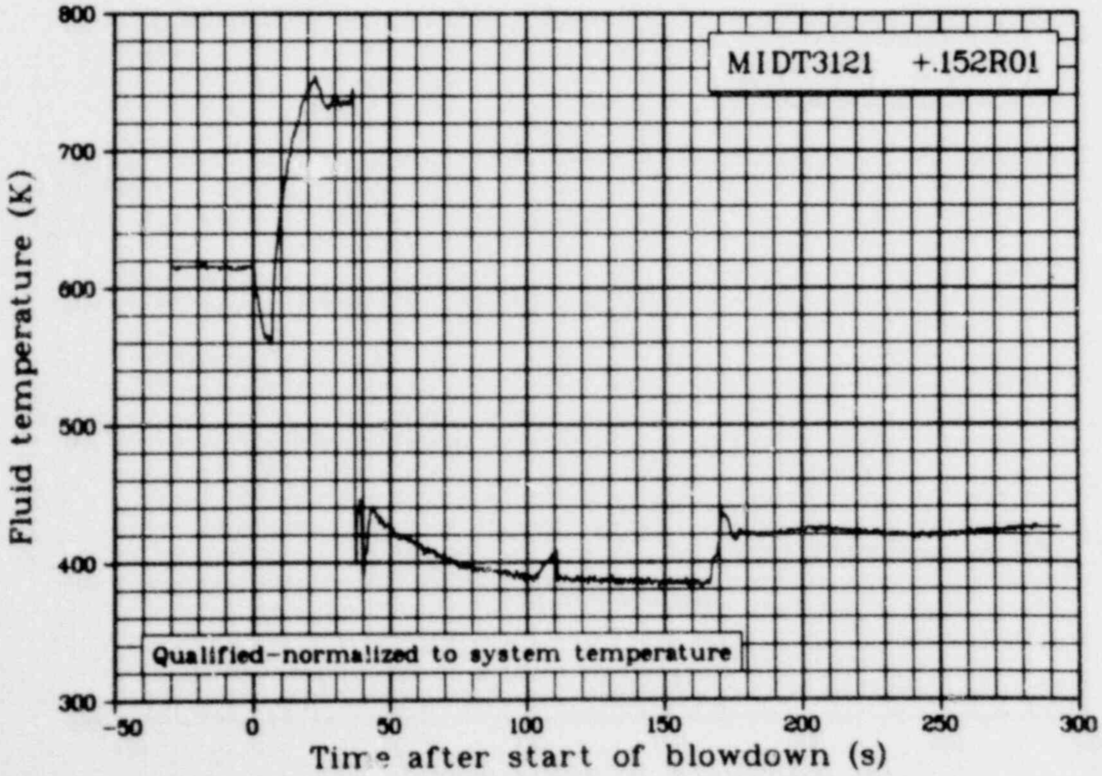

Fig. 178 Fluid temperature of Fuel Rod 312-1, 0.152 m above fuel stack midplane (MIDT3121 +.152R01), from -50 to 300 s.

1405 173

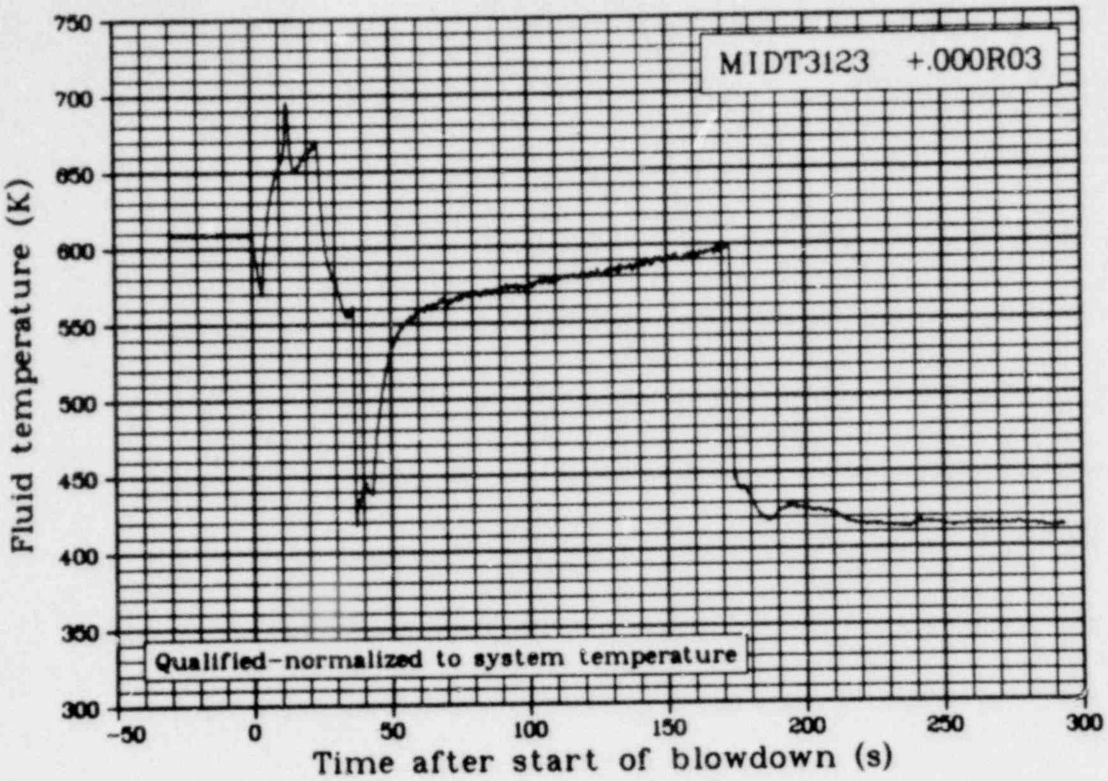

Fig. 179 Fluid temperature of Fuel Rod 312-3, at fuel stack midplane (MIDT3123 + .000R03), from -50 to 300 s.

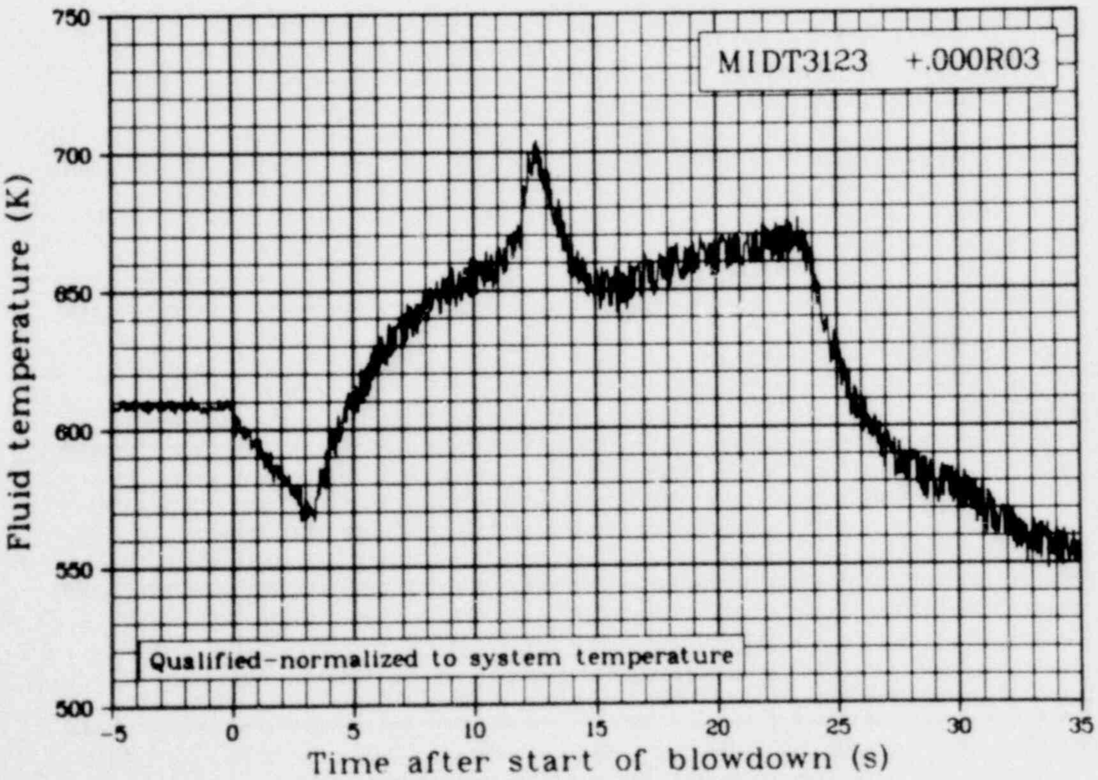

Fig. 180 Fluid temperature of Fuel Rod 312-3, at fuel stack midplane (MIDT3123 + .000R03), from -5 to 35 s.

1405 174

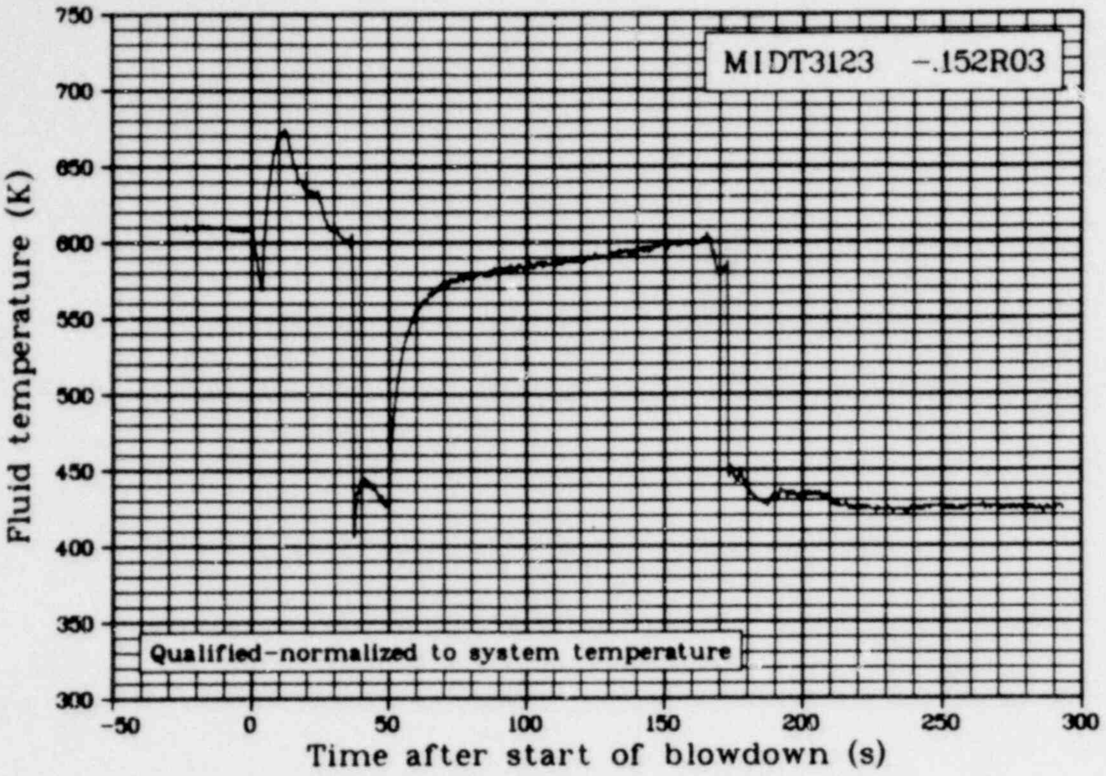

Fig. 181 Fluid temperature of Fuel Rod 312-3, 0.152 m below fuel stack midplane (MIDT3123 -.152R03), from -50 to 300 s.

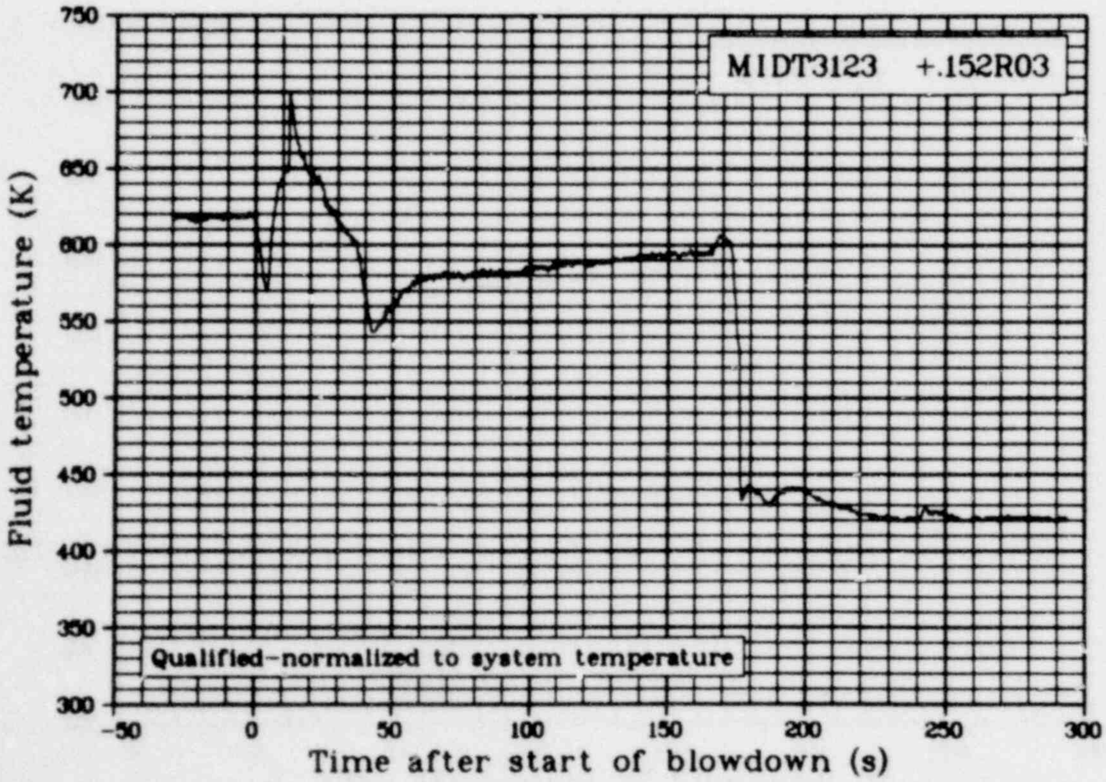

Fig. 182 Fluid temperature of Fuel Rod 312-3, 0.152 m above fuel stack midplane (MIDT3123 +.152R03), from -50 to 300 s.

1405 175

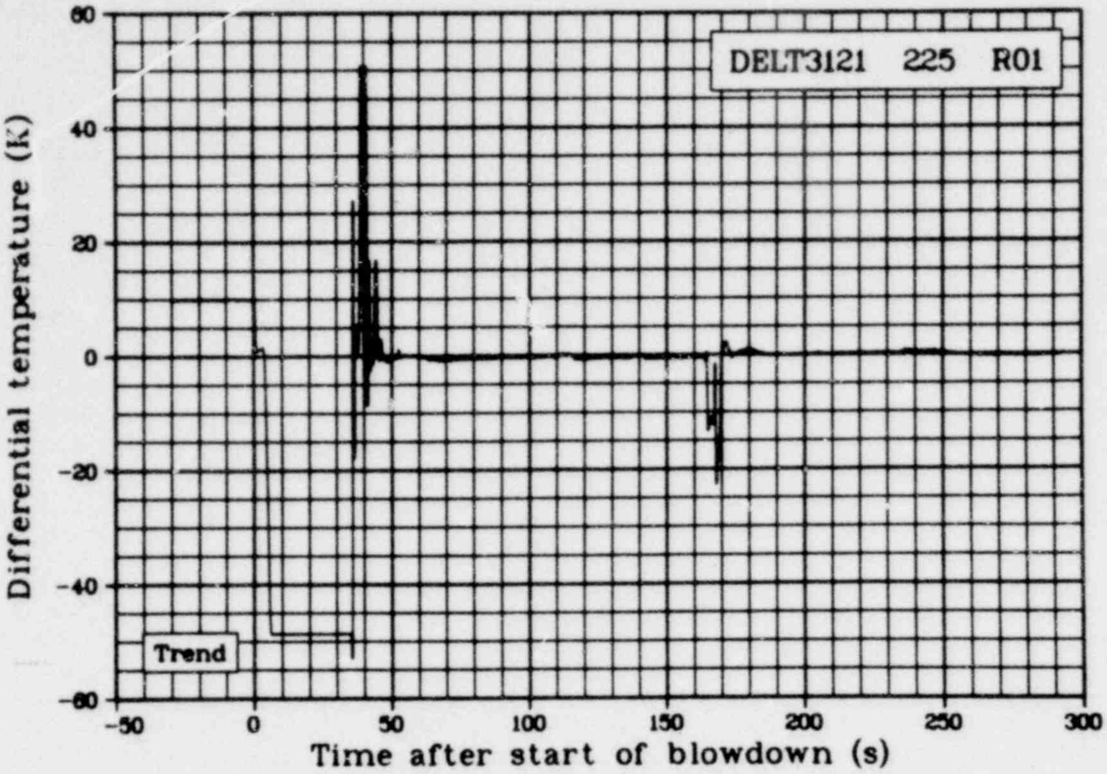

Fig. 183 Differential temperature of Rod 312-1, coolant inlet and outlet (DELT3121 225 R01), from -50 to 300 s.

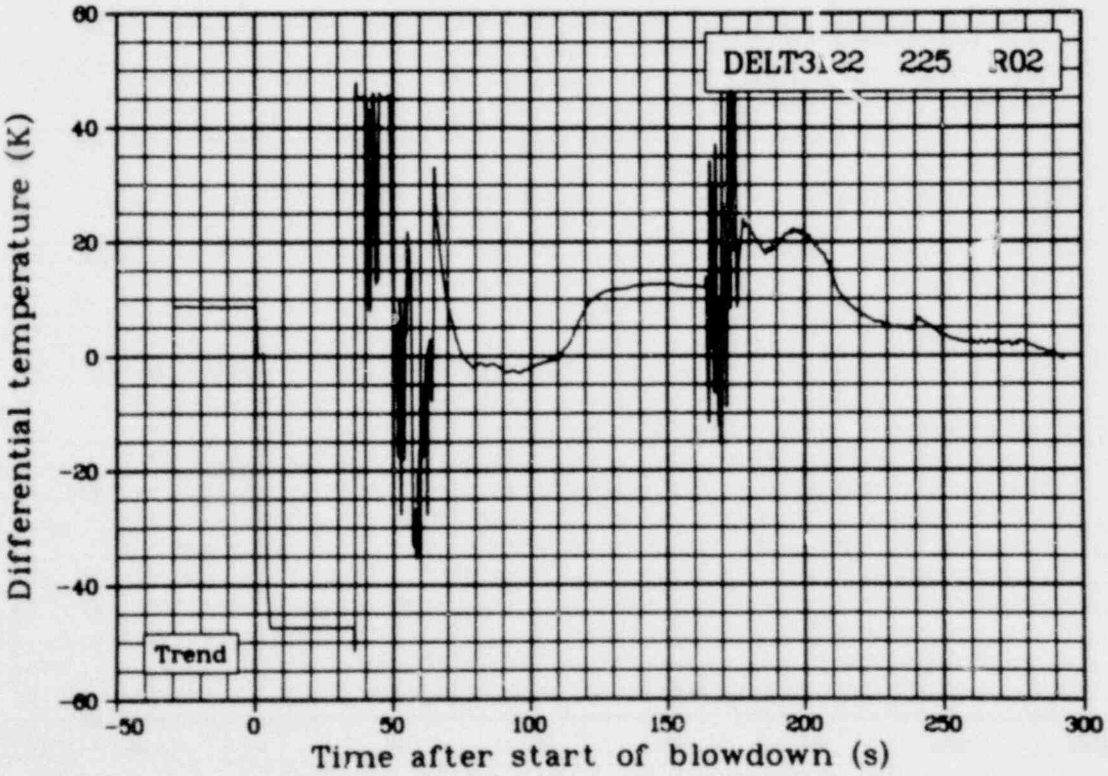

Fig. 184 Differential temperature of Rod 312-2, coolant inlet and outlet (DELT3122 225 R02), from -50 to 300 s.

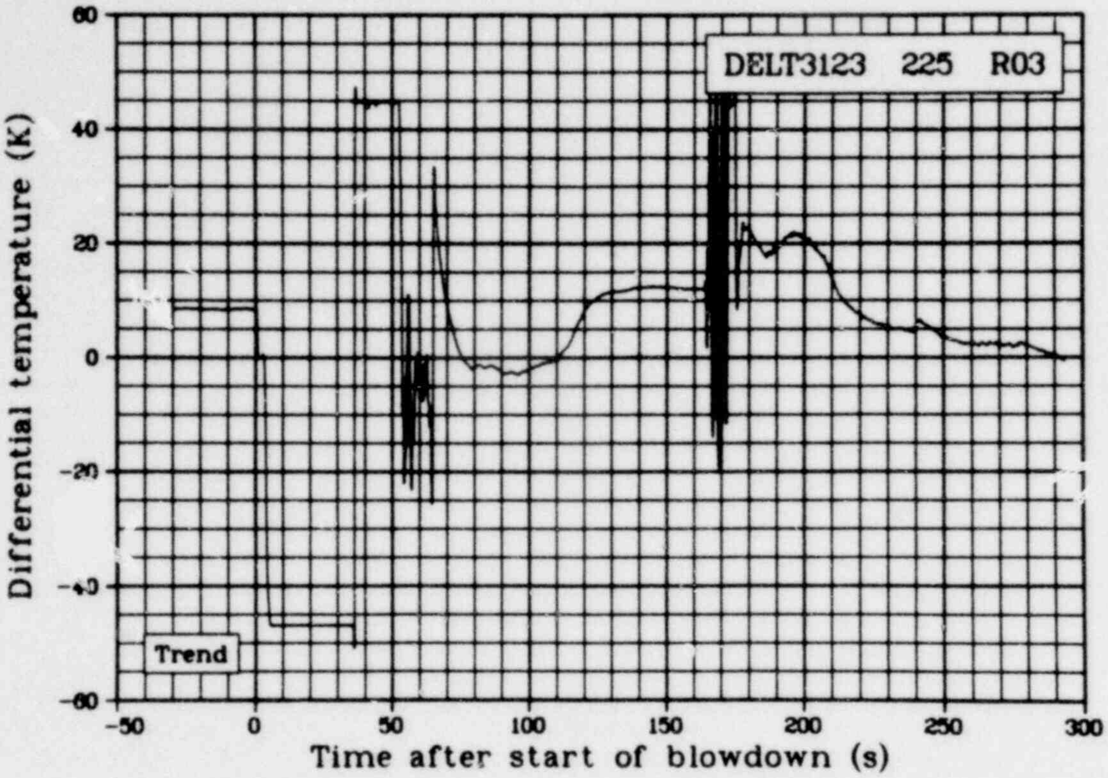

Fig. 185 Differential temperature of Rod 312-3, coolant inlet and outlet (DELT3123 225 R03), from -50 to 300 s.

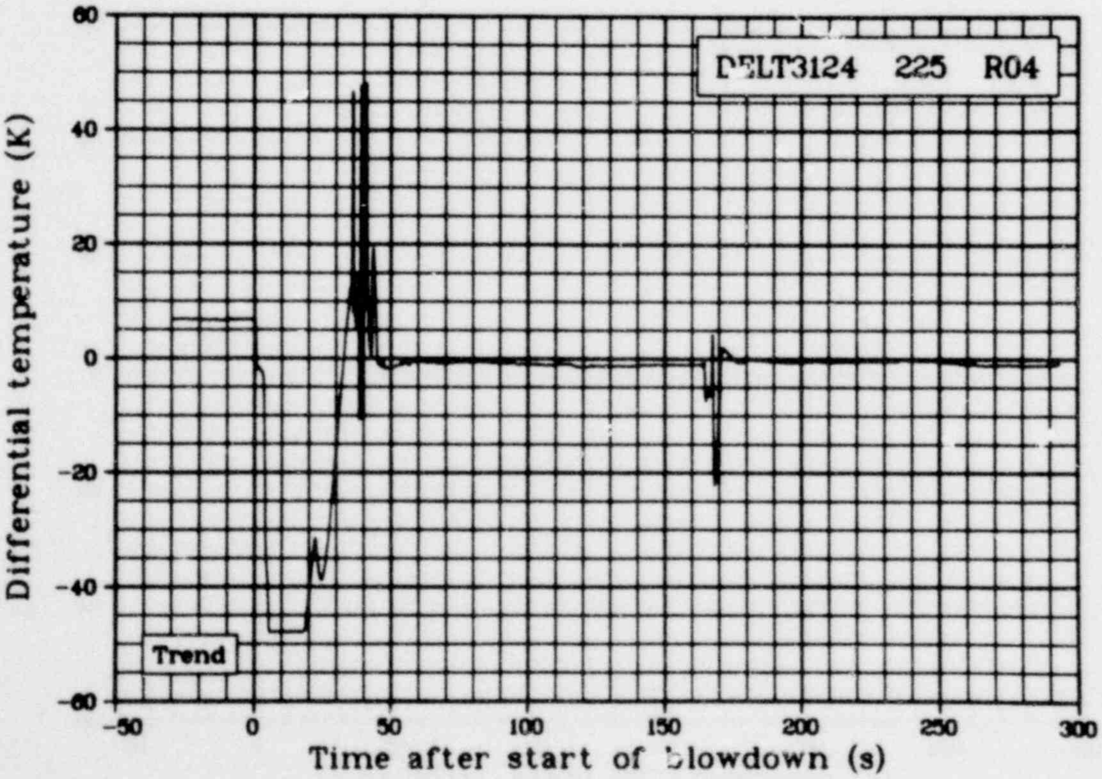

Fig. 186 Differential temperature of Rod 312-4, coolant inlet and outlet (DELT3124 225 R04), from -50 to 300 s.

1405 177

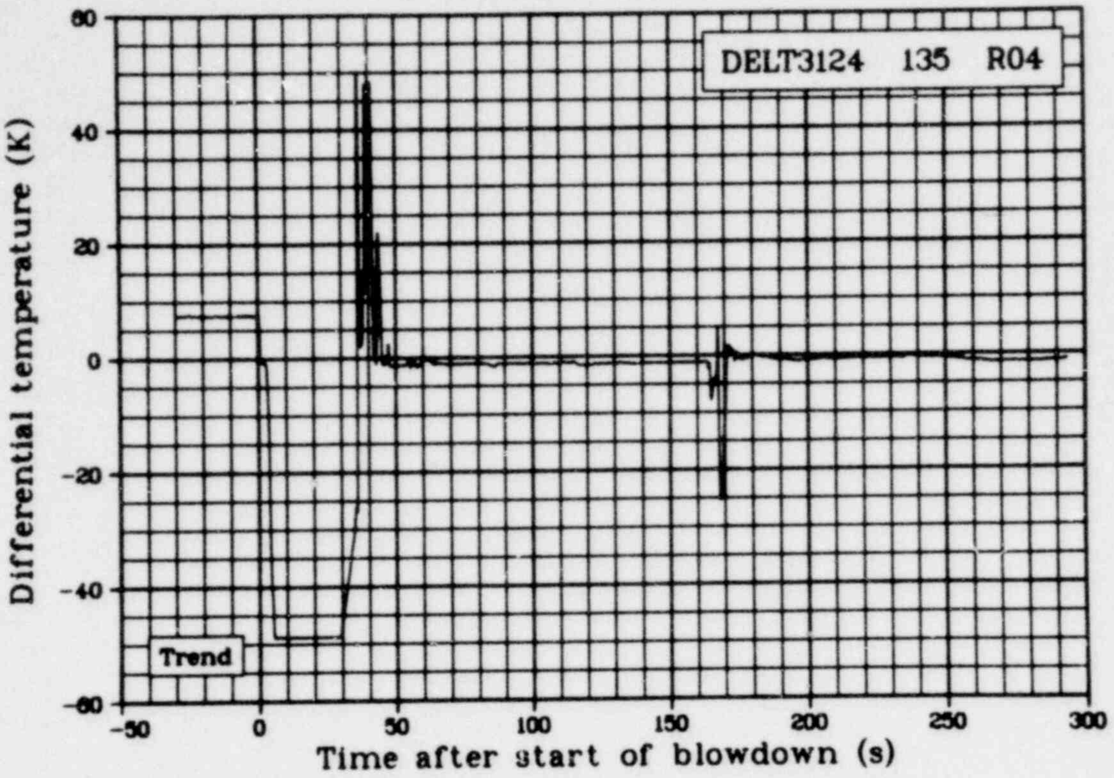

Fig. 187 Differential temperature of Rod 312-4, at 135 degrees, coolant inlet and outlet (DELT3124 135 R04), from -50 to 300 s.

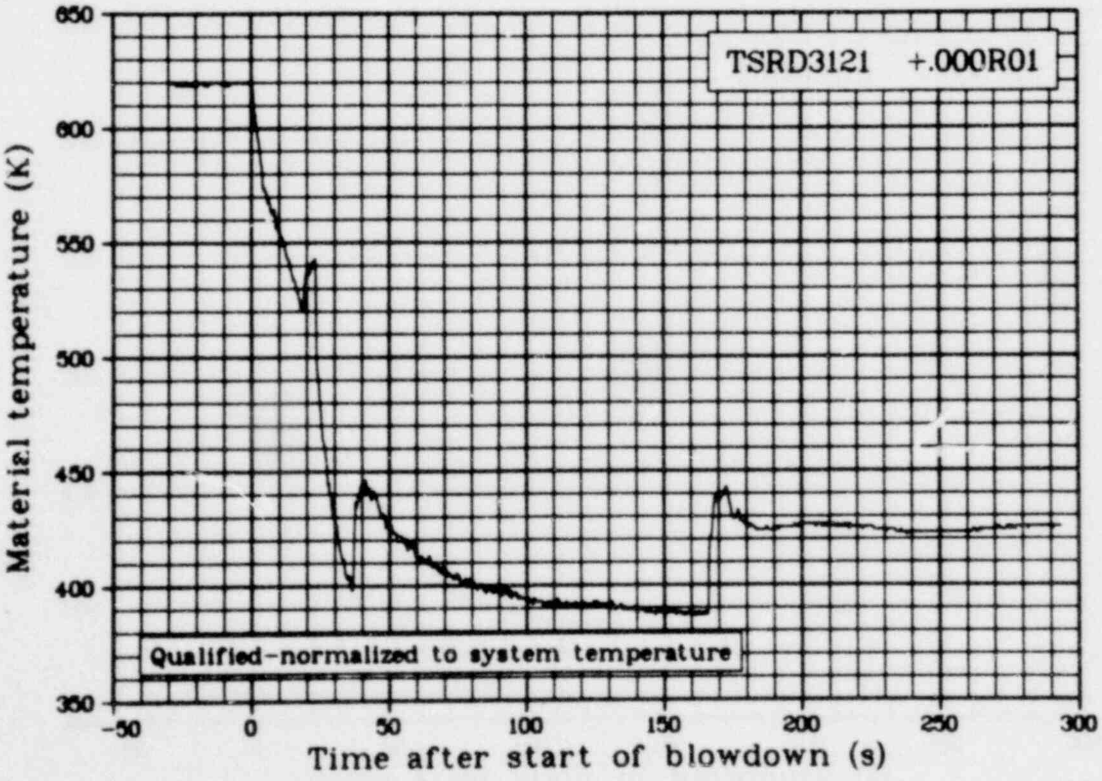

Fig. 188 Material temperature, Rod 312-1 shroud, at fuel stack midplane (TSRD3121 + .000R01), from -50 to 300 s.

1405 178

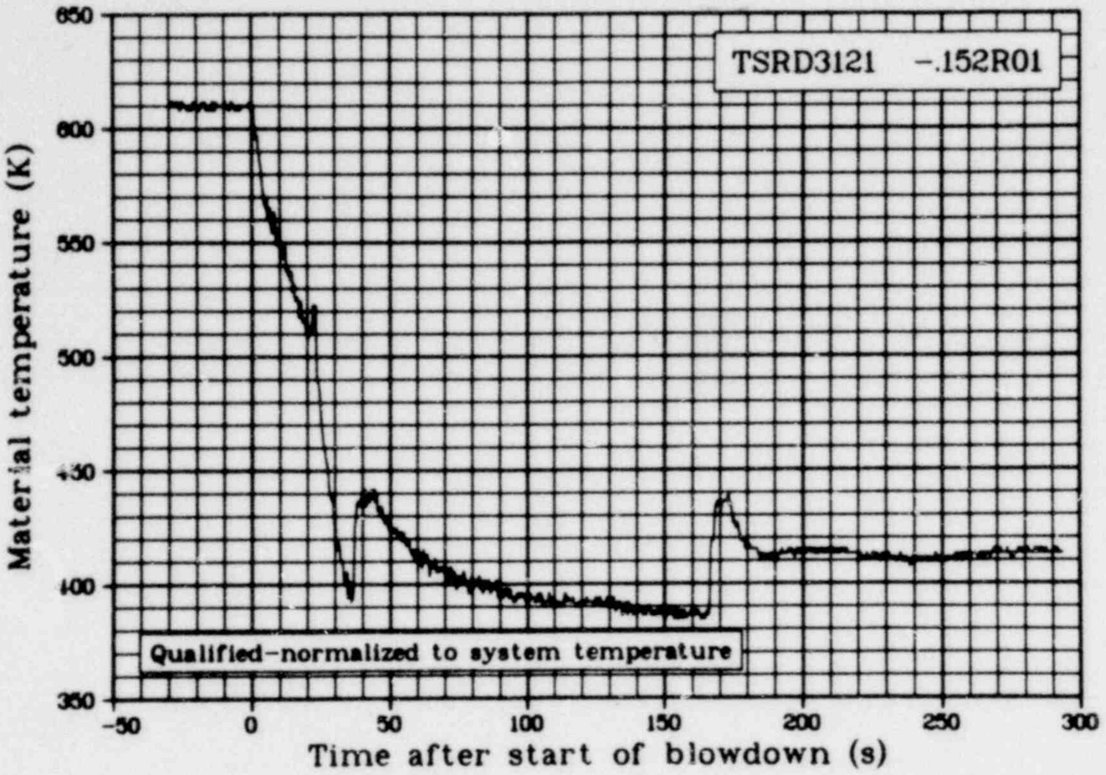

Fig. 189 Material temperature, Rod 312-1 shroud, 0.152 m below fuel stack midplane (TSRD3121 -.152R01), from -50 to 300 s.

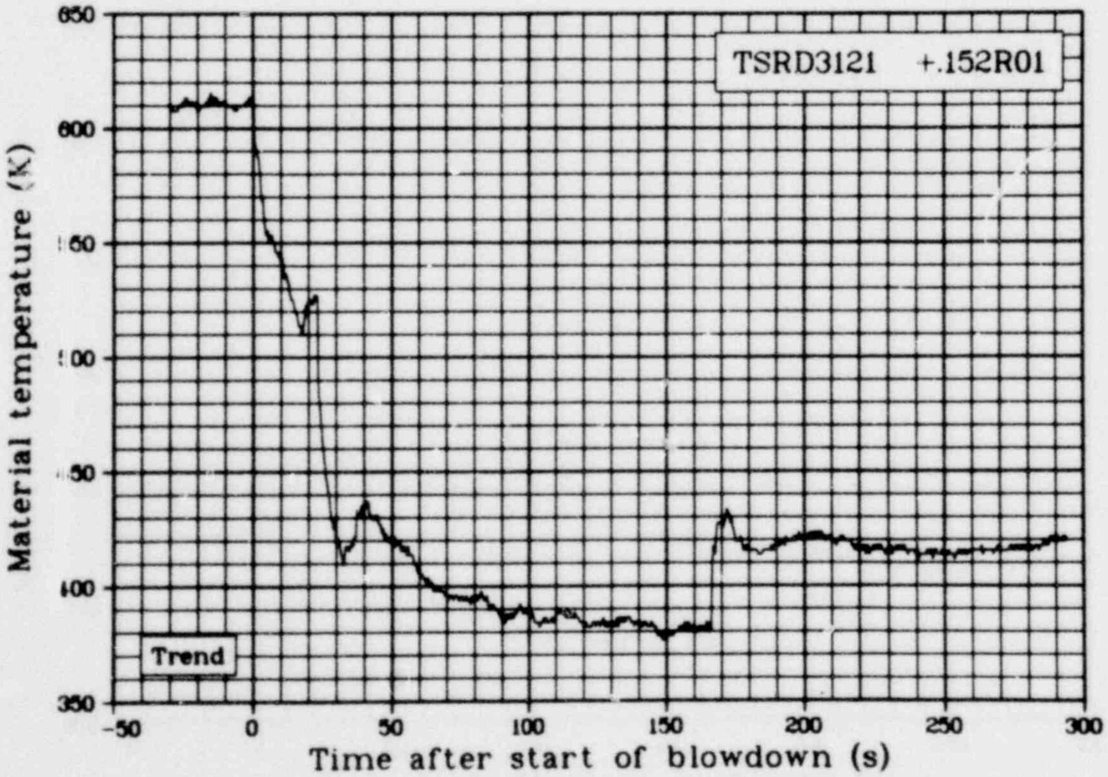

Fig. 190 Material temperature, Rod 312-1 shroud, 0.152 m above fuel stack midplane (TSRD3121 +.152R01), from -50 to 300 s.

1405 179

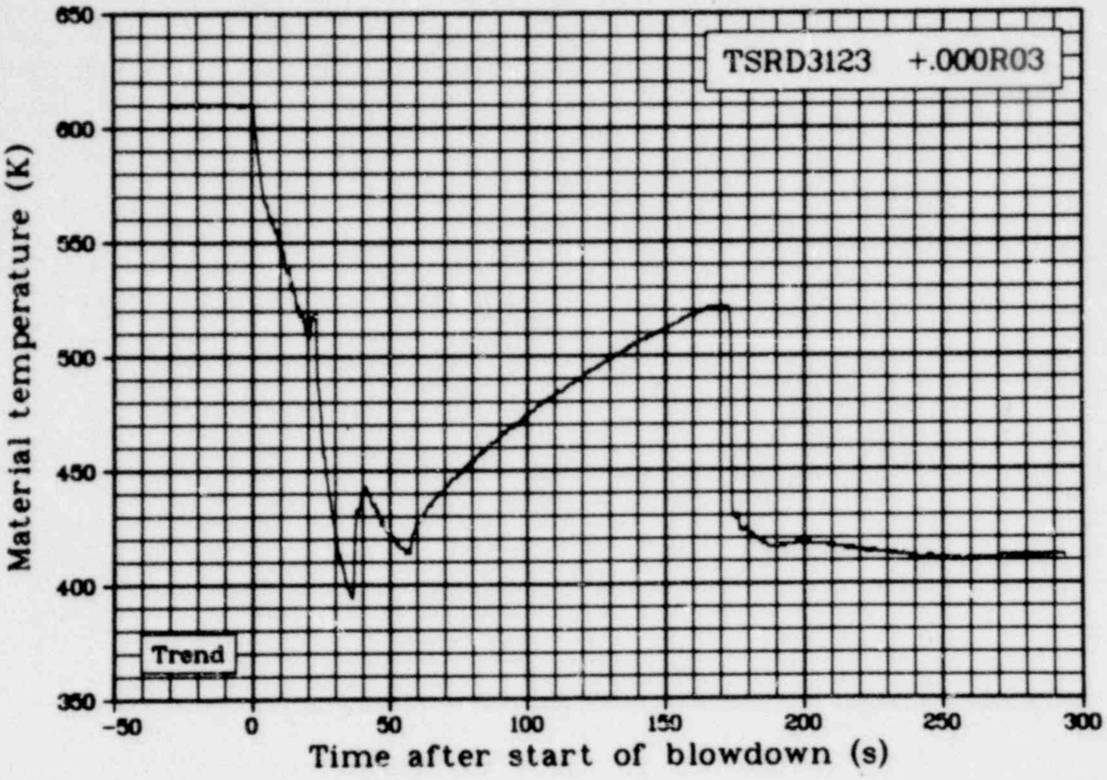

Fig. 191 Material temperature, Rod 312-3 shroud, at fuel stack midplane (TSRD3123 + .000R03), from -50 to 300 s.

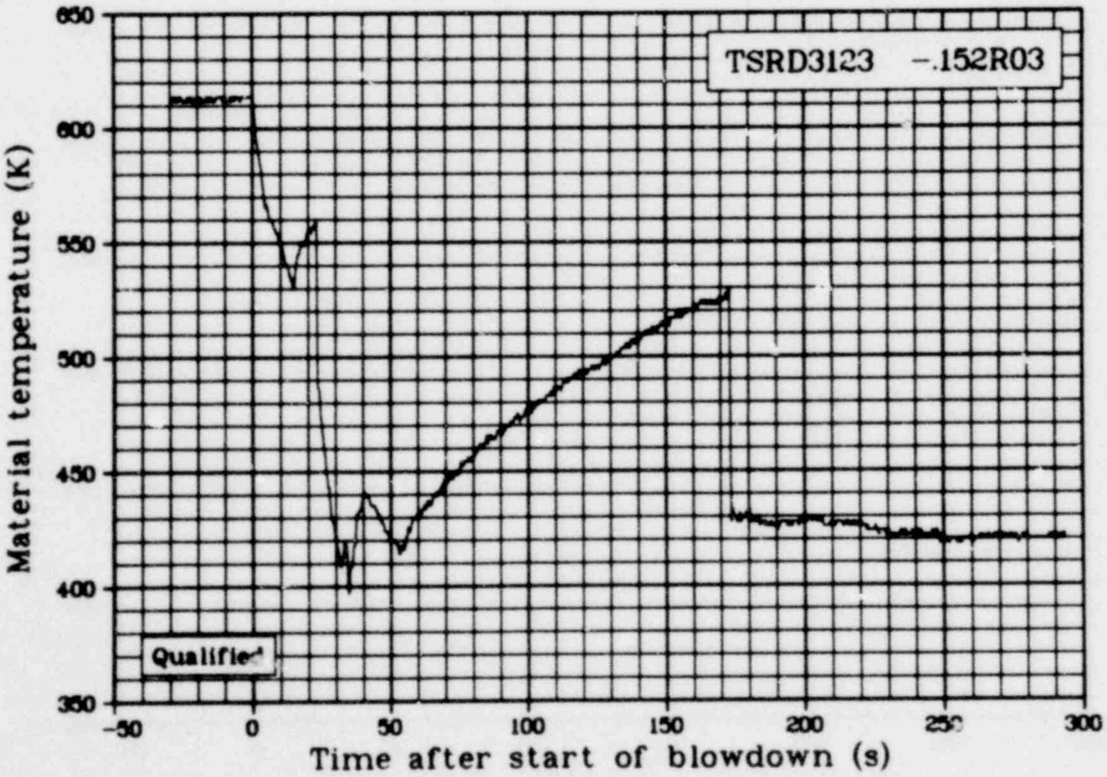

Fig. 192 Material temperature, Rod 312-3 shroud, 0.152 m below fuel stack midplane (TSRD3123 -.152R03), from -50 to 300 s.

1405 180

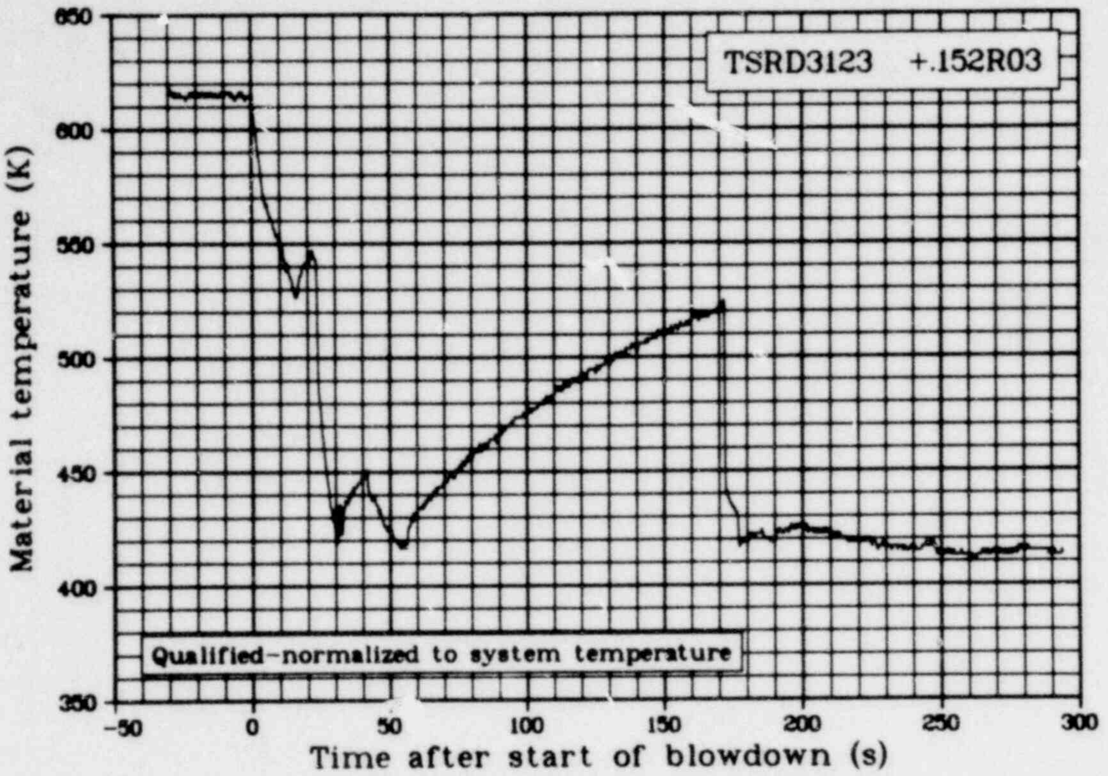

Fig. 193 Material temperature, Rod 312-3 shroud, 0.152 m above fuel stack midplane (TSRD3123 + .152R01), from -50 to 300 s.

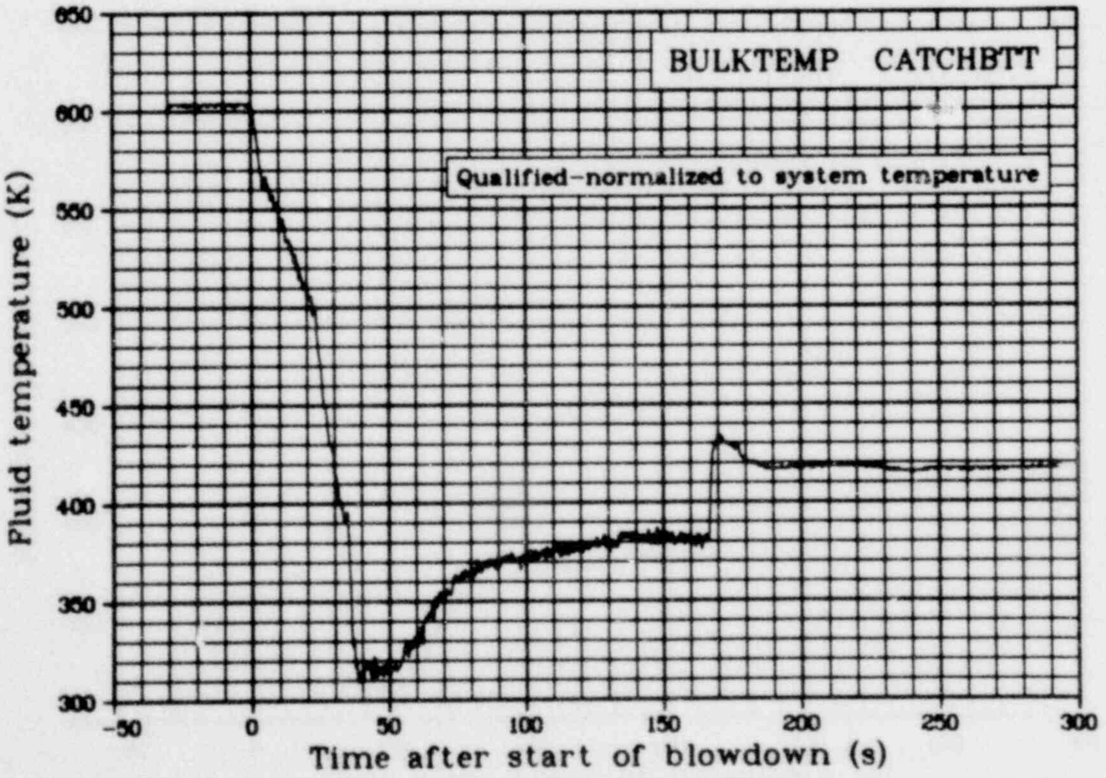

Fig. 194 Fluid temperature in test train catch basket (BULKTEMP CATCHBTT), from -50 to 300 s.

1405 181

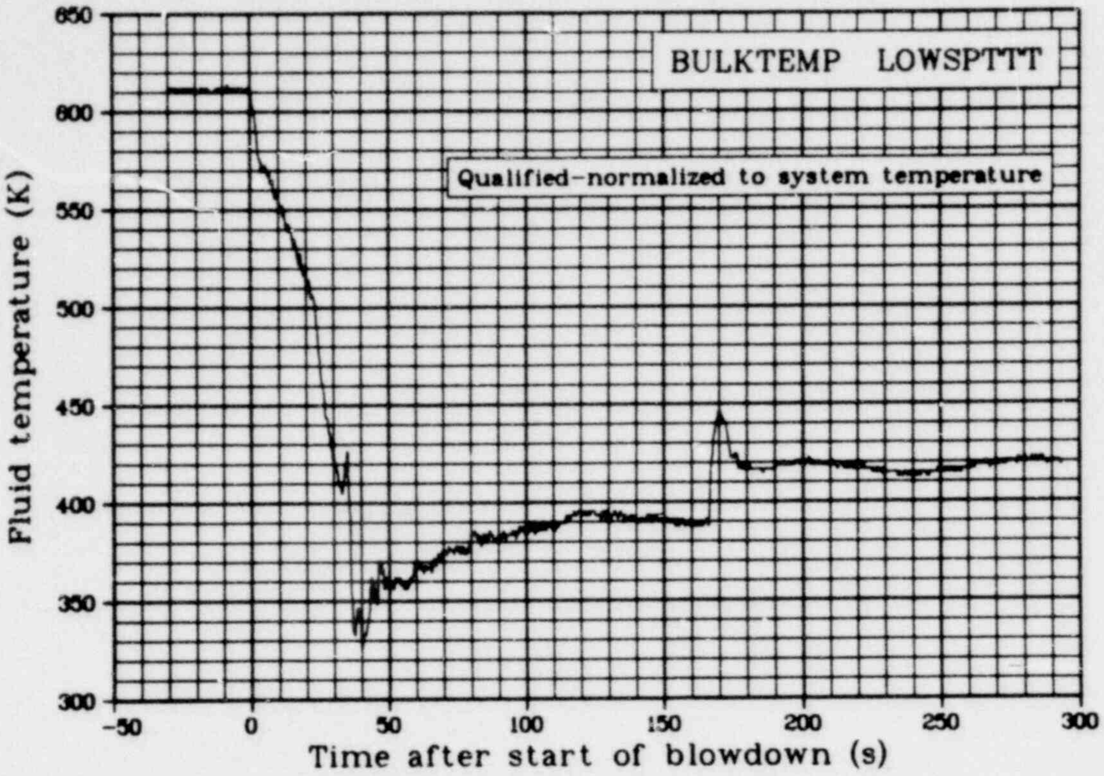

Fig. 195 Fluid temperature below test train lower support plate (BULKTEMP LOWSPTTT), from -50 to 300 s.

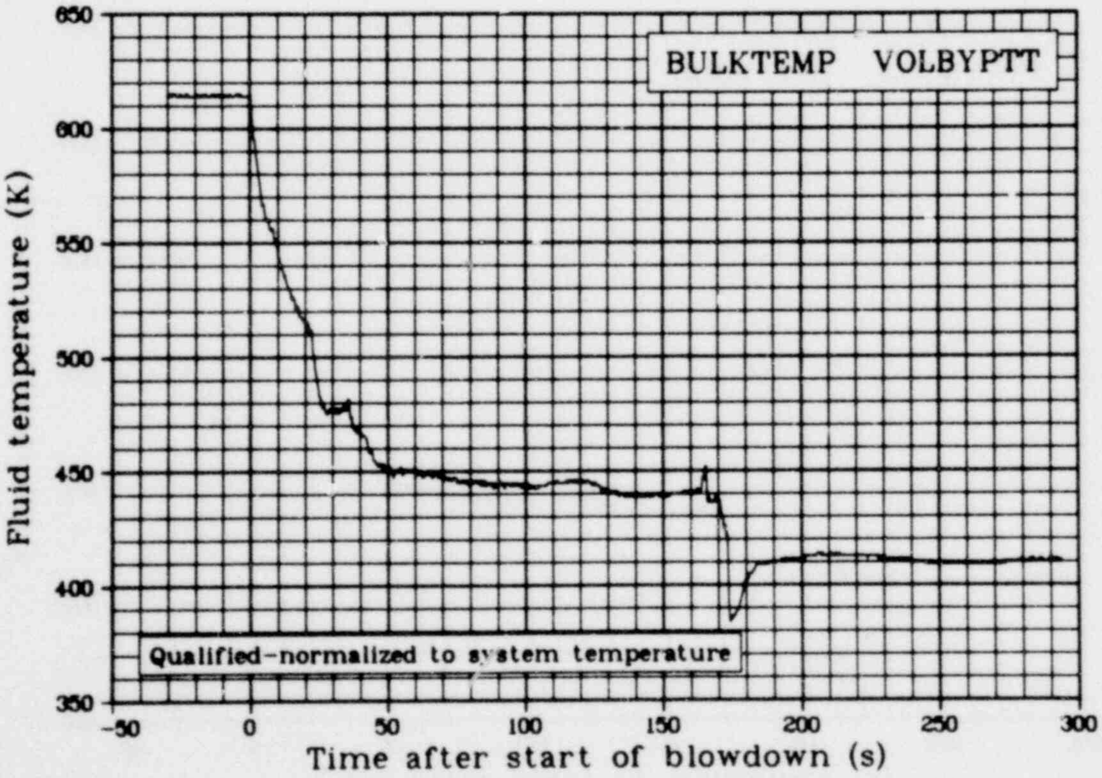

Fig. 196 Fluid temperature in bypass volume at fuel stack midplane (BULKTEMP VOLBYPTT), from -50 to 300 s.

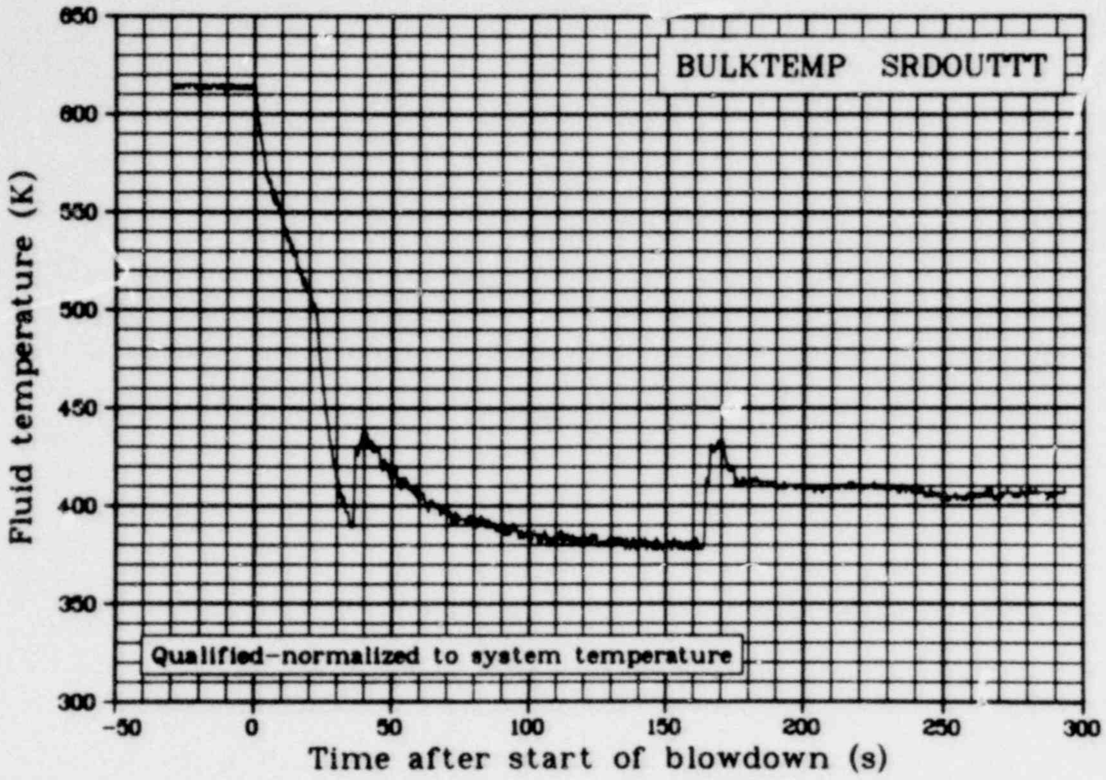

Fig. 197 Fluid temperature 0.05 m above flow shroud outlets (BULKTEMP SRDOUTTT), from -50 to 300 s.

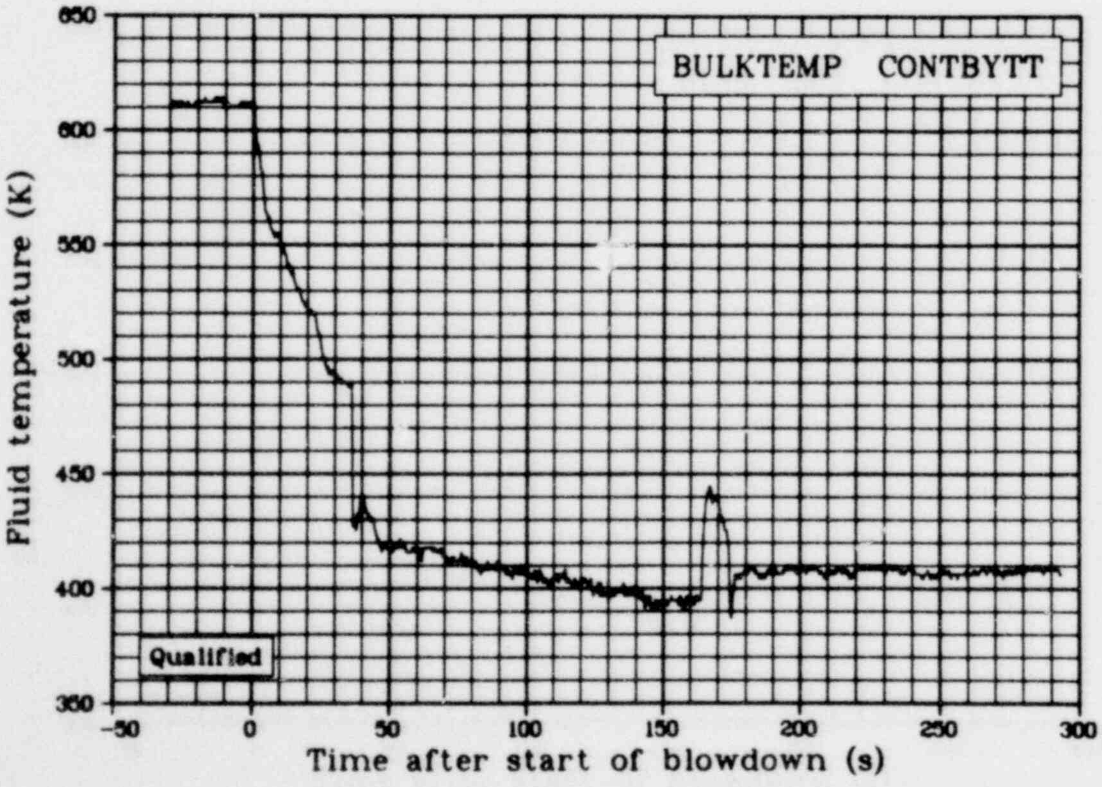

Fig. 198 Fluid temperature at test train controlled bypass inlet (BULKTEMP CONTBYTT), from -50 to 300 s.

1405 183

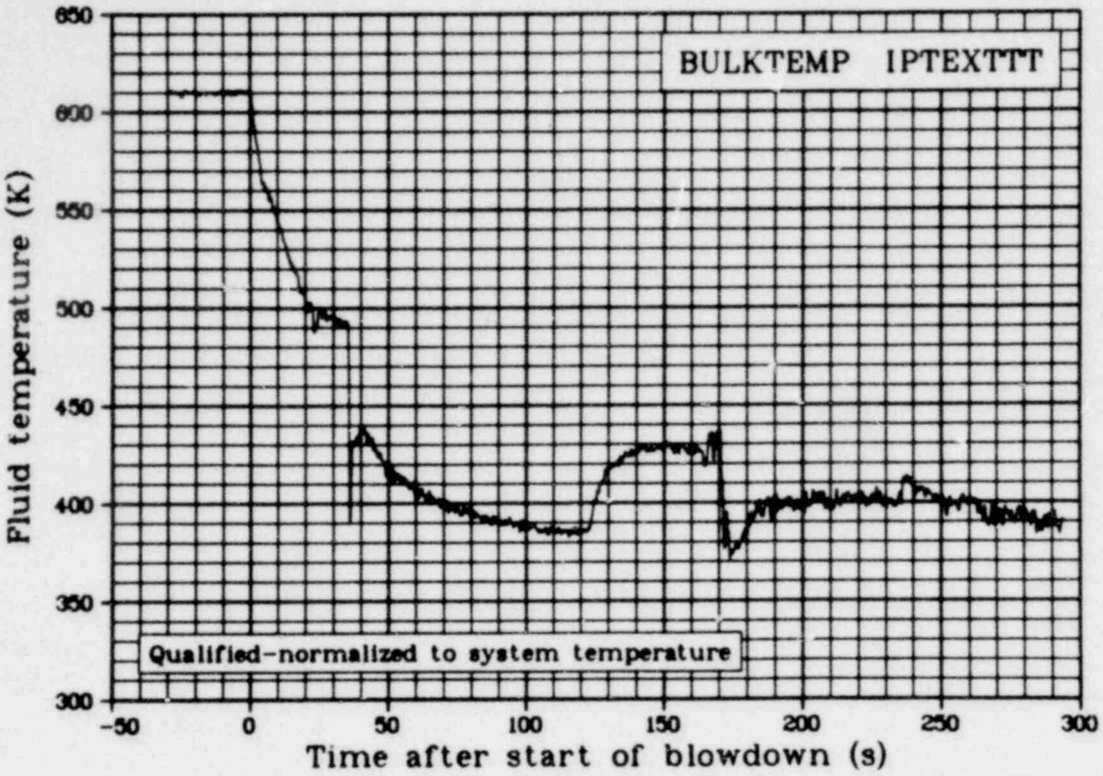

Fig. 199 Fluid temperature at IPT exit (BULKTEMP IPTEXTTT), from -50 to 300 s.

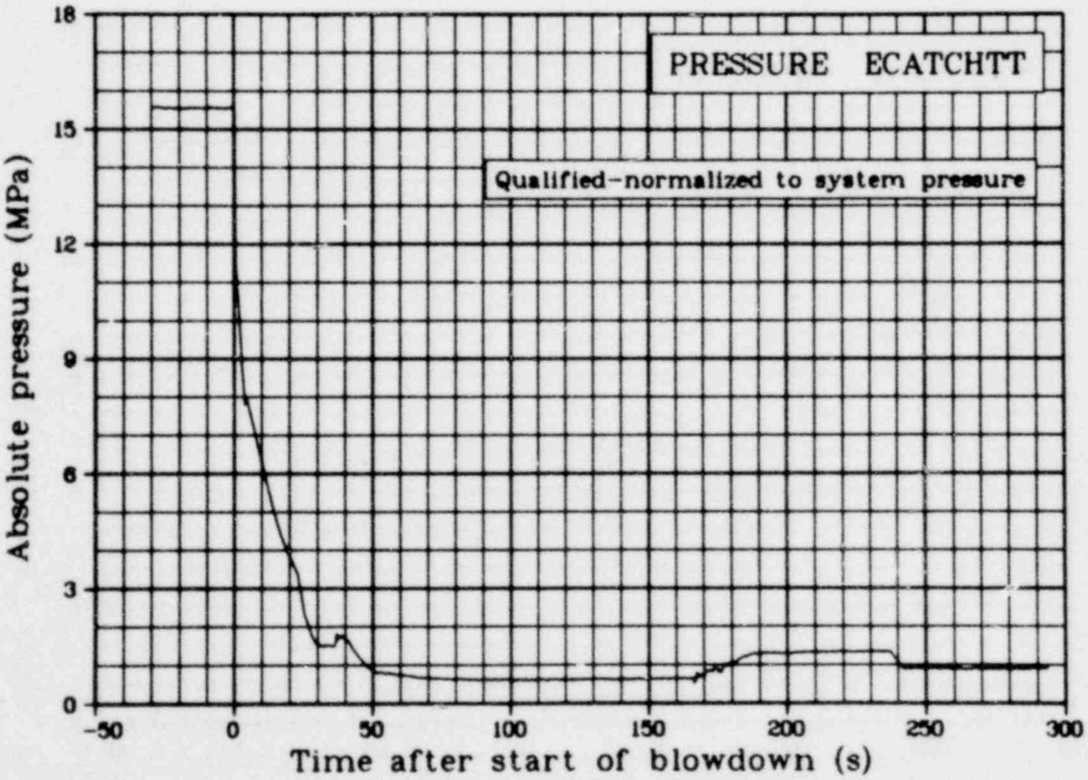

Fig. 200 Absolute pressure in test train catch basket (PRESSURE ECATCHTT), from -50 to 300 s.

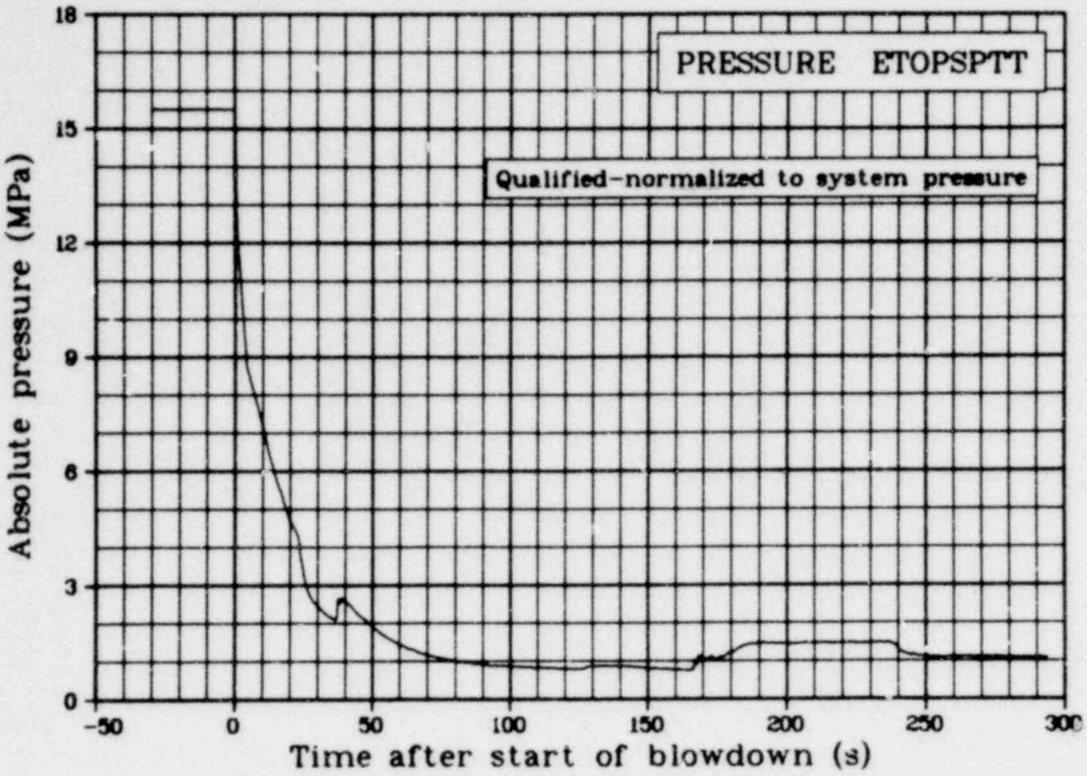

Fig. 201 Absolute pressure above the test train top support plate (PRESSURE ETOPSPTT), from -50 to 300 s.

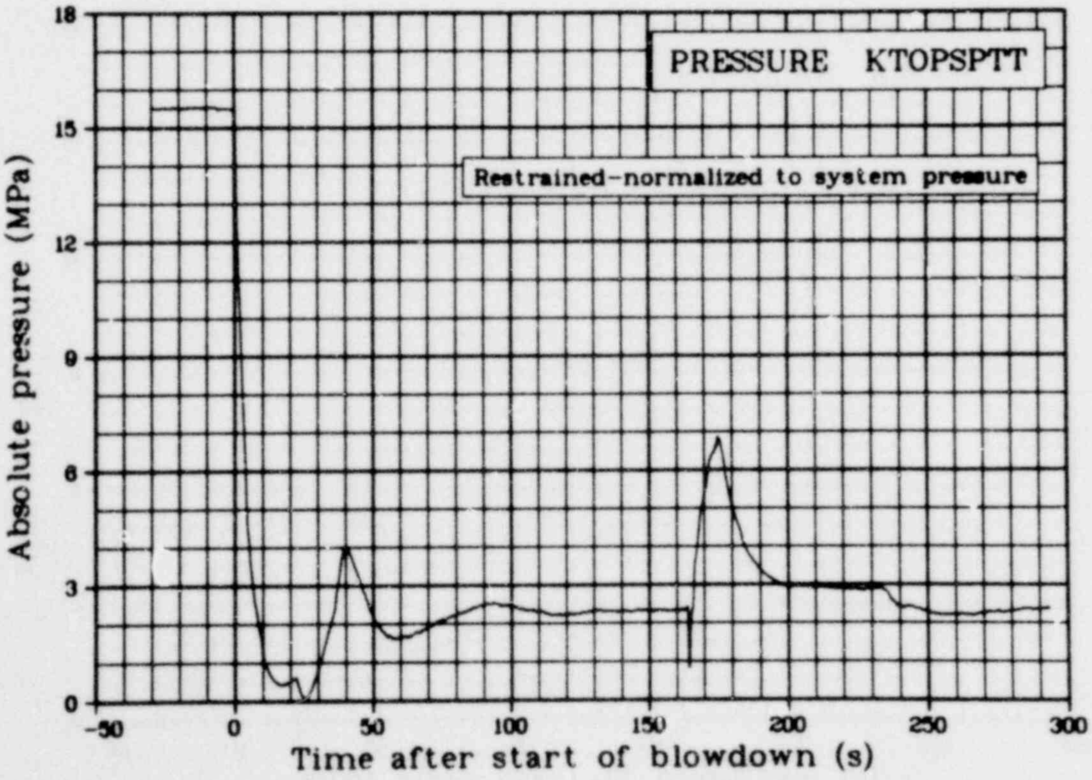

Fig. 202 Absolute pressure above the test train top support plate (PRESSURE KTOPSPTT), from -50 to 300 s.

1405 185

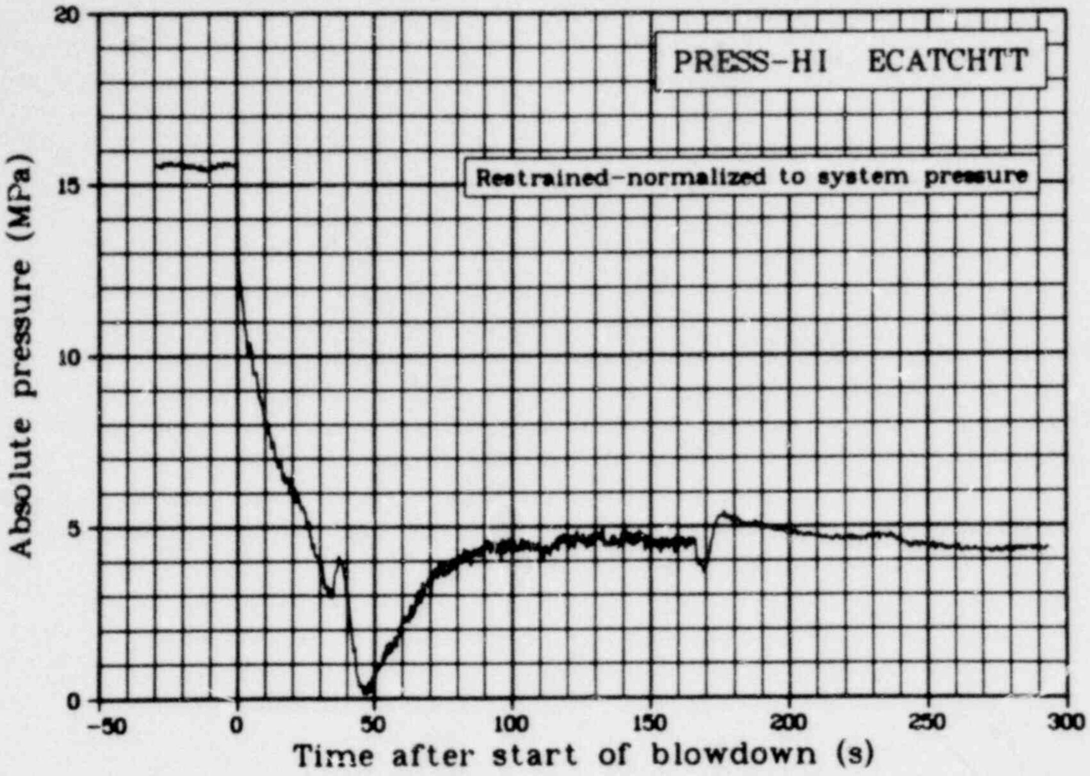

Fig. 203 Absolute pressure in test train catch basket (PRESS-HI ECATCHTT), from -50 to 300 s.

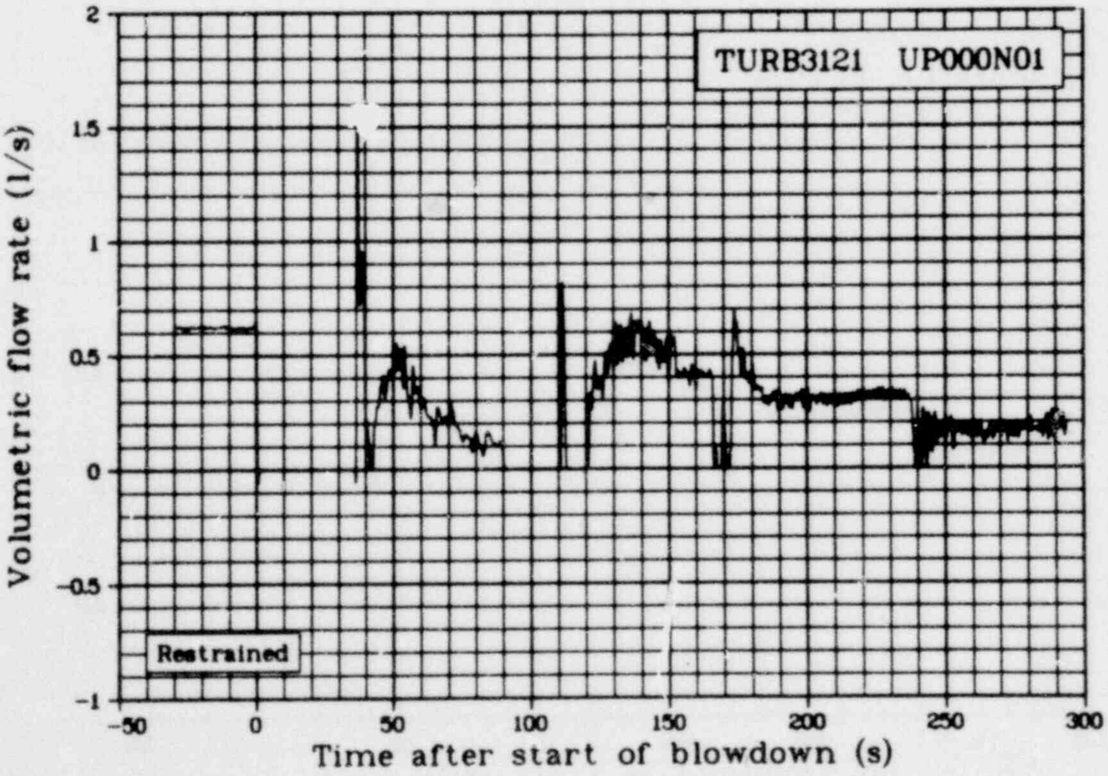

Fig. 204 Volumetric flow rate in Fuel Rod 312-1 upper shroud (TURB3121 UP000N01), from -50 to 300 s.

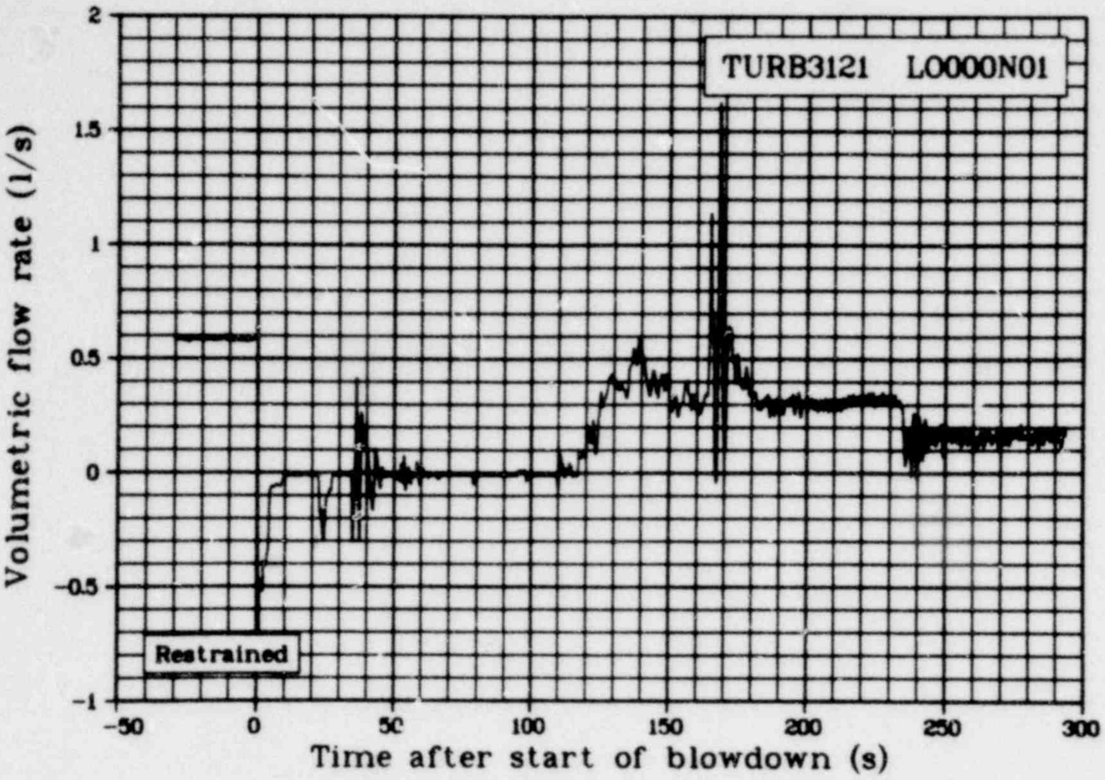

Fig. 205 Volumetric flow rate in Fuel Rod 312-1 lower shroud (TURB3121 L0000N01), from -50 to 300 s.

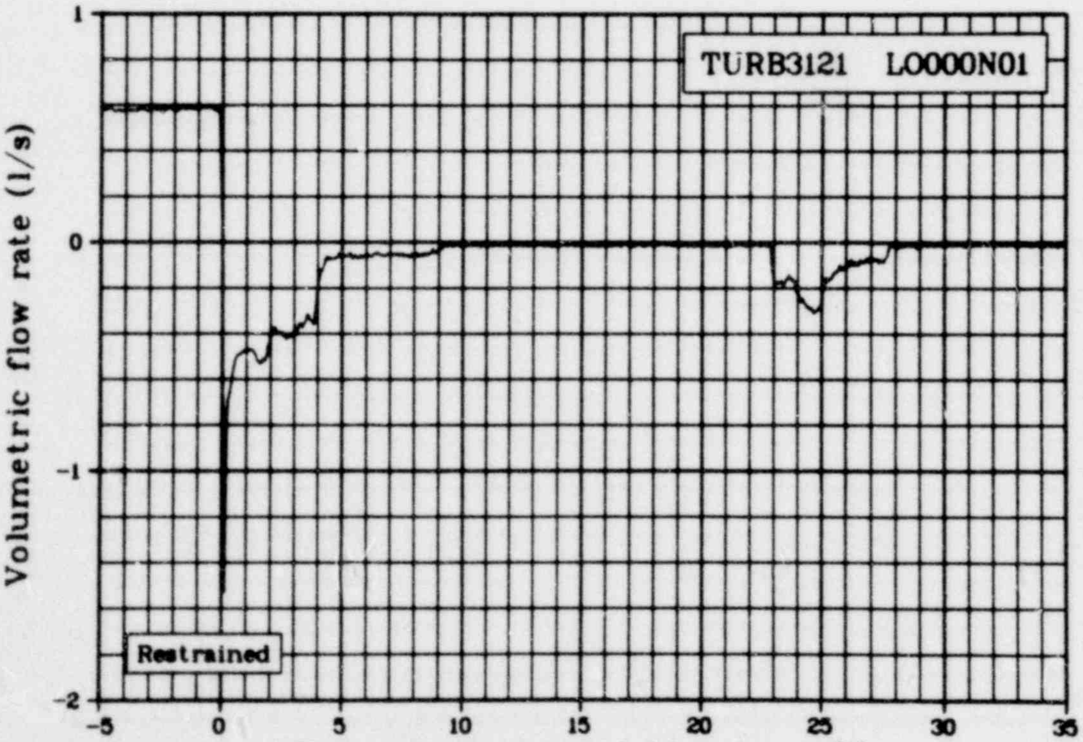

Fig. 206 Volumetric flow rate in Fuel Rod 312-1 lower shroud (TURB3121 L0000N01), from -5 to 35 s.

1405 187

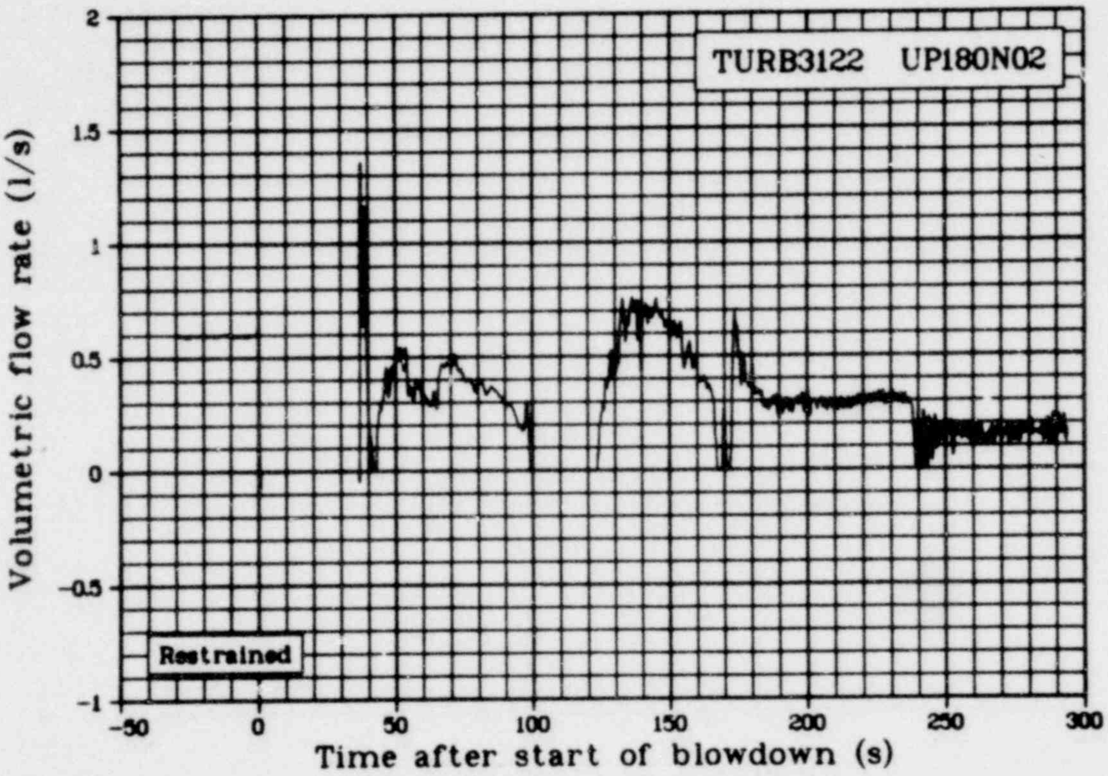

Fig. 207 Volumetric flow rate in Fuel Rod 312-2 upper shroud (TURB3122 UP180N02), from -50 to 300 s.

1405 188

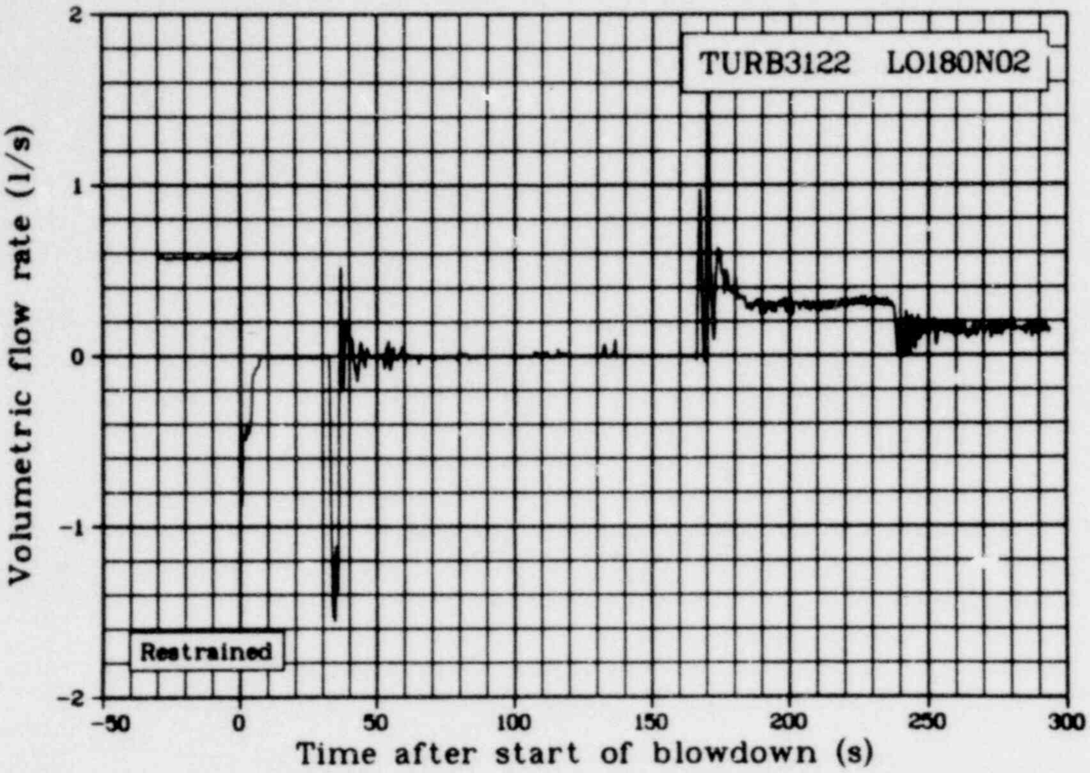

Fig. 208 Volumetric flow rate in Fuel Rod 312-2 lower shroud (TURB3122 L0180N02), from -50 to 300 s.

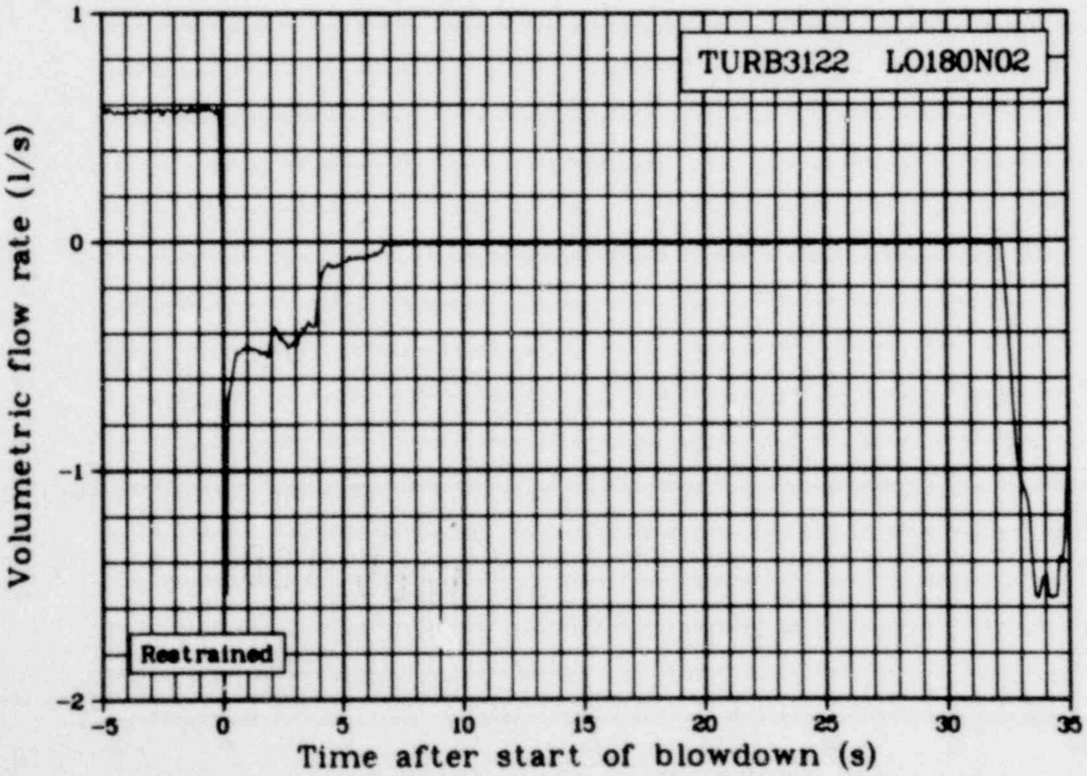

Fig. 209 Volumetric flow rate in Fuel Rod 312-2 lower shroud (TURB3122 L0180N02), from -5 to 35 s.

1405 189

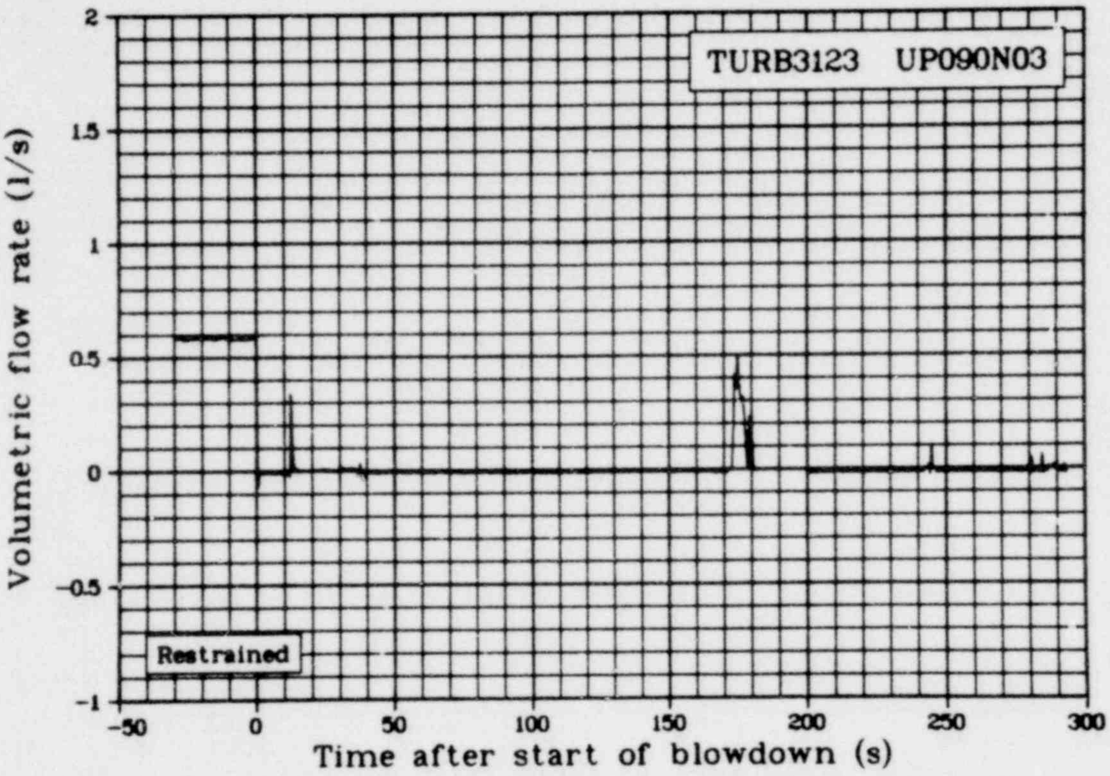

Fig. 210 Volumetric flow rate in Fuel Rod 312-3 upper shroud (TURB3123 UP090N03), from -50 to 300 s.

1405 190

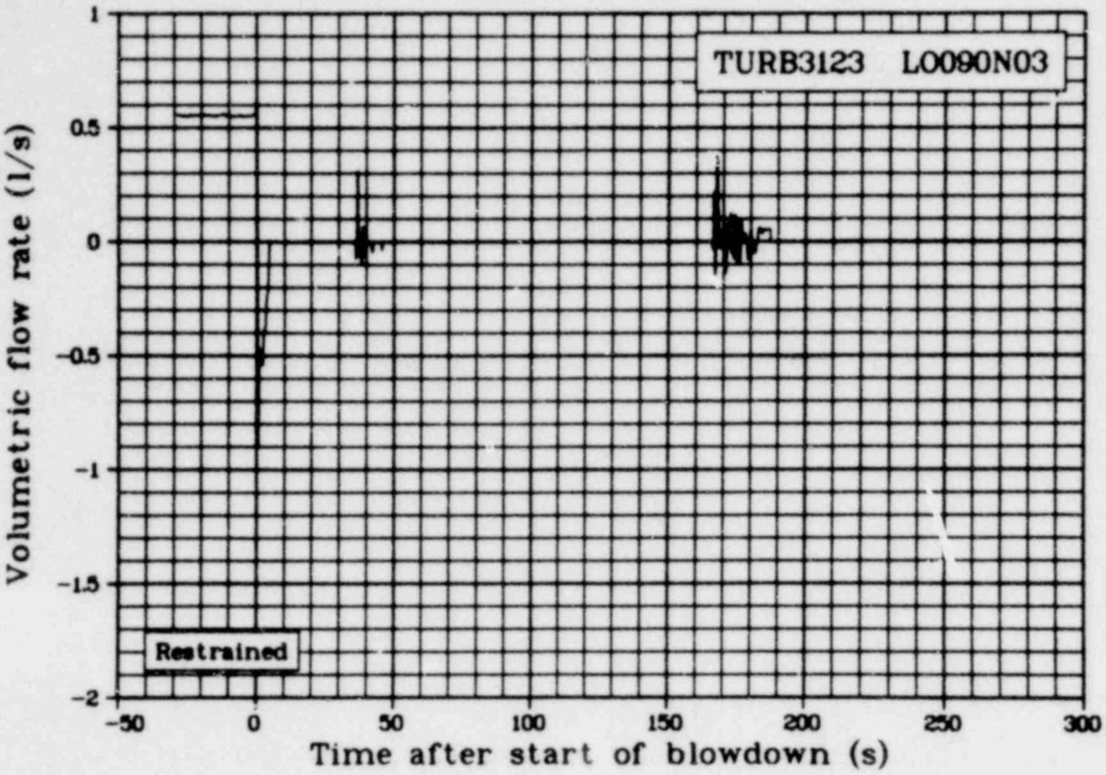

Fig. 211 Volumetric flow rate in Fuel Rod 312-3 lower shroud (TURB3123 L0090N03), from -50 to 300 s.

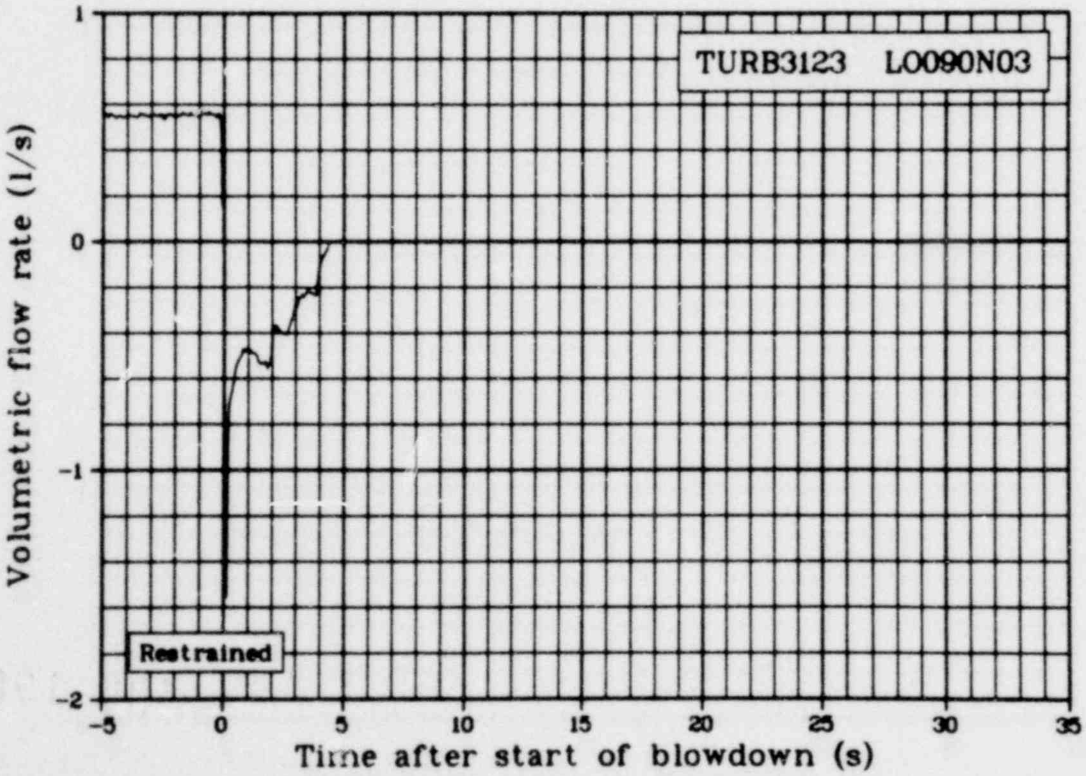

Fig. 212 Volumetric flow rate in Fuel Rod 312-3 lower shroud (TURB3123 L0090N03), from -5 to 35 s.

1405 191

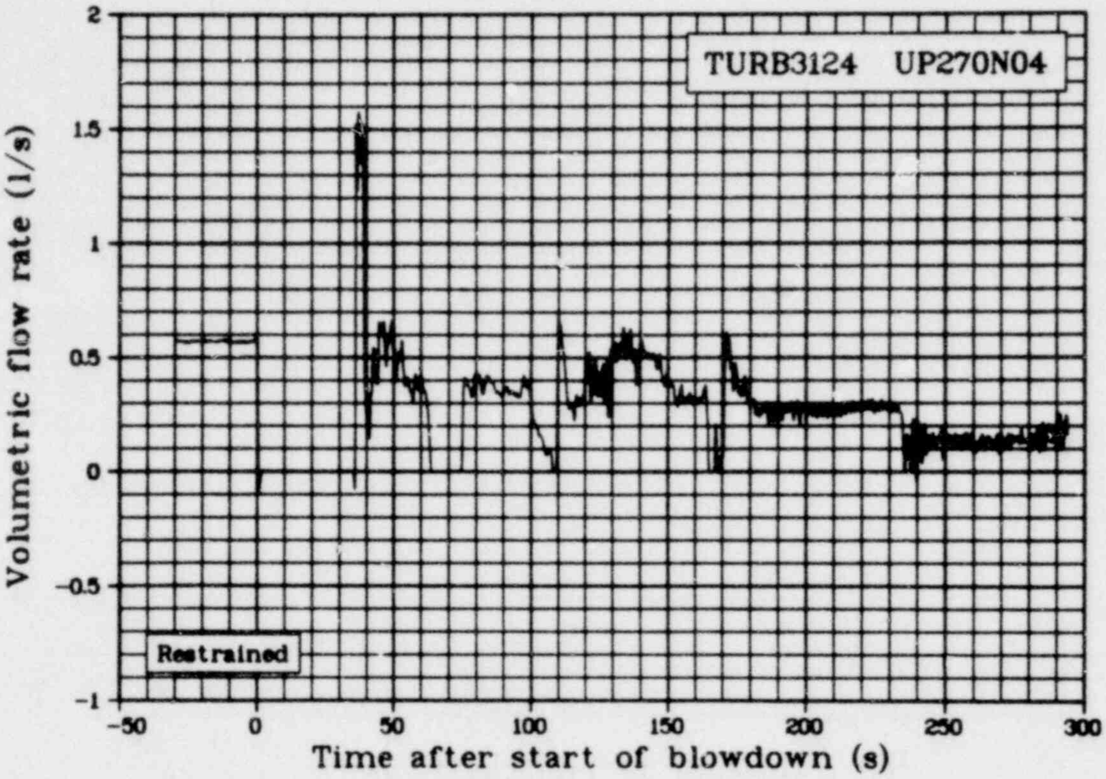

Fig. 213 Volumetric flow rate in Fuel Rod 312-4 upper shroud (TURB3124 UP279N04), from -50 to 300 s.

1405 192

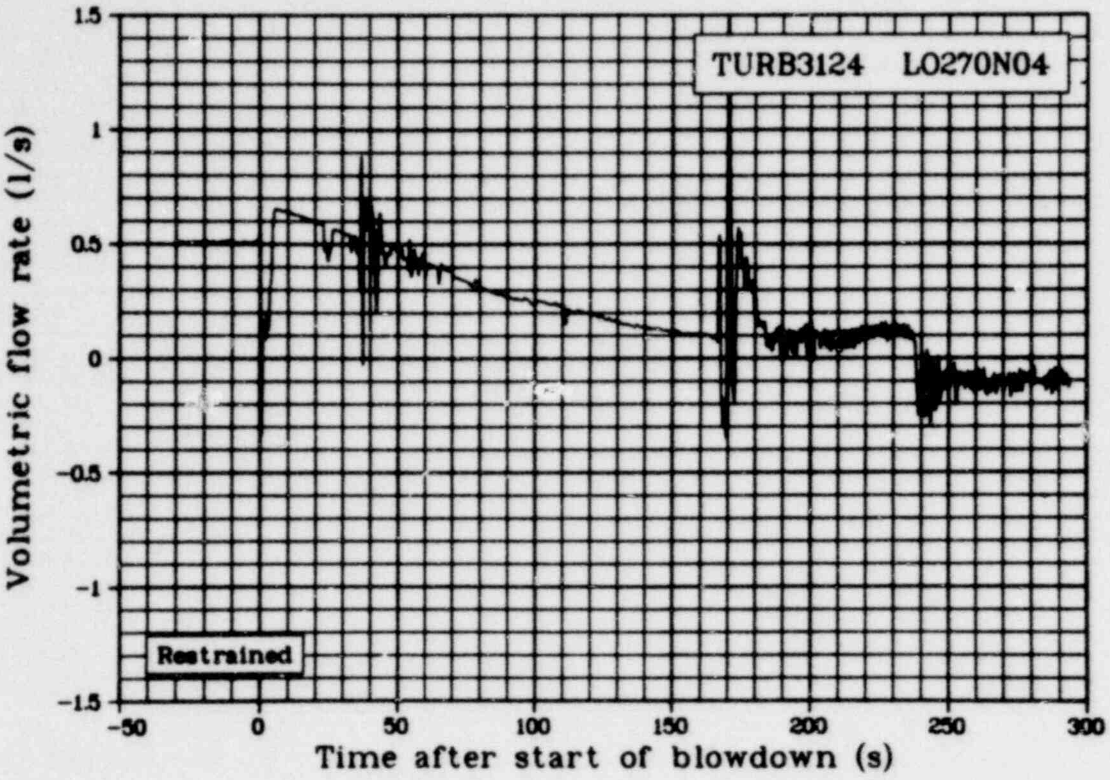

Fig. 214 Volumetric flow rate in Fuel Rod 312-4 lower shroud (TURB3124 L0270N04), from -50 to 300 s.

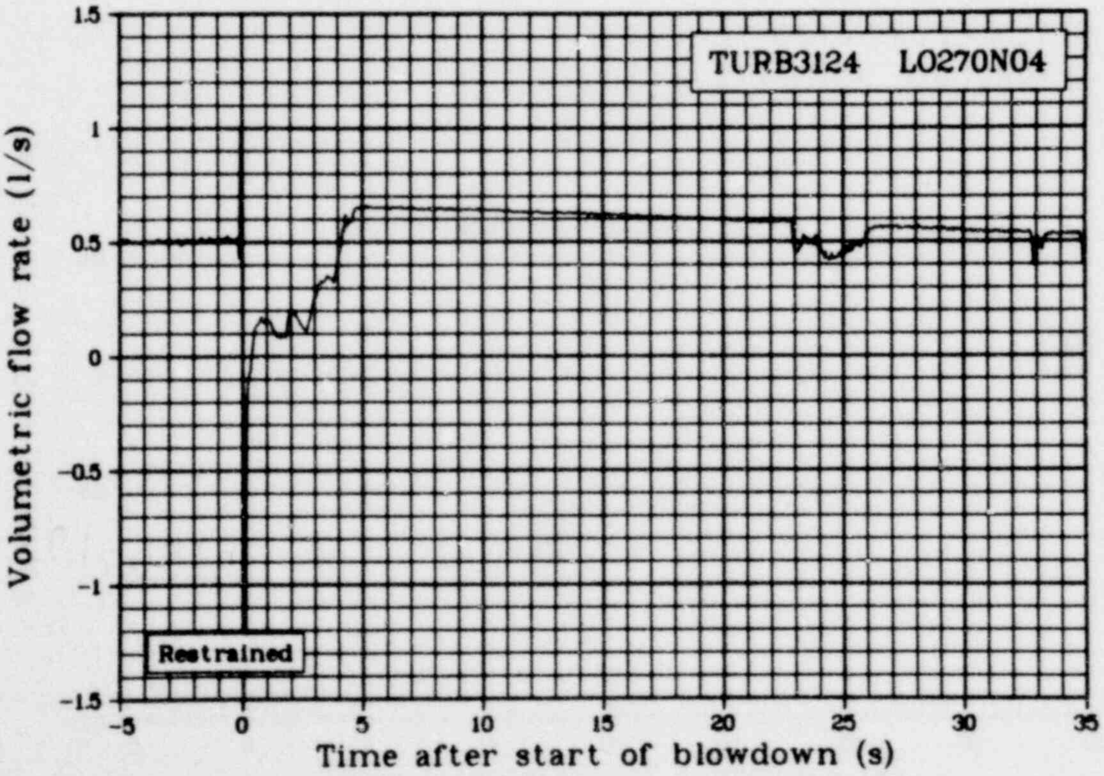

Fig. 215 Volumetric flow rate in Fuel Rod 312-4 lower shroud (TURB3124 L0270N04), from -5 to 35 s.

1405 193

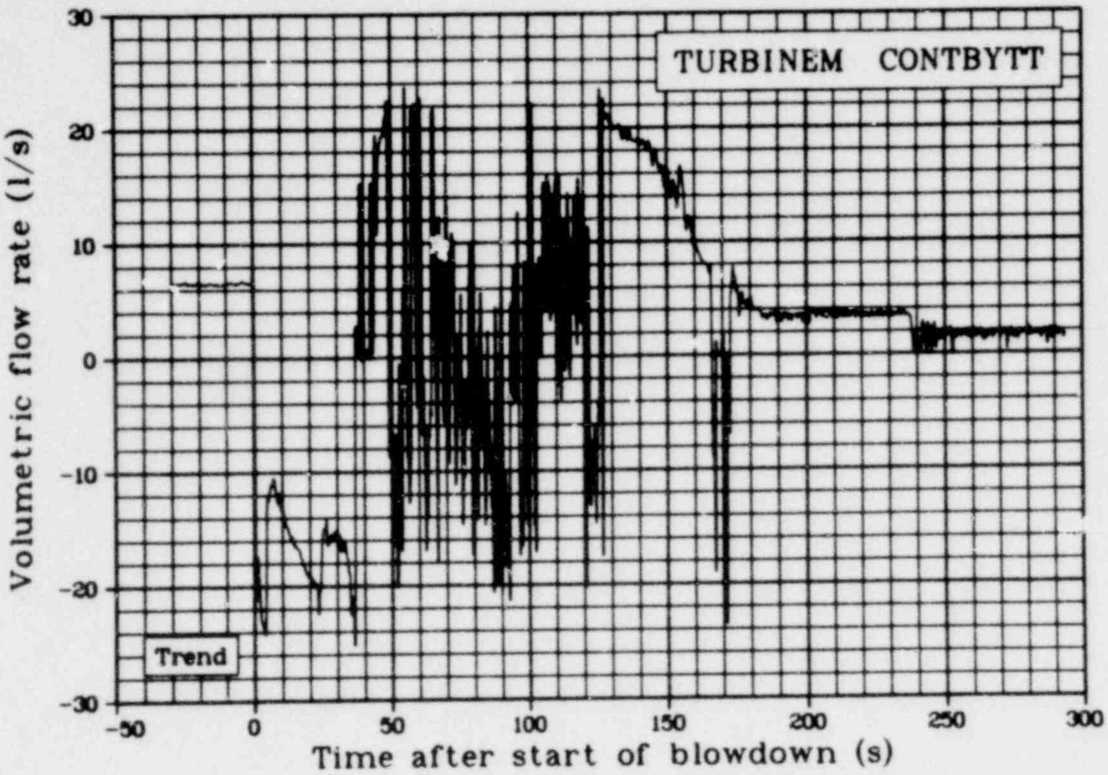

Fig. 216 Volumetric flow rate in test train controlled bypass (TURBINEM CONTBYTT), from -50 to 300 s.

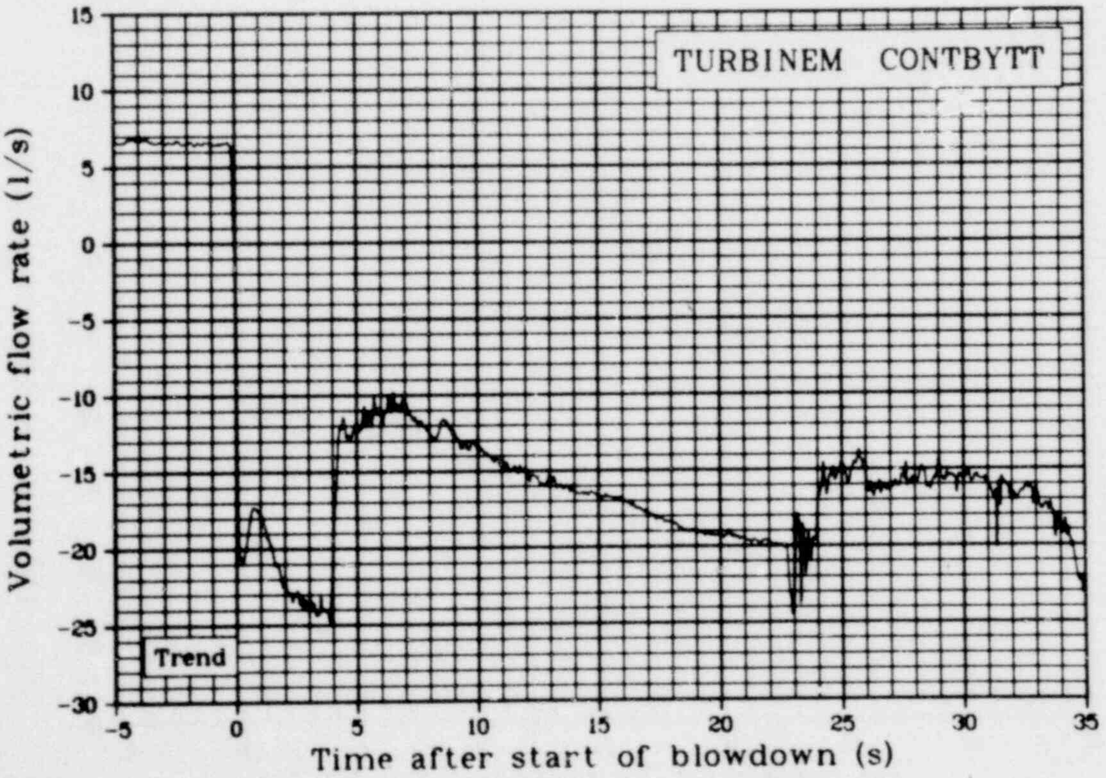

Fig. 217 Volumetric flow rate in test train controlled bypass (TURBINEM CONTBYTT), from -5 to 35 s.

1405 194

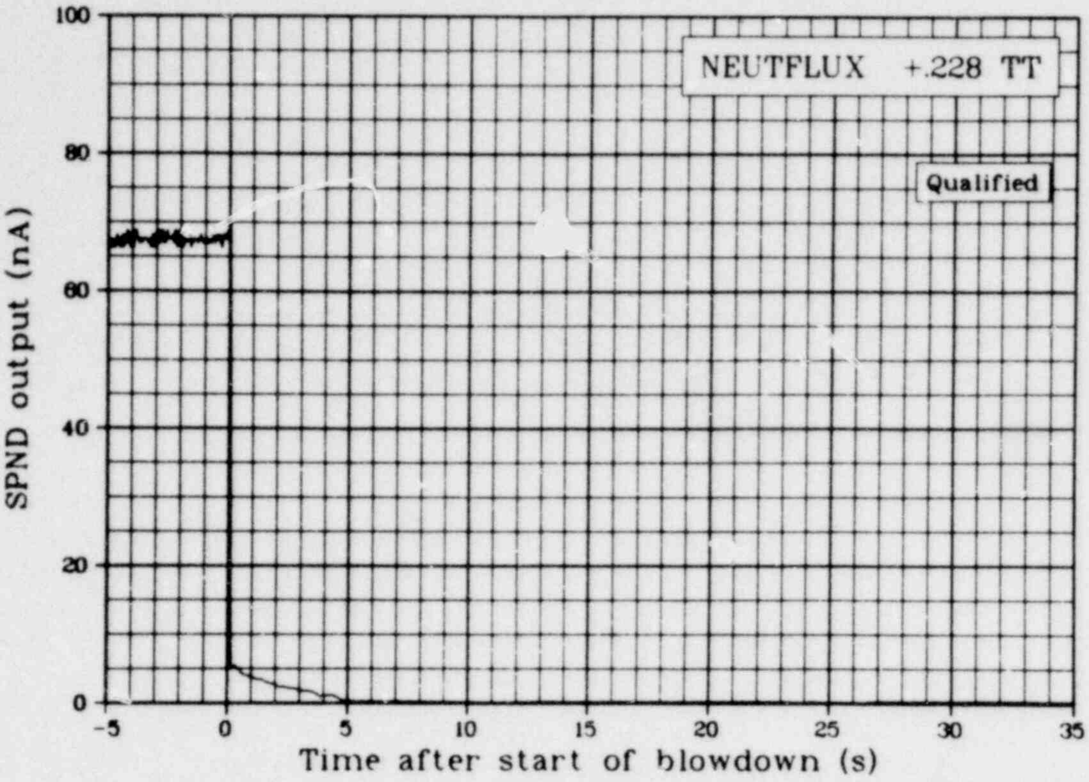

Fig. 218 Neutron flux 0.228 m above fuel stack midplane (NEUTFLUX +.228 TT), from -5 to 35 s.

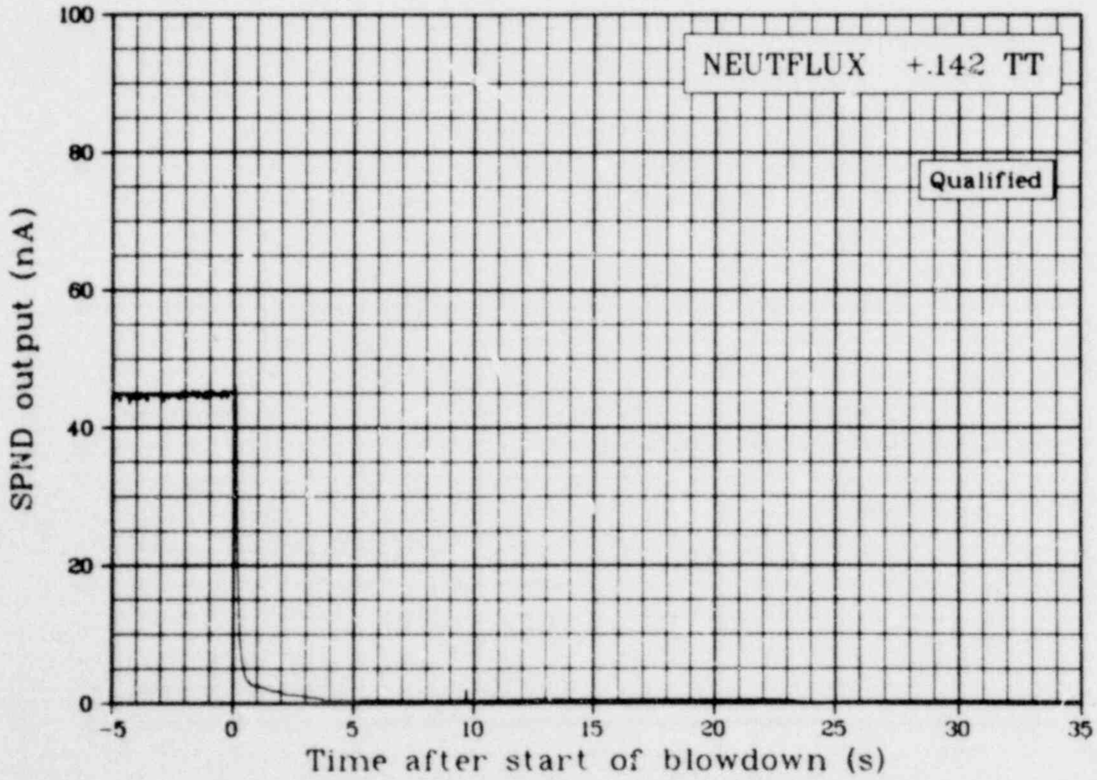

Fig. 219 Neutron flux 0.142 m above fuel stack midplane (NEUTFLUX +.142 TT), from -5 tb 35 s.

1405 195

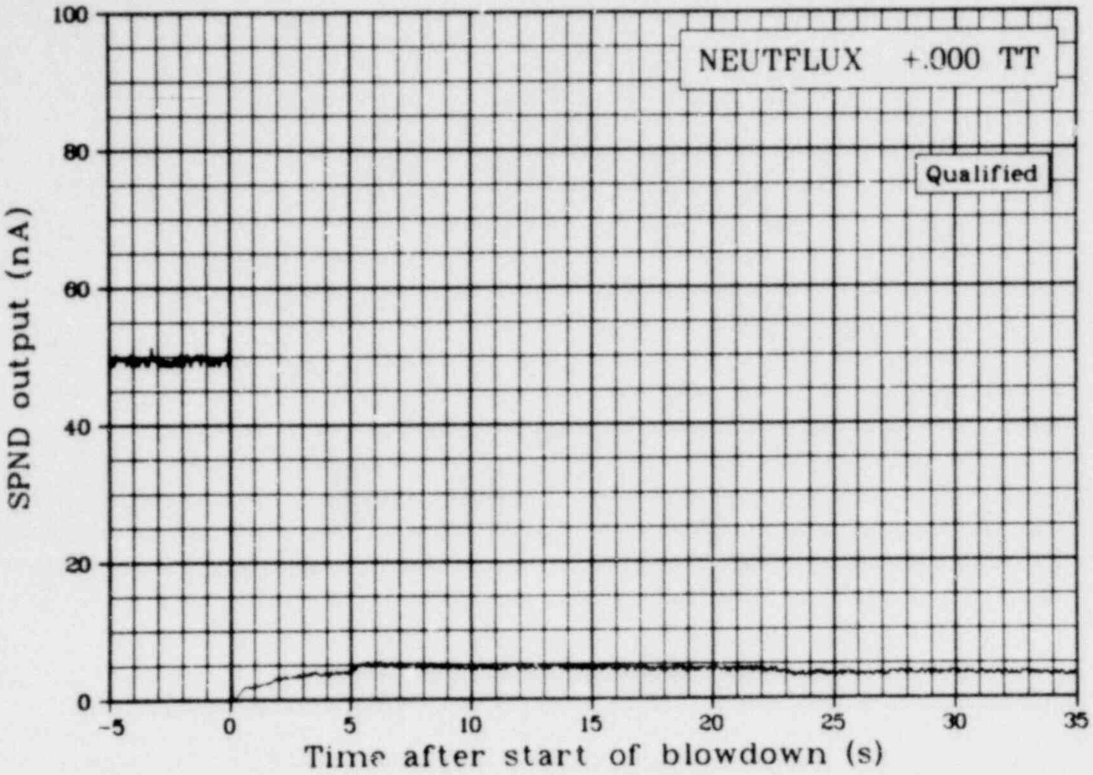

Fig. 220 Neutron flux at fuel stack midplane (NEUTFLUX + .000 TT), from -5 to 35 s.

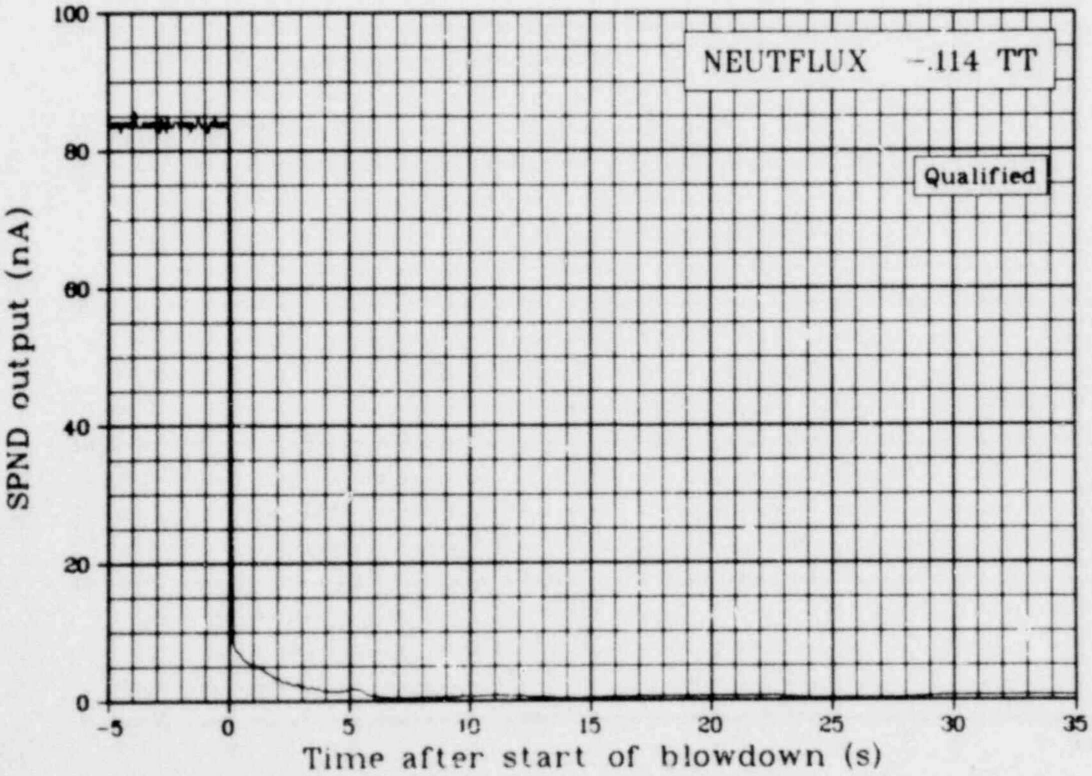

Fig. 221 Neutron flux 0.114 m below fuel stack midplane (NEUTFLUX -.114 TT), from -5 to 35 s.

1405 196

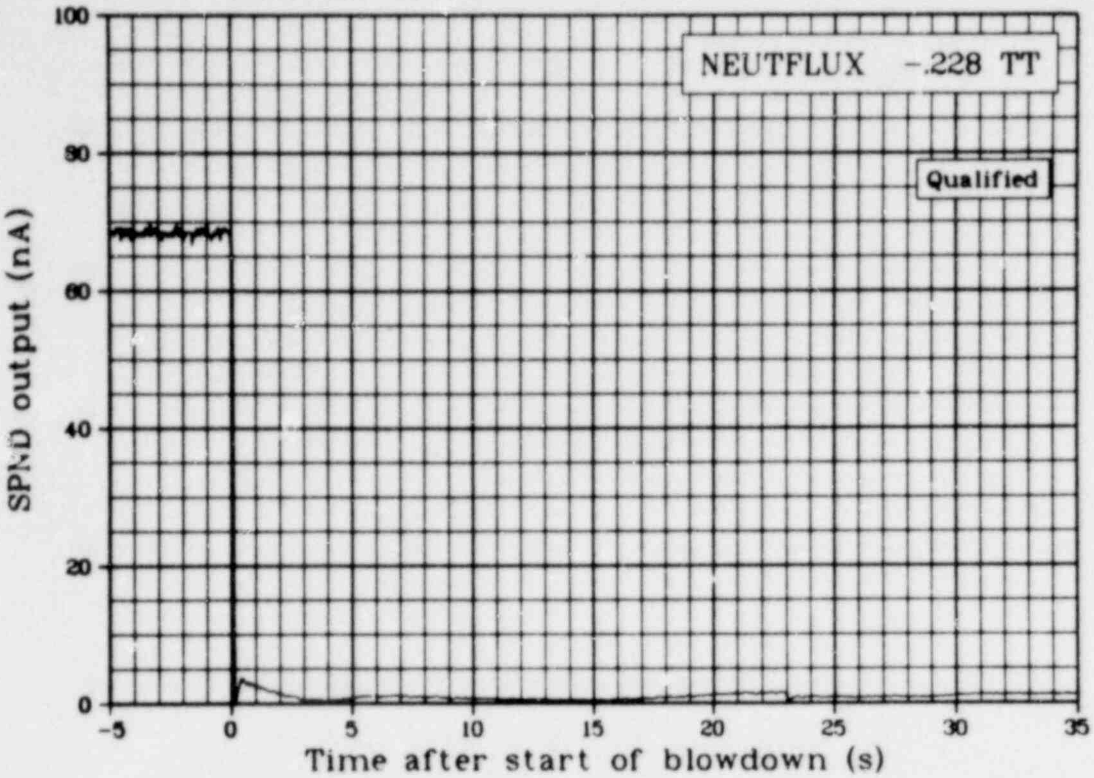

Fig. 222 Neutron flux 0.228 m below fuel stack midplane (NEUTFLUX -.228 TT), from -5 to 35 s.

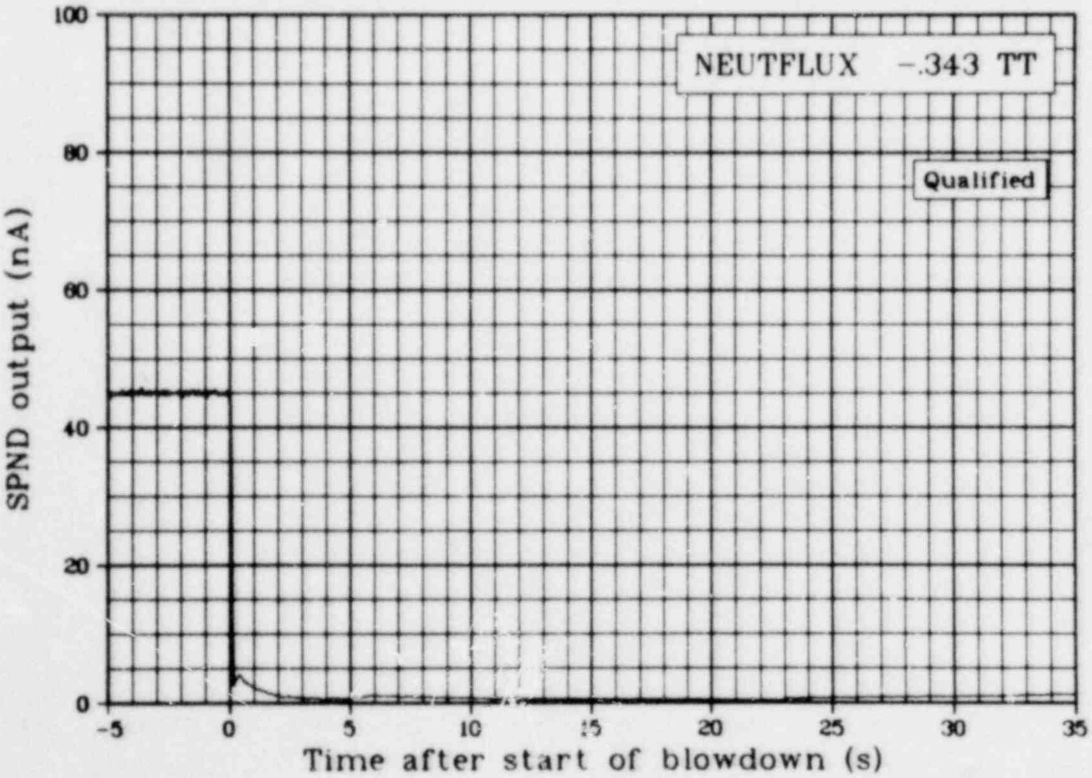

Fig. 223 Neutron flux 0.343 m below fuel stack midplane (NEUTFLUX -.343 TT), from -5 to 35 s.

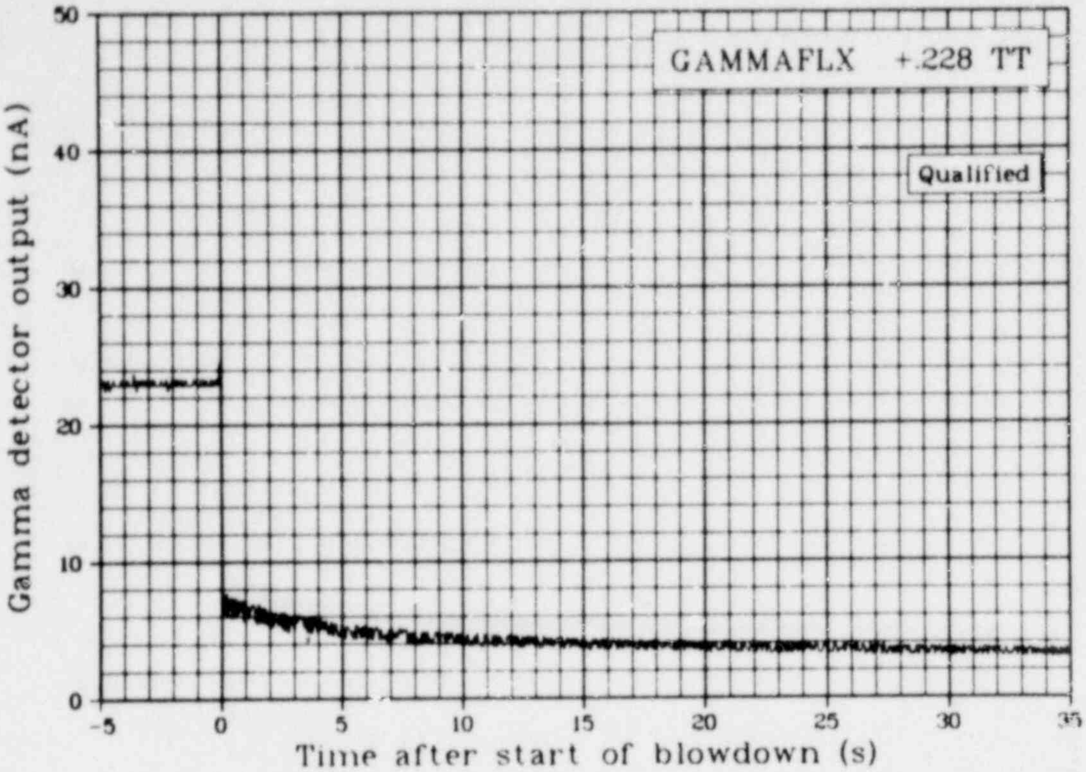

Fig. 224 Gamma flux 0.228 m above fuel stack midplane (GAMMAFLX +.228 TT), from -5 to 35 s.

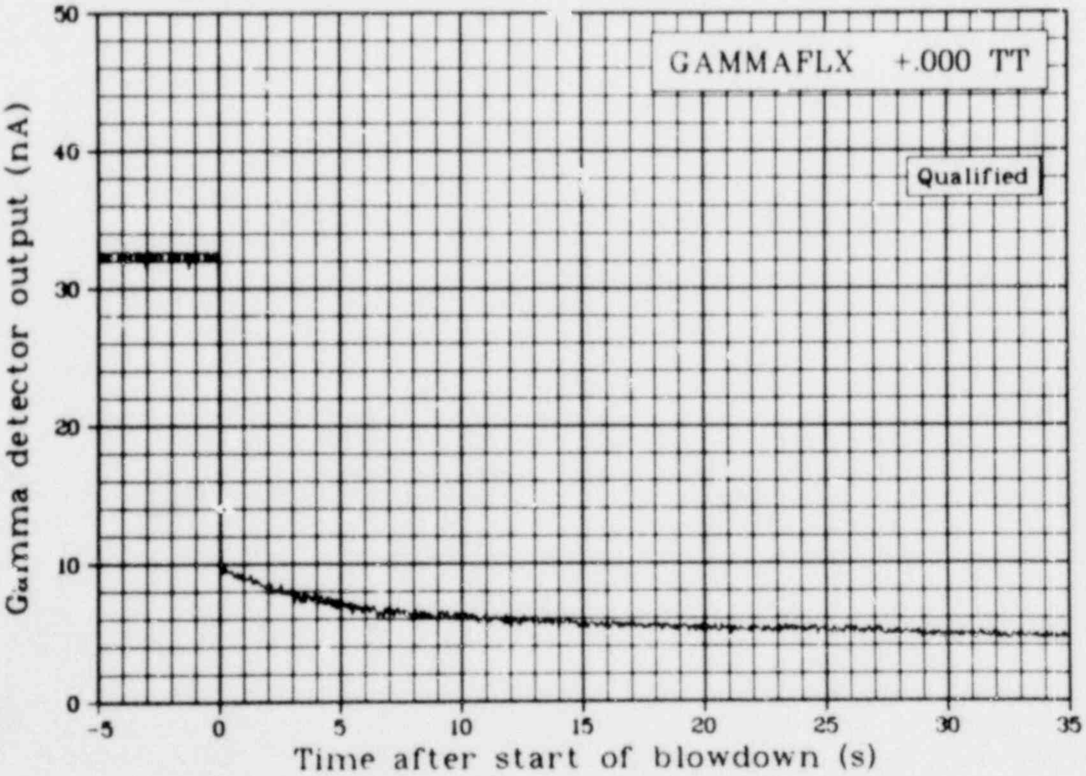

Fig. 225 Gamma flux at fuel stack midplane (GAMMAFLX +.000 TT), from -5 to 35 s.

1405 198

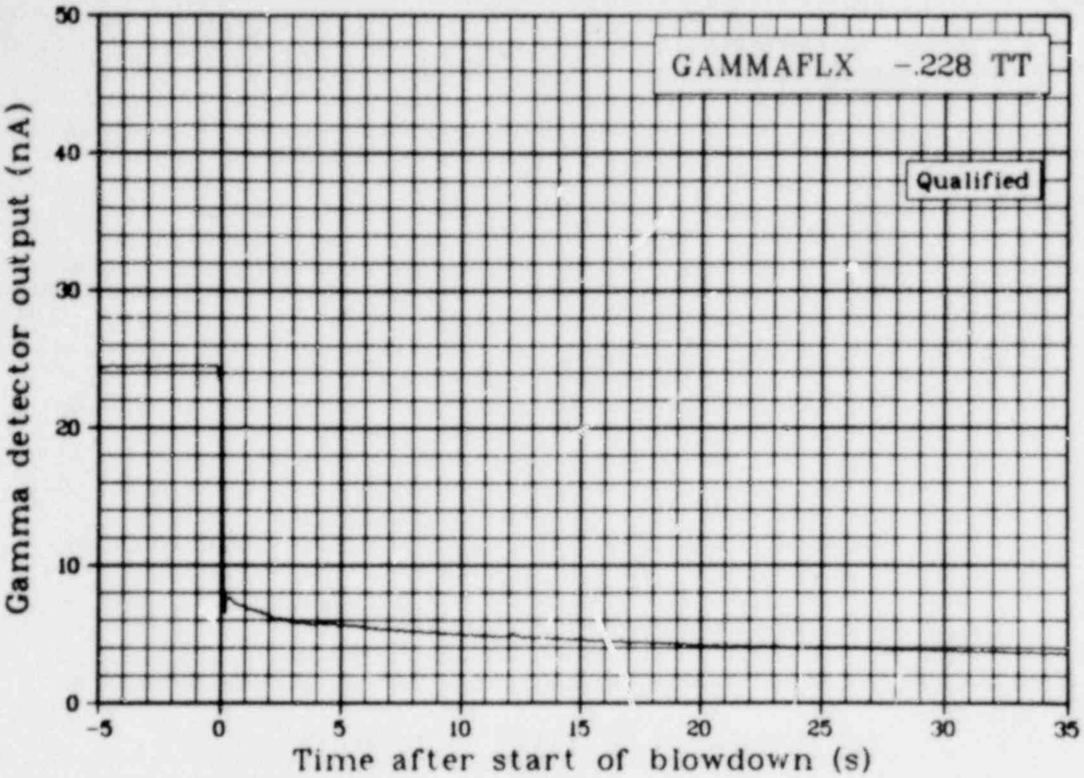

Fig. 226 Gamma flux 0.228 m below fuel stack midplane (GAMMAFLX -.228 TT), from -5 to 35 s.

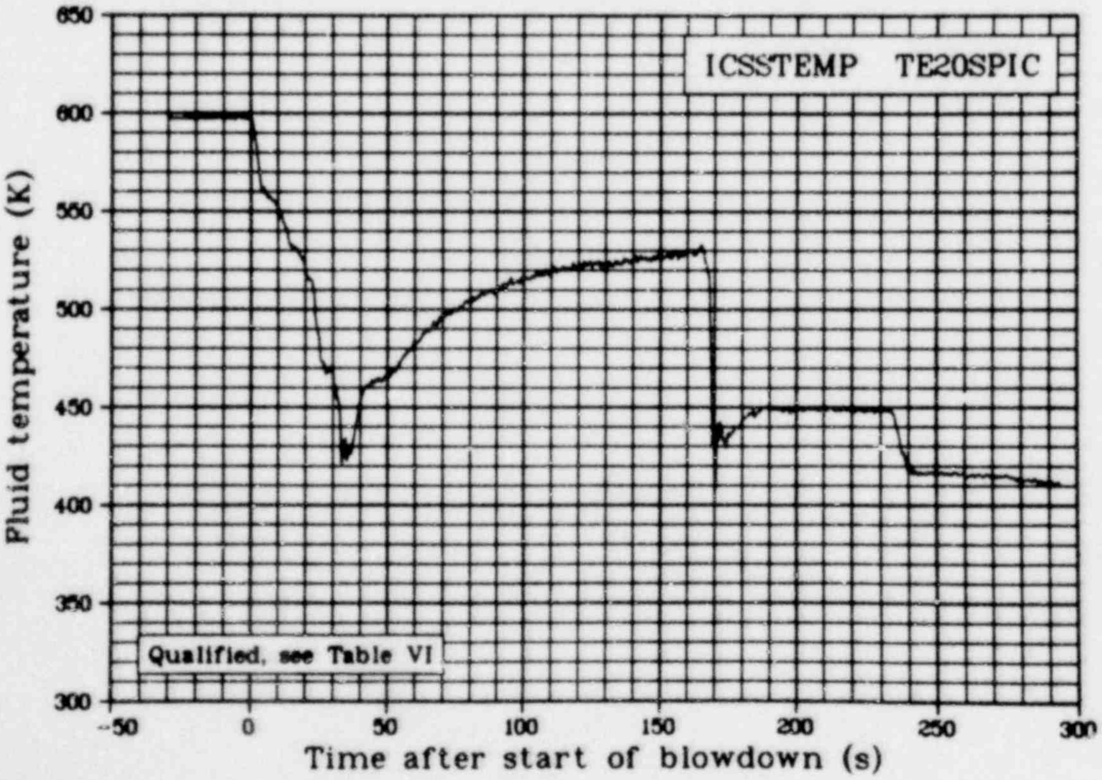

Fig. 227 Fluid temperature in initial condition spool (ICSSTEMP TE20SPIC), from -50 to 300 s.

1405 199

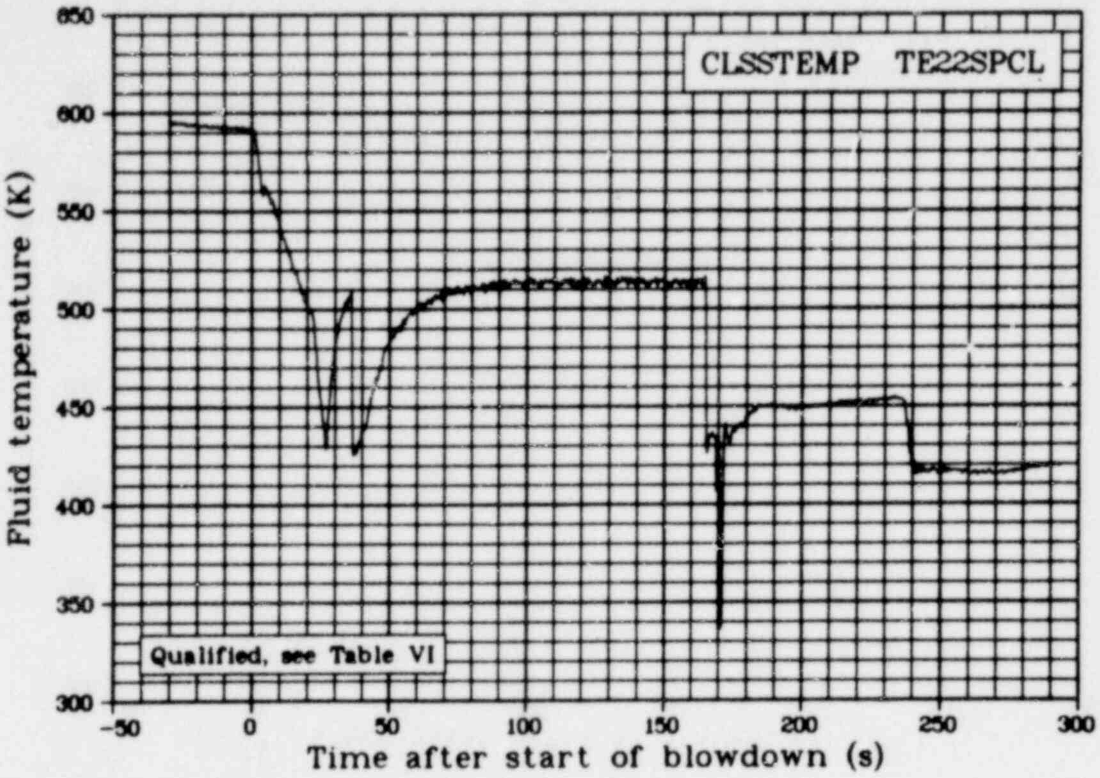

Fig. 228 Fluid temperature in cold leg blowdown spool (CLSSTEMP TE22SPCL), from -50 to 300 s.

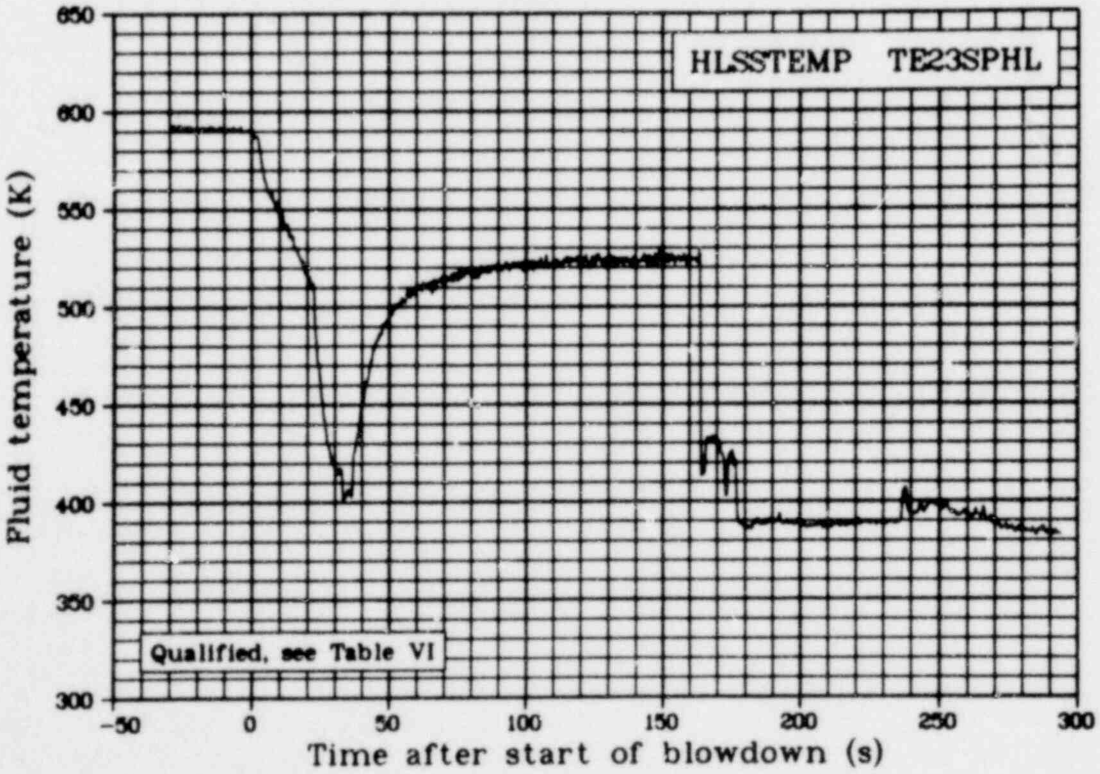

Fig. 229 Fluid temperature in hot leg blowdown spool (HLSSTEMP TE23SPHL), from -50 to 300 s.

1405 200

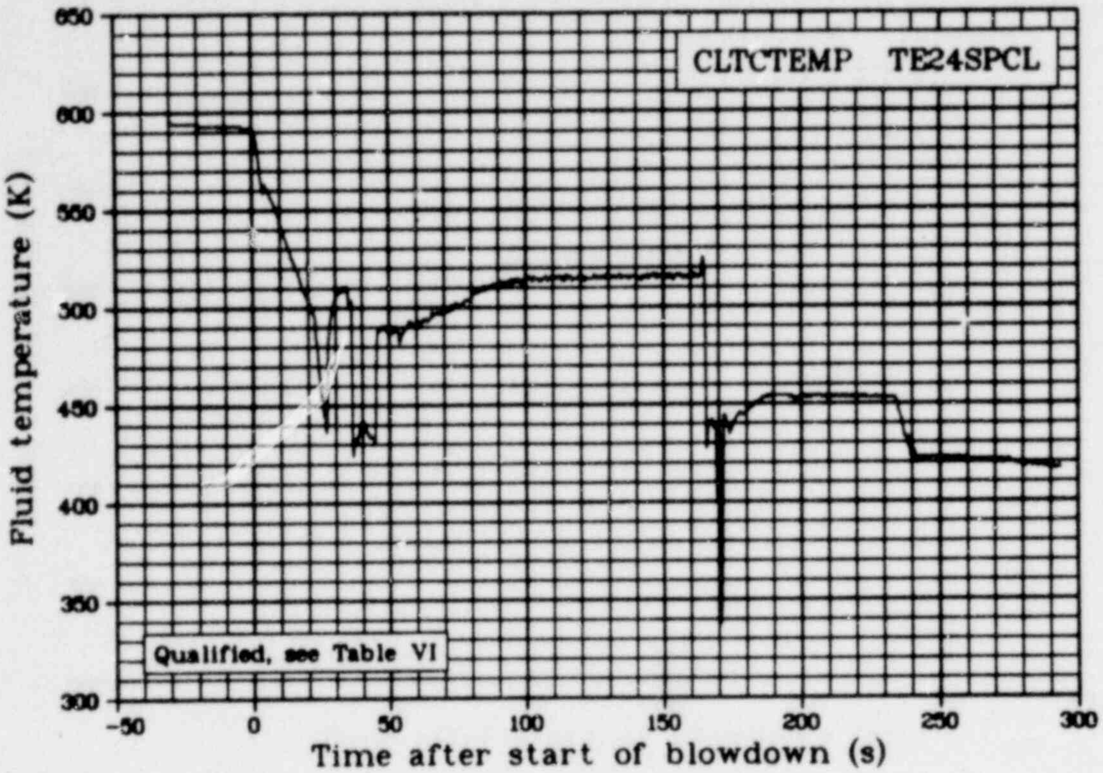

Fig. 230 Fluid temperature in cold leg blowdown spool (CLTCTEMP TE24SPCL), from -50 to 300 s.

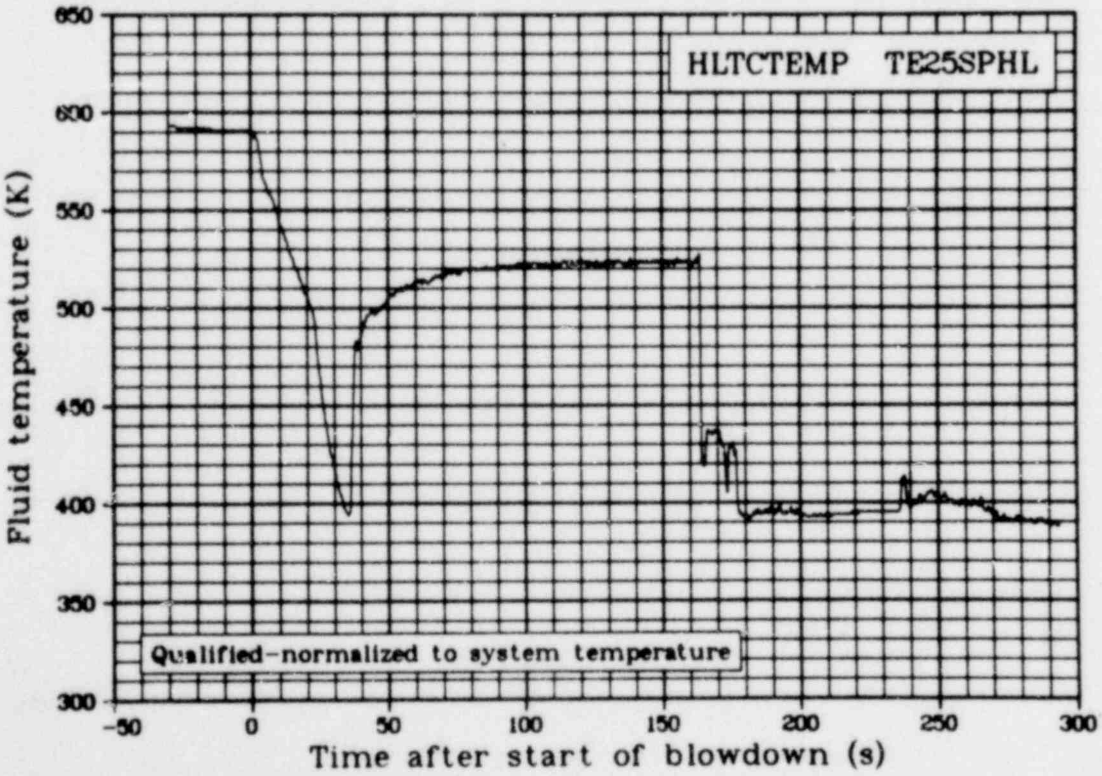

Fig. 231 Fluid temperature in hot leg blowdown spool (HLTCTEMP TE25SPHL), from -50 to 300 s.

1405 201

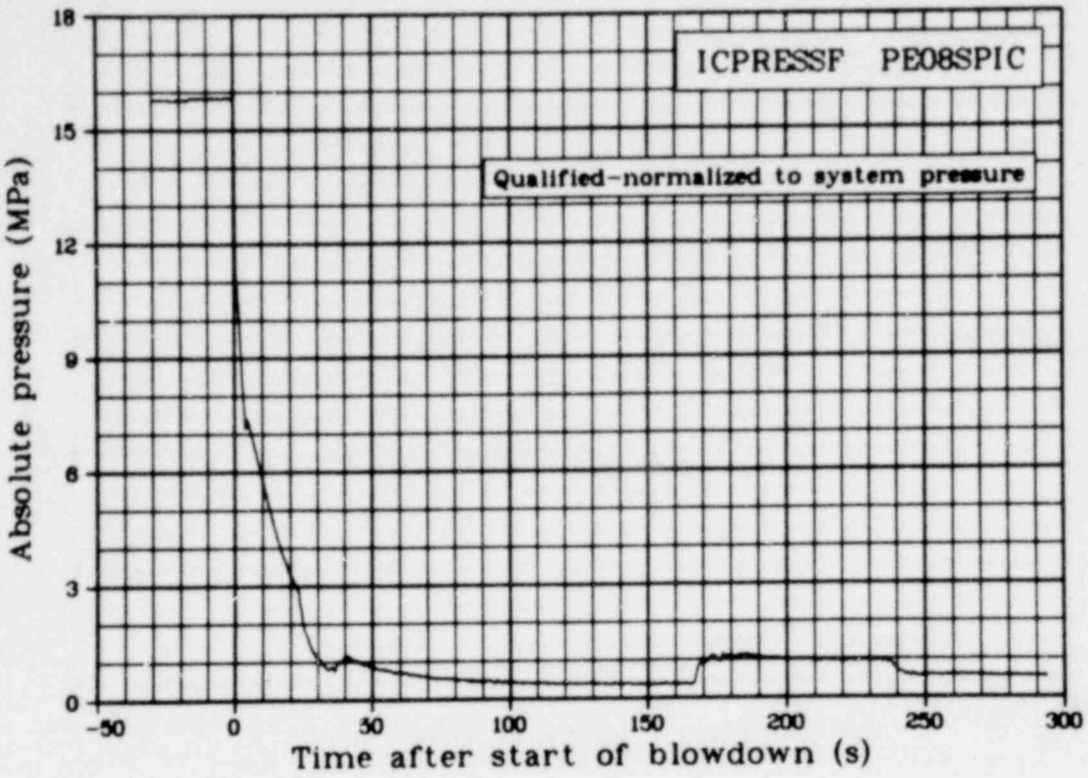

Fig. 232 Absolute pressure in initial condition spool (ICPRESSF PE08SPIC), from -50 to 300 s.

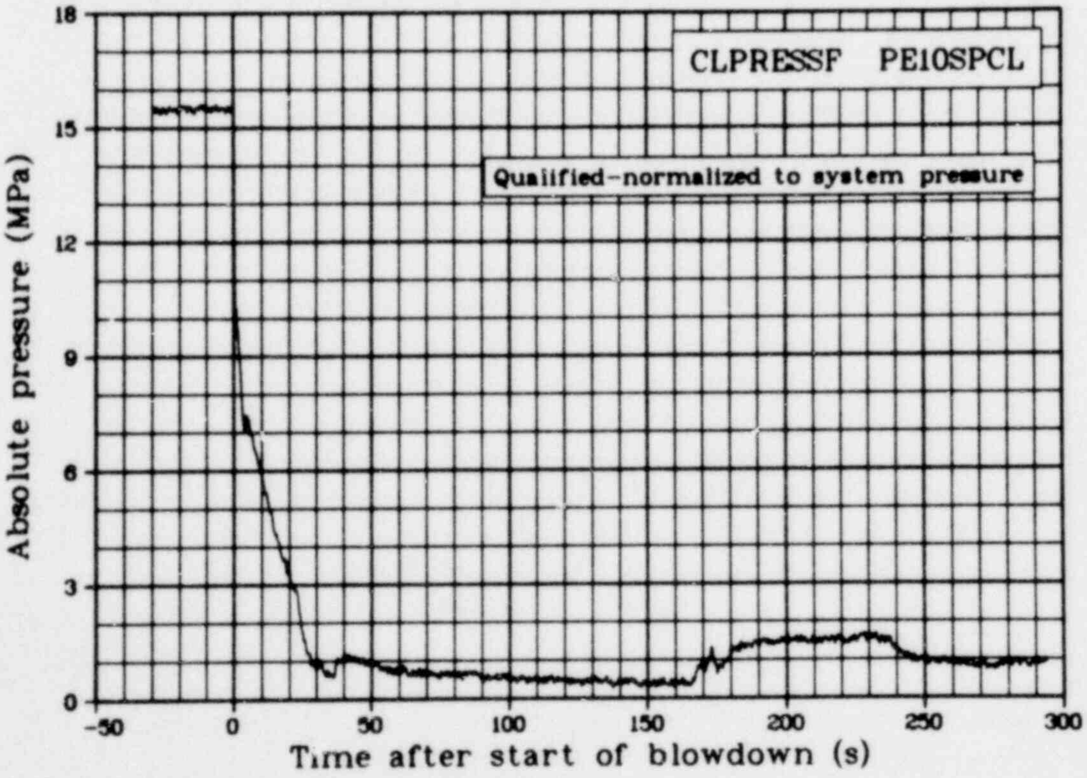

Fig. 233 Absolute pressure in cold leg blowdown spool (CLPRESSF PE10SPCL), from -50 to 300 s.

1405 202

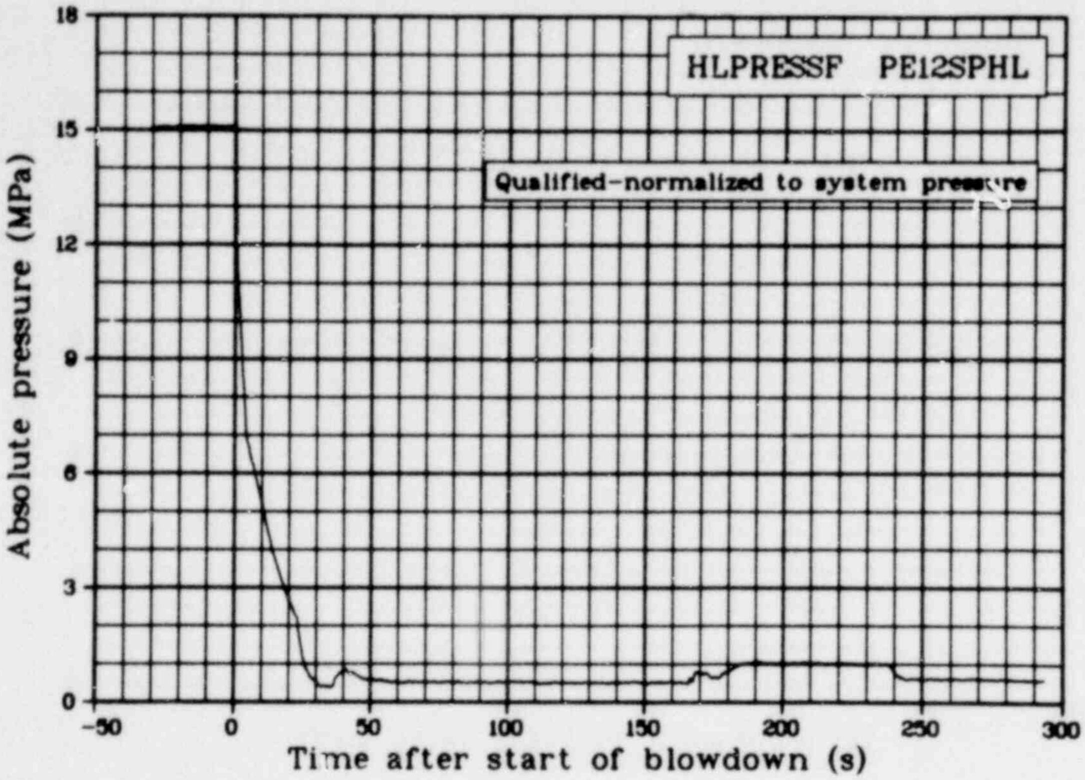

Fig. 234 Absolute pressure in hot leg blowdown spool (HLPRESSF PE12SPHL), from -50 to 300 s.

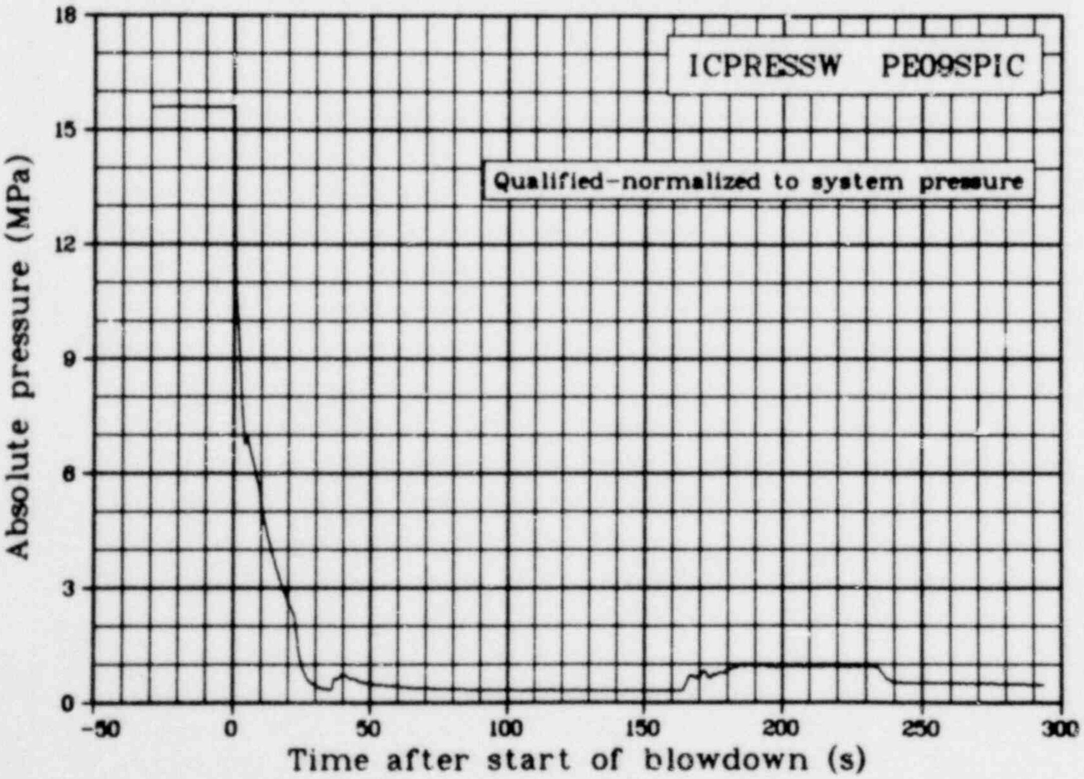

Fig. 235 Absolute pressure in initial condition spool (ICPRESSW PE09SPIC), from -50 to 300 s.

1405 203

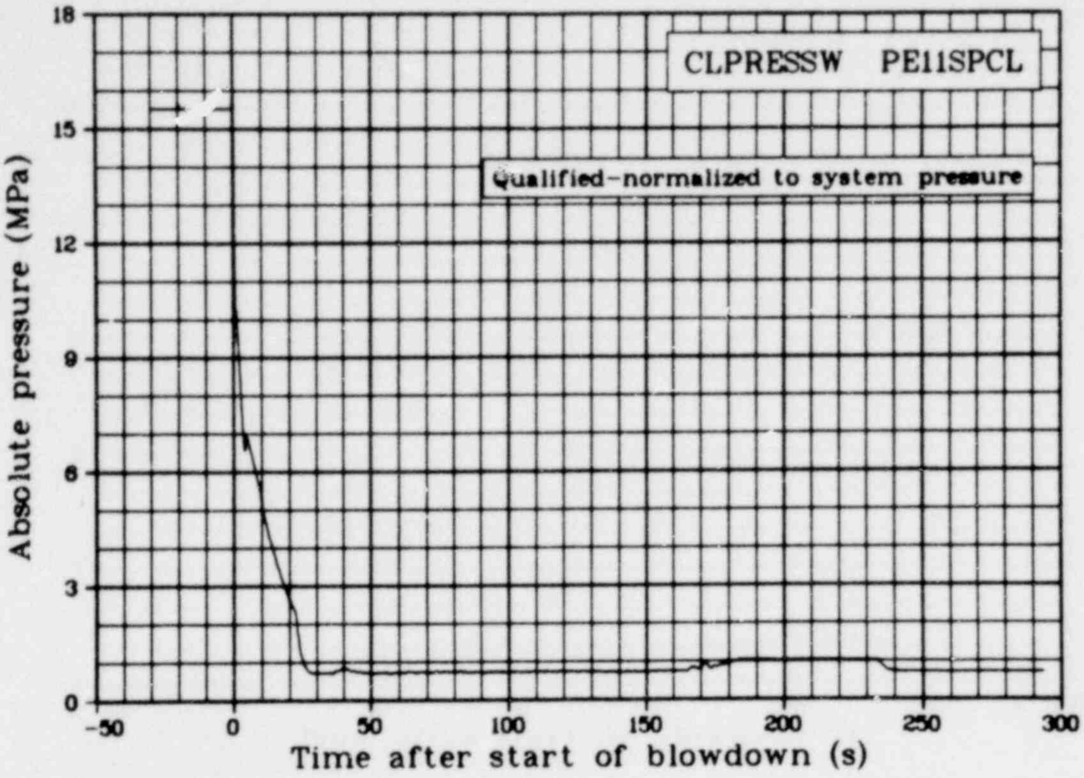

Fig. 236 Absolute pressure in cold leg blowdown spool (CLPRESSW PE11SPCL), from -50 to 300 s.

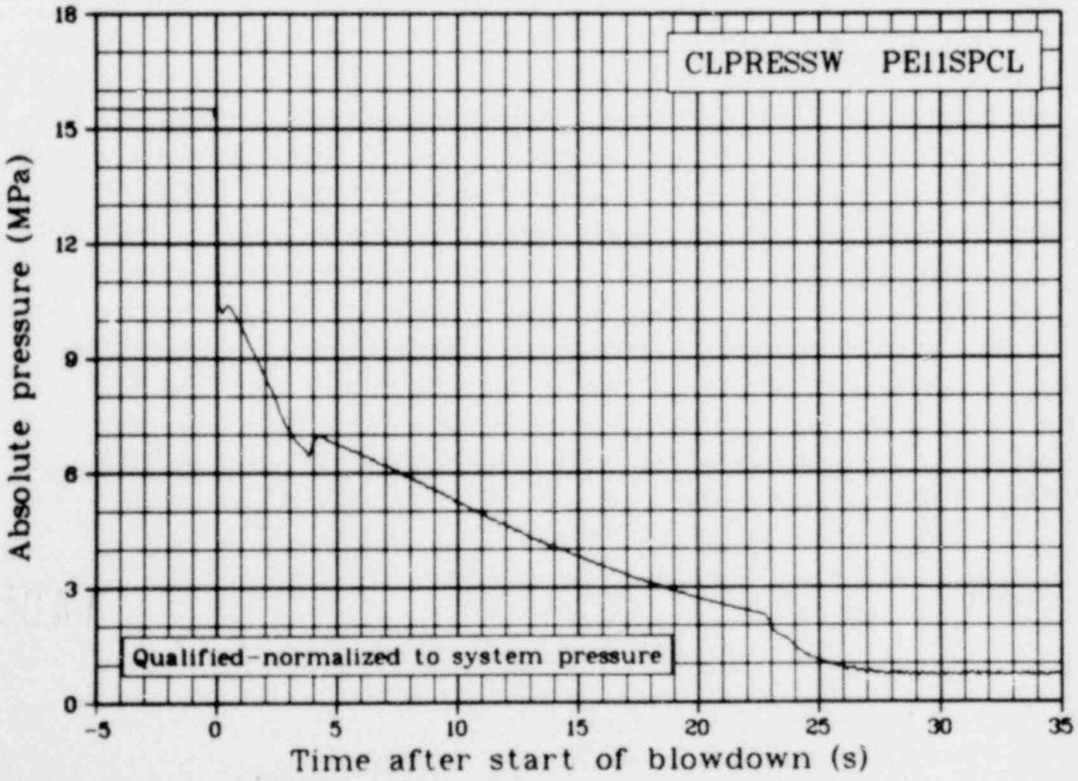

Fig. 237 Absolute pressure in cold leg blowdown spool (CLPRESSW PE11SPCL), from -5 to 35 s.

1405 204

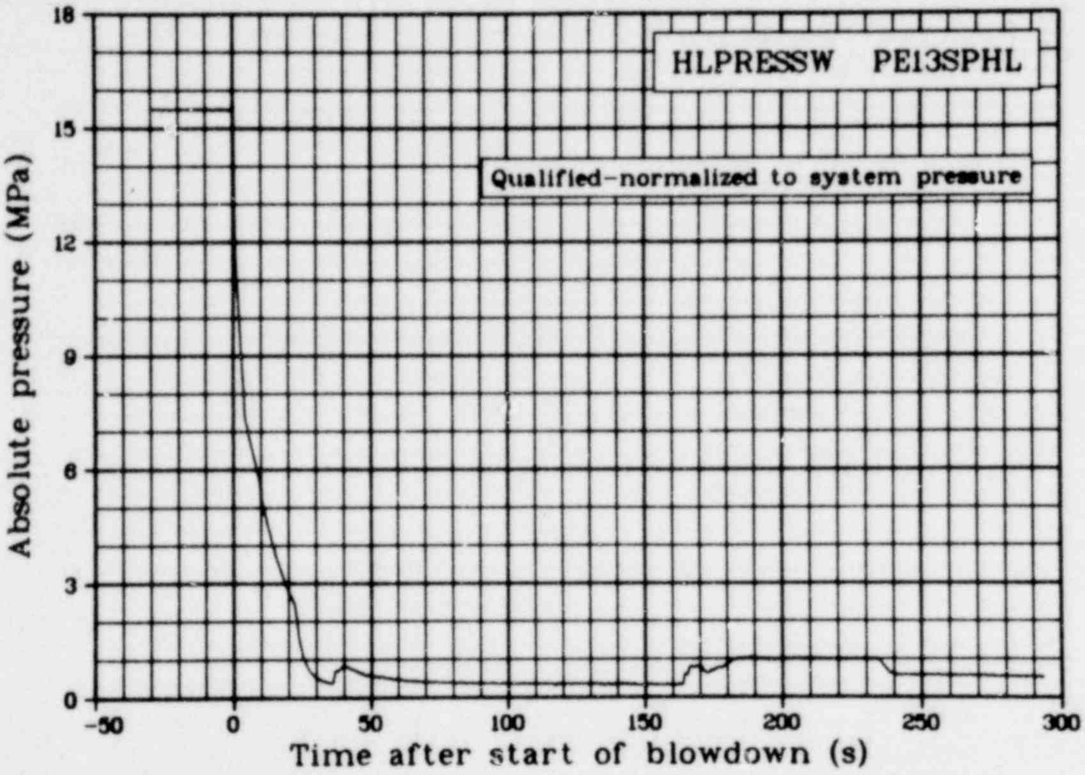

Fig. 238 Absolute pressure in hot leg blowdown spool (HLPRESSW PE13SPHL), from -50 to 300 s.

1405 205

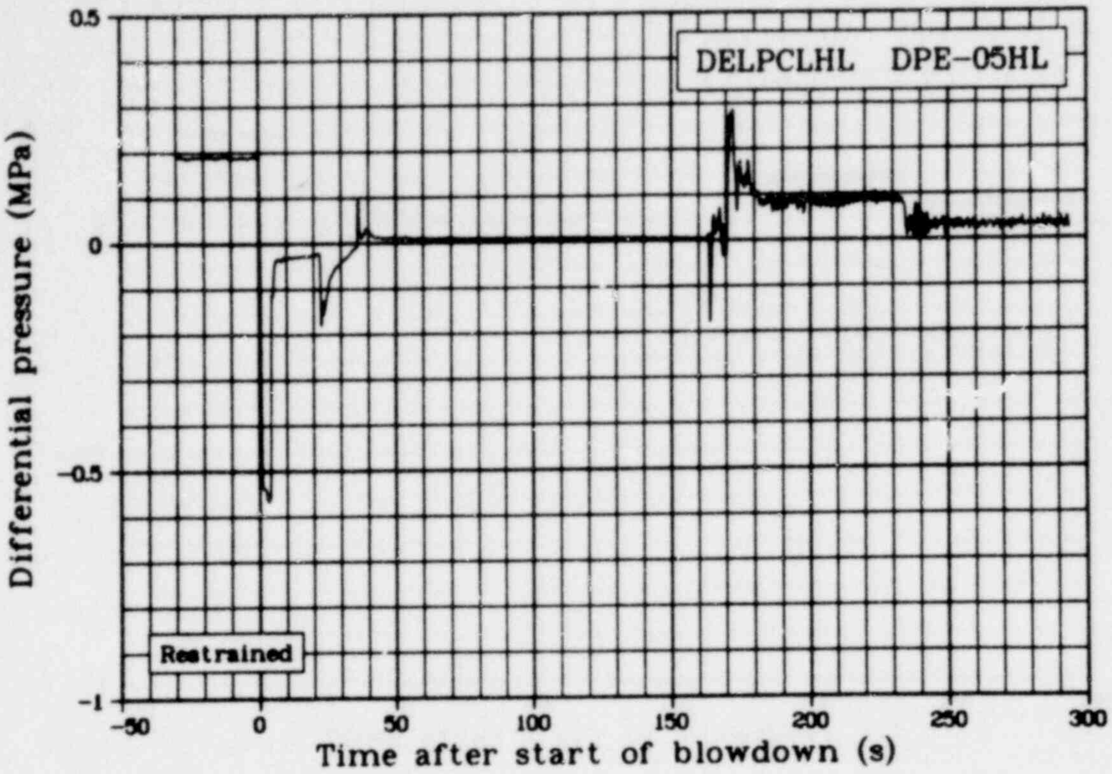

Fig. 239 Differential pressure between blowdown spools (DELPCLHL DPE-05HL), from -50 to 300 s.

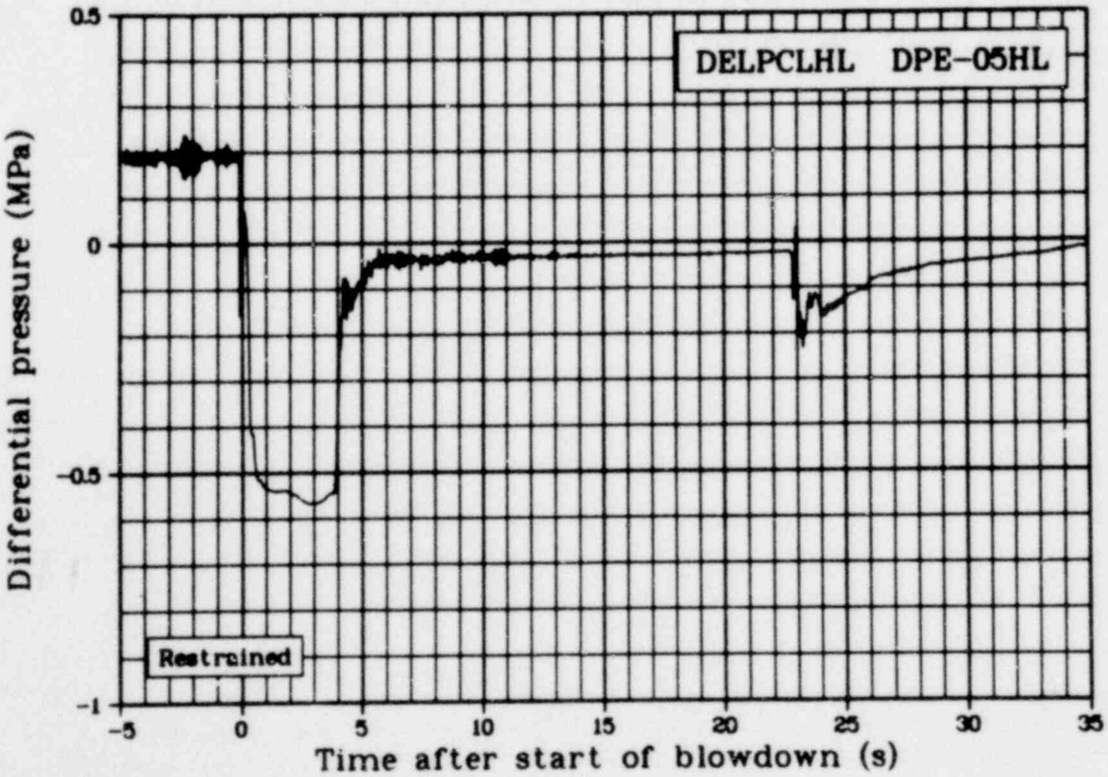

Fig. 240 Differential pressure between blowdown spools (DELPCLHL DPE-05HL), from -5 to 35 s.

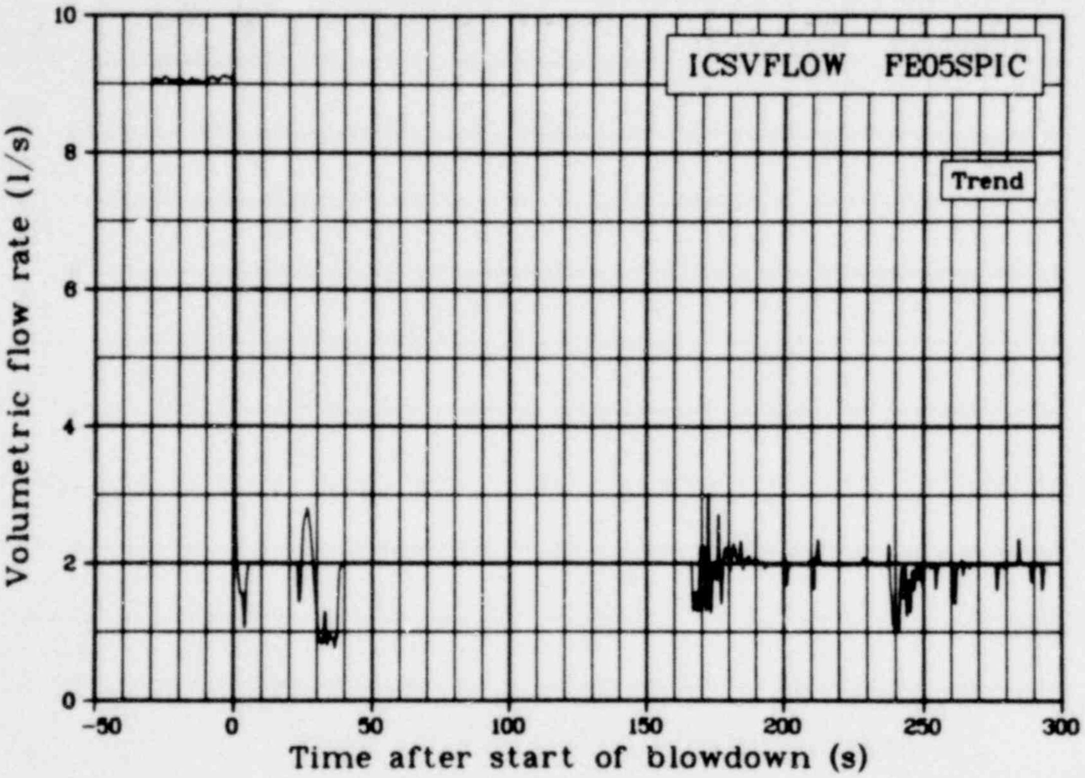

Fig. 241 Volumetric flow rate in initial condition spool (ICSVFLOW FE05SPIC), from -50 to 300 s.

1405 207

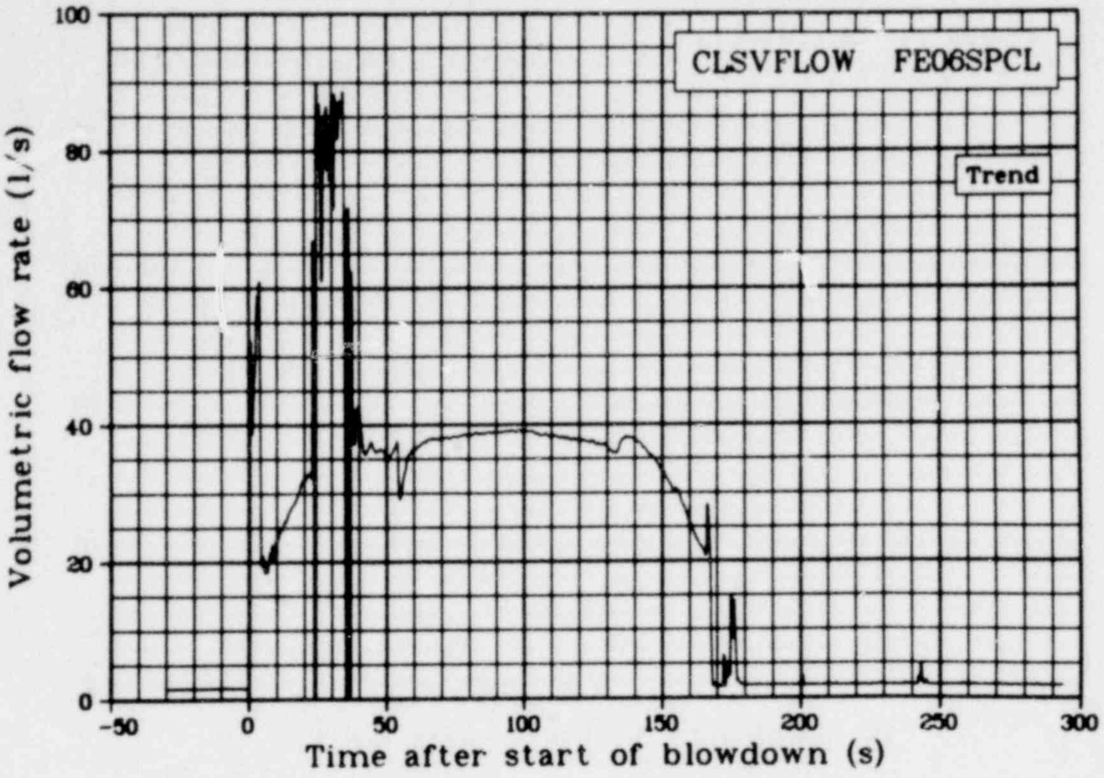

Fig. 242 Volumetric flow rate in cold leg blowdown spool (CLSVFLOW FE06SPCL), from -50 to 300 s.

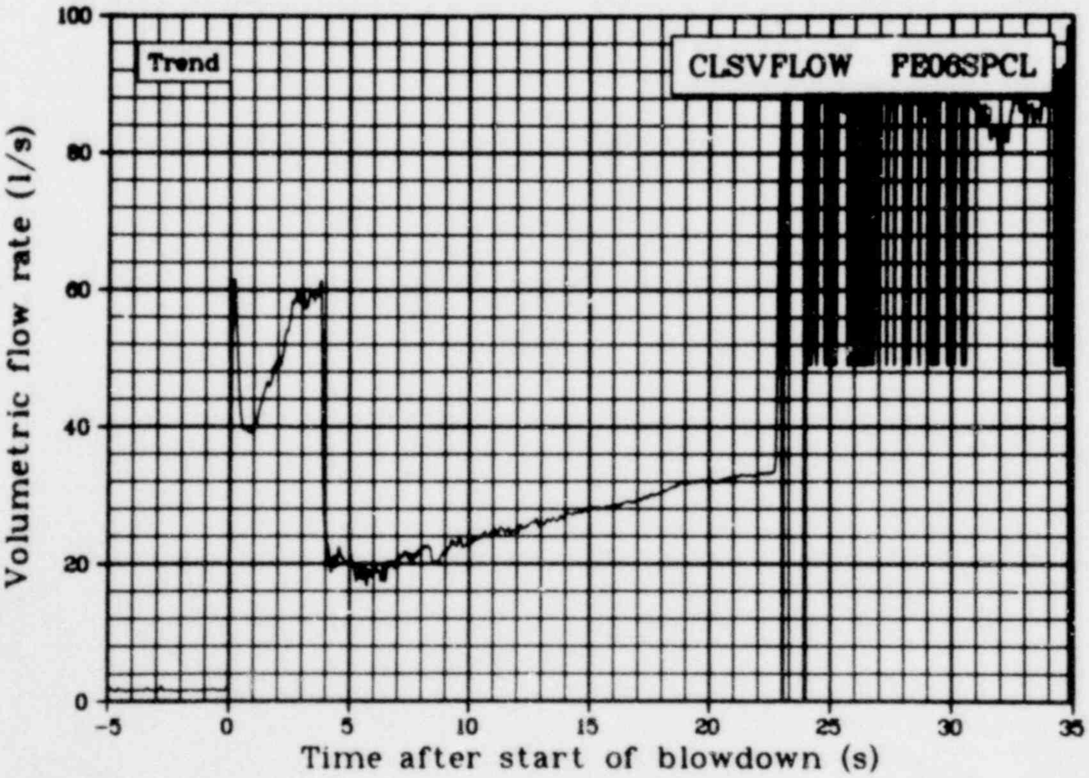

Fig. 243 Volumetric flow rate in cold leg blowdown spool (CLSVFLOW FE06SPCL), from -5 to 35 s.

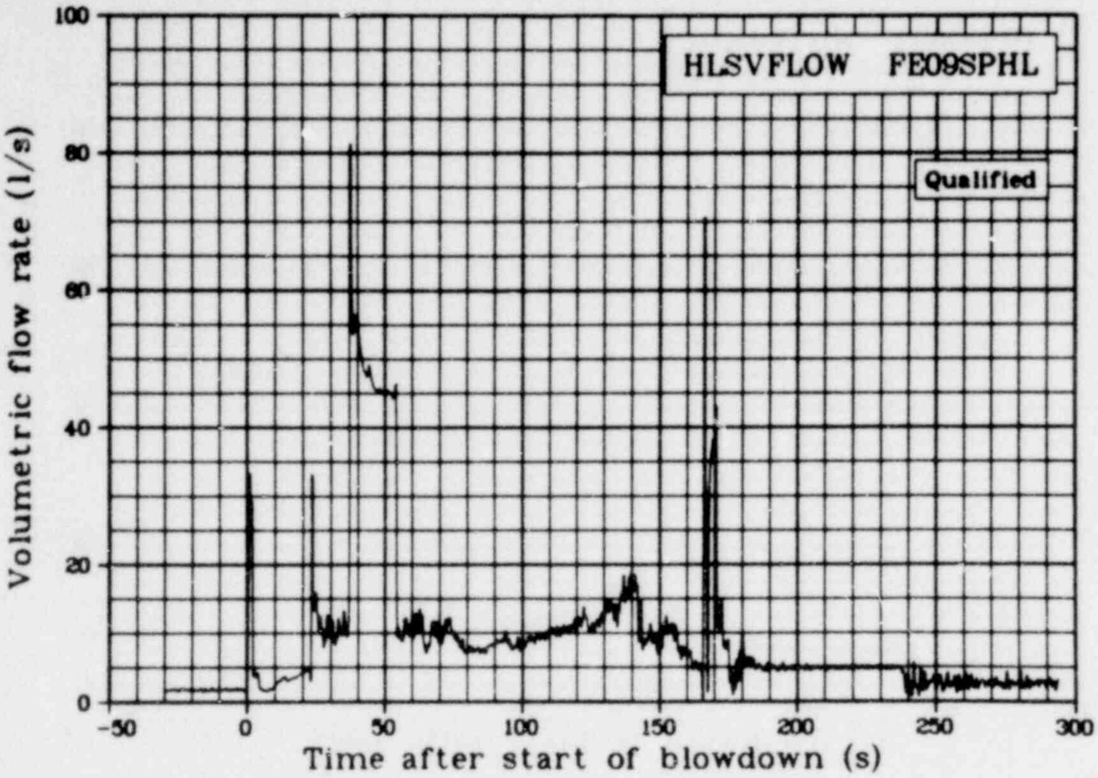

Fig. 244 Volumetric flow rate in hot leg blowdown spool (HLSVFLOW FE09SPHL), from -50 to 300 s.

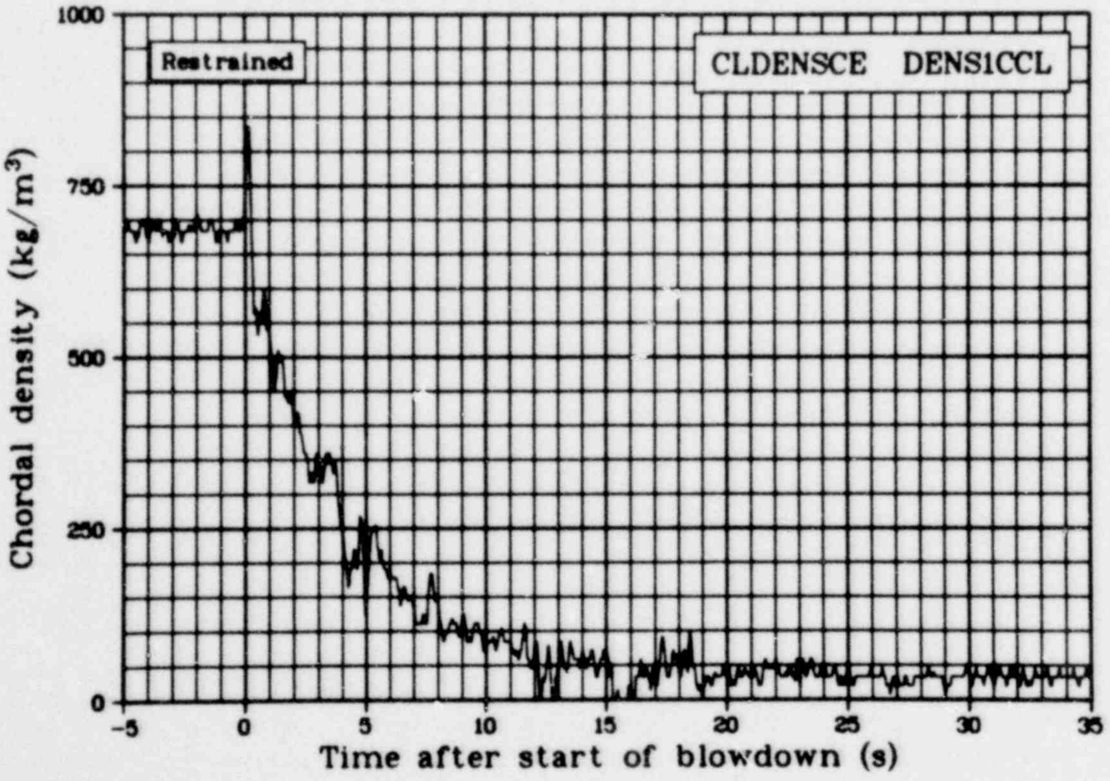

Fig. 245 Chordal density of center beam in cold leg blowdown spool (CLDENSCE DENS1CCL), from -5 to 35 s.

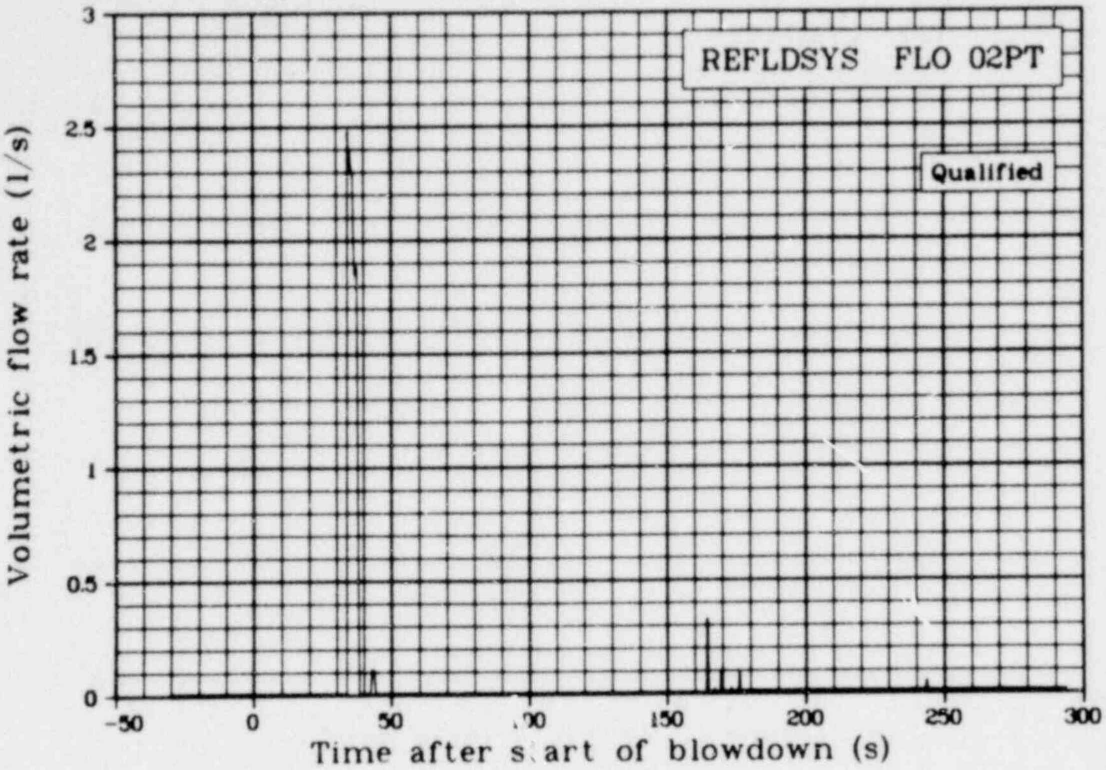

Fig. 246 Volumetric flow rate in reflood line No. 2 (REFLDSYS FLO 02PT), from -50 to 300 s.

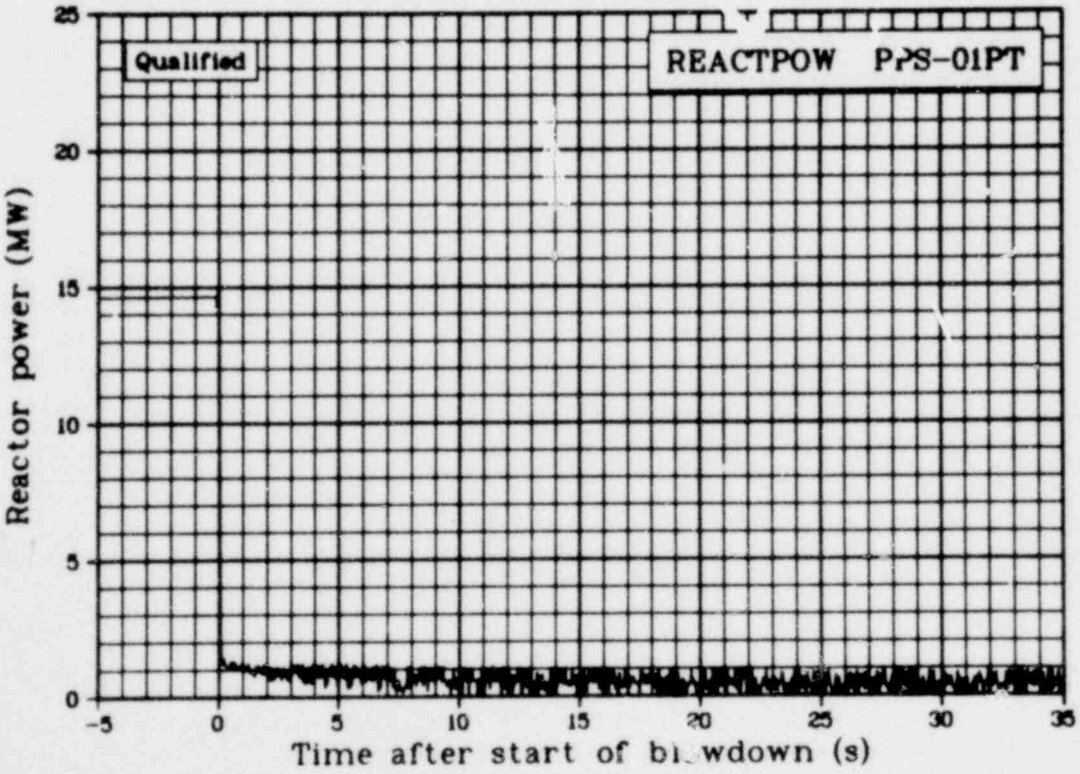

Fig. 247 Reactor power from Core Ionization Chamber PPS 1 (REACTPOW PPS-01PT), from -5 to 35 s.

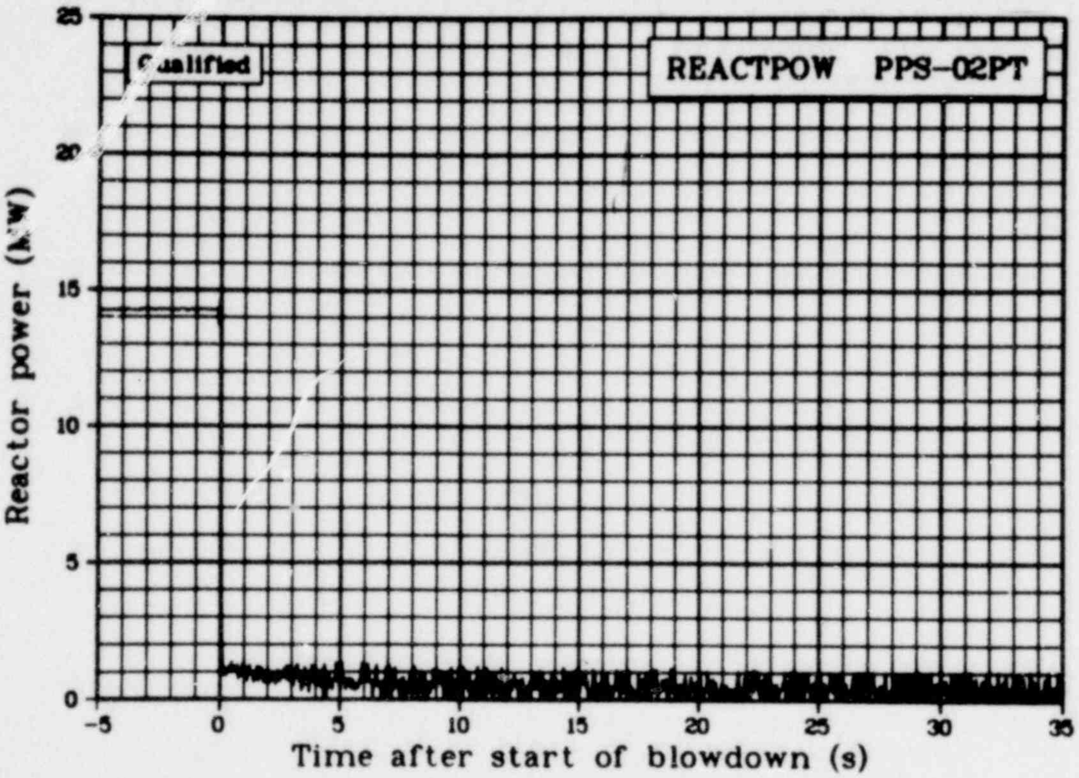

Fig. 248 Reactor power from Core Ionization Chamber PPS 2 (REACTPOW PPS-02PT), from -5 to 35 s.

1405 211

TEST LLR-5

1405 212

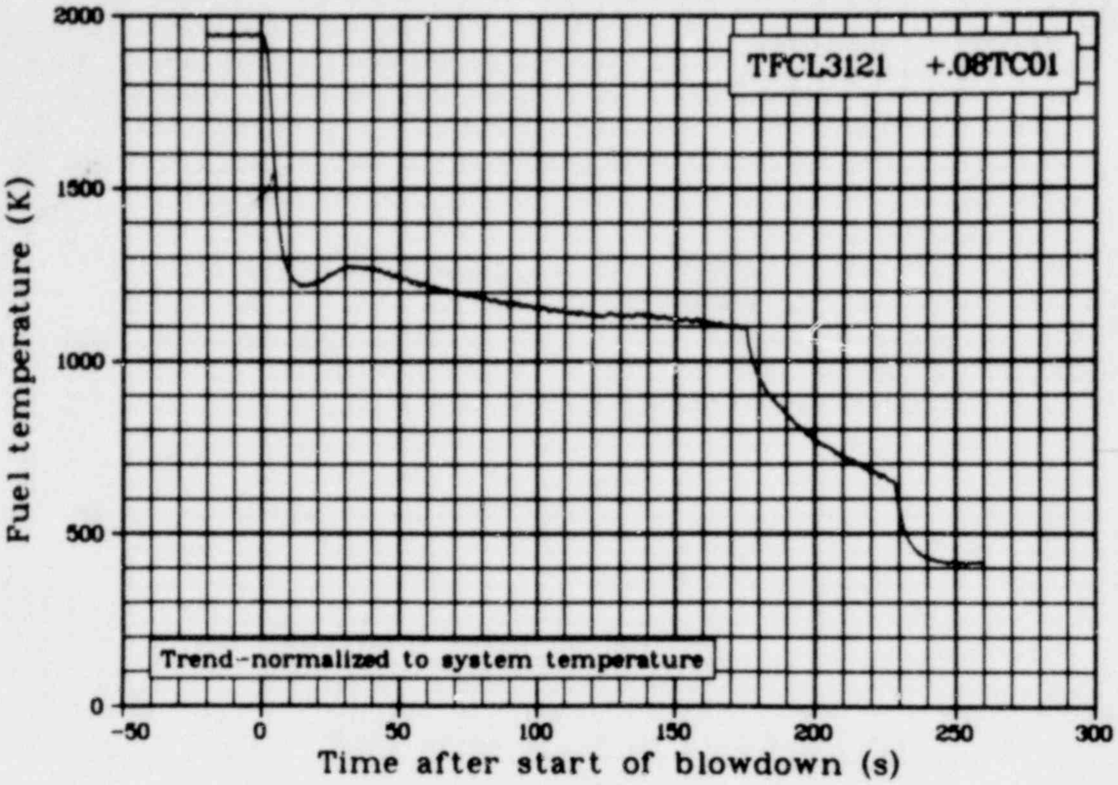

Fig. 249 Fuel temperature in Rod 312-1, 0.08 m above the fuel stack midplane (TFCL3121 +.08TC01), from -50 to 300 s.

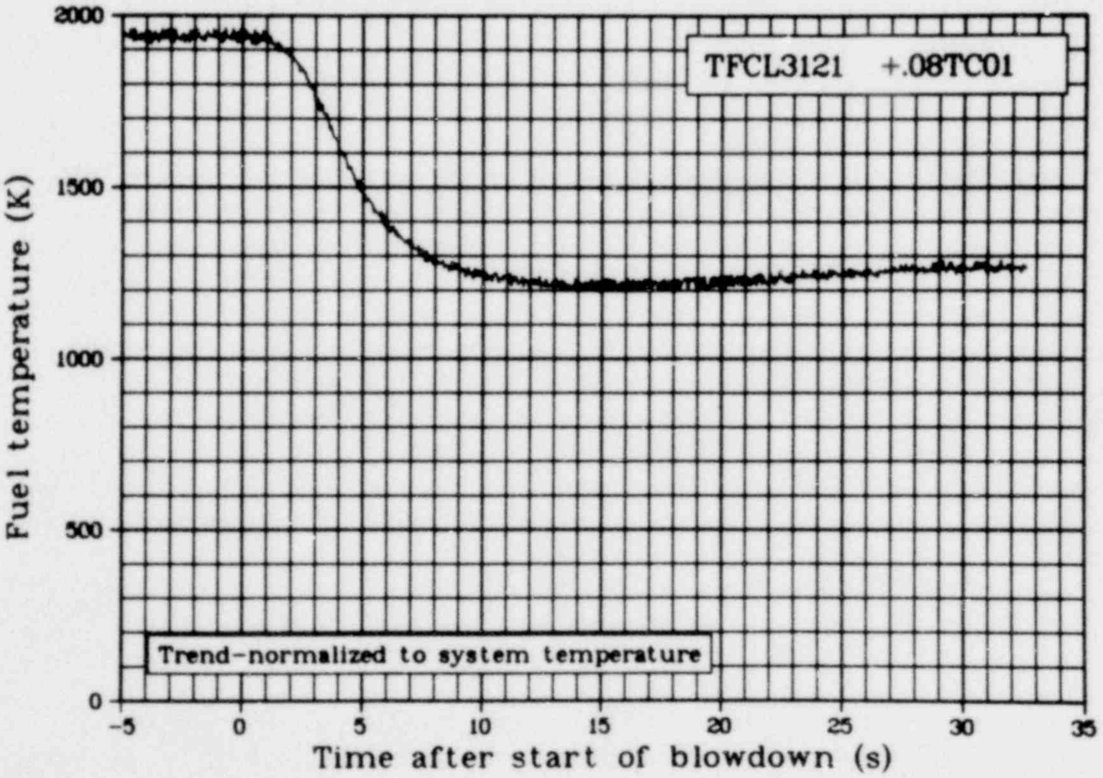

Fig. 250 Fuel temperature in Rod 312-1, 0.08 m above the fuel stack midplane (TFCL3121 +.08TC01), from -5 to 35 s.

1405 213

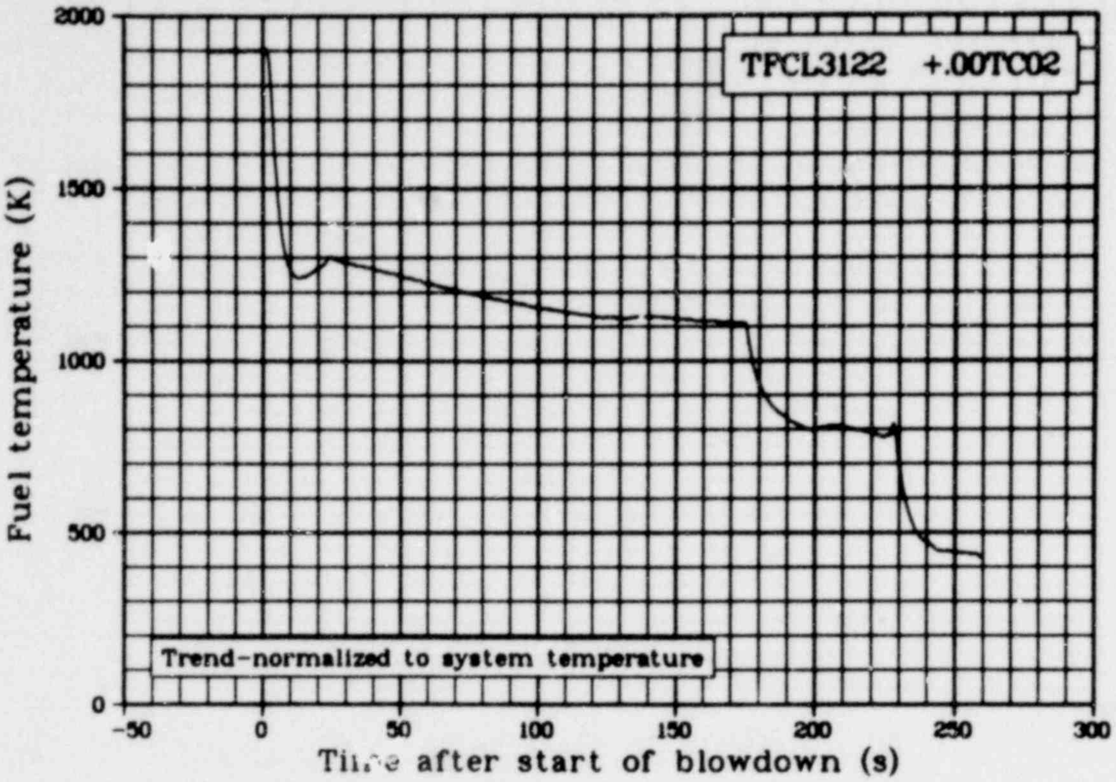

Fig. 251 Fuel temperature in Rod 312-2, at fuel stack midplane (TFCL3122 +.00TC02), from -50 to 300 s.

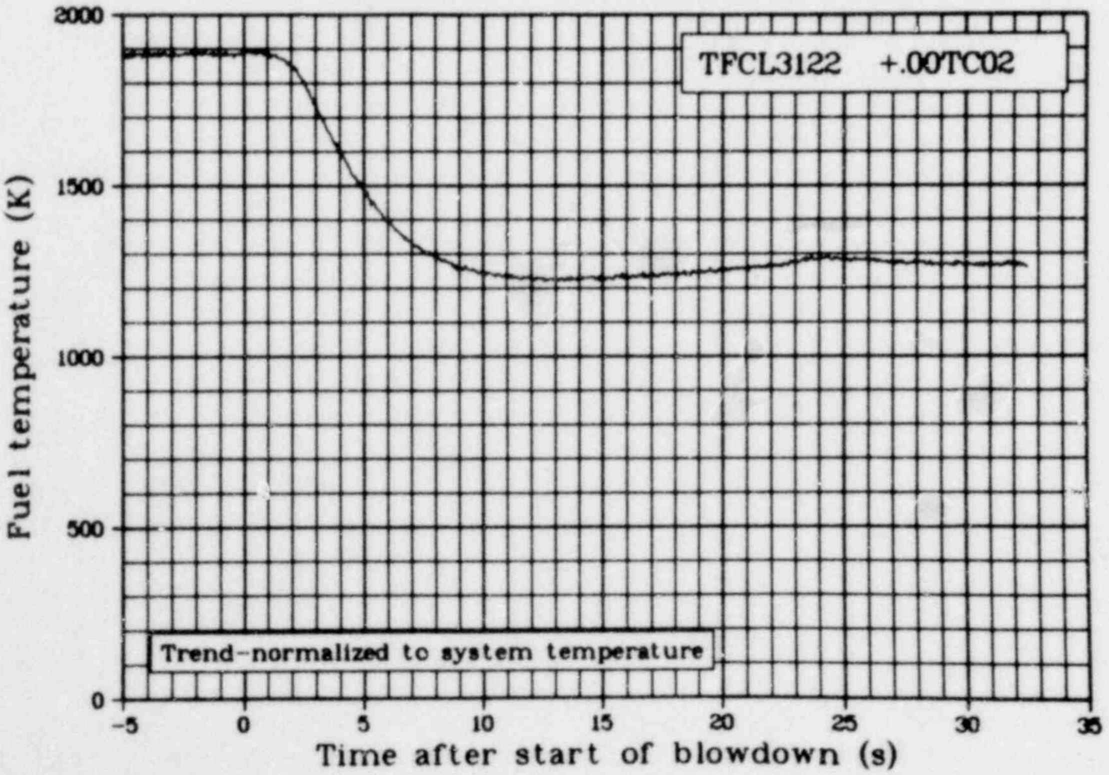

Fig. 252 Fuel temperature in Rod 312-2, at fuel stack midplane (TFCL3122 +.00TC02), from -5 to 35 s.

1405 214

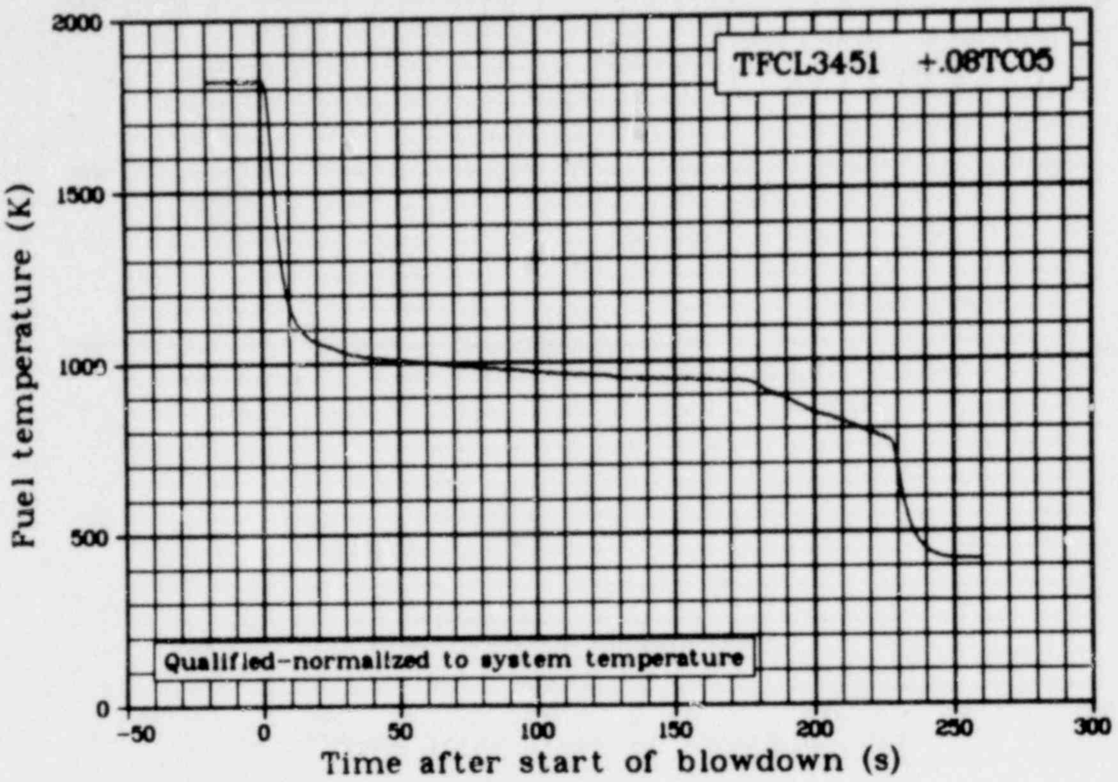

Fig. 253 Fuel temperature in Rod 345-1, 0.08 m above the fuel stack midplane (TFCL3451 + .08TC05), from -50 to 300 s.

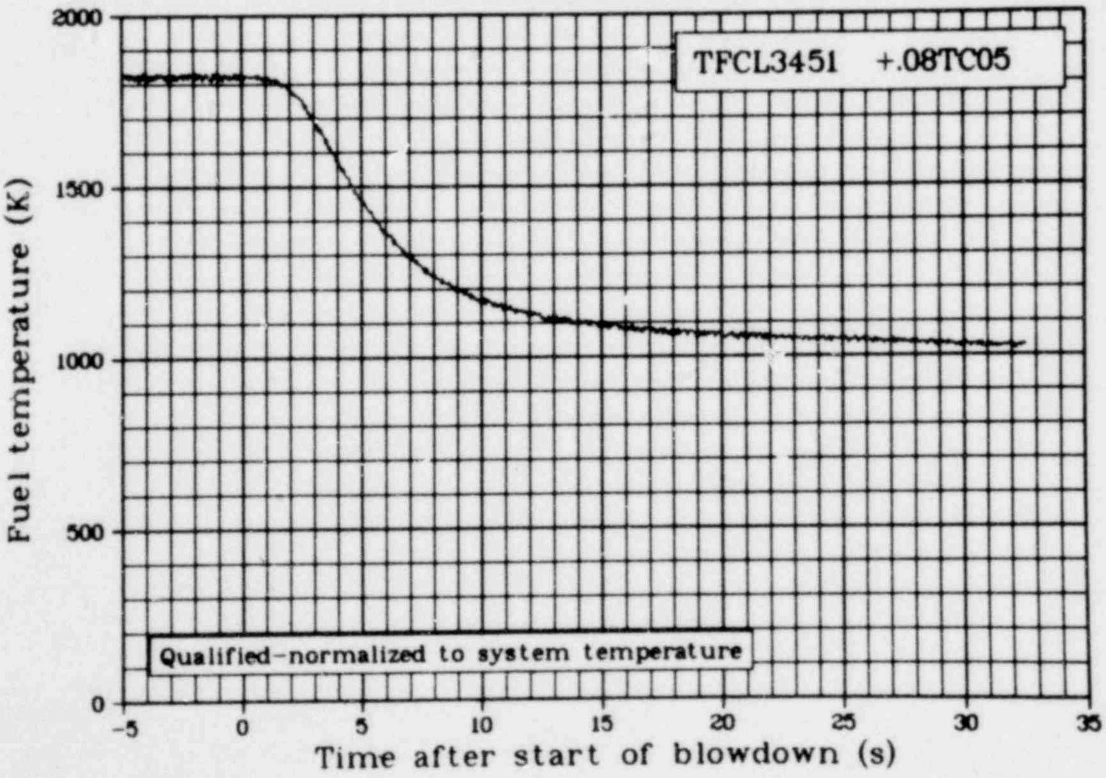

Fig. 254 Fuel temperature in Rod 345-1, 0.08 m above the fuel stack midplane (TFCL3451 + .08TC05), from -5 to 35 s.

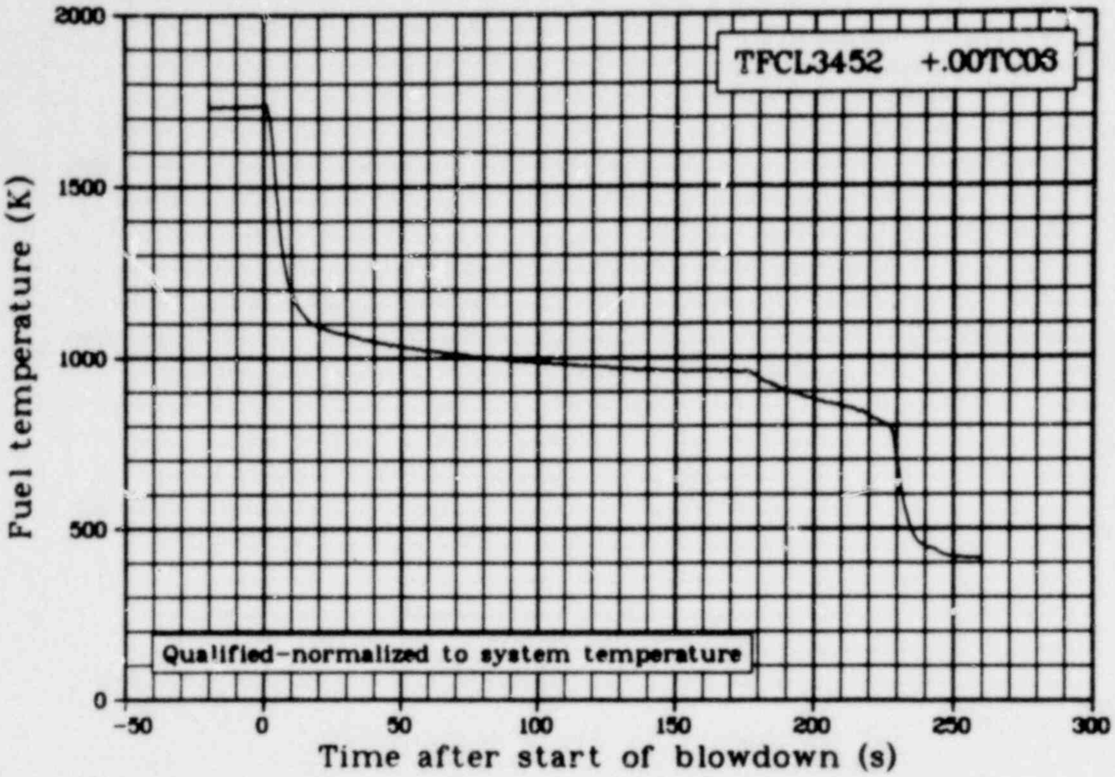

Fig. 255 Fuel temperature in Rod 345-2, at fuel stack midplane (TFCL3452 + .00TC06), from -50 to 300 s.

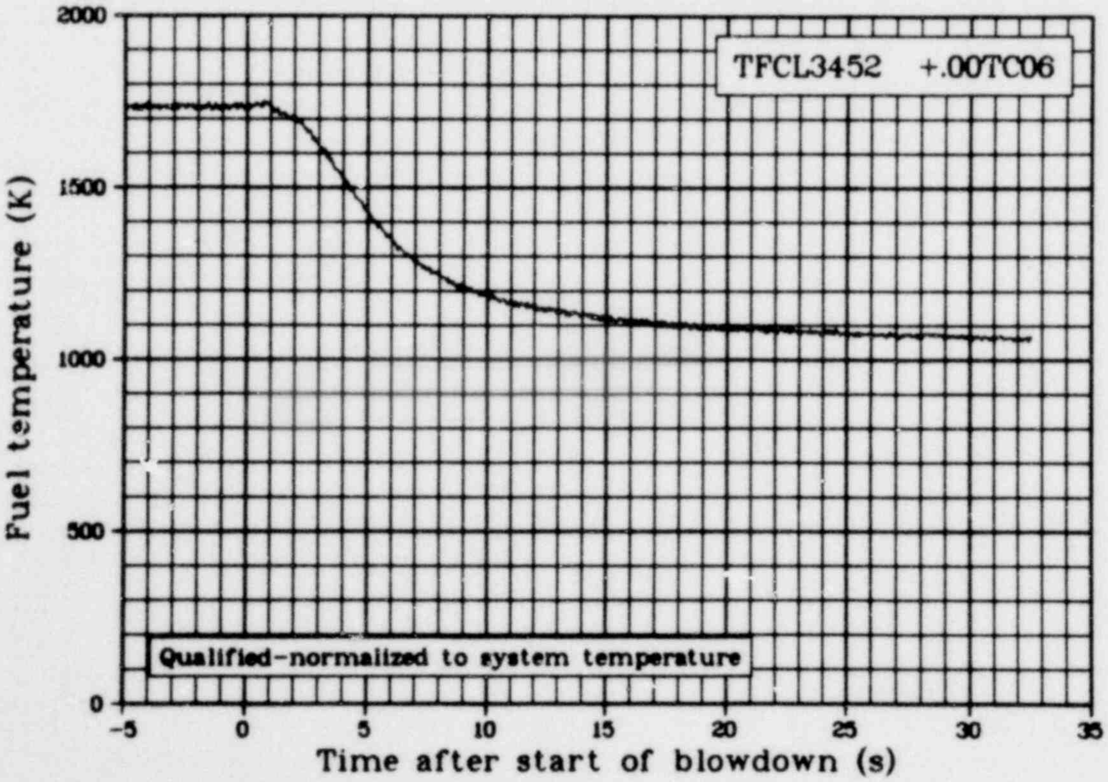

Fig. 256 Fuel temperature in Rod 345-2, at fuel stack midplane (TFCL3452 + .00TC06), from -5 to 35 s.

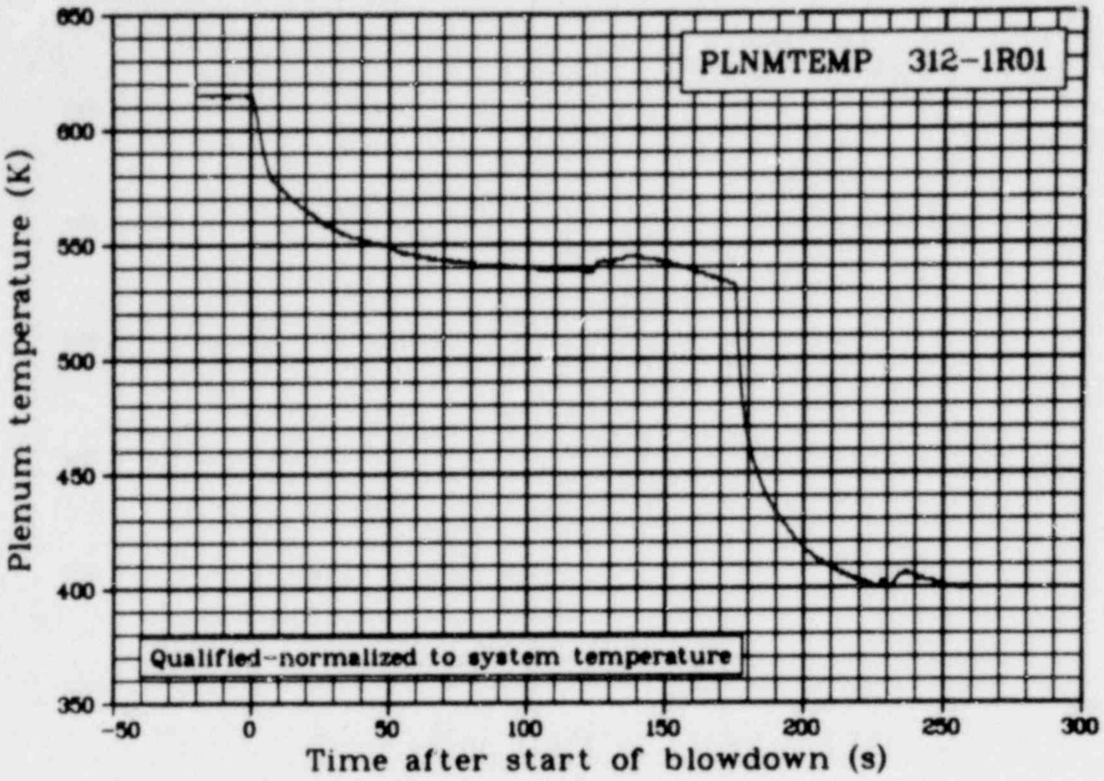

Fig. 257 Plenum temperature in Fuel Rod 312-1 (PLNMTEMP 312-1R01), from -50 to 300 s.

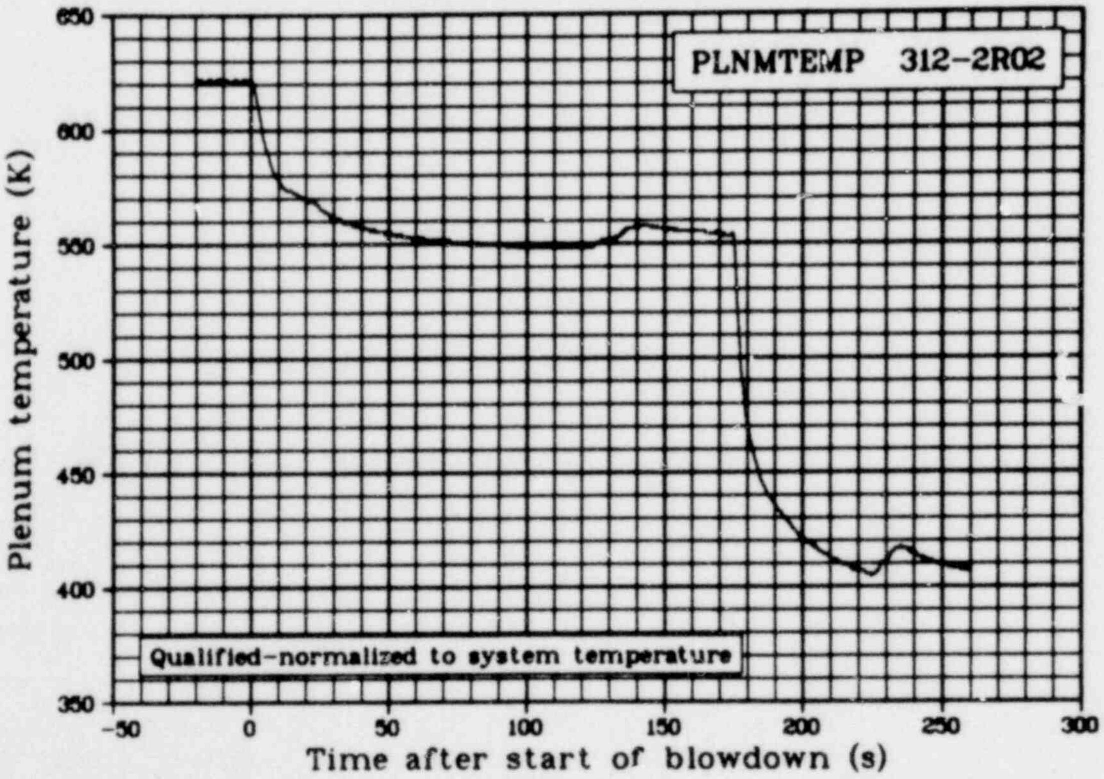

Fig. 258 Plenum temperature in Fuel Rod 312-2 (PLNMTEMP 312-2R02), from -50 to 300 s.

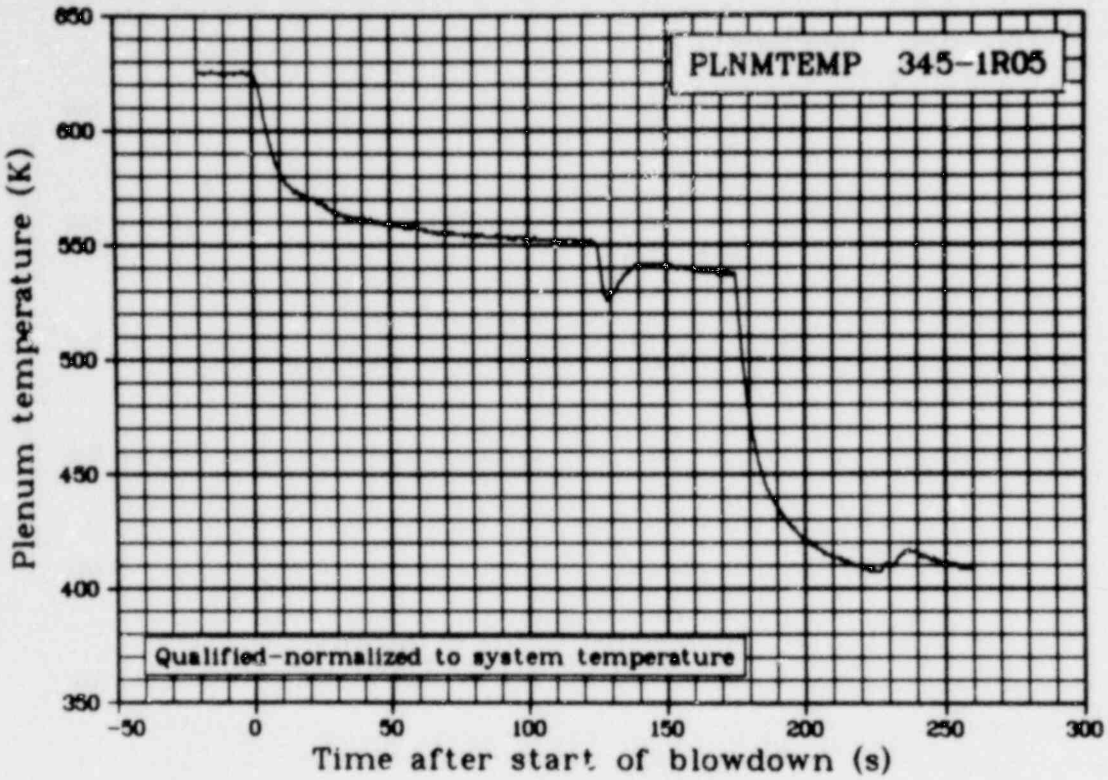

Fig. 259 Plenum temperature in Fuel Rod 345-1 (PLNMTEMP 345-1R05), from -50 to 300 s.

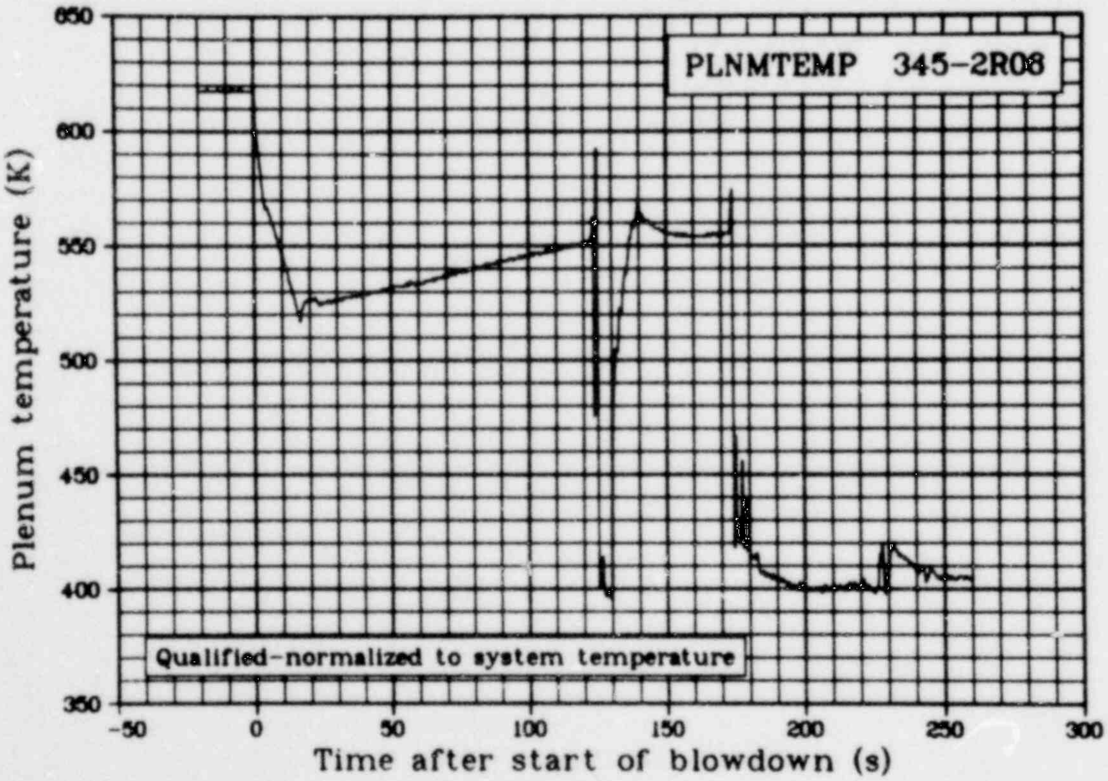

Fig. 260 Plenum temperature in Fuel Rod 345-2 (PLNMTEMP 345-2R06), from -50 to 300 s.

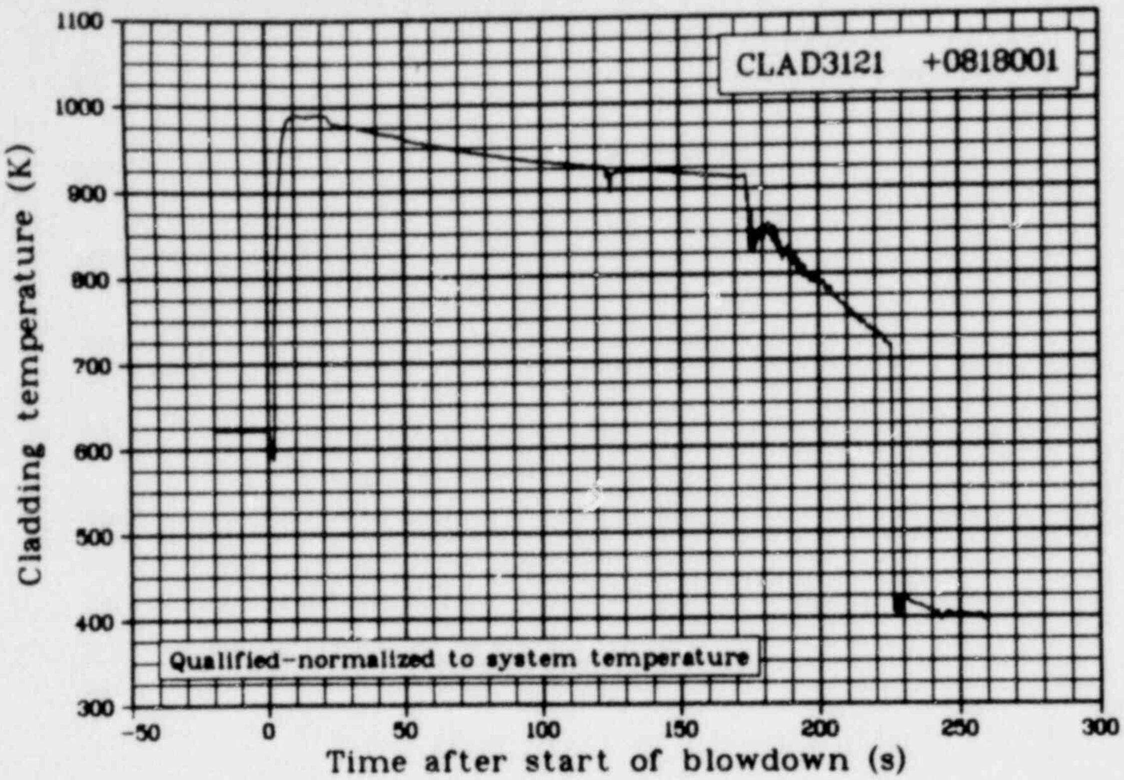

Fig. 261 Cladding temperature, Rod 312-1, at 180 degrees and 0.08 m above fuel stack midplane (CLAD3121 +0818001), from -50 to 300 s.

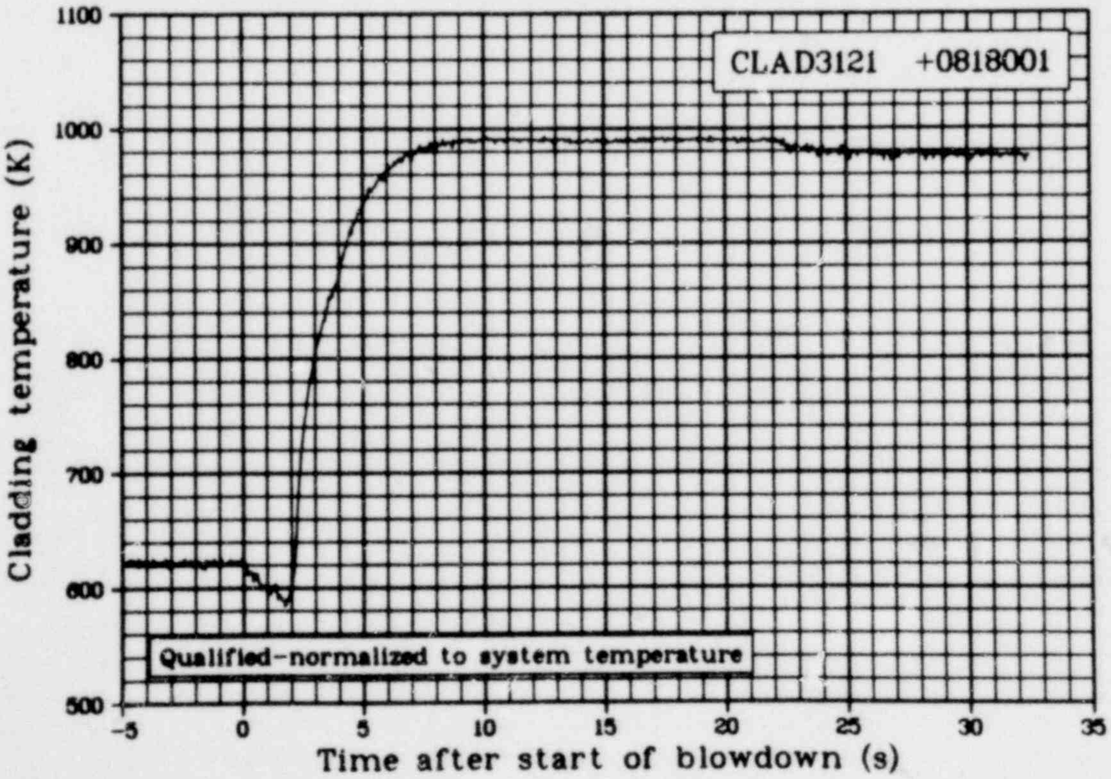

Fig. 262 Cladding temperature, Rod 312-1, at 180 degrees and 0.08 m above fuel stack midplane (CLAD3121 +0818001), from -5 to 35 s.

1405 219

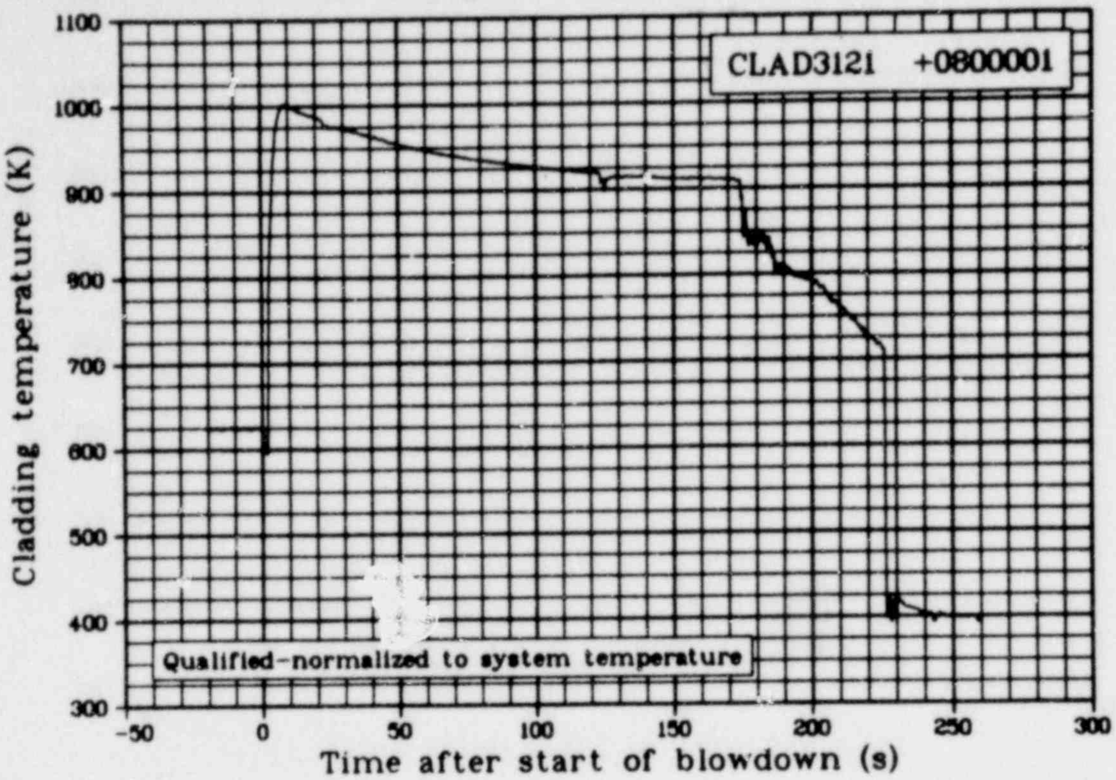

Fig. 263 Cladding temperature, Rod 312-1, at 0 degrees and 0.08 m above fuel stack midplane (CLAD3121 +0800001), from -50 to 300 s.

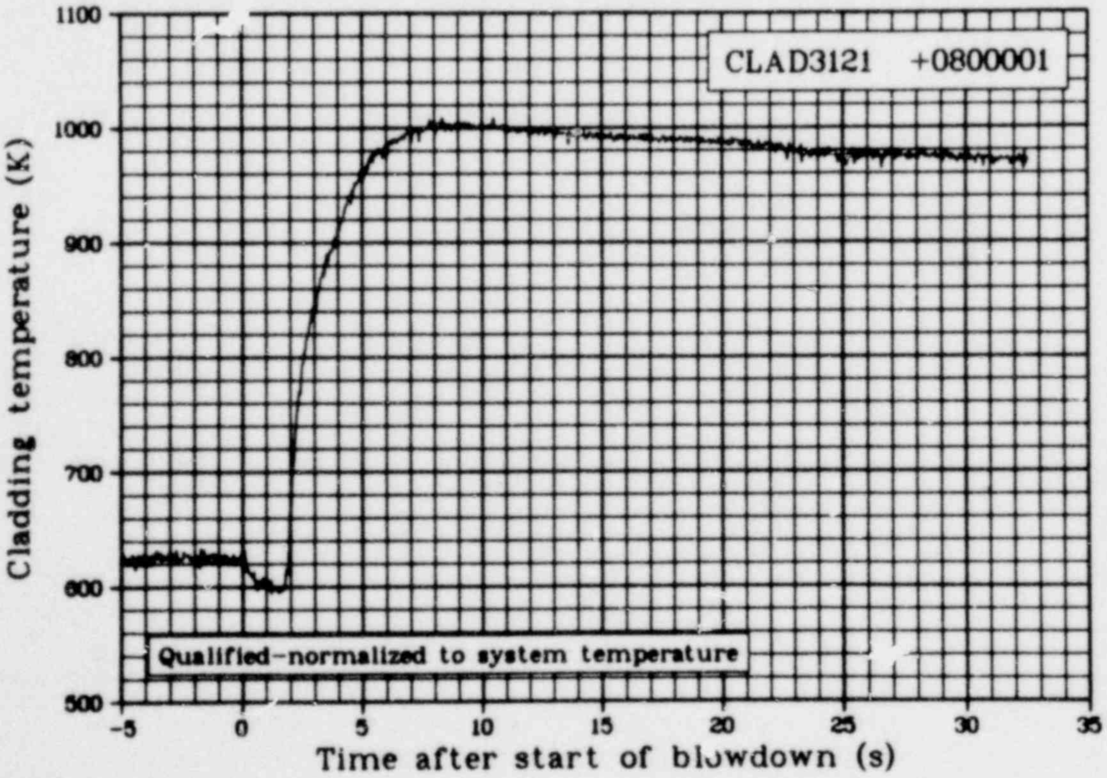

Fig. 264 Cladding temperature, Rod 312-1, at 0 degrees and 0.08 m above fuel stack midplane (CLAD3121 +0800001), from -5 to 35 s.

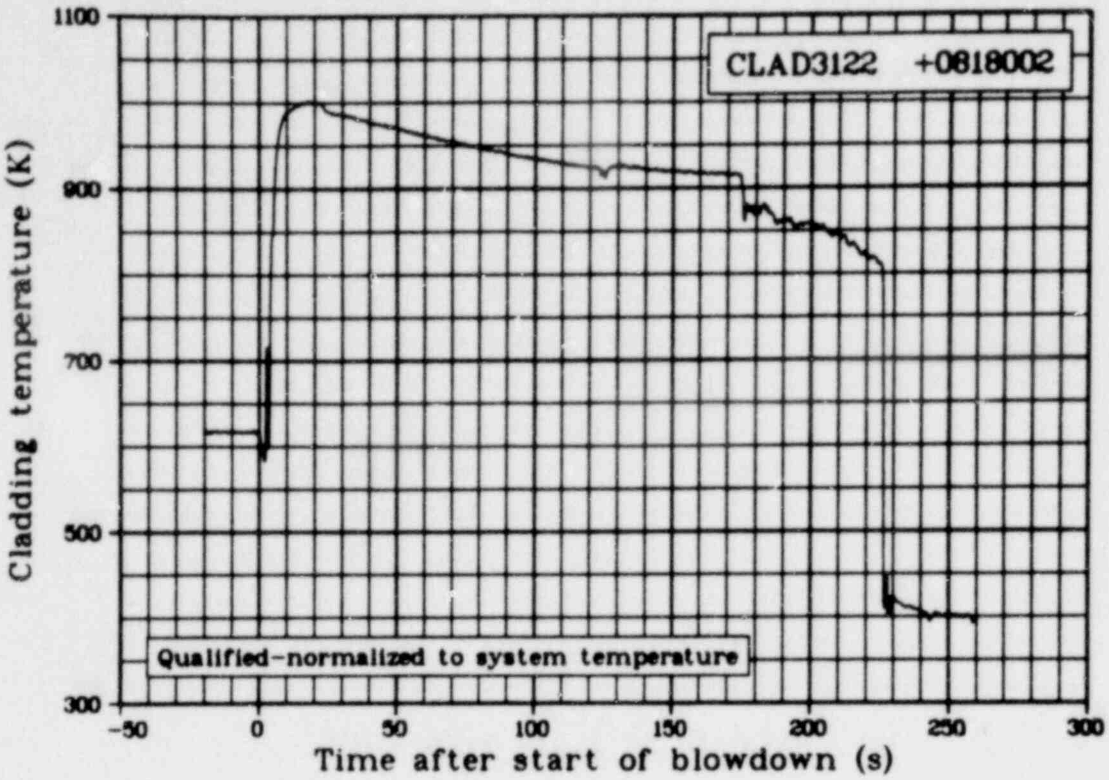

Fig. 265 Cladding temperature, Rod 312-2, at 180 degrees and 0.08 m above fuel stack midplane (CLAD3122 + 0818002), from -50 to 300 s.

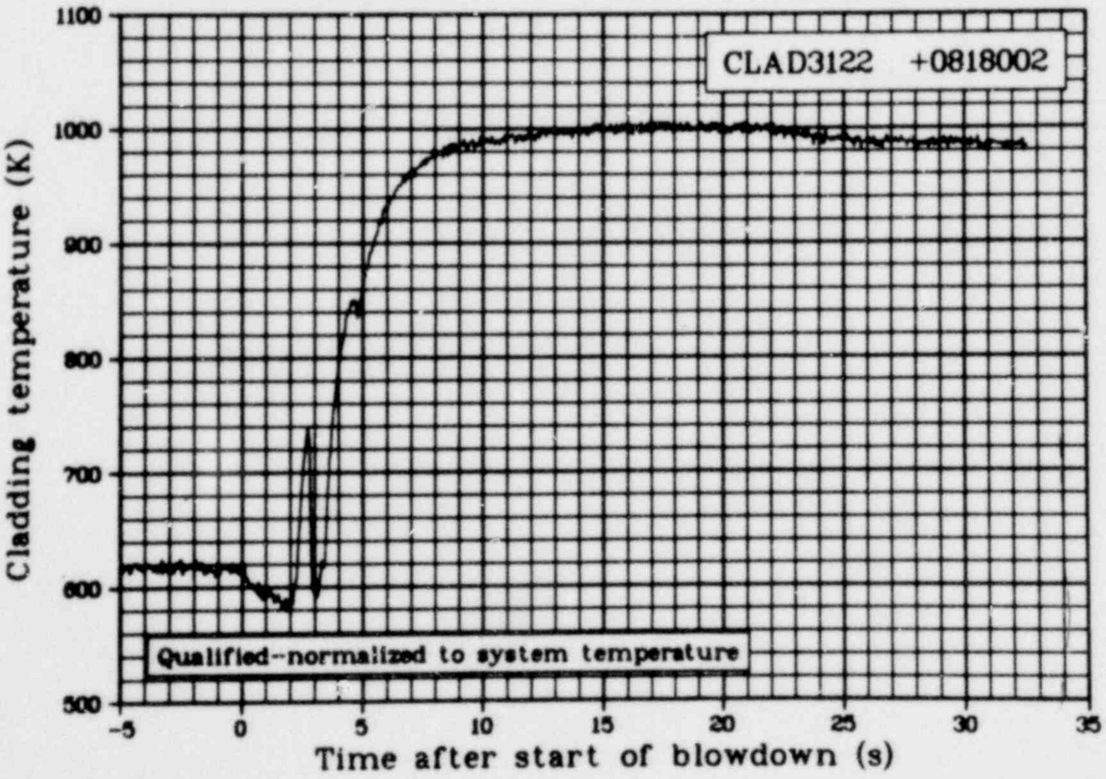

Fig. 266 Cladding temperature, Rod 312-2, at 180 degrees and 0.08 m above fuel stack midplane (CLAD3122 + 0818002), from -5 to 35 s.

1405 221

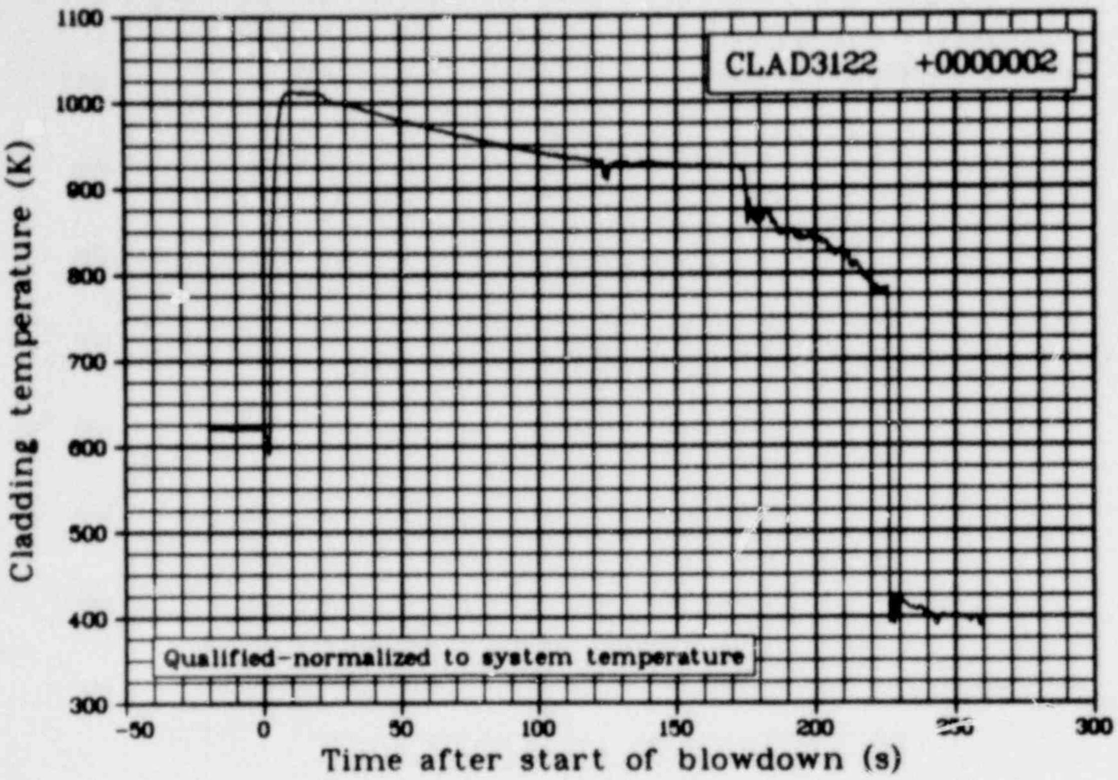

Fig. 267 Cladding temperature, Rod 312-2, at 0 degrees and fuel stack midplane (CLAD3122 + 0000002), from -50 to 300 s.

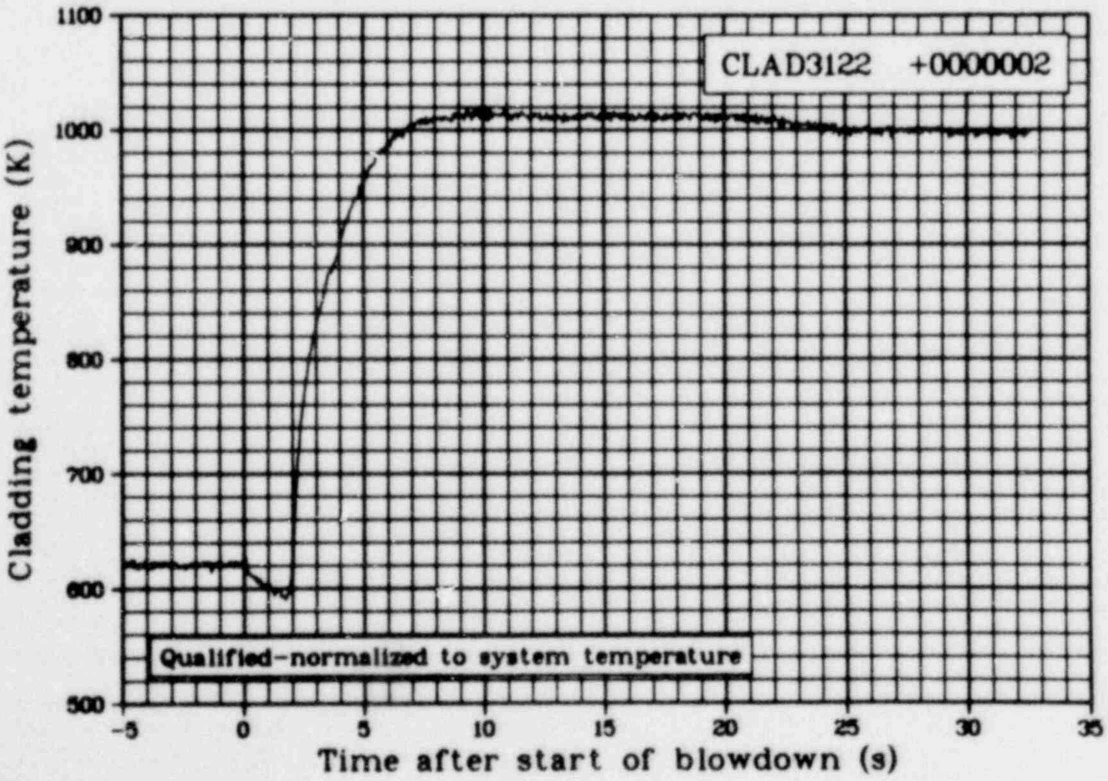

Fig. 268 Cladding temperature, Rod 312-2, at 0 degrees and fuel stack midplane (CLAD3122 + 0000002), from -5 to 35 s.

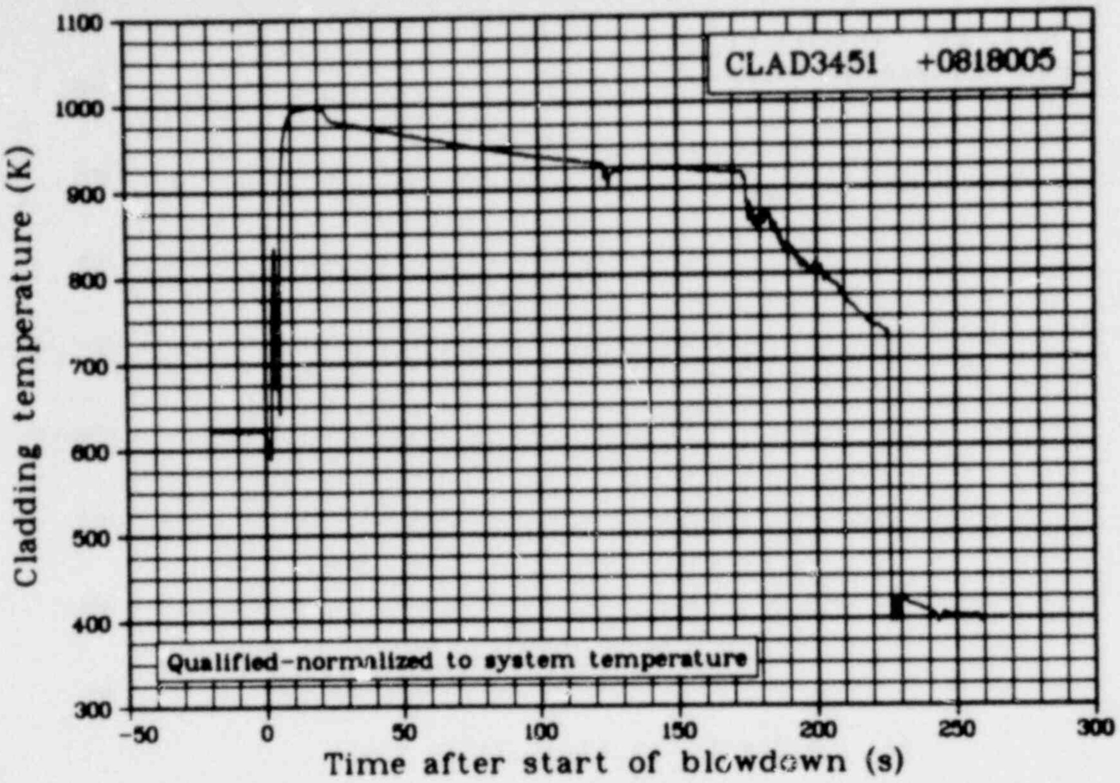

Fig. 269 Cladding temperature, Rod 345-1, at 180 degrees and 0.08 m above fuel stack midplane (CLAD3451 +0818005), from -50 to 300 s.

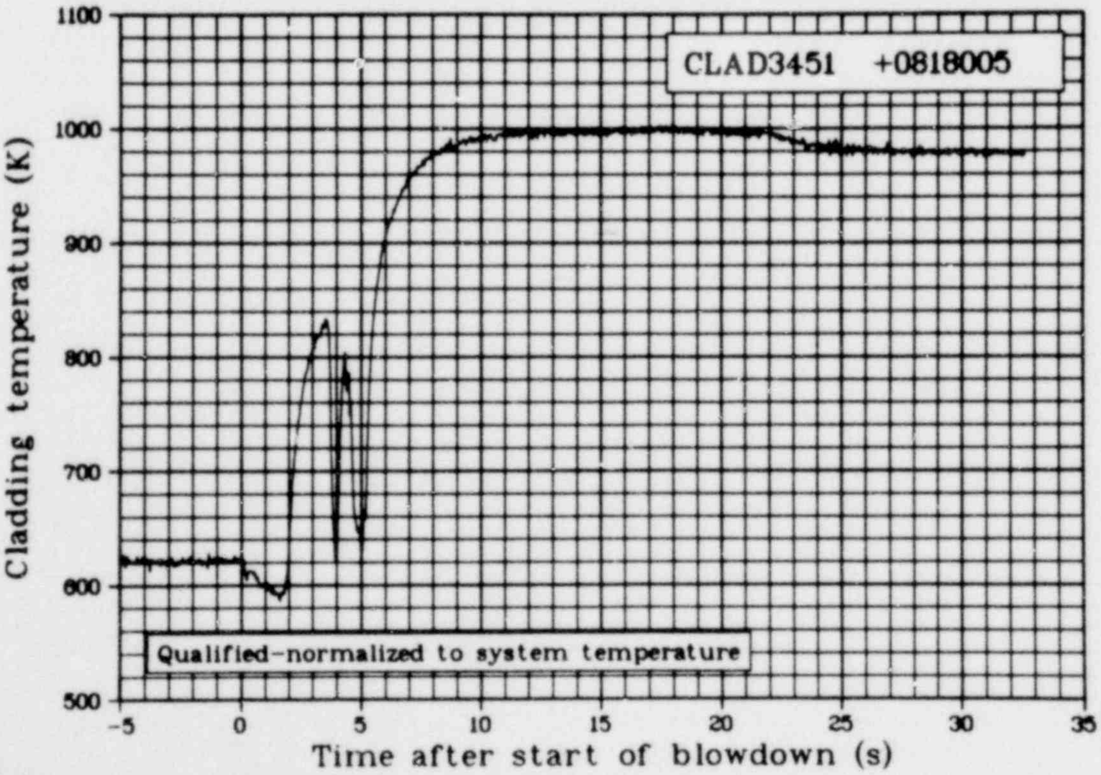

Fig. 270 Cladding temperature, Rod 345-1, at 180 degrees and 0.08 m above fuel stack midplane (CLAD3451 +0818005), from -5 to 35 s.

1405 223

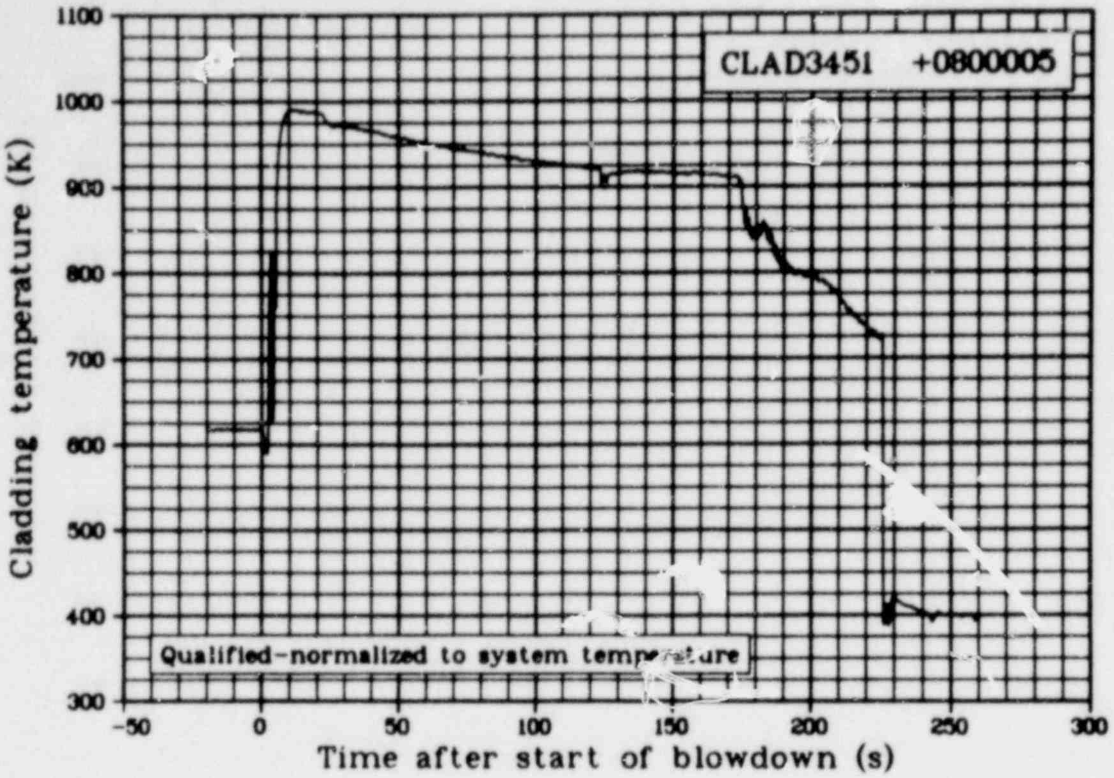

Fig. 271 Cladding temperature, Rod 345-1, at 0 degrees and 0.08 m above fuel stack midplane (CLAD3451 +0800005), from -50 to 360 s.

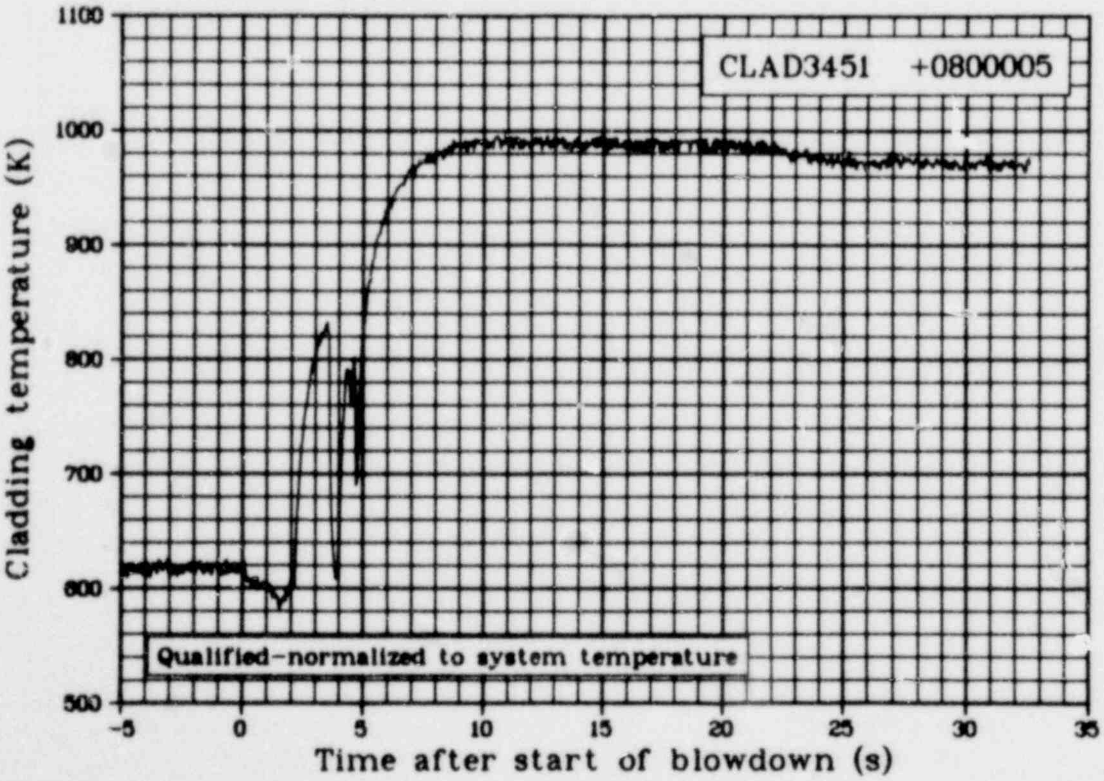

Fig. 272 Cladding temperature, Rod 345-1, at 0 degrees and 0.08 m above fuel stack midplane (CLAD3451 +0800005), from -5 to 35 s.

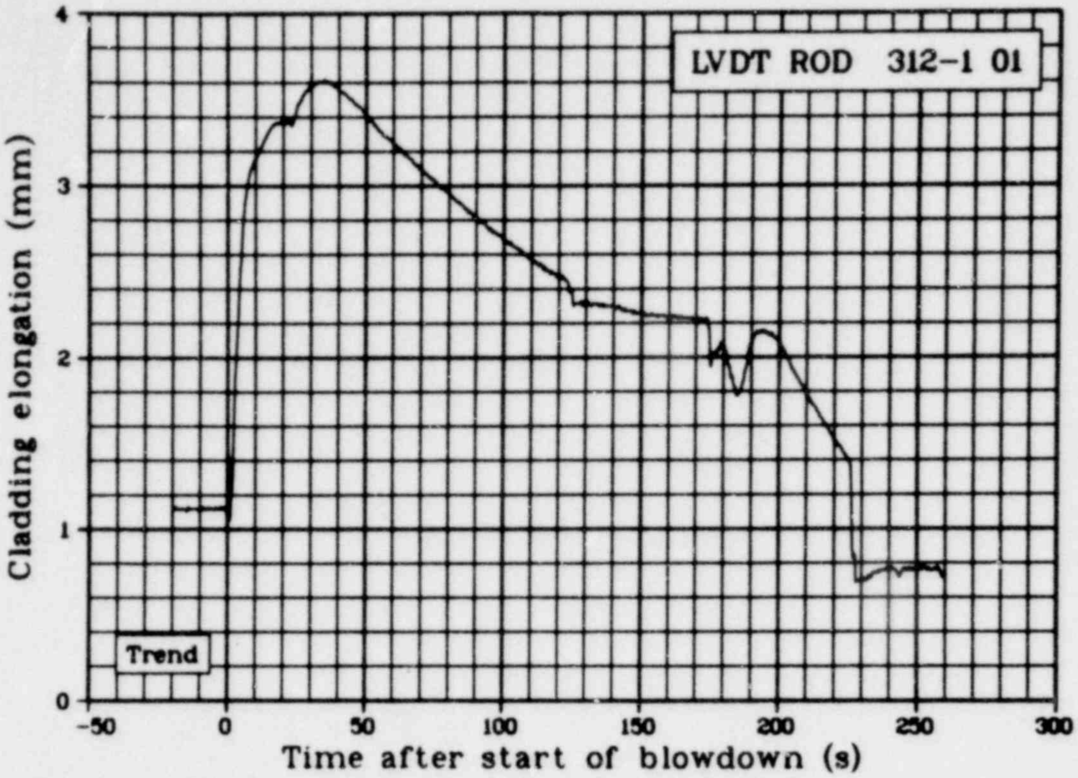

Fig. 273 Cladding elongation of Fuel Rod 312-1, (LVDT ROD 312-1 01), from -50 to 300 s.

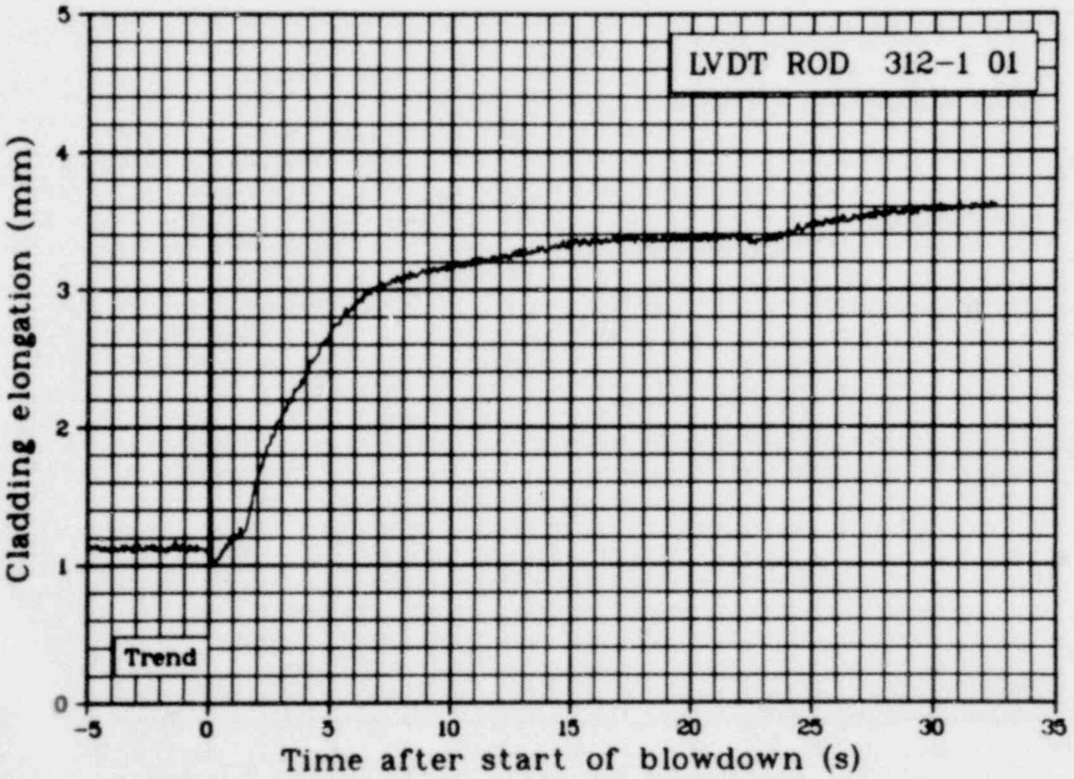

Fig. 274 Cladding elongation of Fuel Rod 312-1, (LVDT ROD 312-1 01), from -5 to 35 s.

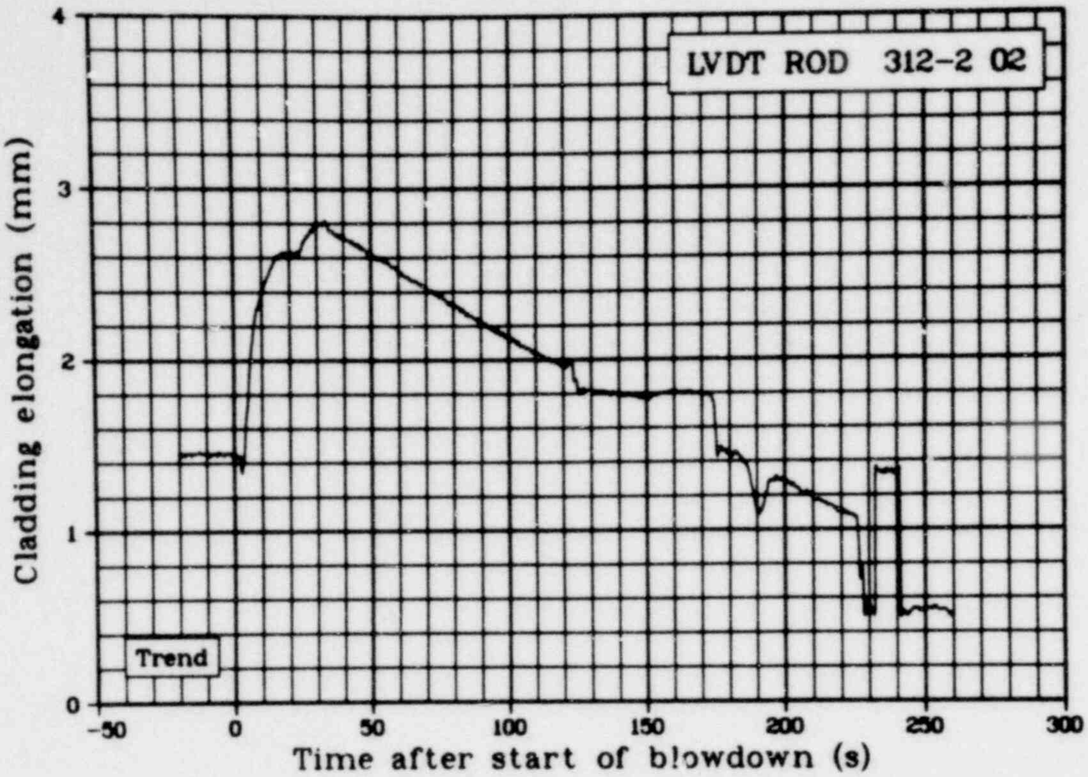

Fig. 275 Cladding elongation of Fuel Rod 312-2, (LVDT ROD 312-2 02), from -50 to 300 s.

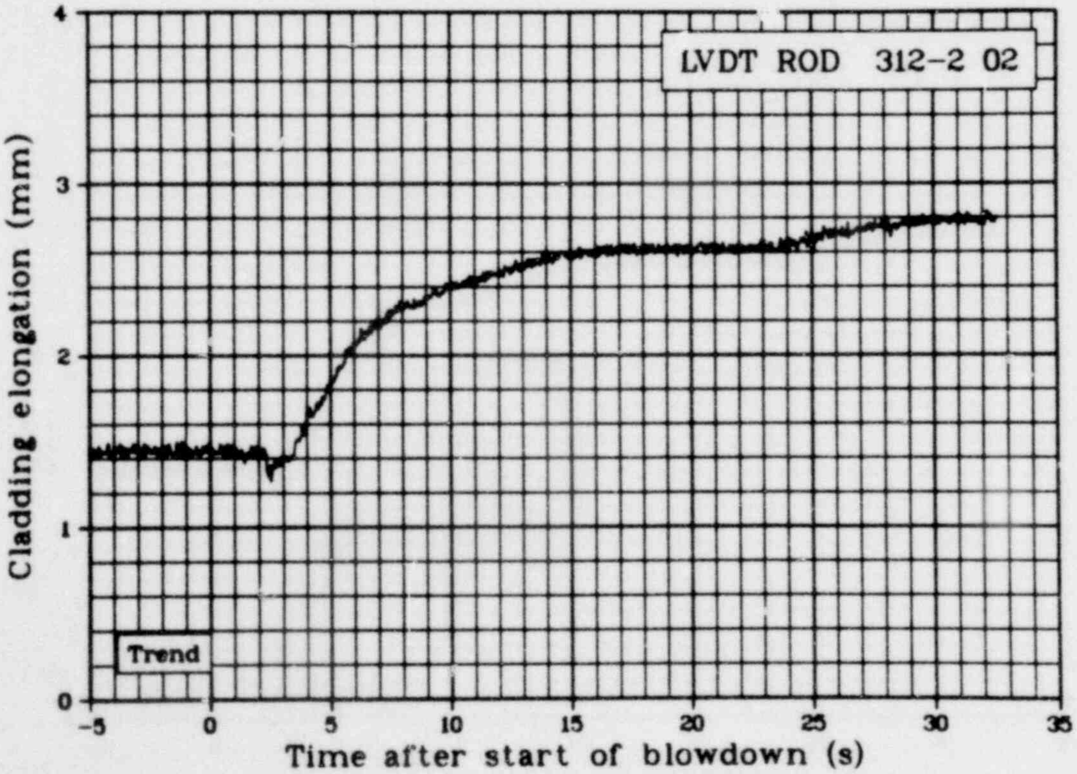

Fig. 276 Cladding elongation of Fuel Rod 312-2, (LVDT ROD 312-2 02), from -5 to 35 s.

1405 226

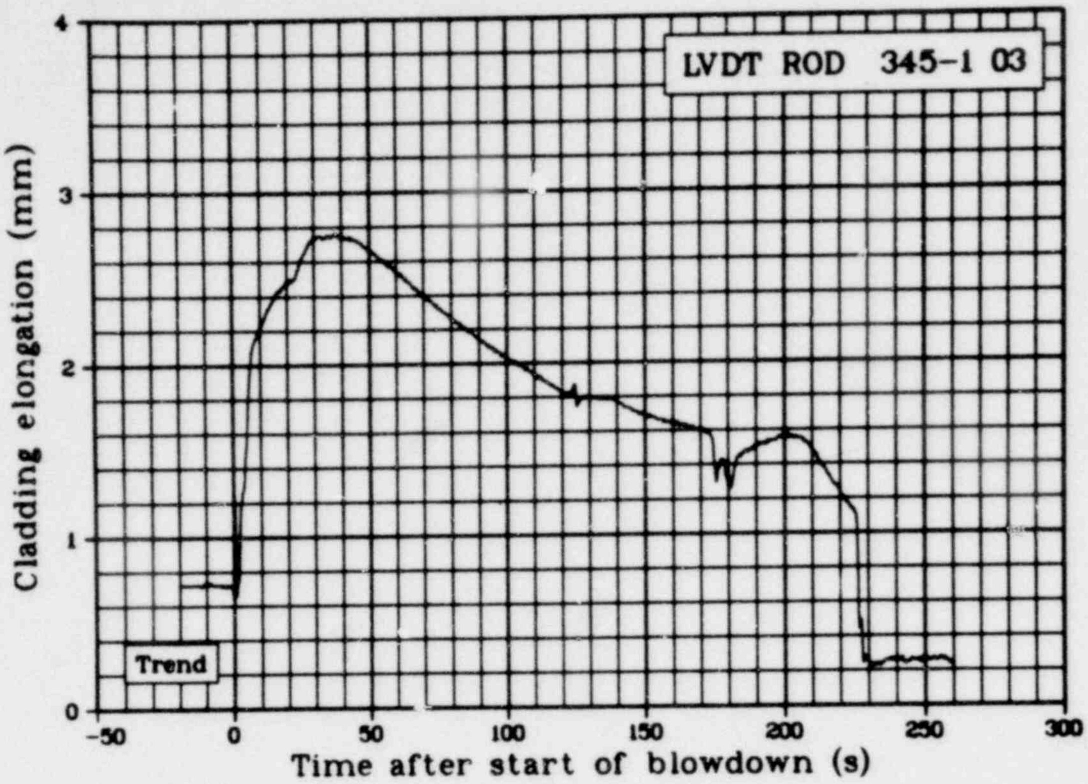

Fig. 277 Cladding elongation of Fuel Rod 345-1, (LVDT ROD 345-1 03), from -50 to 300 s.

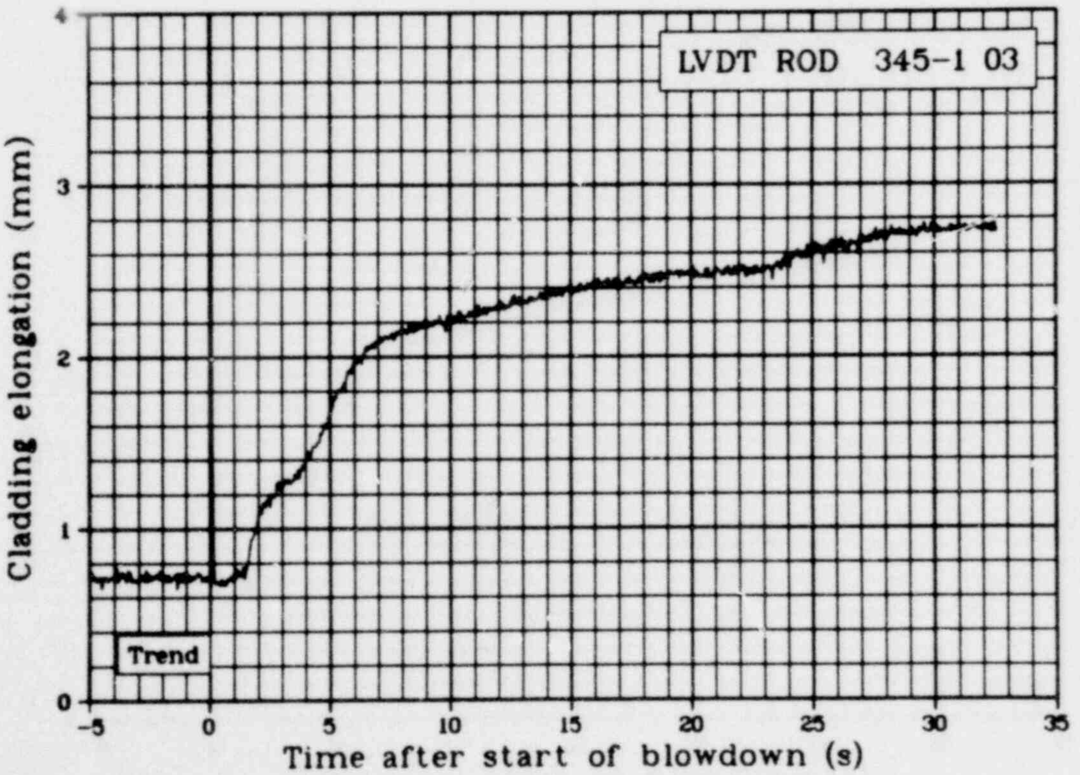

Fig. 278 Cladding elongation of Fuel Rod 345-1, (LVDT ROD 345-1 03), from -5 to 35 s.

1405 227

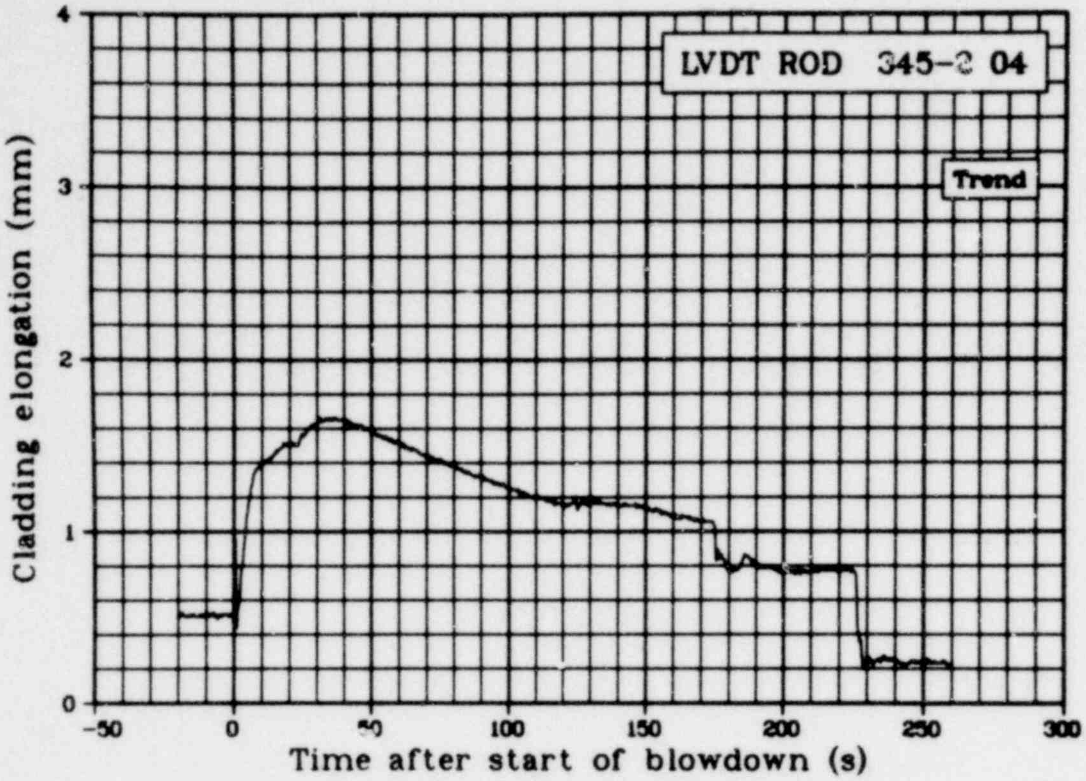

Fig. 279 Cladding elongation of Fuel Rod 345-2, (LVDT ROD 345-2 04), from -50 to 300 s.

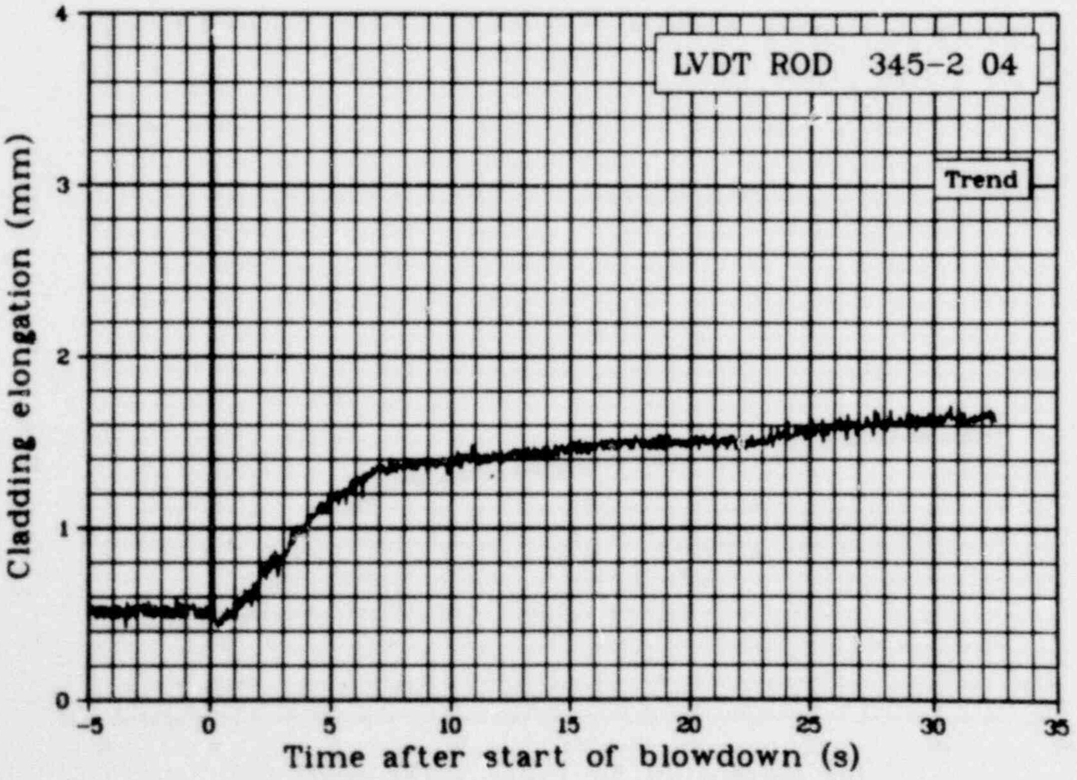

Fig. 280 Cladding elongation of Fuel Rod 345-2, (LVDT ROD 345-2 04), from -5 to 35 s.

1405 228

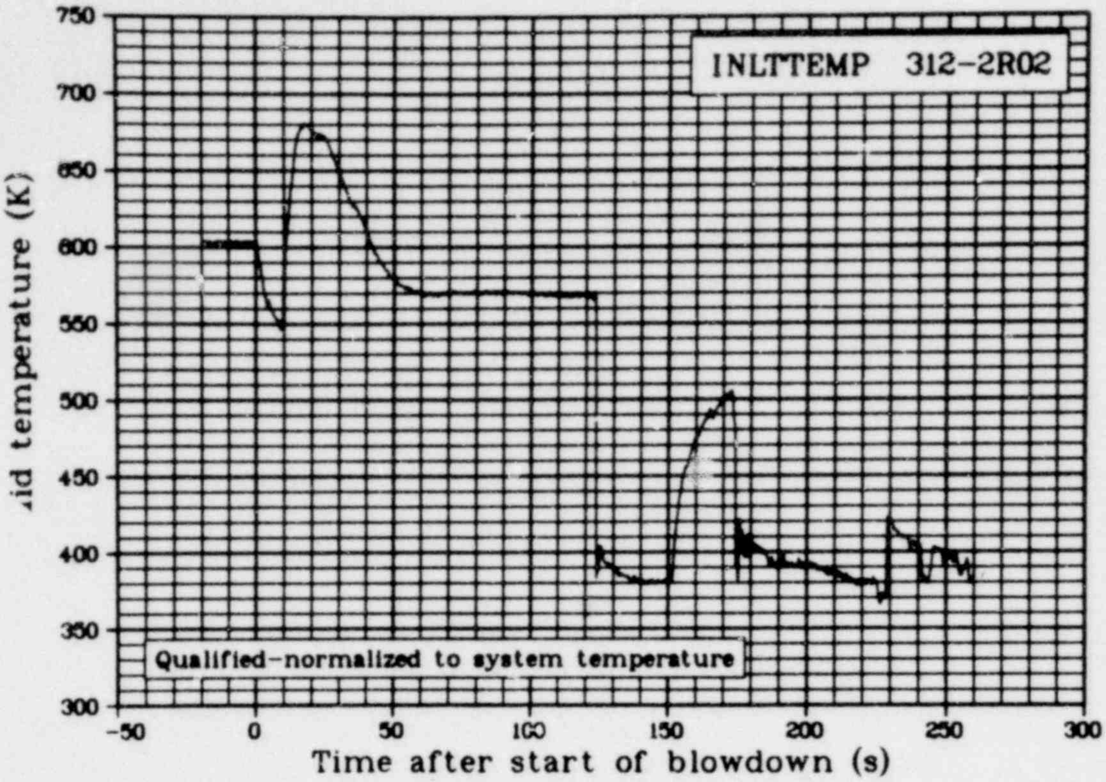

Fig. 281 Fluid temperature of Fuel Rod 312-3 coolant inlet (INLTTEMP 312-2RO2), from -50 to 300 s.

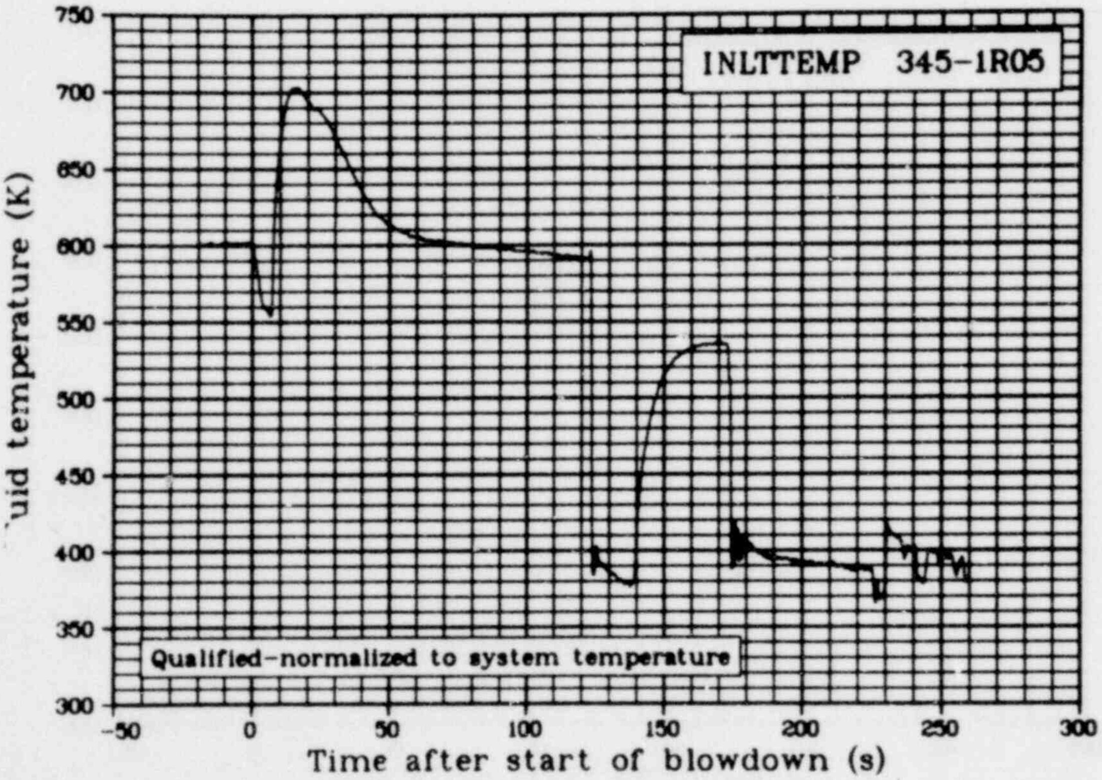

Fig. 282 Fluid temperature of Fuel Rod 345-1 coolant inlet (INLTTEMP 345-1RO5), from -50 to 300 s.

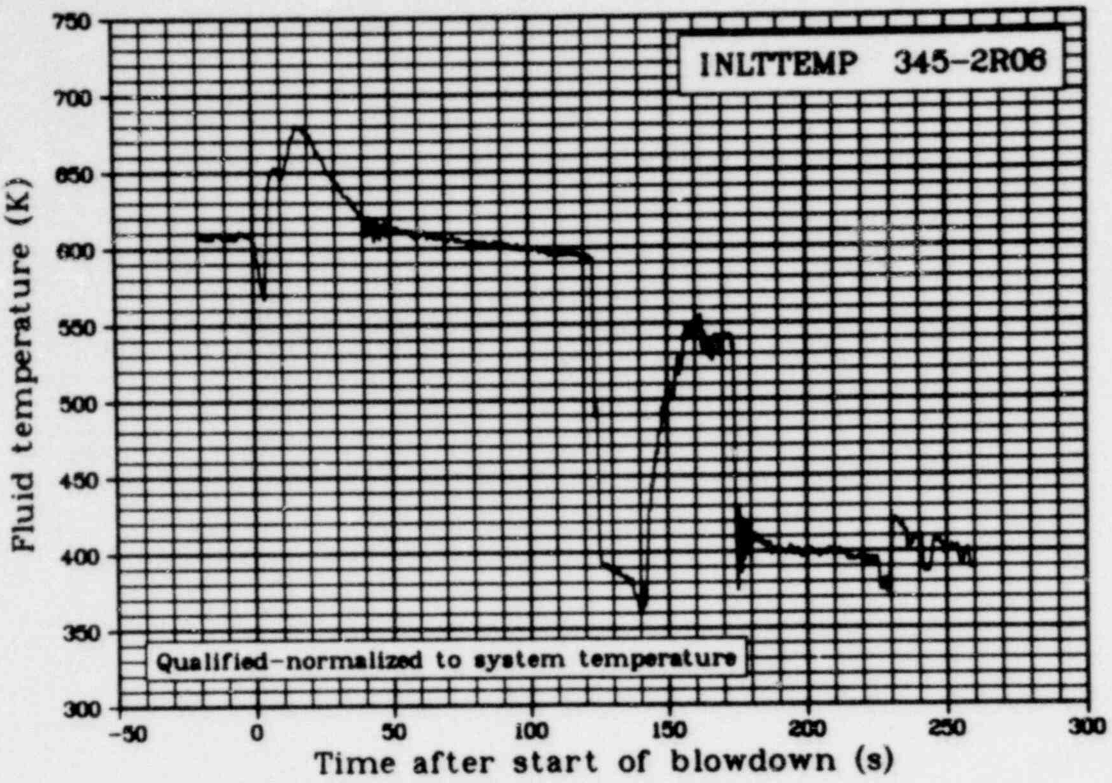

Fig. 283 Fluid temperature of Fuel Rod 345-2 coolant inlet (INLTTEMP 345-2RO6), from -50 to 300 s.

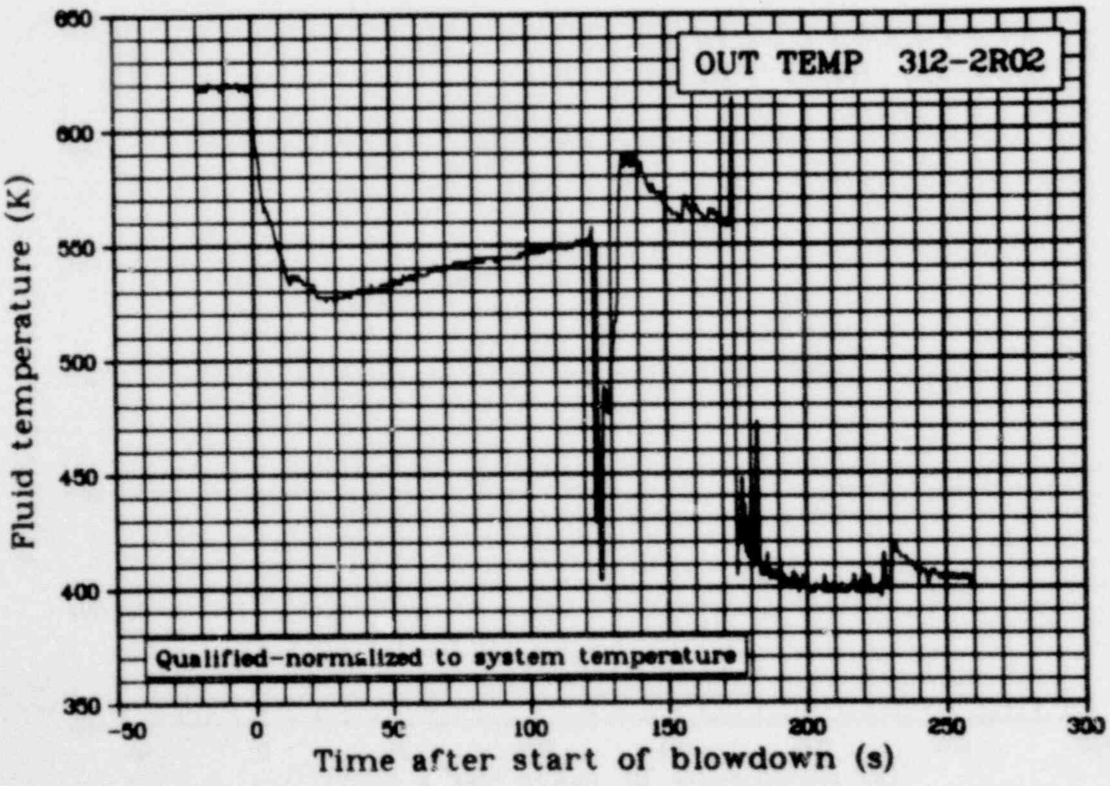

Fig. 284 Fluid temperature of Fuel Rod 312-2 coolant outlet (OUT TEMP 312-2RO2), from -50 to 300 s.

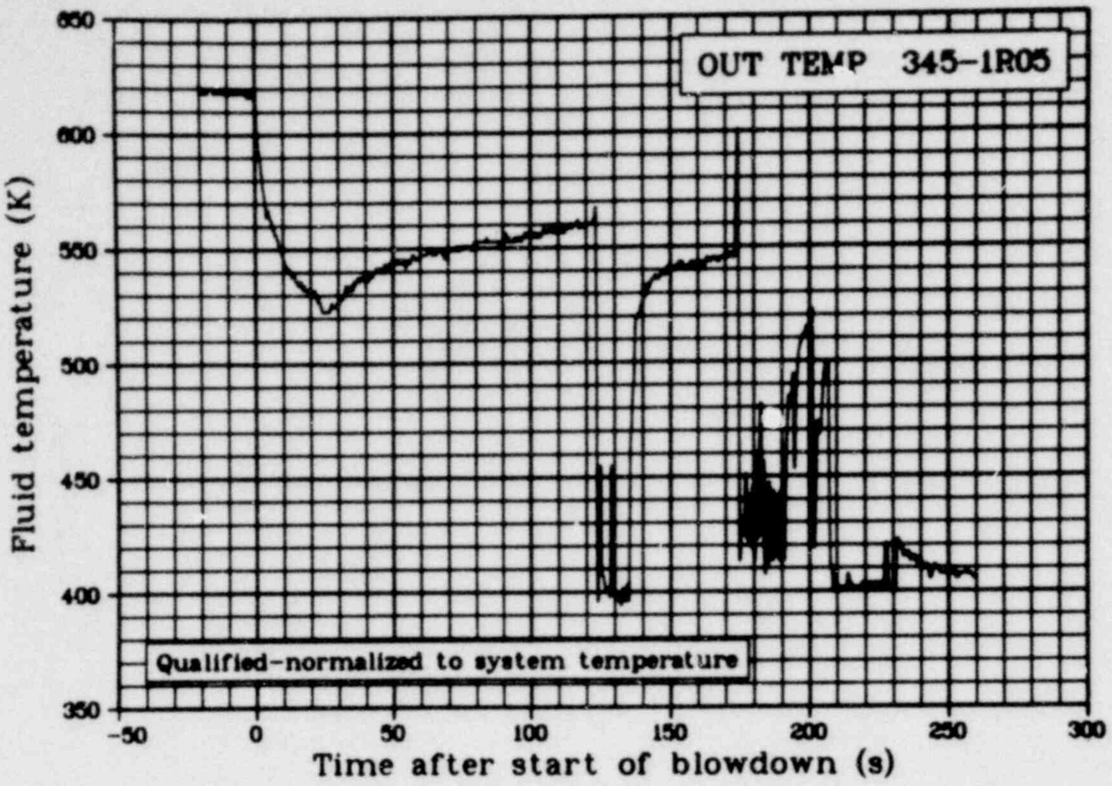

Fig. 285 Fluid temperature of Fuel Rod 345-1 coolant outlet (OUT TEMP 345-1RO5), from -50 to 300 s.

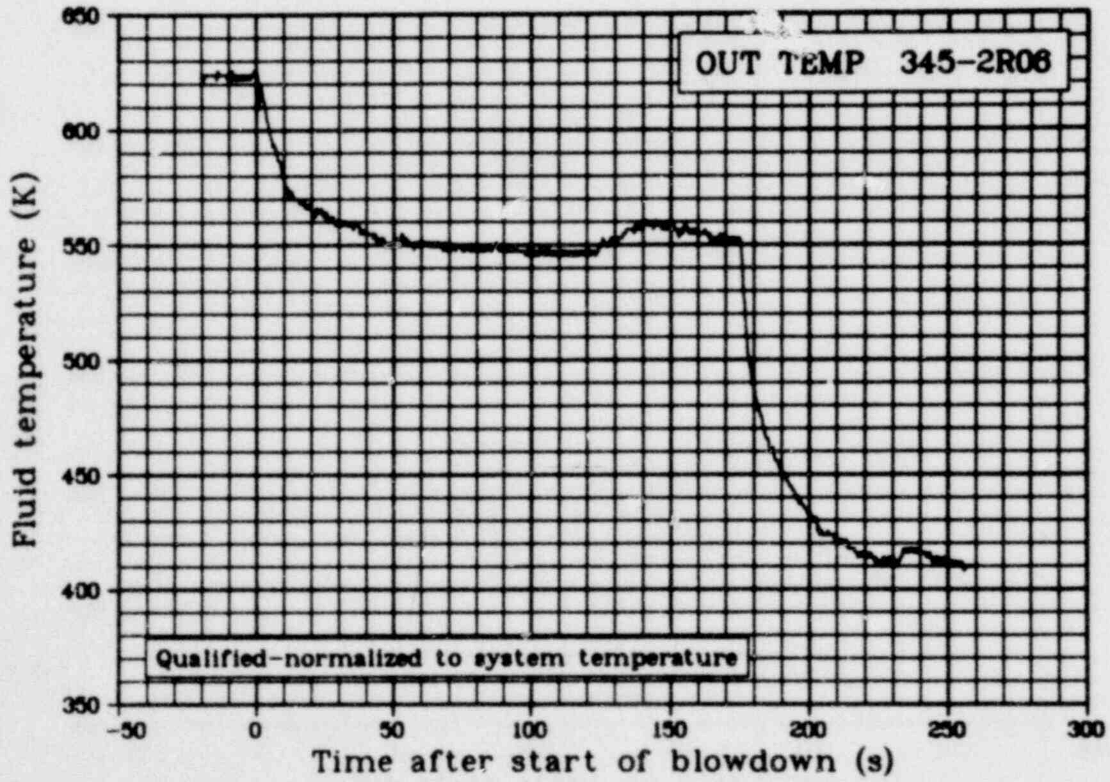

Fig. 286 Fluid temperature of Fuel Rod 345-2 coolant outlet (OUT TEMP 345-2RO6), from -50 to 300 s.

1405 231

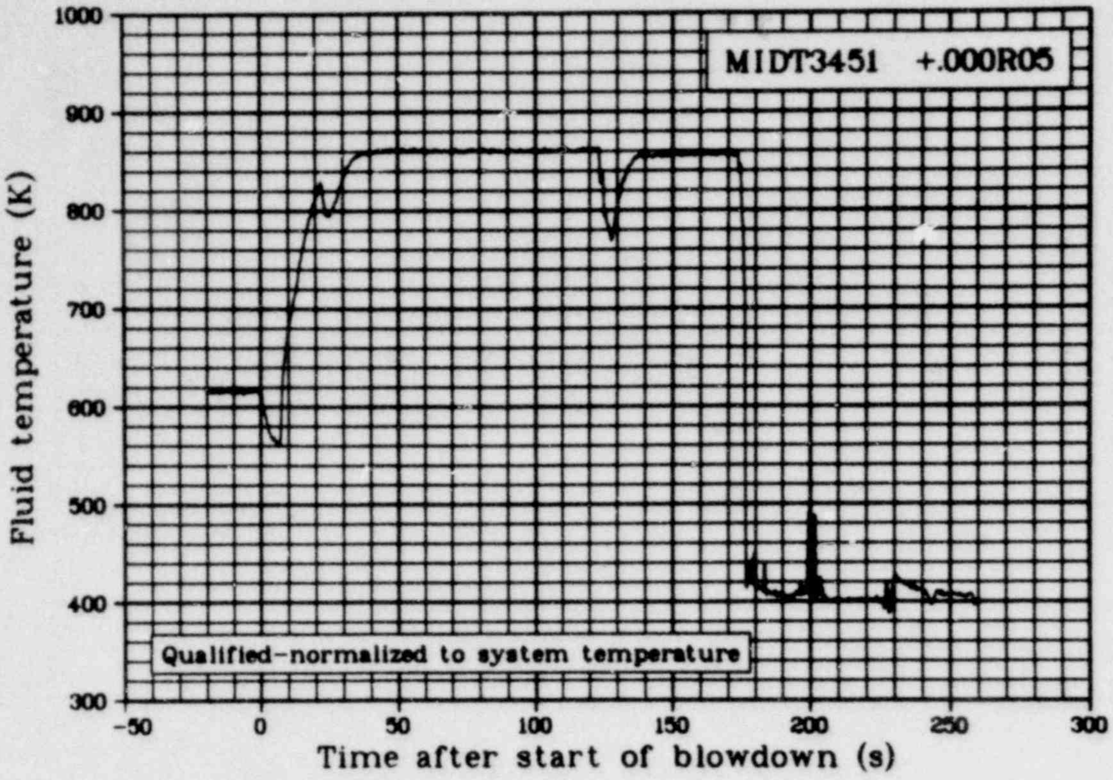

Fig. 287 Fluid temperature of Fuel Rod 345-1, at fuel stack midplane (MIDT3451 + .000R05), from -50 to 300 s.

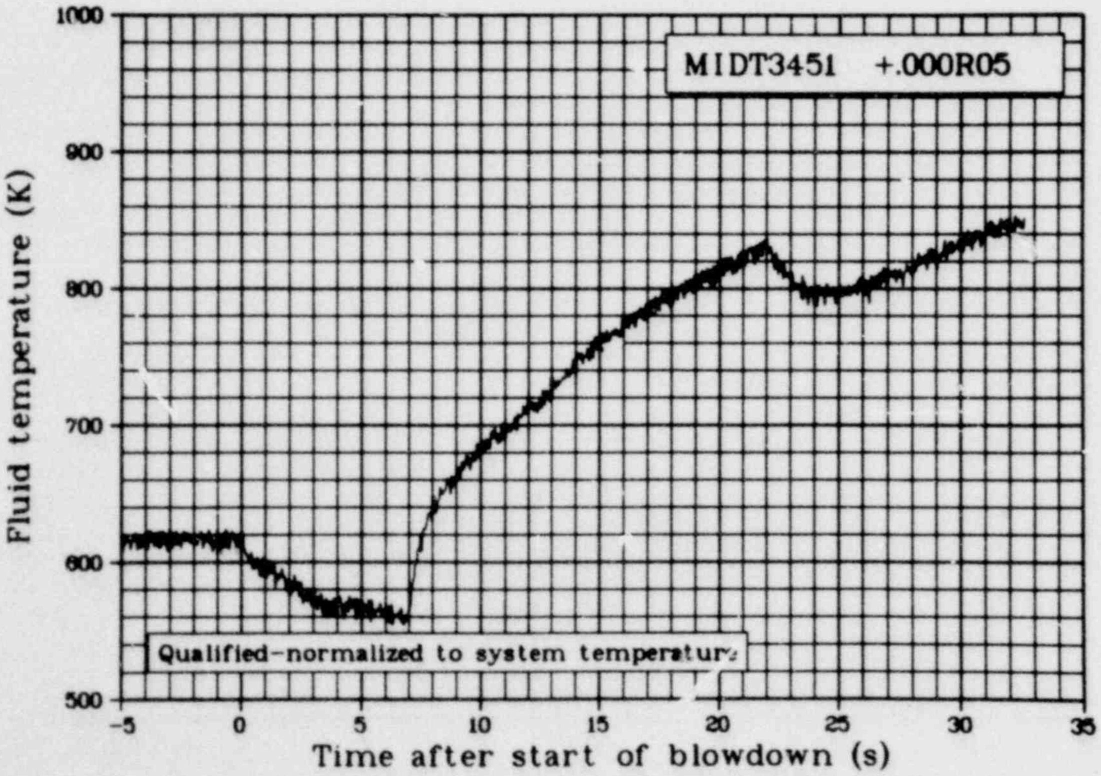

Fig. 288 Fluid temperature of Fuel Rod 345-1, at fuel stack midplane (MIDT3451 + .000R05), from -5 to 35 s.

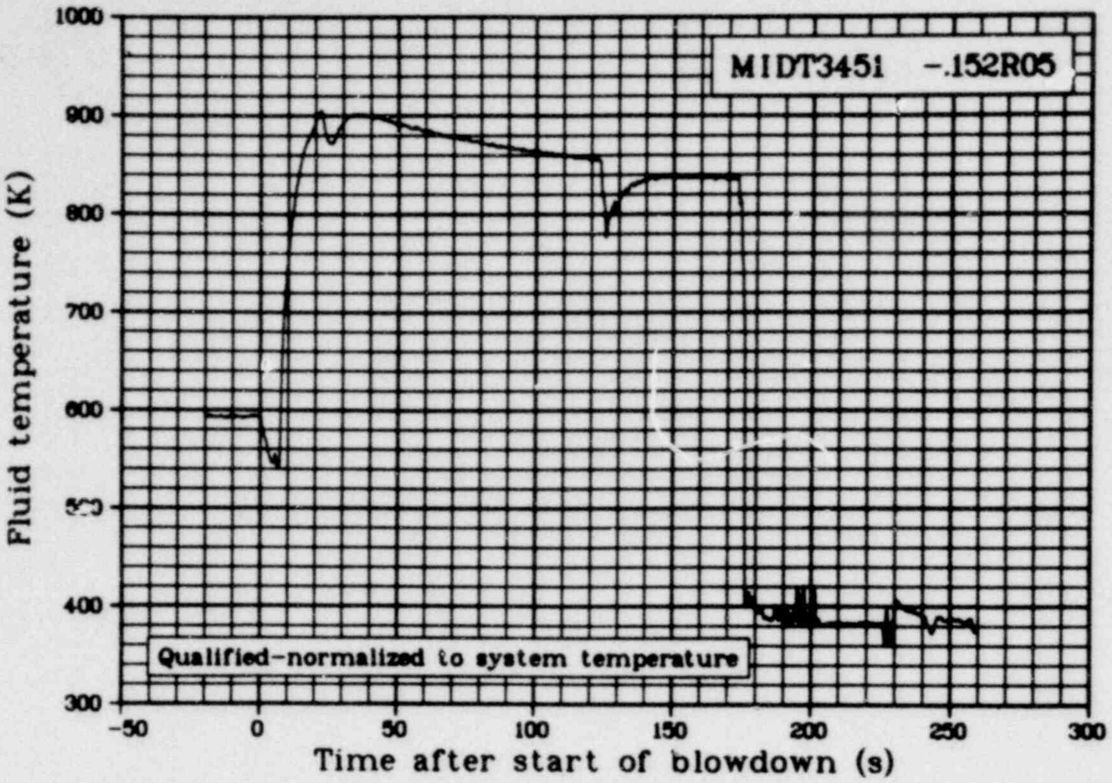

Fig. 289 Fluid temperature of Fuel Rod 345-1, 0.152 m below fuel stack midplane (MIDT3451 -.152R05), from -50 to 300 s.

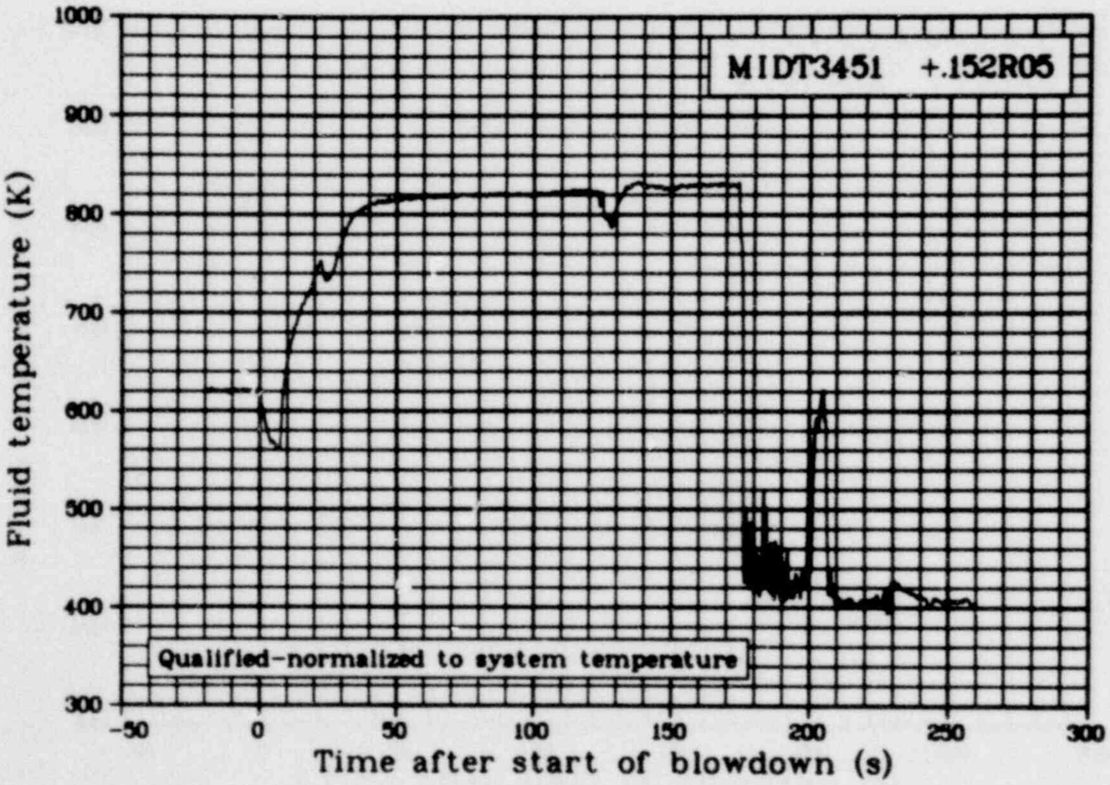

Fig. 290 Fluid temperature of Fuel Rod 345-1, 0.152 m above fuel stack midplane (MIDT3451 +.152R05), from -50 to 300 s.

1405 233

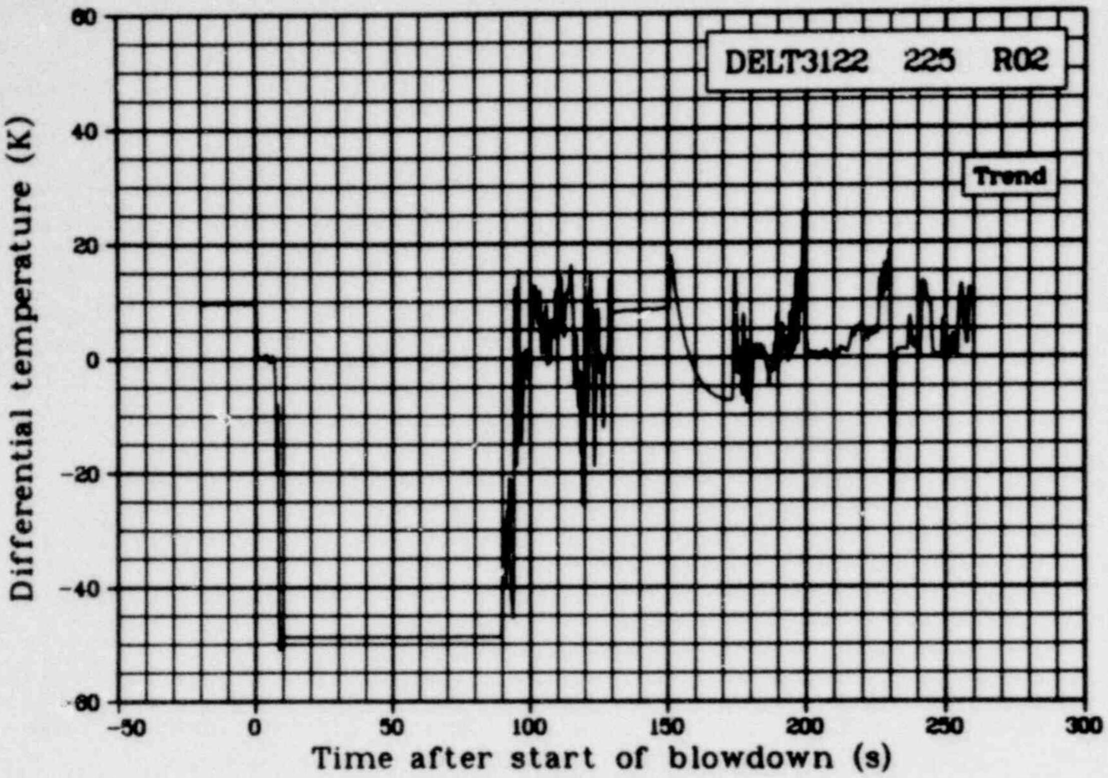

Fig. 291 Differential temperature of Rod 312-2 coolant inlet and outlet (DELT3122 225 R02), from -50 to 300 s.

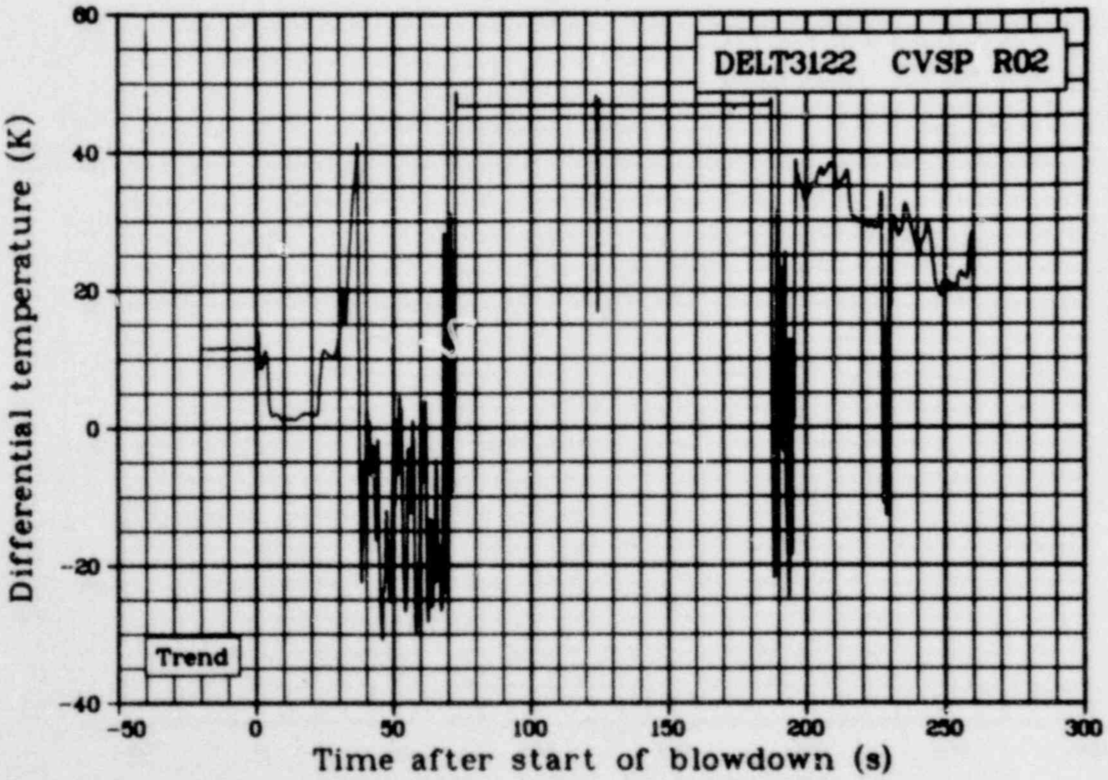

Fig. 292 Differential temperature of Rod 312-2, from support plate to outlet check valve (DELT3122 CVSP R02), from -50 to 300 s.

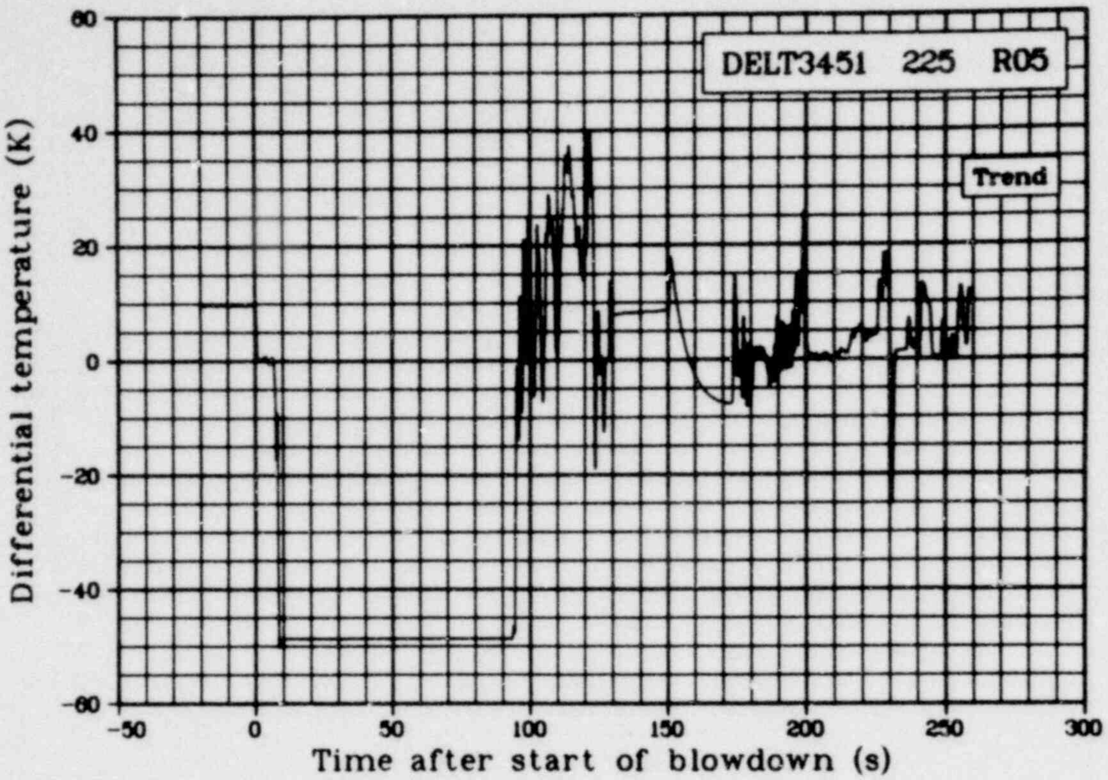

Fig. 293 Differential temperature of Rod 345-1 coolant inlet and outlet (DELT3451 225 R05), from -50 to 300 s.

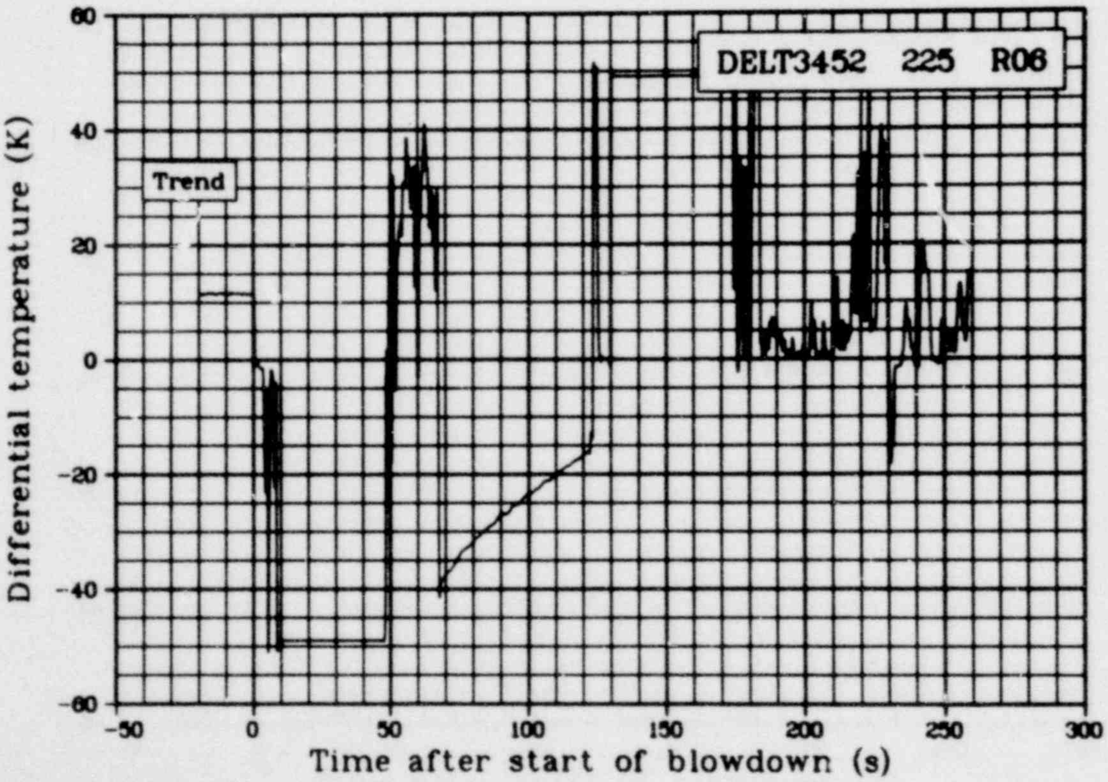

Fig. 294 Differential temperature of Rod 345-2, coolant inlet and outlet (DELT3452 225 R06), from -50 to 300 s.

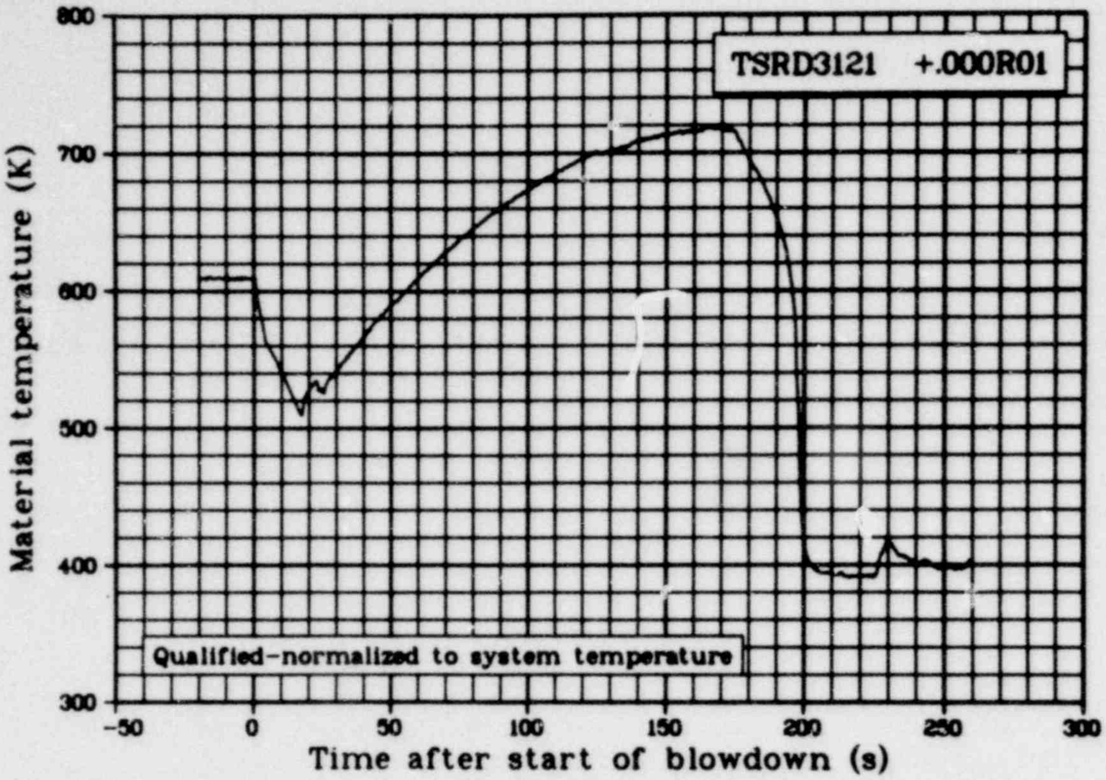

Fig. 295 Material temperature, Rod 312-1 shroud, at fuel stack midplane (TSRD3121 + .000R01), from -50 to 300 s.

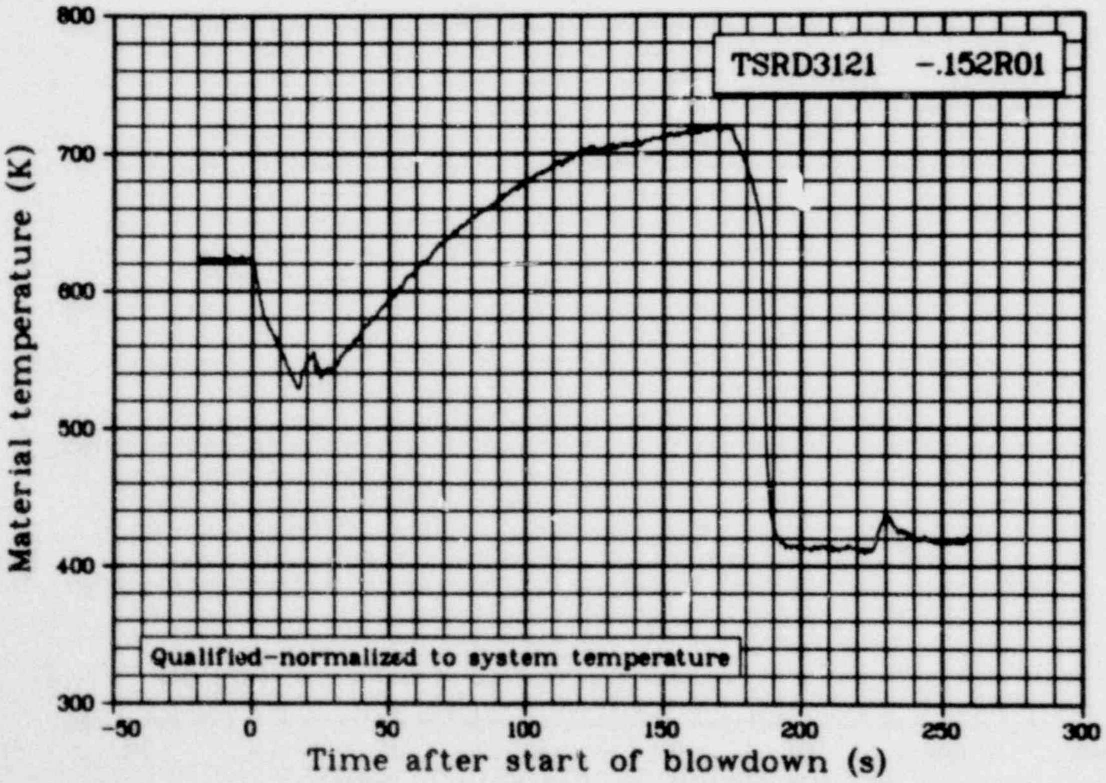

Fig. 296 Material temperature, Rod 312-1 shroud, 0.152 m below fuel stack midplane (TSRD3121 -.152R01), from -50 to 300 s.

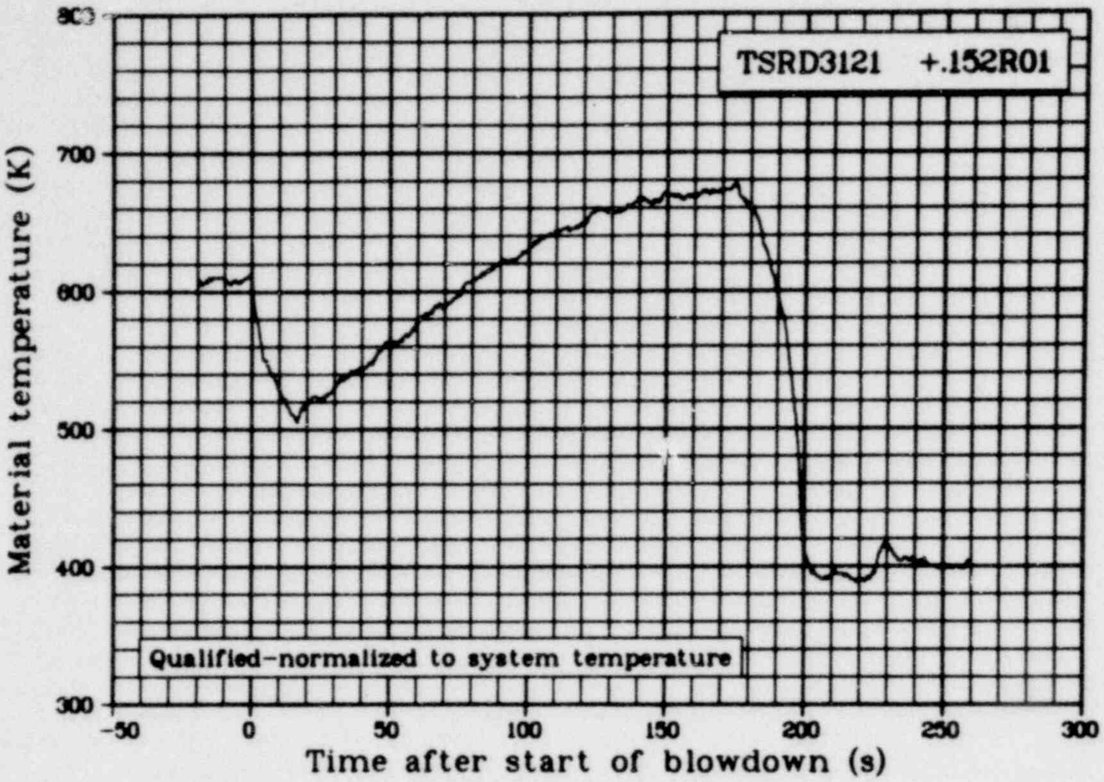

Fig. 297 Material temperature, Rod 312-1 shroud, 0.152 m above fuel stack midplane (TSRD3121 +.152R01), from -50 to 300 s.

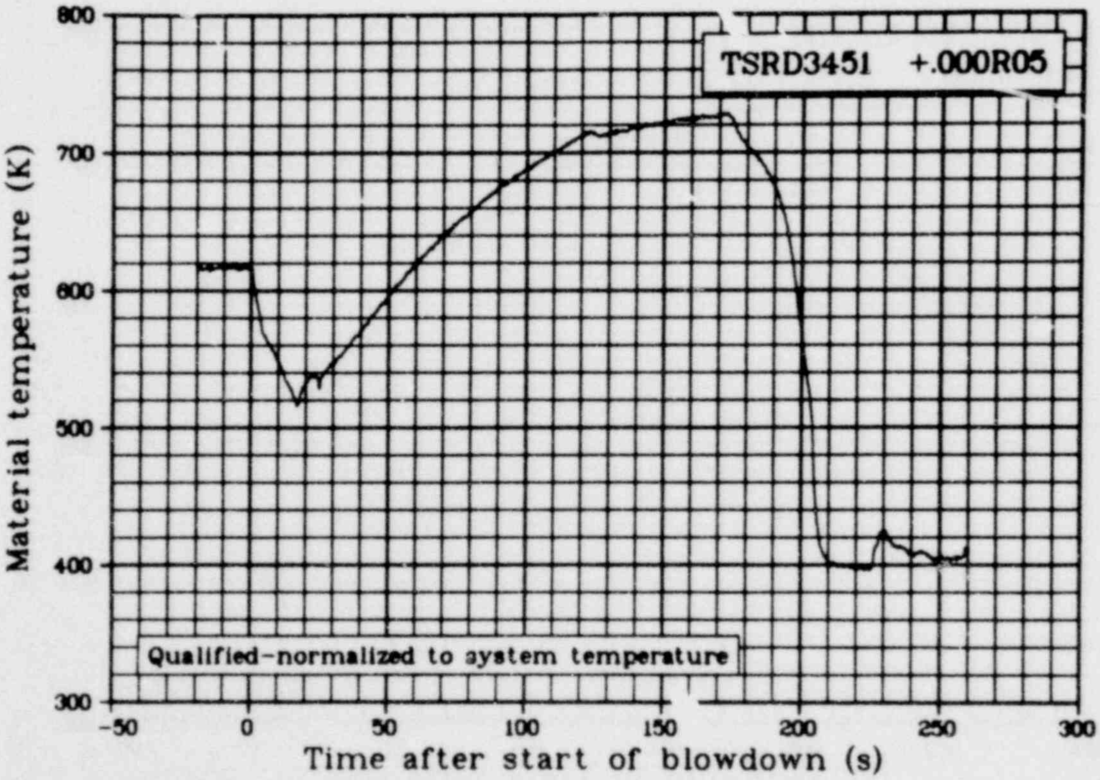

Fig. 298 Material temperature, Rod 345-1 shroud, at fuel stack midplane (TSRD3451 +.000R05), from -50 to 300 s.

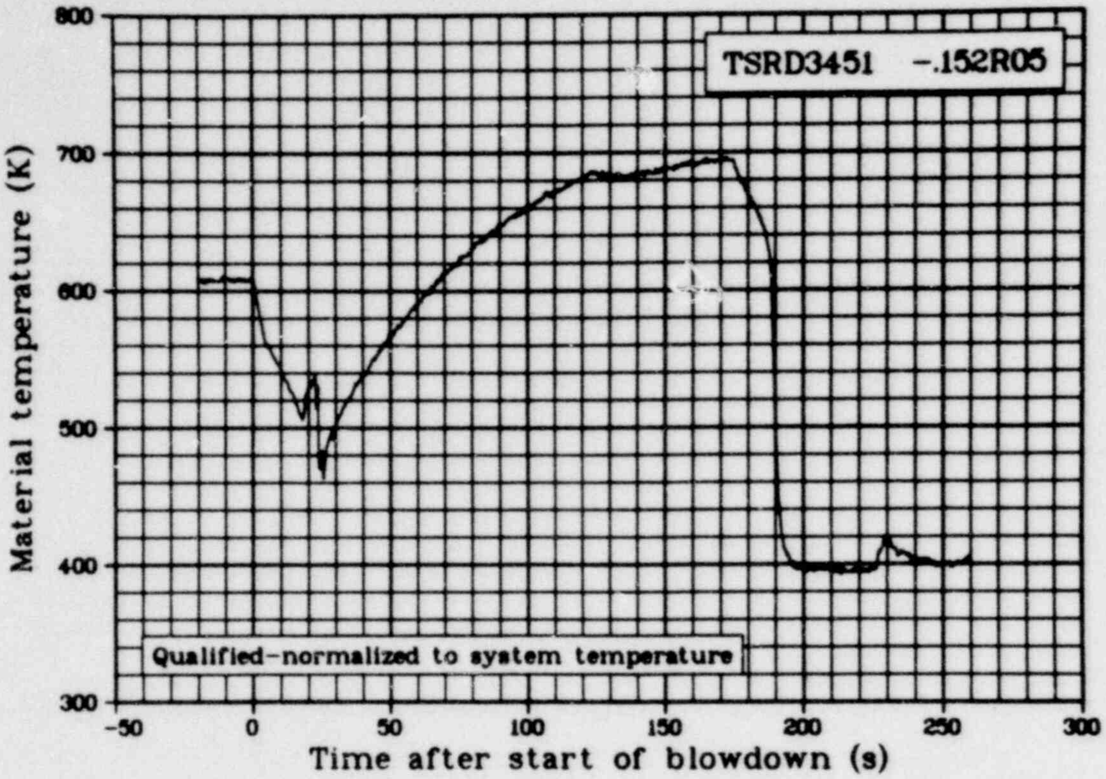

Fig. 299 Material temperature, Rod 345-1 shroud, 0.152 m below fuel stack midplane (TSRD3451 -.152R05), from -50 to 300 s.

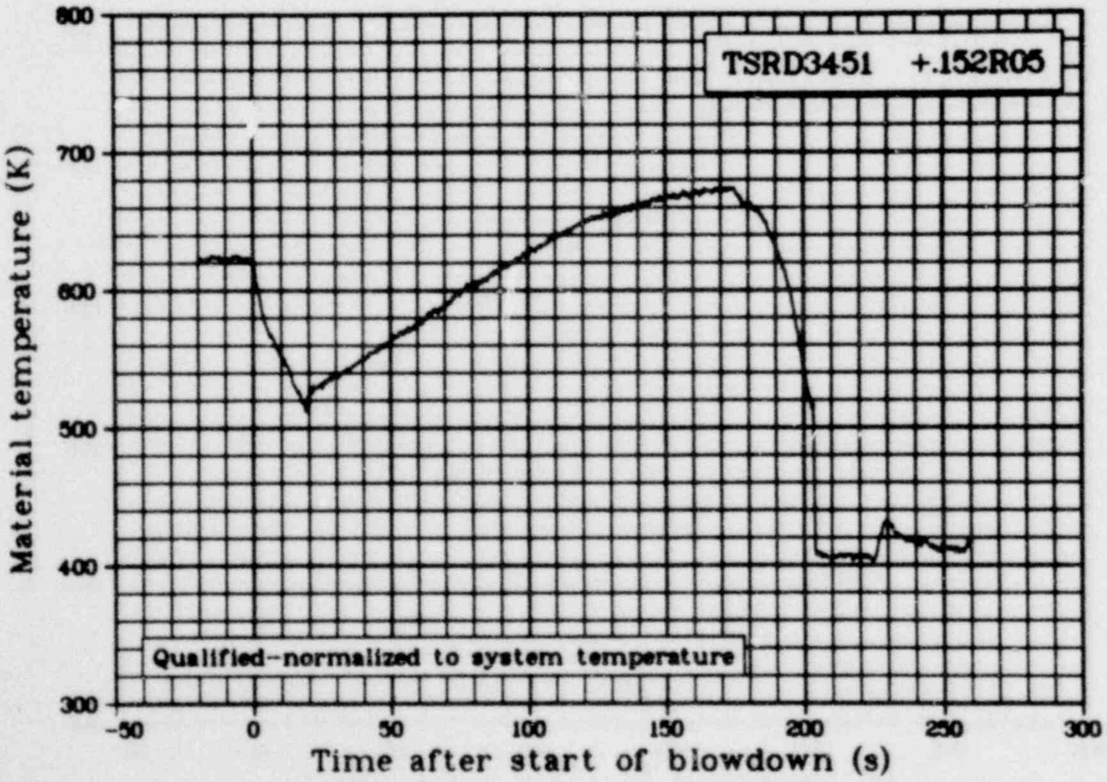

Fig. 300 Material temperature, Rod 345-1 shroud, 0.152 m above fuel stack midplane (TSRD3451 +.152R05), from -50 to 300 s.

1405 238

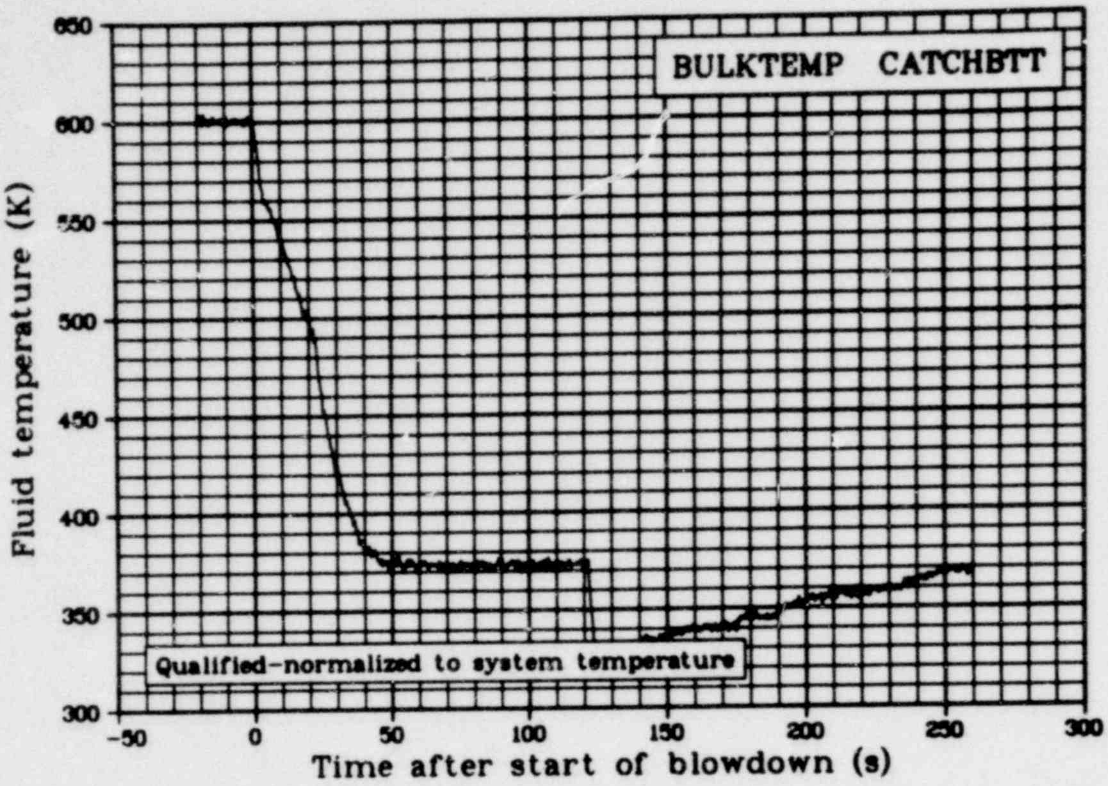

Fig. 301 Fluid temperature in test train catch basket (BULKTEMP CATCHBTT), from -50 to 300 s.

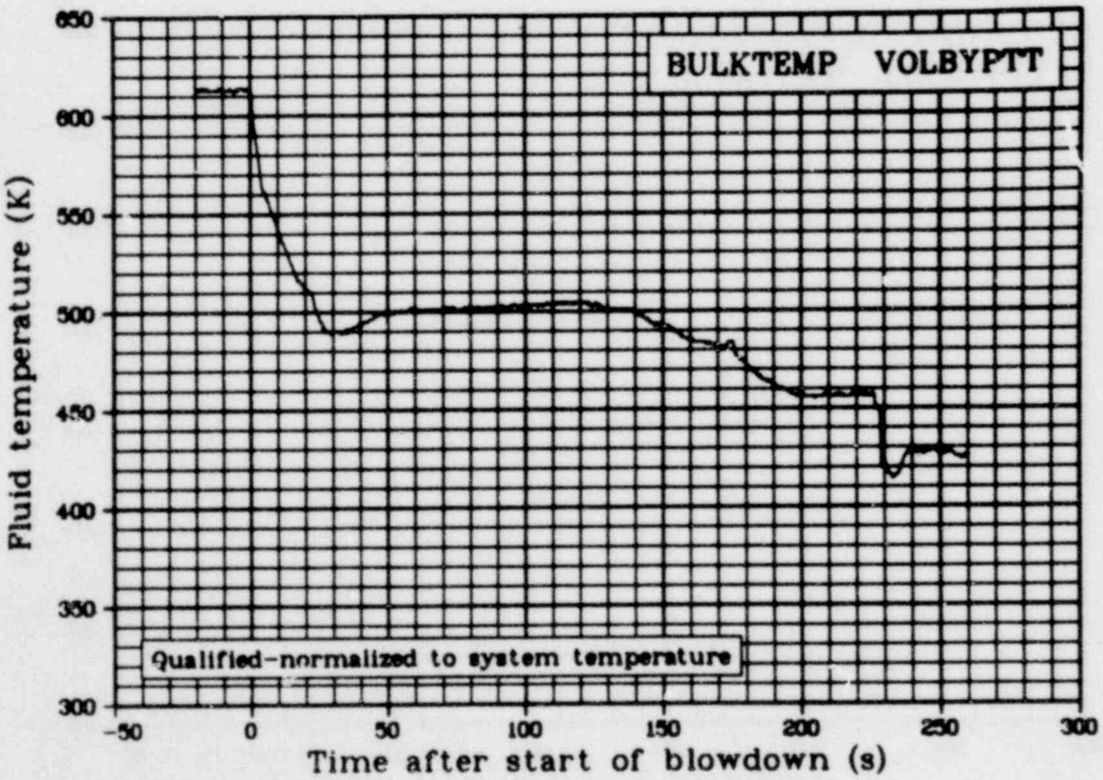

Fig. 302 Fluid temperature in bypass volume at fuel stack midplane (BULKTEMP VOLBYPTT), from -50 to 300 s.

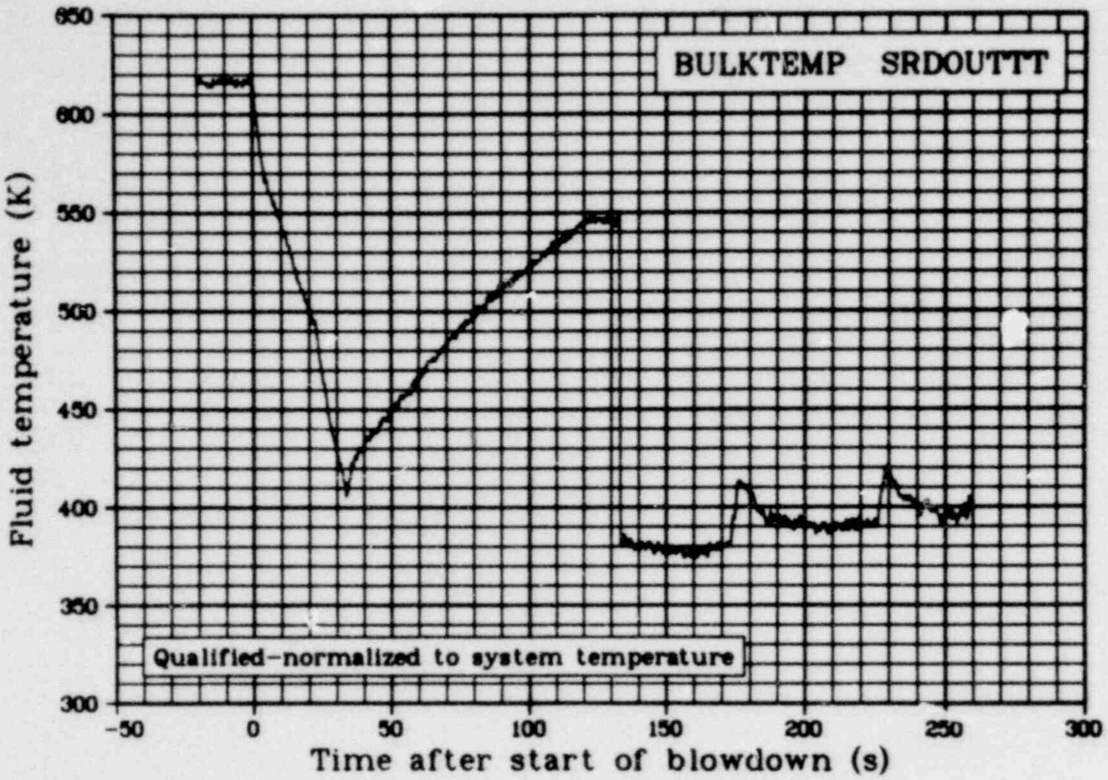

Fig. 303 Fluid temperature 0.05 m above flow shroud outlets (BULKTEMP SRDOUTTT), from -50 to 300 s.

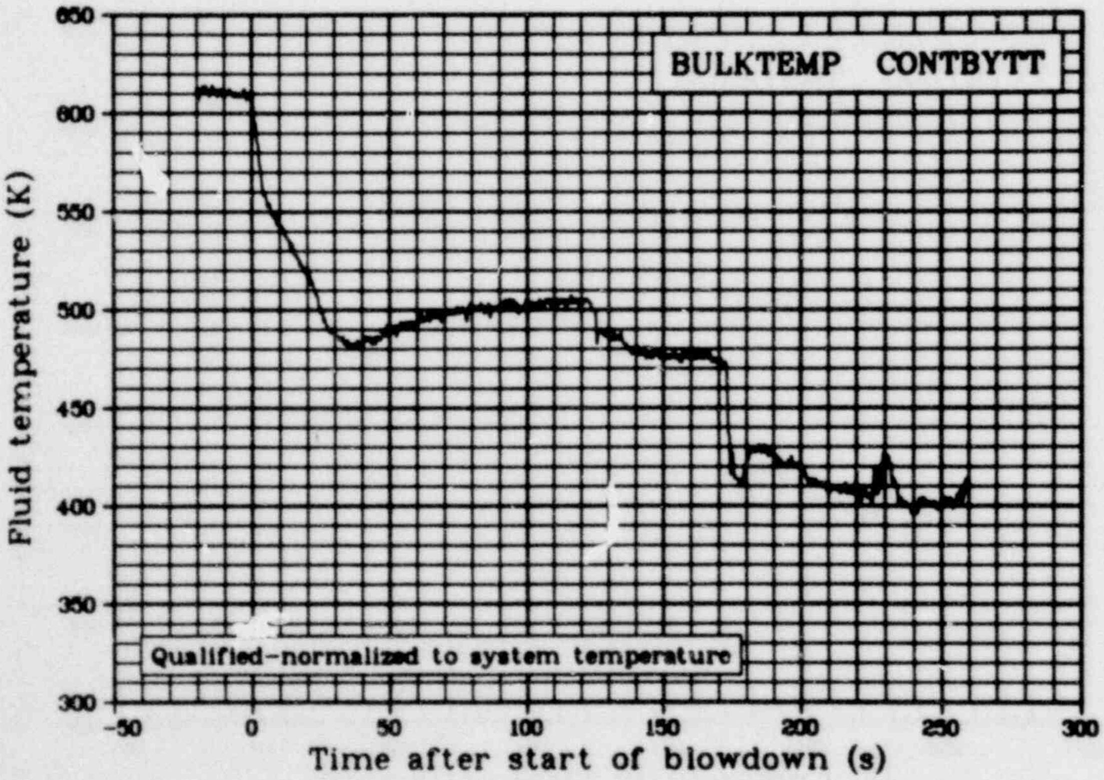

Fig. 304 Fluid temperature at test train controlled bypass inlet (BULKTEMP CONTBYTT), from -50 to 300 s.

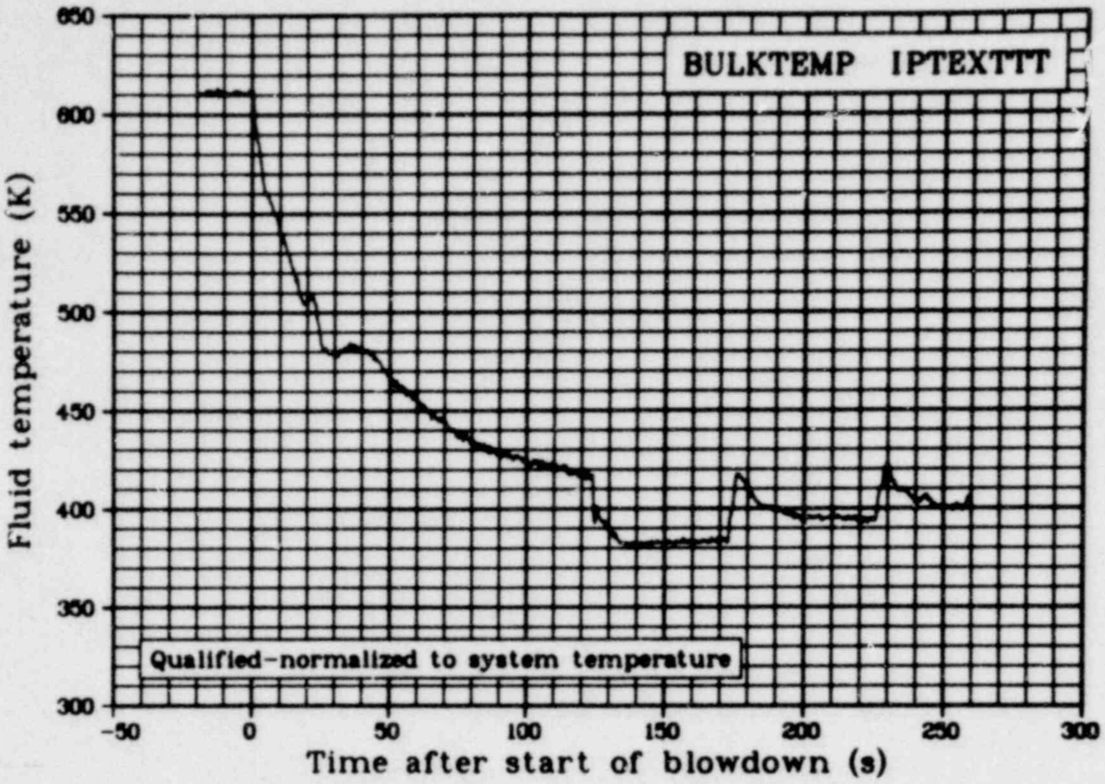

Fig. 305 Fluid temperature at IPT exit (BULKTEMP IPTEXTTT), from -50 to 300 s.

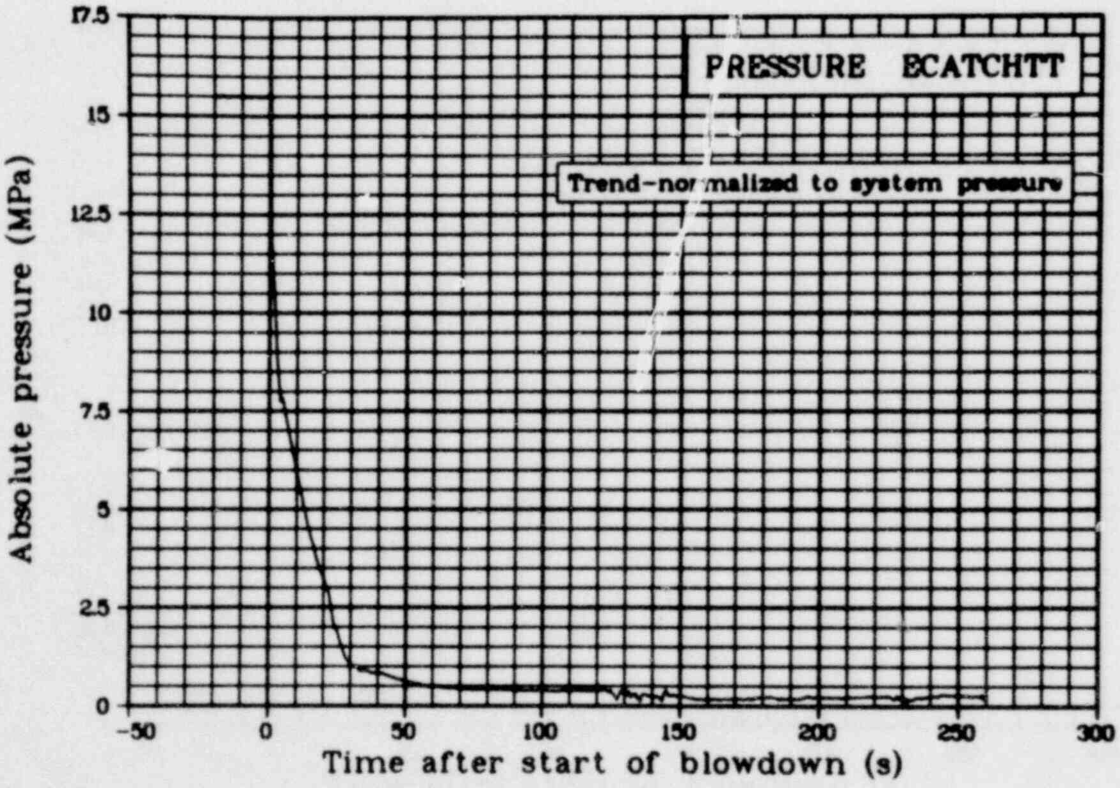

Fig. 306 Absolute pressure in test train catch basket (PRESSURE ECATCHTT), from -50 to 300 s.

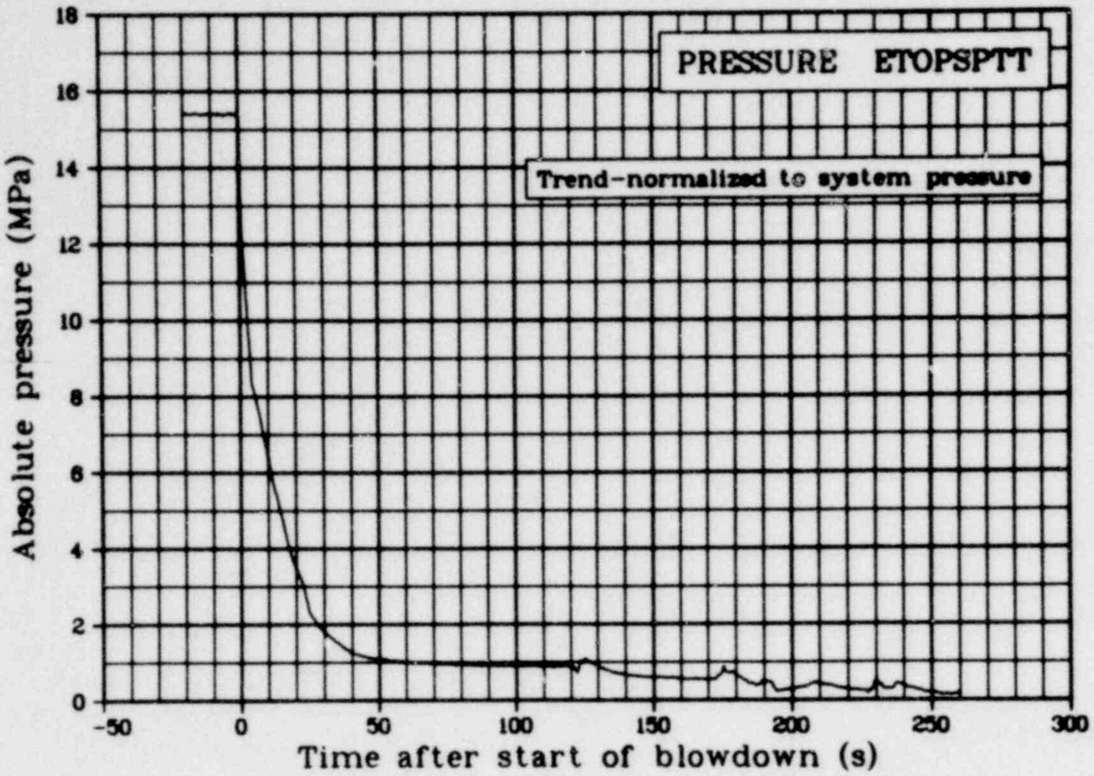

Fig. 307 Absolute pressure above test train top support plate (PRESSURE ETOPSPTT), from -50 to 300 s.

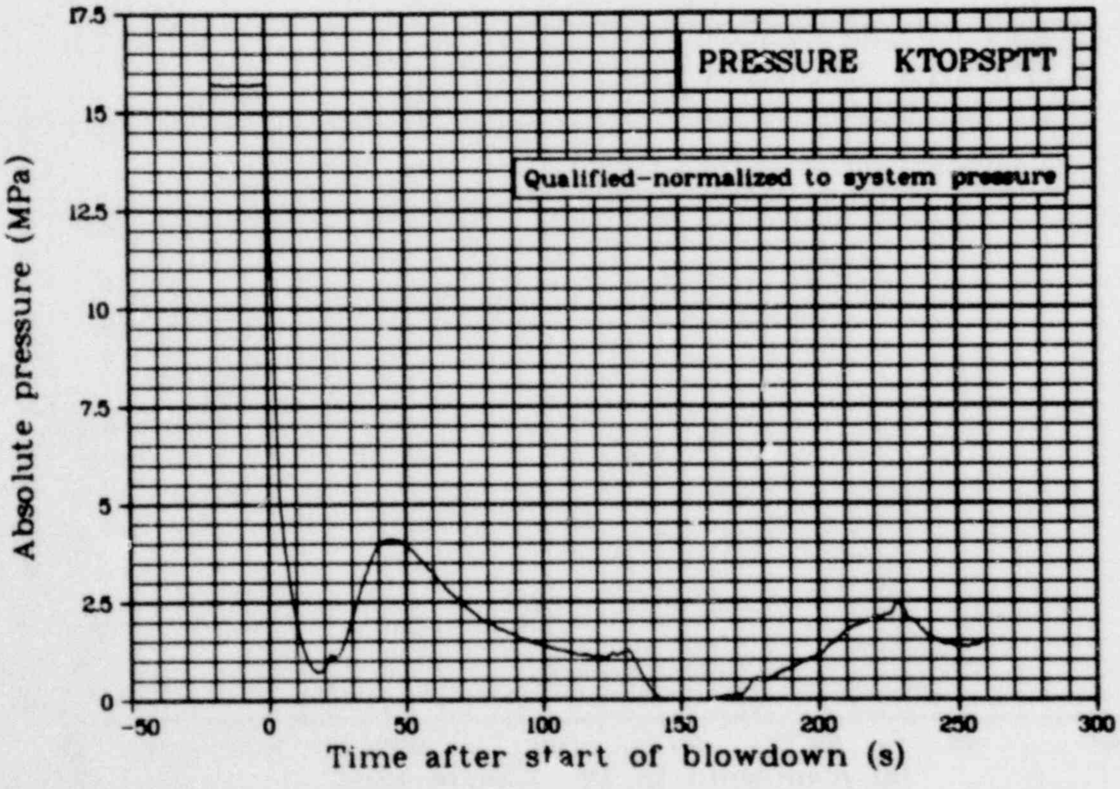

Fig. 308 Absolute pressure above the test train top support plate (PRESSURE KTOPSPTT), from -50 to 300 s.

1405 242

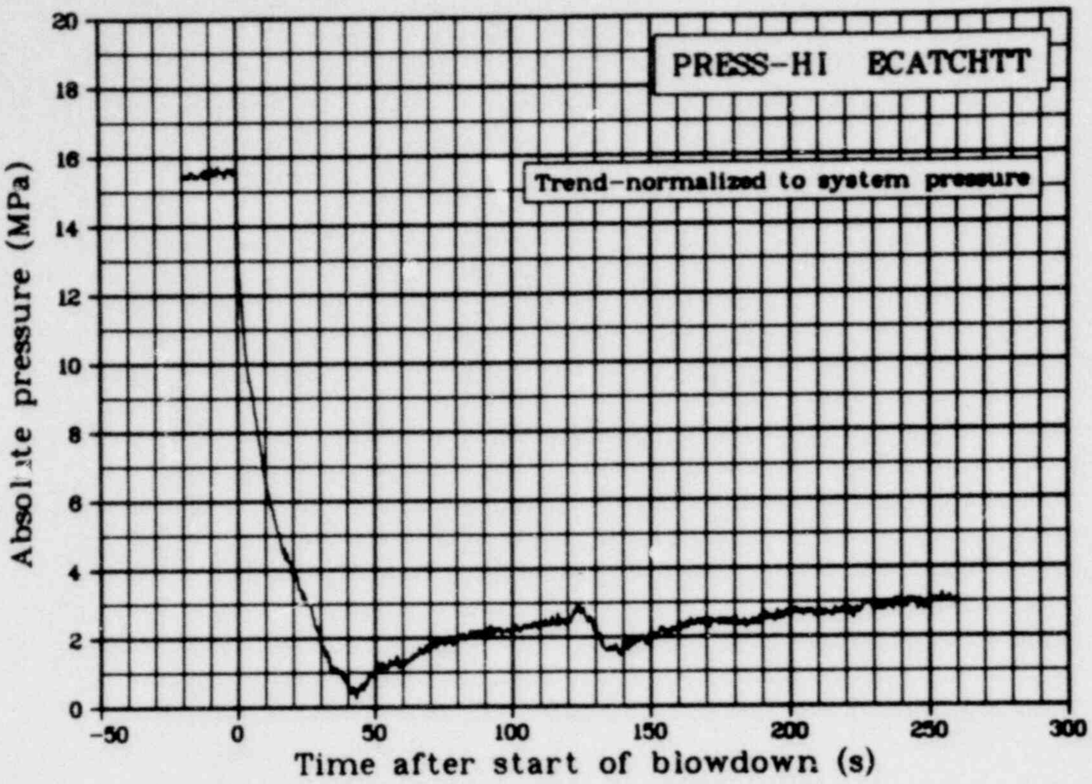

Fig. 309 Absolute pressure in test train catch basket (PRESS-HI ECATCHTT), from -50 to 300 s.

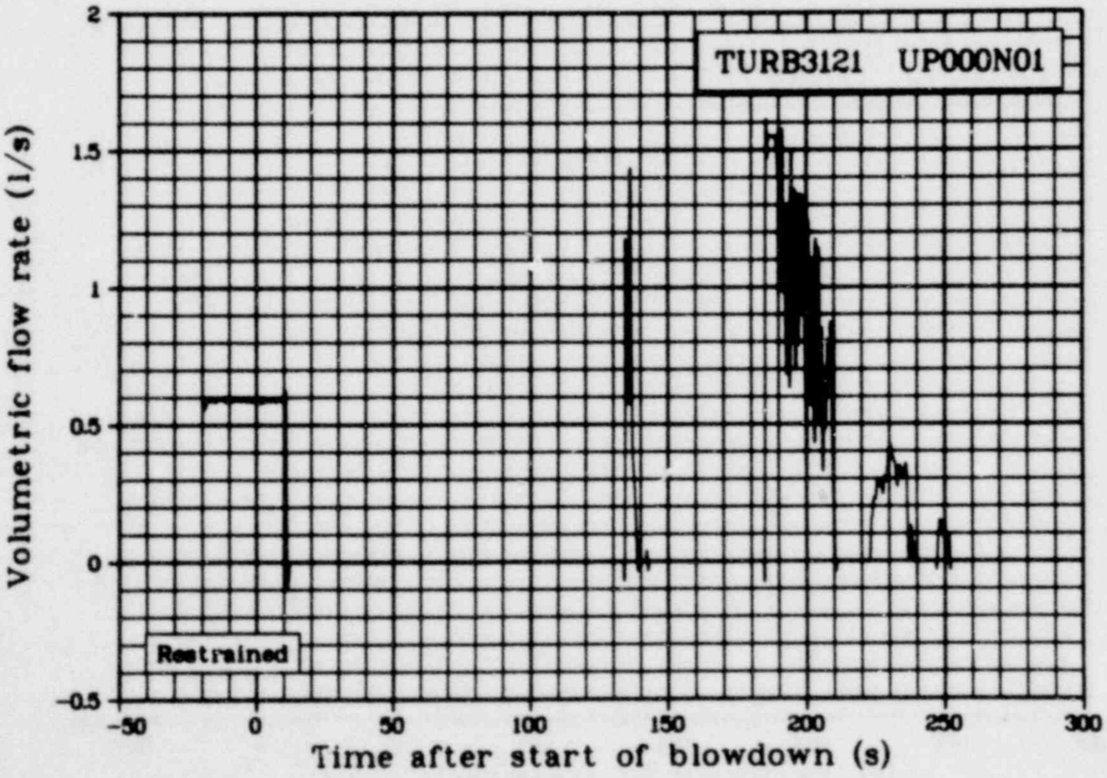

Fig. 310 Volumetric flow rate in Fuel Rod 312-1 upper shroud (TURB3121 UP000N01), from -50 to 300 s.

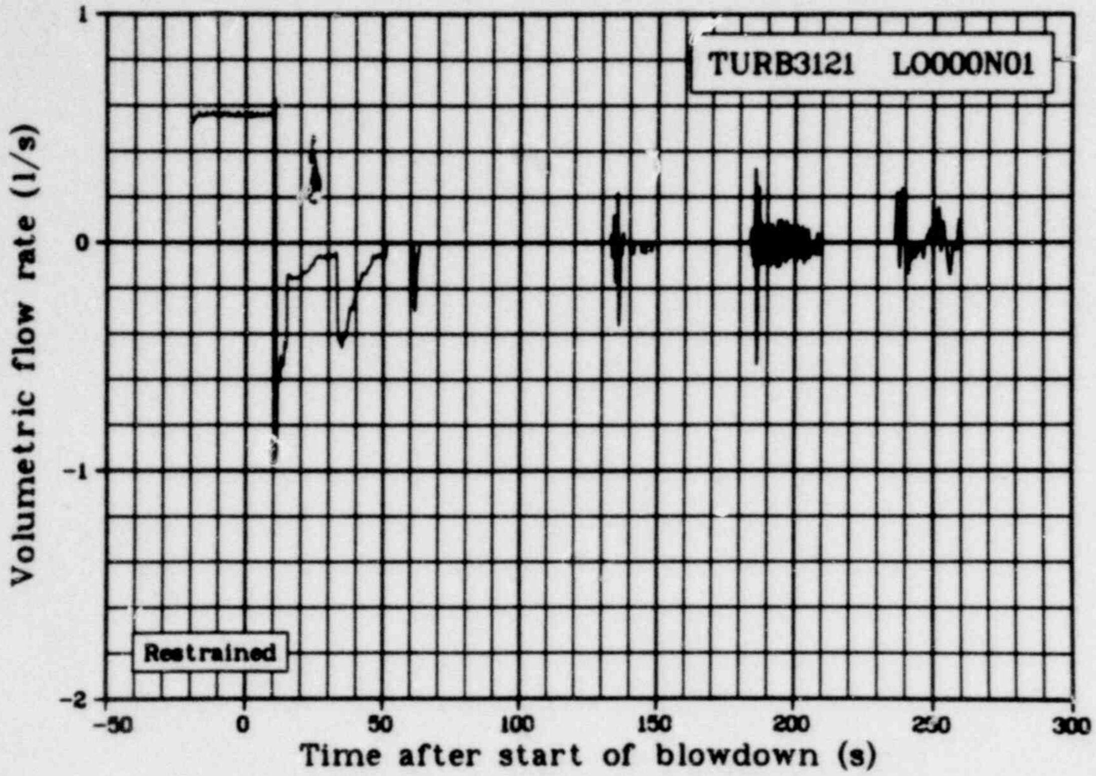

Fig. 311 Volumetric flow rate in Fuel Rod 312-1 lower shroud (TURB3121 L0000N01), from -50 to 300 s.

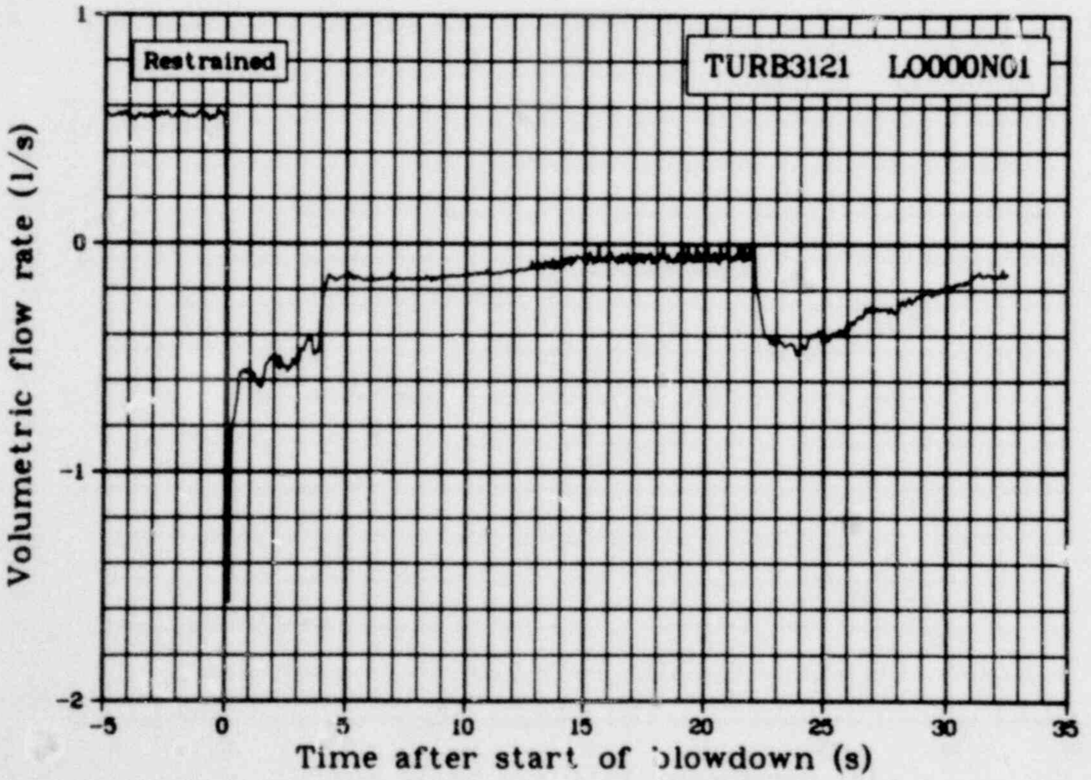

Fig. 312 Volumetric flow rate in Fuel Rod 312-1 lower shroud (TURB3121 L0000N01), from -5 to 35 s.

1405 244

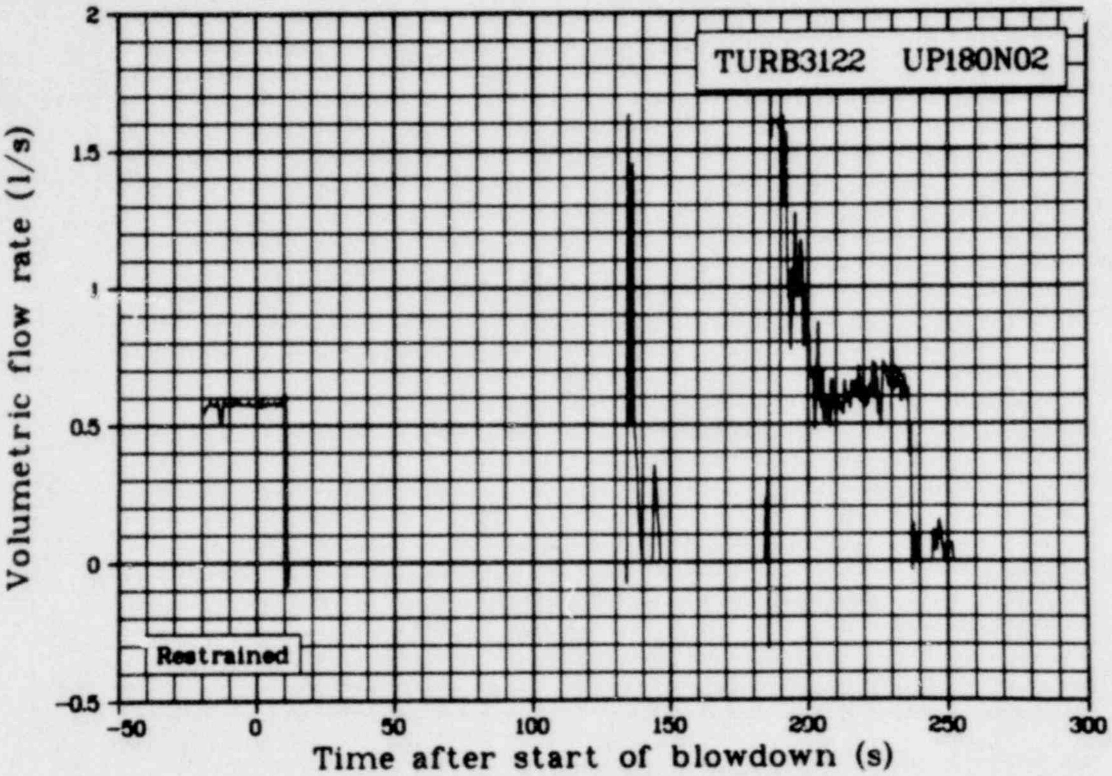

Fig. 313 Volumetric flow rate in Fuel Rod 312-2 upper shroud (TURB3122 UP180N02), from -50 to 300 s.

1405 245

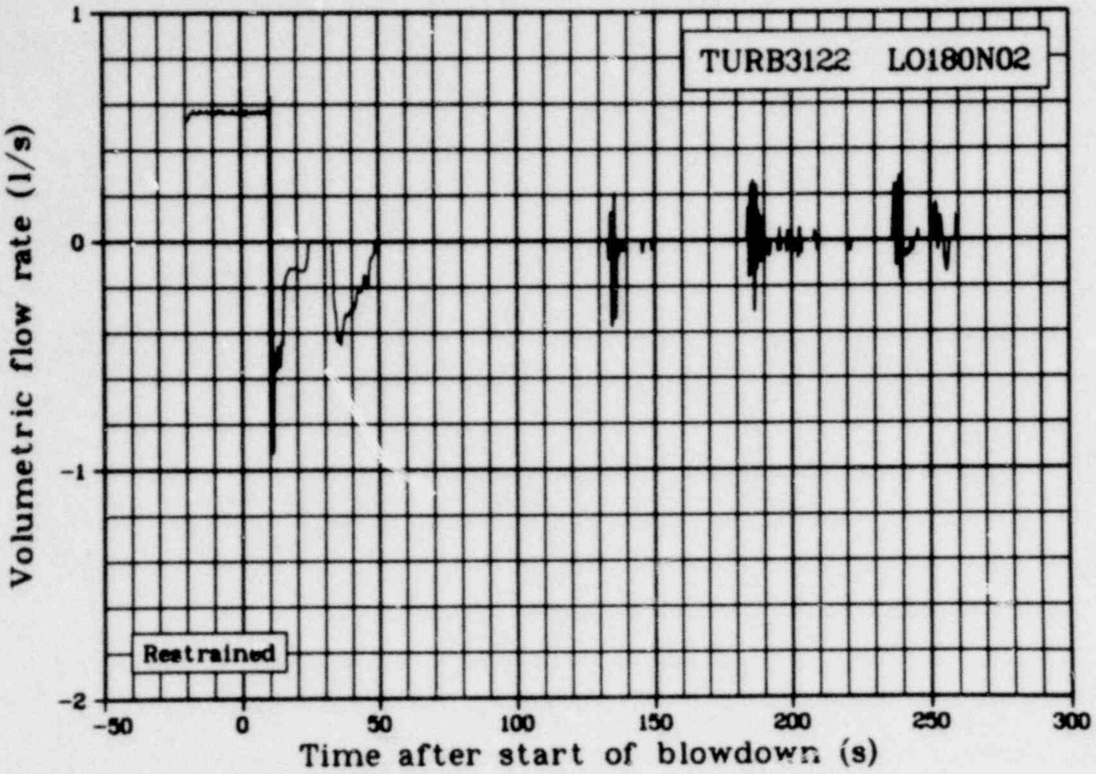

Fig. 314 Volumetric flow rate in Fuel Rod 312-2 lower shroud (TURB3122 L0180N02), from -50 to 300 s.

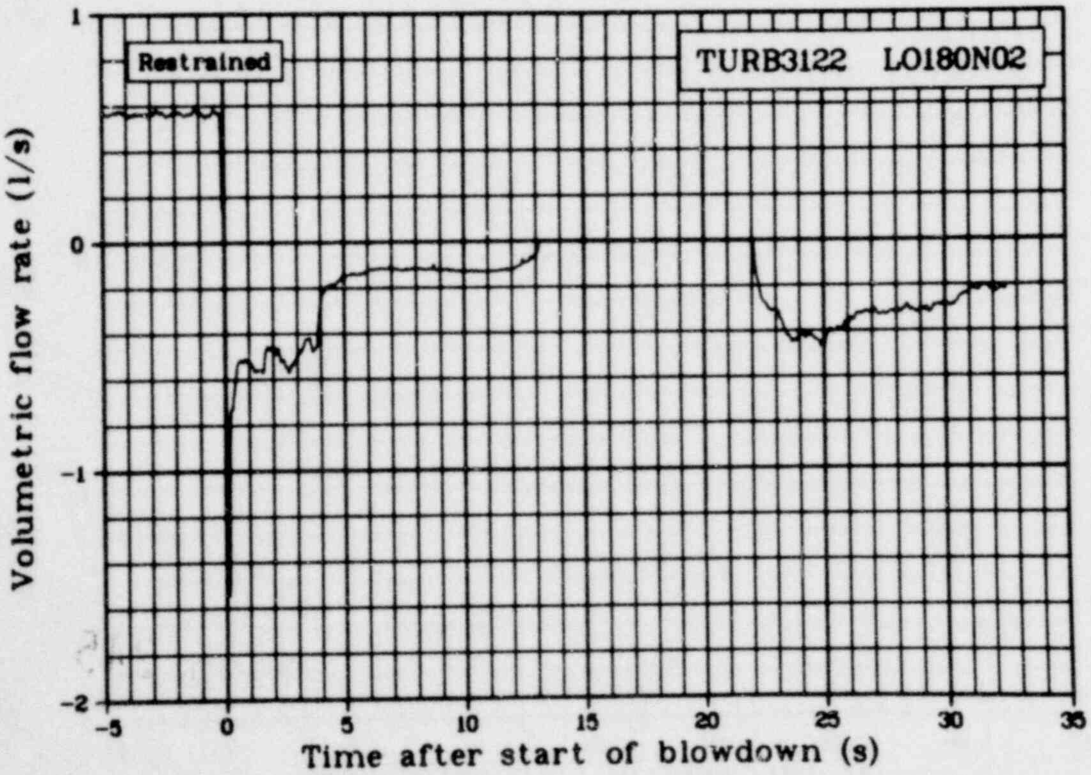

Fig. 315 Volumetric flow rate in Fuel Rod 312-2 lower shroud (TURB3122 L0180N02), from -5 to 35 s.

1405 246

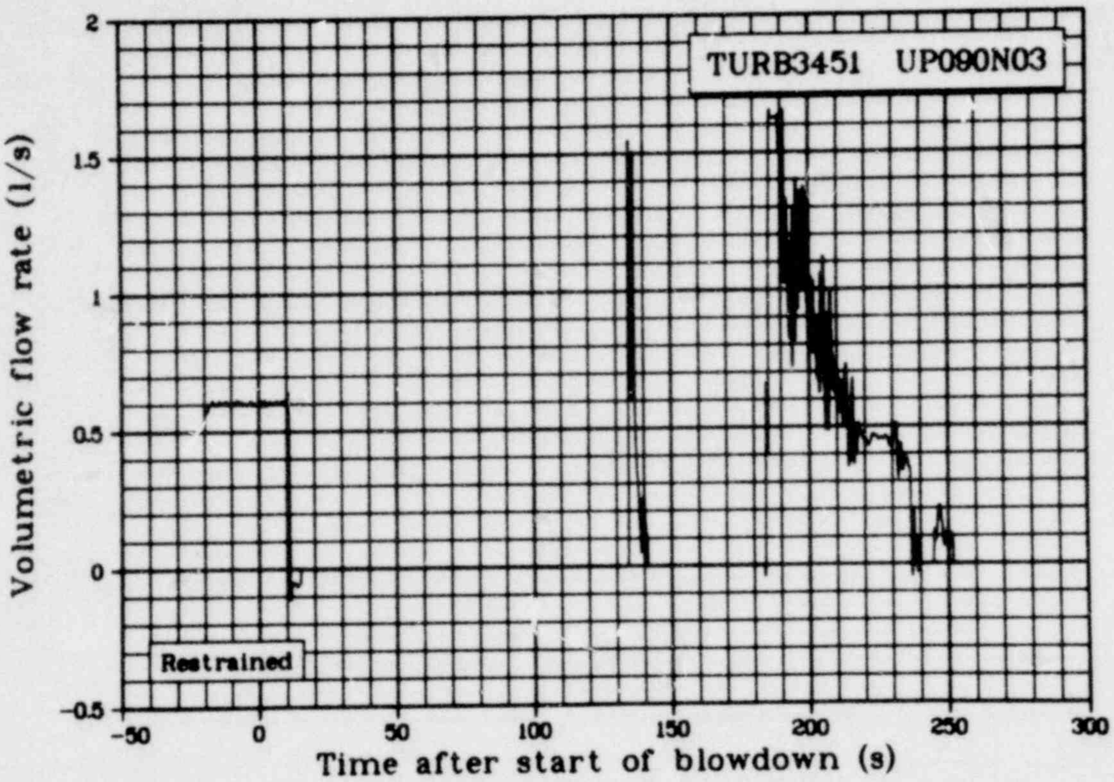

Fig. 316 Volumetric flow rate in Fuel Rod 345-1 upper shroud (TURB3451 UP090N03), from -50 to 300 s.

1405 247

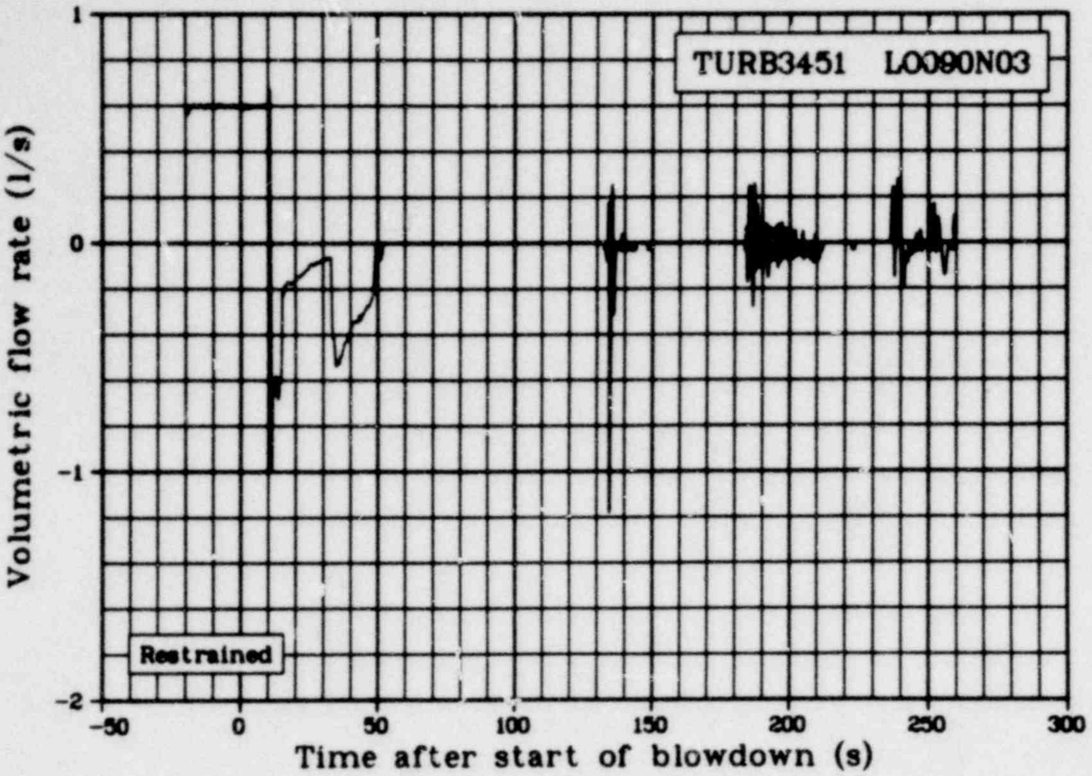

Fig. 317 Volumetric flow rate in Fuel Rod 345-1 lower shroud (TURB3451 L0090N03), from -50 to 300 s.

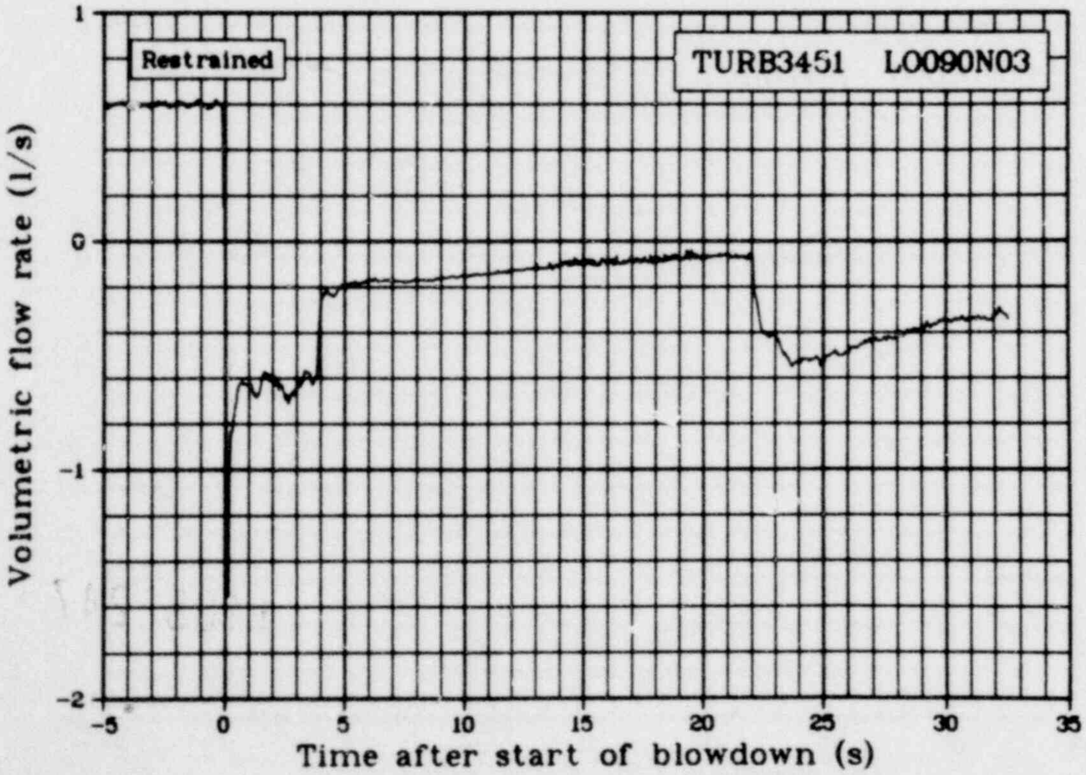

Fig. 318 Volumetric flow rate in Fuel Rod 345-1 lower shroud (TURB3451 L0090N03), from -5 to 35 s.

1405 248

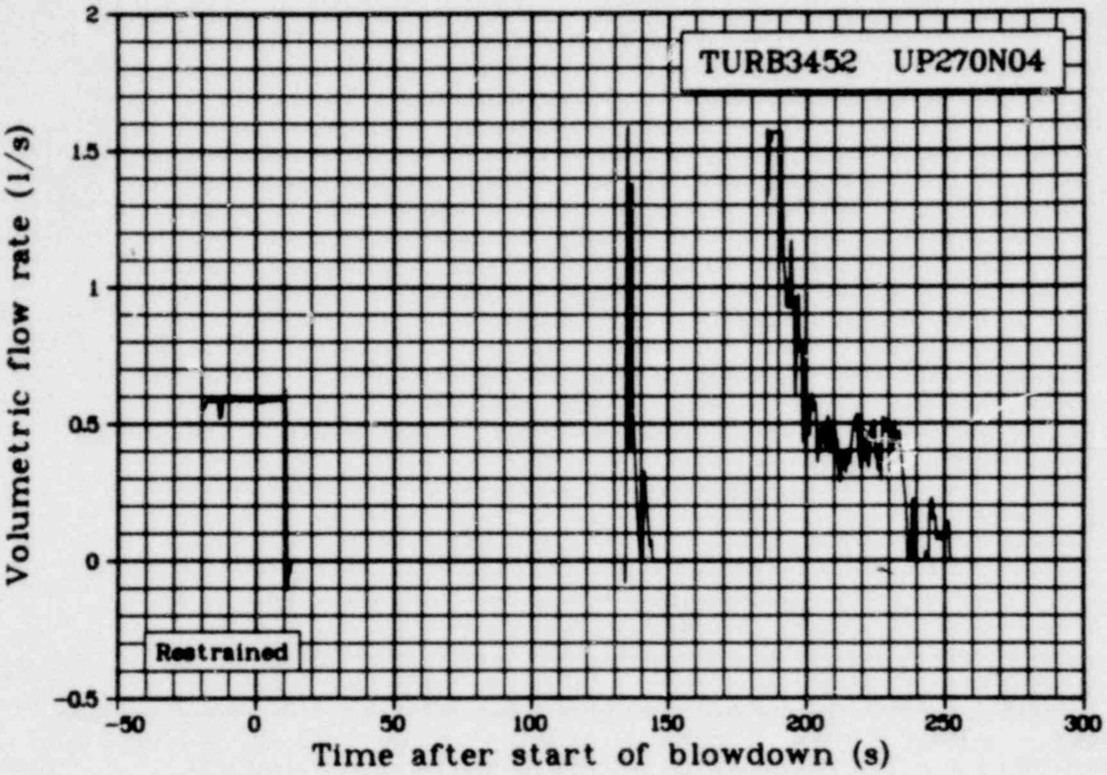

Fig. 319 Volumetric flow rate in Fuel Rod 345-2 upper shroud (TURB3452 UP270N04), from -50 to 300 s.

Y405 249

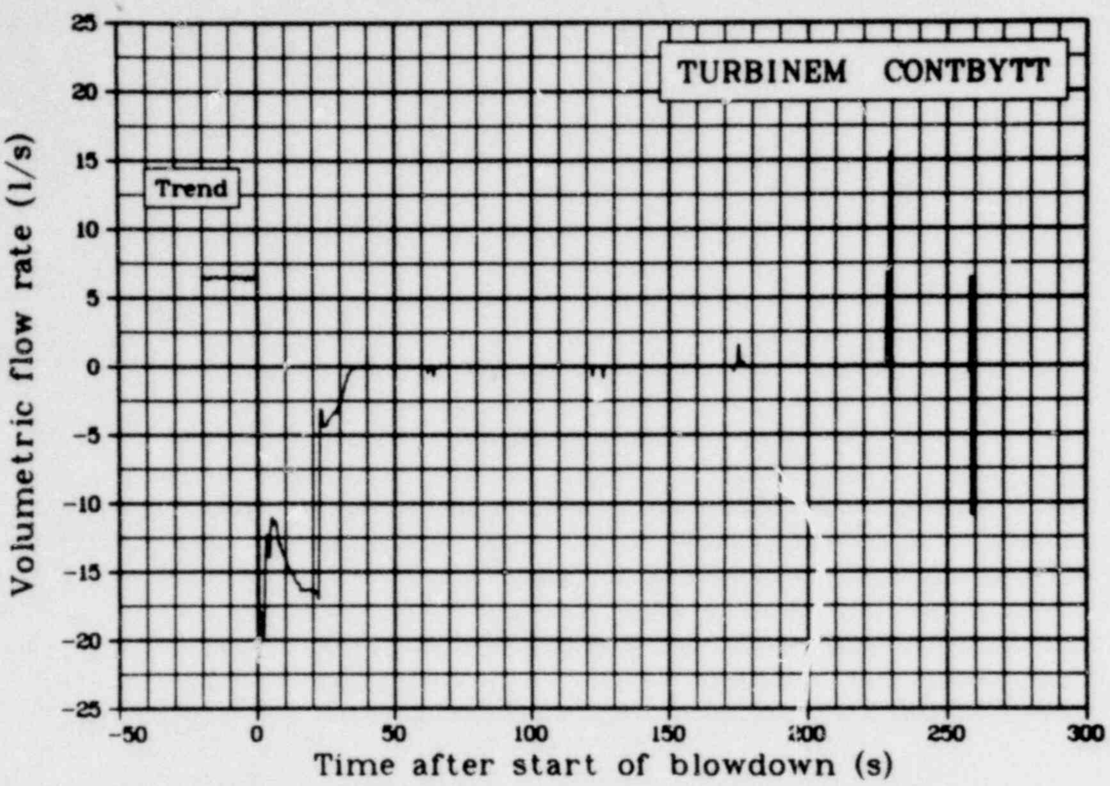

Fig. 320 Volumetric flow rate in test train controlled bypass (TURBINEM CONTBYTT), from -50 to 300 s.

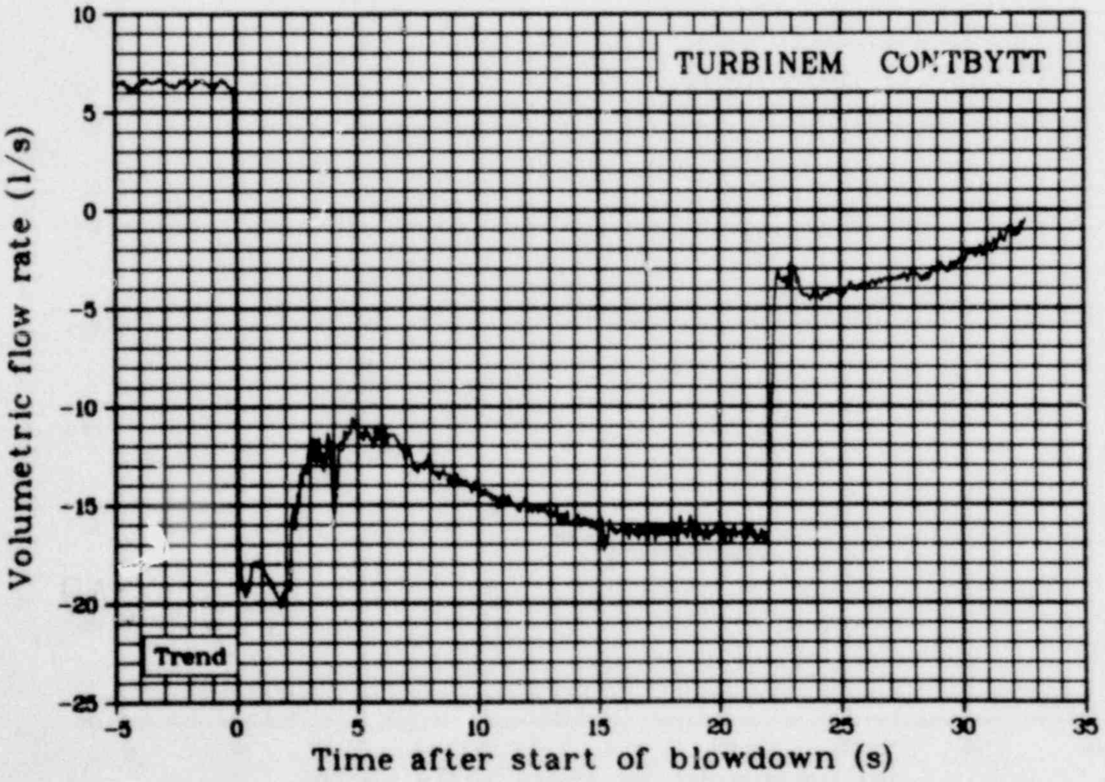

Fig. 321 Volumetric flow rate in test train controlled bypass (TURBINEM CONTBYTT), from -5 to 35 s.

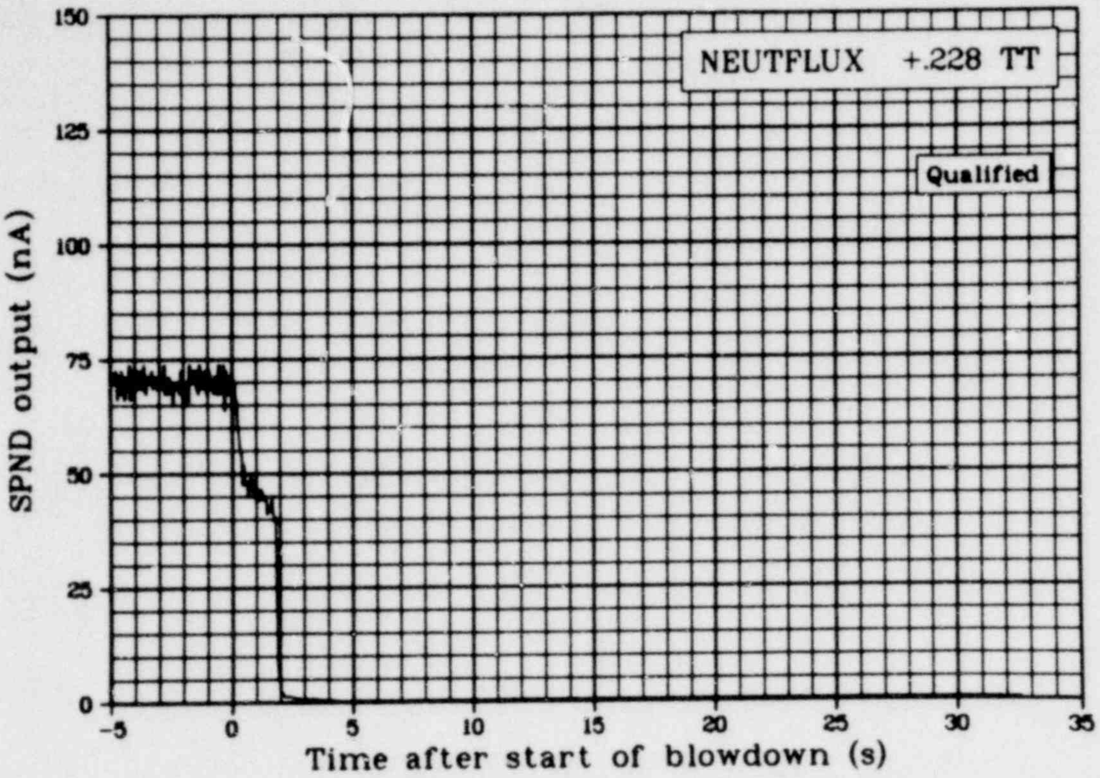

Fig. 322 Neutron flux 0.228 m above fuel stack midplane (NEUTFLUX +.228 TT), from -5 to 35 s.

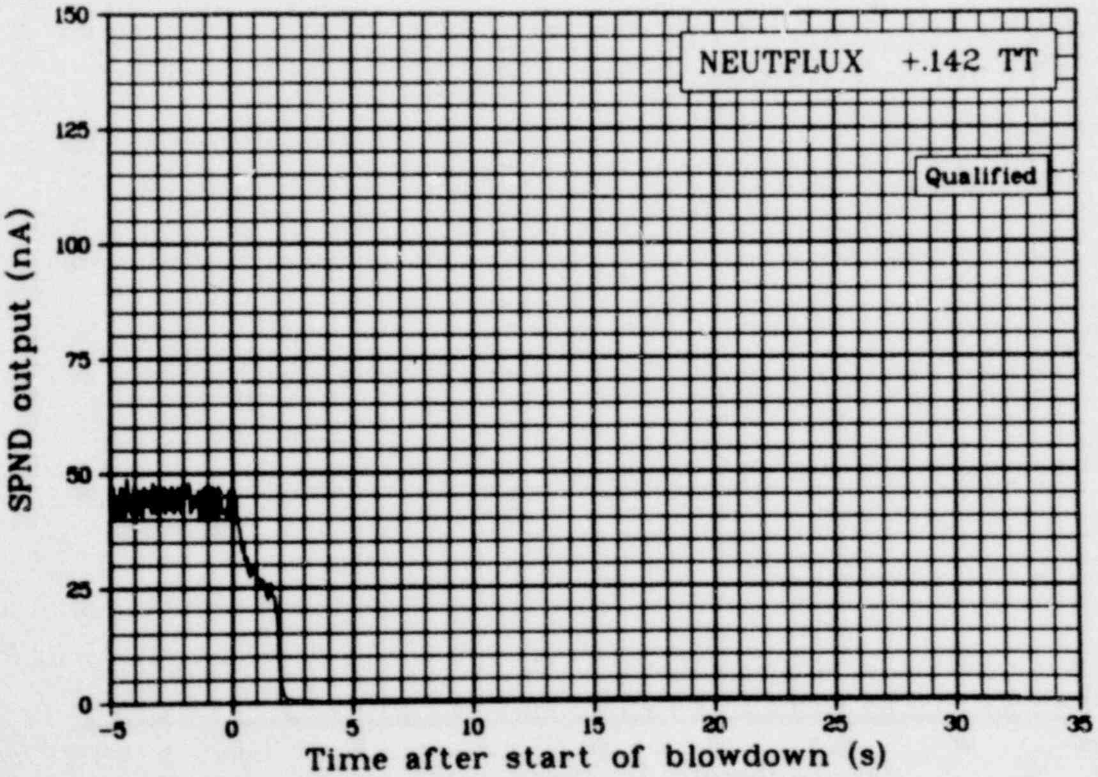

Fig. 323 Neutron flux 0.142 m above fuel stack midplane (NEUTFLUX +.142 TT), from -5 to 35 s.

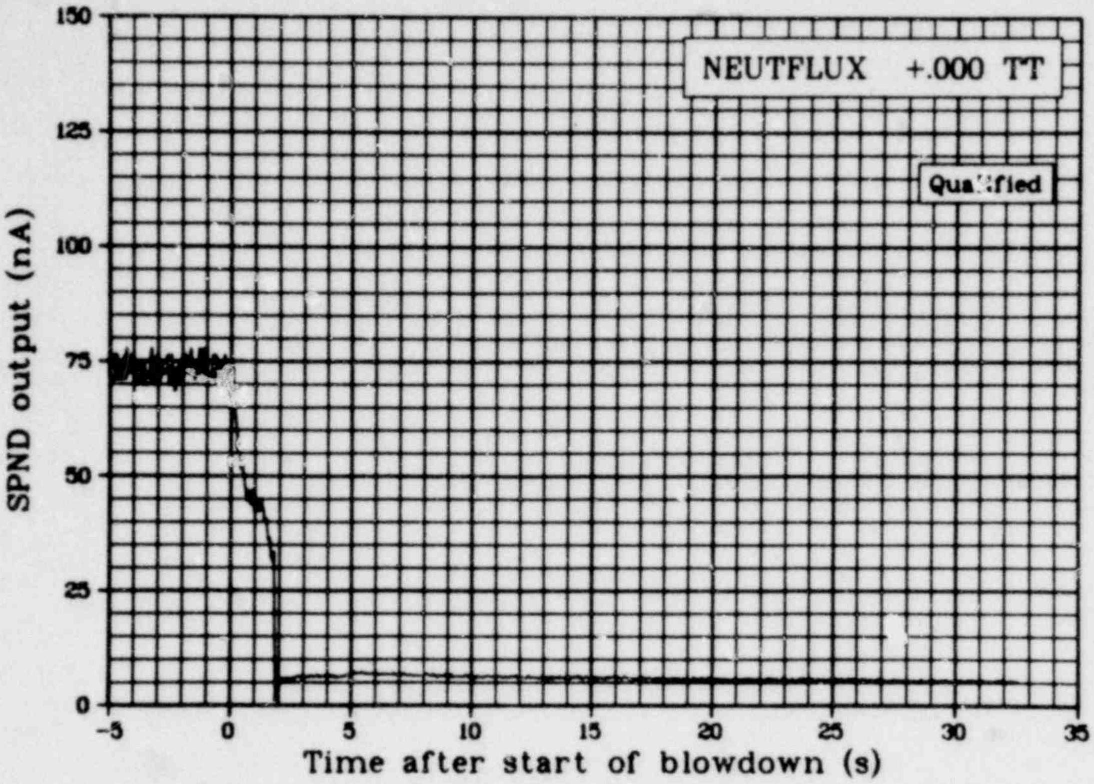

Fig. 324 Neutron flux at fuel stack midplane (NEUTFLUX +.000 TT), from -5 to 35 s.

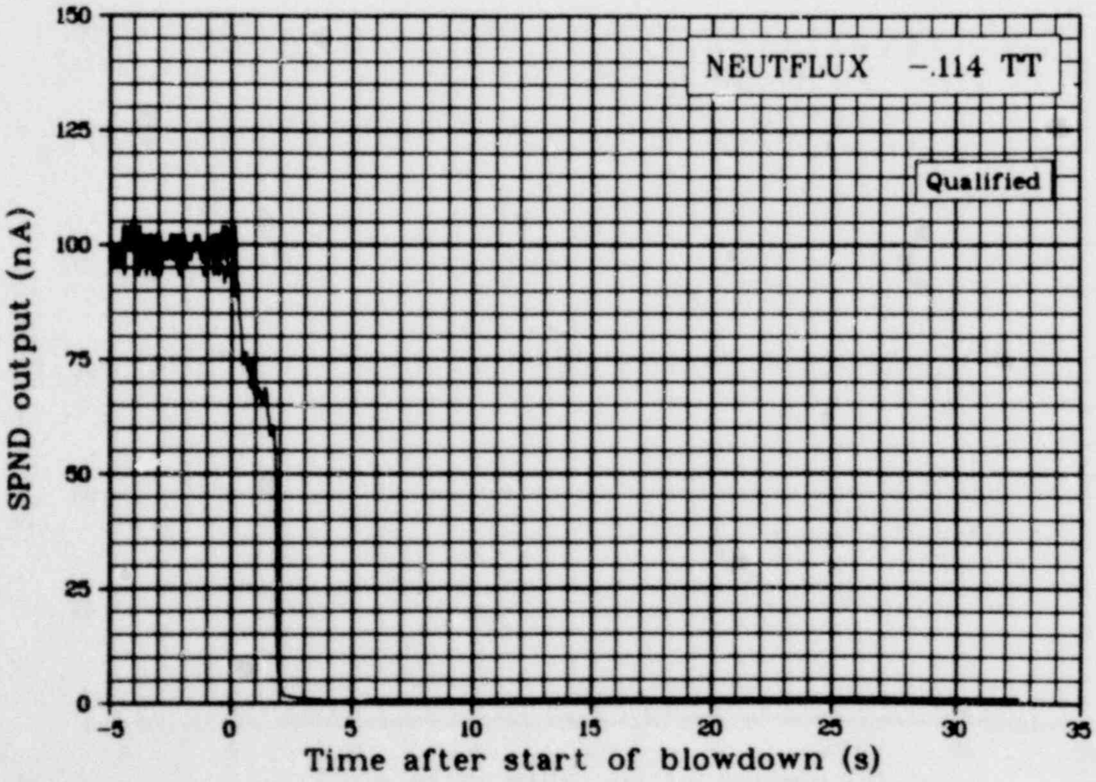

Fig. 325 Neutron flux 0.114 m below fuel stack midplane (NEUTFLUX -.114 TT), from -5 to 35 s.

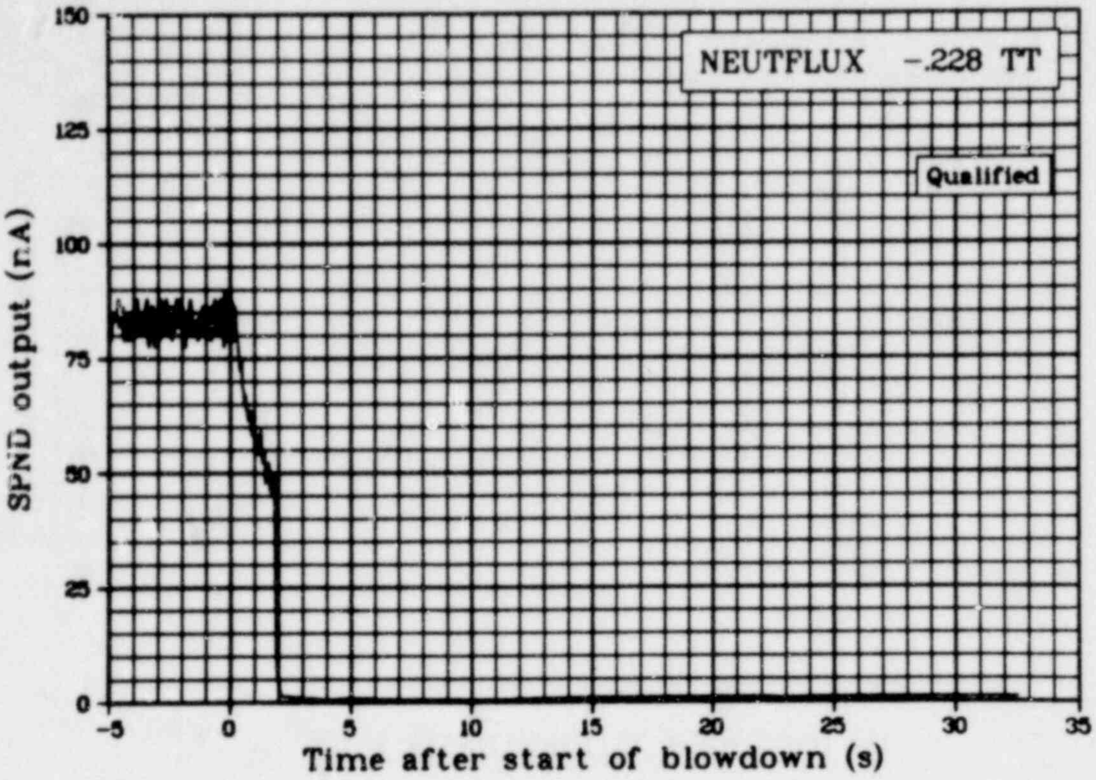

Fig. 326 Neutron flux 0.228 m below fuel stack midplane (NEUTFLUX -.228 TT), from -5 to 35 s.

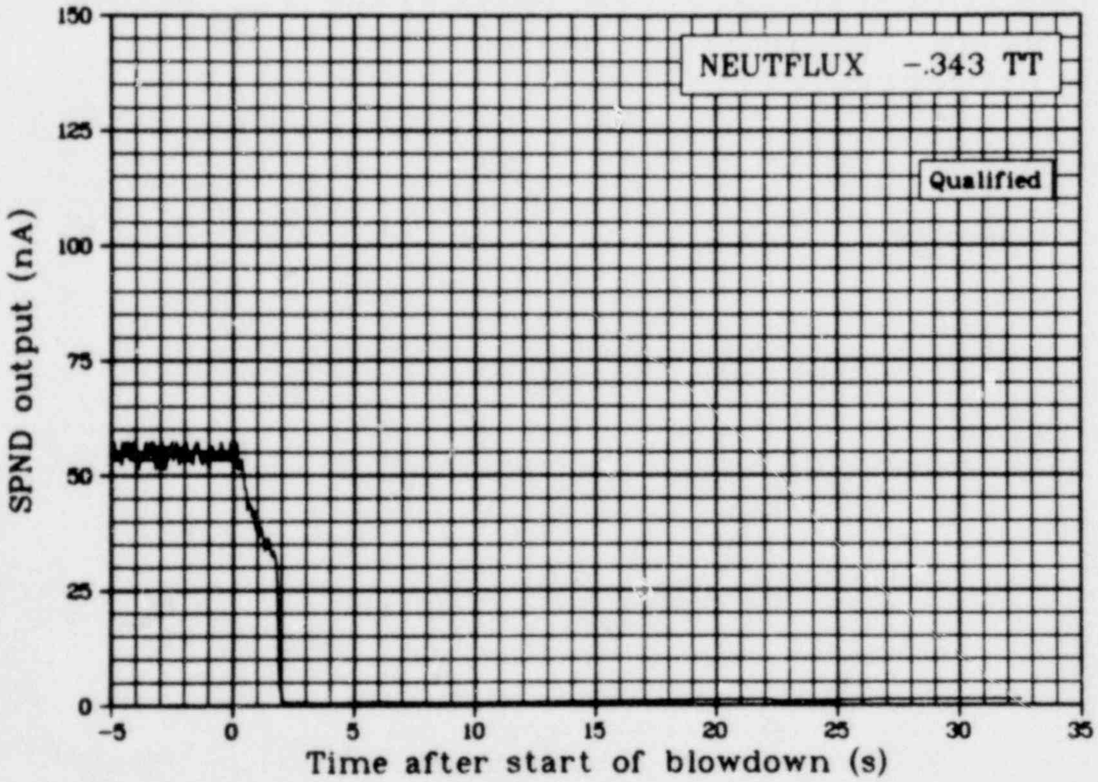

Fig. 327 Neutron flux 0.343 m below fuel stack midplane (NEUTFLUX -.343 TT), from -5 to 35 s.

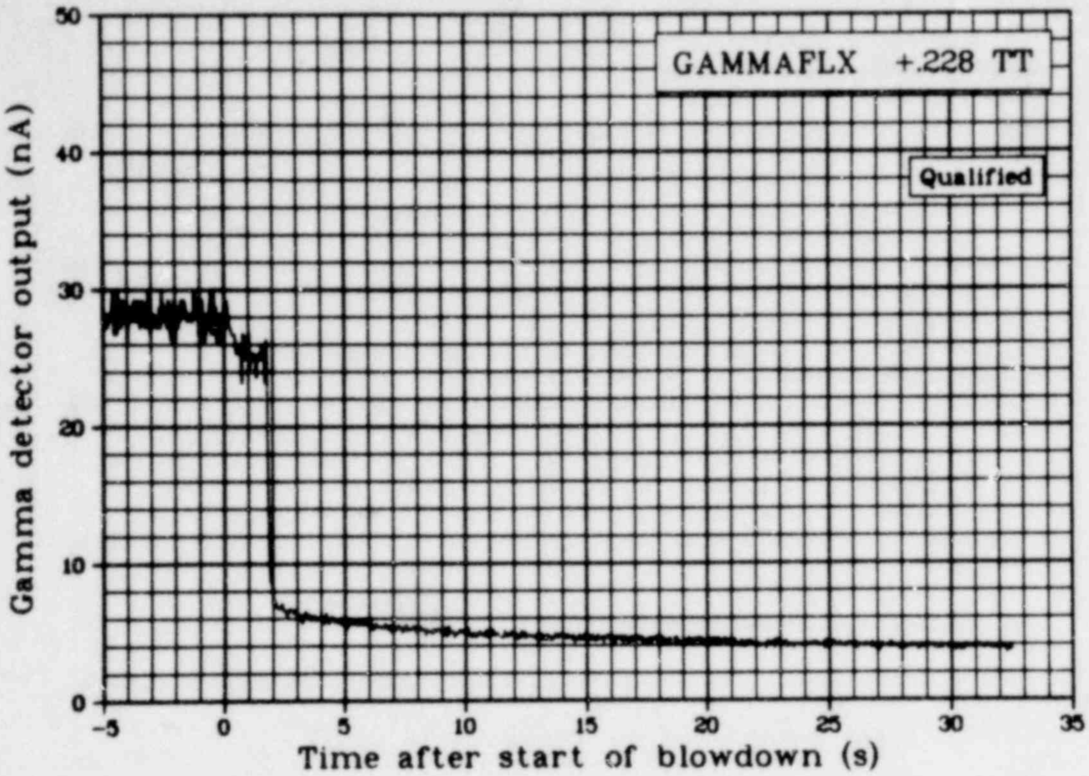

Fig. 328 Gamma flux 0.228 m above fuel stack midplane (GAMMAFLX +.228 TT), from -5 to 35 s.

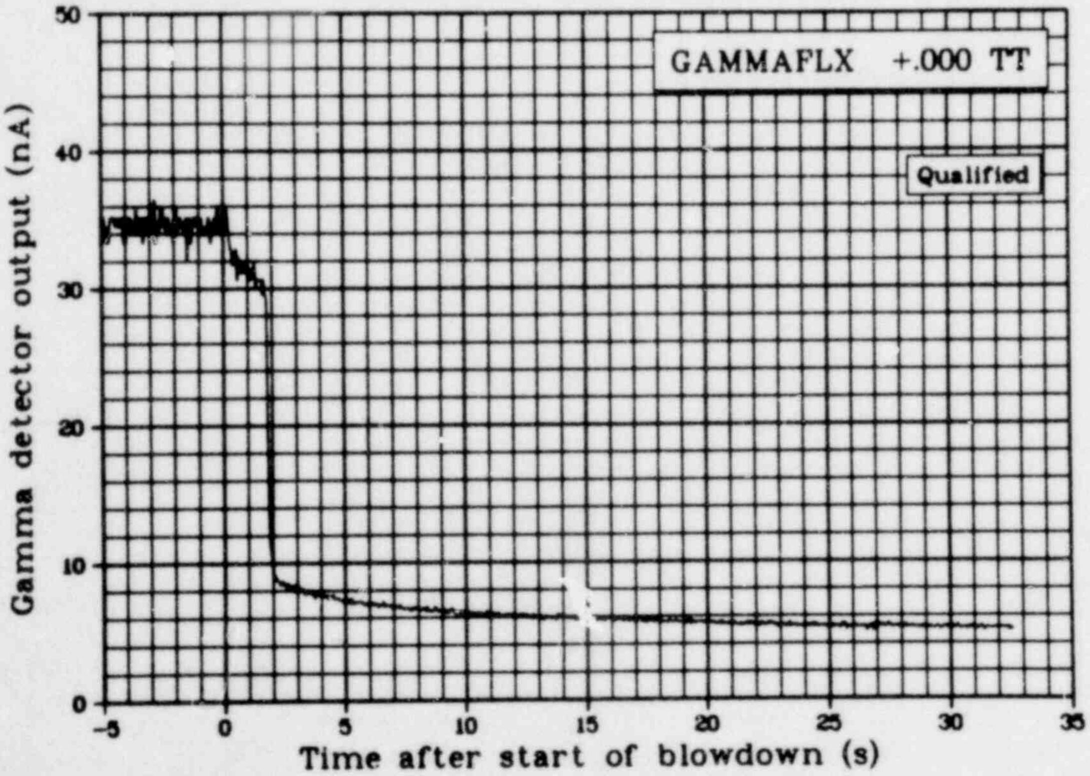

Fig. 329 Gamma flux at fuel stack midplane (GAMMAFLX +.000 TT), from -5 to 35 s.

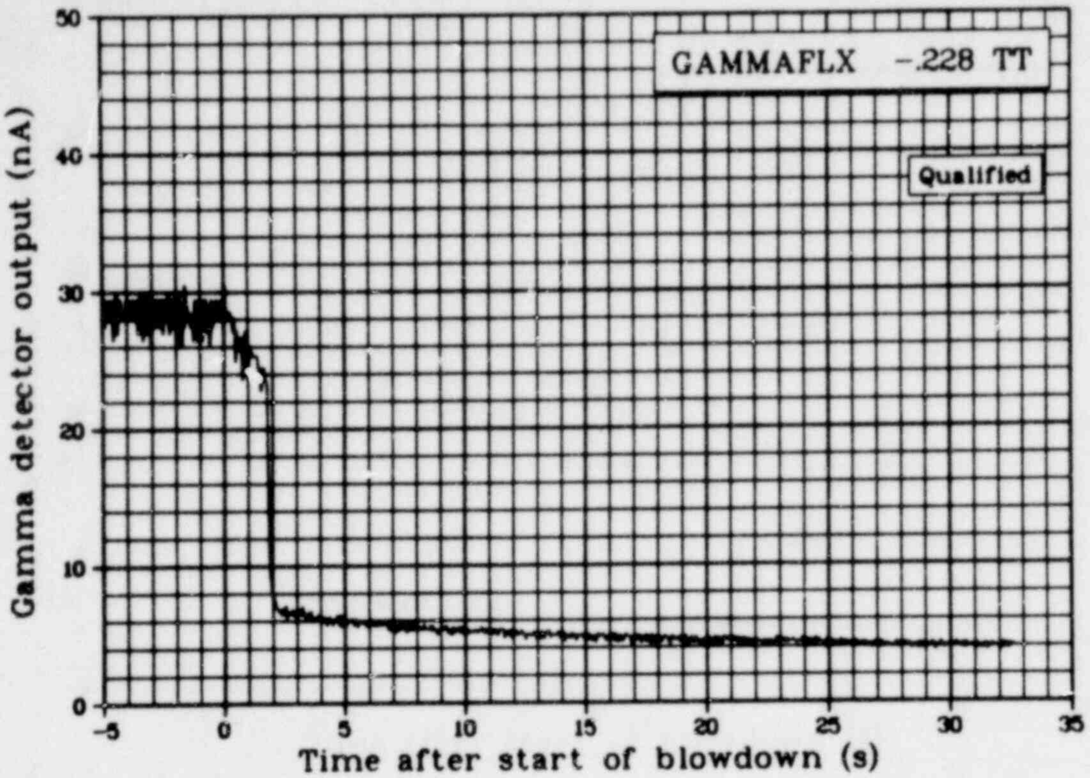

Fig. 330 Gamma flux 0.228 m below fuel stack midplane (GAMMAFLX -.228 TT), from -5 to 35 s.

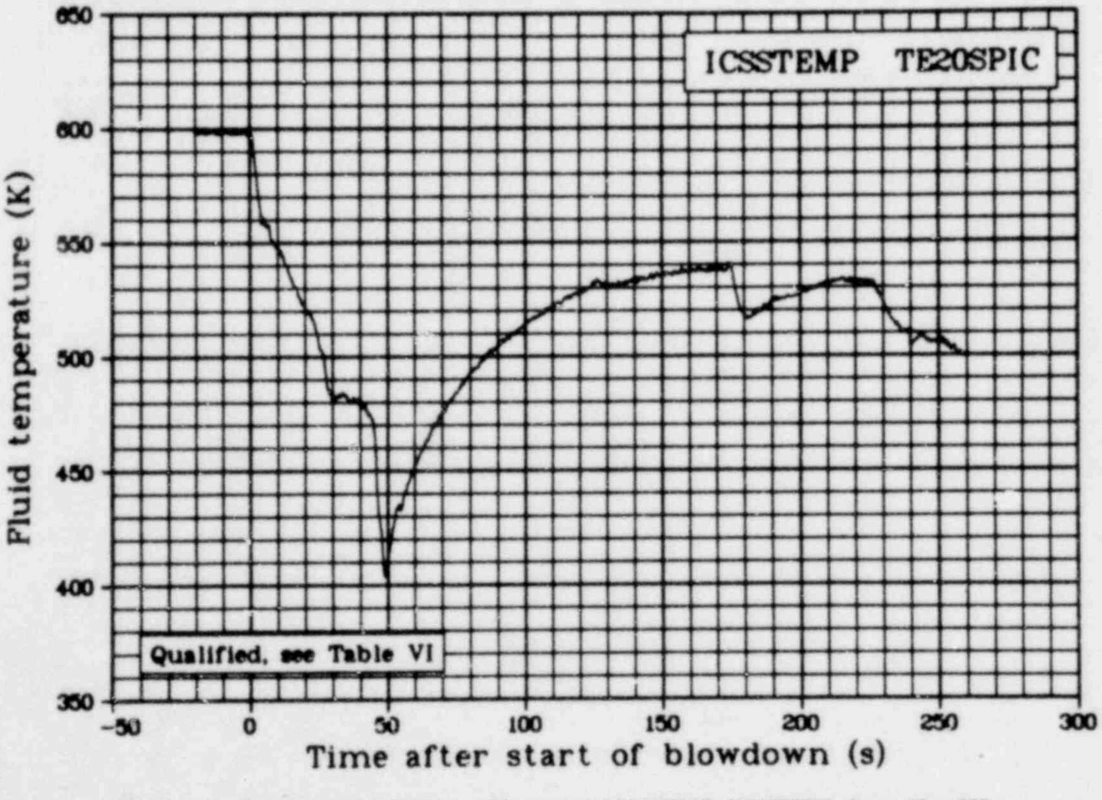

Fig. 331 Fluid temperature in initial condition spool (ICSSTEMP TE20SPIC), from -50 to 300 s.

1405 255

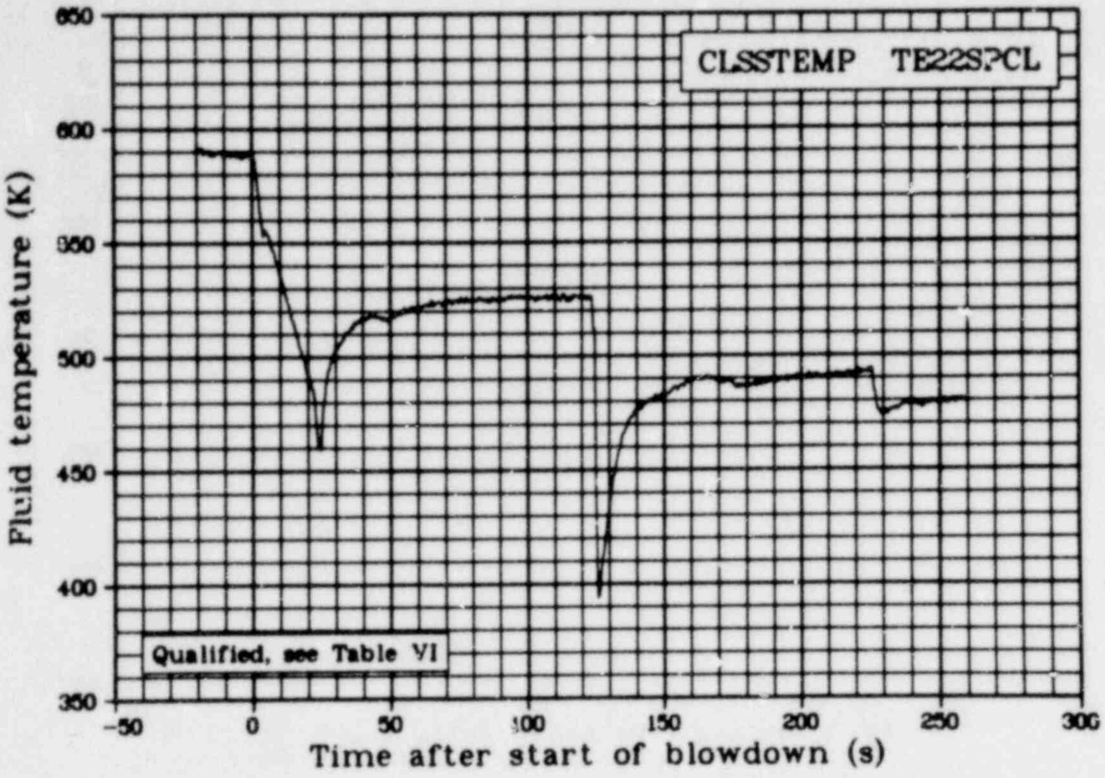

Fig. 332 Fluid temperature in cold leg blowdown spool (CLSSTEMP TE22SPCL), from -50 to 300 s.

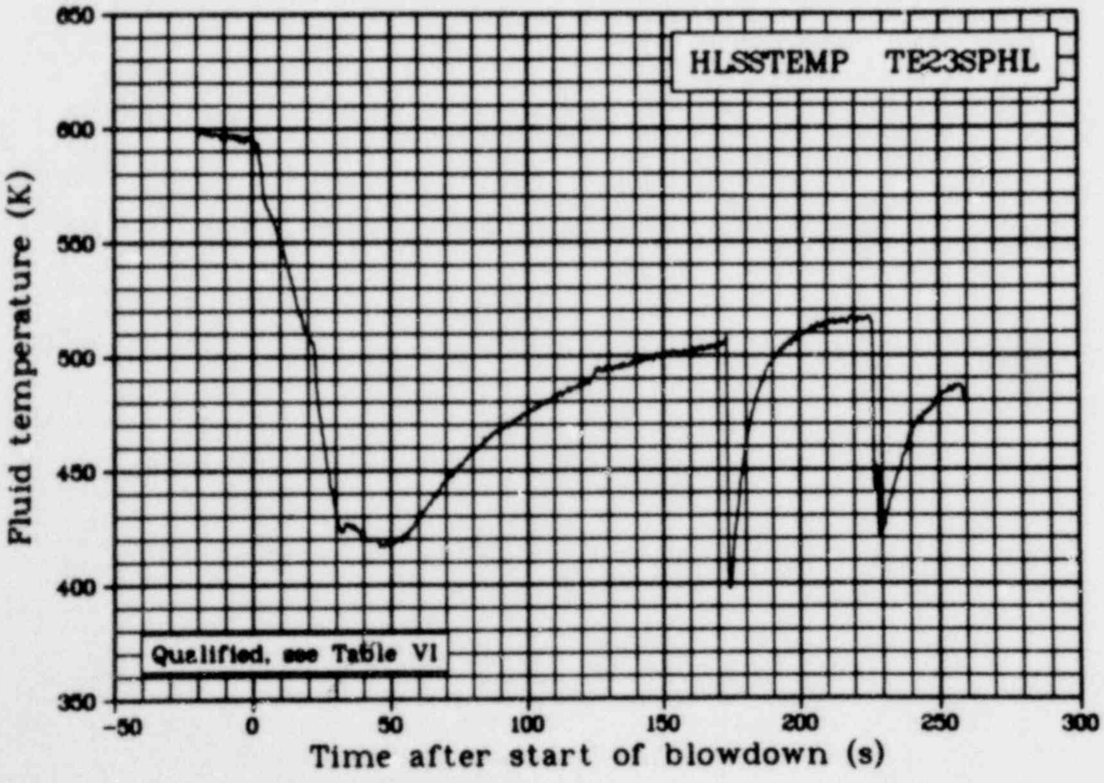

Fig. 333 Fluid temperature in hot leg blowdown spool (HLSSTEMP TE23SPHL), from -50 to 300 s.

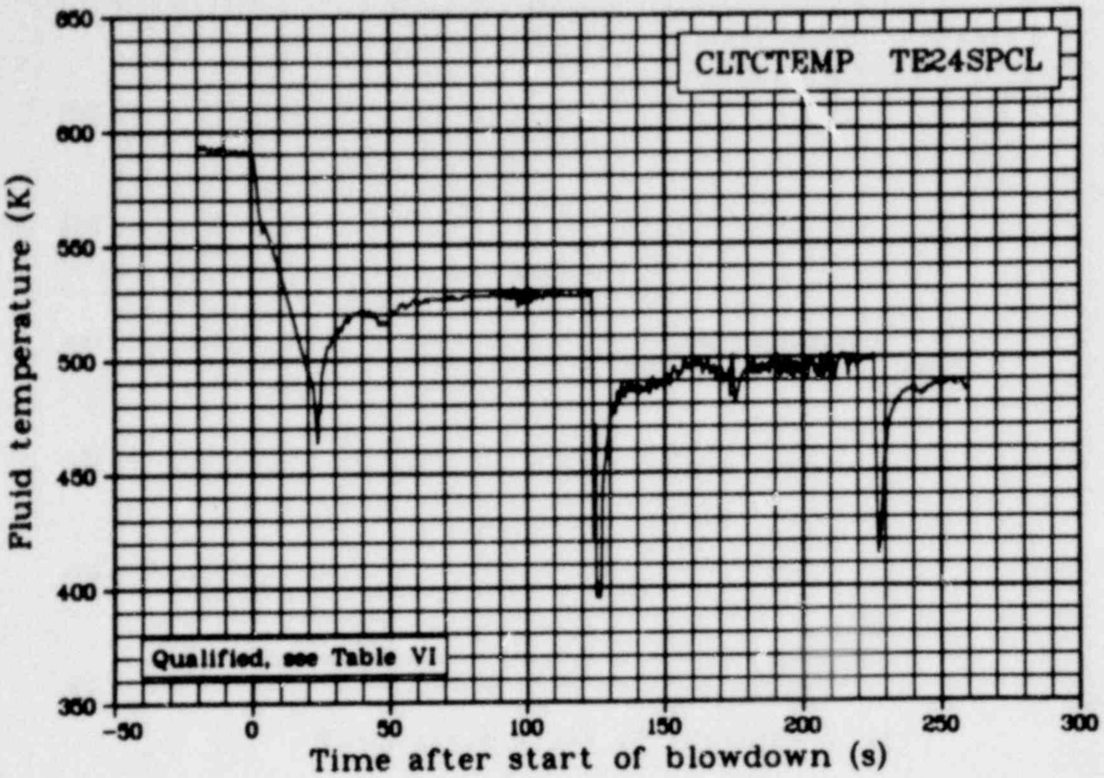

Fig. 334 Fluid temperature in cold leg blowdown spool (CLTCTEMP TE24SPCL), from -50 to 300 s.

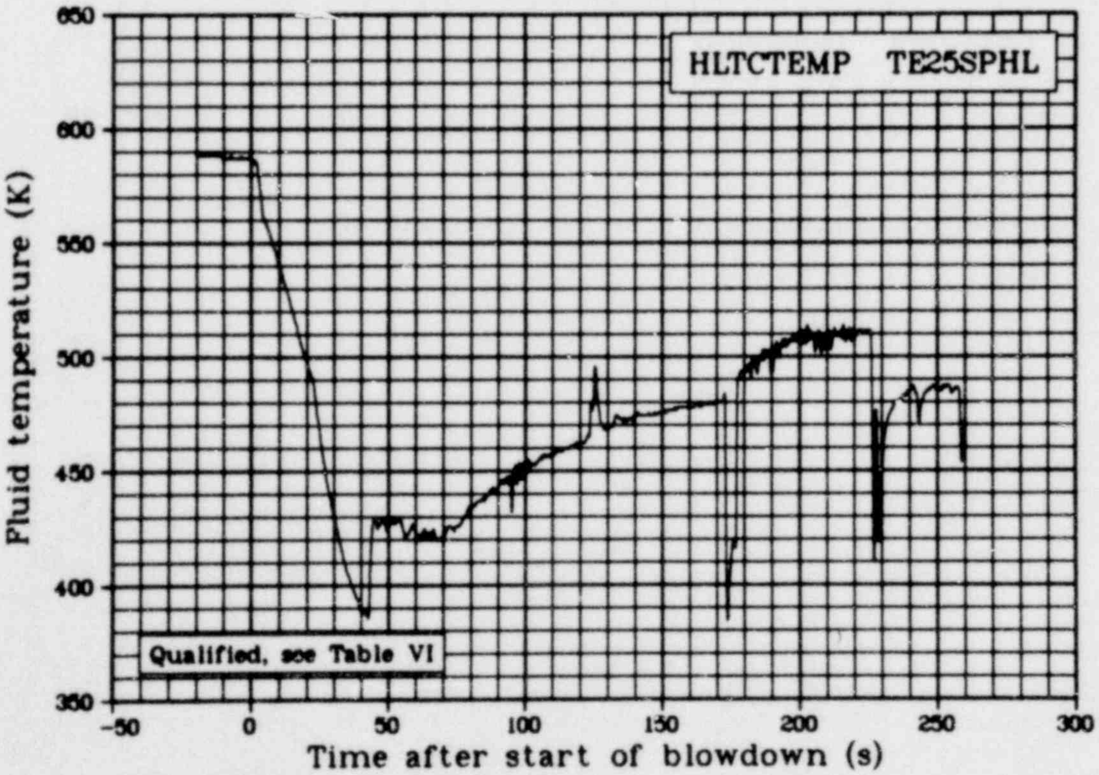

Fig. 335 Fluid temperature in hot leg blowdown spool (HLTCTEMP TE25SPHL), from -50 to 300 s.

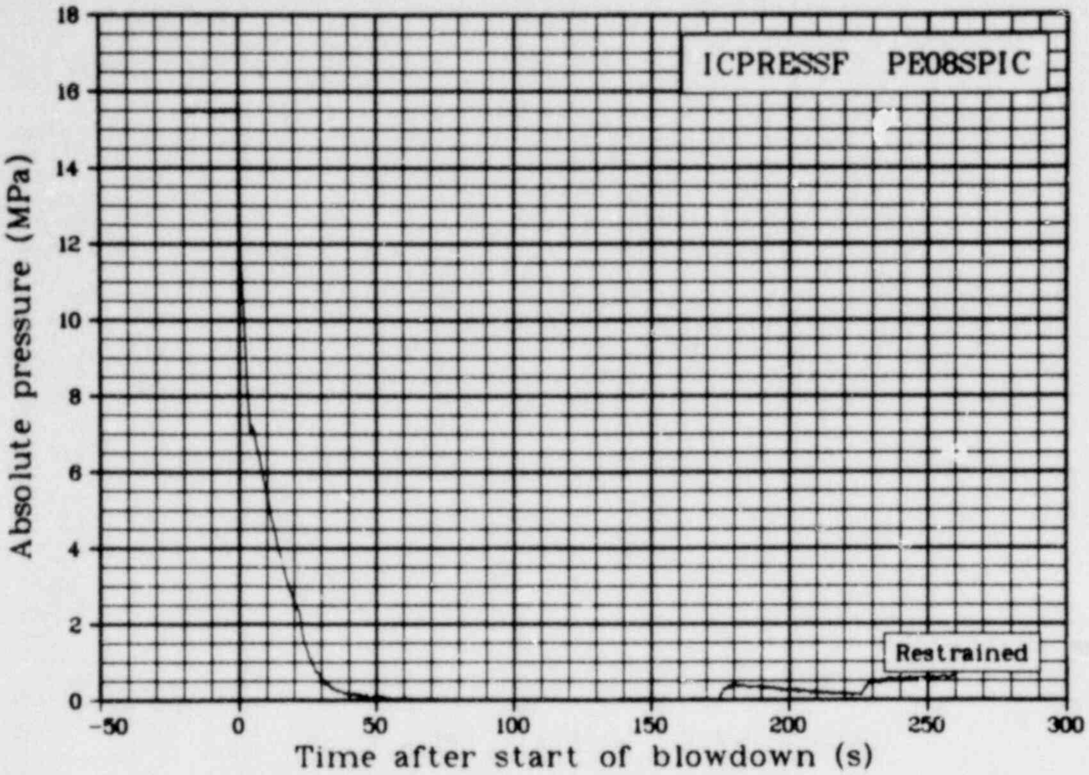

Fig. 336 Absolute pressure in initial condition spool (ICPRESSF PE08SPIC), from -50 to 300 s.

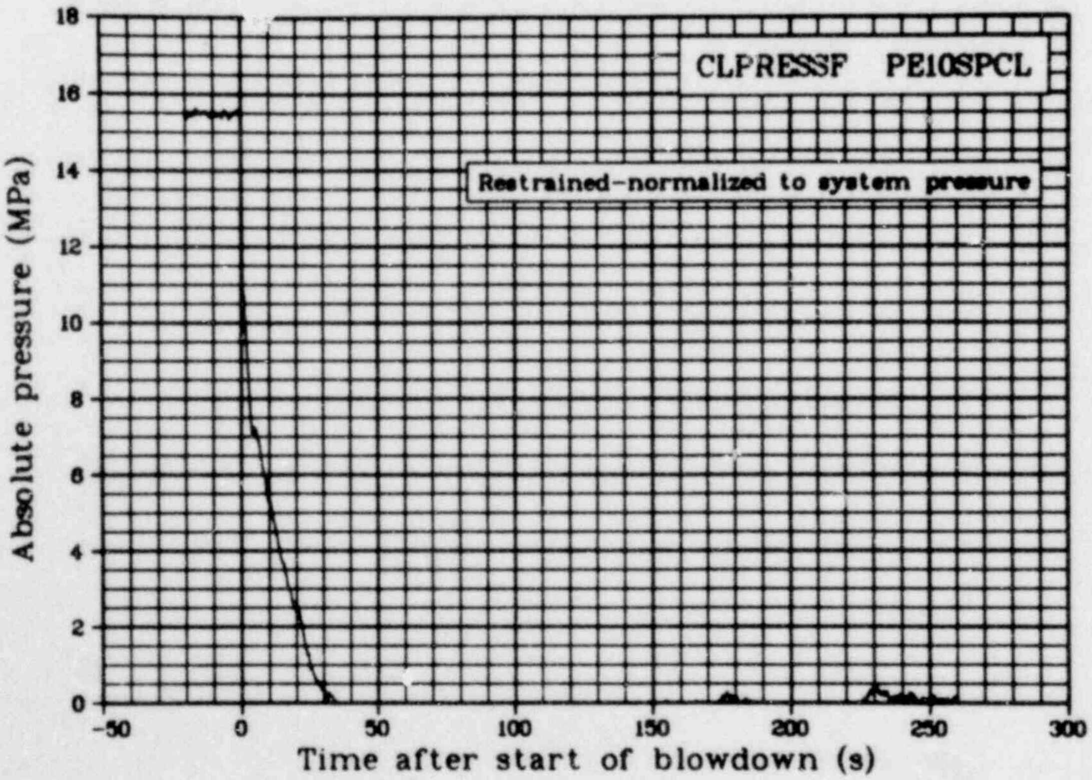

Fig. 337 Absolute pressure in cold leg blowdown spool (CLPRESSF PE10SPCL), from -50 to 300 s.

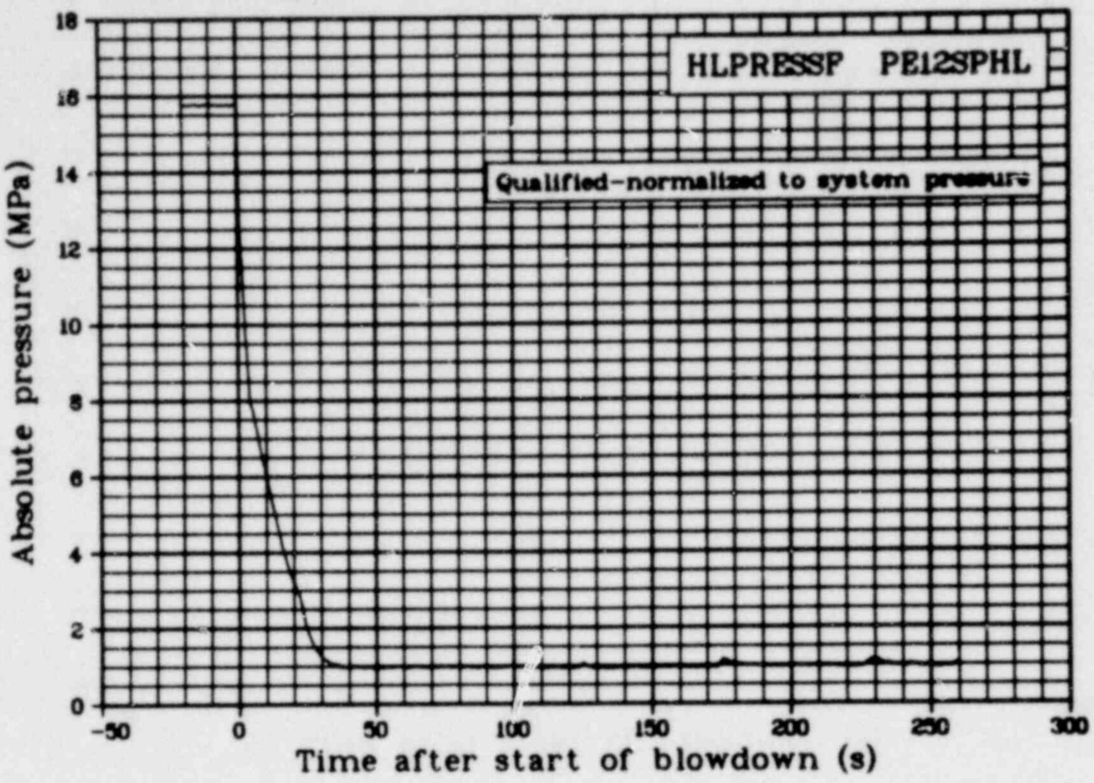

Fig. 338 Absolute pressure in hot leg blowdown spool (HLPRESSF PE12SPHL), from -50 to 300 s.

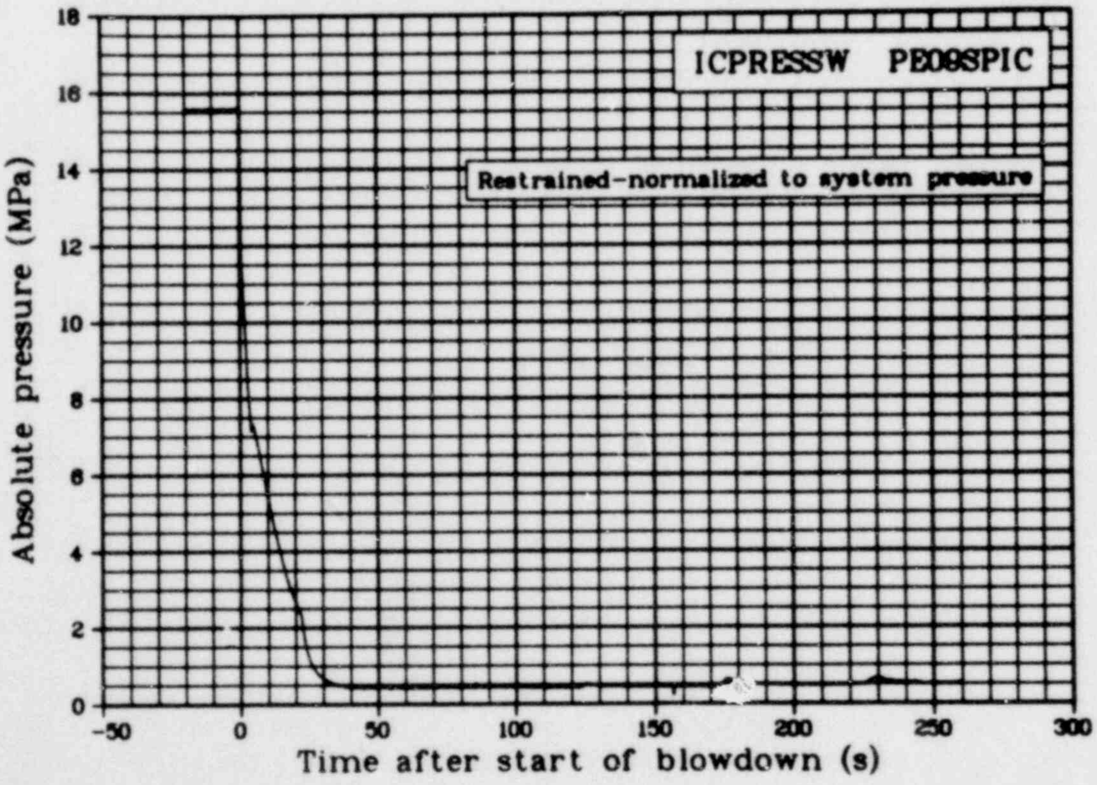

Fig. 339 Absolute pressure in initial condition spool (ICPRESSW PE09SPIC), from -50 to 300 s.

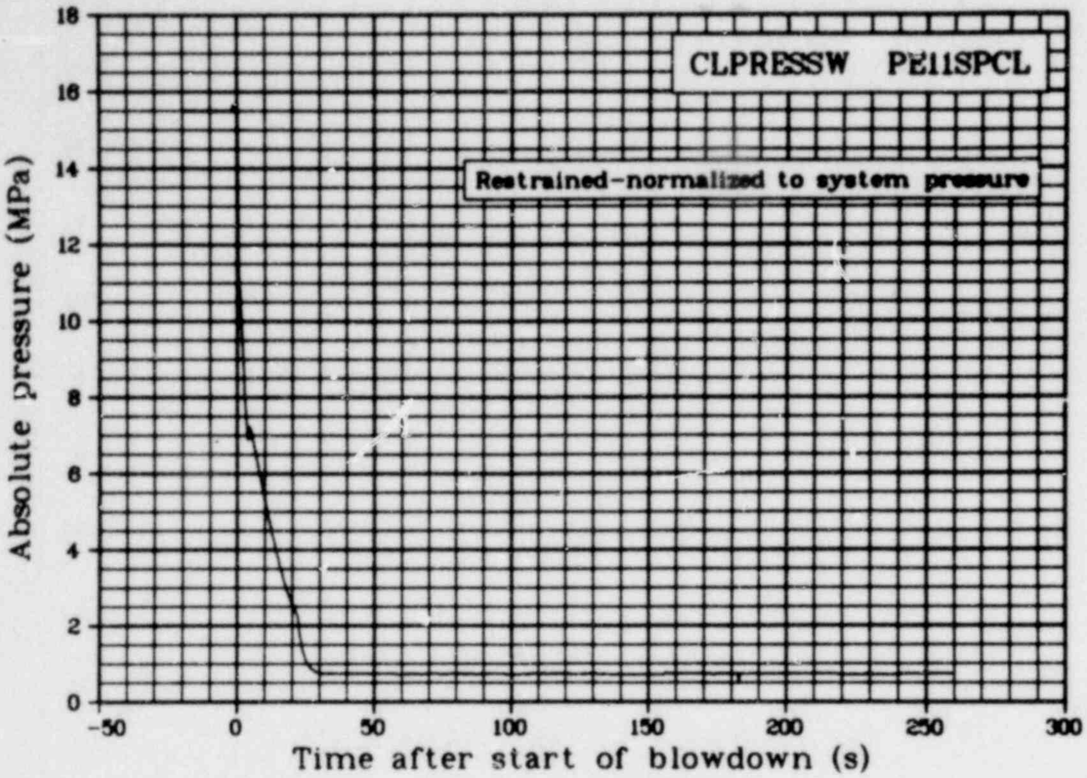

Fig. 340 Absolute pressure in cold leg blowdown spool (CLPRESSW PE11SPCL), from -50 to 300 s.

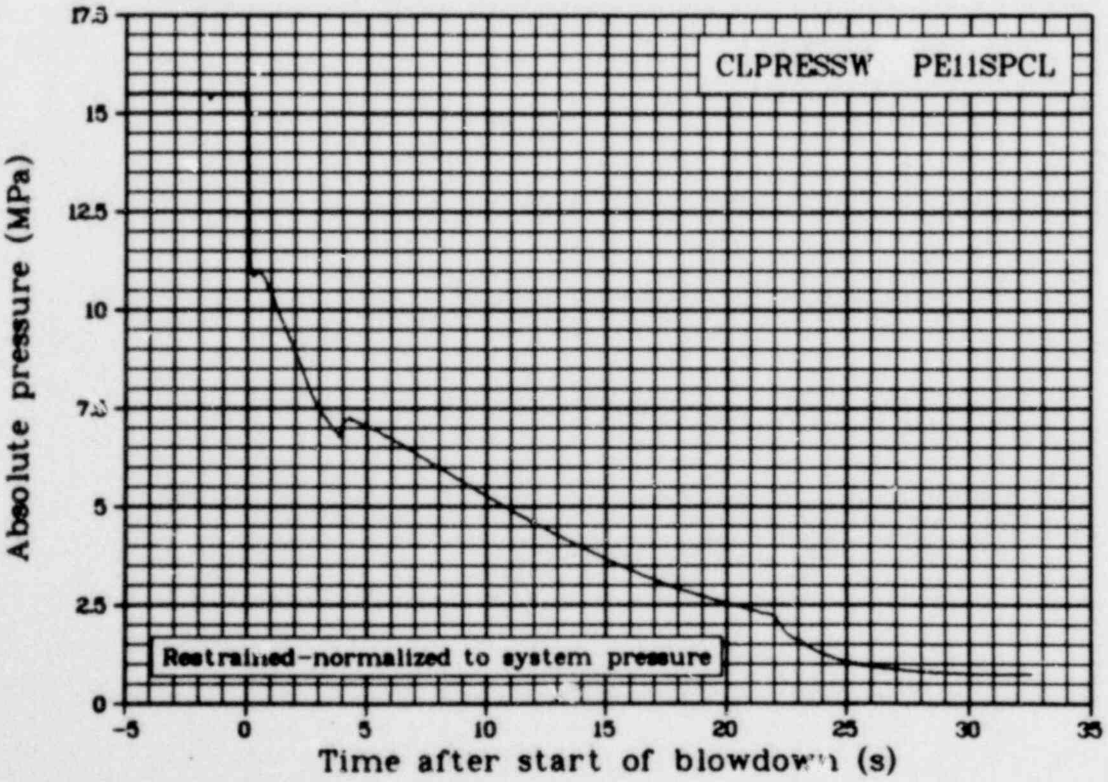

Fig. 341 Absolute pressure in cold leg blowdown spool (CLPRESSW PE11SPCL), from -5 to 35 s.

1405 260

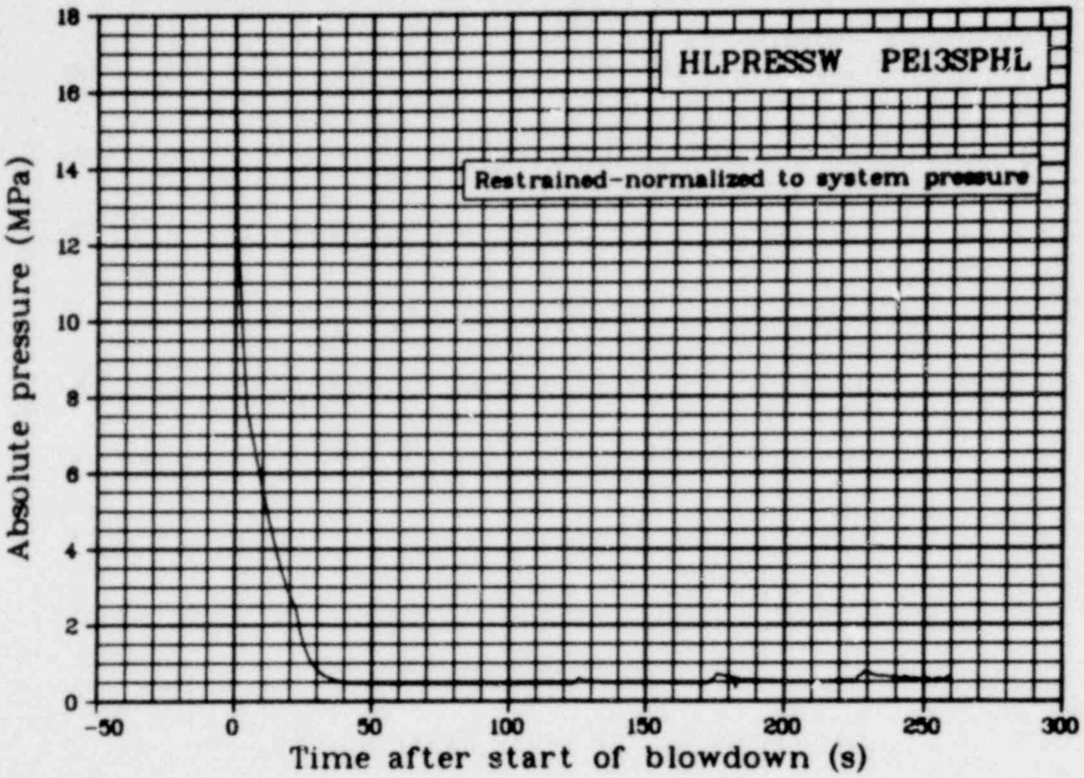

Fig. 342 Absolute pressure in hot leg blowdown spool (HLPRESSW PE13SPHL), from -50 to 300 s.

1405 261

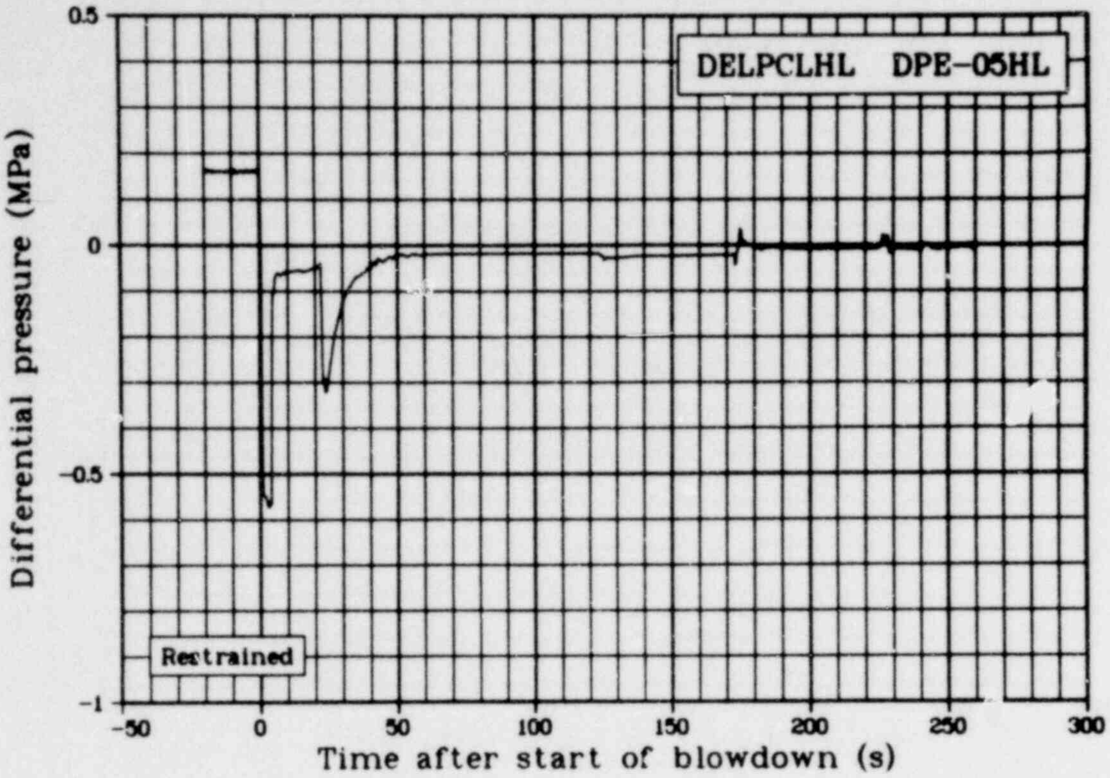

Fig. 343 Differential pressure between blowdown spools (DELPCLHL DPE-05HL), from -50 to 300 s.

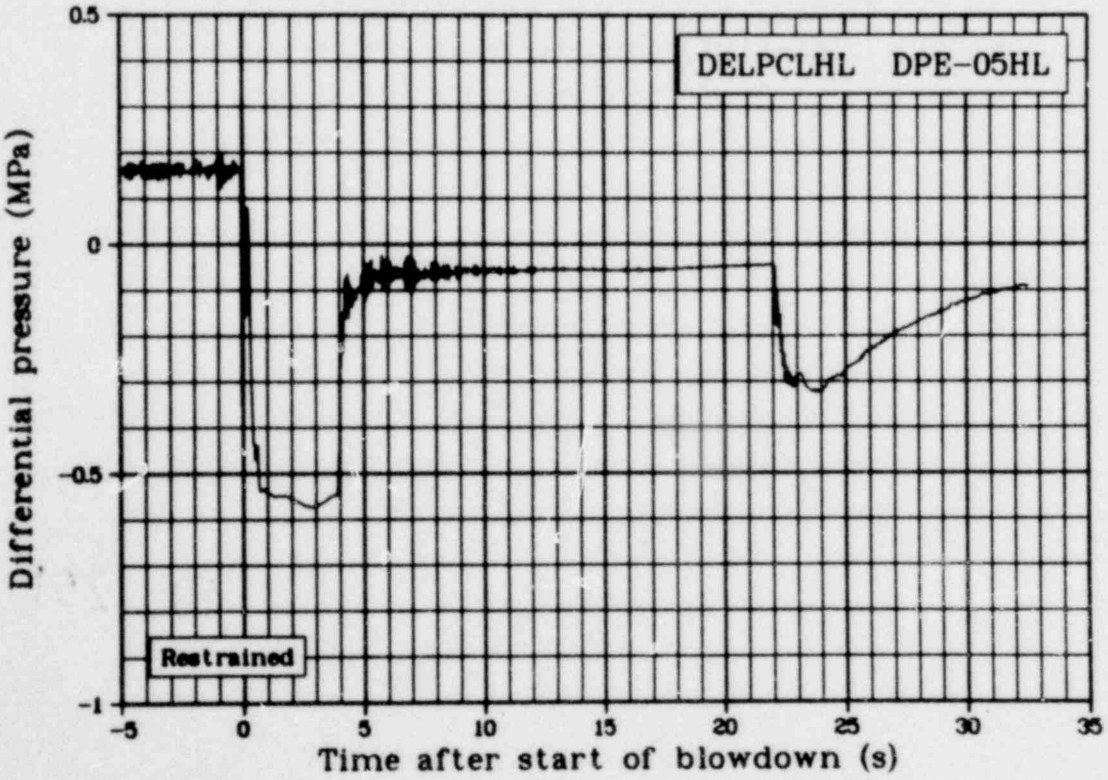

Fig. 344 Differential pressure between blowdown spools (DELPCLHL DPE-05HL), from -5 to 35 s.

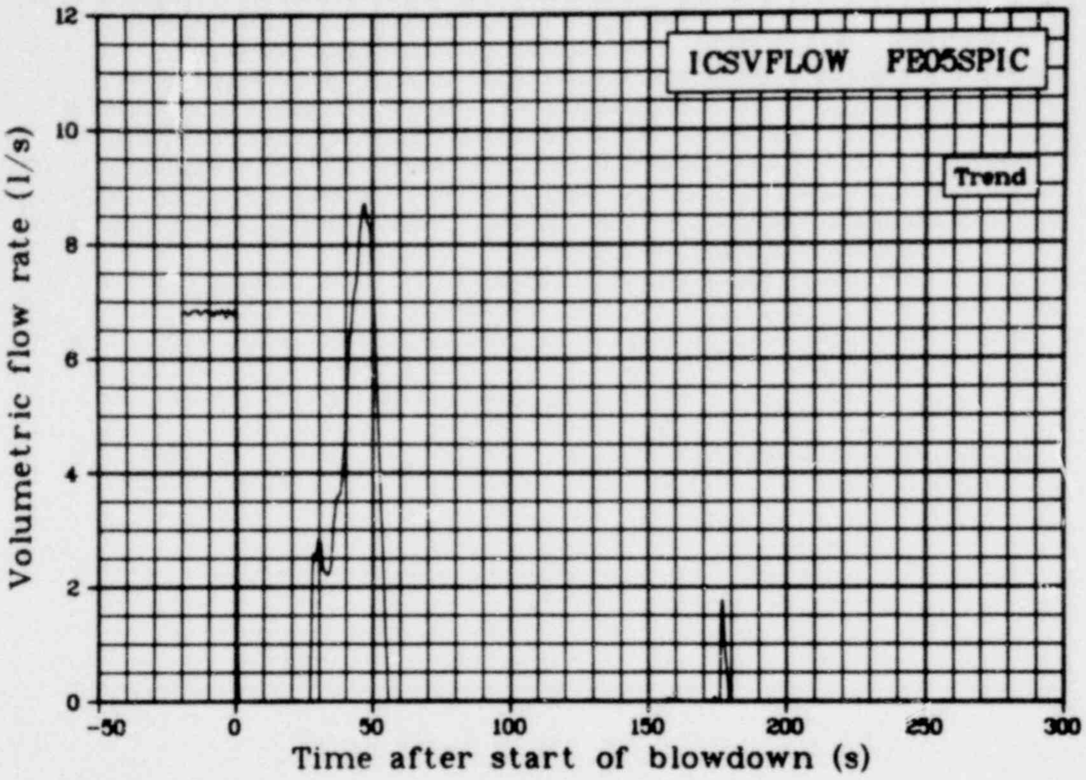

Fig. 345 Volumetric flow rate in initial condition spool (ICSVFLOW FE05SPIC), from -50 to 300 s.

1405 263

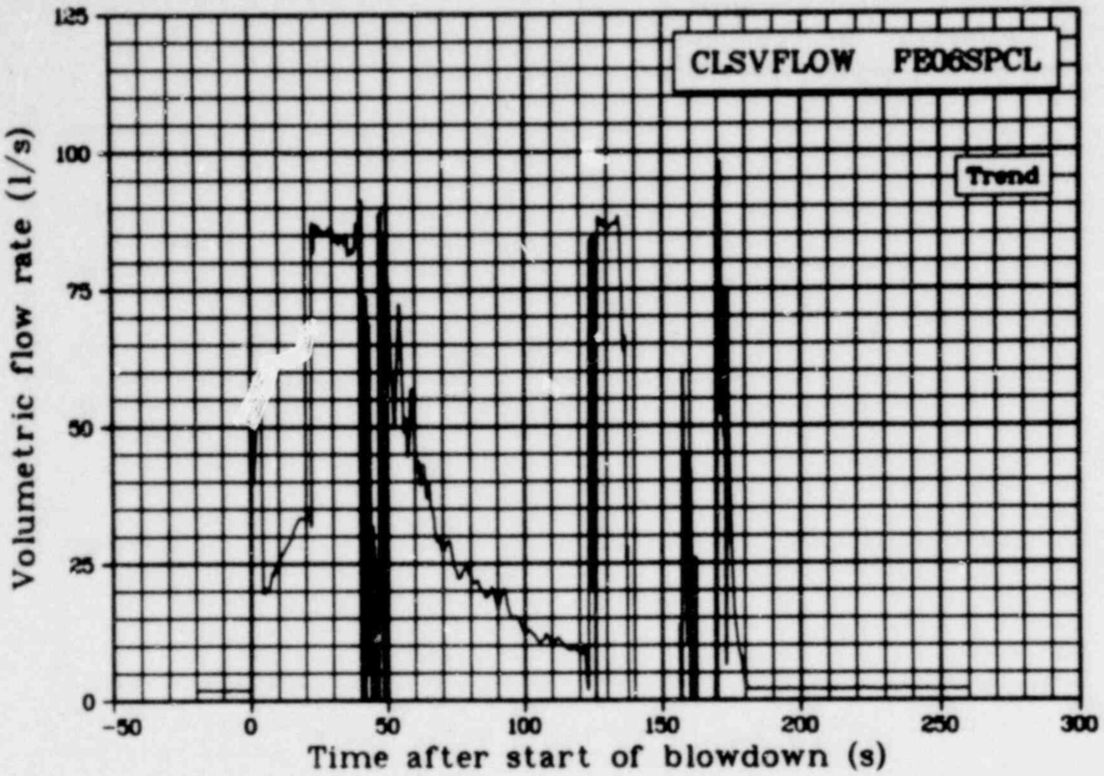

Fig. 346 Volumetric flow rate in cold leg blowdown spool (CLSVFLOW FE06SPCL), from -50 to 300 s.

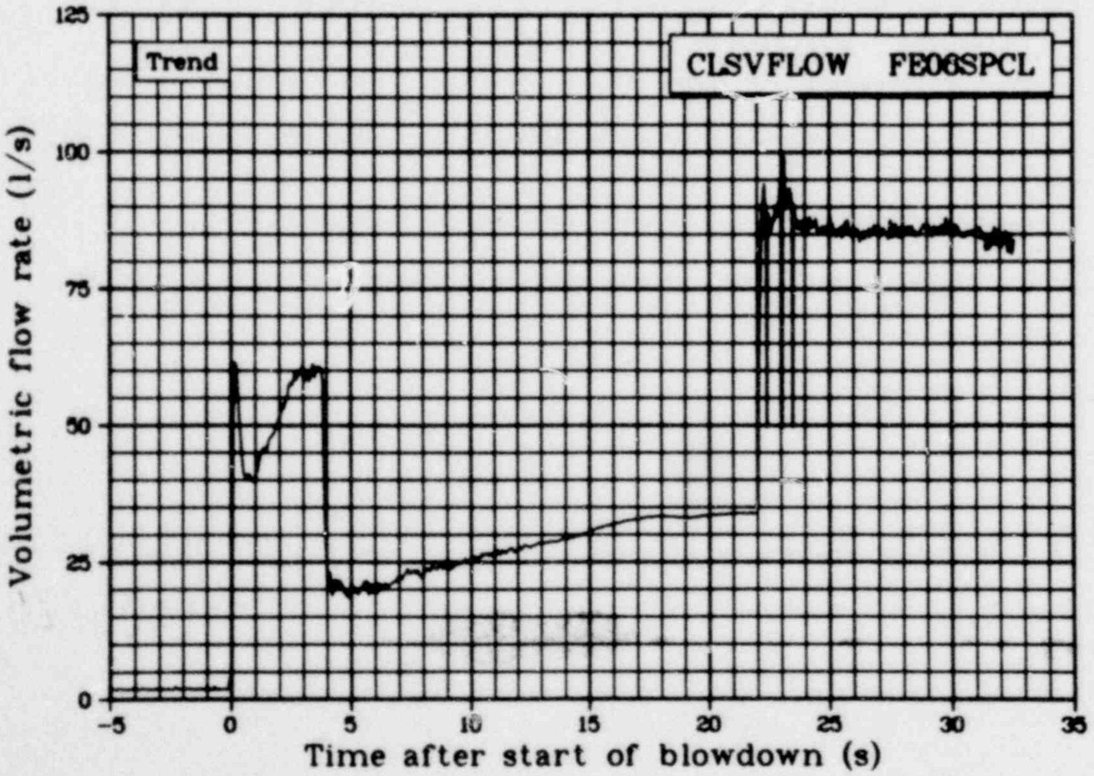

Fig. 347 Volumetric flow rate in cold leg blowdown spool (CLSVFLOW FE06SPCL), from -5 to 35 s.

1405 264

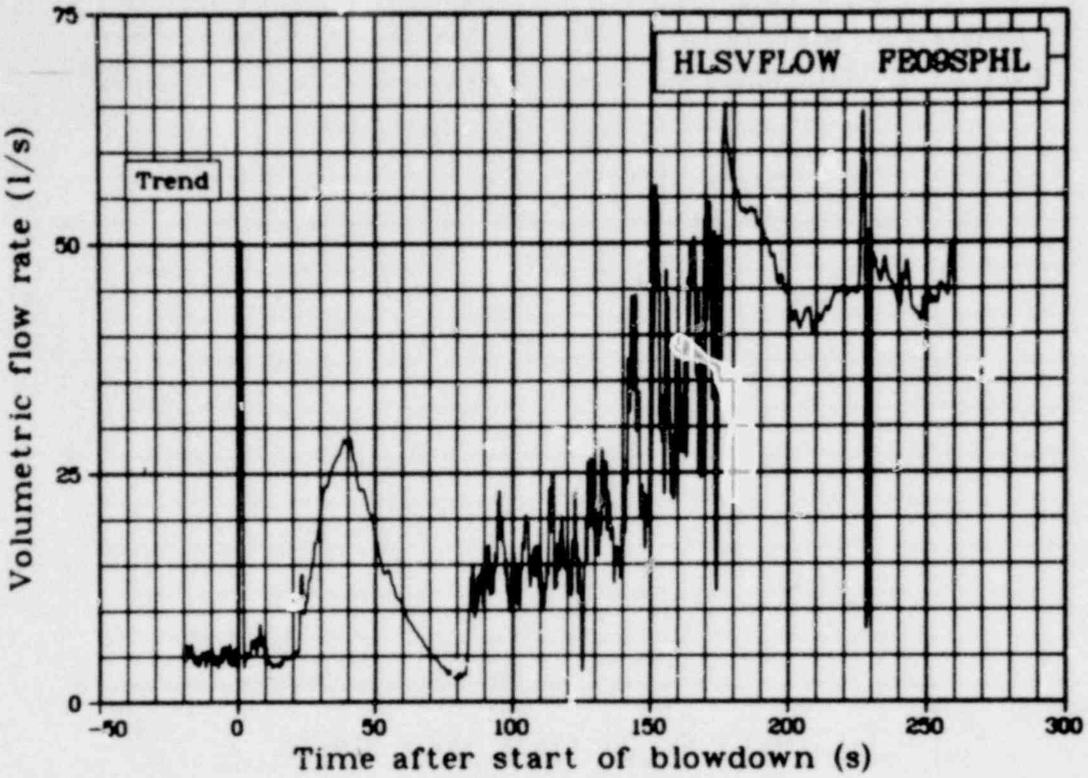

Fig. 348 Volumetric flcw rate in hot leg blowdown spool (HLSVFLOW FE09SPHL), from -50 to 300 s.

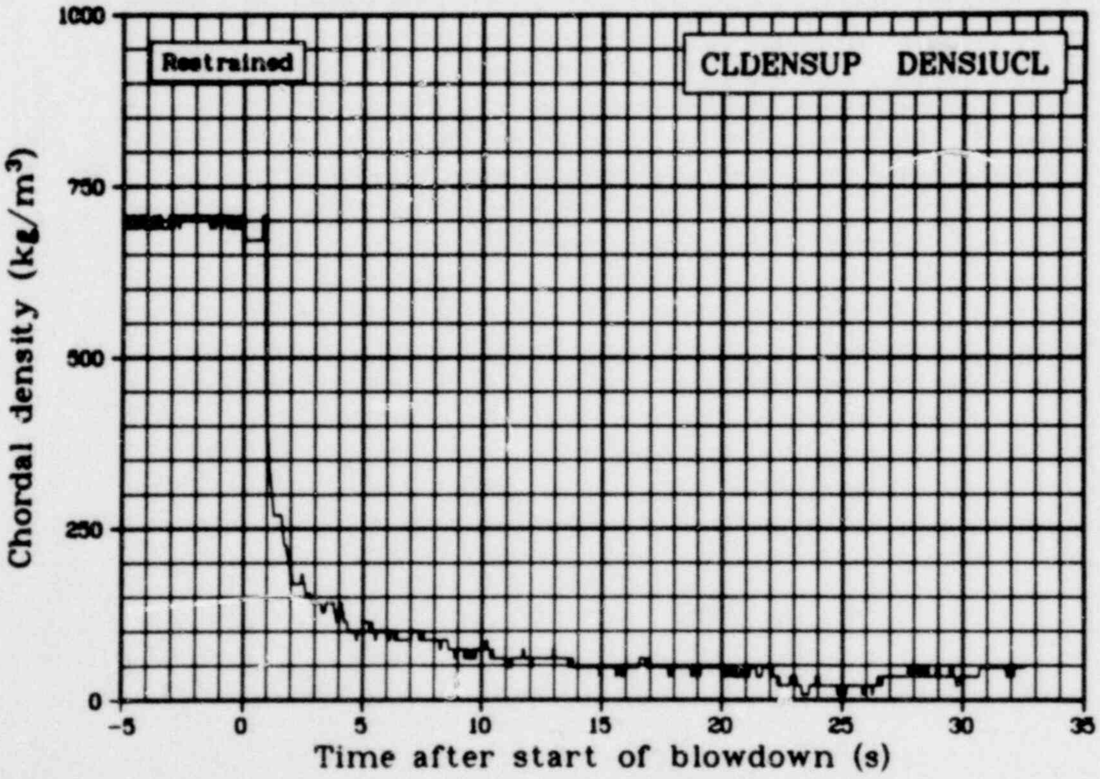

Fig. 349 Chordal density of upper beam in cold leg blowdown spool (CLDENSUP DENS1UCL), from -5 to 35 s.

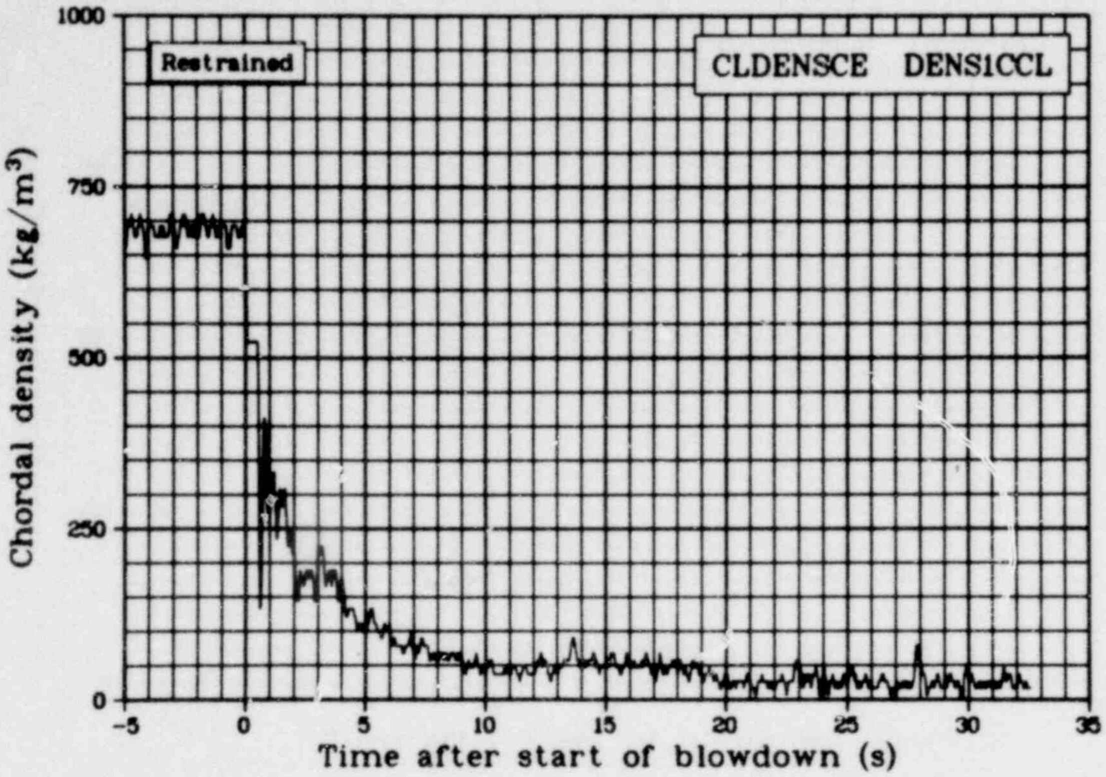

Fig. 350 Chordal density of center beam in cold leg blowdown spool (CLDENSCE DENS1CCL), from -5 to 35 s.

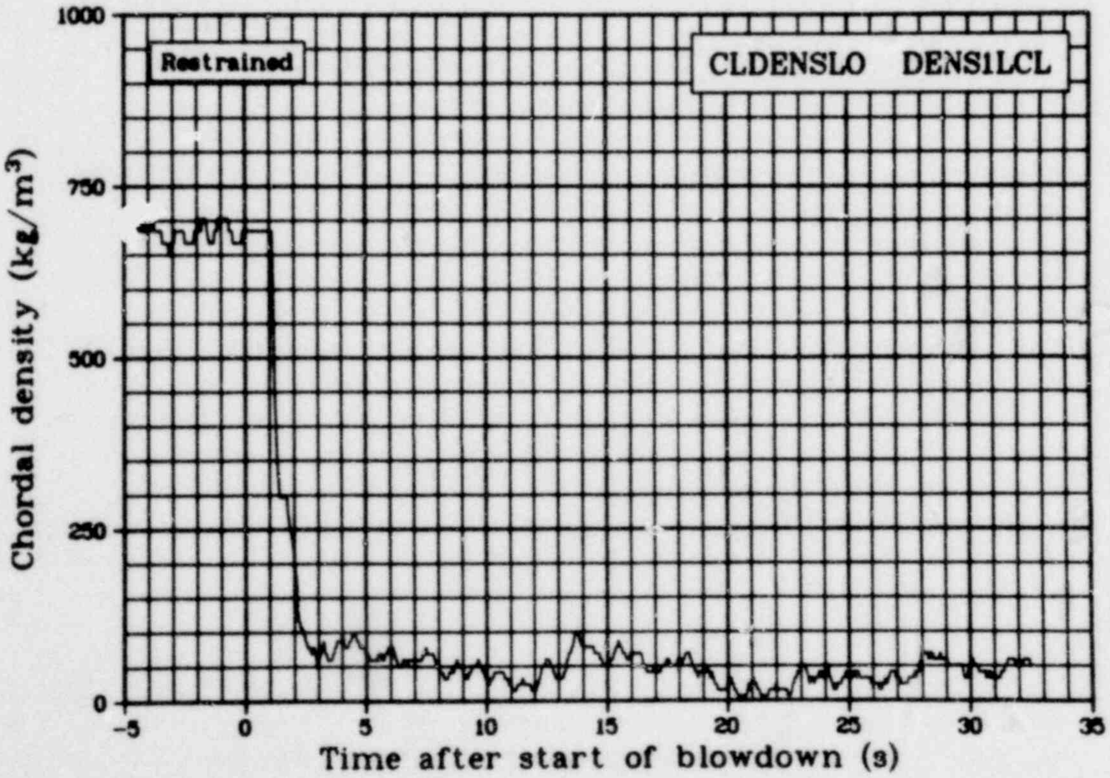

Fig. 351 Chordal density of lower beam in cold leg blowdown spool (CLDENSLO DENS1LCL), from -5 to 35 s.

1405 266

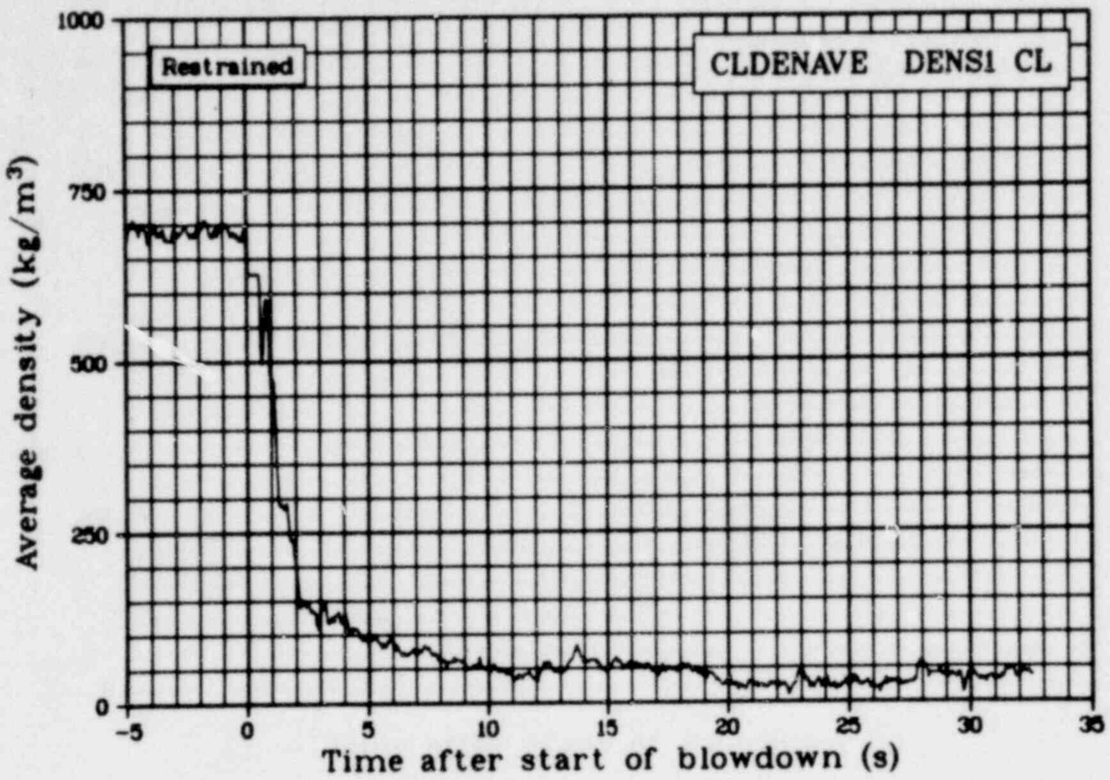

Fig. 352 Average density of cold leg blowdown spool (CLDENAVE DENS1 CL), from -5 to 35 s.

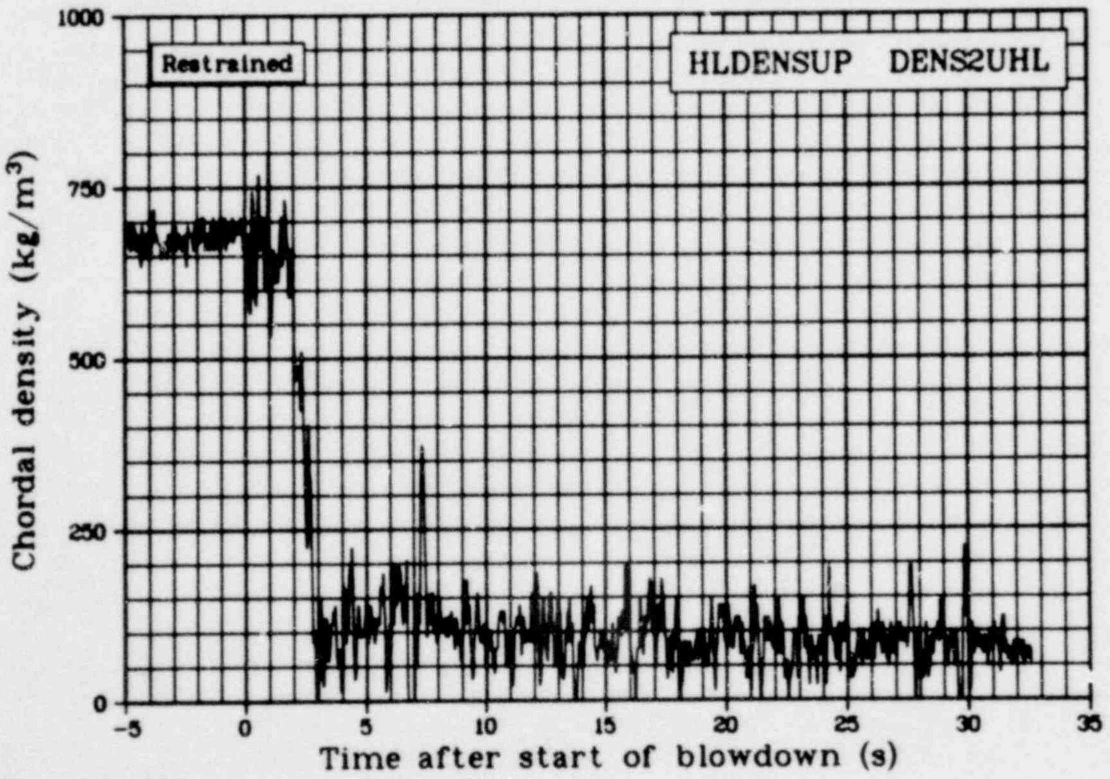

Fig. 353 Chordal density of upper beam in hot leg blowdown spool (HLDENSUP DENS2UHL), from -5 to 35 s.

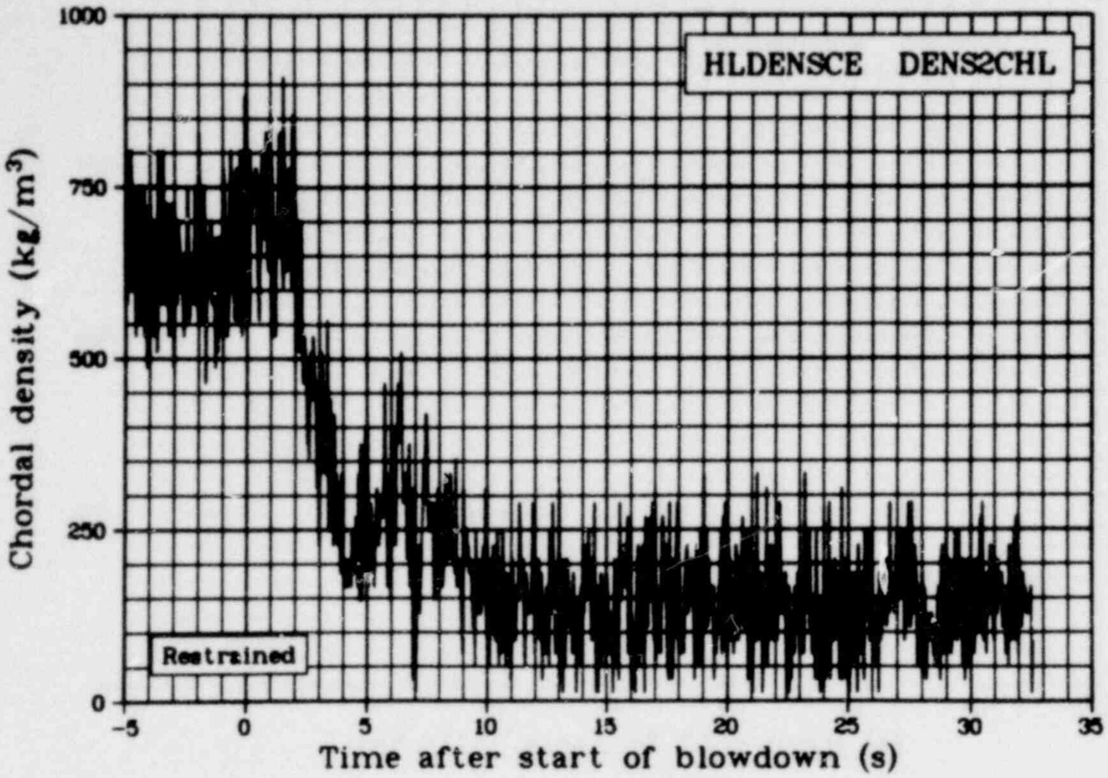

Fig. 354 Chordal density of center beam in hot leg blowdown spool (HLDENSCE DENS2CHL), from -5 to 35 s.

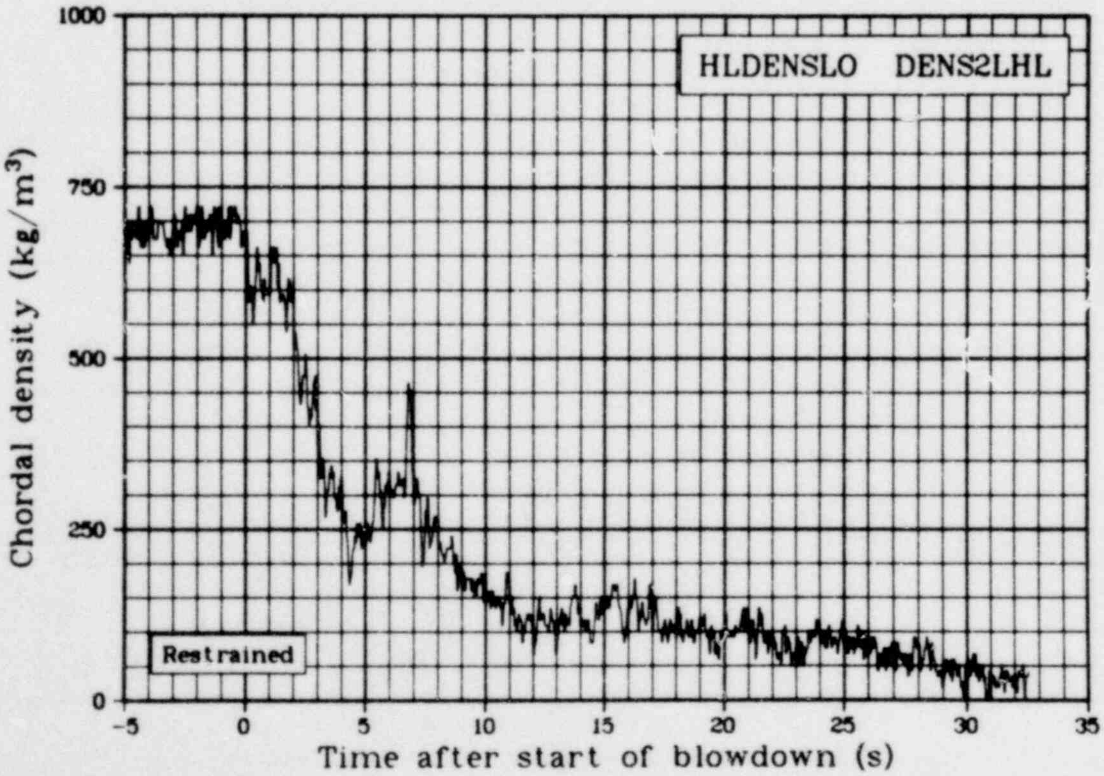

Fig. 355 Chordal density of lower beam in hot leg blowdown spool (HLDENSLO DENS2LHL), from -5 to 35 s.

1405 268

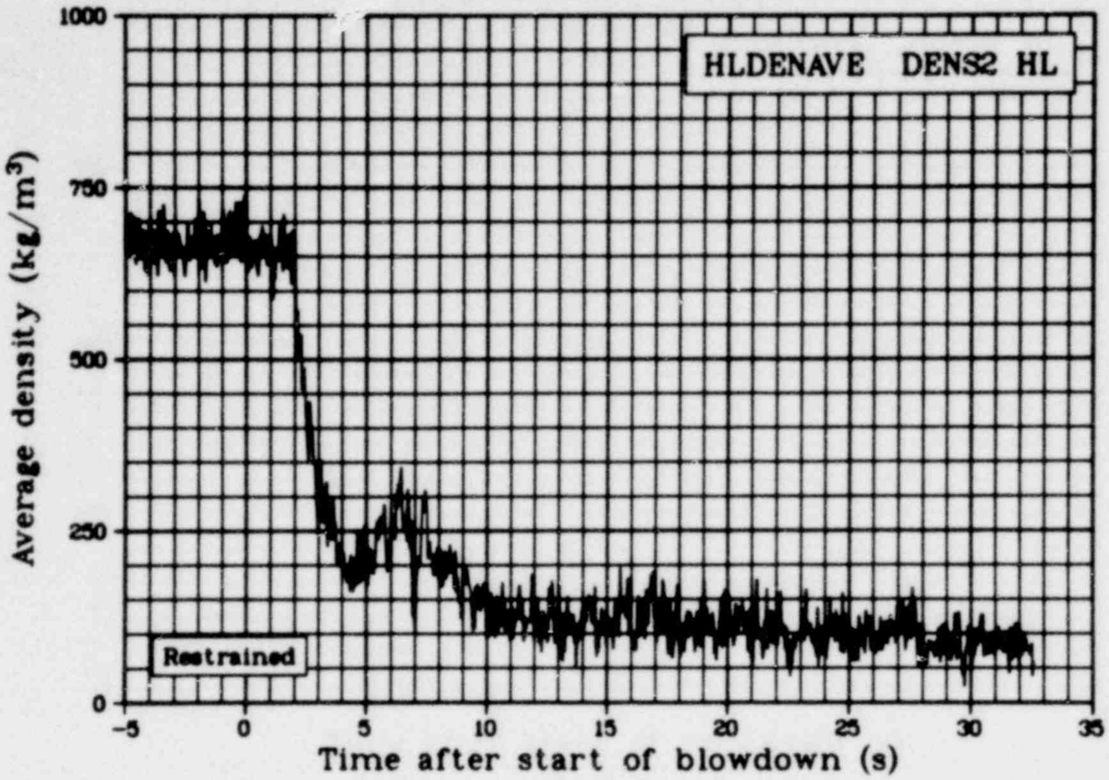

Fig. 356 Average density of hot leg blowdown spool (HLDENAVE DENS2 HL), from -5 to 35 s.

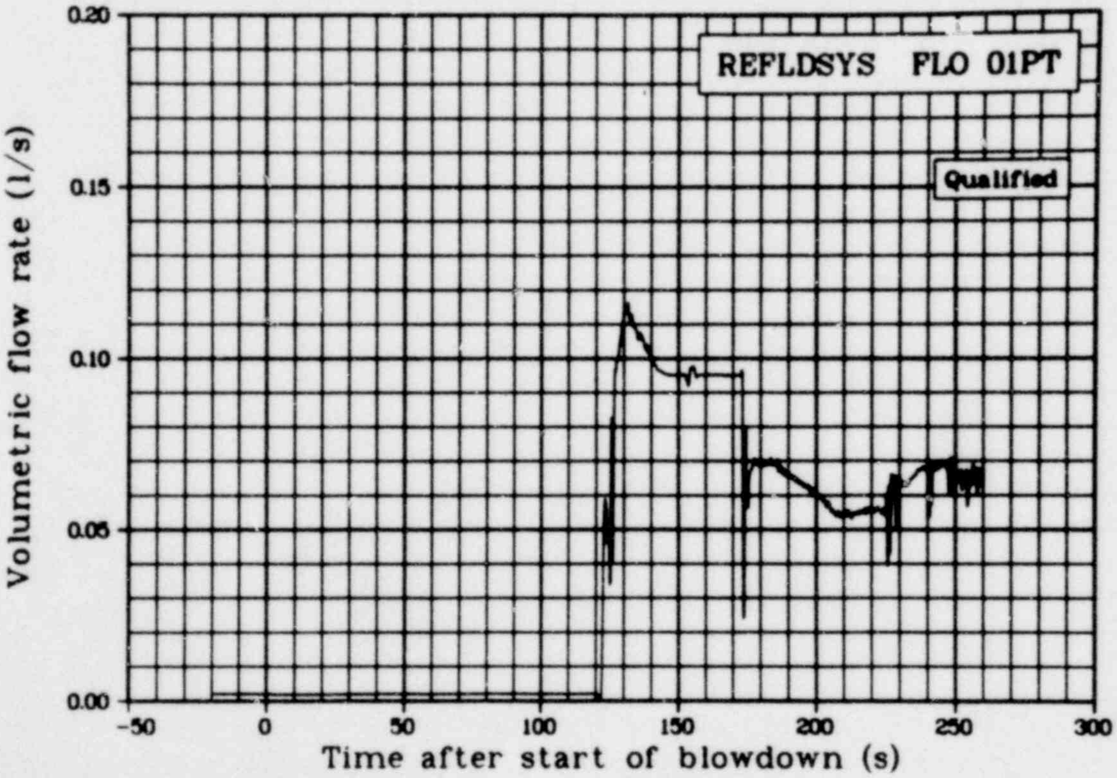

Fig. 357 Volumetric flow rate in reflood line No. 1 (REFLDSYS FLO 01PT), from -50 to 300 s.

1405 269

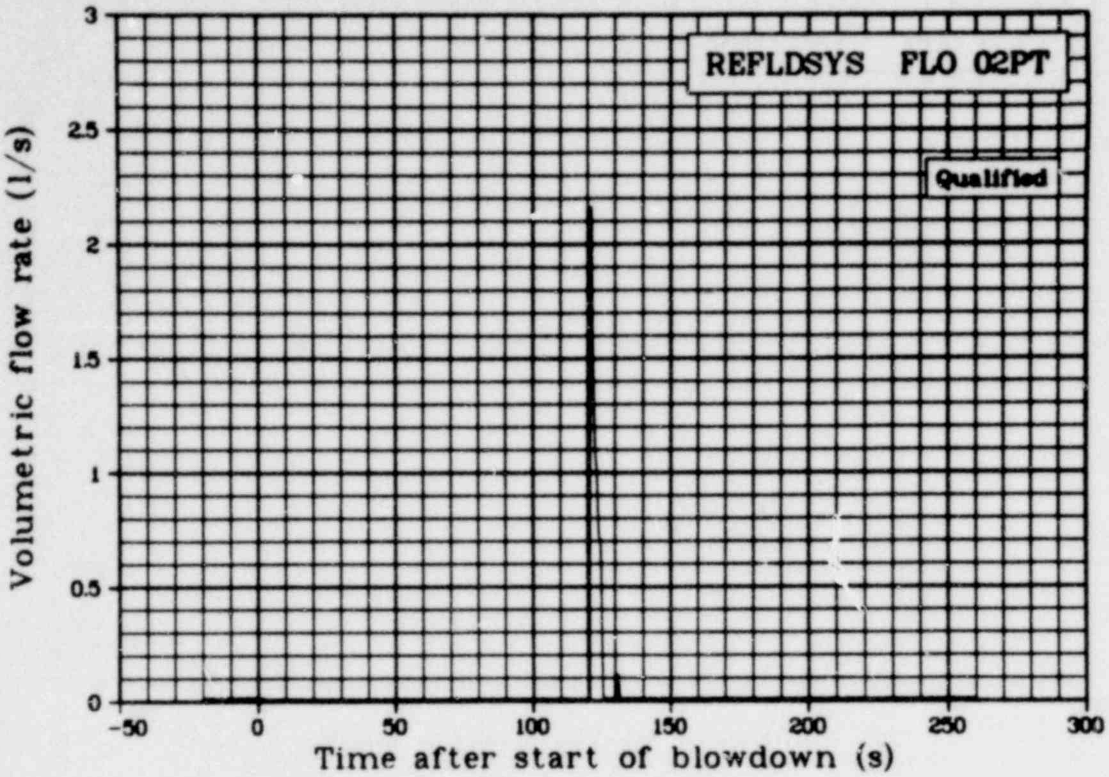

Fig. 358 Volumetric flow rate in reflood line No. 2 (REFLDSYS FLO 02PT), from -50 to 300 s.

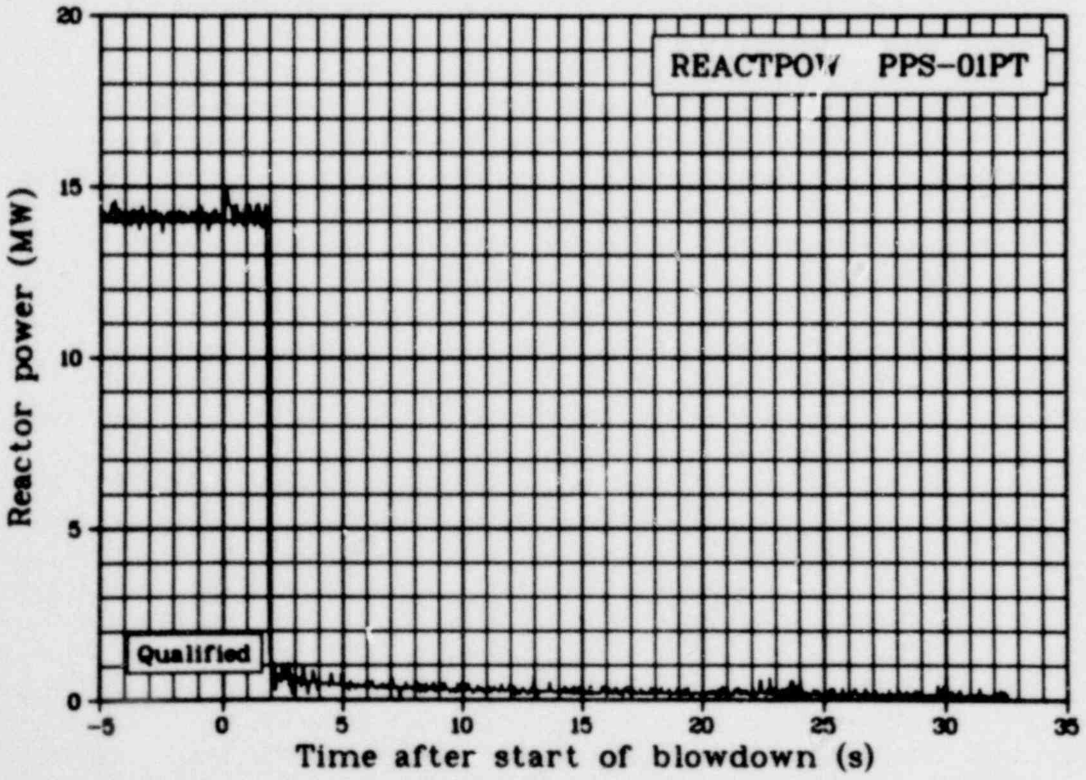

Fig. 359 Reactor power from Core Ionization Chamber PPS 1 (REACTPOW PPS-01PT), from -5 to 35 s.

1405 270

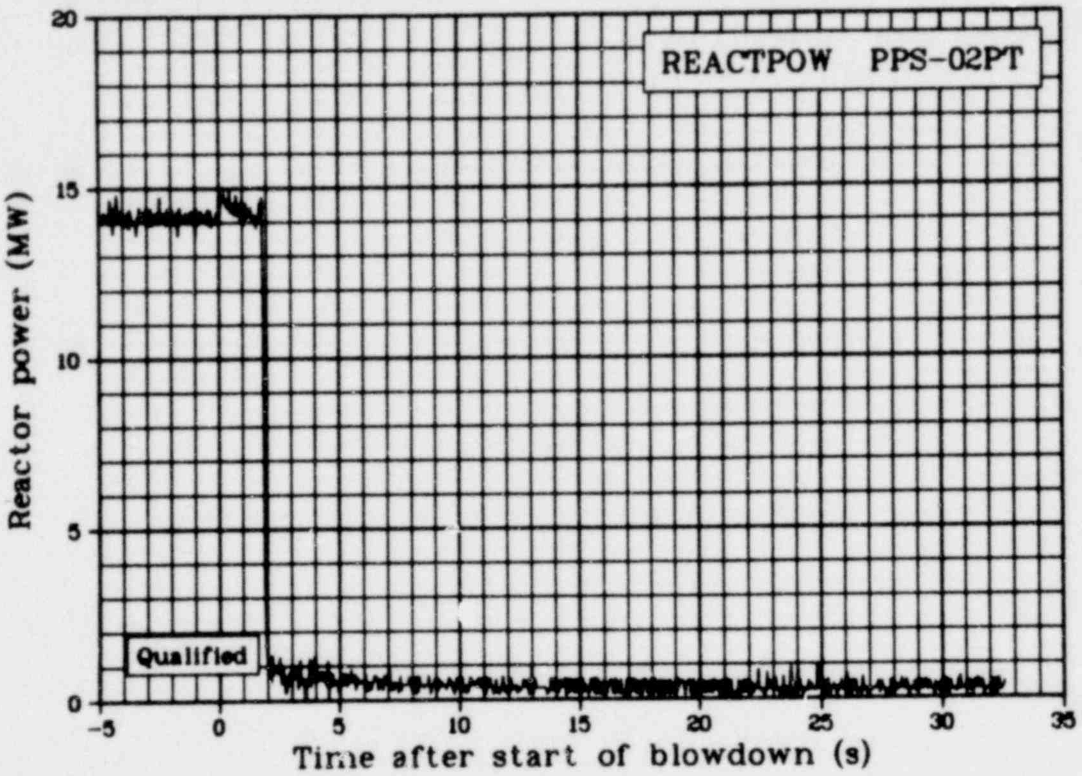

Fig. 360 Reactor power from Core Ionization Chamber PPS 2 (REACTPOW PPS-02PT), from -5 to 35 s.

1405 271

272

1405 27~~2~~3

TEST LLR-4

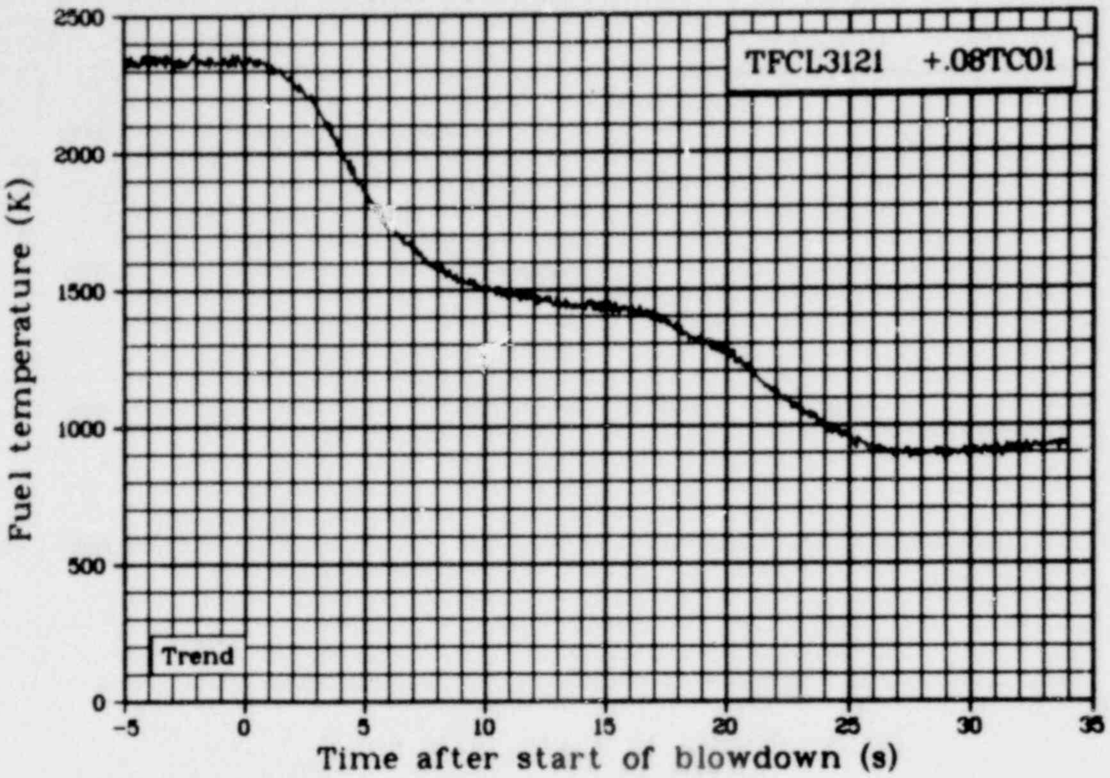

Fig. 361 Fuel temperature in Rod 312-1, 0.08 m above the fuel stack midplane (TFCL3121 +.08TC01), from -5 to 35 s.

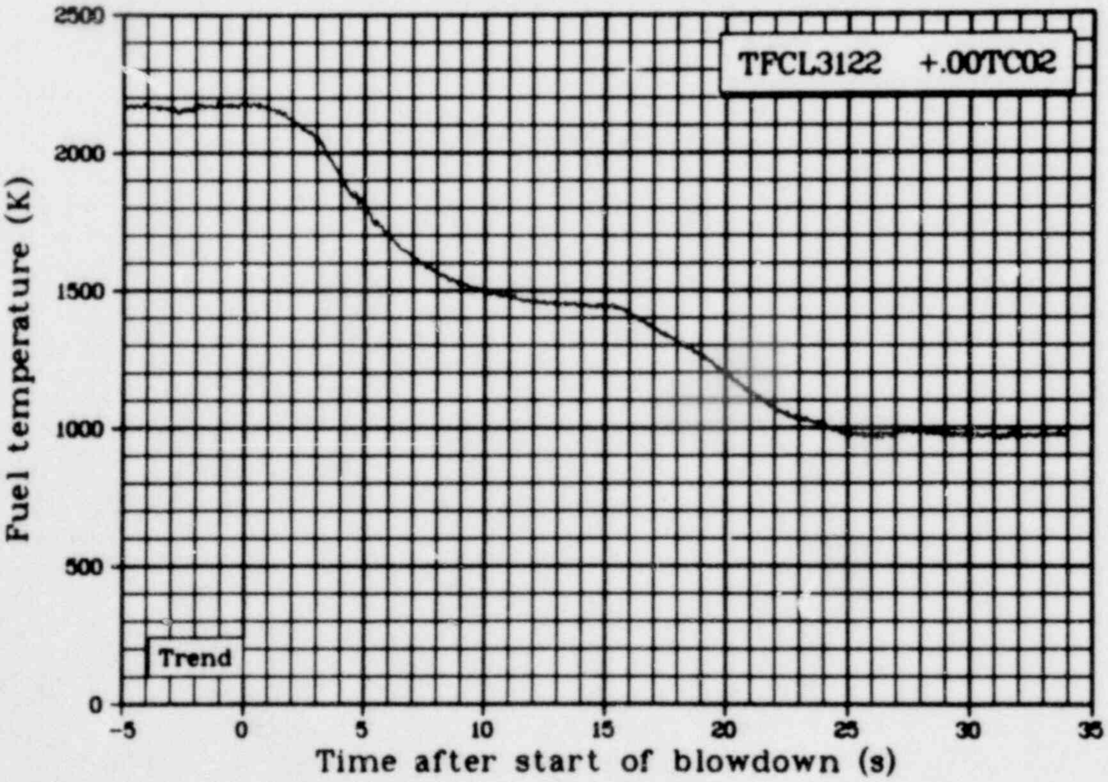

Fig. 362 Fuel temperature in Rod 312-2, at fuel stack midplane (TFCL3122 +.00TC02), from -5 to 35 s.

~~1405 273~~ 4

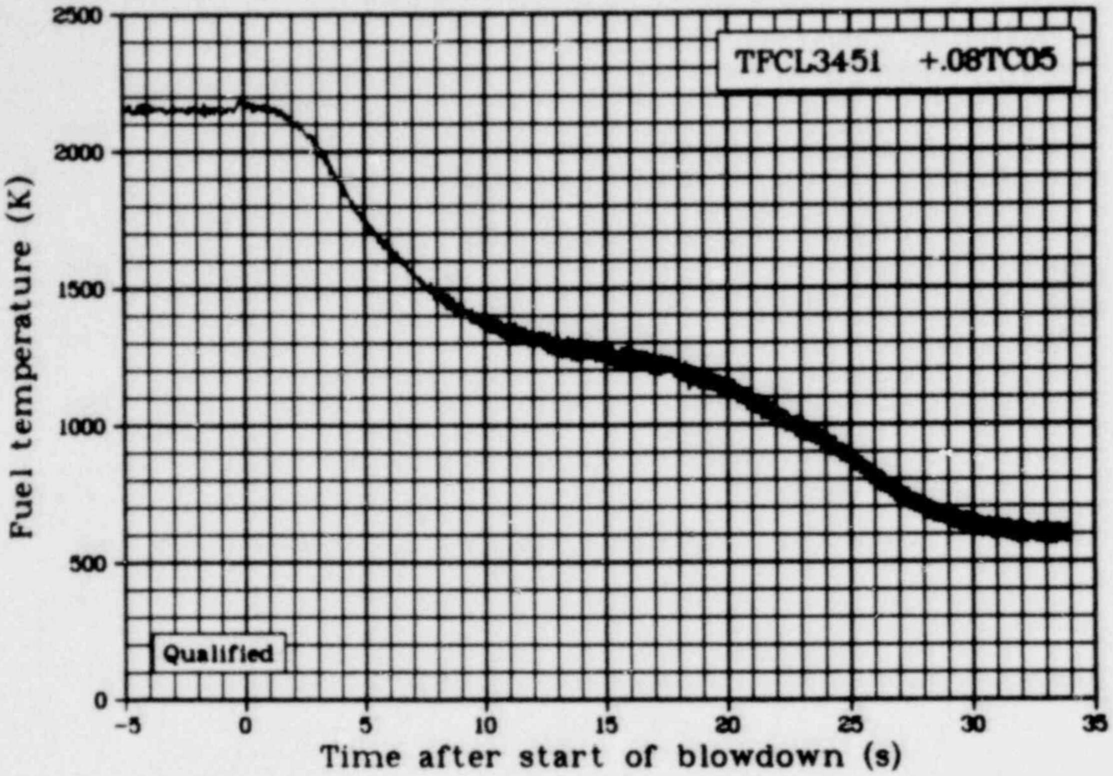

Fig. 363 Fuel temperature in Rod 345-1, 0.08 m above the fuel stack midplane (TFCL3451 +.08TC05), from -5 to 35 s.

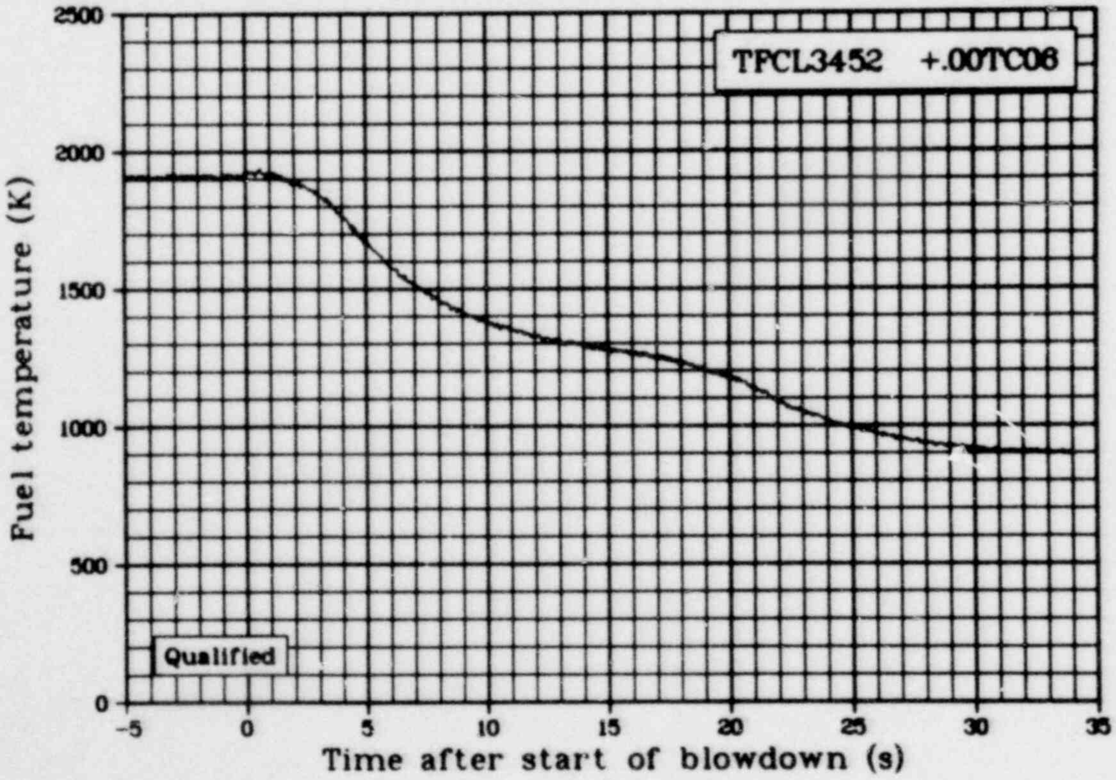

Fig. 364 Fuel temperature in Rod 345-2, at fuel stack midplane (TFCL3452 +.00TC06), from -5 to 35 s.

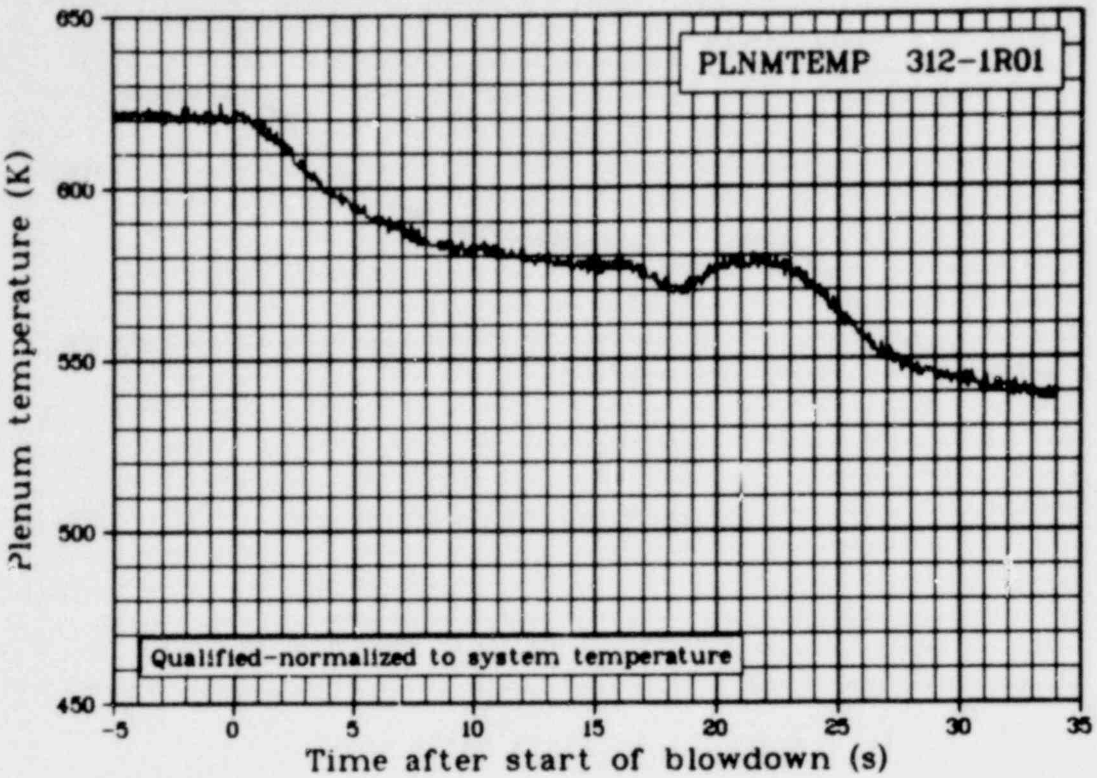

Fig. 365 Plenum temperature in Fuel Rod 312-1 (PLNMTEMP 312-1R01), from -5 to 35 s.

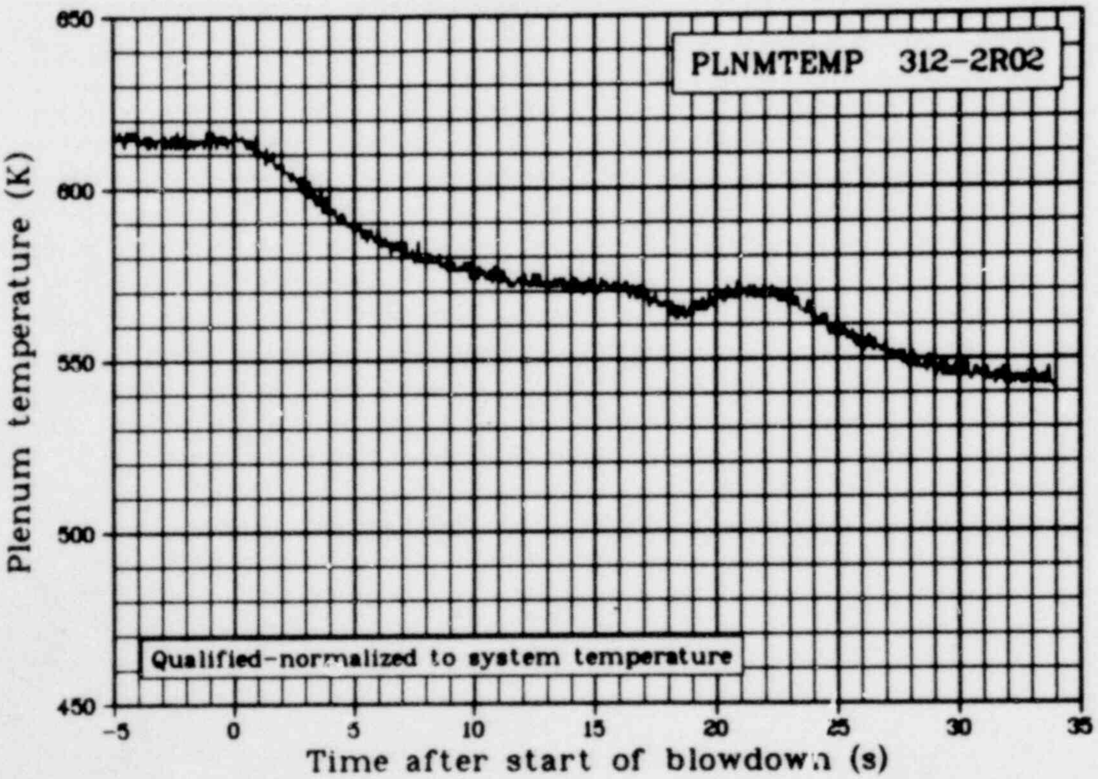

Fig. 366 Plenum temperature in Fuel Rod 312-2 (PLNMTEMP 312-2R02), from -5 to 35 s.

1405 ~~275~~ 276

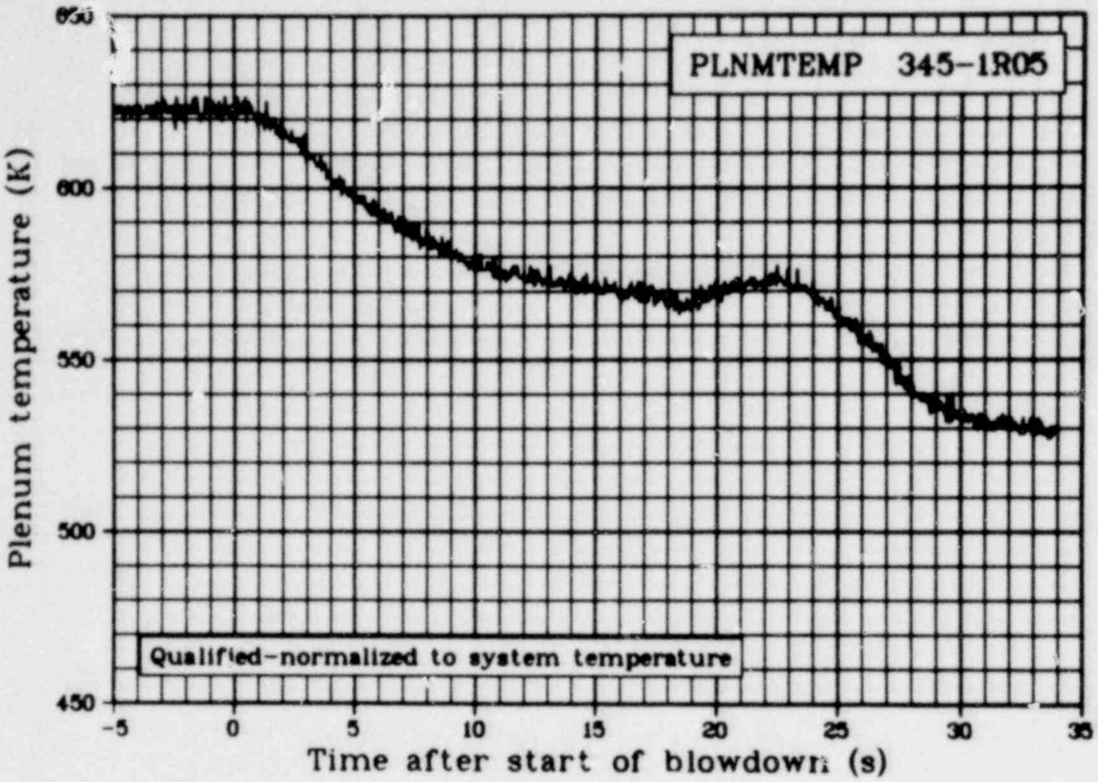

Fig. 367 Plenum temperature in Fuel Rod 345-1 (PLNMTEMP 345-1R05), from -5 to 35 s.

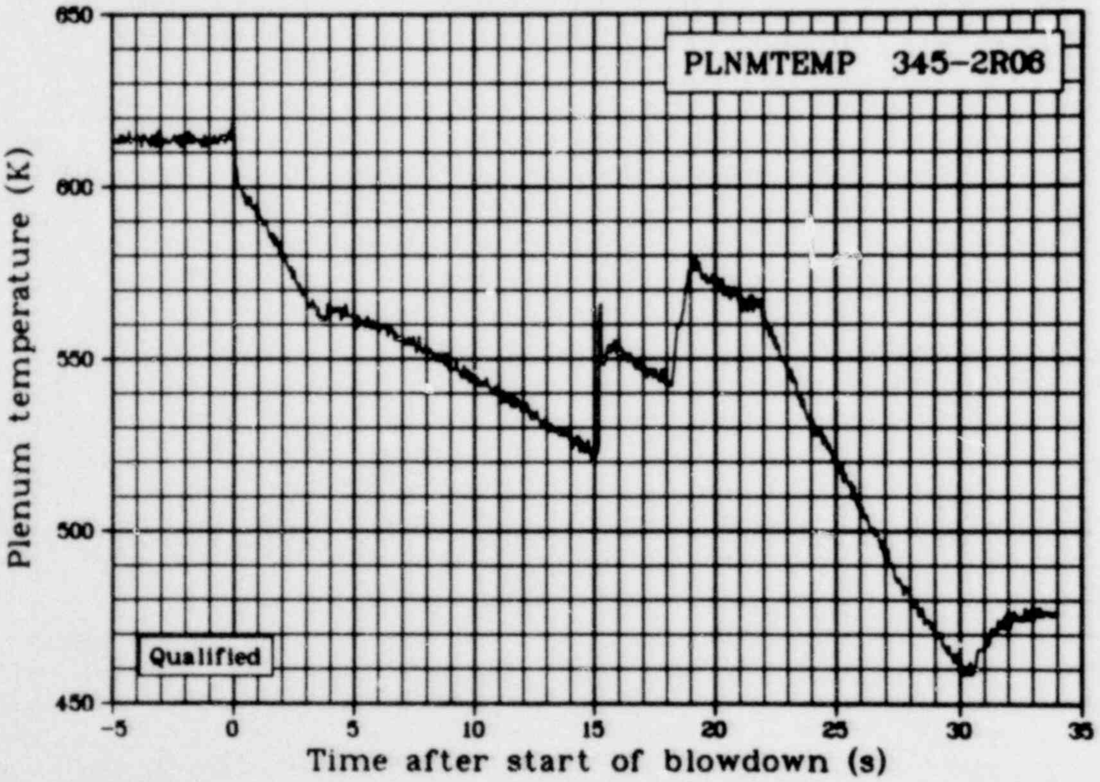

Fig. 368 Plenum temperature in Fuel Rod 345-2 (PLNMTEMP 345-2R06), from -5 to 35 s.

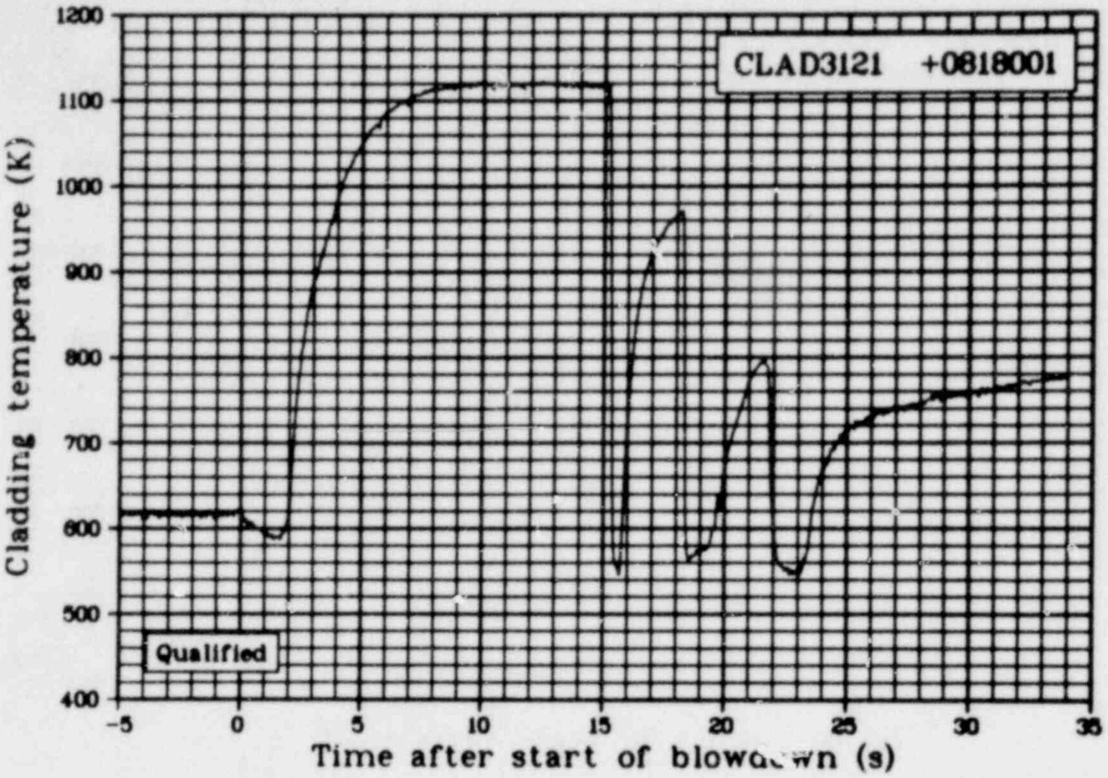

Fig. 369 Cladding temperature, Rod 312-1, at 180 degrees and 0.08 m above fuel stack midplane (CLAD3121 +0818001), from -5 to 35 s.

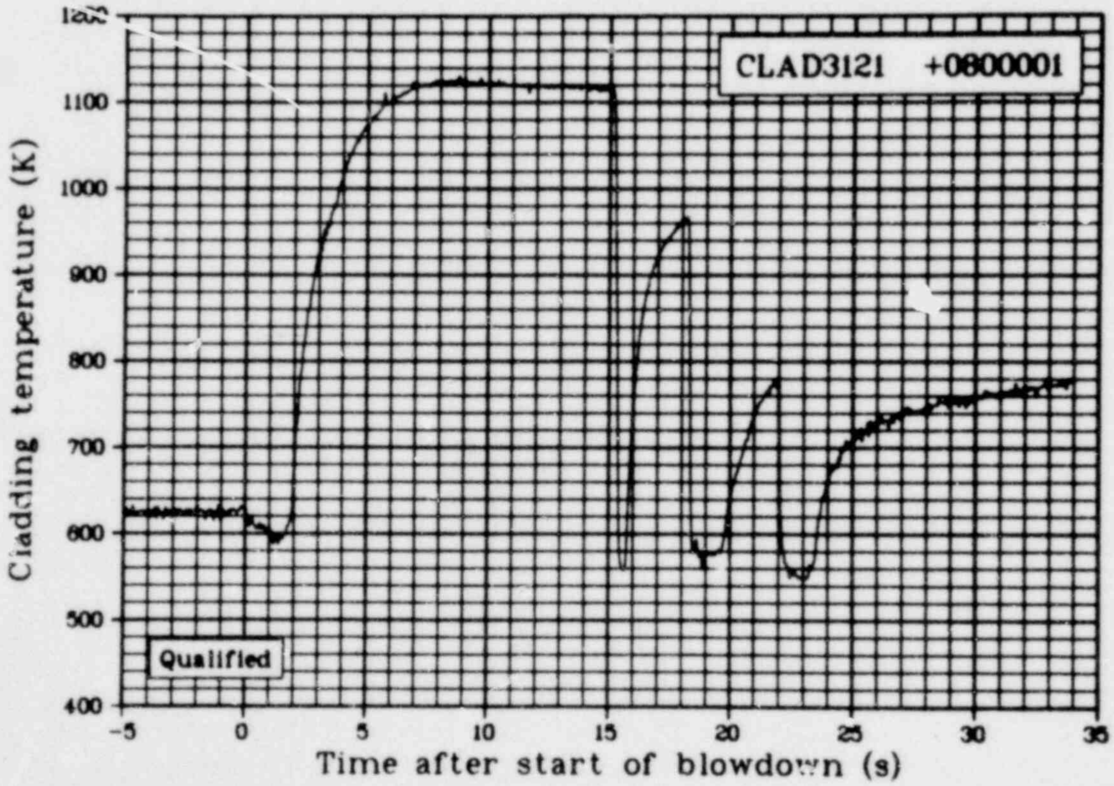

Fig. [illegible] Cladding temperature, Rod 312-1, at 0 degrees and 0.08 m above fuel stack midplane (CLAD3121 +0800001), fro[illegible] to 35 s.

1405 278

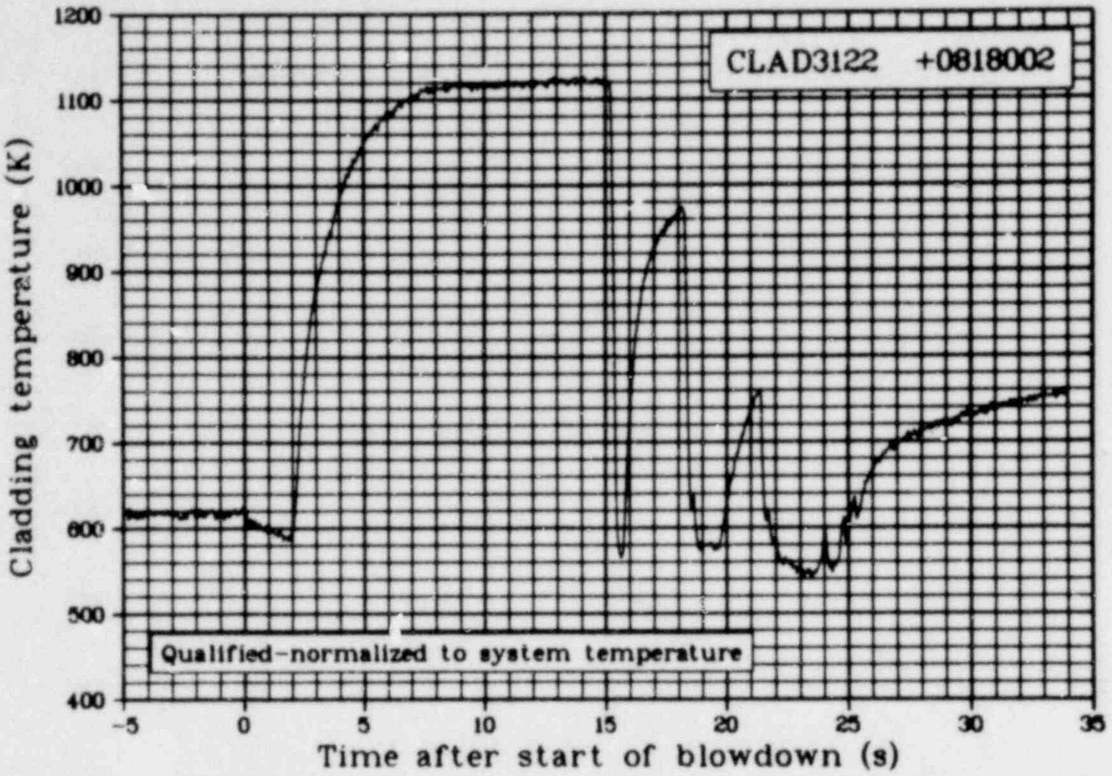

Fig. 371 Cladding temperature, Rod 312-2, at 180 degrees and 0.08 m above fuel stack midplane (CLAD3122 +0818002), from -5 to 35 s.

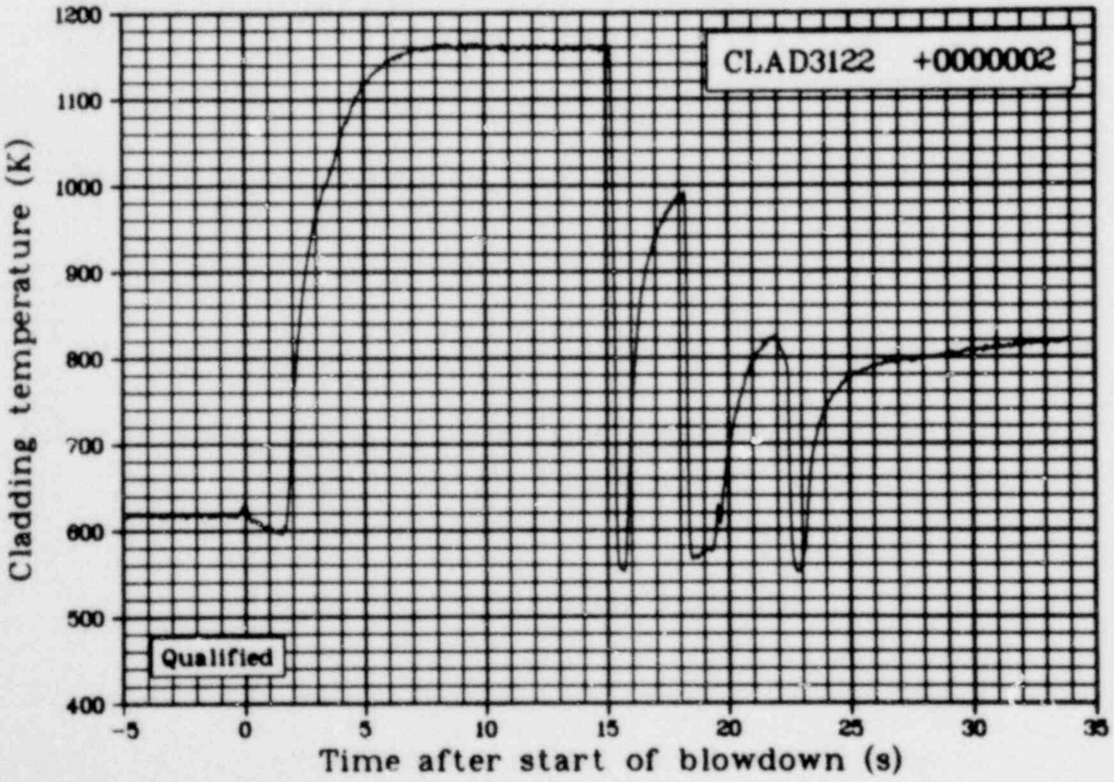

Fig. 372 Cladding temperature, Rod 312-2, at 0 degrees and fuel stack midplane (CLAD3122 +0000002), from -5 to 35 s.

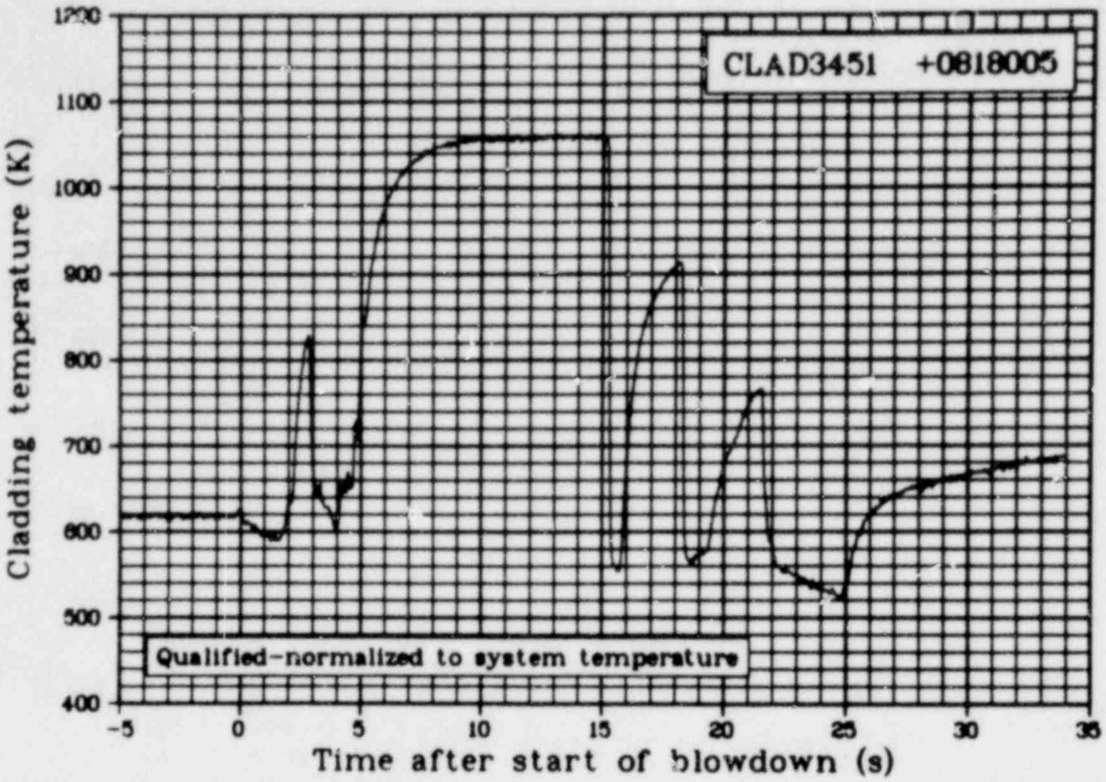

Fig. 373 Cladding temperature, Rod 345-1, at 180 degrees and 0.08 m above fuel stack midplane (CLAD3451 +0818005), from -5 to 35 s.

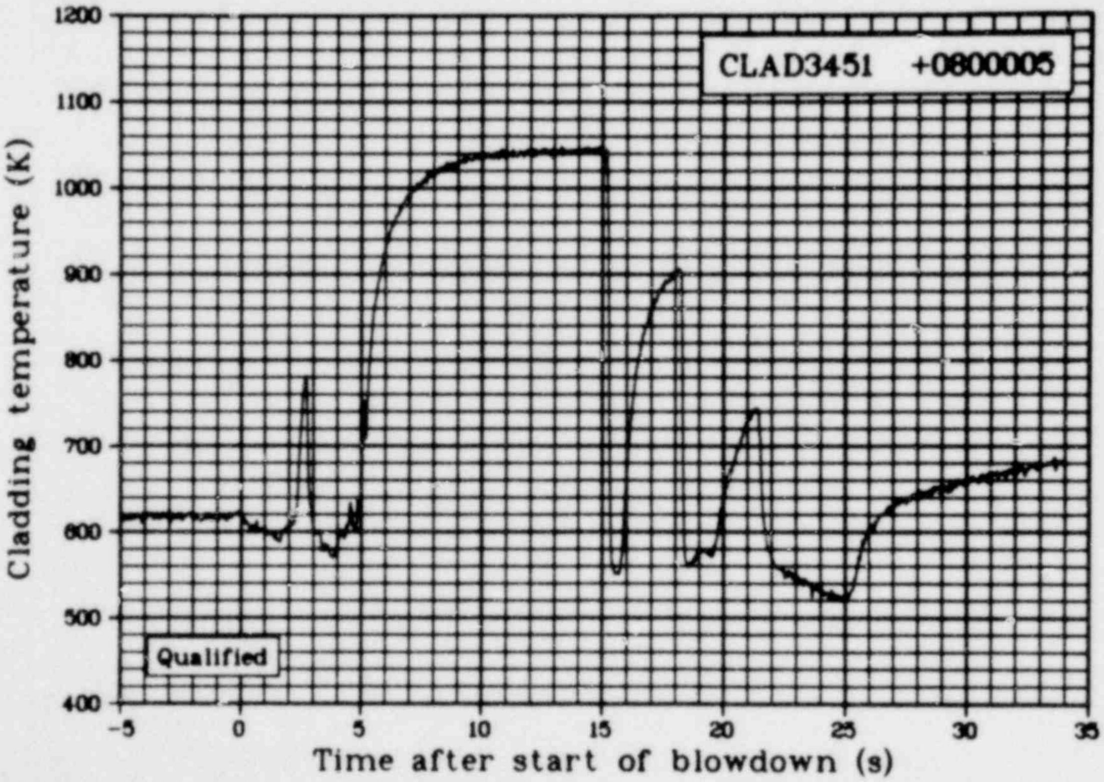

Fig. 374 Cladding temperature, Rod 345-1, at 0 degrees and 0.08 m above fuel stack midplane (CLAD3451 +0800005), from -5 to 35 s.

1405 280

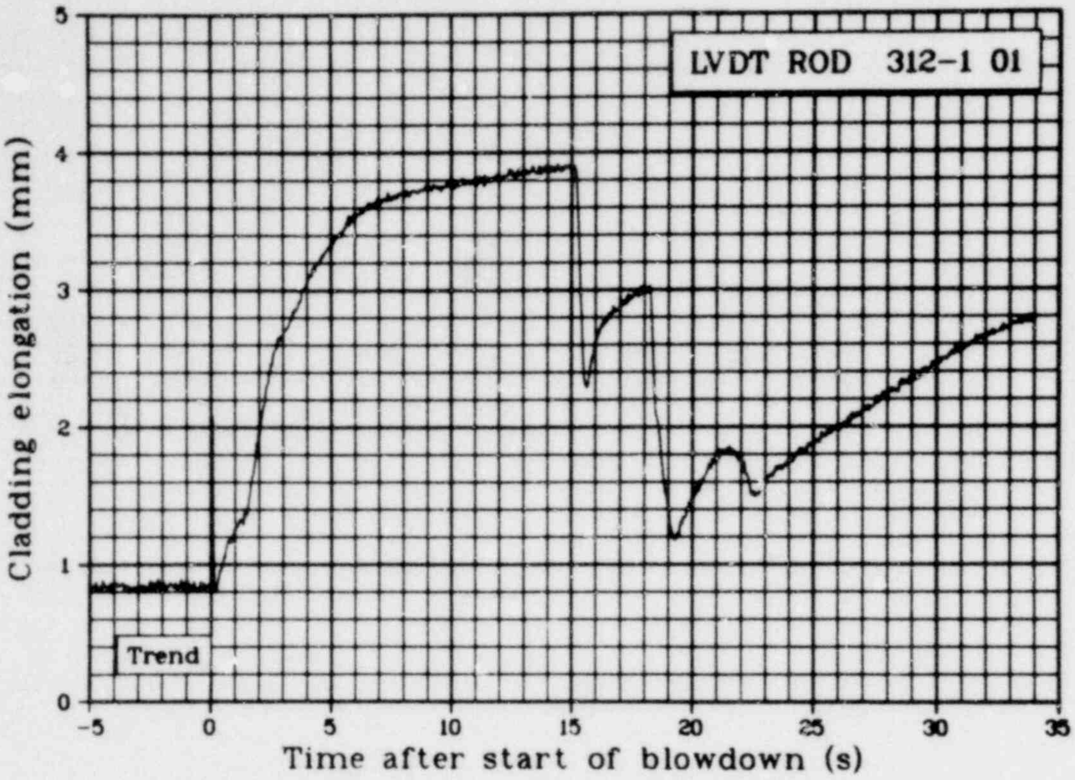

Fig. 375 Cladding elongation of Fuel Rod 312-1, (LVDT ROD 312-1 01), from -5 to 35 s.

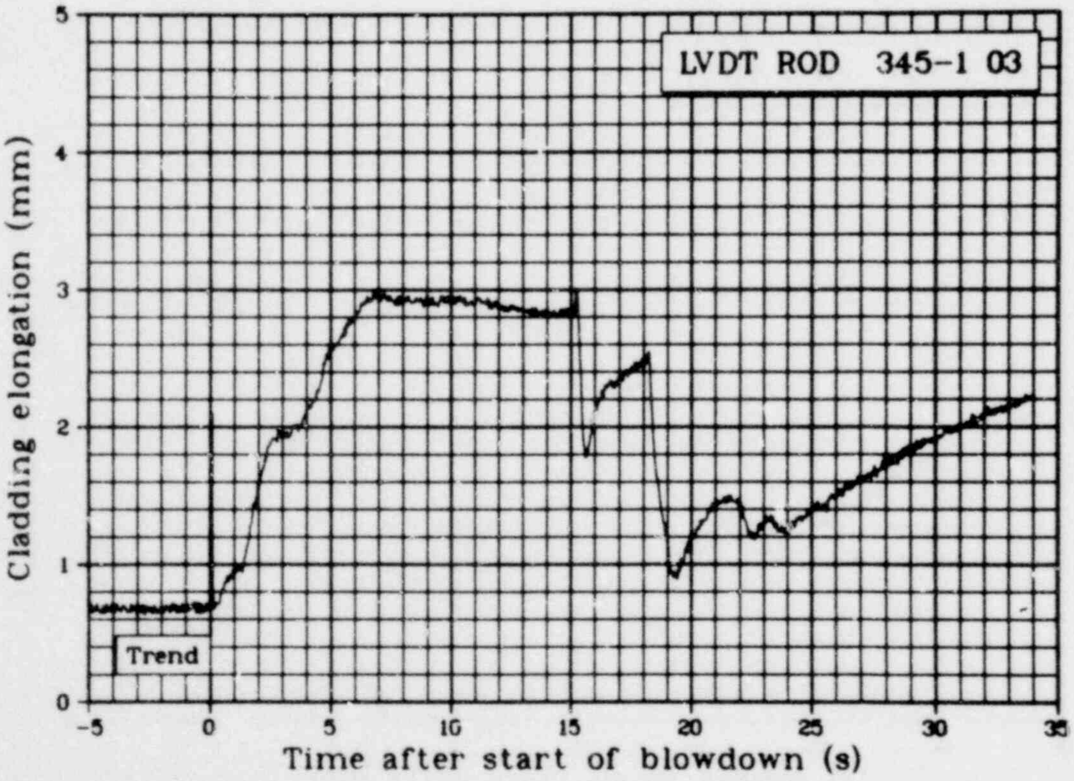

Fig. 376 Cladding elongation of Fuel Rod 345-1, (LVDT ROD 345-1 03), from -5 to 35 s.

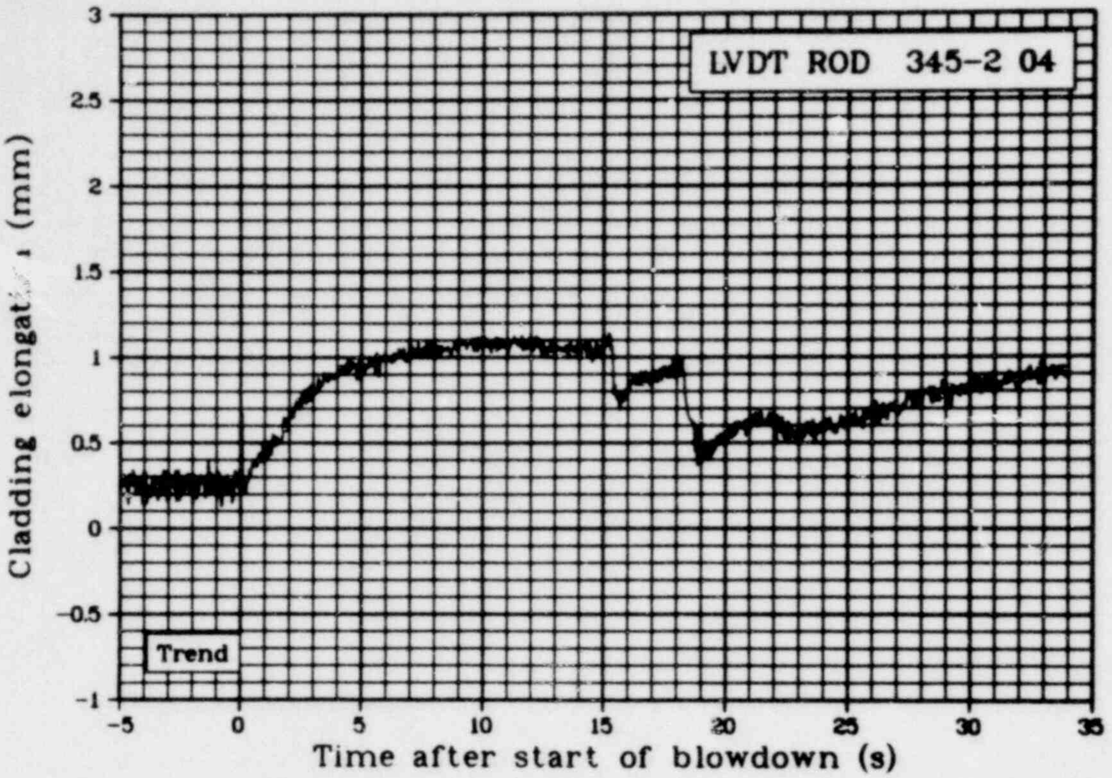

Fig. 377 Cladding elongation of Fuel Rod 345-2, (LVDT ROD 345-2 04), from -5 to 35 s.

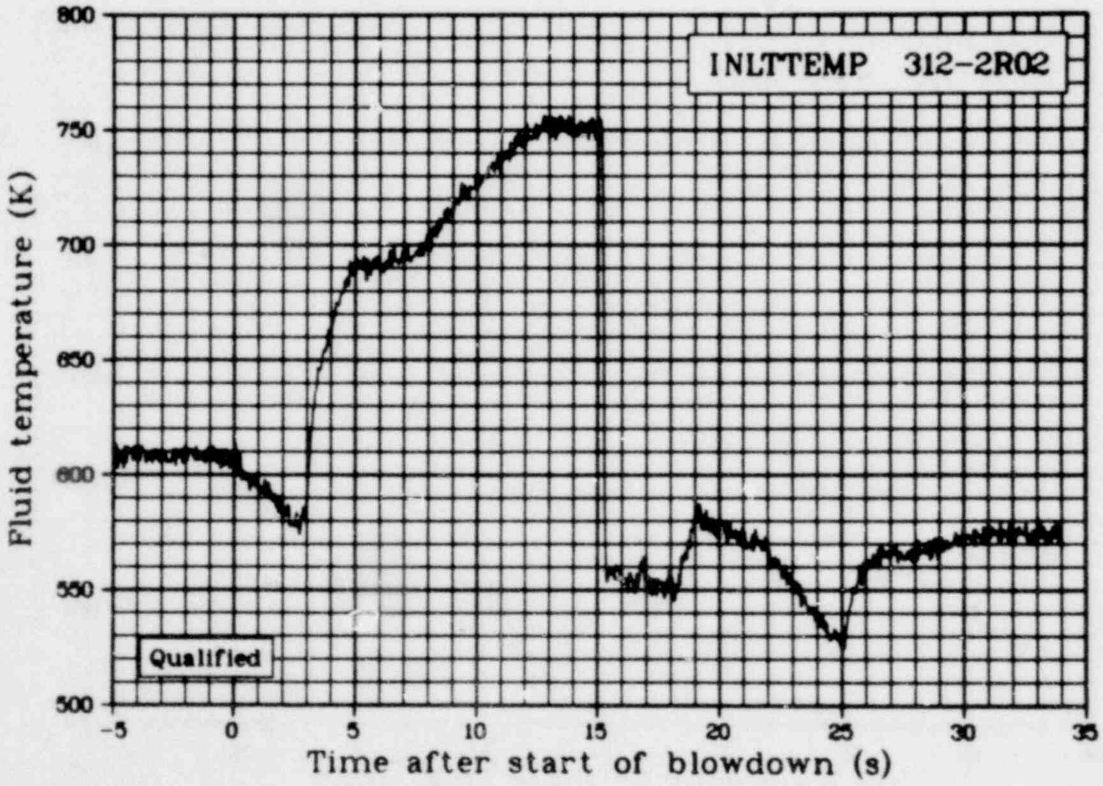

Fig. 378 Fluid temperature of Fuel Rod 312-2 coolant inlet (INLTTEMP 312-2R02), from -5 to 35 s.

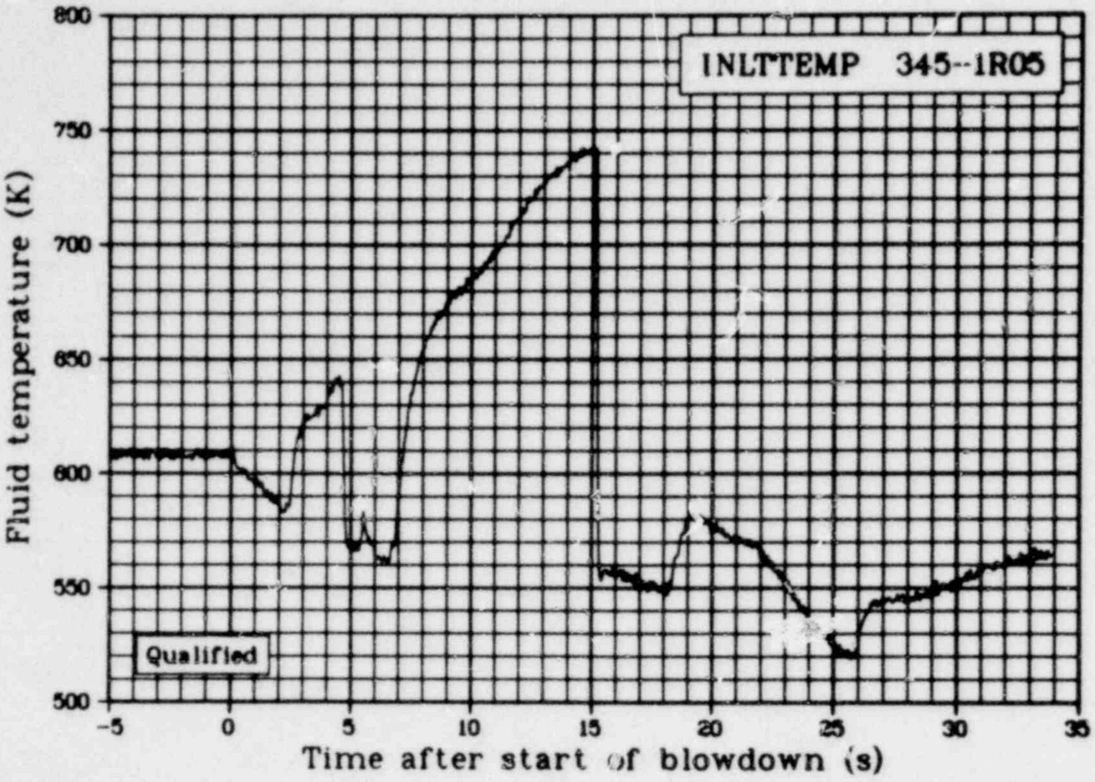

Fig. 379 Fluid temperature of Fuel Rod 345-1 coolant inlet (INLTTEMP 345-1R05), from -5 to 35 s.

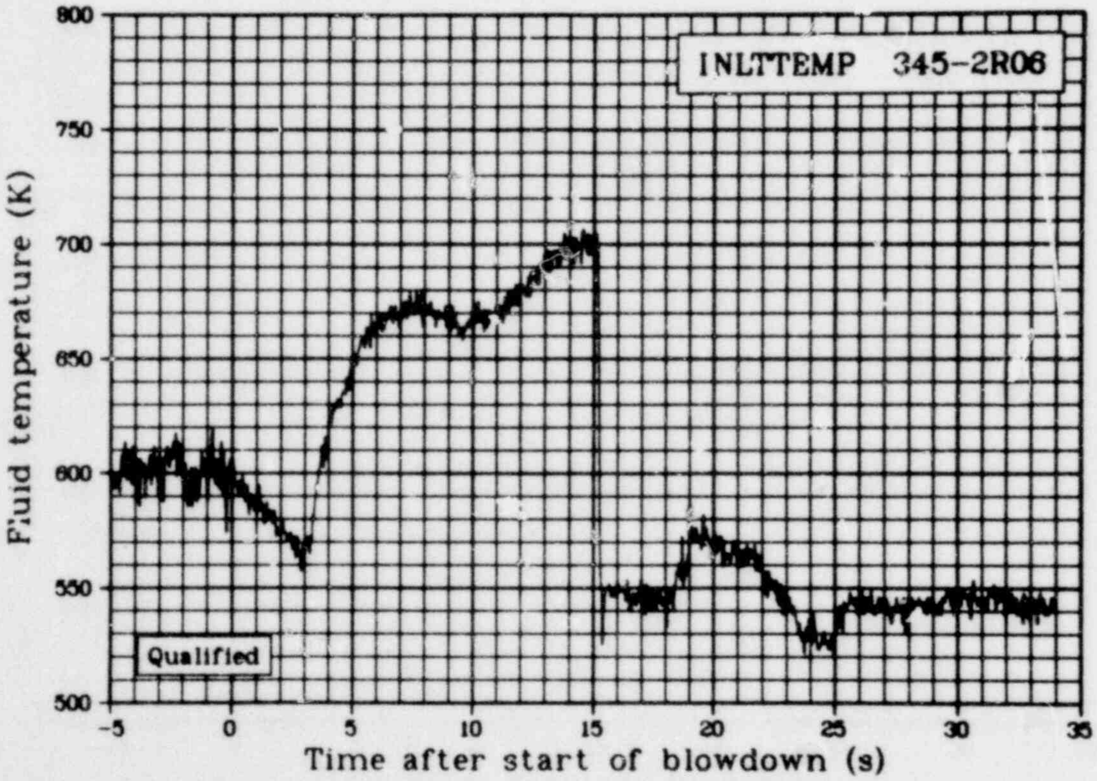

Fig. 380 Fluid temperature of Fuel Rod 345-2 coolant inlet (INLTTEMP 345-2R06), from -5 to 35 s.

1405 ~~282~~ 283

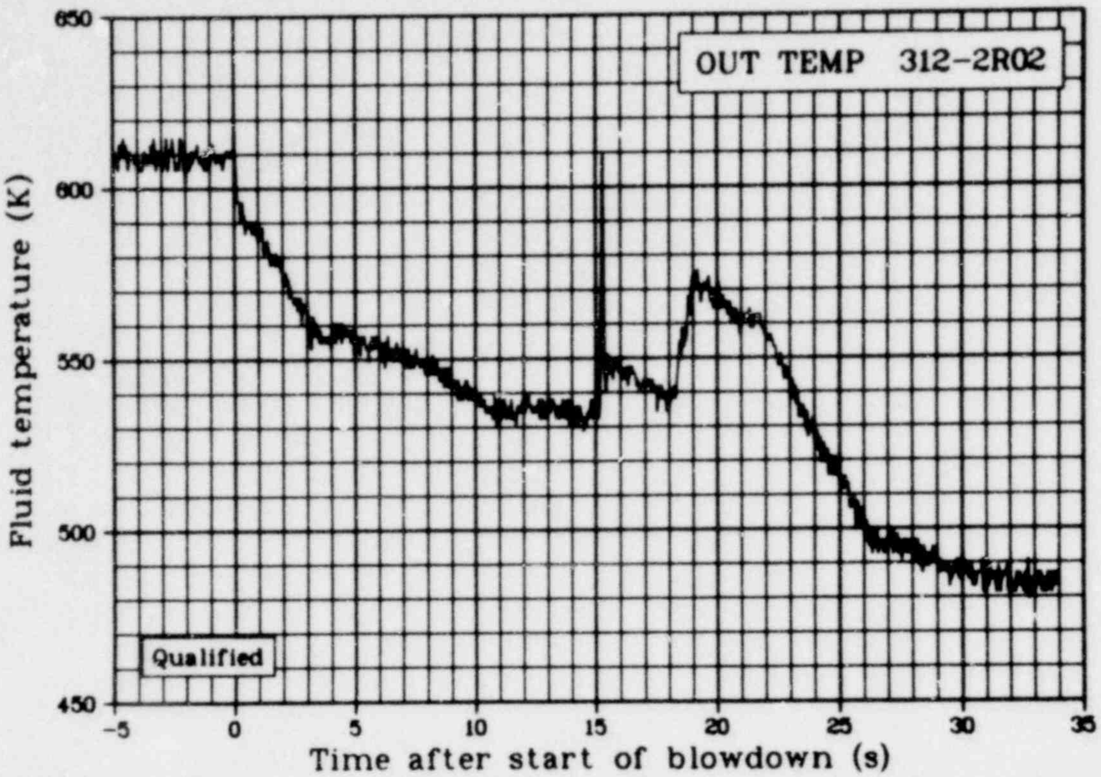

Fig. 381 Fluid temperature of Fuel Rod 312-2 coolant outlet (OUT TEMP 312-2R02), from -5 to 35 s.

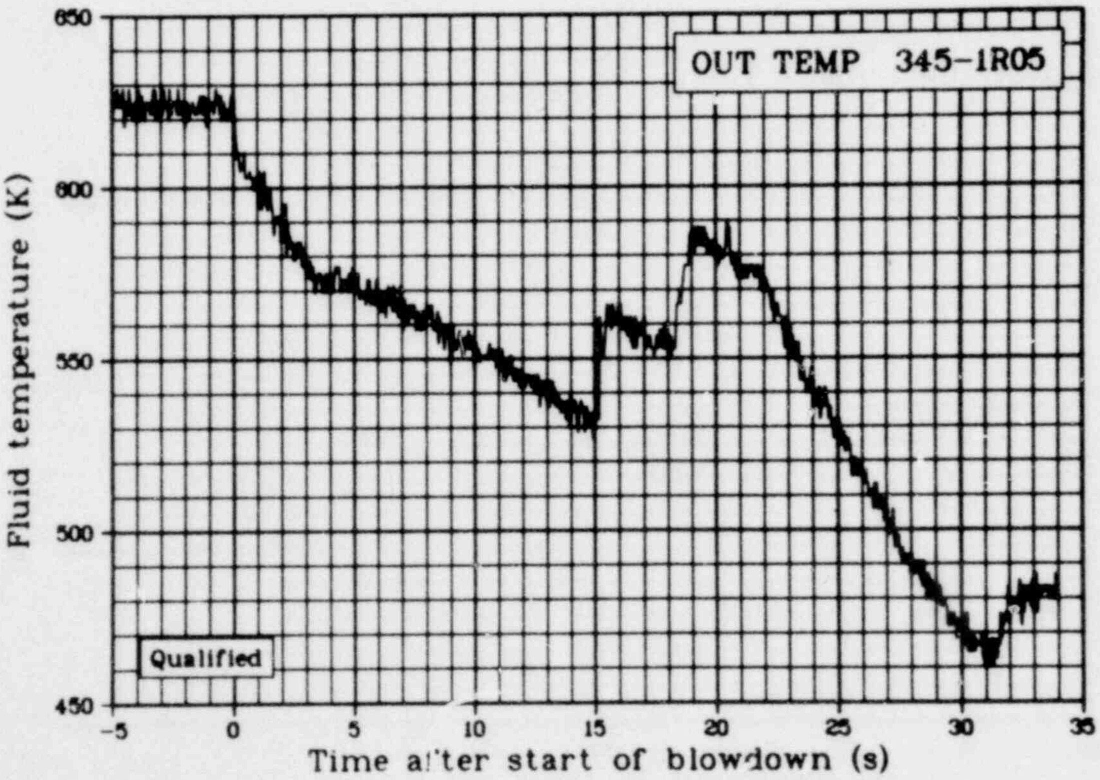

Fig. 382 Fluid temperature of Fuel Rod 345-1 coolant outlet (OUT TEMP 345-1R05), from -5 to 35 s.

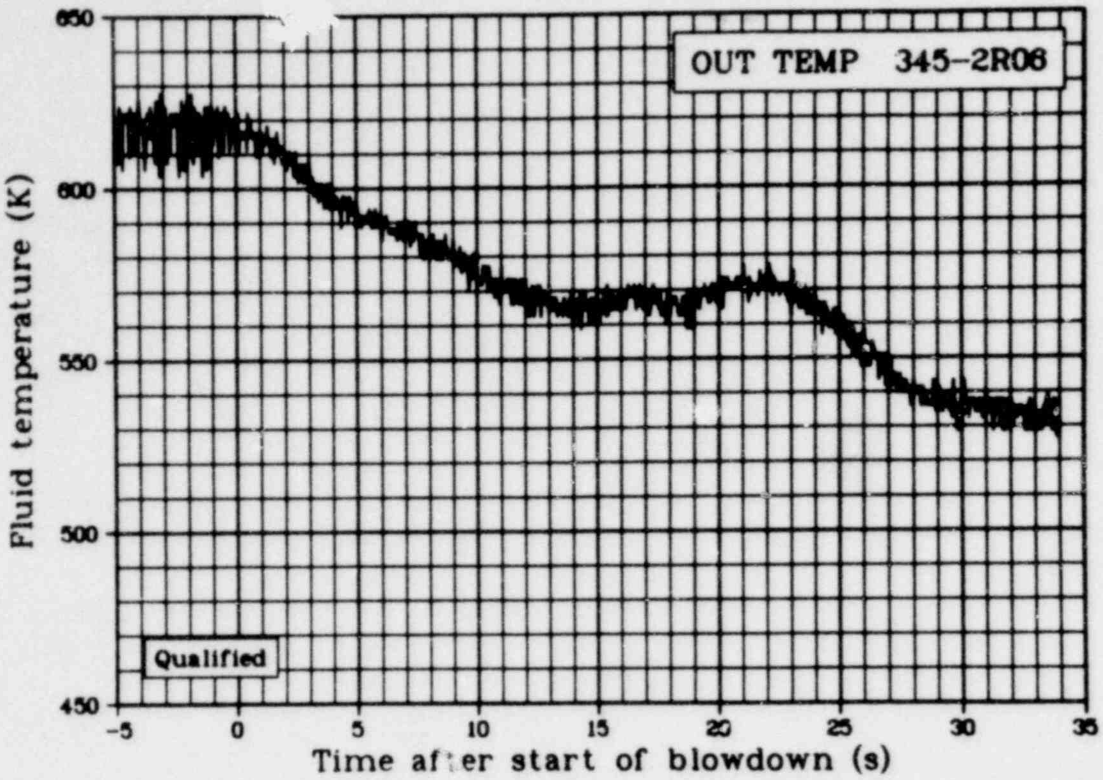

Fig. 383 Fluid temperature of Fuel Rod 345-2 coolant outlet (OUT TEMP 345-2R06), from -5 to 35 s.

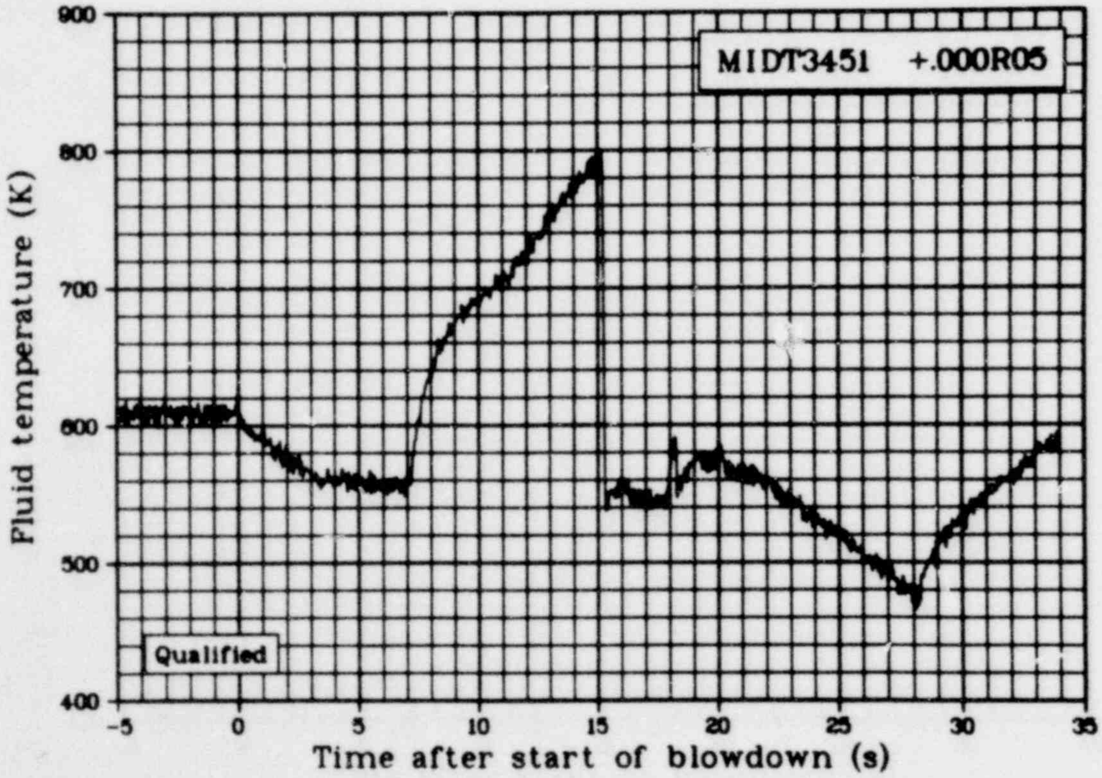

Fig. 384 Fluid temperature of Fuel Rod 345-1, at fuel stack midplane (MIDT3451 + .000R05), from -5 to 35 s.

1405 28~~4~~5

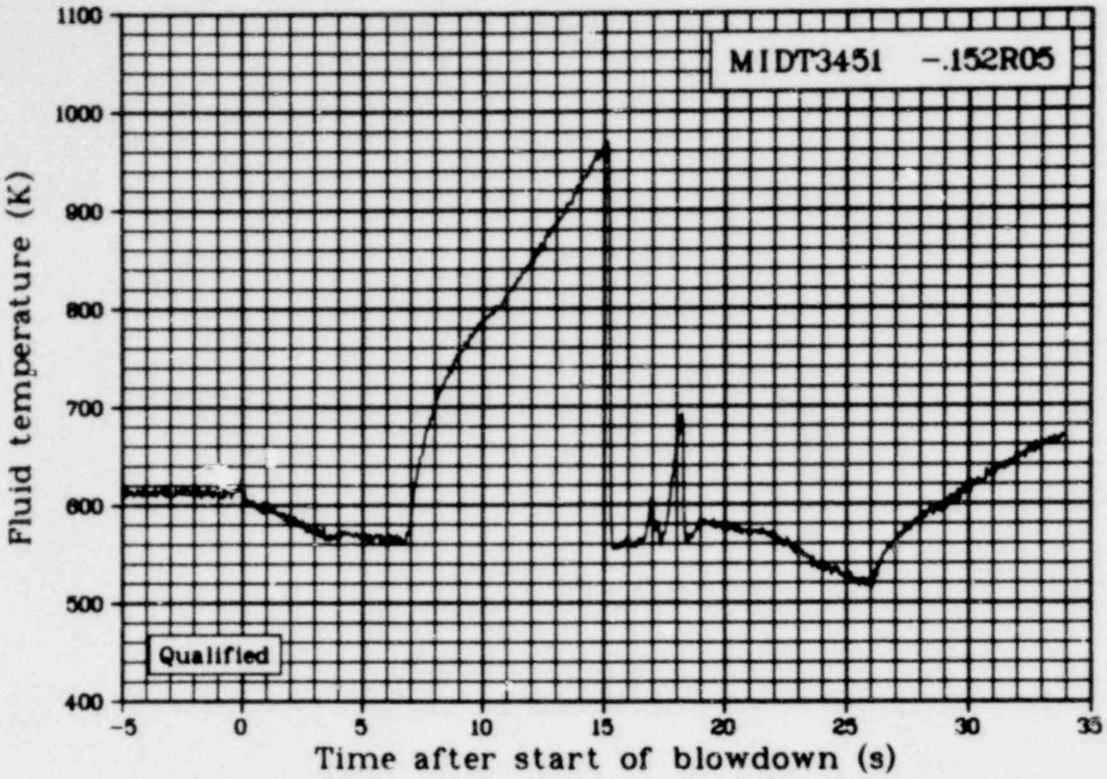

Fig. 385 Fluid temperature of Fuel Rod 345-1, 0.152 m below fuel stack midplane (MIDT3451 -.152R05), from -5 to 35 s.

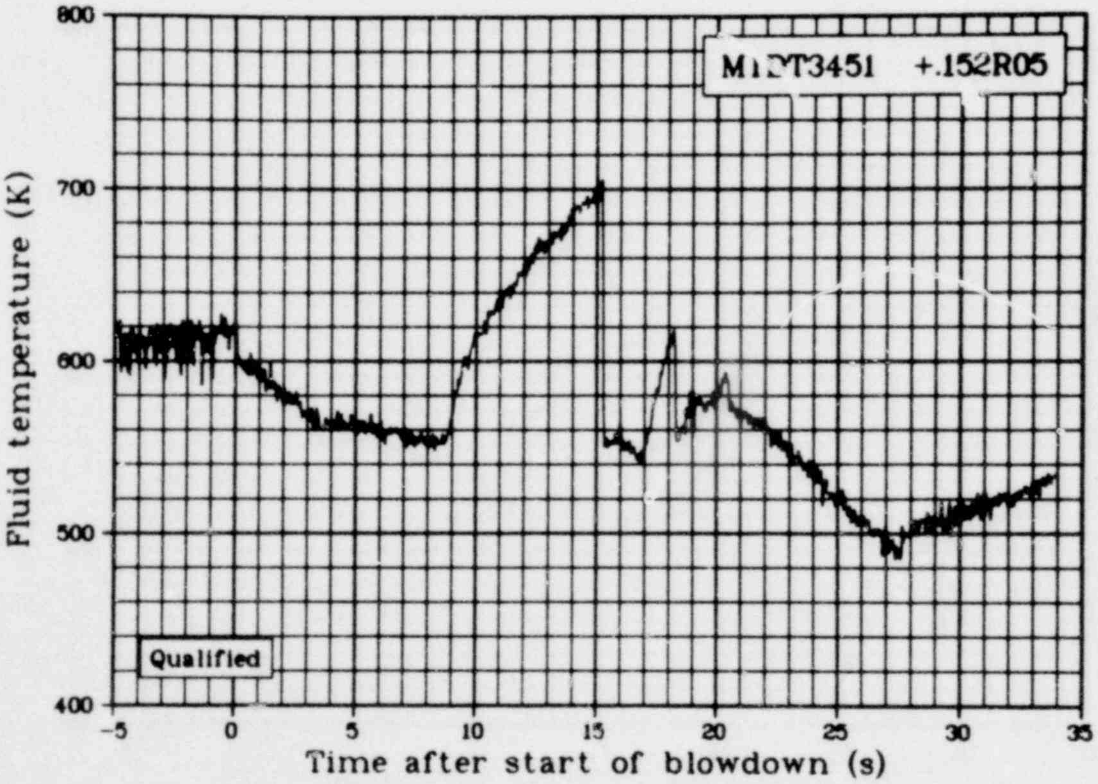

Fig. 386 Fluid temperature of Fuel Rod 345-1, 0.152 m above fuel stack midplane (MIDT3451 + .152R05), from -5 to 35 s.

1405 28~~5~~6

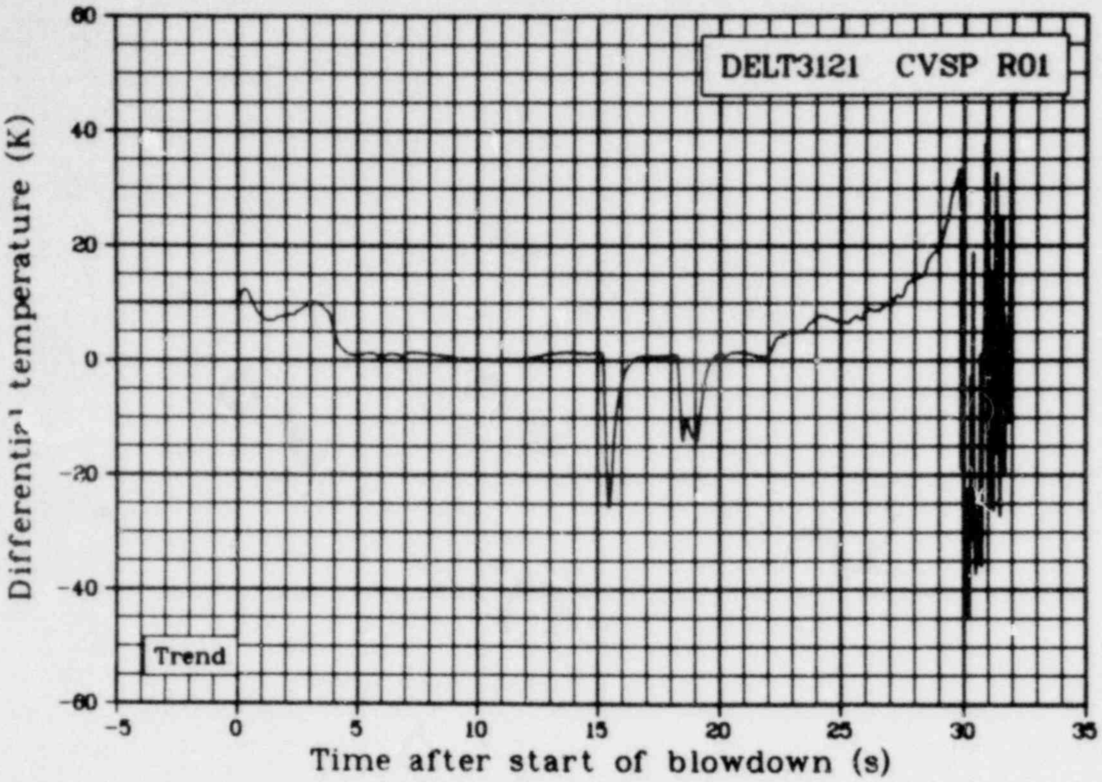

Fig. 387 Differential temperature of Rod 312-1, from support plate to outlet check valve (DELT3121 CVSP R01), from -5 to 35 s.

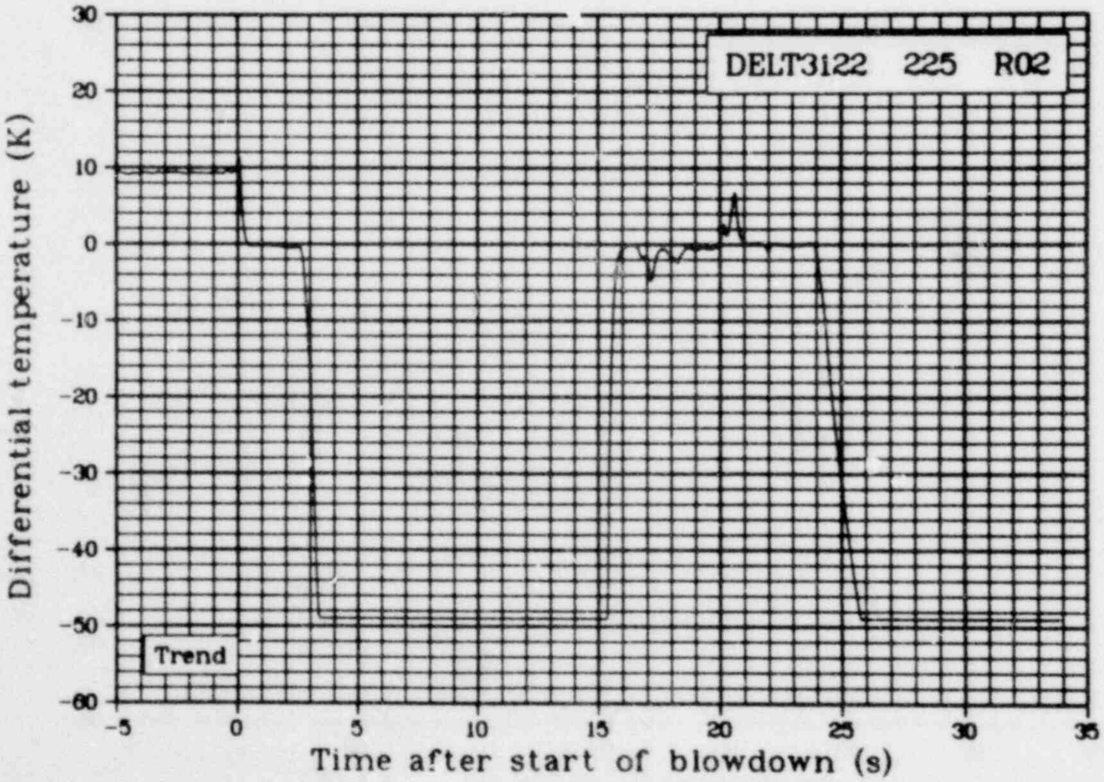

Fig. 388 Differential temperature of Rod 312-2, coolant inlet and outlet (DELT3122 225 R02), from -5 to 35 s.

1405 28~~6~~7

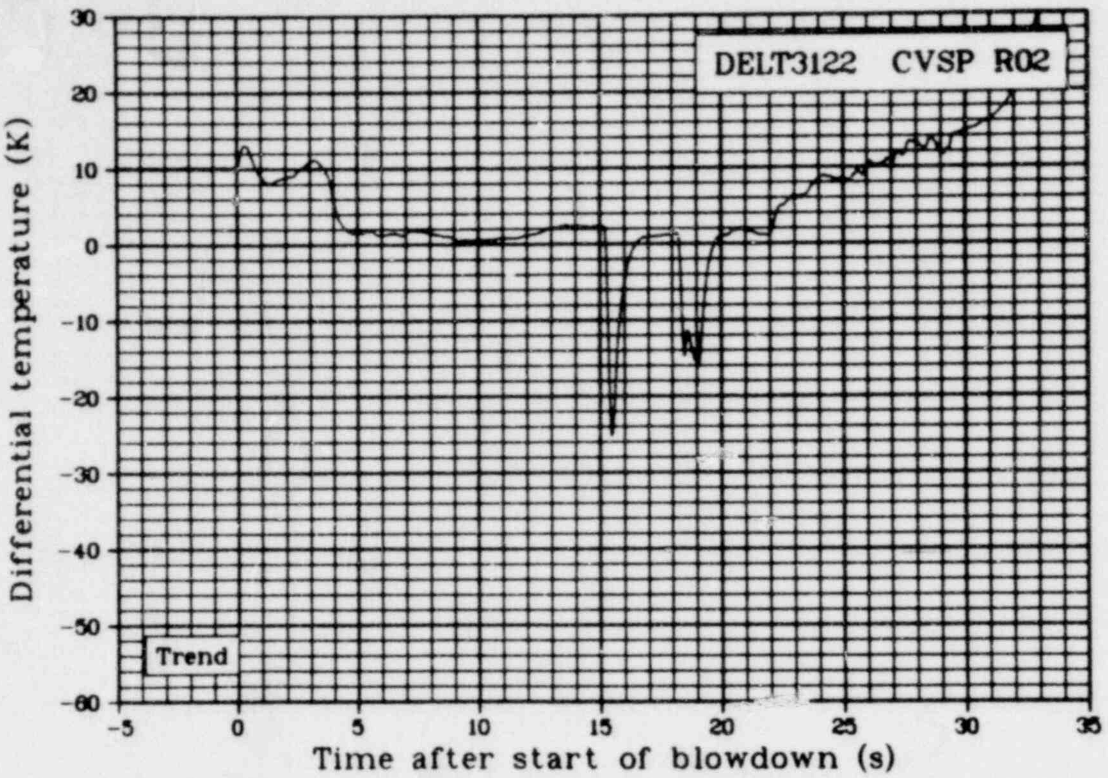

Fig. 389 Differential temperature of Rod 312-2, from support plate to outlet check valve (DELT3122 CVSP R02), from -5 to 35 s.

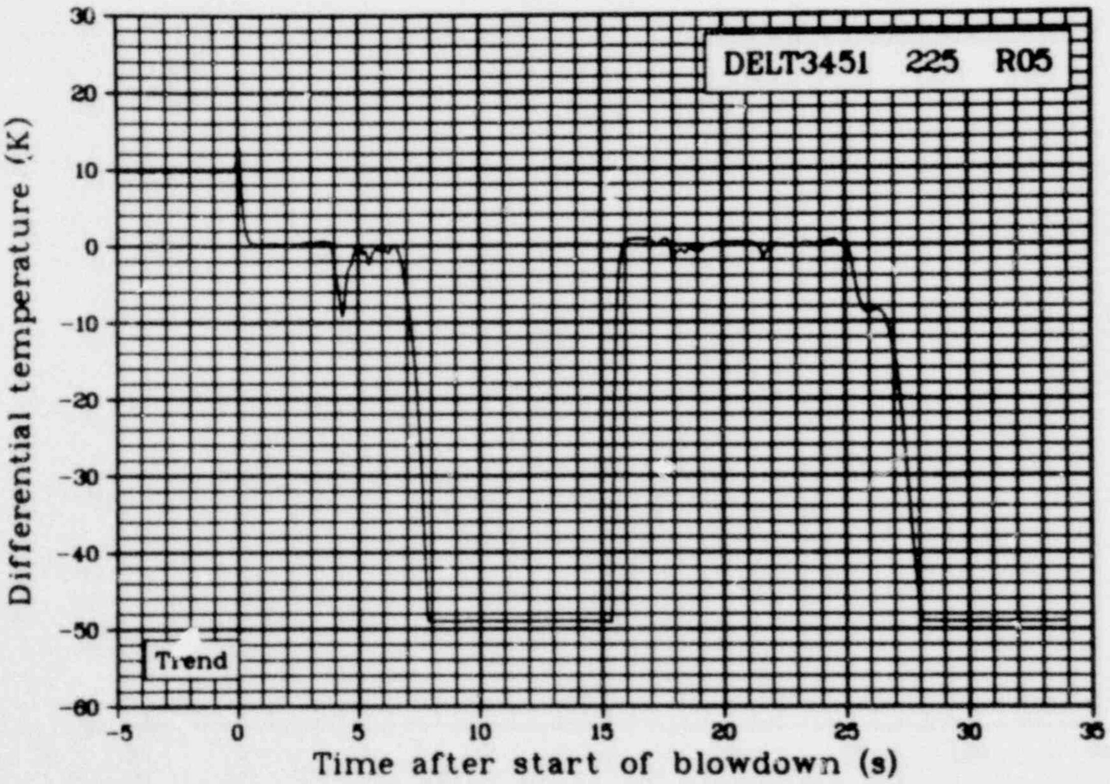

Fig. 390 Differential temperature of Rod 345-1 coolant inlet and outlet (DELT3451 225 R05), from -5 to 35 s.

1405 288

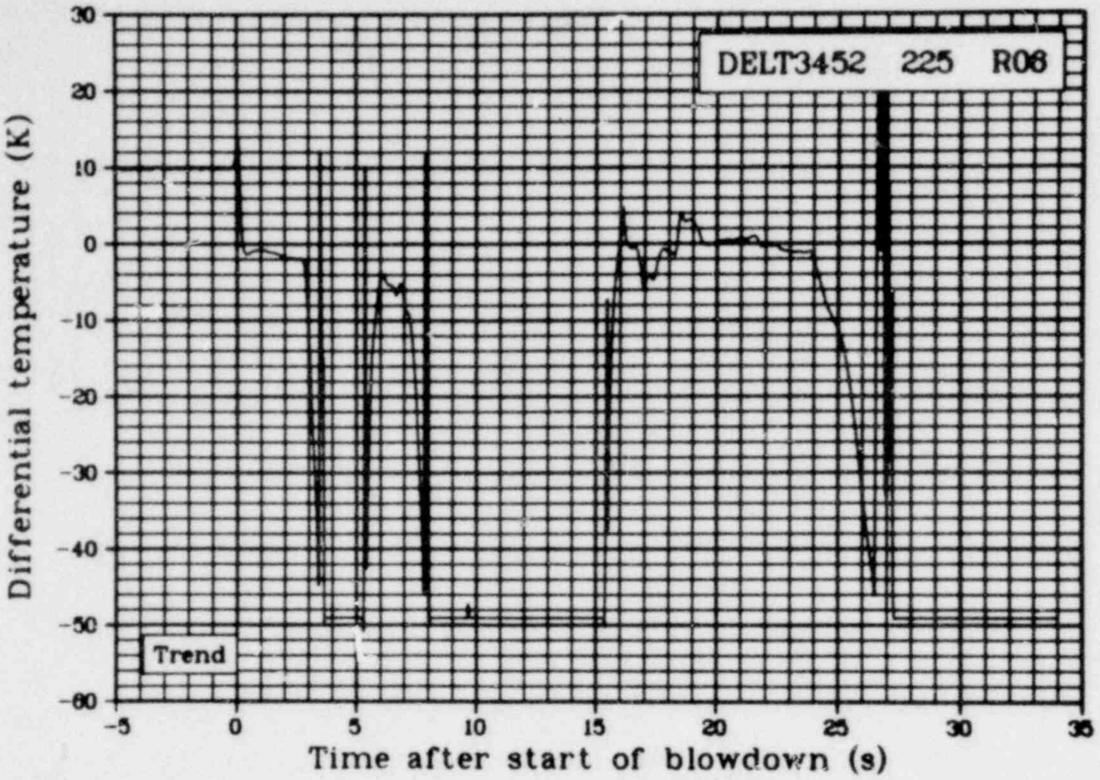

Fig. 391 Differential temperature of Rod 345-2, coolant inlet and outlet (DELT3452 225 R06), from -5 to 35 s.

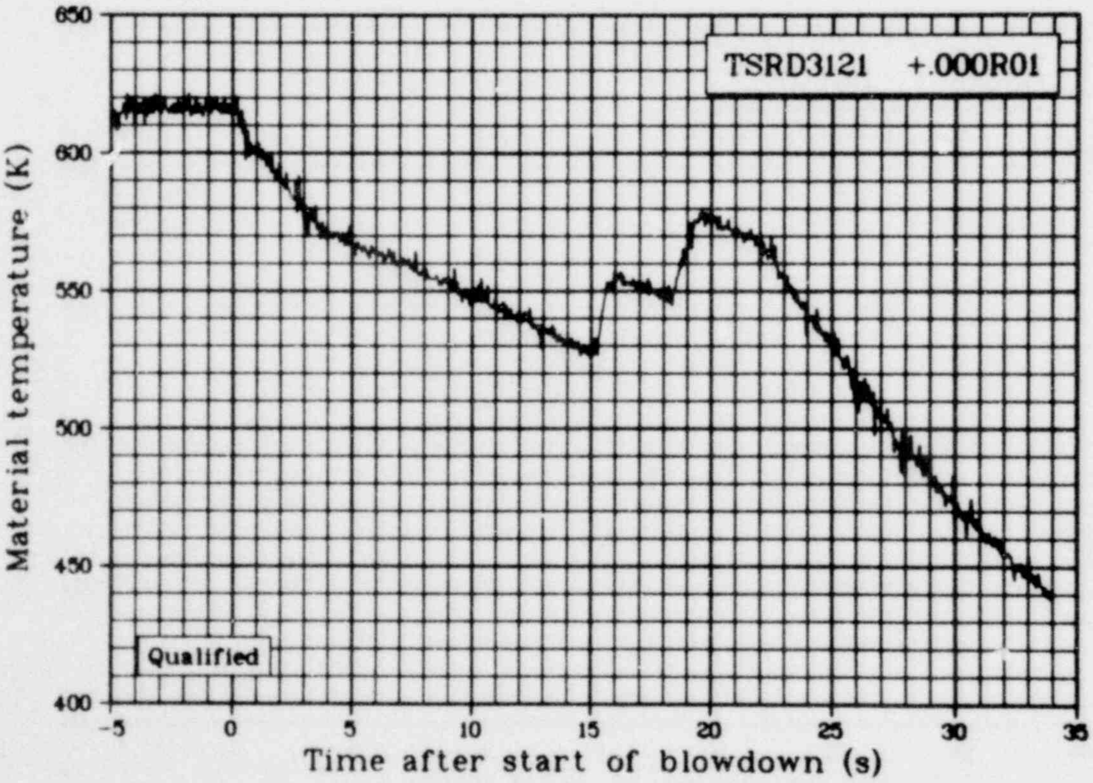

Fig. 392 Material temperature, Rod 312-1 shroud, at fuel stack midplane (TSRD3121 + .000R01), from -5 to 35 s.

1405 289

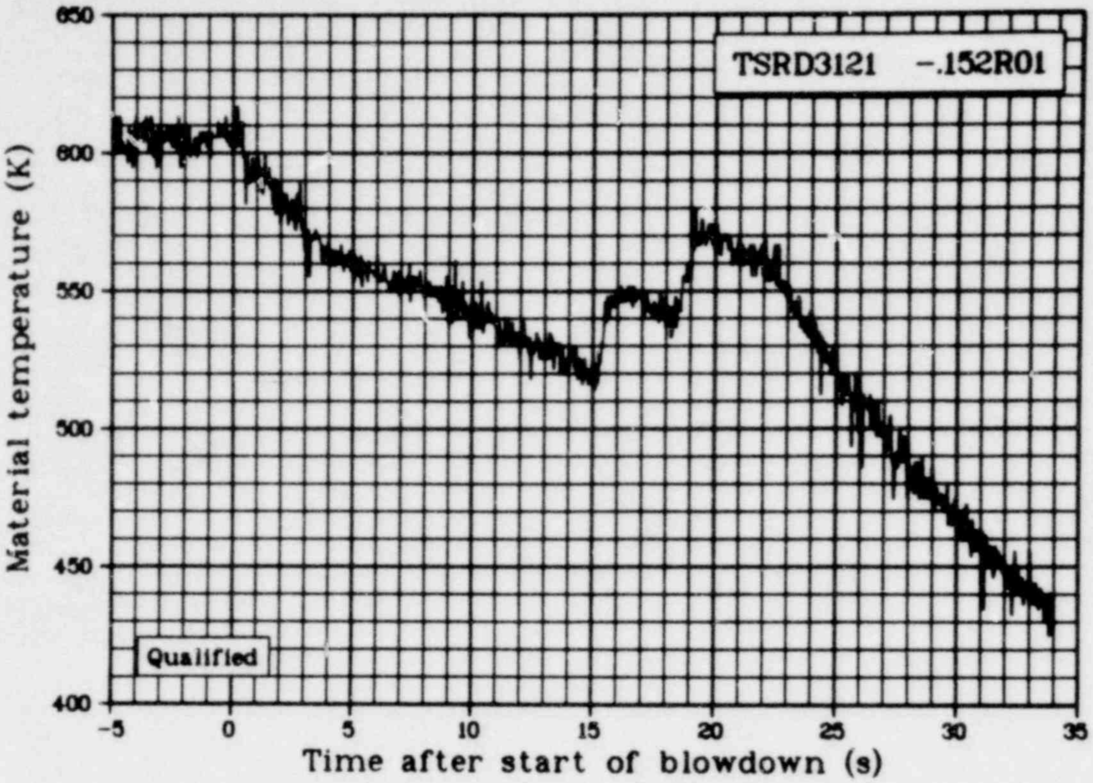

Fig. 393 Material temperature, Rod 312-1 shroud, 0.152 m below fuel stack midplane (TSRD3121 -.152R01), from -5 to 35 s.

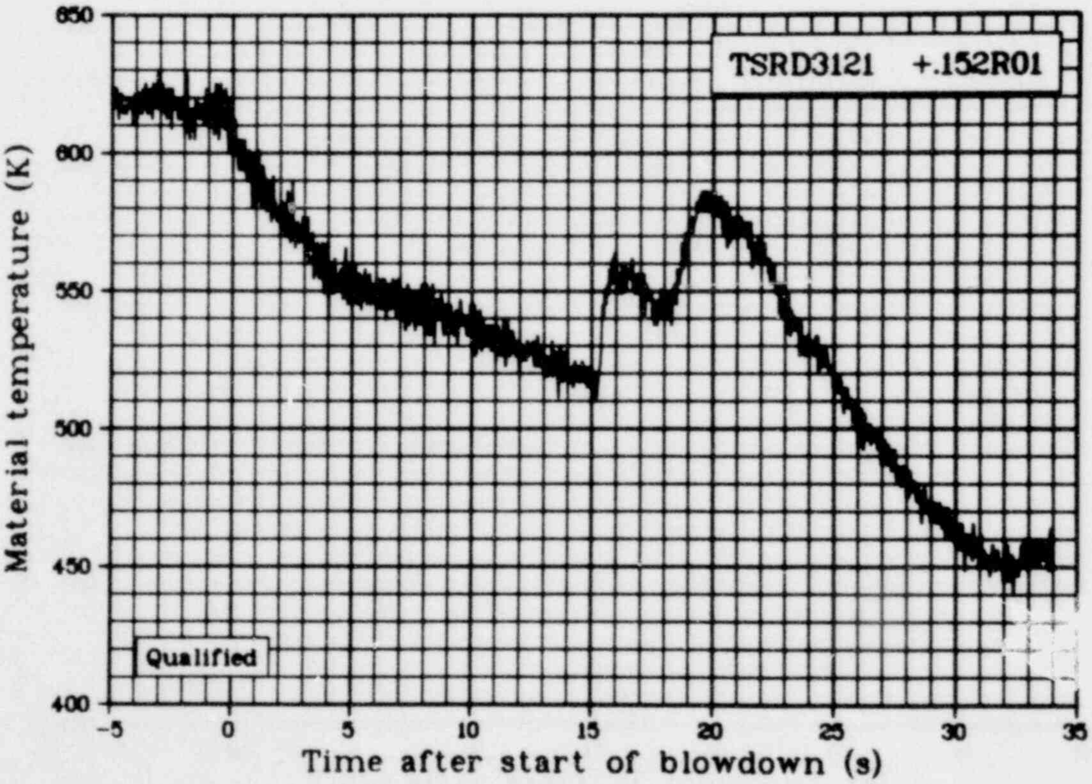

Fig. 394 Material temperature, Rod 312-1 shroud, 0.152 m above fuel stack midplane (TSRD3121 +.152R01), from -5 to 35 s.

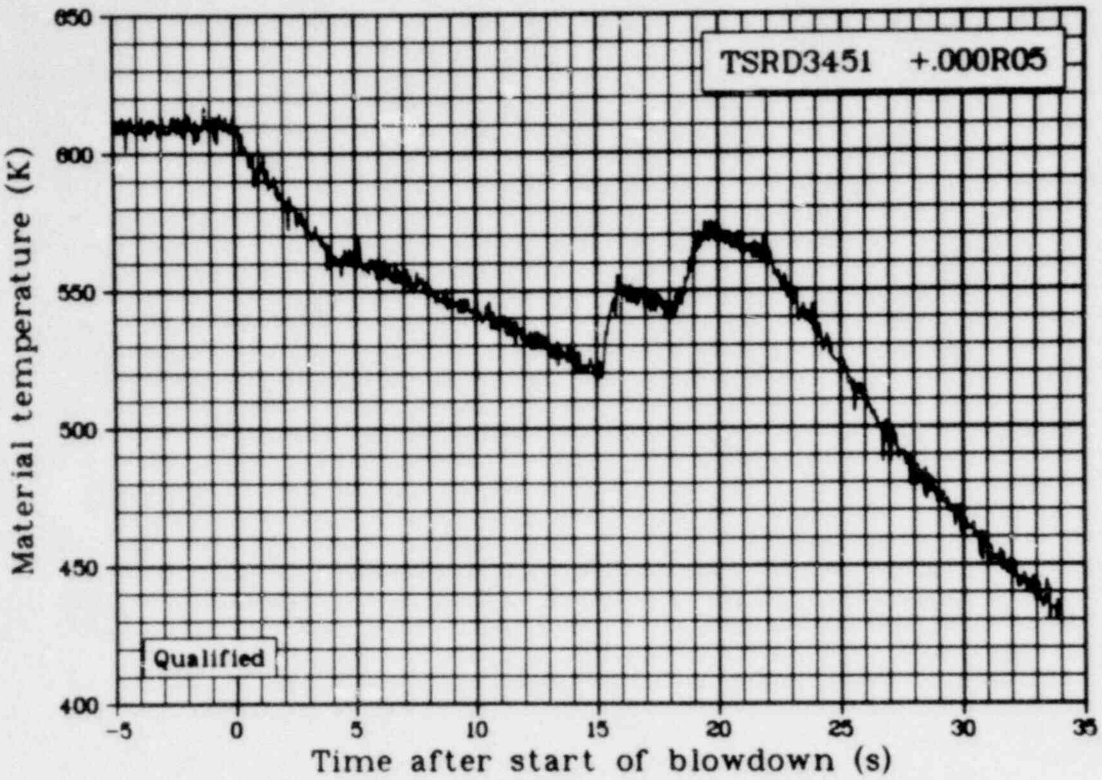

Fig. 395 Material temperature, Rod 345-1 shroud, at fuel stack midplane (TSRD3451 + .000R05), from -5 to 35 s.

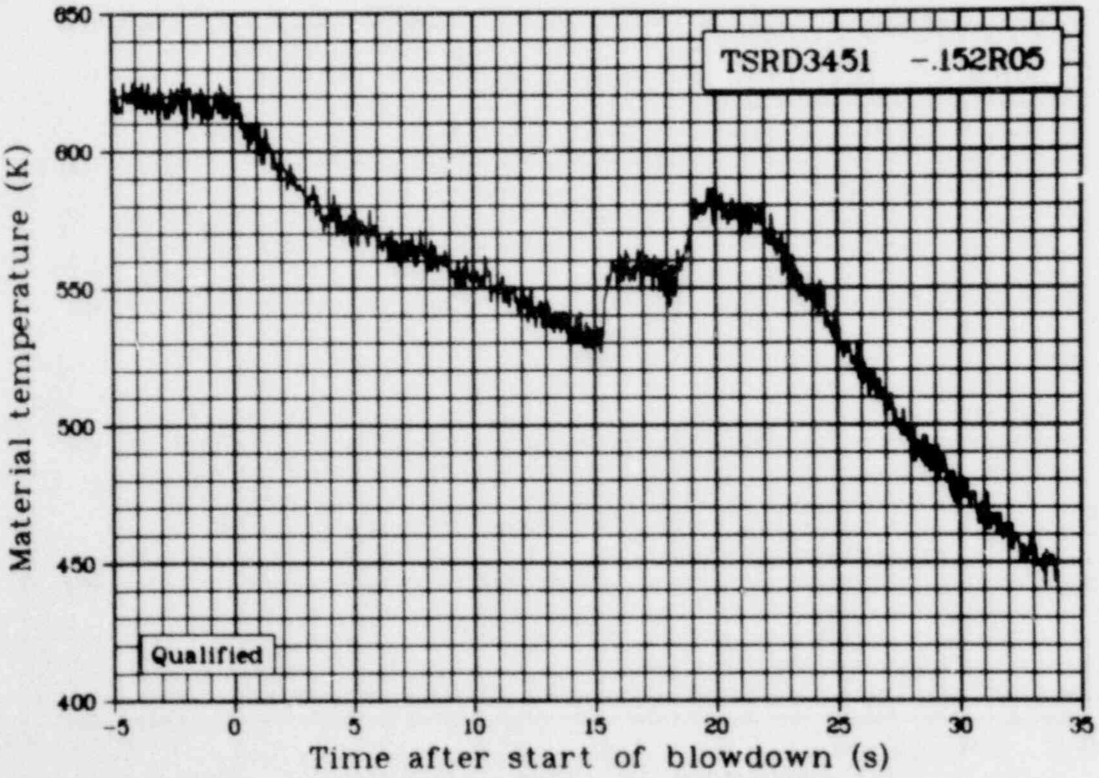

Fig. 396 Material temperature, Rod 345-1 shroud, 0.152 m below fuel stack midplane (TSRD3451 -.152R05), from -5 to 35 s.

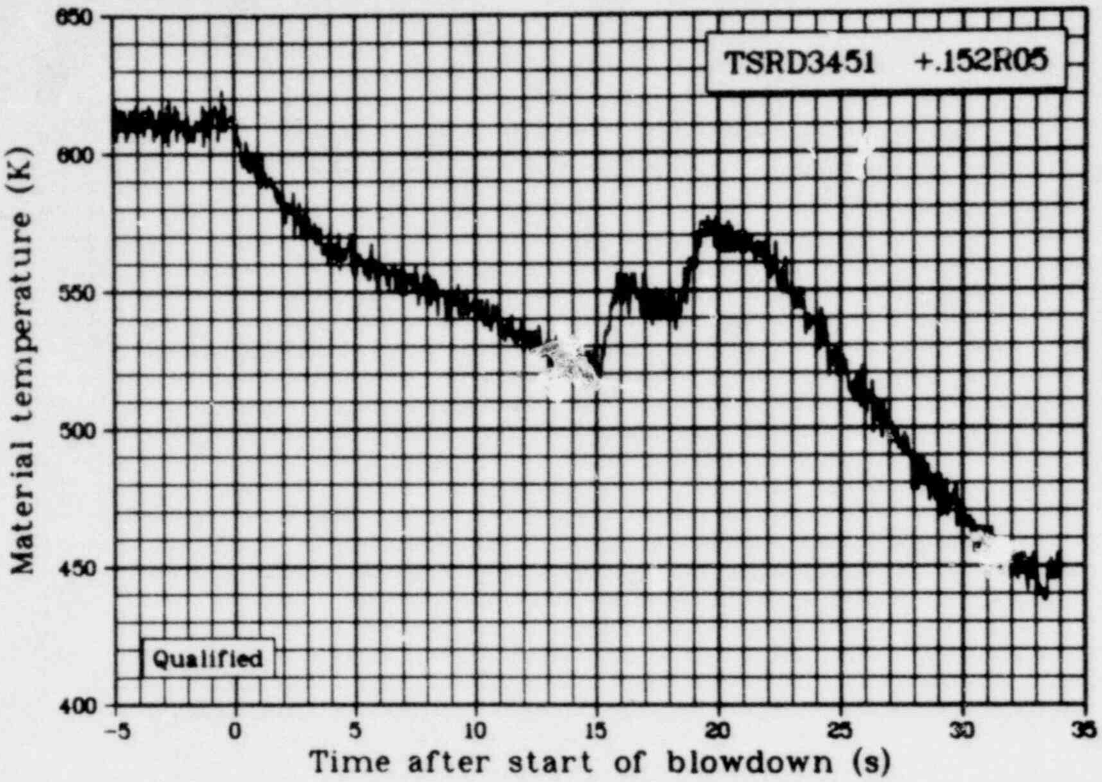

Fig. 397 Material temperature, Rod 345-1 shroud, 0.152 m above fuel stack midplane (TSRD3451 +.152R05), from -5 to 35 s.

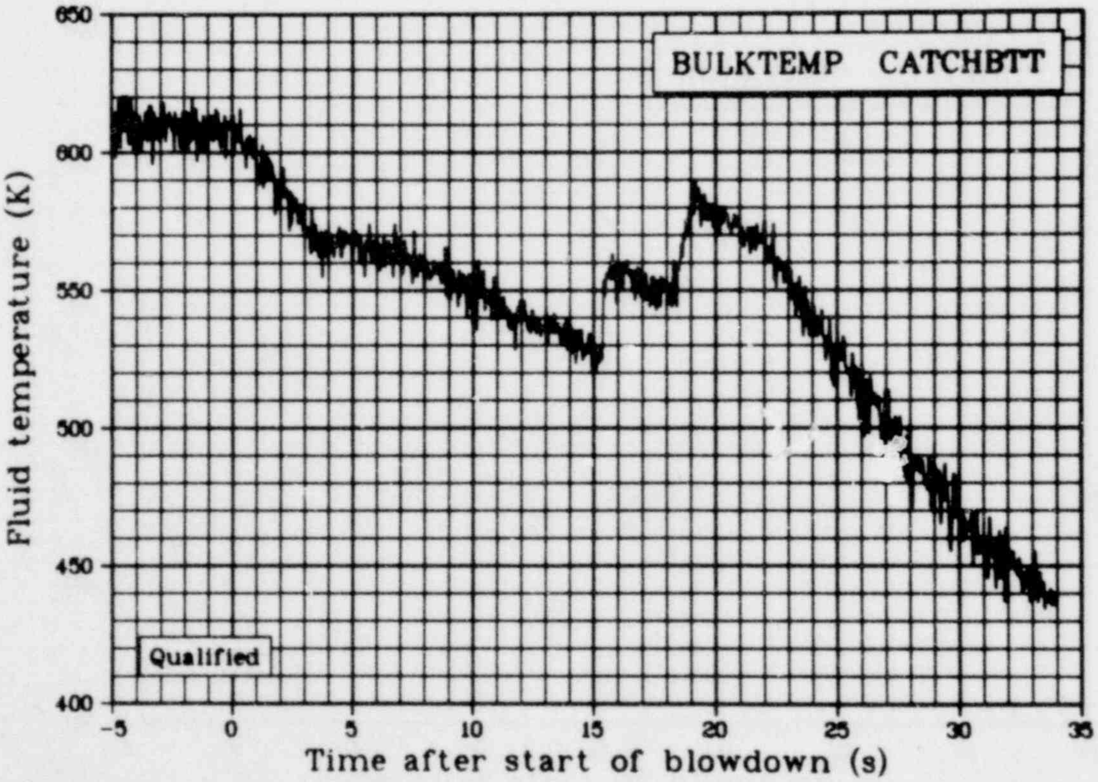

Fig. 398 Fluid temperature in test train catch basket (BULKTEMP CATCHBTT), from -5 to 35 s.

1405 292

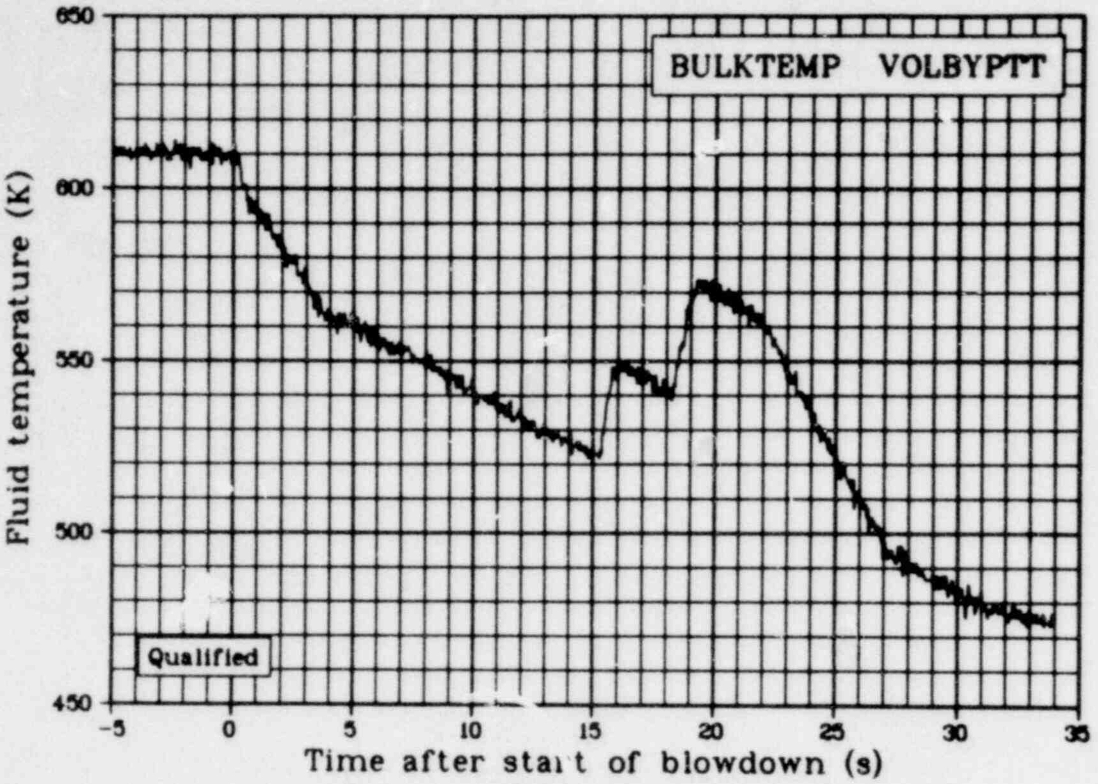

Fig. 399 Fluid temperature in bypass volume at fuel stack midplane (BULKTEMP VOLBYPTT), from -5 to 35 s.

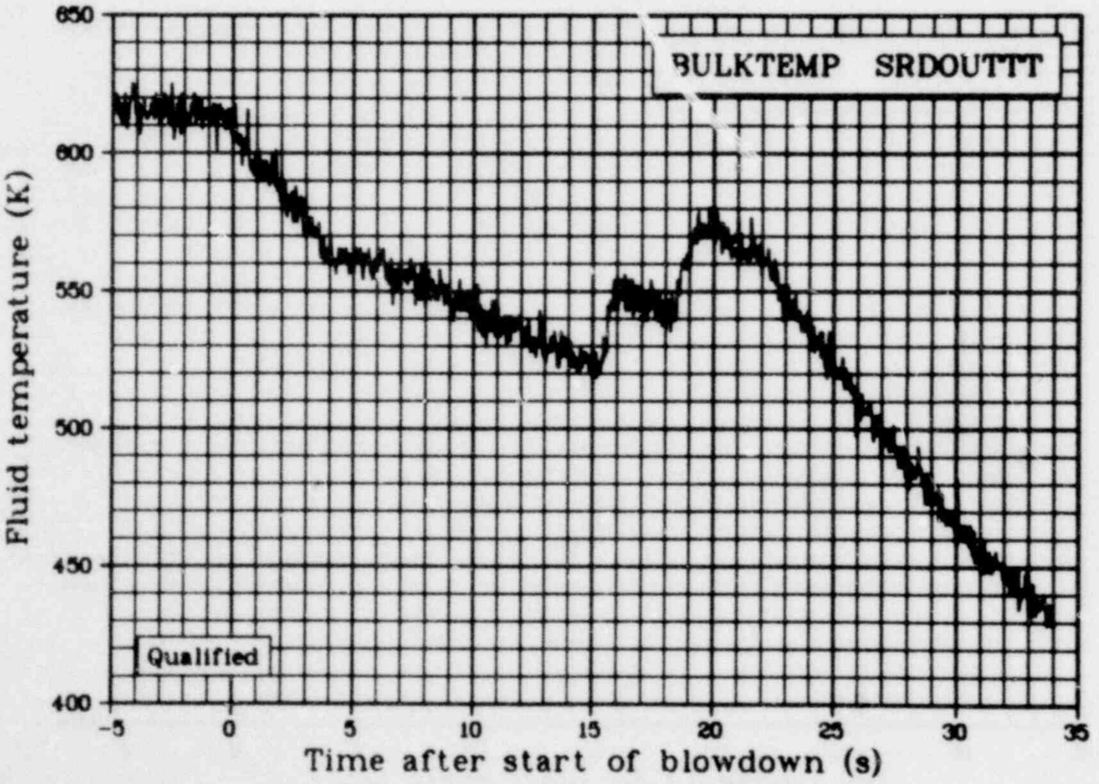

Fig. 400 Fluid temperature 0.05 m above flow shroud outlets (BULKTEMP SRDOUTTT), from -5 to 35 s.

1405 293

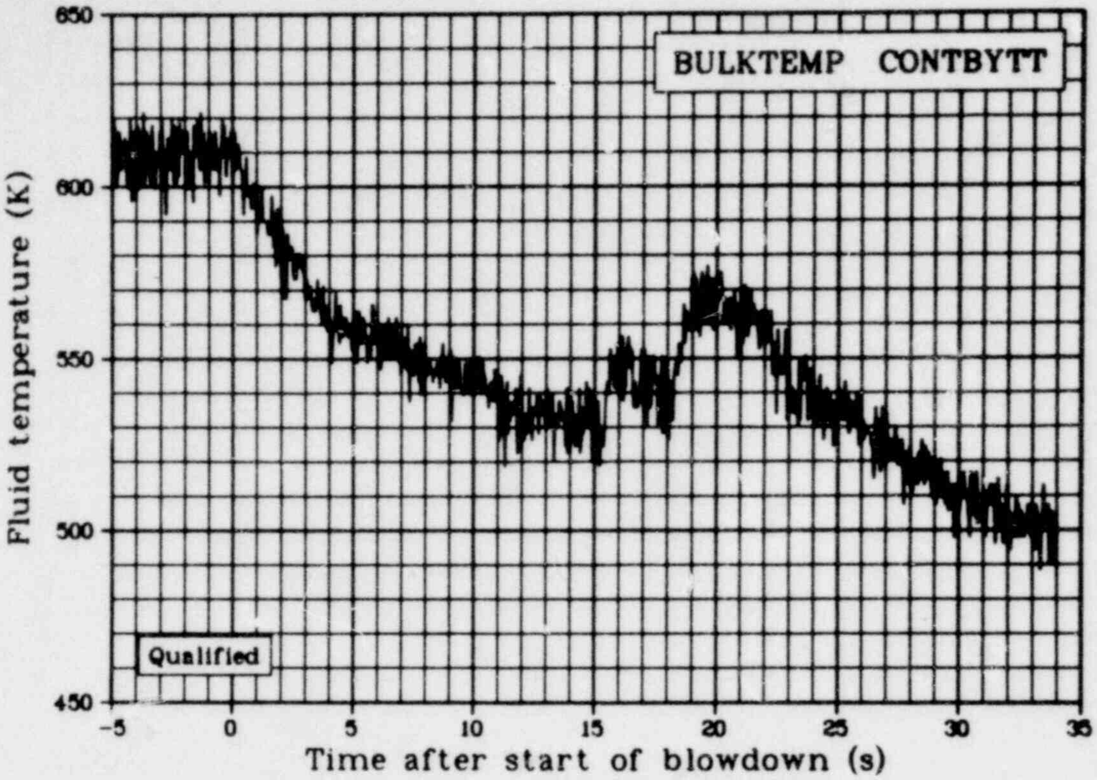

Fig. 401 Fluid temperature at test train controlled bypass inlet (BULKTEMP CONTBYTT), from -5 to 35 s.

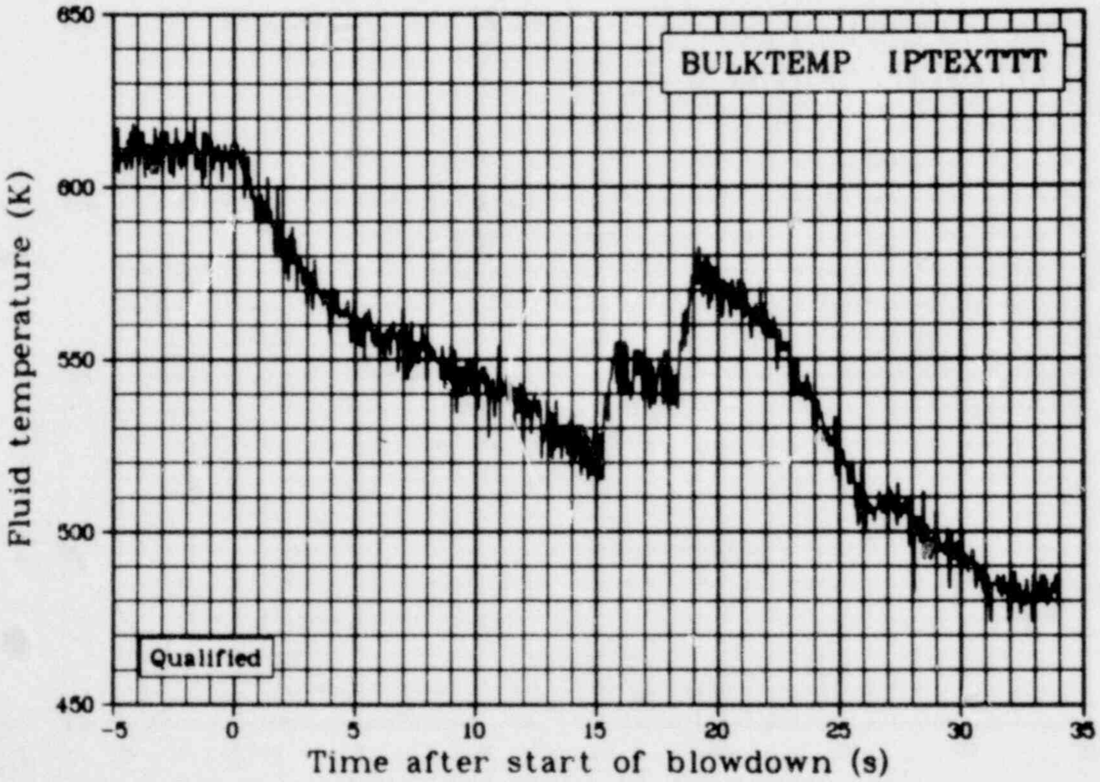

Fig. 402 Fluid temperature at IPT exit (BULKTEMP IPTEXTTT), from -5 to 35 s.

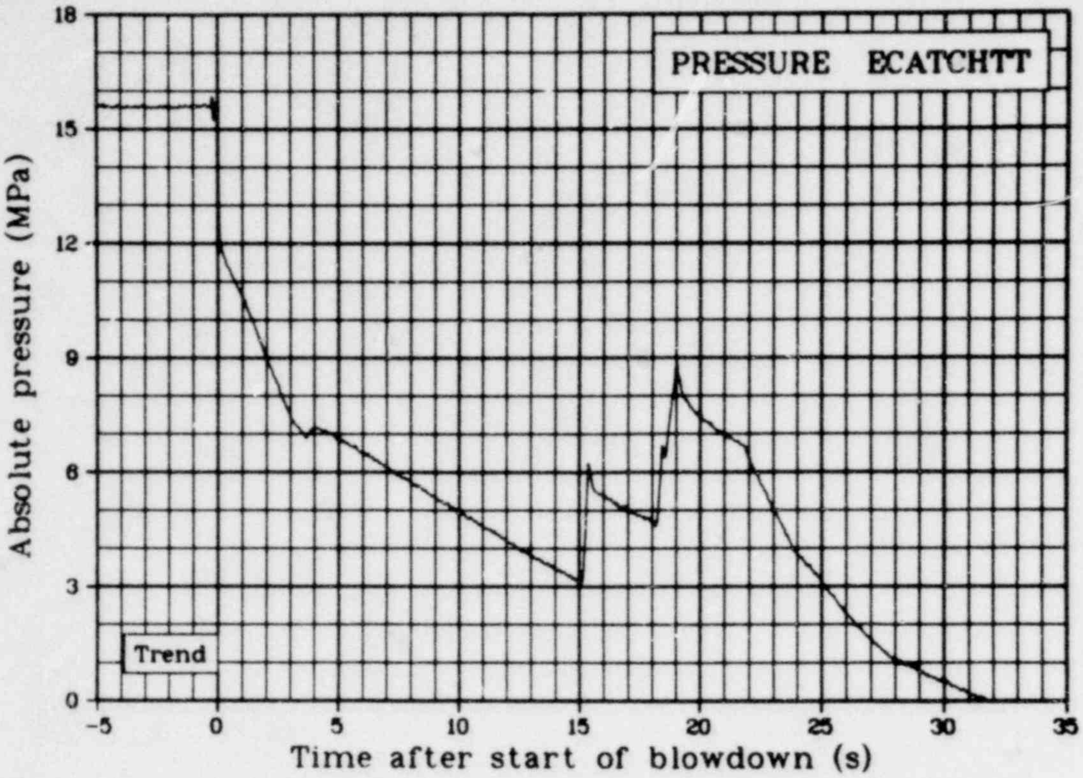

Fig. 403 Absolute pressure in test train catch basket (PRESSURE ECATCHTT), from -5 to 35 s.

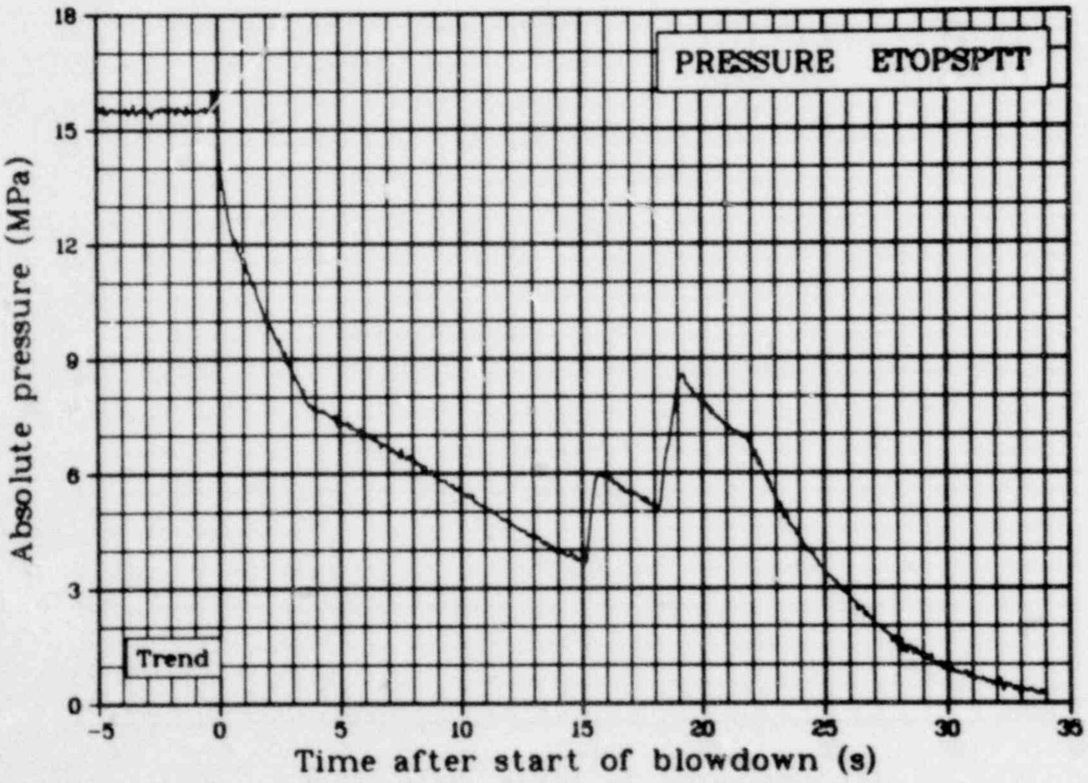

Fig. 404 Absolute pressure above the test train top support plate (PRESSURE ETOPSPTT), from -5 to 35 s.

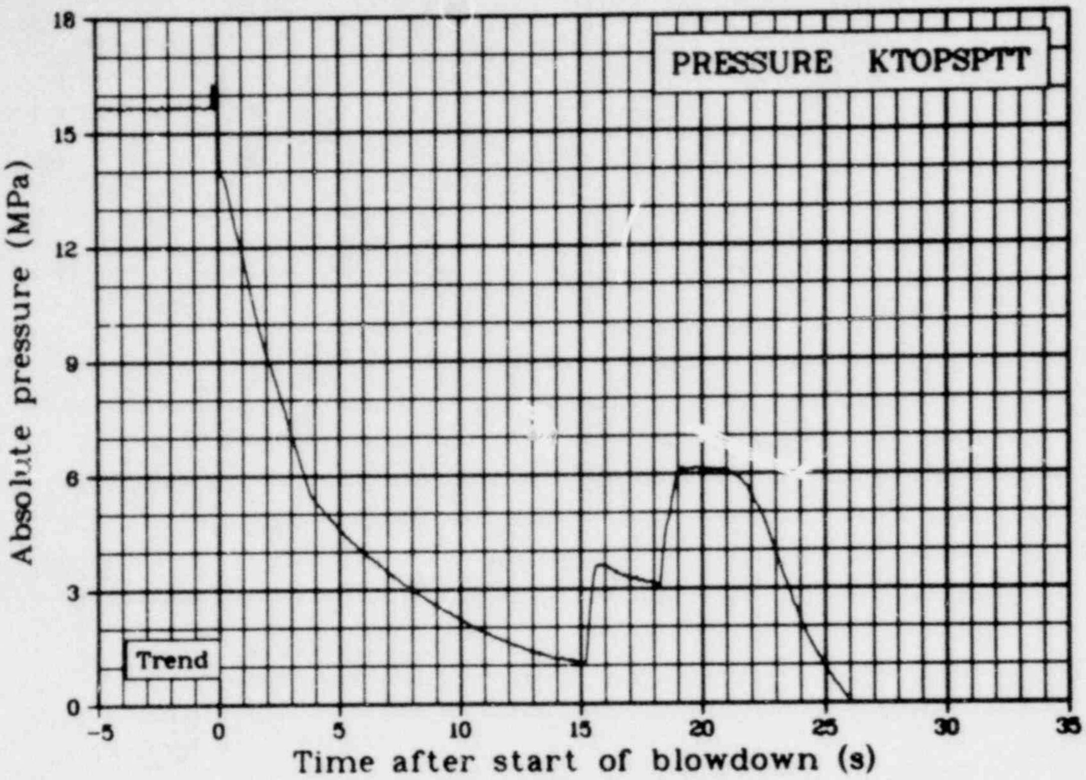

Fig. 405 Absolute pressure above the test train top support plate (PRESSURE KTOPSPTT), from -5 to 35 s.

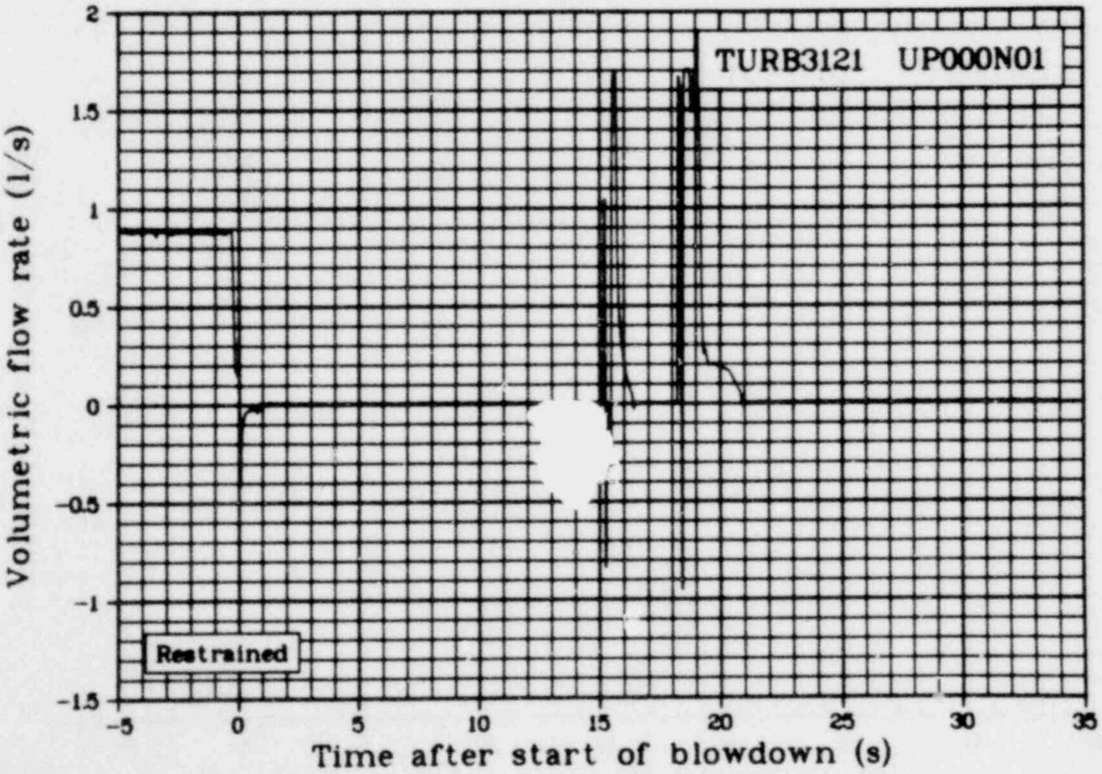

Fig. 406 Volumetric flow rate in Fuel Rod 312-1 upper shroud (TURB3121 UP000N01), from -5 to 35 s.

1405 296

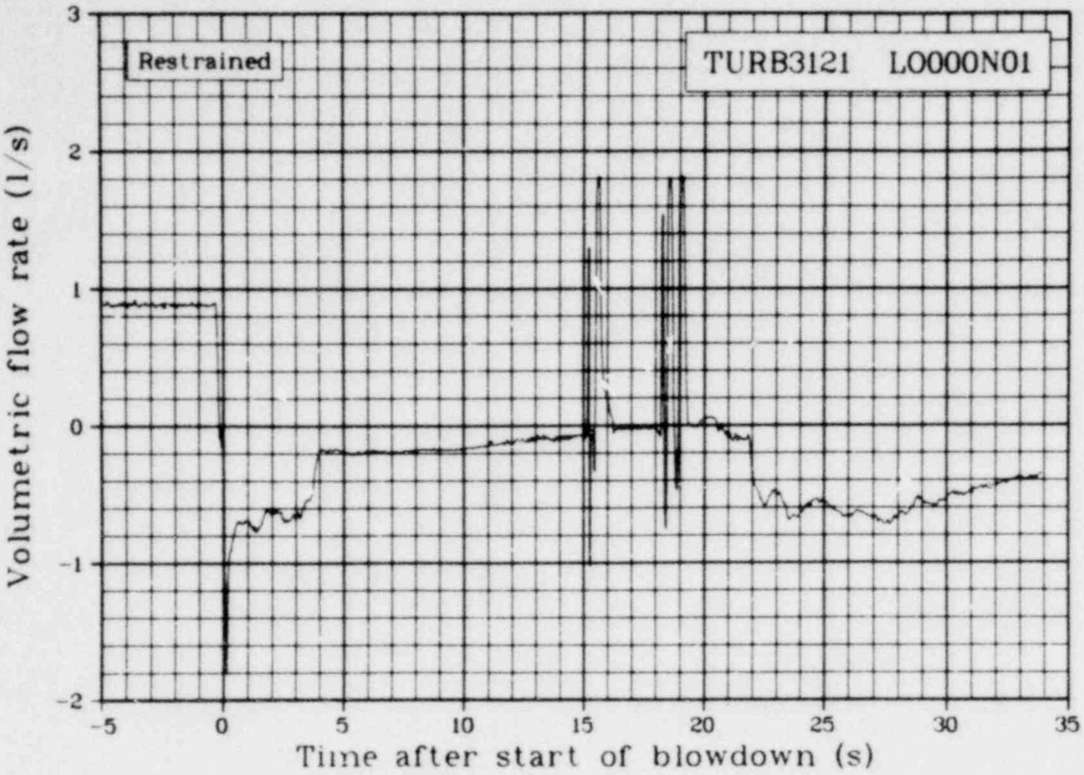

Fig. 407 Volumetric flow rate in Fuel Rod 312-1 lower shroud (TURB3121 L0000N01), from -5 to 35 s.

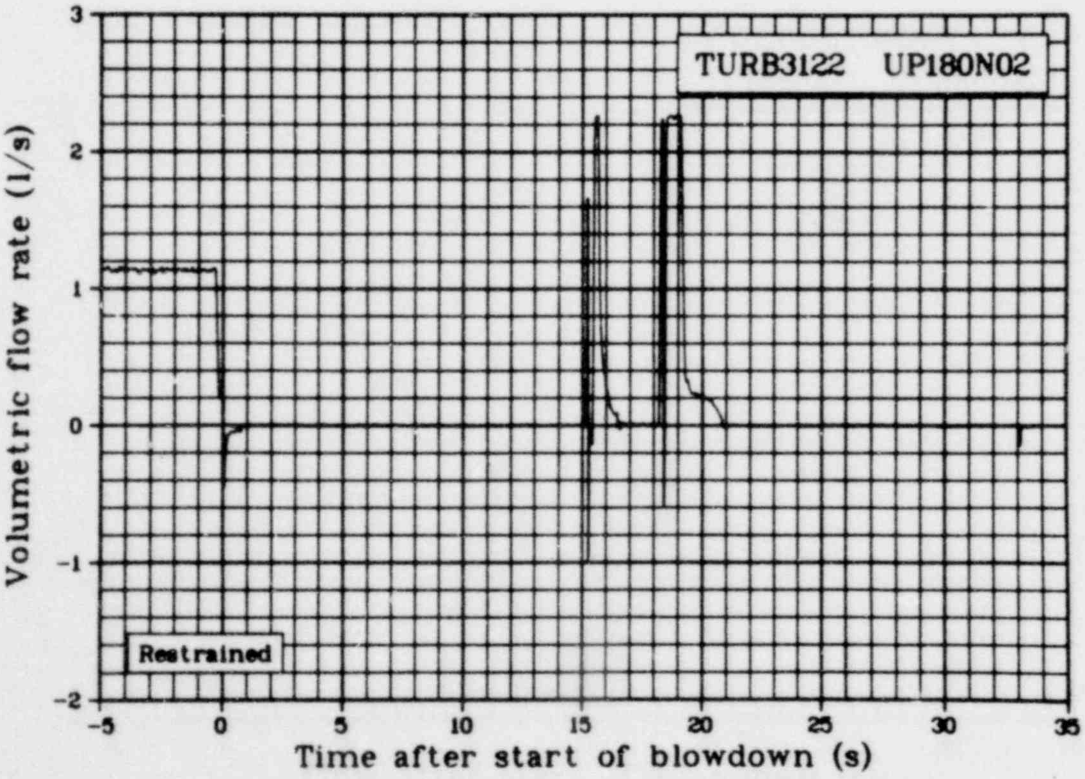

Fig. 408 Volumetric flow rate in Fuel Rod 312-2 upper shroud (TURB3122 UP180N02), from -5 to 35 s.

1405 296

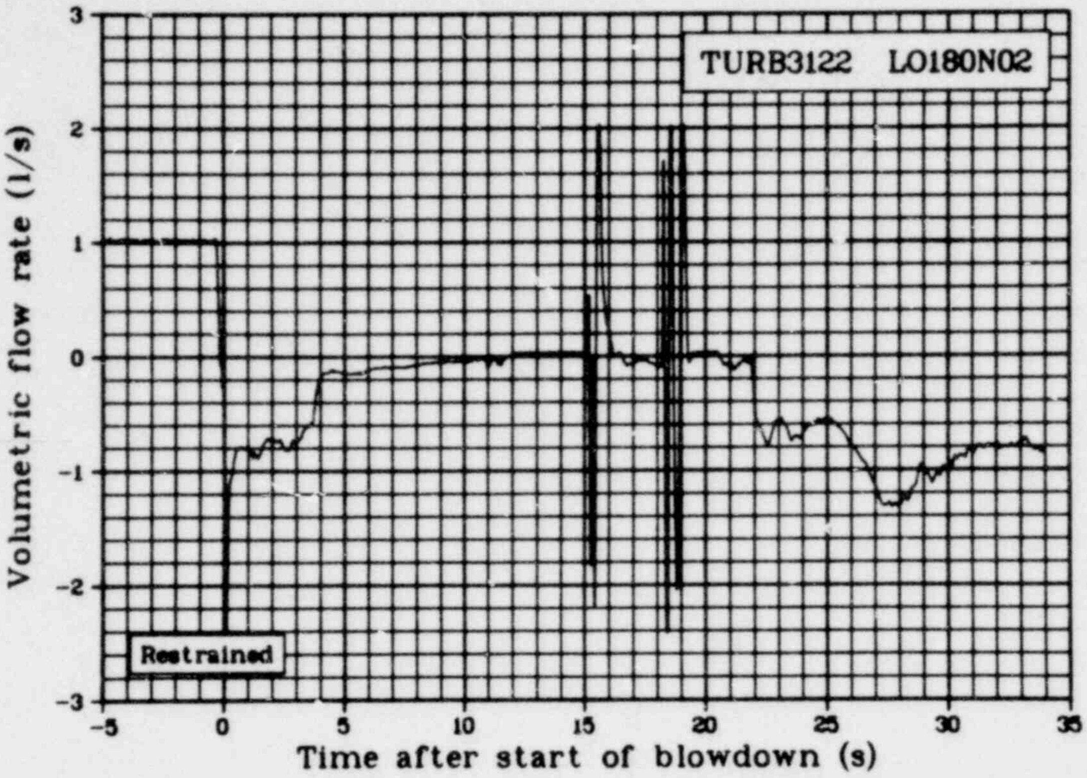

Fig. 409 Volumetric flow rate in Fuel Rod 312-2 lower shroud (TURB3122 L0180N02), from -5 to 35 s.

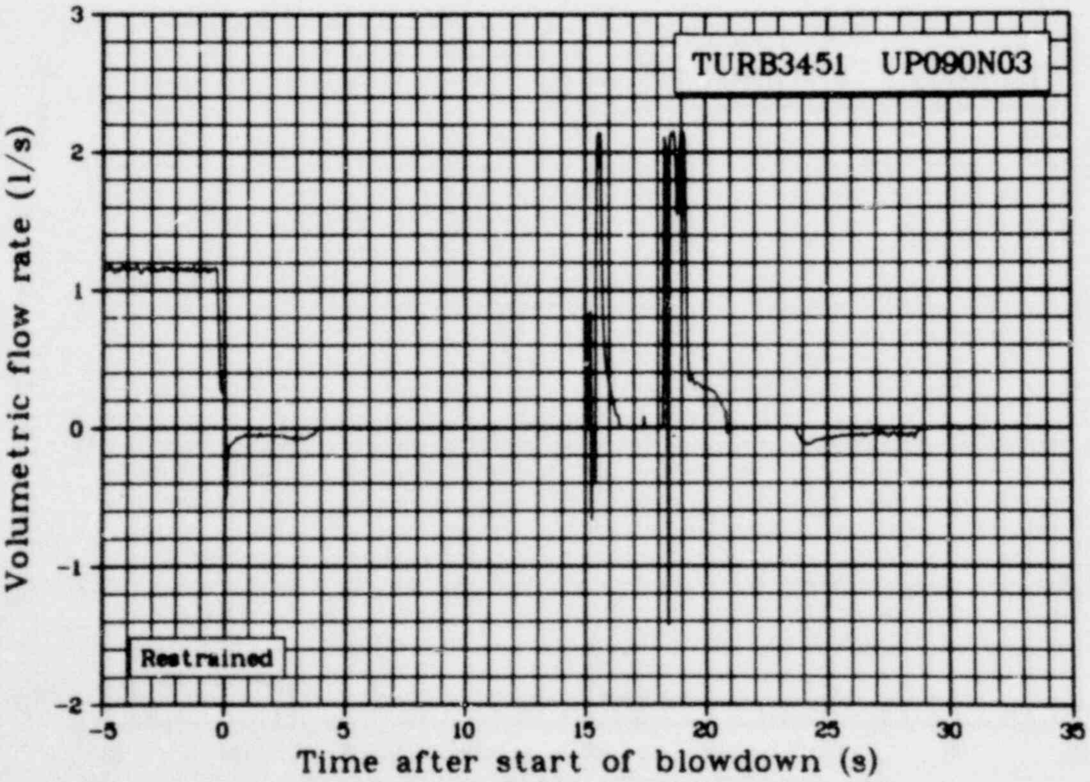

Fig. 410 Volumetric flow rate in Fuel Rod 345-1 upper shroud (TURB3451 UP090N03), from -5 to 35 s.

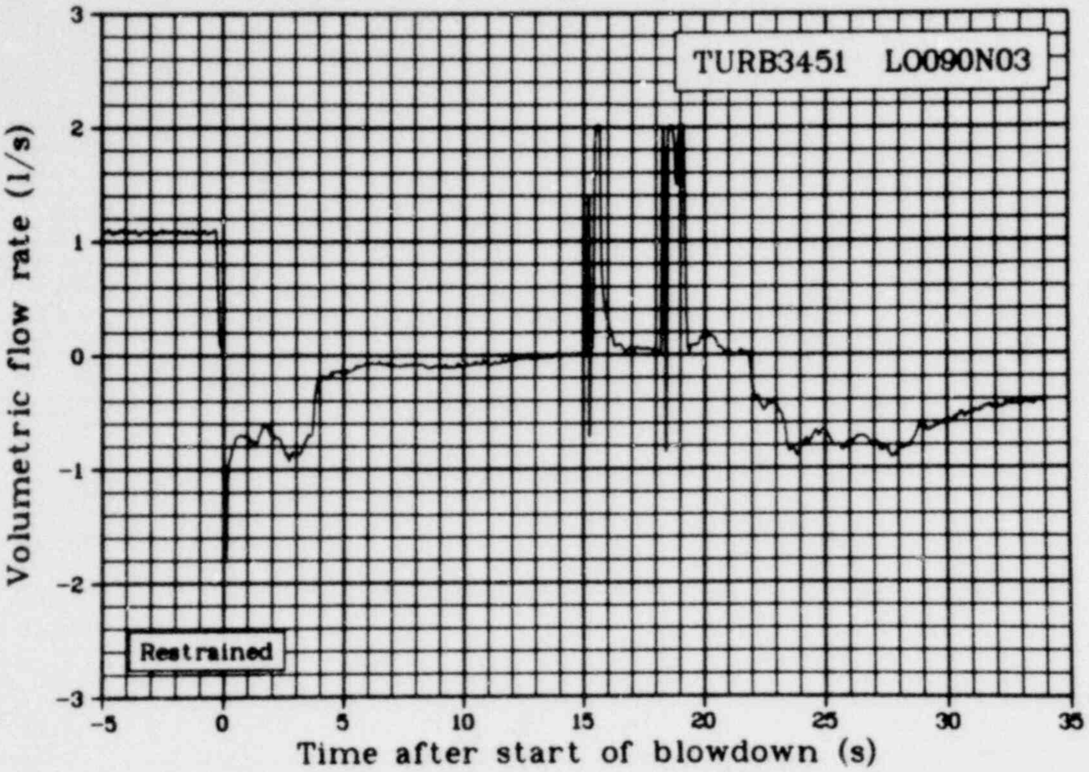

Fig. 411 Volumetric flow rate in Fuel Rod 345-1 lower shroud (TURB3451 L0090N03), from -5 to 35 s.

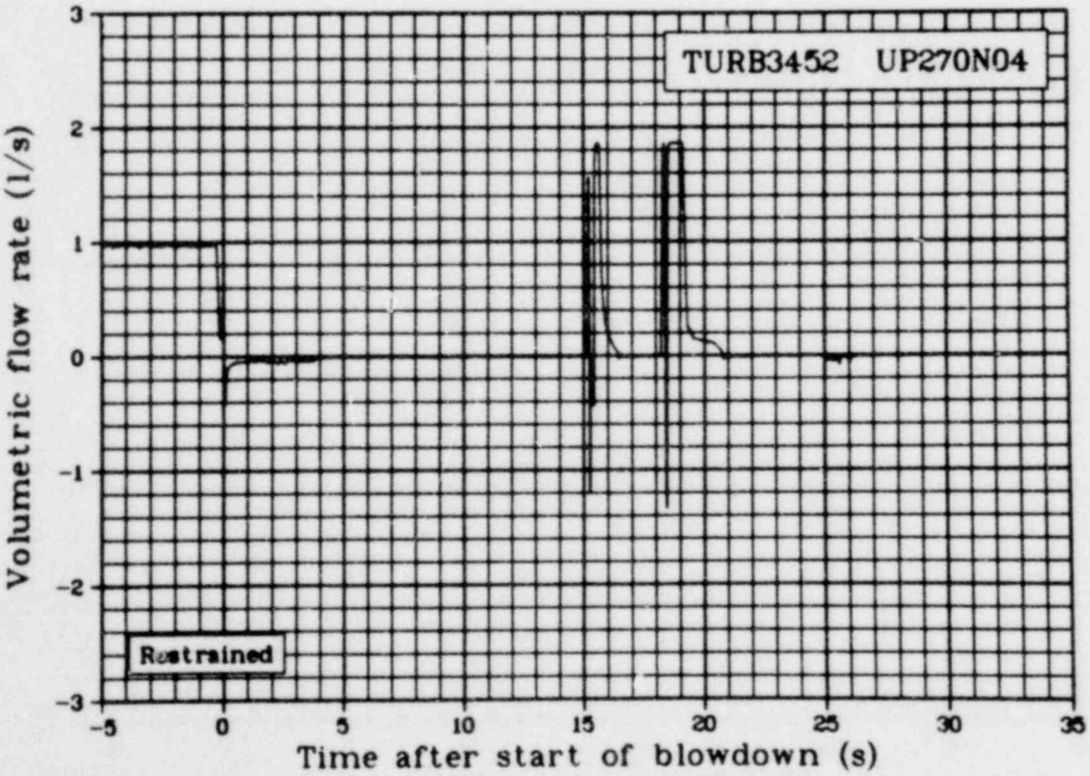

Fig. 412 Volumetric flow rate in Fuel Rod 345-2 upper shroud (TURB3452 UP270N04), from -5 to 35 s.

9
1405 298

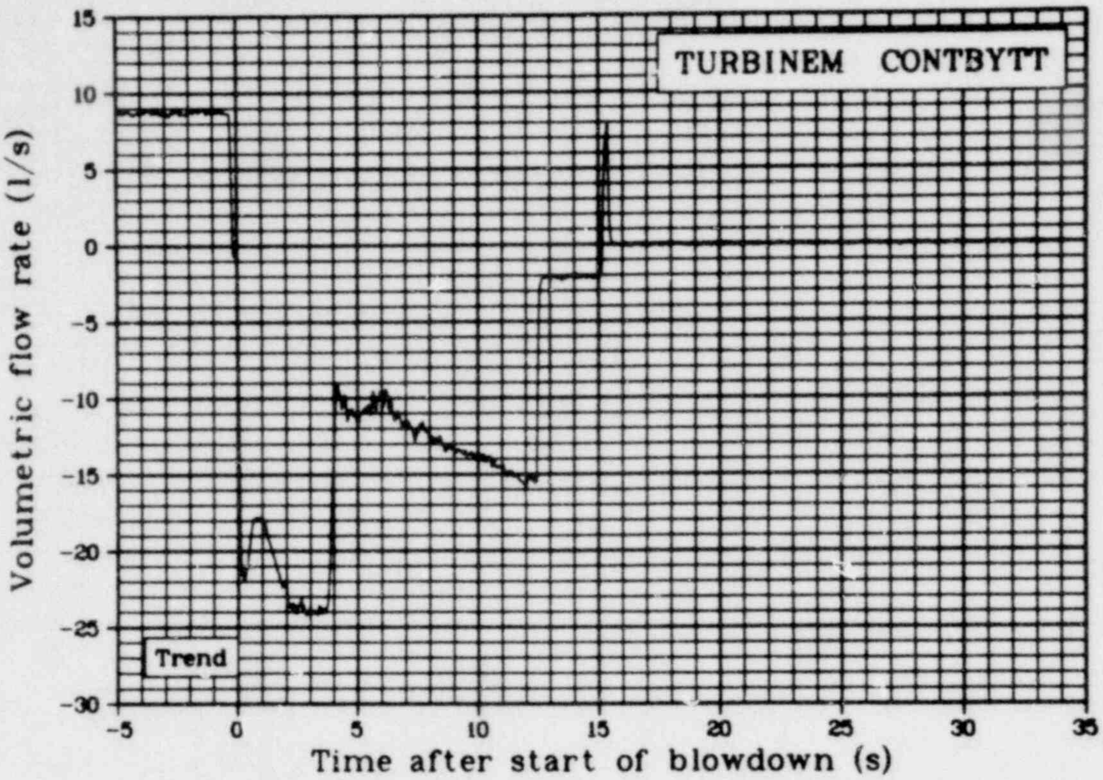

Fig. 413 Volumetric flow rate in test train controlled bypass (TURBINEM CONTBYTT), from -5 to 35 s.

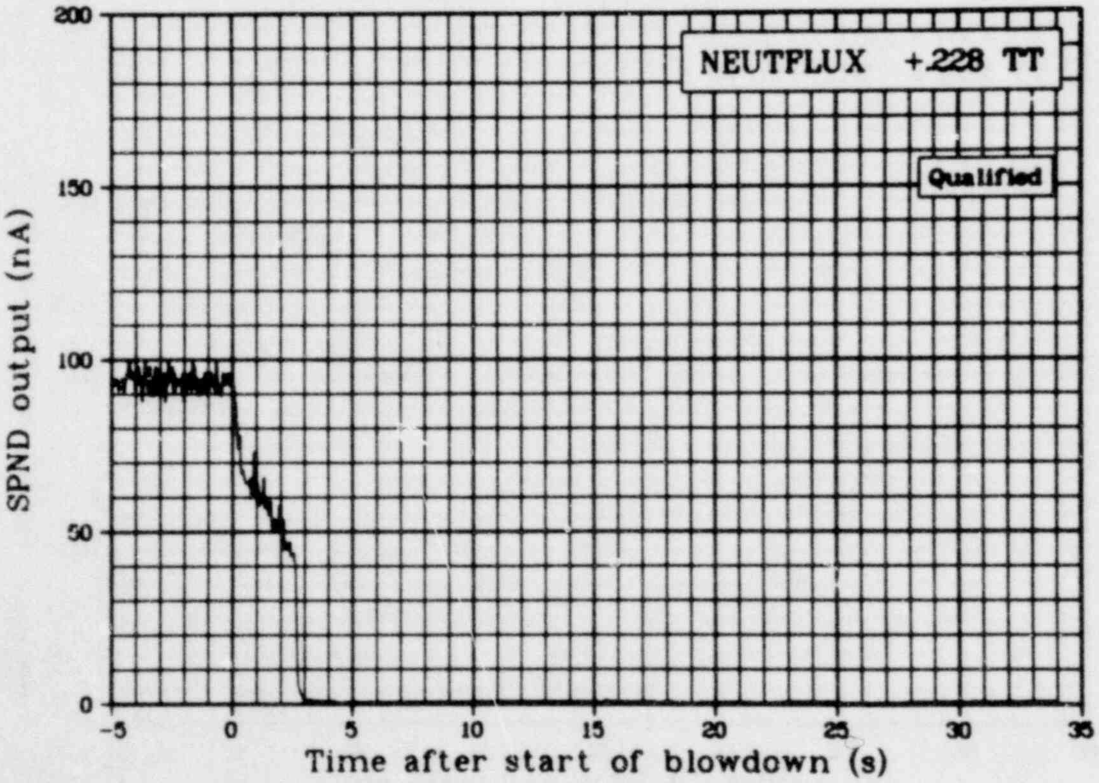

Fig. 414 Neutron flux 0.228 m above fuel stack midplane (NEUTFLUX + .228 TT), from -5 to 35 s.

1405 ~~299~~ 300

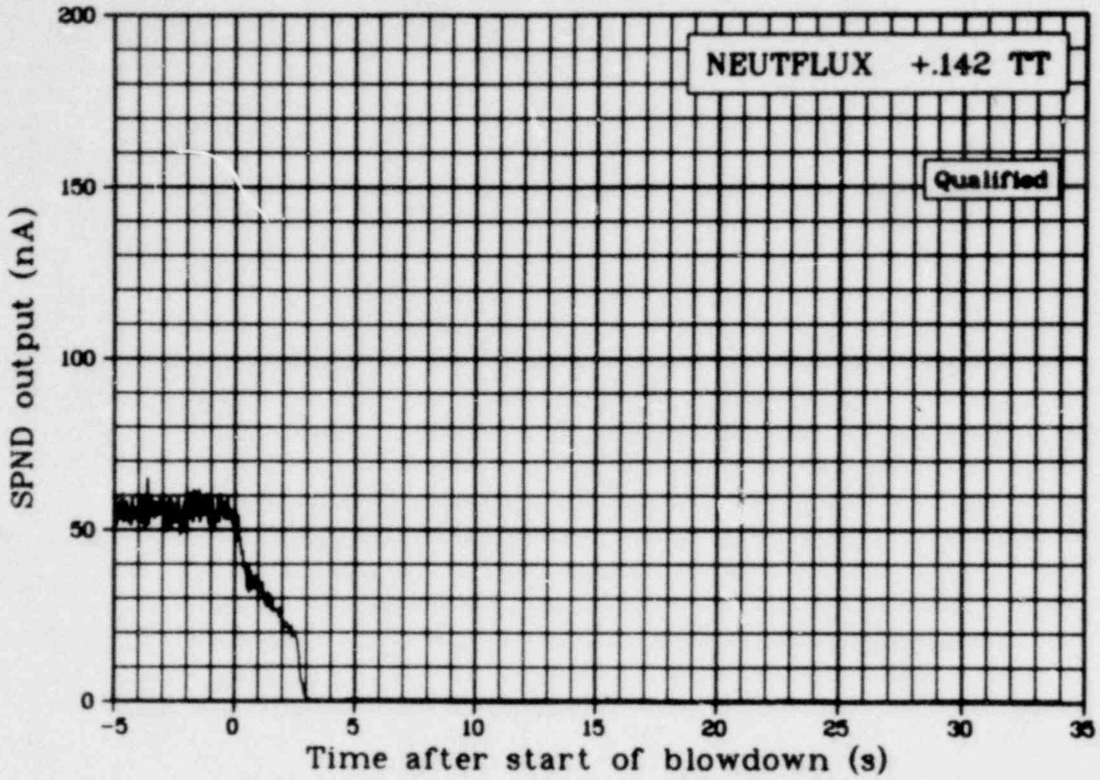

Fig. 415 Neutron flux 0.142 m above fuel stack midplane (NEUTFLUX +.142 TT), from -5 to 35 s.

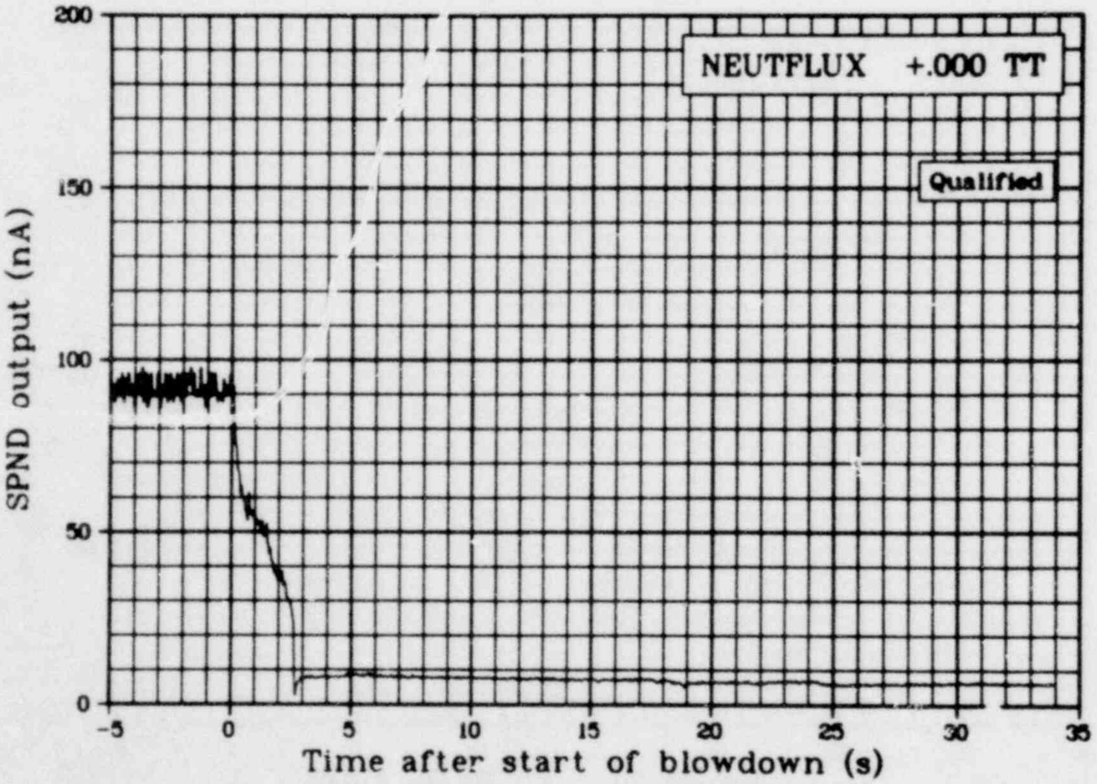

Fig. 416 Neutron flux at fuel stack midplane (NEUTFLUX +.000 TT), from -5 to 35 s.

1405 308

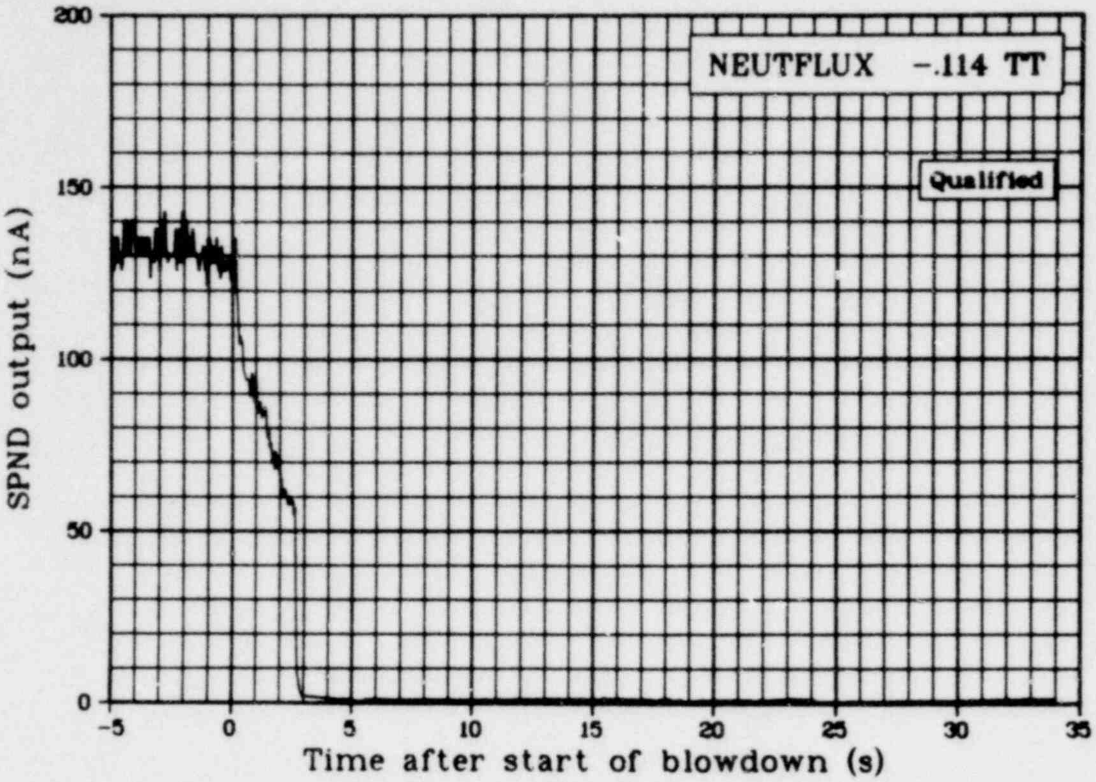

Fig. 417 Neutron flux 0.114 m below fuel stack midplane (NEUTFLUX -.114 TT), from -5 to 35 s.

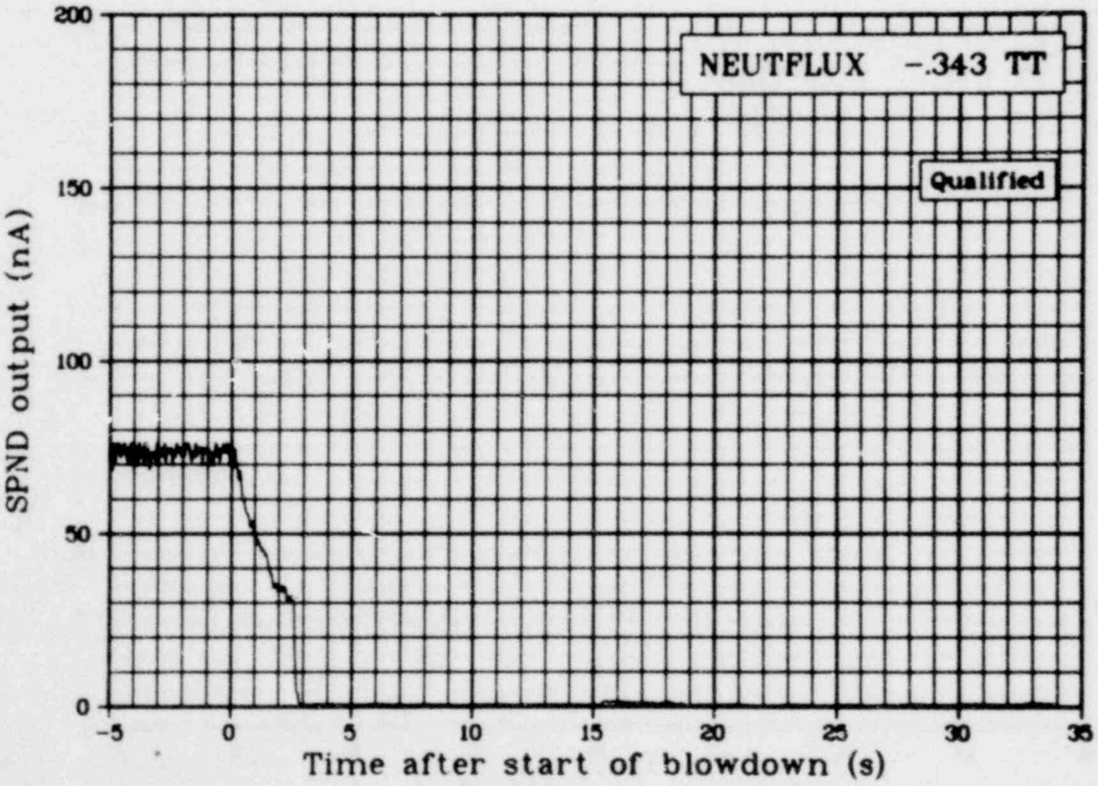

Fig. 418 Neutron flux 0.343 m below fuel stack midplane (NEUTFLUX -.343 TT), from -5 to 35 s.

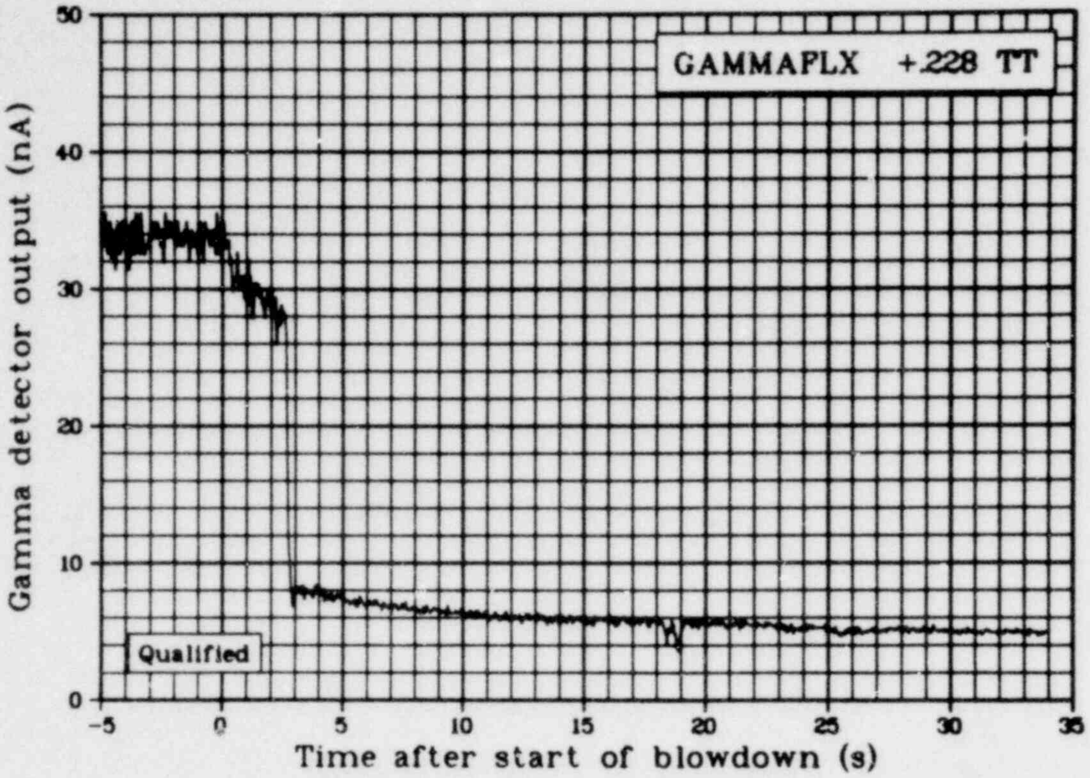

Fig. 419 Gamma flux 0.228 m above fuel stack midplane (GAMMAFLX + .228 TT), from -5 to 35 s.

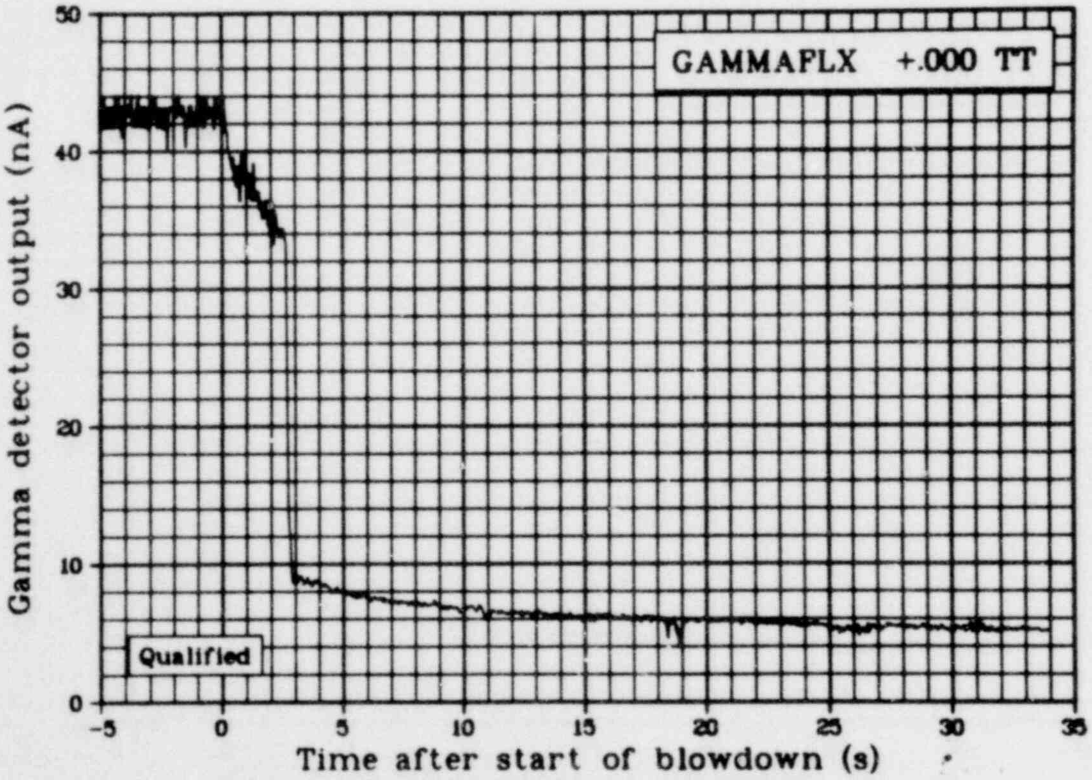

Fig. 420 Gamma flux at fuel stack midplane (GAMMAFLX + .000 TT), from -5 to 35 s.

3
1405 302

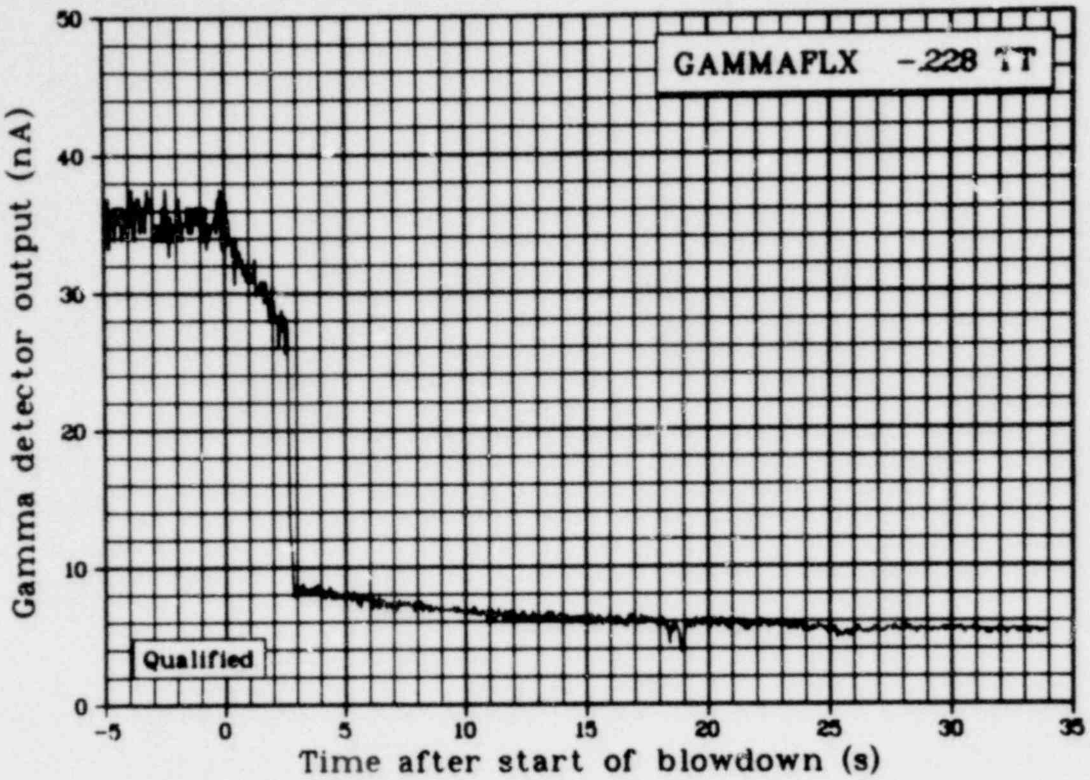

Fig. 421 Neutron flux 0.228 m below fuel stack midplane (NEUTFLUX -.228 TT), from -5 to 35 s.

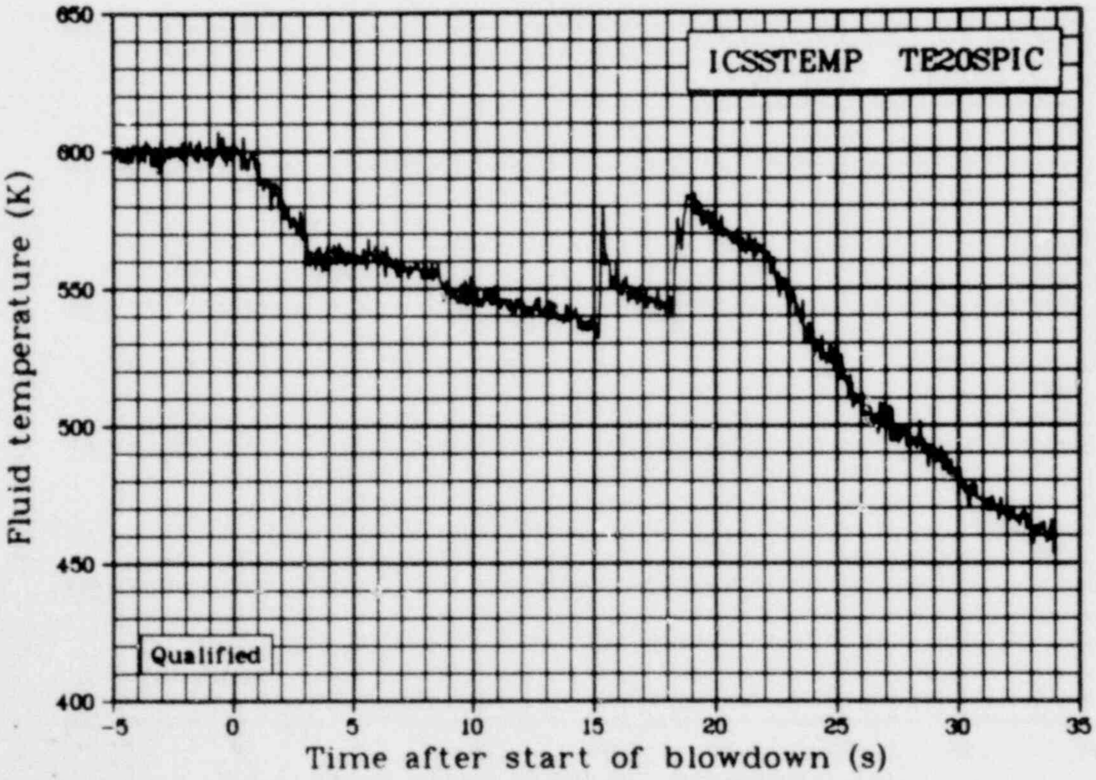

Fig. 422 Fluid temperature in initial condition spool (ICSSTEMP TE20SPIC), from -5 to 35 s.

1405 30~~3~~4

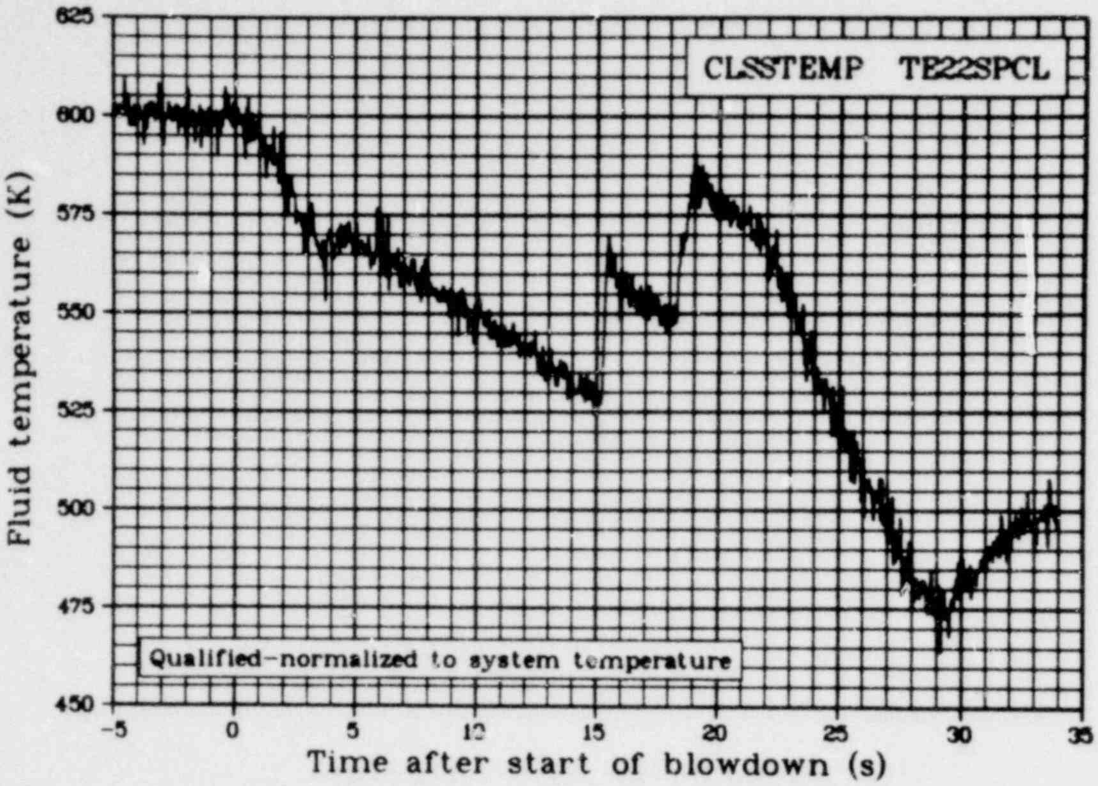

Fig. 423 Fluid temperature in cold leg blowdown spool (CLSSTEMP TE22SPCL), from -5 to 35 s.

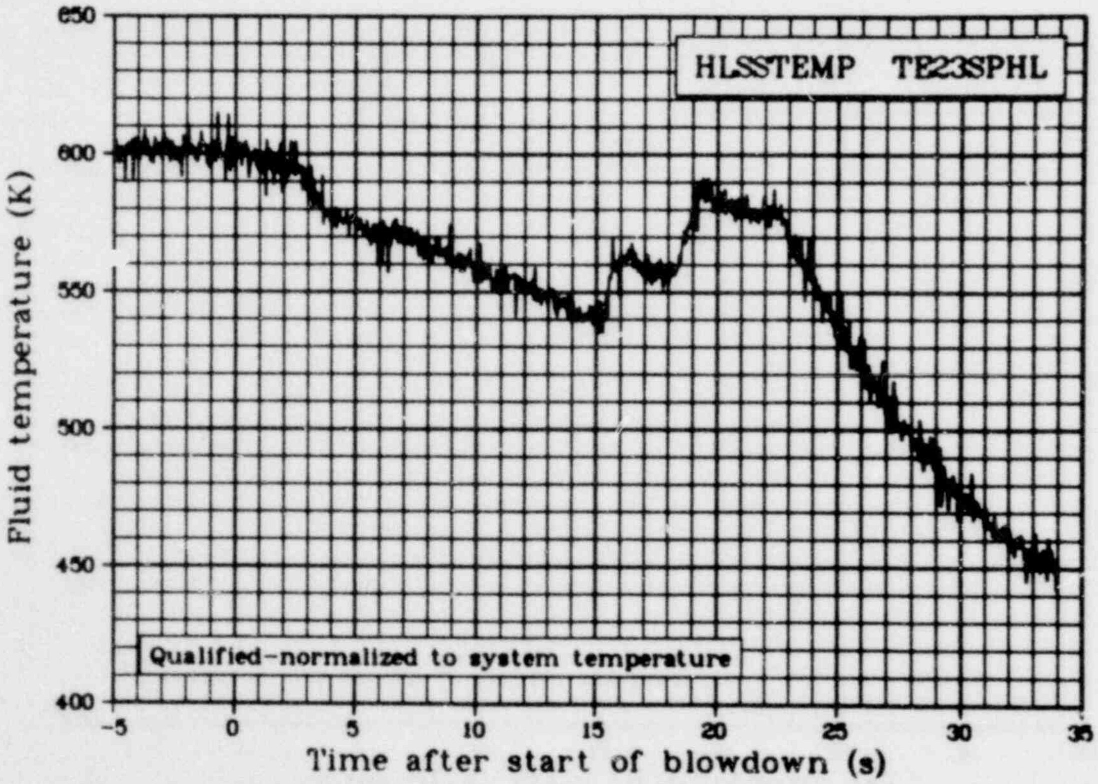

Fig. 424 Fluid temperature in hot leg blowdown spool (HLSSTEMP TE23SPHL), from -5 to 35 s.

5
1405 30~~4~~

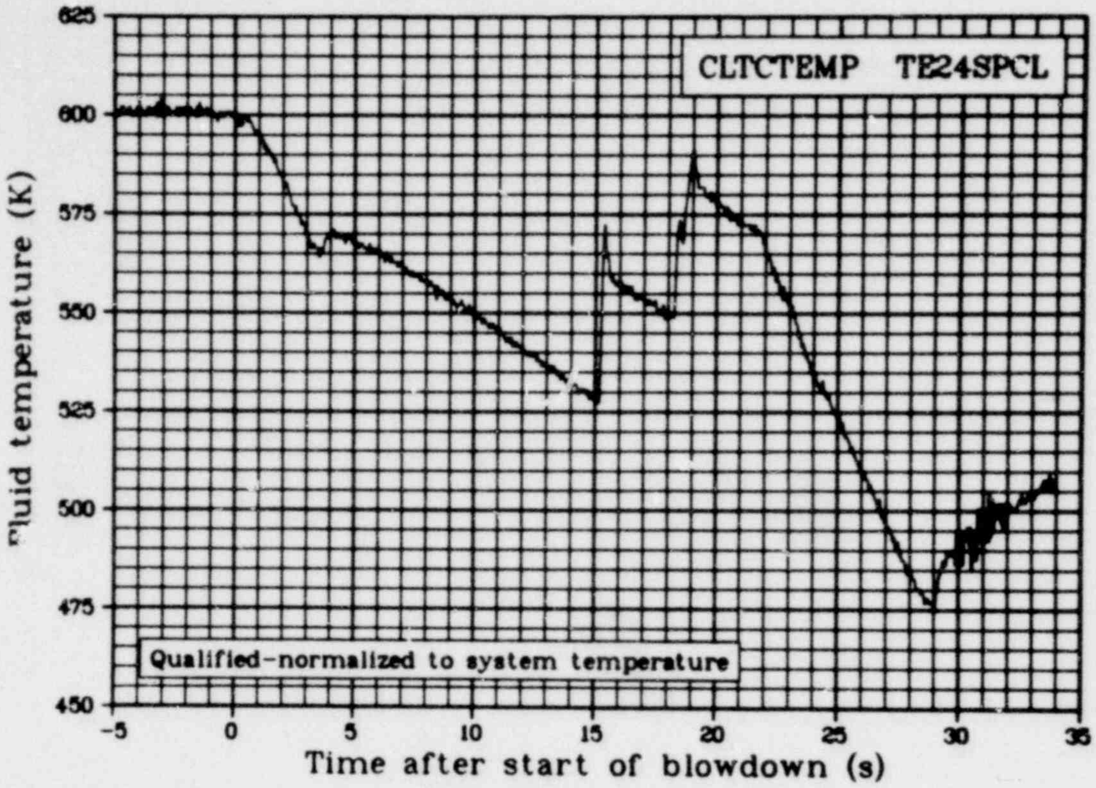

Fig. 425 Fluid temperature in cold leg blowdown spool (CLTCTEMP TE24SPCL), from -5 to 35 s.

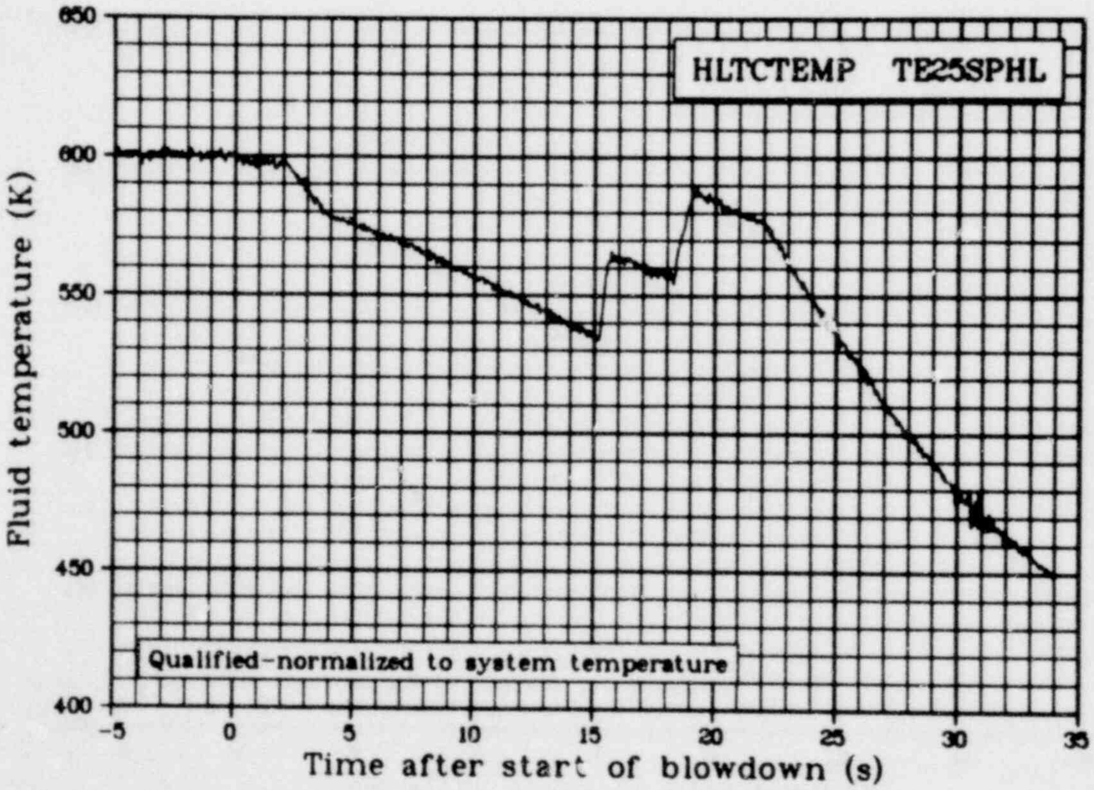

Fig. 426 Fluid temperature in hot leg blowdown spool (HLTCTEMP TE25SPHL), from -5 to 35 s.

1405 305 6

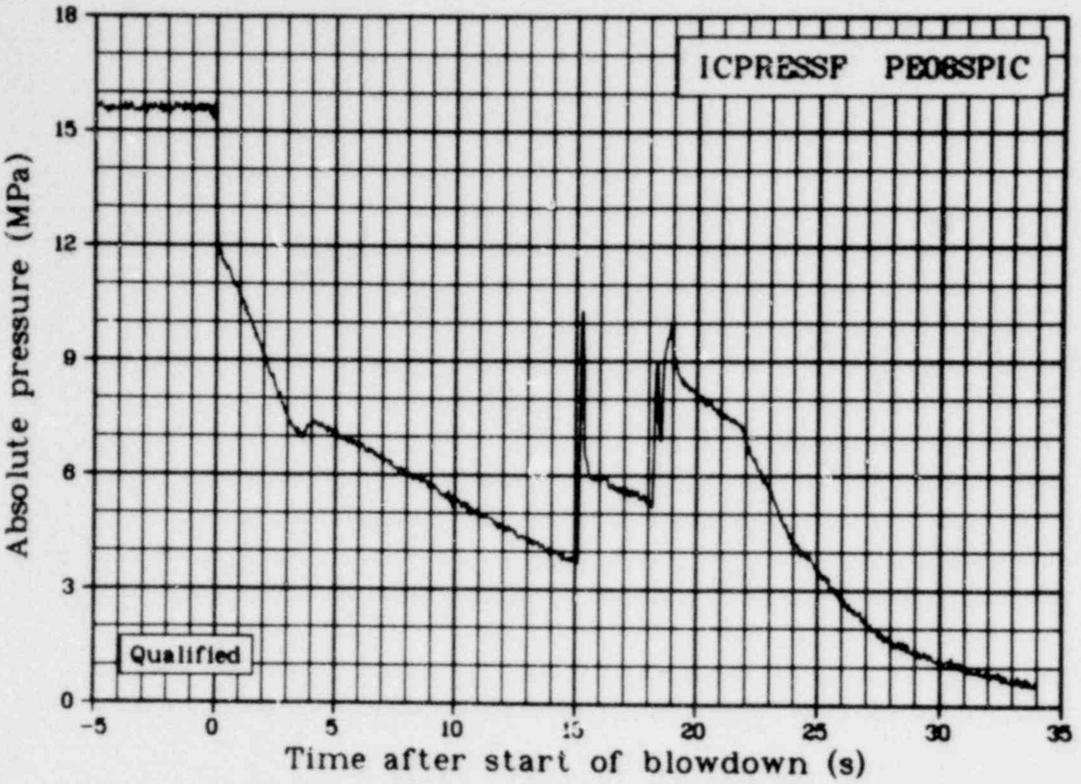

Fig. 427 Absolute pressure in initial condition spool (ICPRESSF PE08SPIC), from -5 to 35 s.

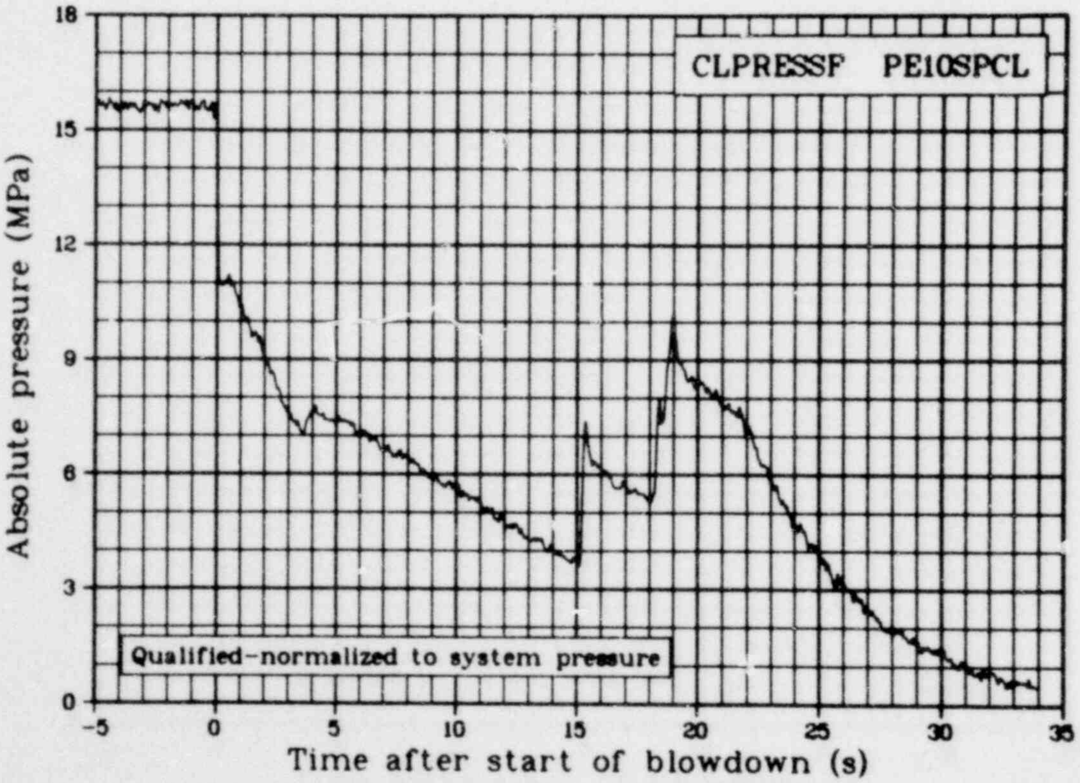

Fig. 428 Absolute pressure in cold leg blowdown spool (CLPRESSF PE10SPCL), from -5 to 35 s.

1405 307

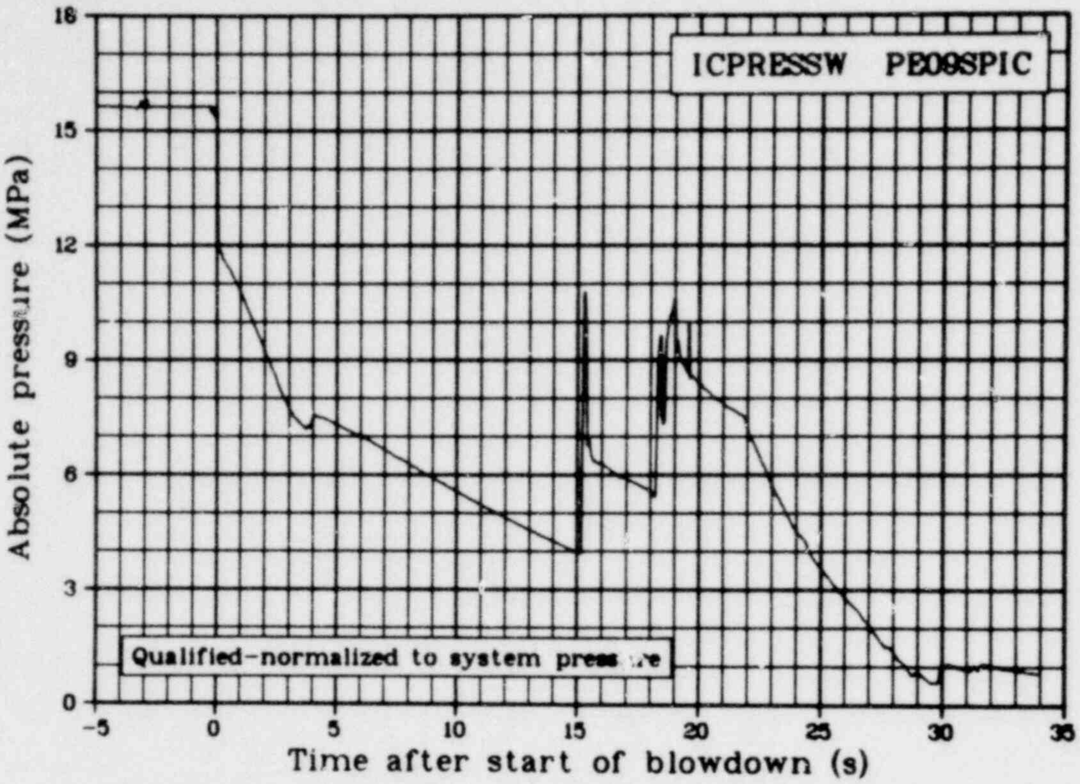

Fig. 429 Absolute pressure in initial condition spool (ICPRESSW PE09SPIC), from -5 to 35 s.

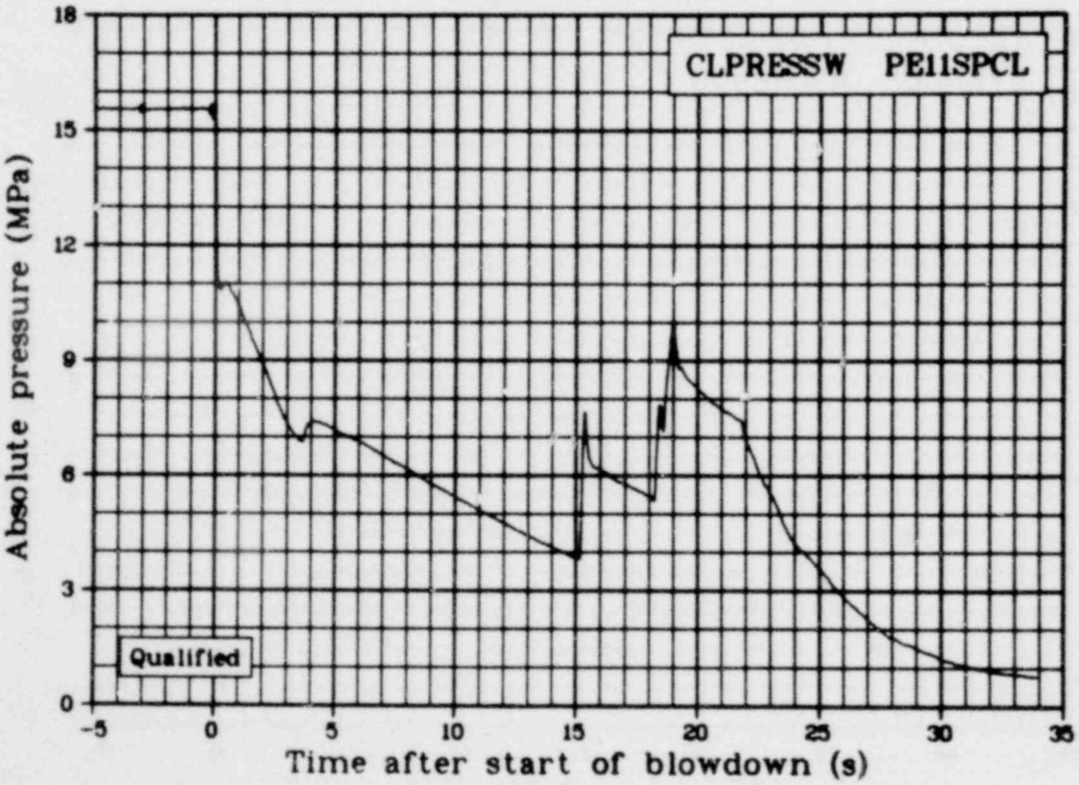

Fig. 430 Absolute pressure in cold leg blowdown spool (CLPRESSW PE11SPCL), from -5 to 35 s.

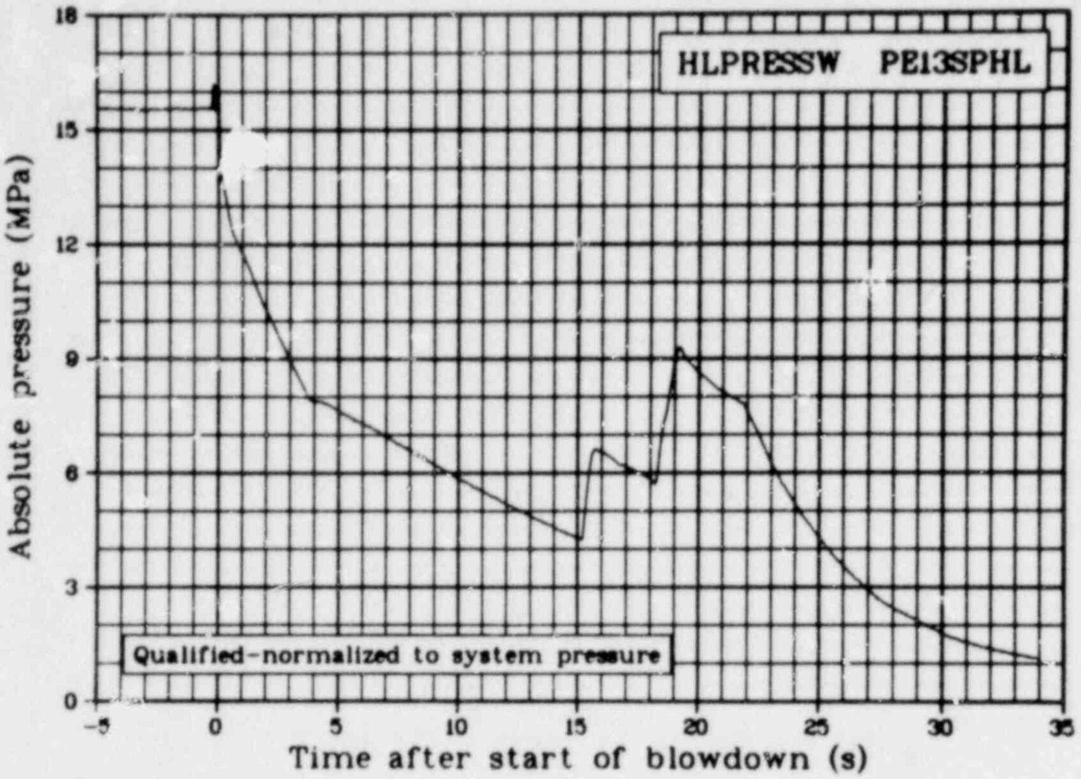

Fig. 431 Absolute pressure in hot leg blowdown spool (HLPRESSW PE13SPHL), from -5 to 35 s.

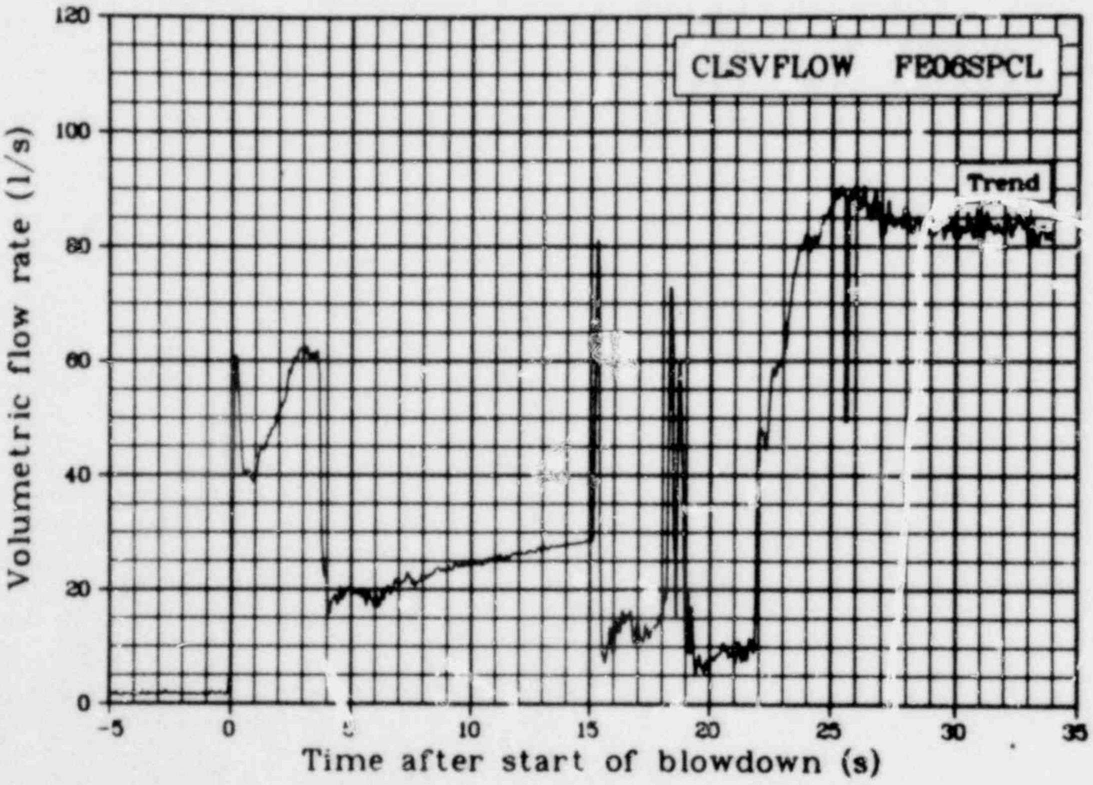

Fig. 432 Volumetric flow rate in cold leg blowdown spool (CLSVFLOW FE06SPCL from -5 to 35 s.

9
1405 308

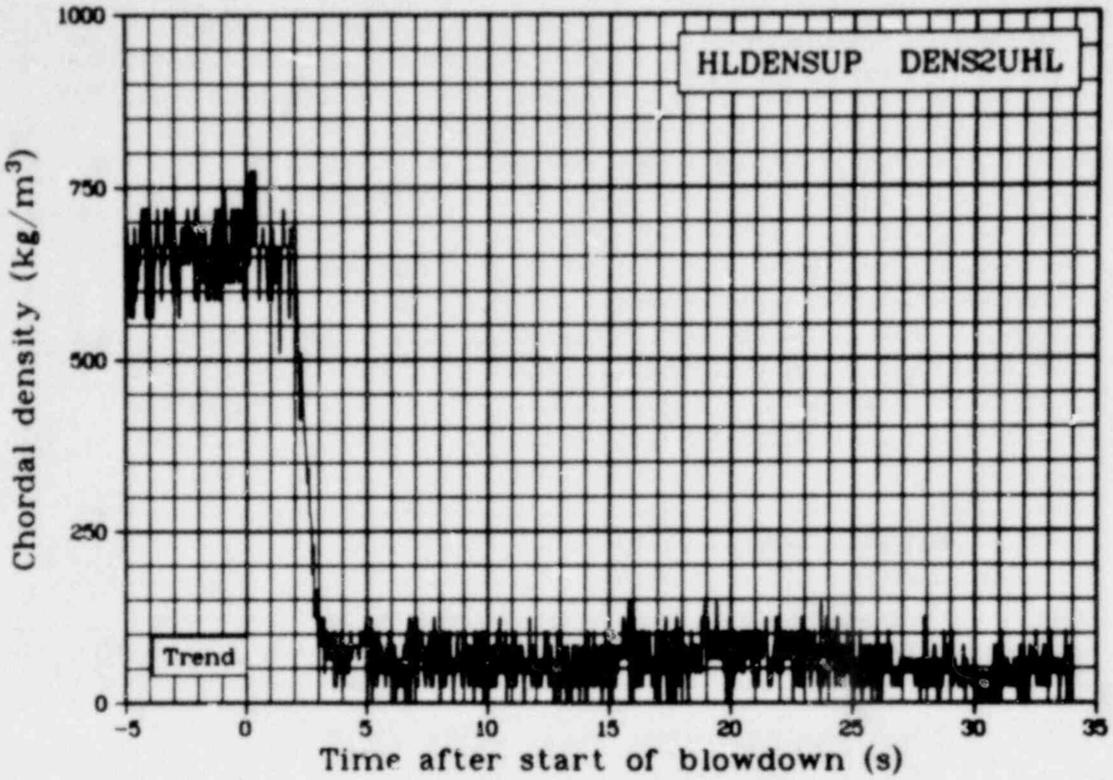

Fig. 433 Chordal density of upper beam in hot leg blowdown spool (HLDENSUP DENS2UHL), from -5 to 35 s.

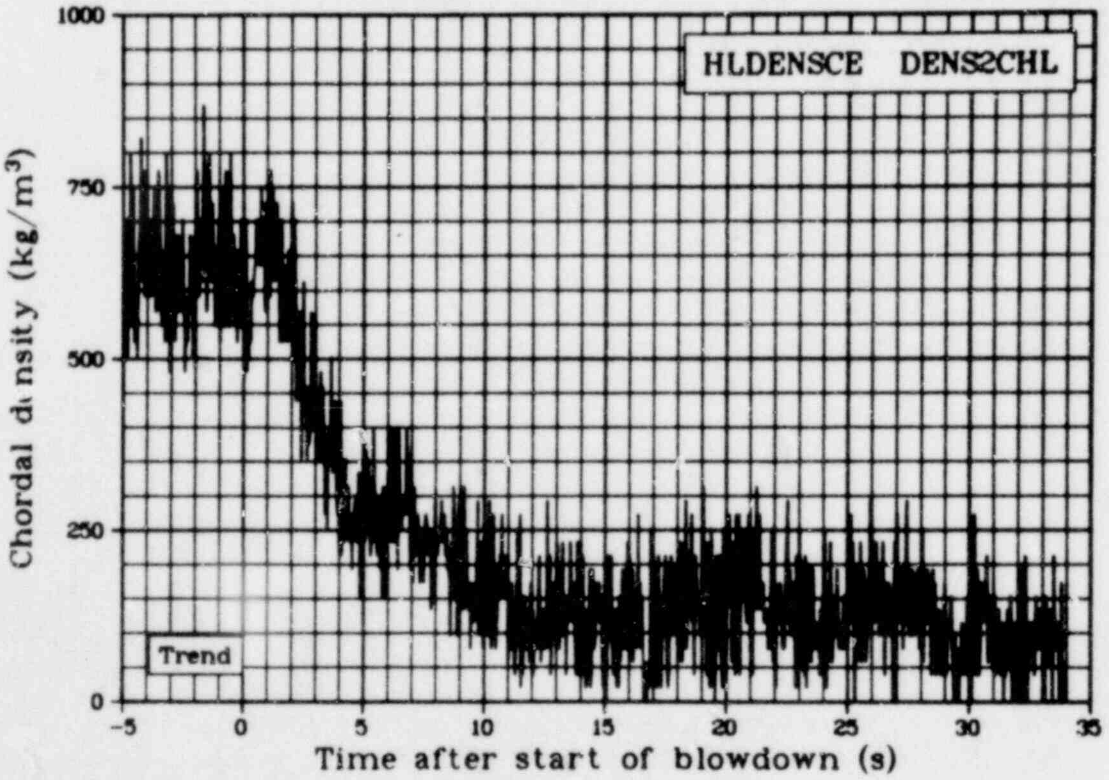

Fig. 434 Chordal density of center beam in hot leg blowdown spool (HLDENSCE DENS2CHL), from -5 to 35 s.

10
1405 3~~09~~

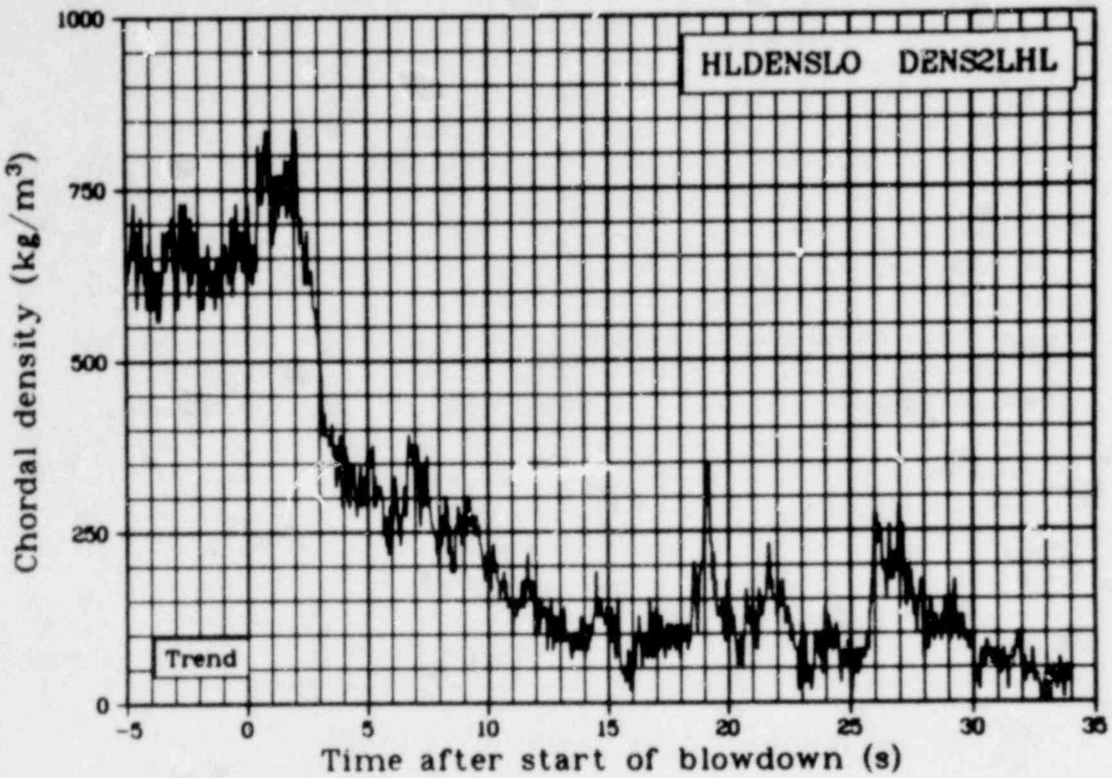

Fig. 435 Chordal density of lower beam in hot leg blowdown spool (HLDENSLO DENS2LHL), from -5 to 35 s.

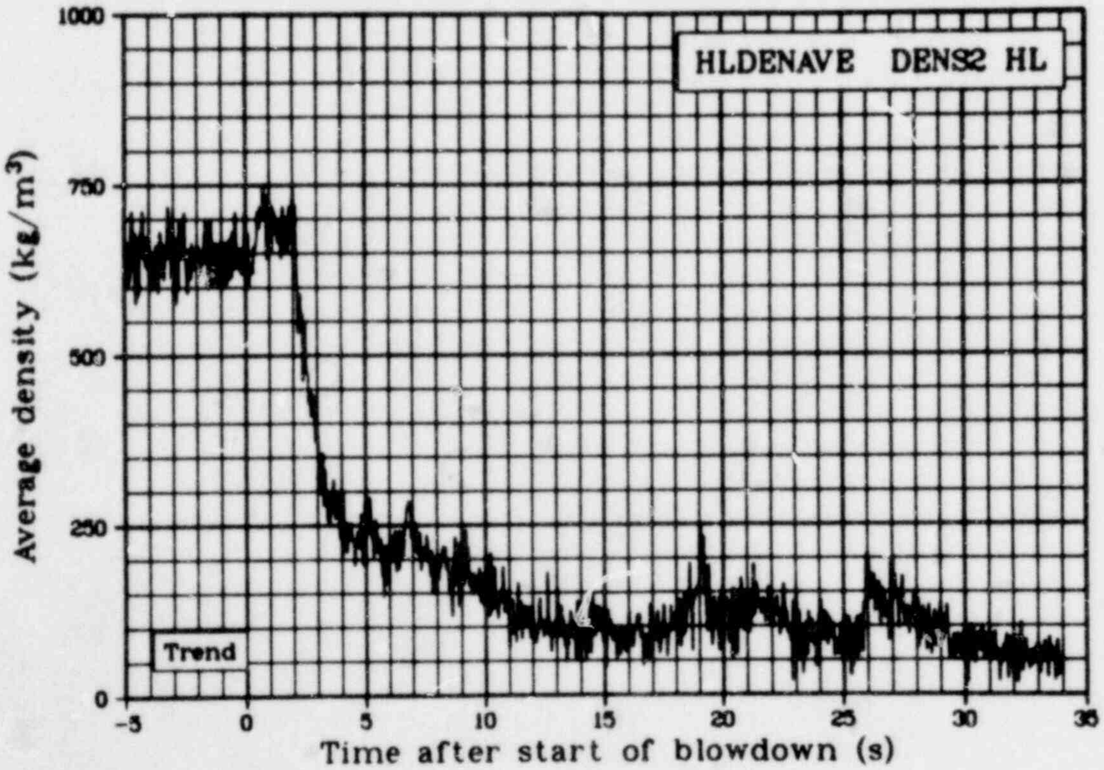

Fig. 436 Average density of hot leg blowdown spool (HLDENAVE DENS2 HL), from -5 to 35 s.

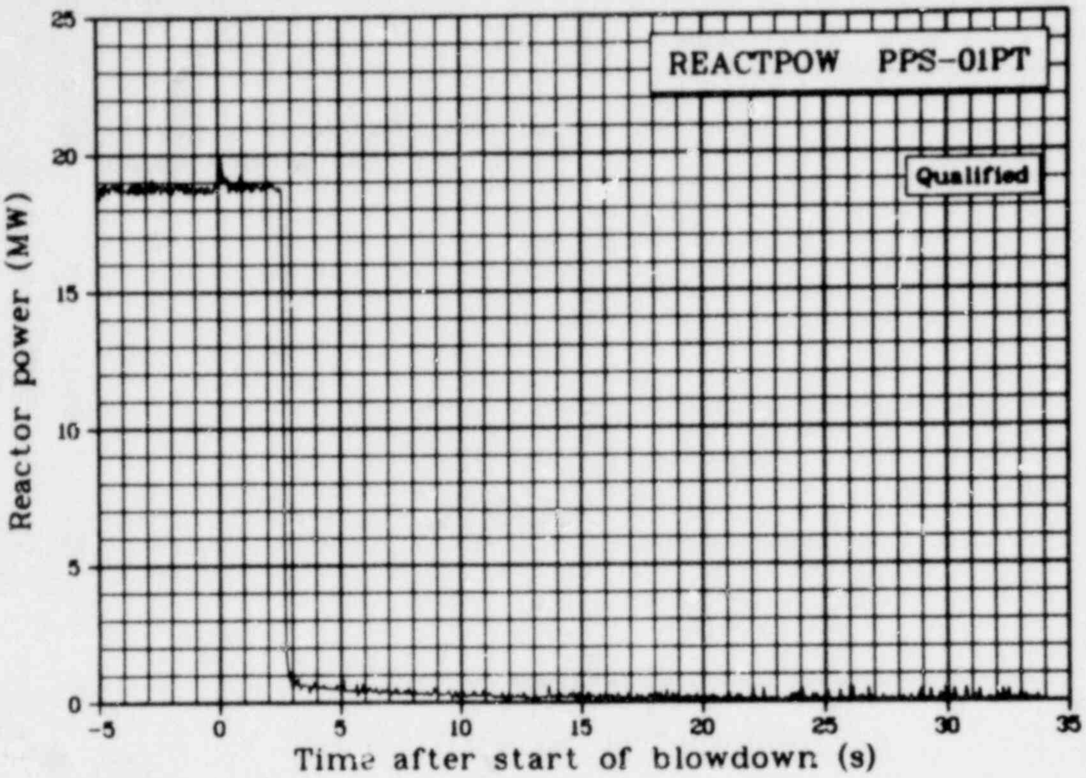

Fig. 437 Reactor power from Core Ionization Chamber PPS 1 (REACTPOW PPS-01PT), from -5 to 35 s.

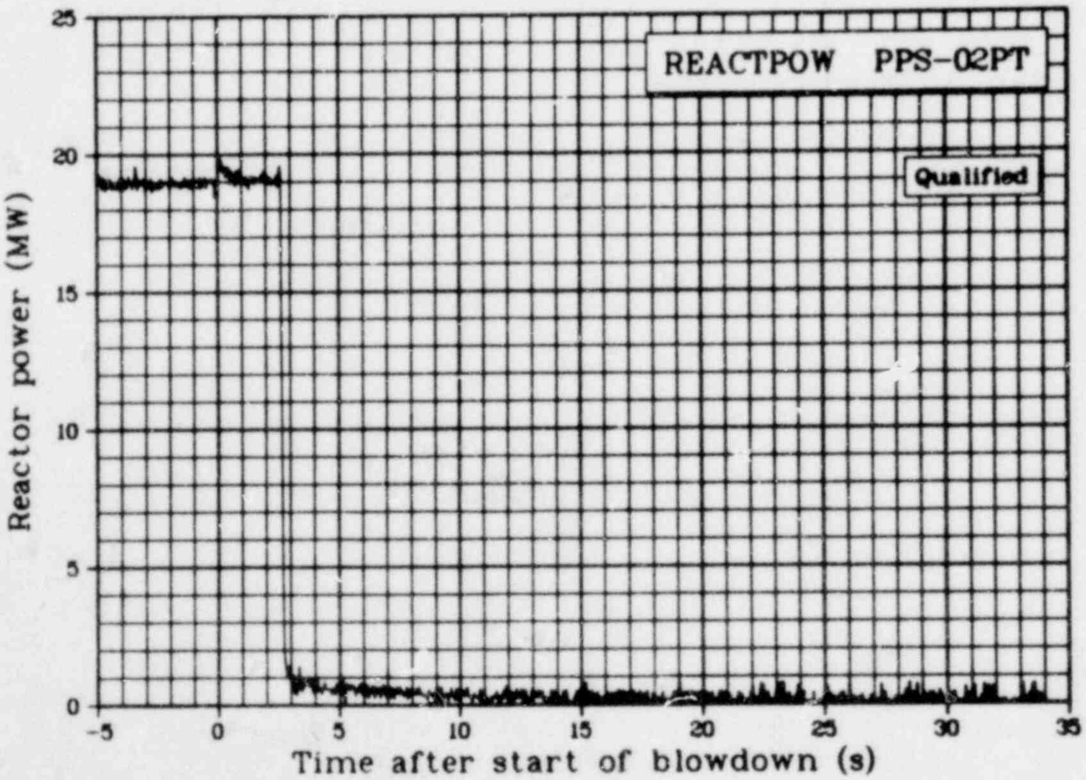

Fig. 438 Reactor power from Core Ionization Chamber PPS 2 (REACTPOW PPS-02PT), from -5 to 35 s.

1405 312

1405 31~~2~~3

~~3~~

1405 31~~8~~

4

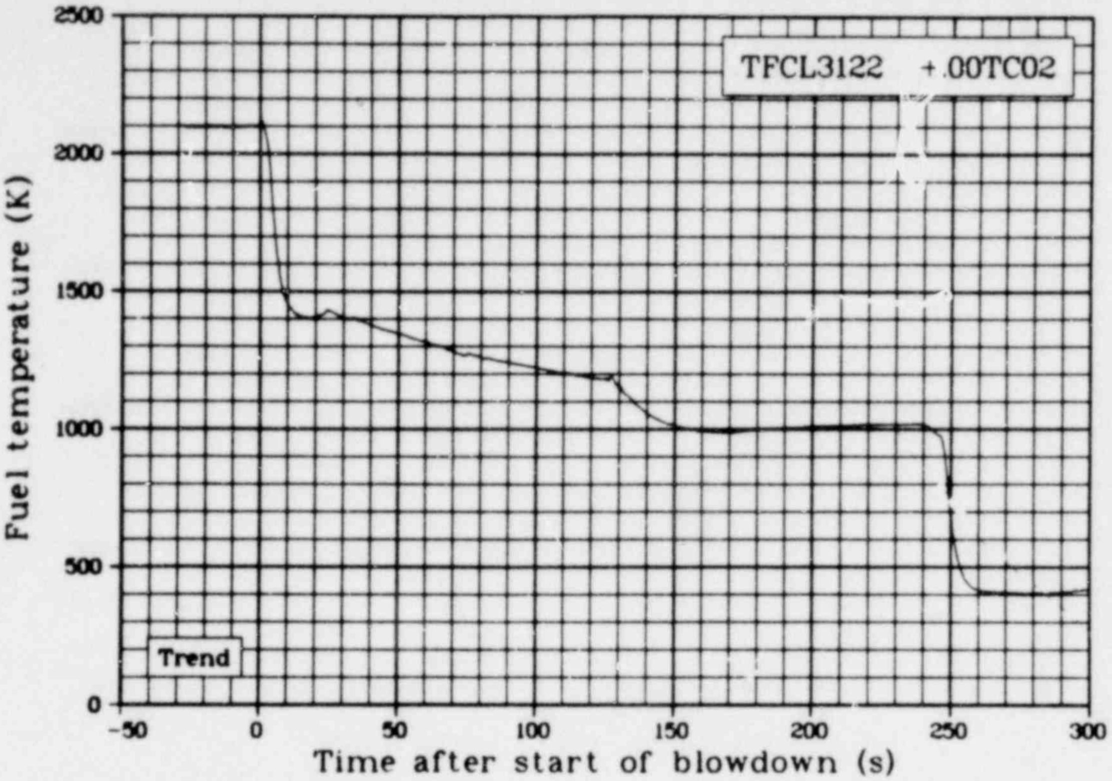

Fig. 439 Fuel temperature in Rod 312-2, at fuel stack midplane (TFCL3122 +.00TC02), from -50 to 300 s.

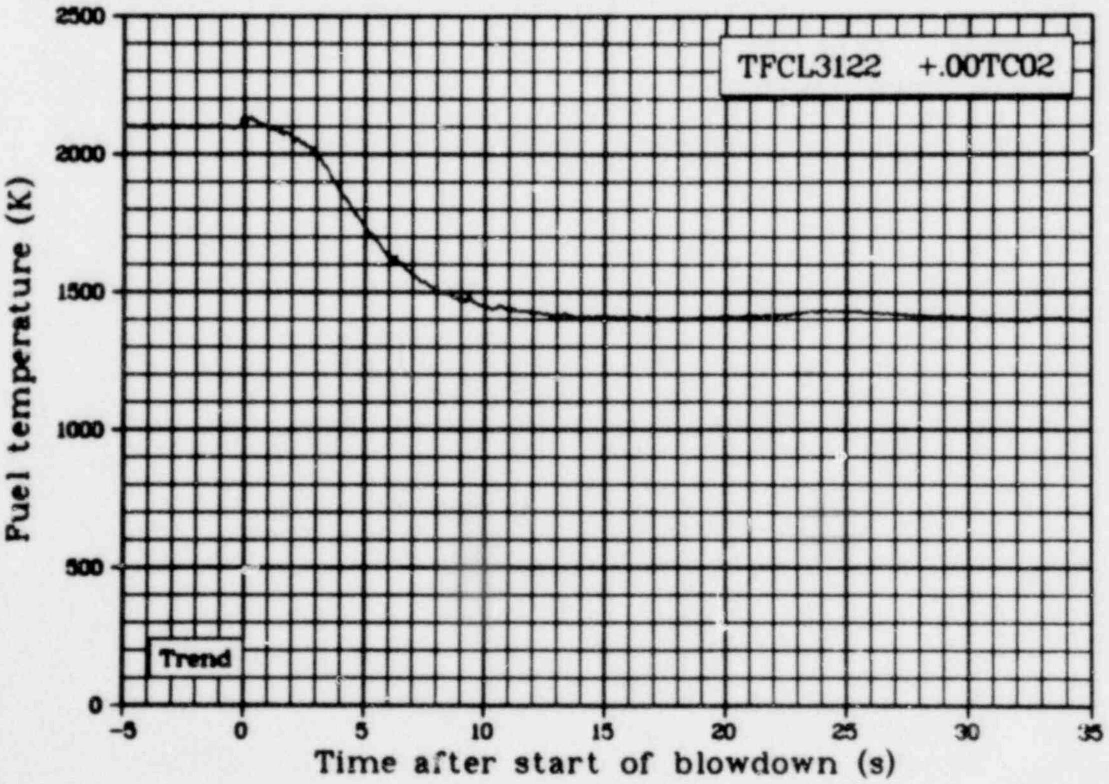

Fig. 440 Fuel temperature in Rod 312-2, at fuel stack midplane (TFCL3122 +.00TC02), from -5 to 35 s.

1405 315

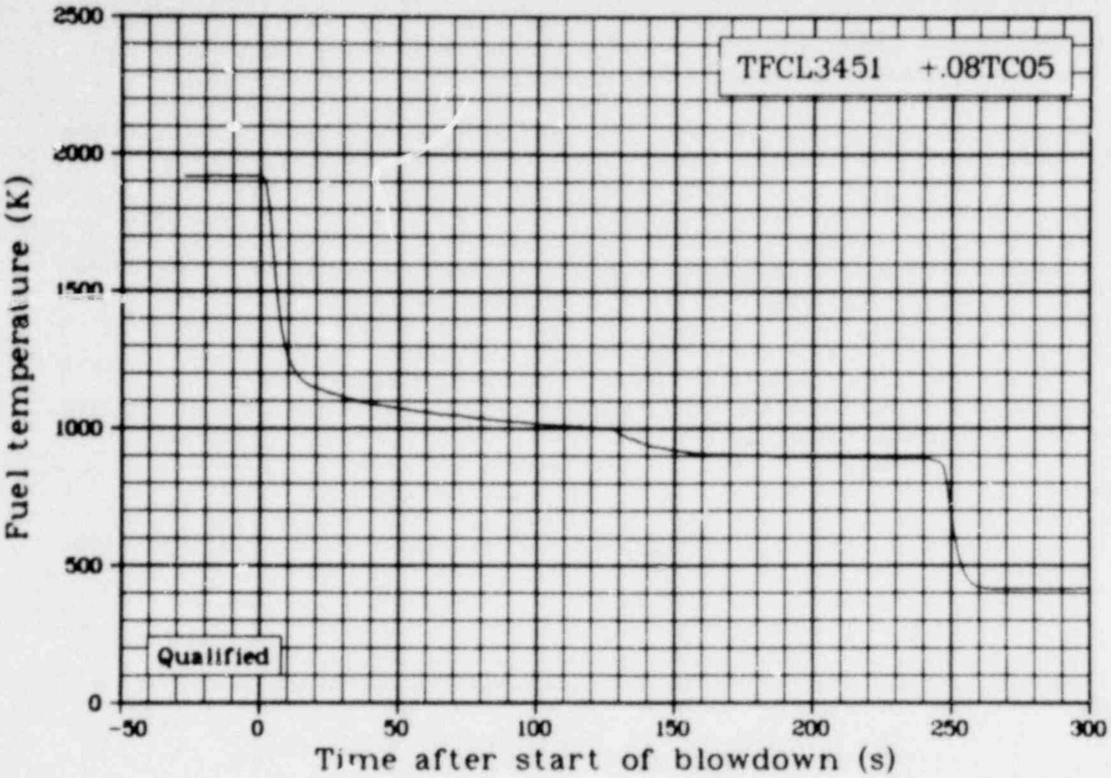

Fig. 441 Fuel temperature in Rod 345-1, 0.08 m above the fuel stack midplane (TFCL3451 + .08TC05), from -50 to 300 s.

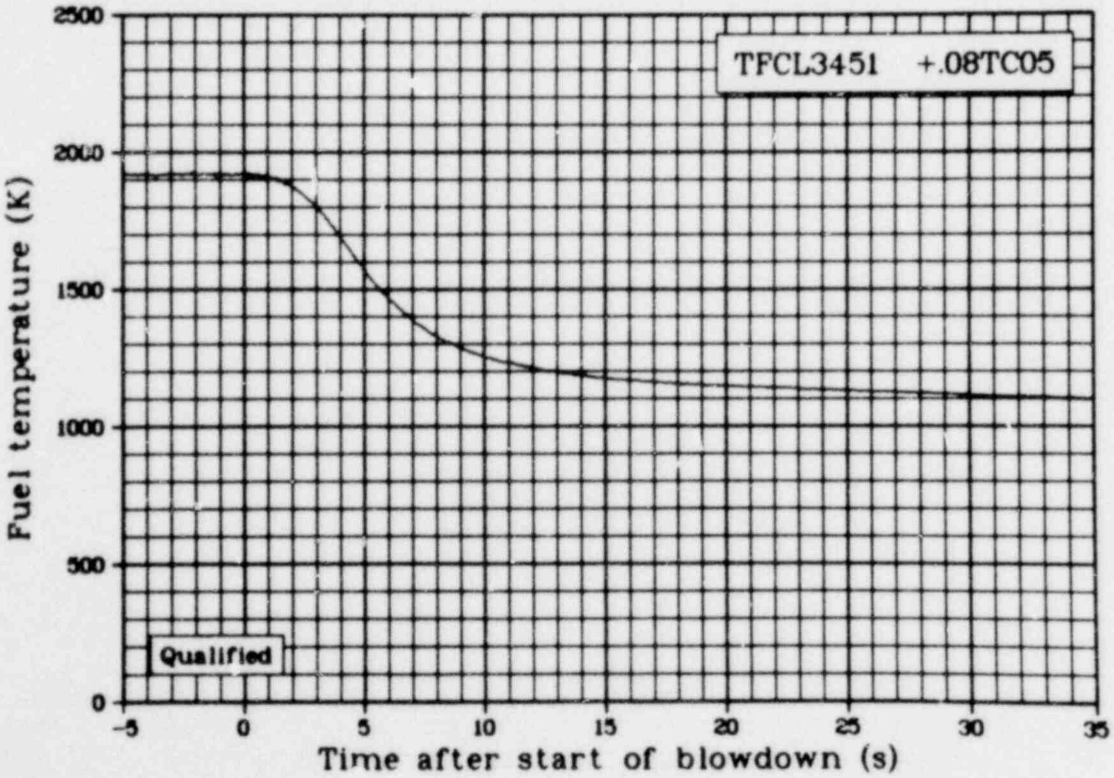

Fig. 442 Fuel temperature in Rod 345-1, 0.08 m above the fuel stack midplane (TFCL3451 + .08TC05), from -5 to 35 s.

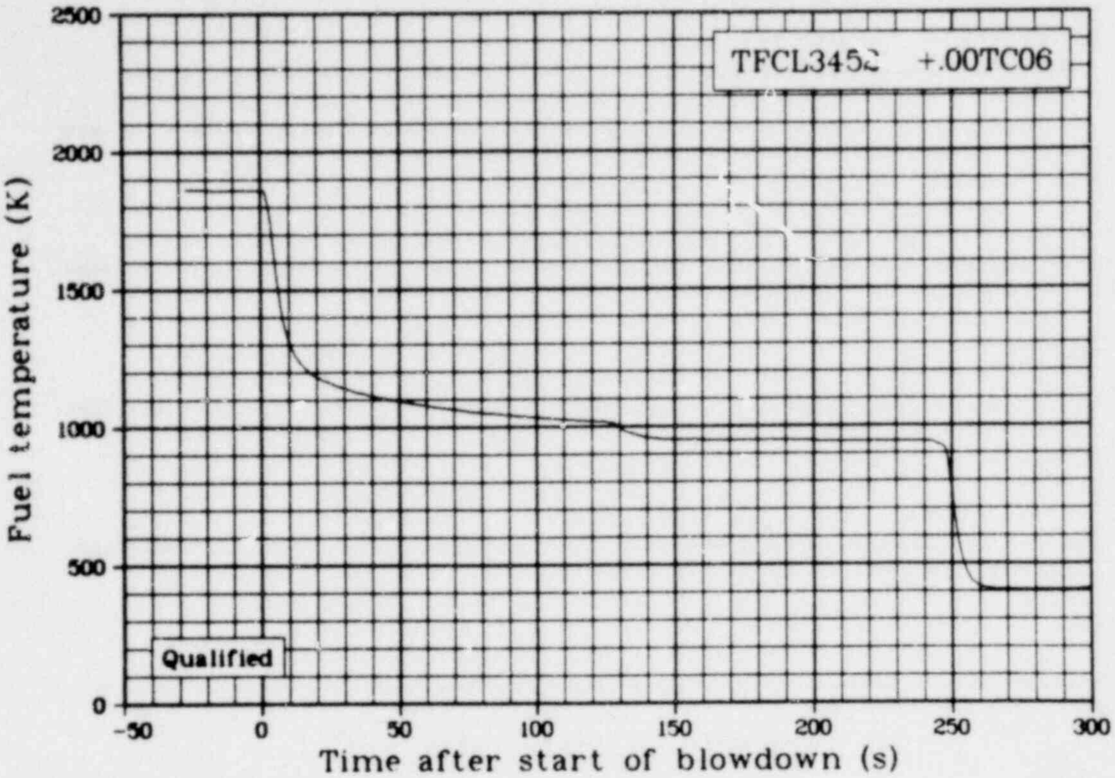

Fig. 443 Fuel temperature in Rod 345-2, at fuel stack midplane (TFCL3452 +.00TC06), from -50 to 300 s.

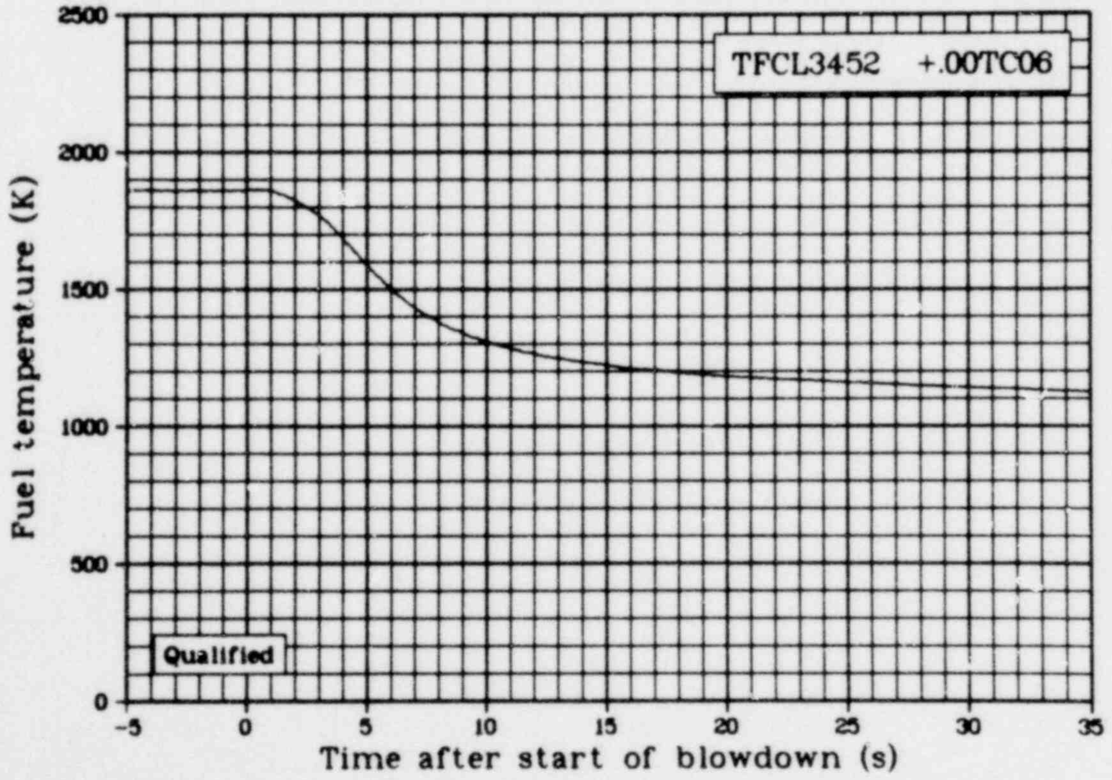

Fig. 444 Fuel temperature in Rod 345-2, at fuel stack midplane (TFCL3452 + .00TC06), from -5 to 35 s.

1405 317

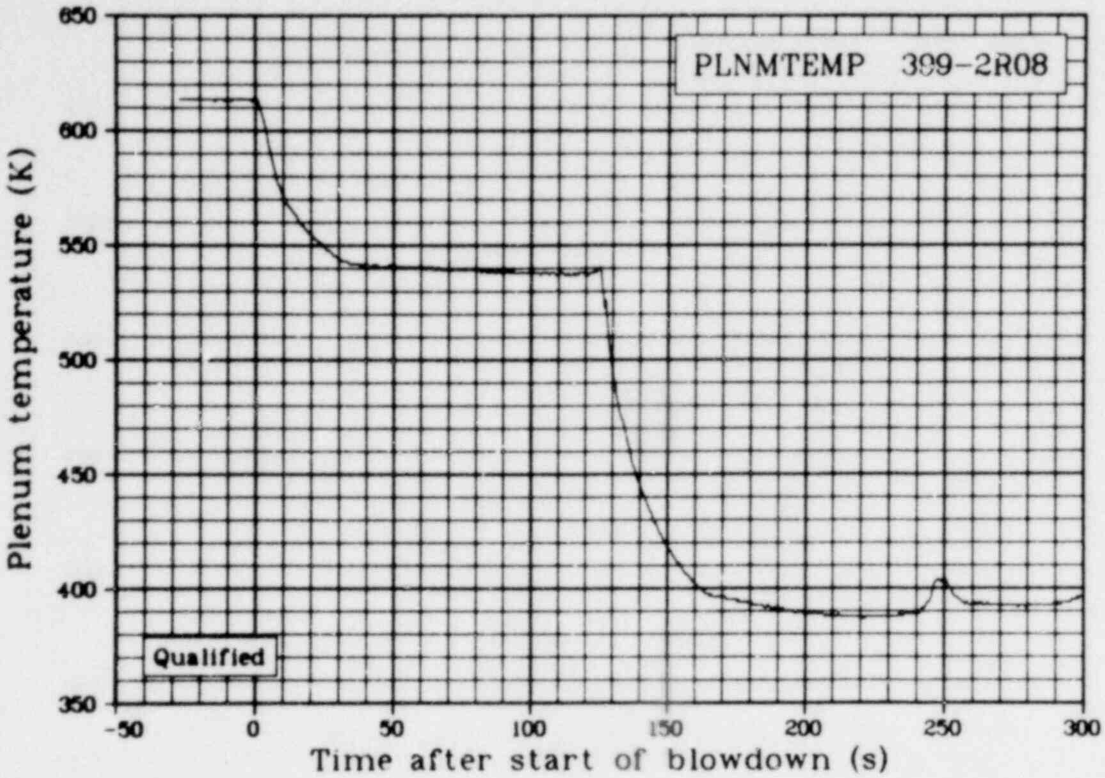

Fig. 445 Plenum temperature in Fuel Rod 399-2 (PLNMTEMP 399-2R08), from -50 to 300 s.

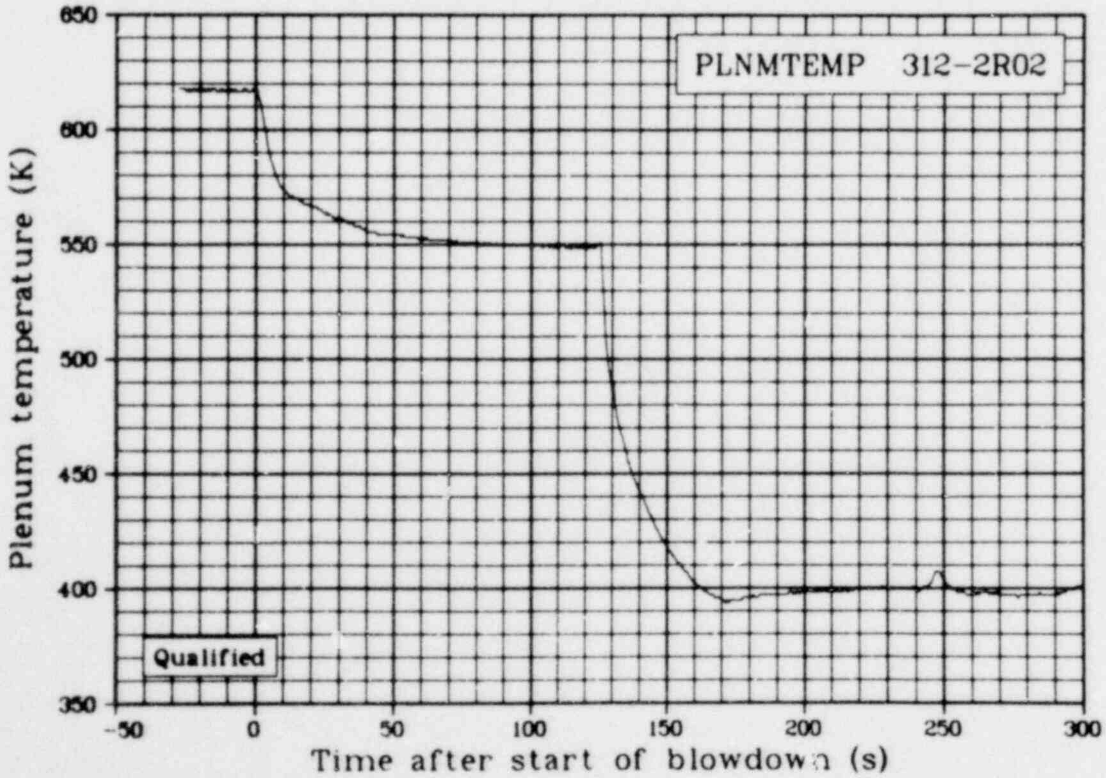

Fig. 446 Plenum temperature in Fuel Rod 312-2 (PLNMTEMP 312-2R02), from -50 to 300 s.

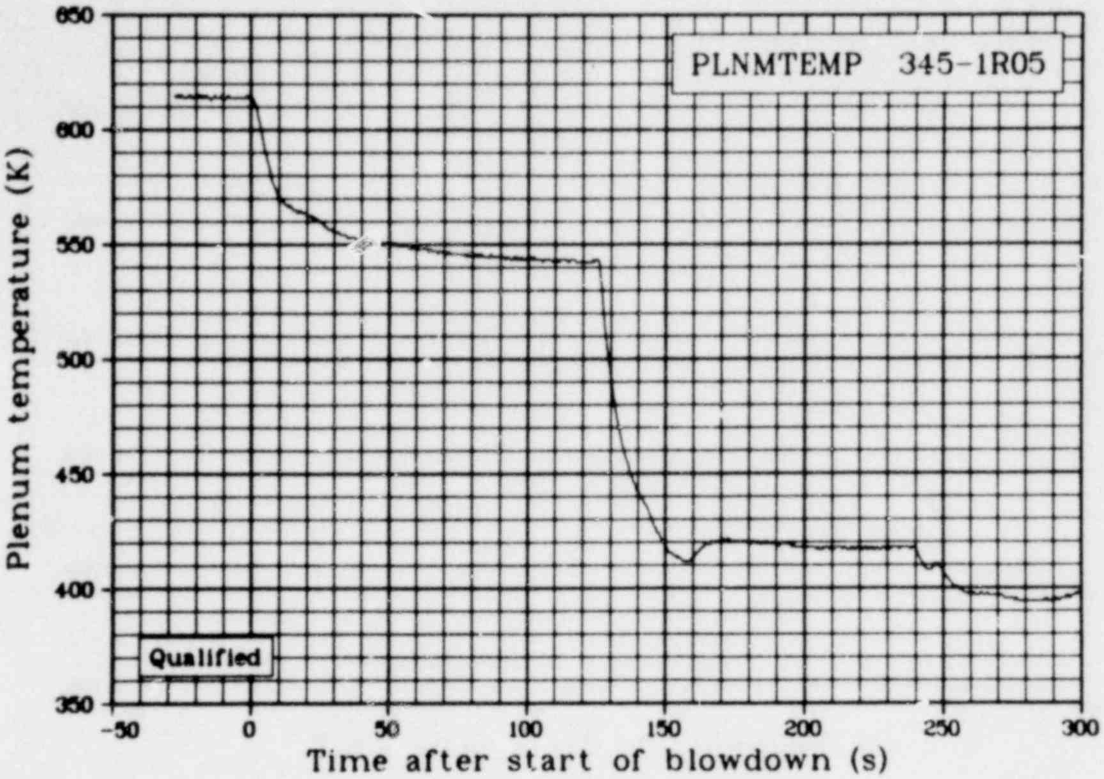

Fig. 447 Plenum temperature in Fuel Rod 345-1 (PLNMTEMP 345-1R05), from -50 to 300 s.

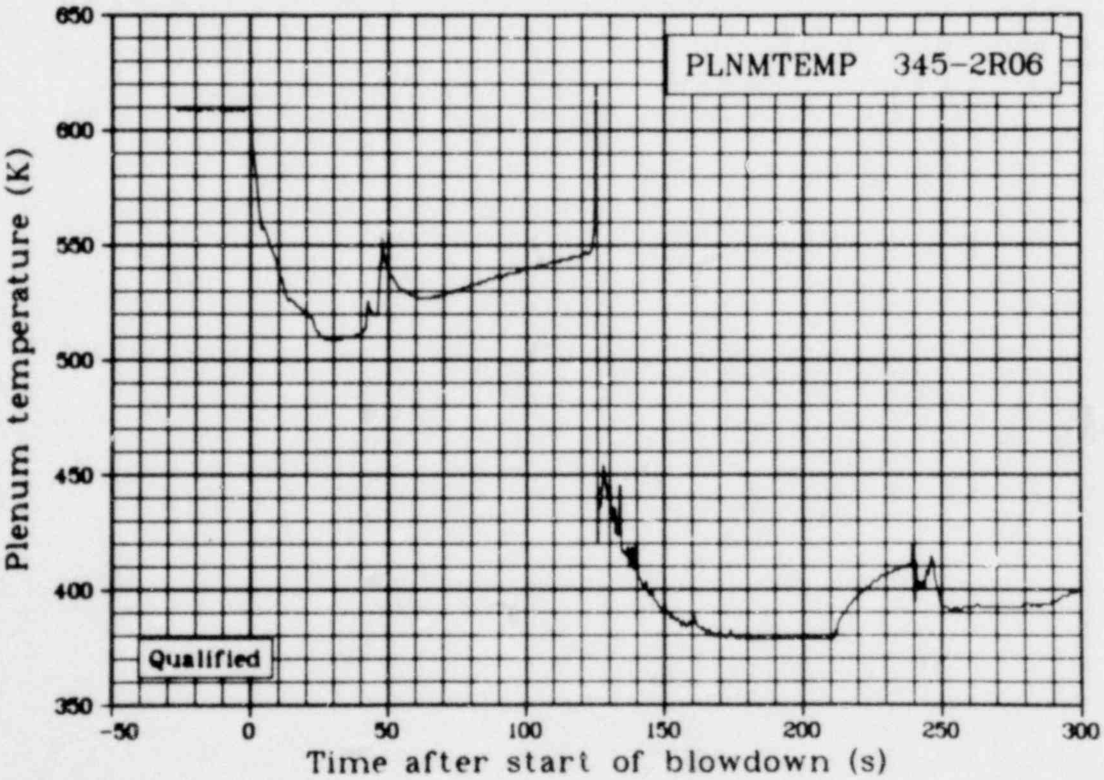

Fig. 448 Plenum temperature in Fuel Rod 345-2 (PLNMTEMP 345-2R06), from -50 to 300 s.

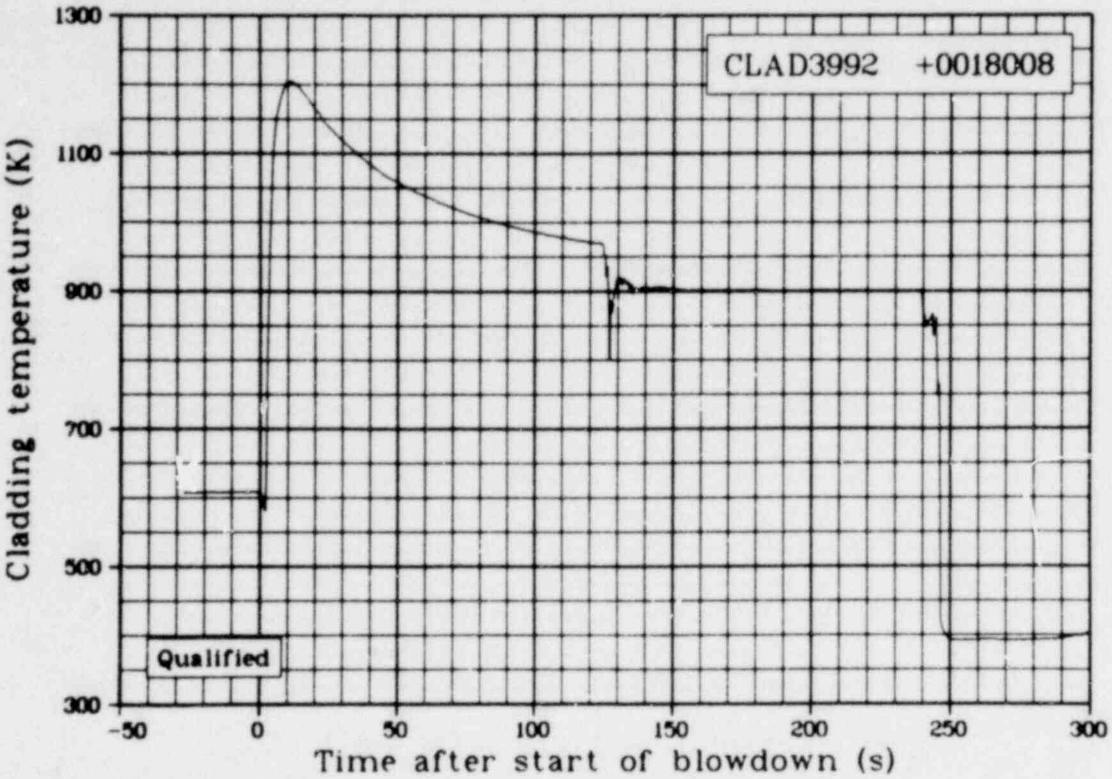

Fig. 449 Cladding temperature, Rod 399-2, at 180 degrees and fuel stack midplane (CLAD3992 + 0018008), from -50 to 300 s.

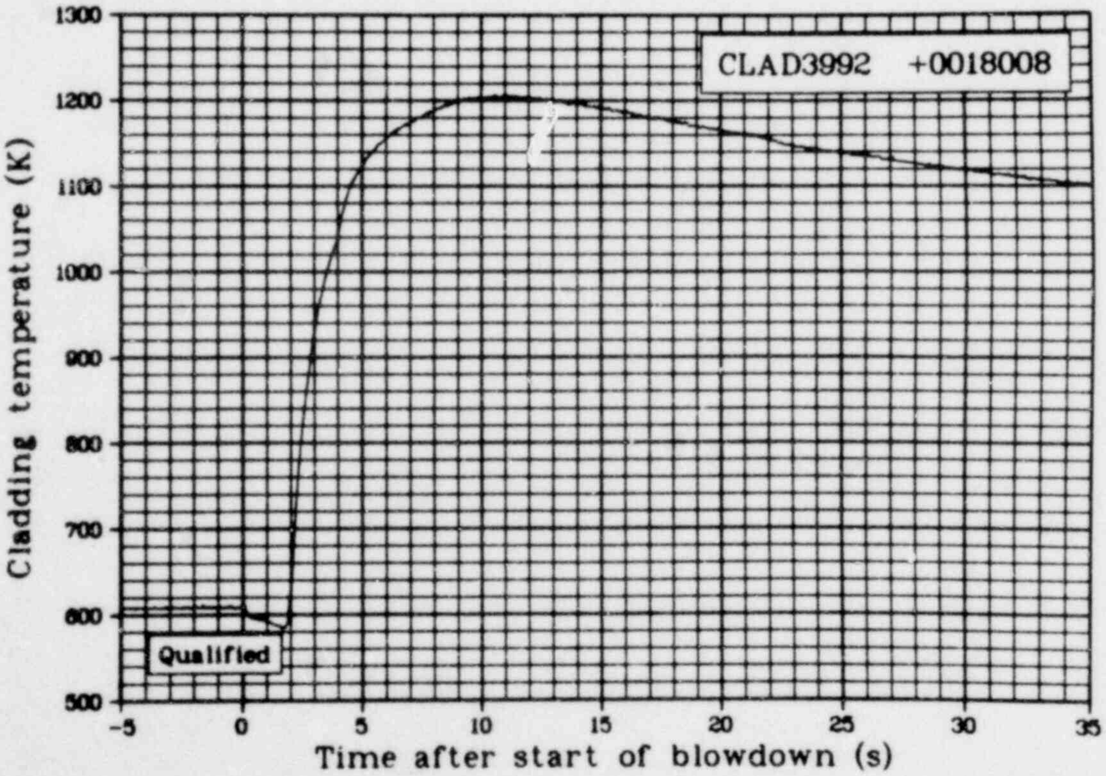

Fig. 450 Cladding temperature, Rod 399-2, at 180 degrees and fuel stack midplane (CLAD3992 + 0018008), from -5 to 35 s.

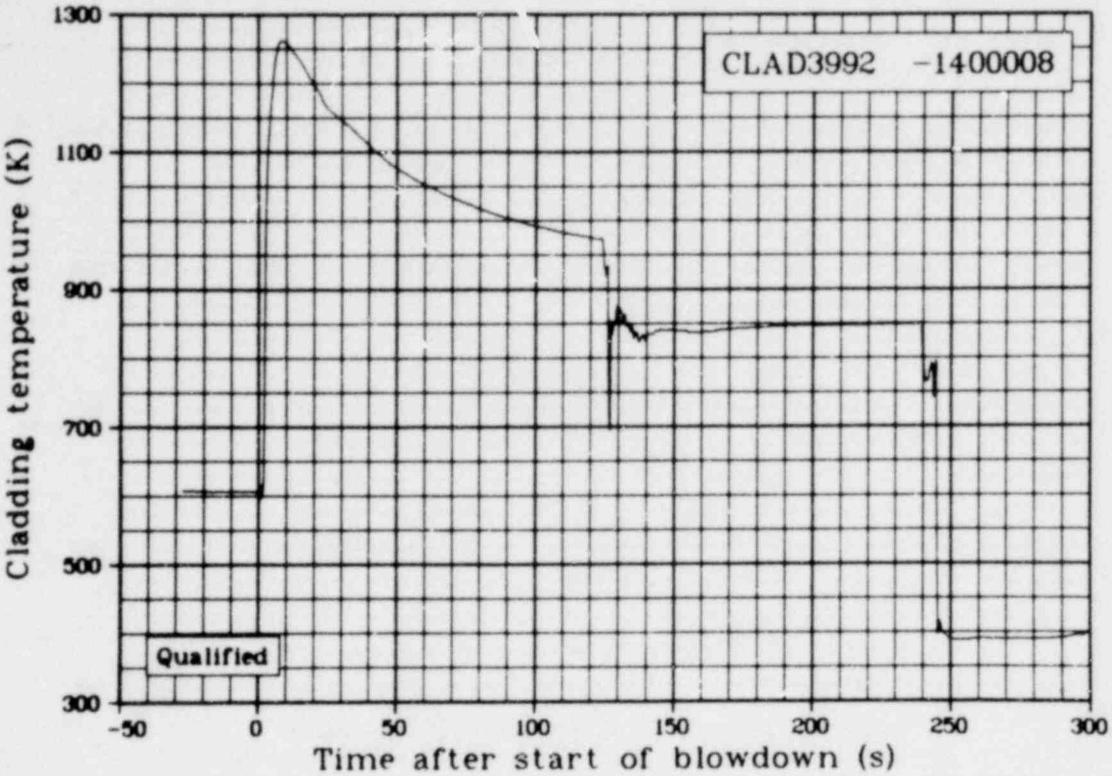

Fig. 451 Cladding temperature, Rod 399-2, at 0 degrees and 0.14 m below fuel stack midplane (CLAD3992 -1400008), from -50 to 300 s.

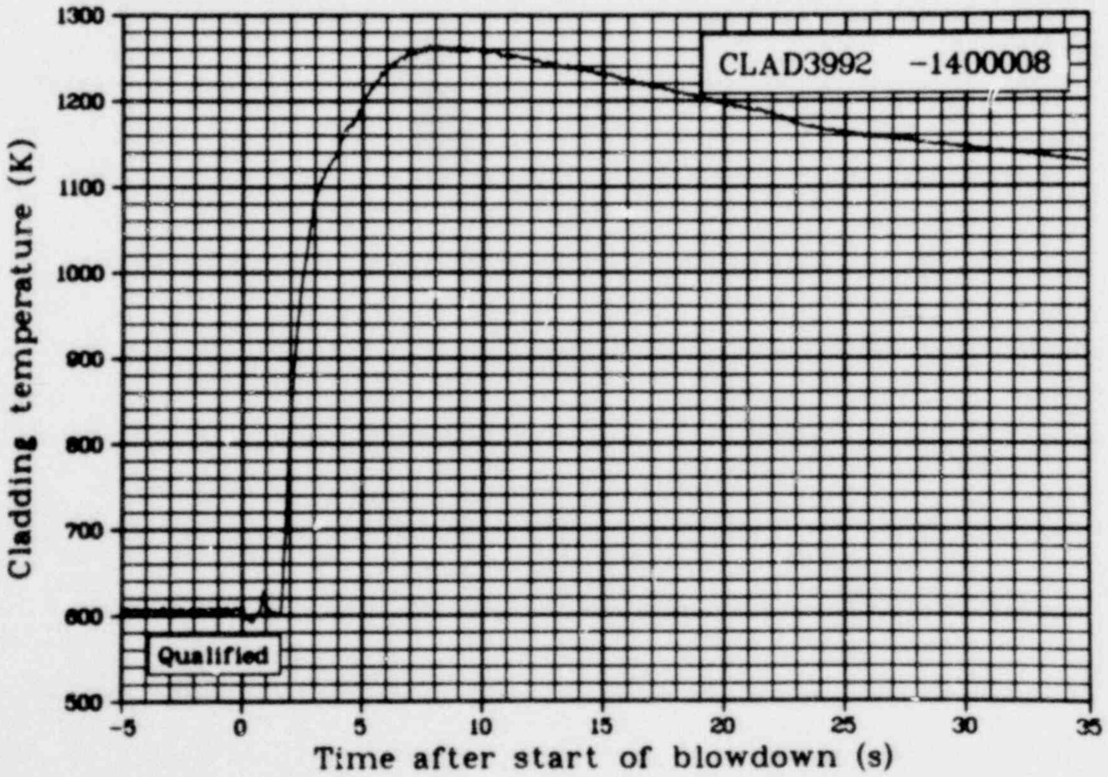

Fig. 452 Cladding temperature, Rod 399-2, at 0 degrees and 0.14 m below fuel stack midplane (CLAD3992 -1400008), from -5 to 35 s.

1405 321

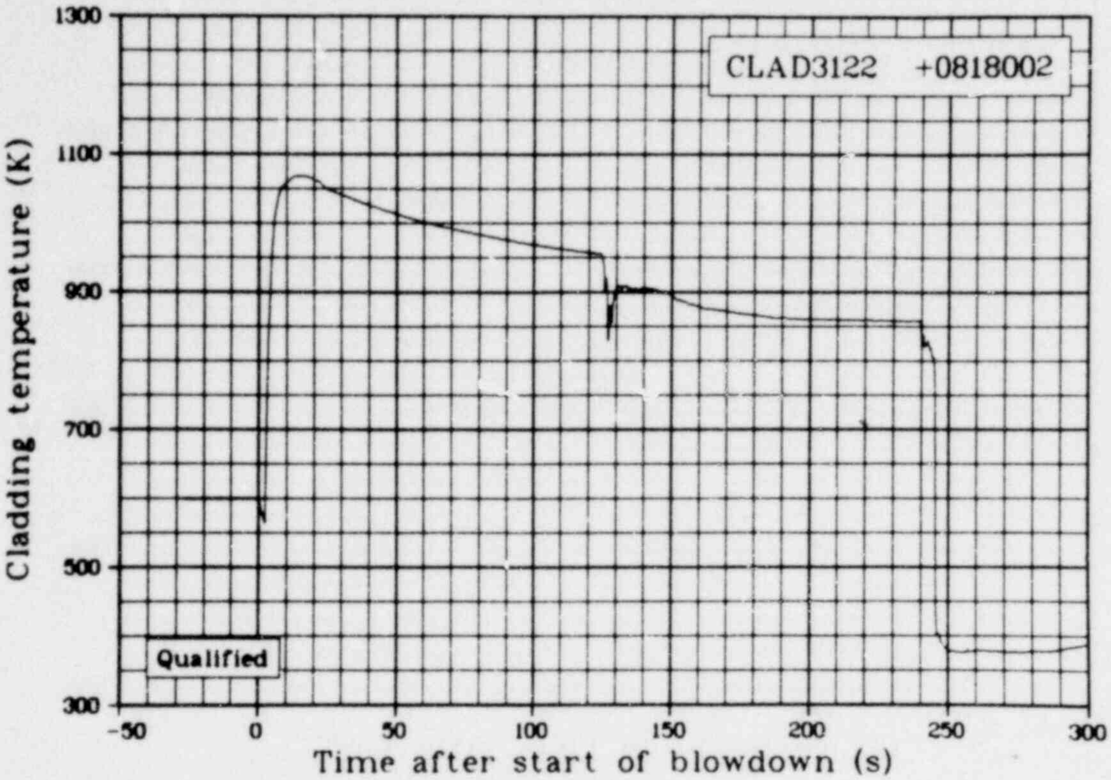

Fig. 453 Cladding temperature, Rod 312-2, at 180 degrees and 0.08 m above fuel stack midplane (CLAD3122 +0818002), from -50 to 300 s.

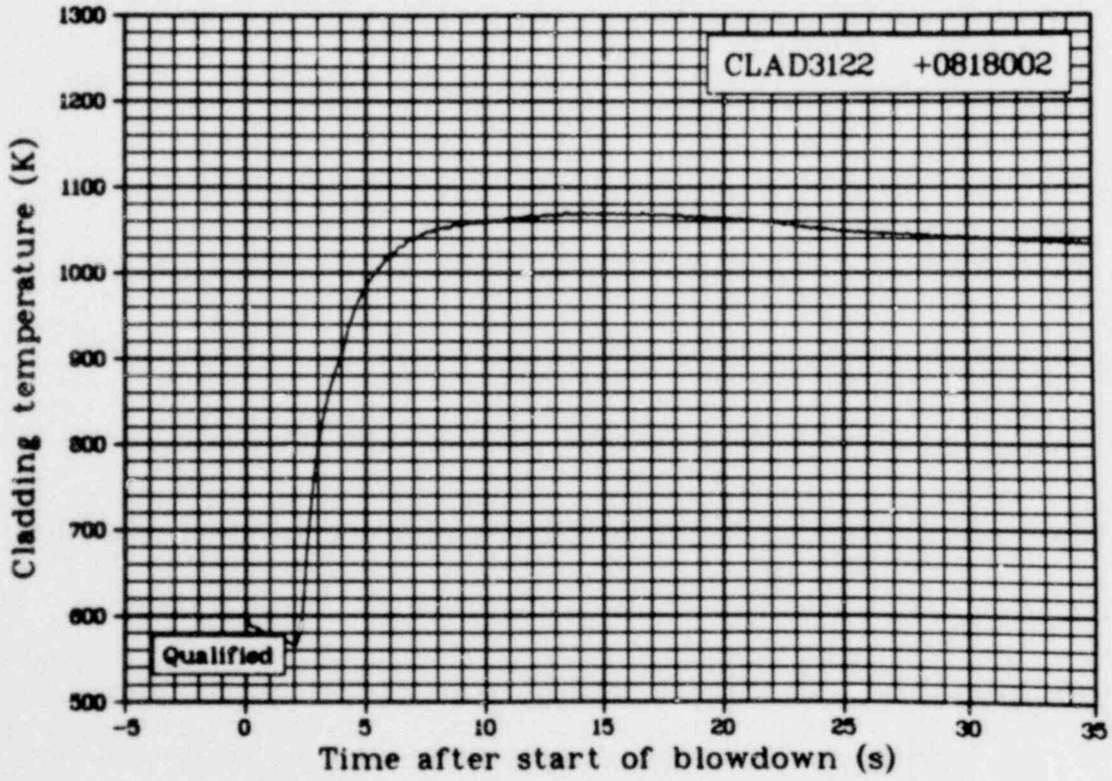

Fig. 454 Cladding temperature, Rod 312-2, at 180 degrees and 0.08 m above fuel stack midplane (CLAD3122 +0818002), from -5 to 35 s.

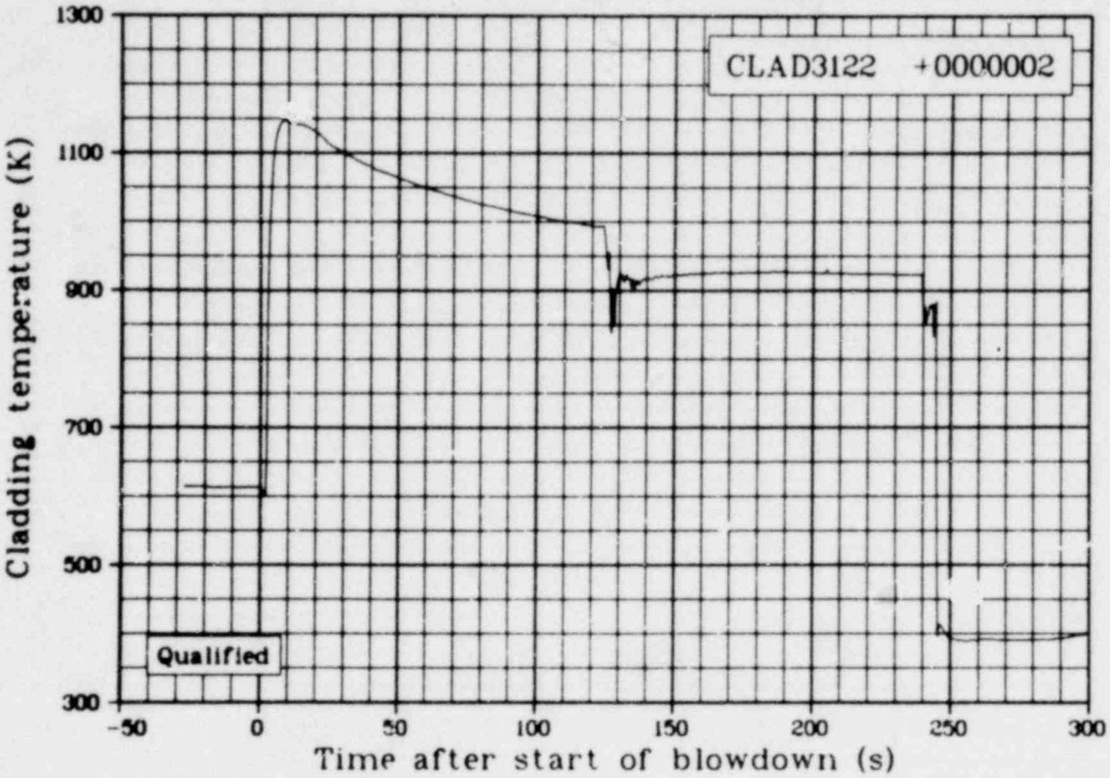

Fig. 455 Cladding temperature, Rod 312-2, at 0 degrees and fuel stack midplane (CLAD3122 + 0000002), from -50 to 300 s.

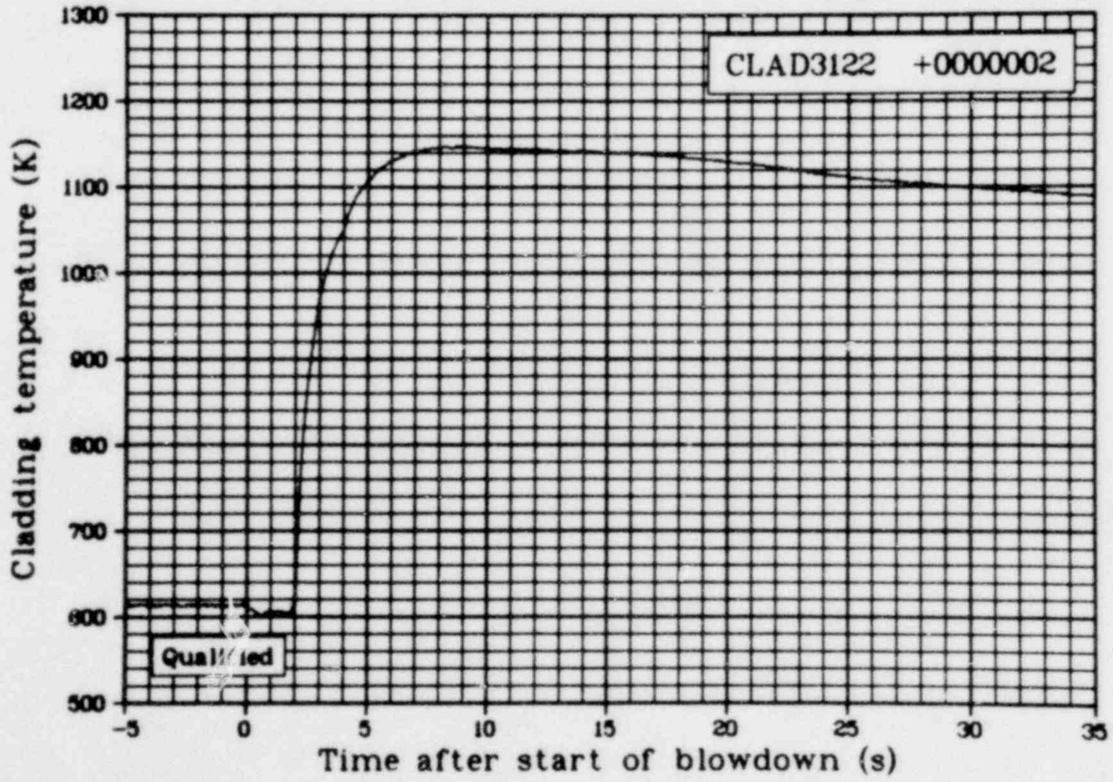

Fig. 456 Cladding temperature, Rod 312-2, at 0 degrees and fuel stack midplane (CLAD3122 + 0000002), from -5 to 35 s.

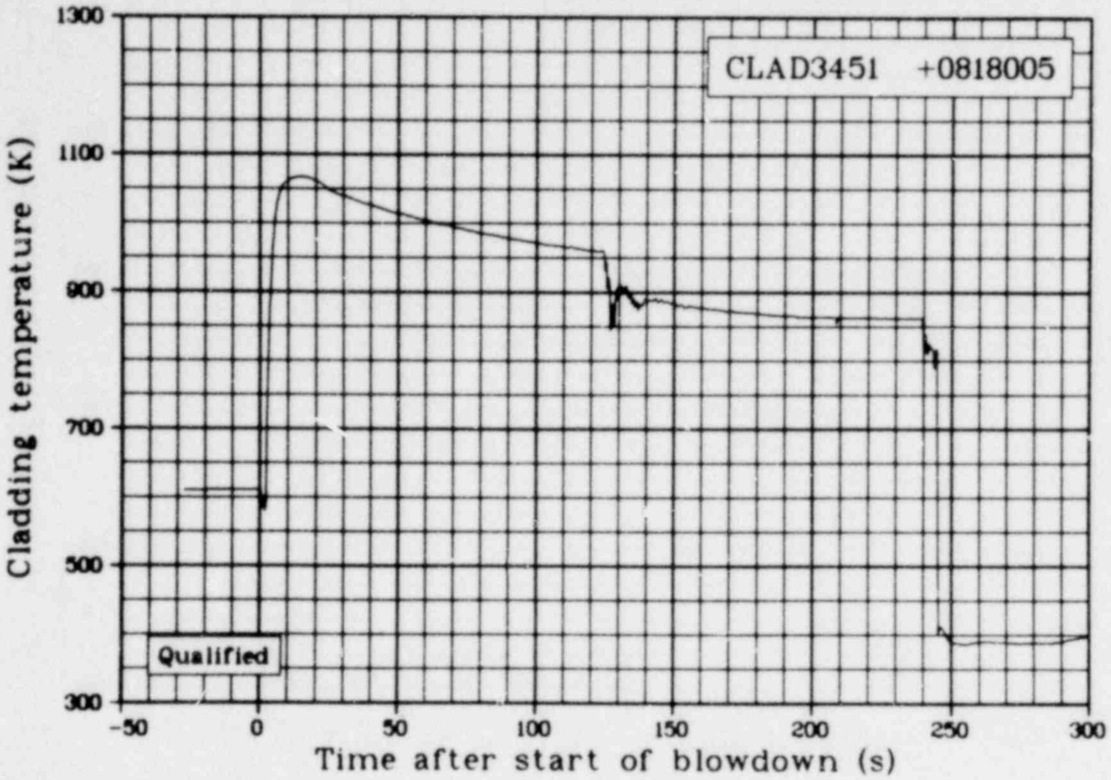

Fig. 457 Cladding temperature, Rod 345-1, at 180 degrees and 0.08 m above fuel stack midplane (CLAD3451 +0818005), from -50 to 300 s.

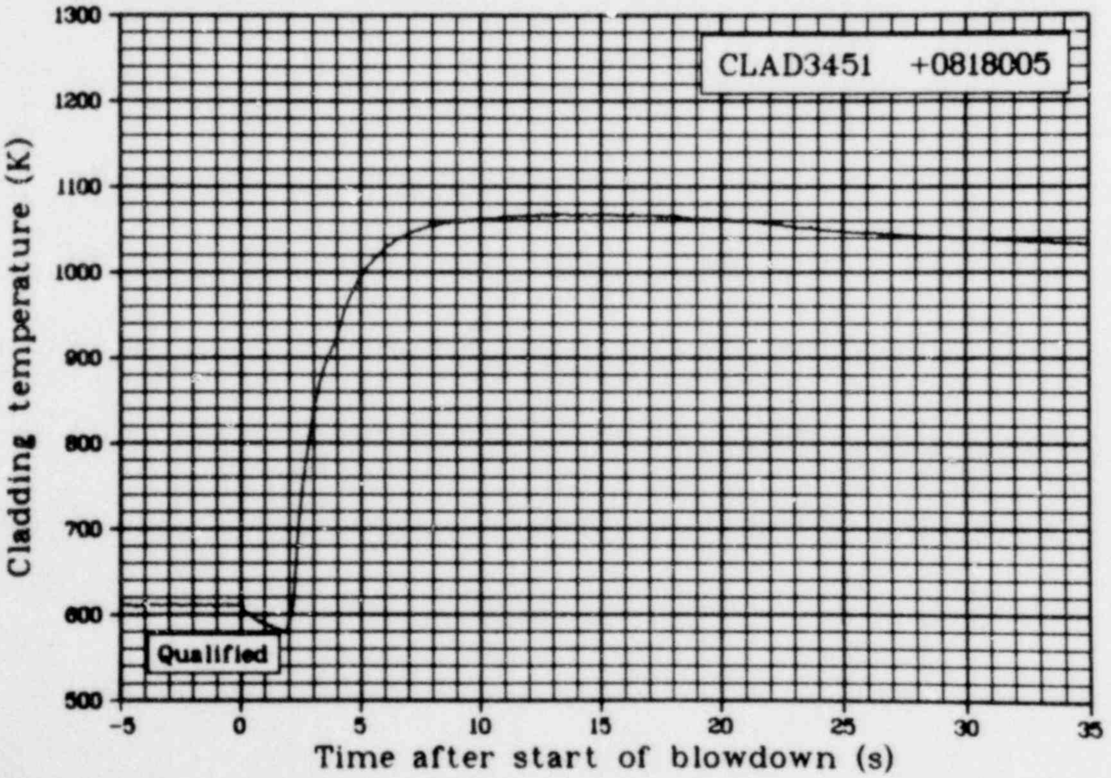

Fig. 458 Cladding temperature, Rod 345-1, at 180 degrees and 0.08 m above fuel stack midplane (CLAD3451 +0818005), from -5 to 35 s.

1405 324

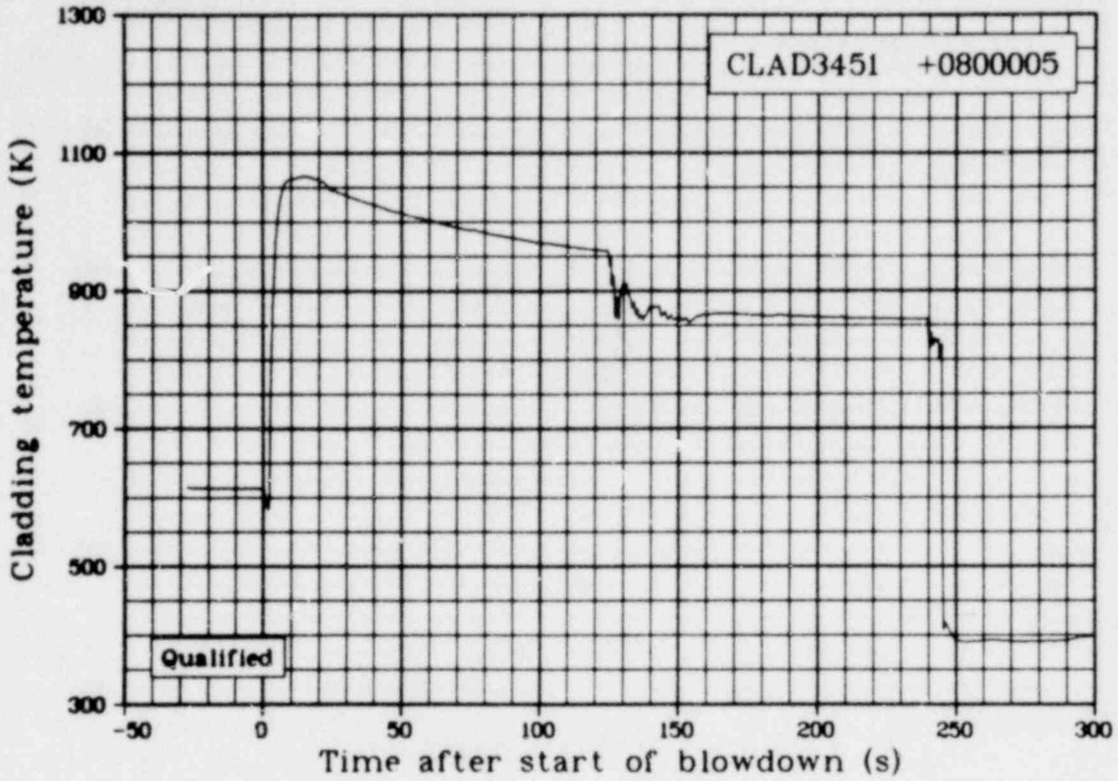

Fig. 459 Cladding temperature, Rod 345-1, at 0 degrees and 0.08 m above fuel stack midplane (CLAD3451 +0800005), from -50 to 300 s.

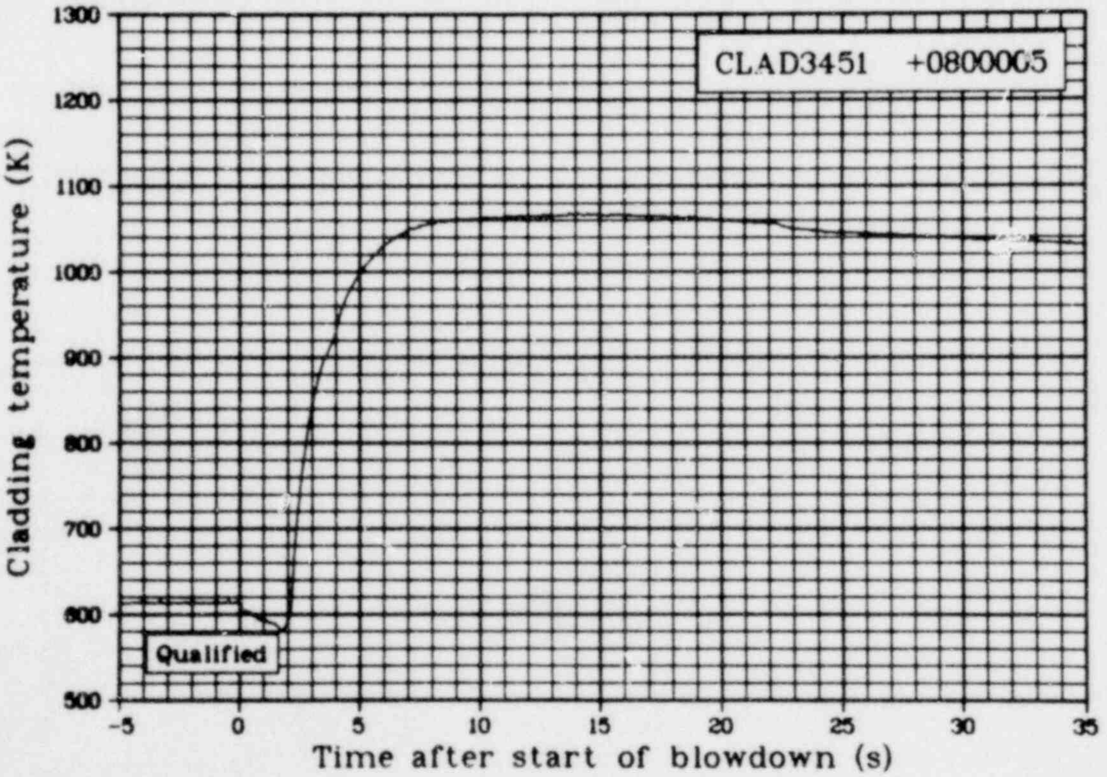

Fig. 460 Cladding temperature, Rod 345-1, at 0 degrees and 0.08 m above fuel stack midplane (CLAD3451 +0800005), from -5 to 35 s.

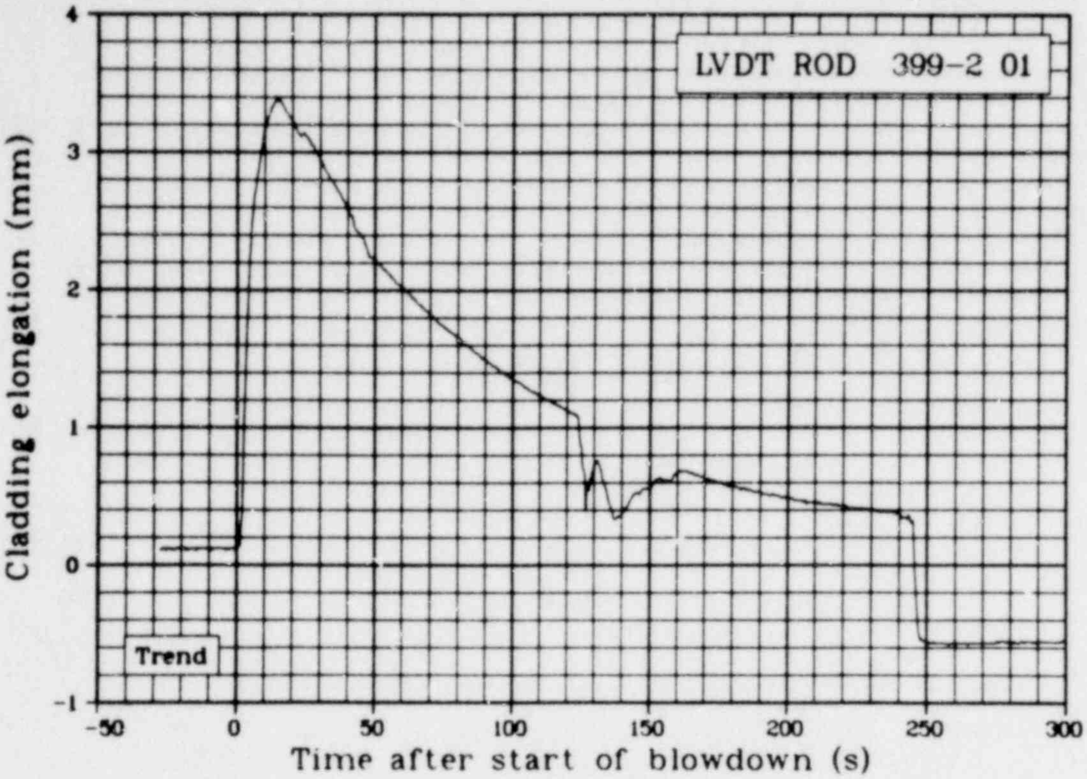

Fig. 461 Cladding elongation of Fuel Rod 399-2, (LVDT ROD 399-2 01), from -50 to 300 s.

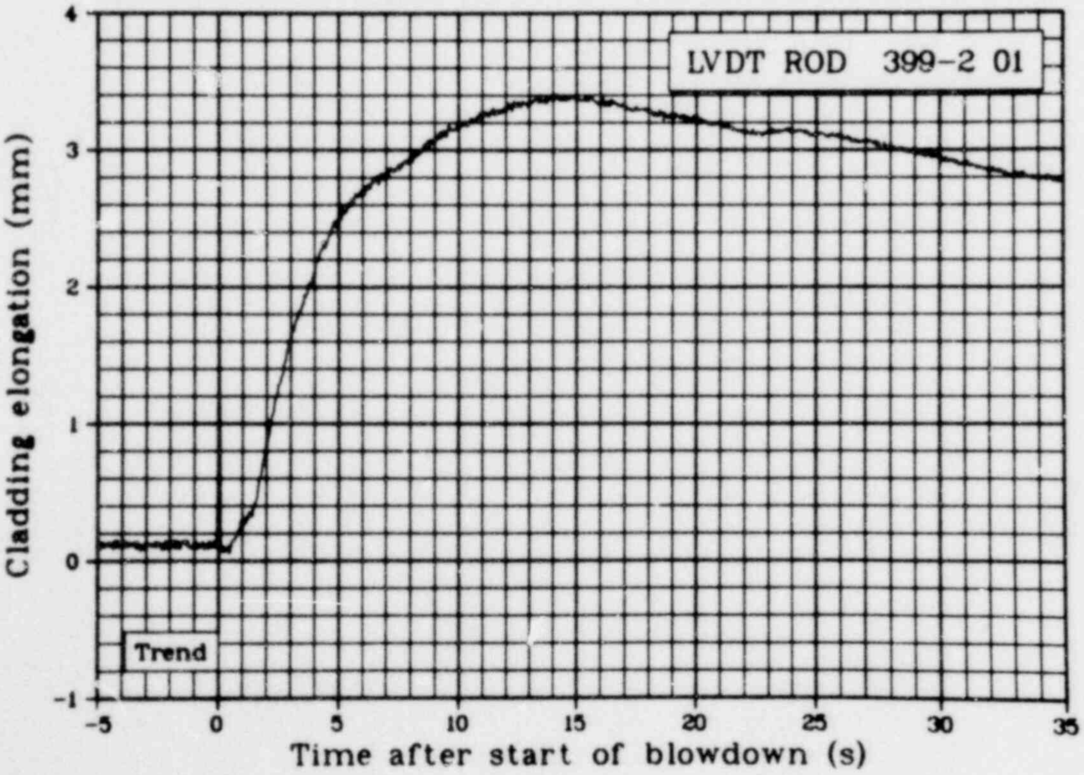

Fig. 462 Cladding elongation of Fuel Rod 399-2, (LVDT ROD 399-2 01), from -5 to 35 s.

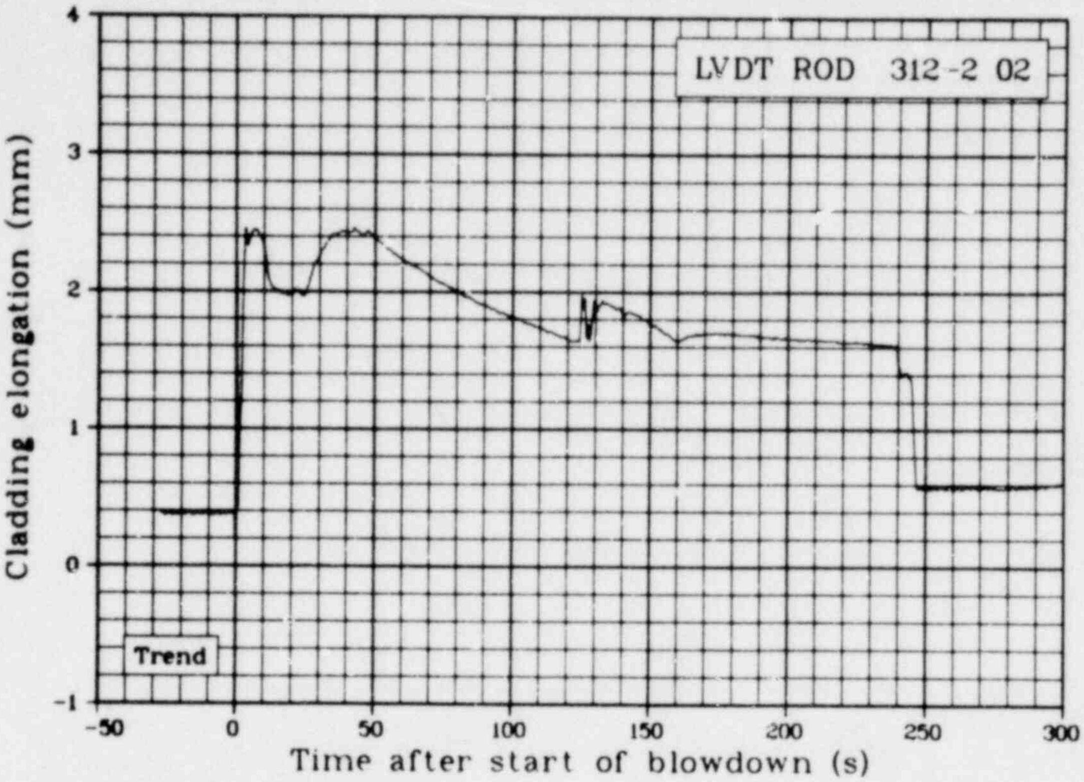

Fig. 463 Cladding elongation of Fuel Rod 312-2, (LVDT ROD 312-2 02), from -50 to 300 s.

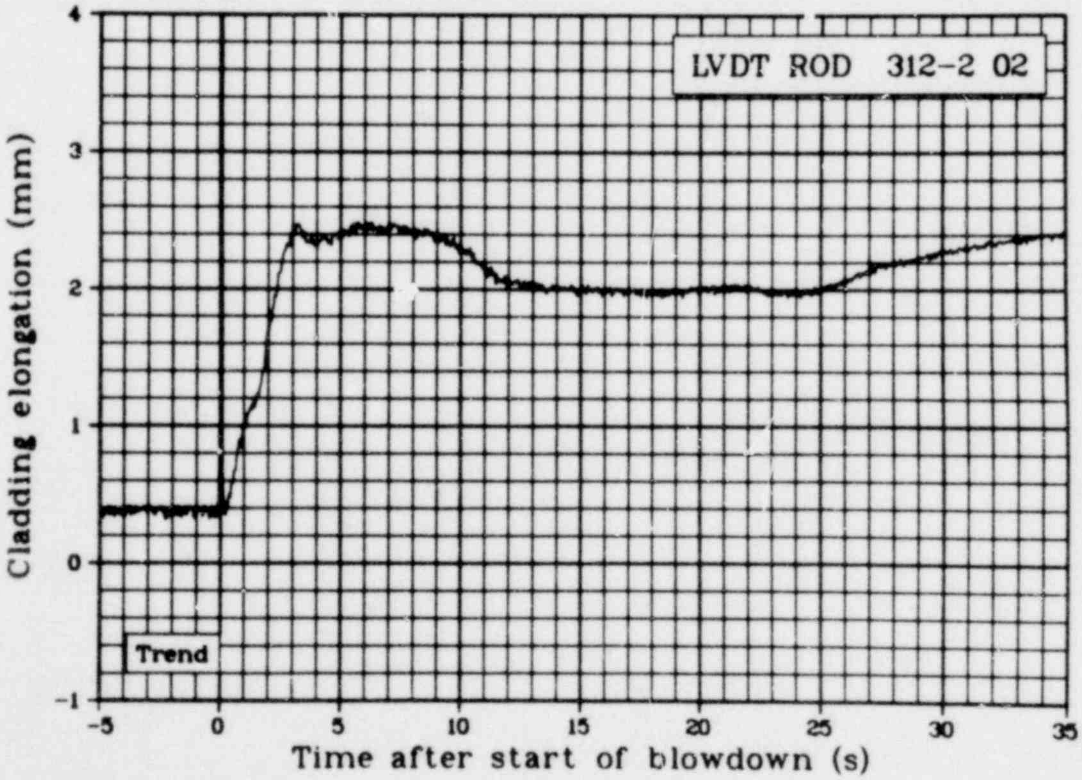

Fig. 464 Cladding elongation of Fuel Rod 312-2, (LVDT ROD 312-2 02), from -5 to 35 s.

1405 327

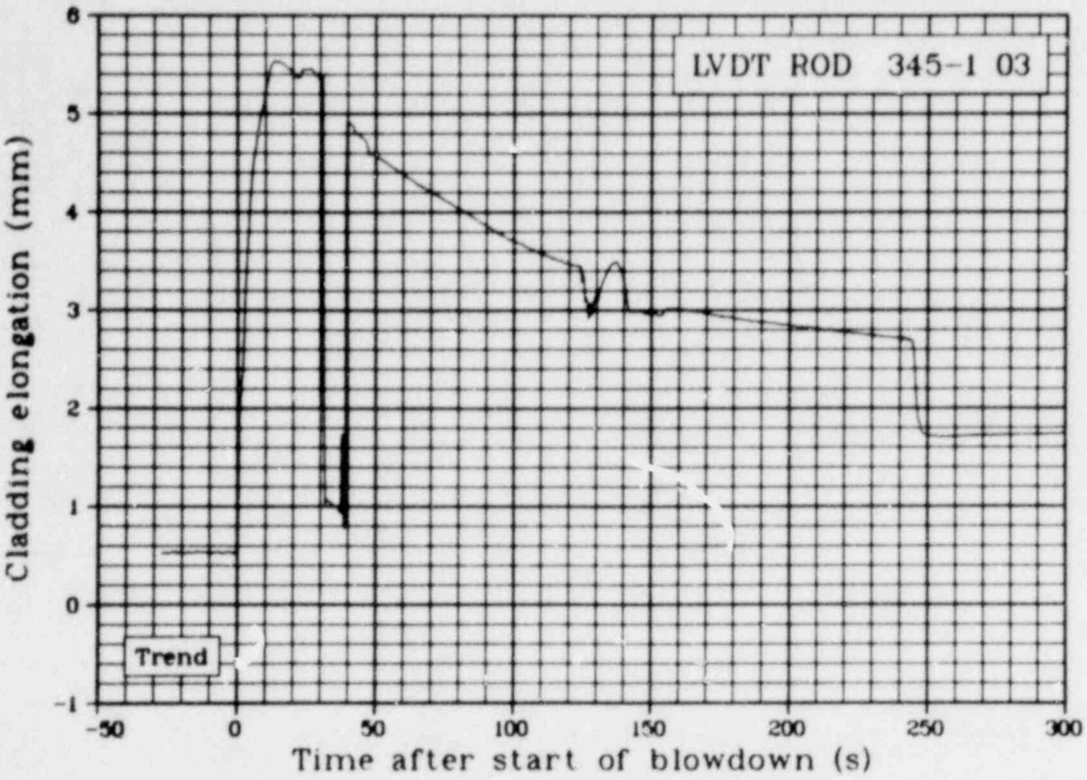

Fig. 465 Cladding elongation of Fuel Rod 345-1, (LVDT ROD 345-1 03), from -50 to 300 s.

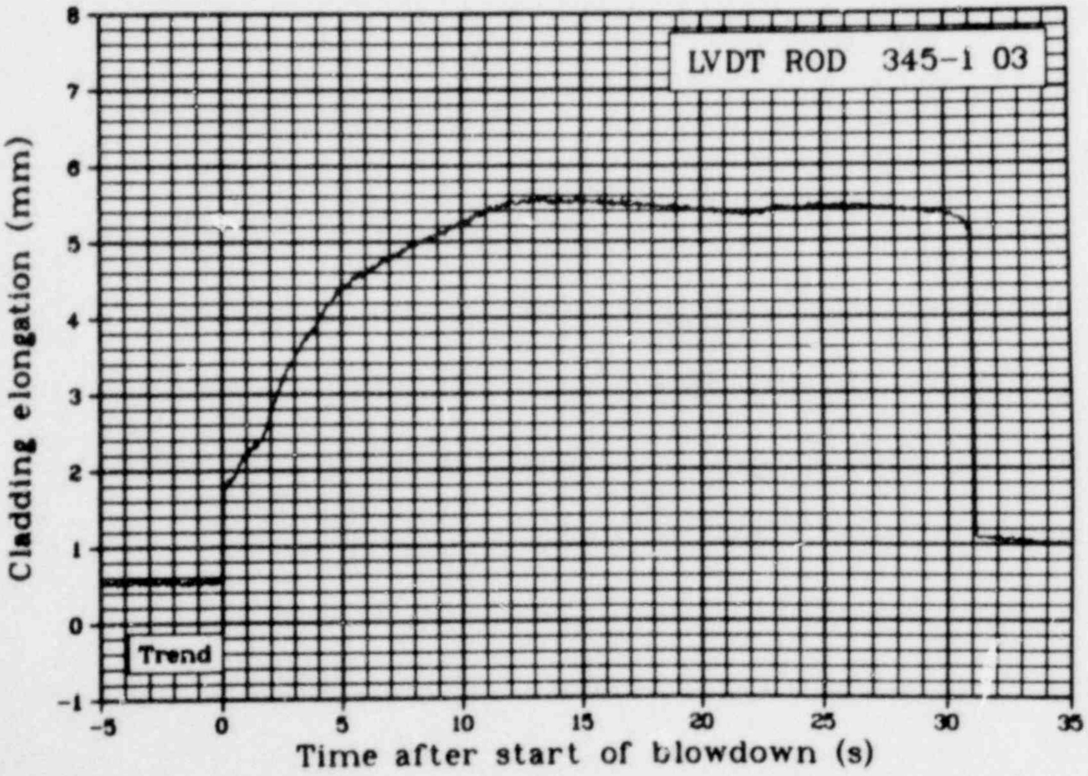

Fig. 466 Cladding elongation of Fuel Rod 345-1, (LVDT ROD 345-1 03), from -5 to 35 s.

1405 328

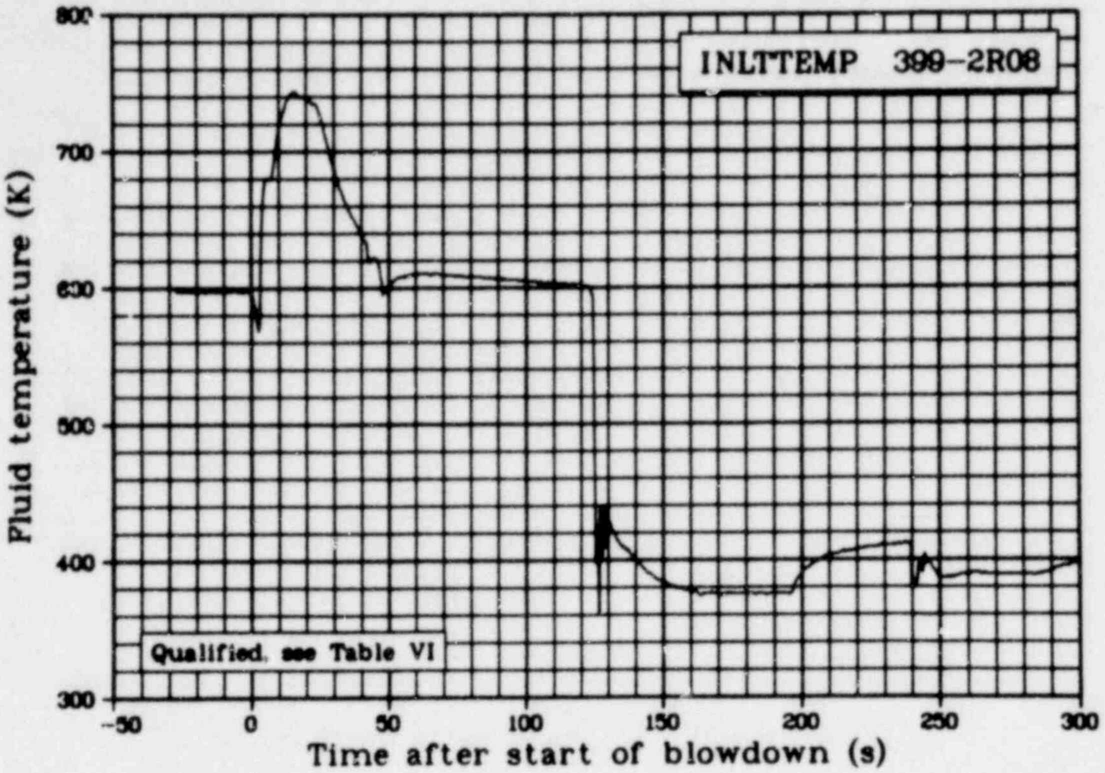

Fig. 467 Fluid temperature of Fuel Rod 399-2 coolant inlet (INLTTEMP 399-2RO8), from -50 to 300 s.

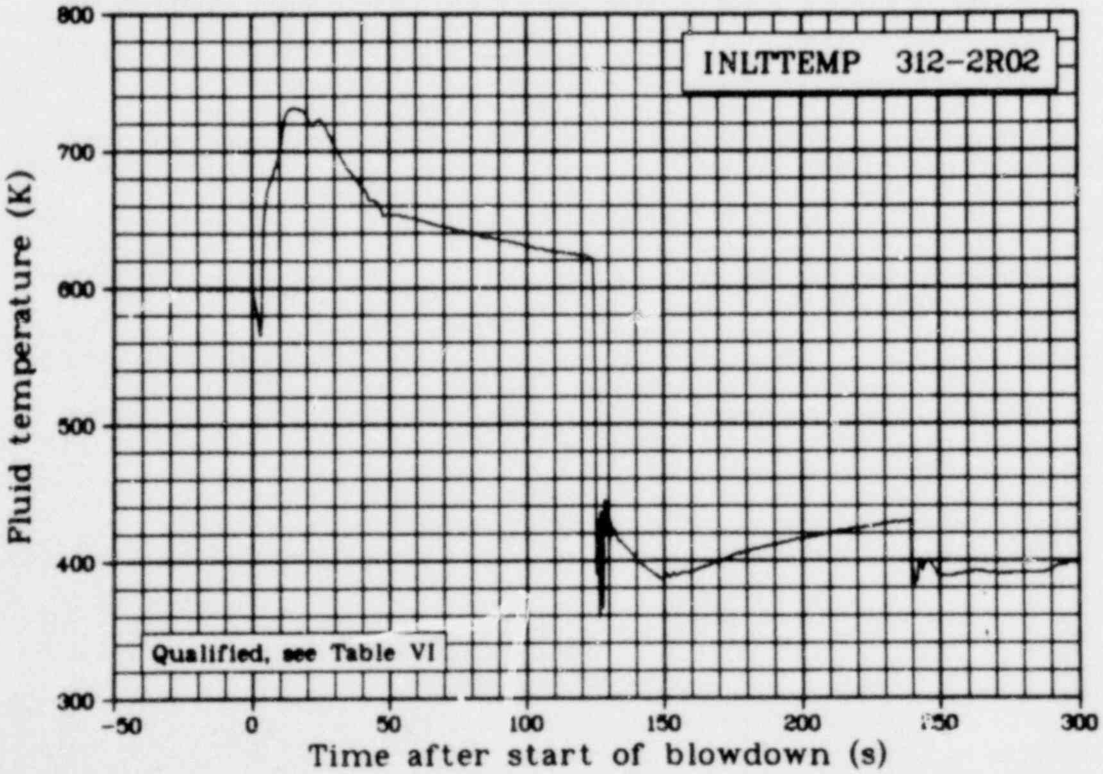

Fig. 468 Fluid temperature of Fuel Rod 312-2 coolant inlet (INLTTEMP 312-2RO2), from -50 to 300 s.

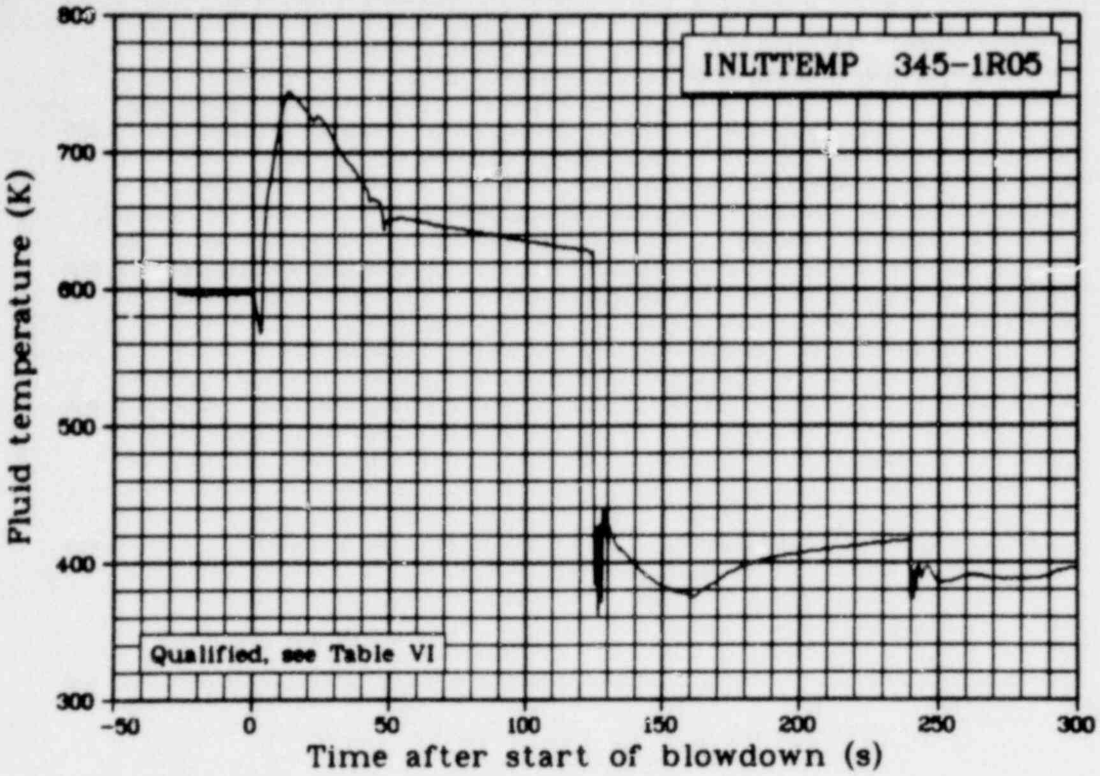

Fig. 469 Fluid temperature of Fuel Rod 345-1 coolant inlet (INLTTEMP 345-1RO5), from -50 to 300 s.

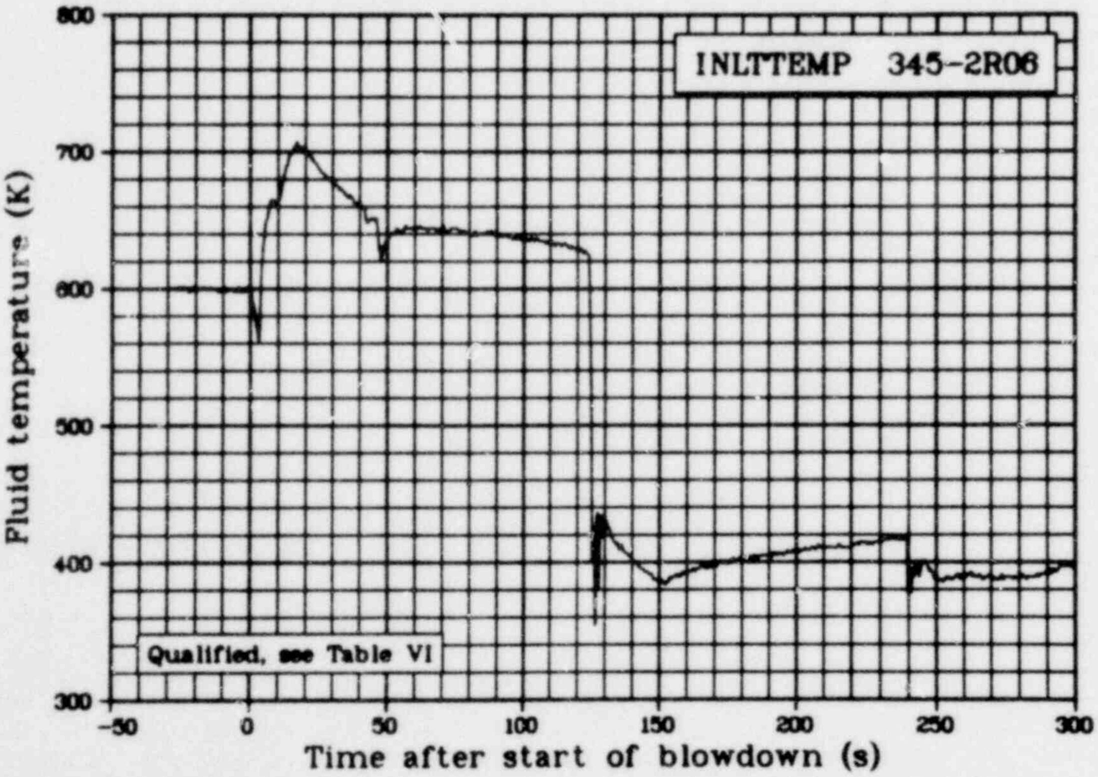

Fig. 470 Fluid temperature of Fuel Rod 34 i-2 coolant inlet (INLTTEMP 345-2RO6), from -50 to 300 s.

1405 330

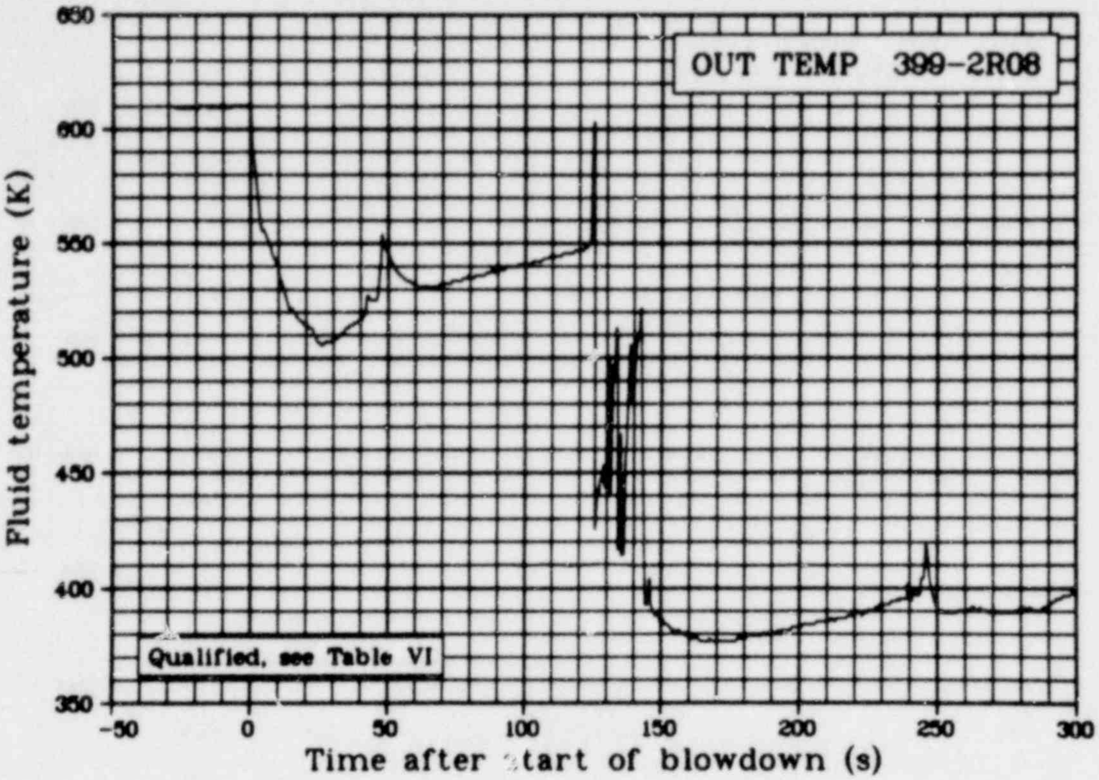

Fig. 471 Fluid temperature of Fuel Rod 399-2 coolant outlet (OUT TEMP 399-2RO8), from -50 to 300 s.

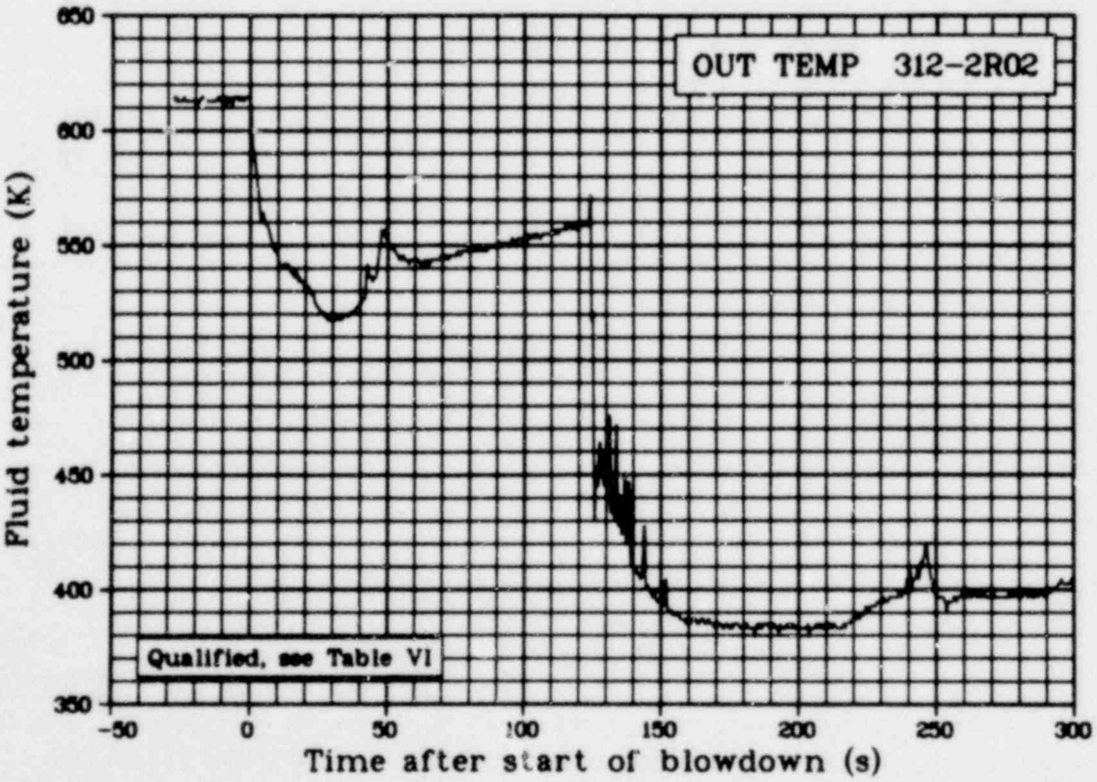

Fig. 472 Fluid temperature of Fuel Rod 312-2 coolant outlet (OUT TEMP 312-2RO2), from -50 to 300 s.

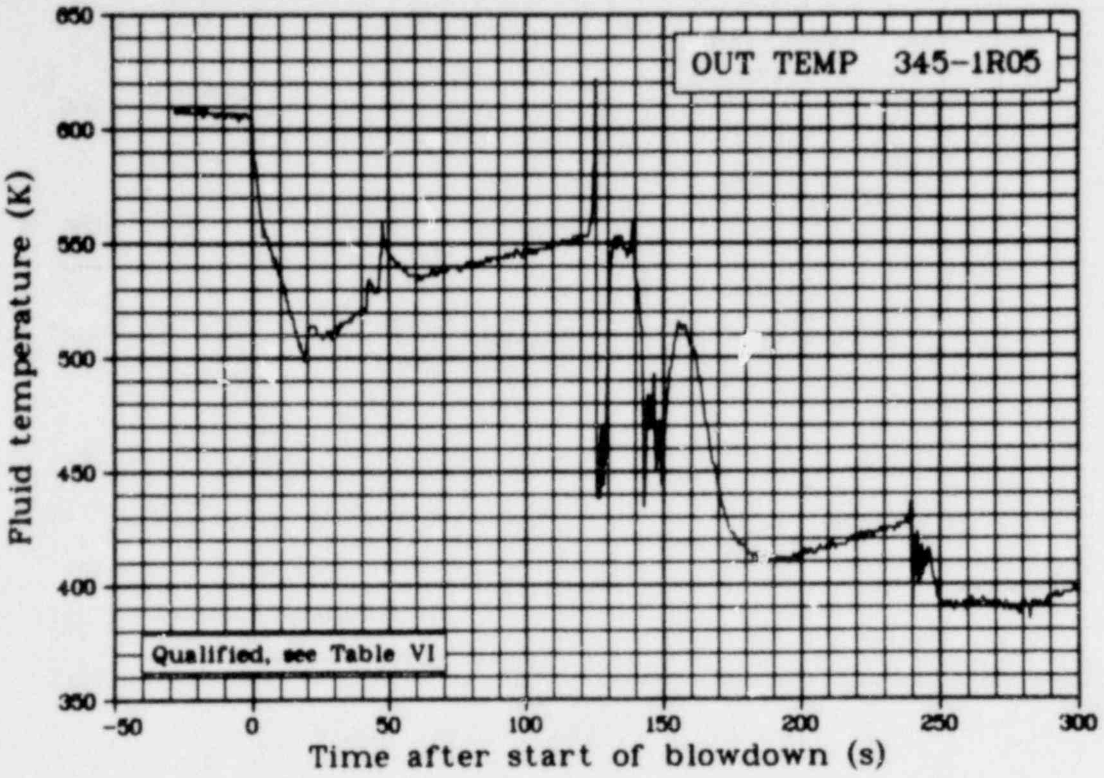

Fig. 473 Fluid temperature of Fuel Rod 345-1 coolant outlet (OUT TEMP 345-1RO5), from -50 to 300 s.

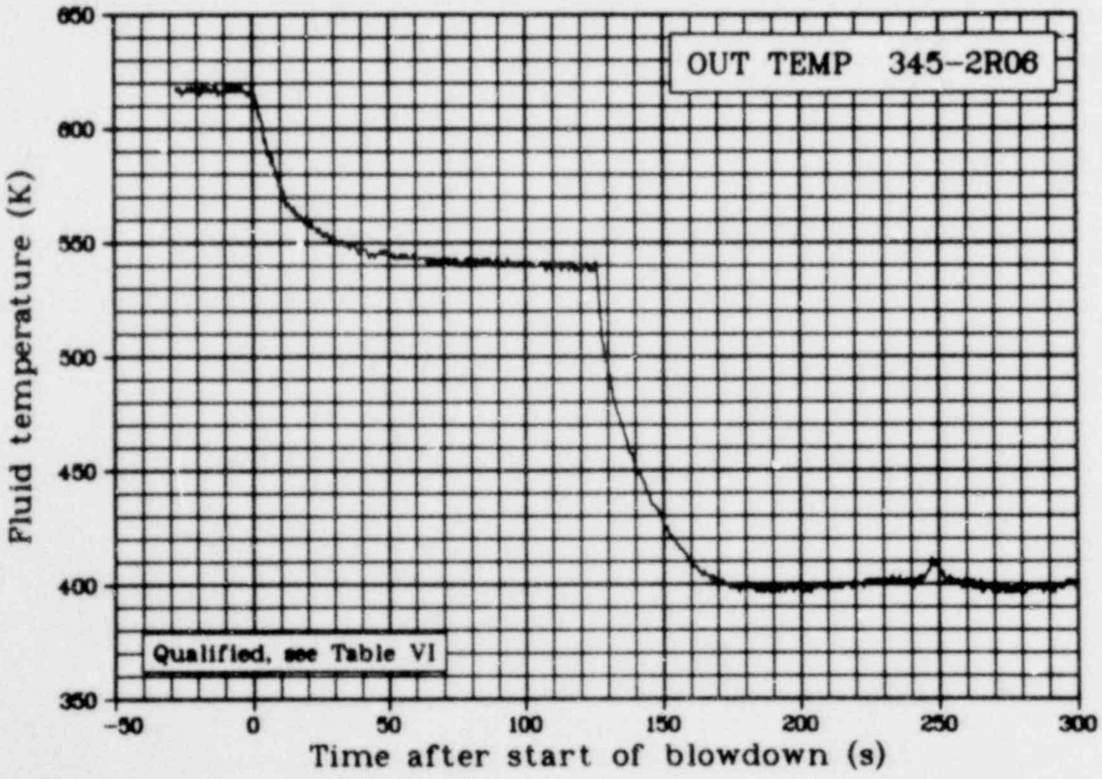

Fig. 474 Fluid temperature of Fuel Rod 345-2 coolant outlet (OUT TEMP 345-2RO6), from -50 to 300 s.

1405 332

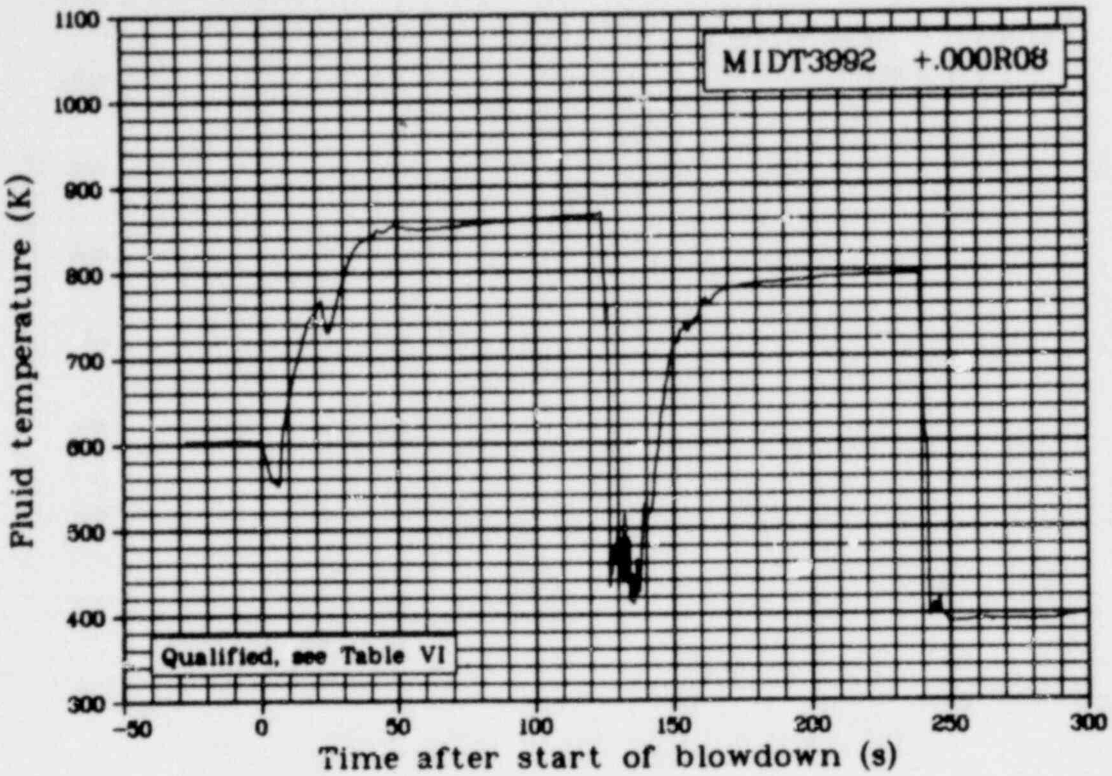

Fig. 475 Fluid temperature of Fuel Rod 399-2, at fuel stack midplane (MIDT3992 + .000R08), from -50 to 300 s.

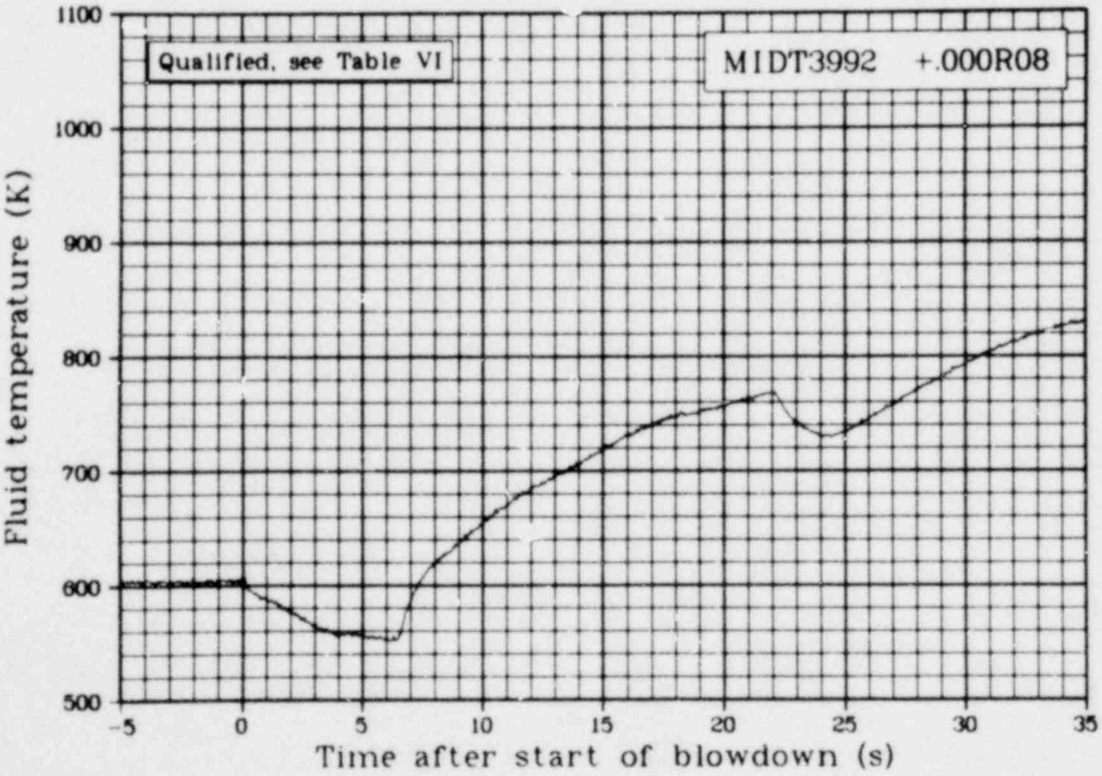

Fig. 476 Fluid temperature of Fuel Rod 399-2, at fuel stack midplane (MIDT3992 + .000R08), from -5 to 35 s.

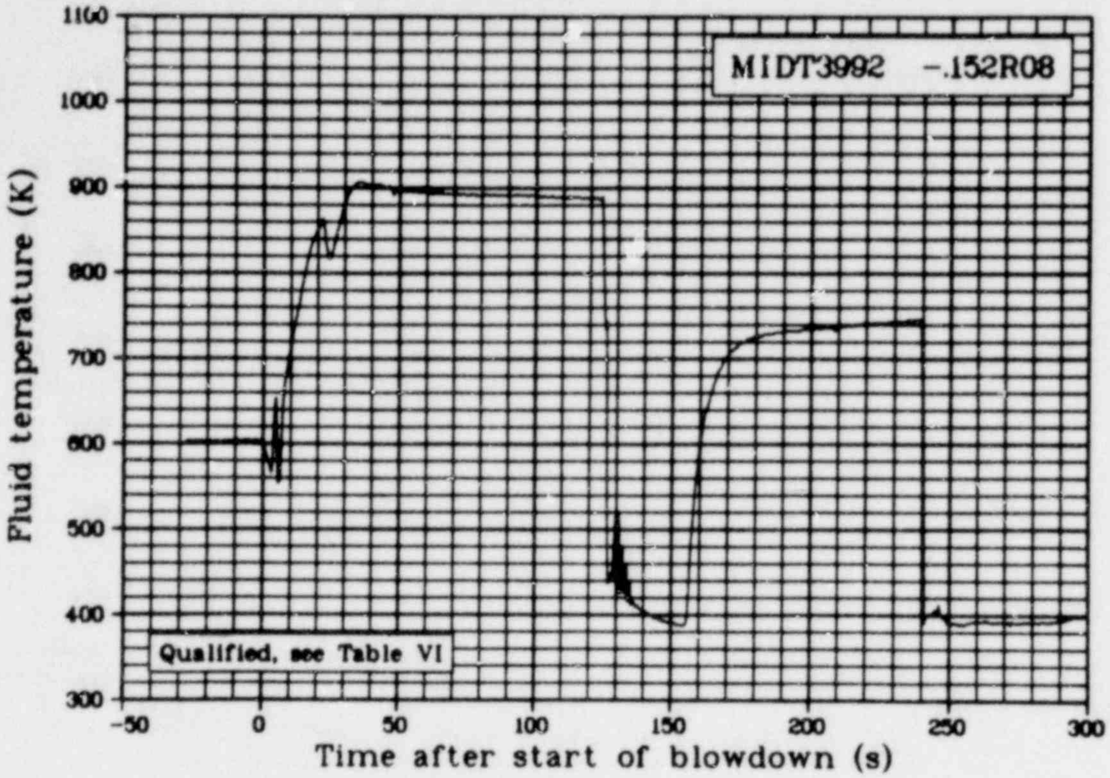

Fig. 477 Fluid temperature of Fuel Rod 399-2, 0.152 m below fuel stack midplane (MIDT3992 -.152R08), from -50 to 300 s.

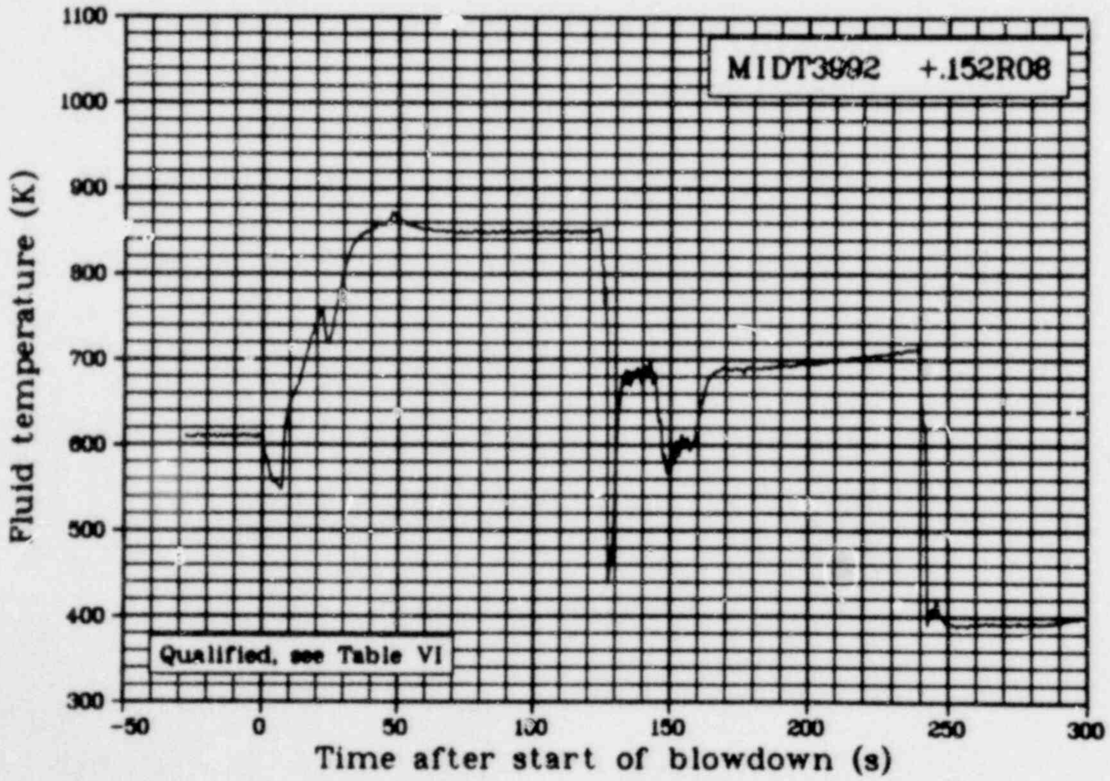

Fig. 478 Fluid temperature of Fuel Rod 399-2, 0.152 m above fuel stack midplane (MIDT3992 +.152R08), from -50 to 300 s.

1405 334

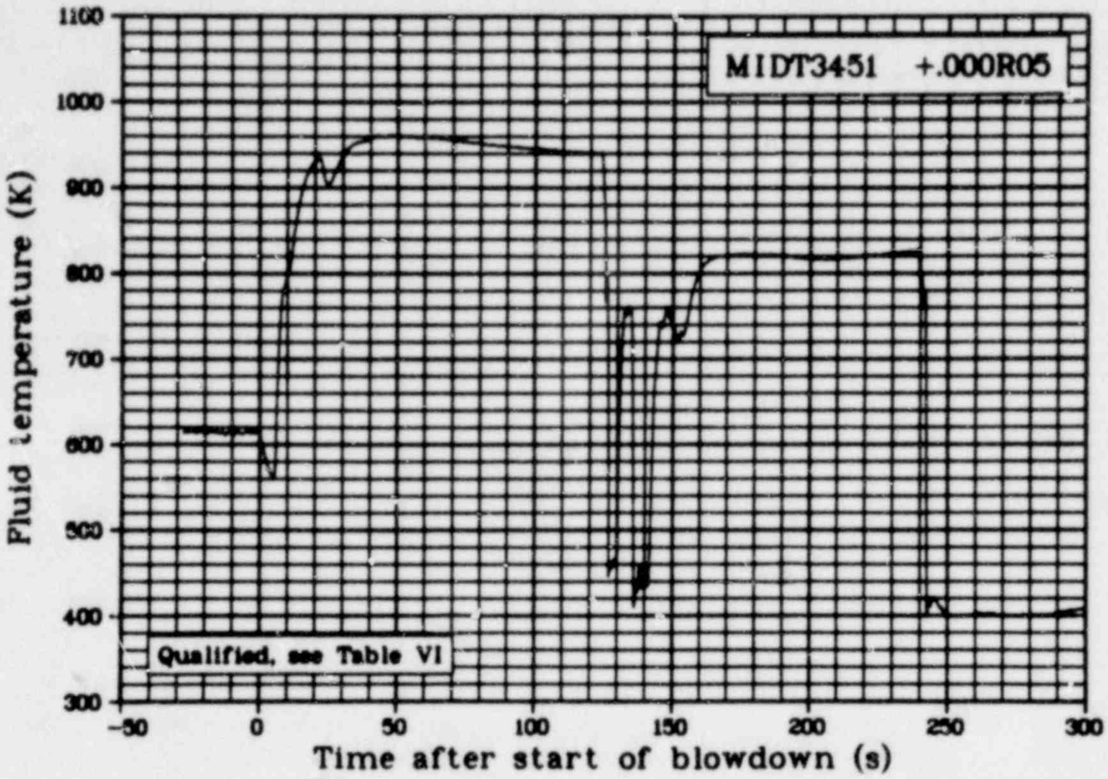

Fig. 479 Fluid temperature of Fuel Rod 345-1, at fuel stack midplane (MIDT3451 + .000R05), from -50 to 300 s.

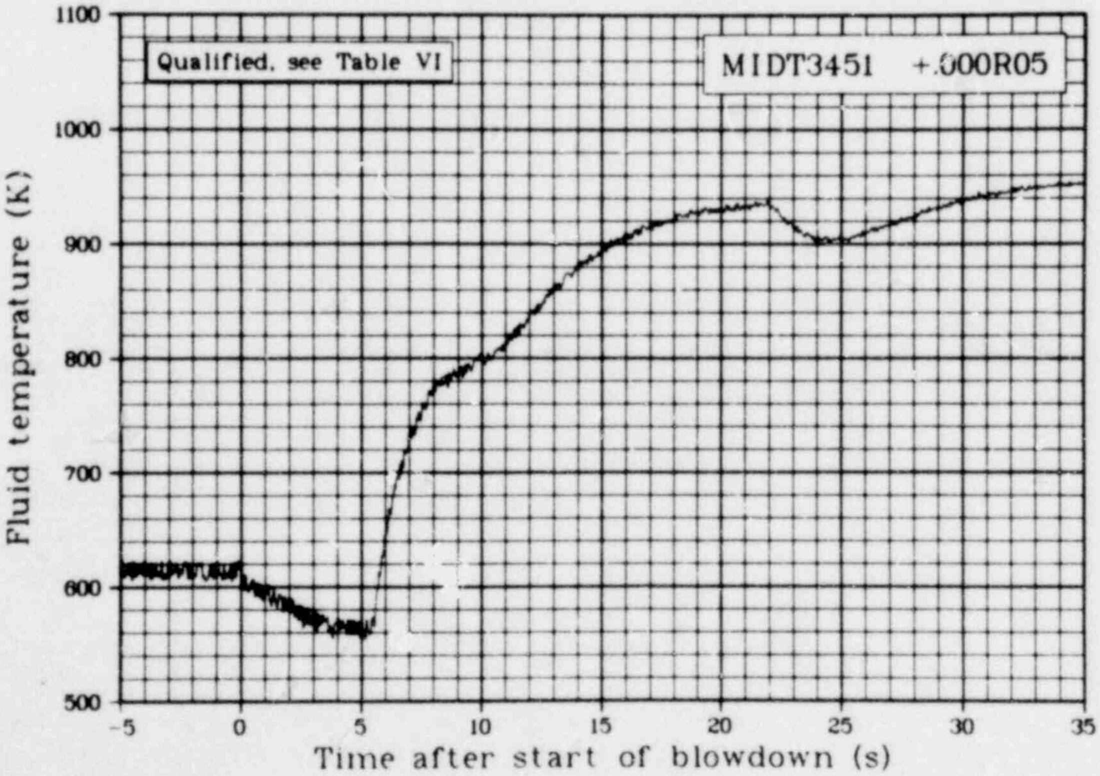

Fig. 480 Fluid temperature of Fuel Rod 345-1, at fuel stack midplane (MIDT3451 + .000R05), from -5 to 35 s.

1405 335

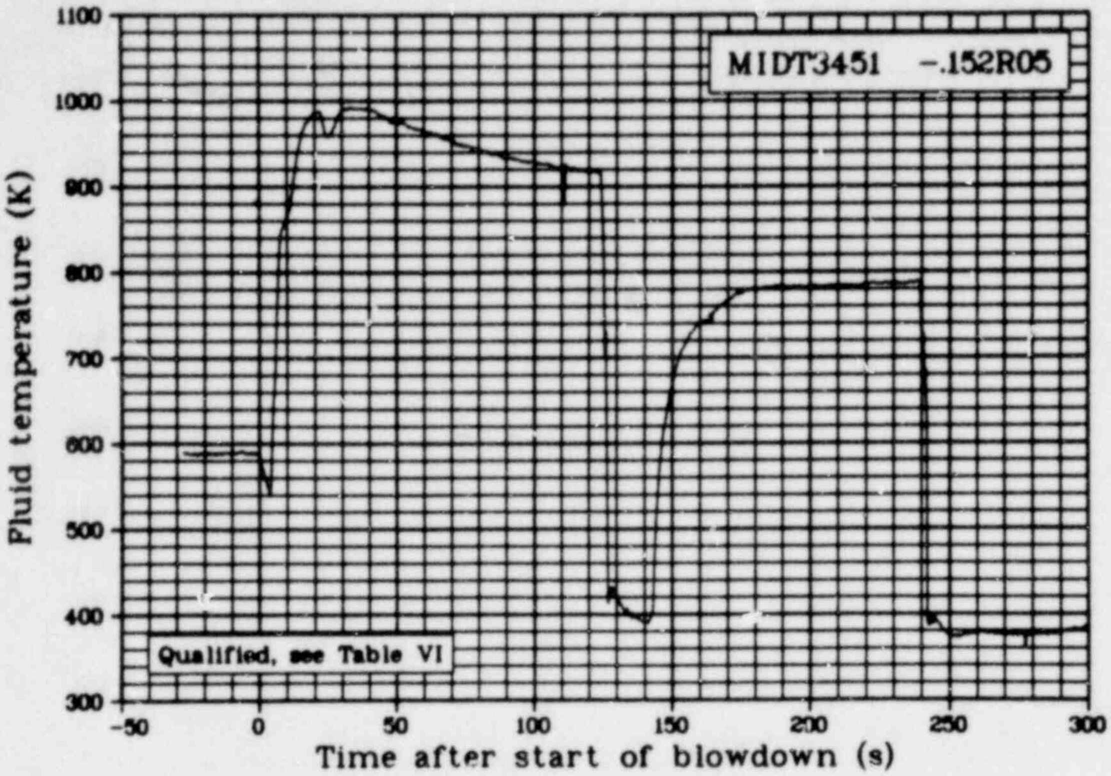

Fig. 481 Fluid temperature of Fuel Rod 345-1, 0.152 m below fuel stack midplane (MIDT3451 -.152R05), from -50 to 300 s.

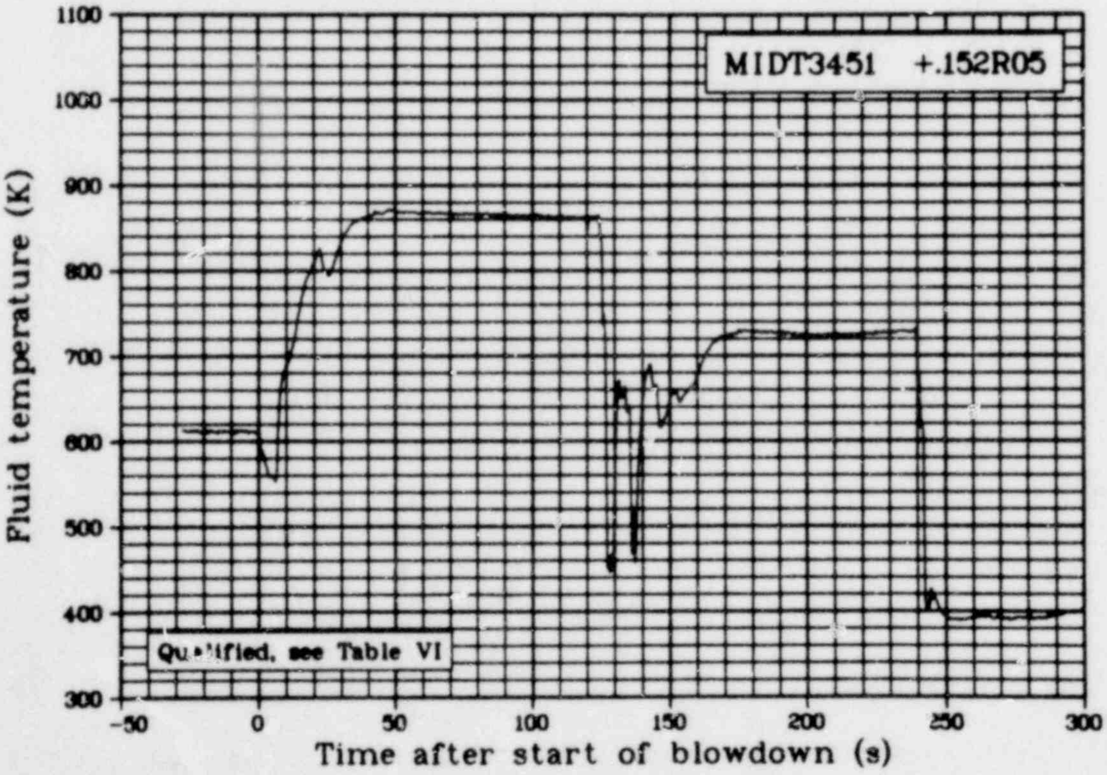

Fig. 482 Fluid temperature of Fuel Rod 345-1, 0.152 m above fuel stack midplane (MIDT3451 +.152R05), from -50 to 300 s.

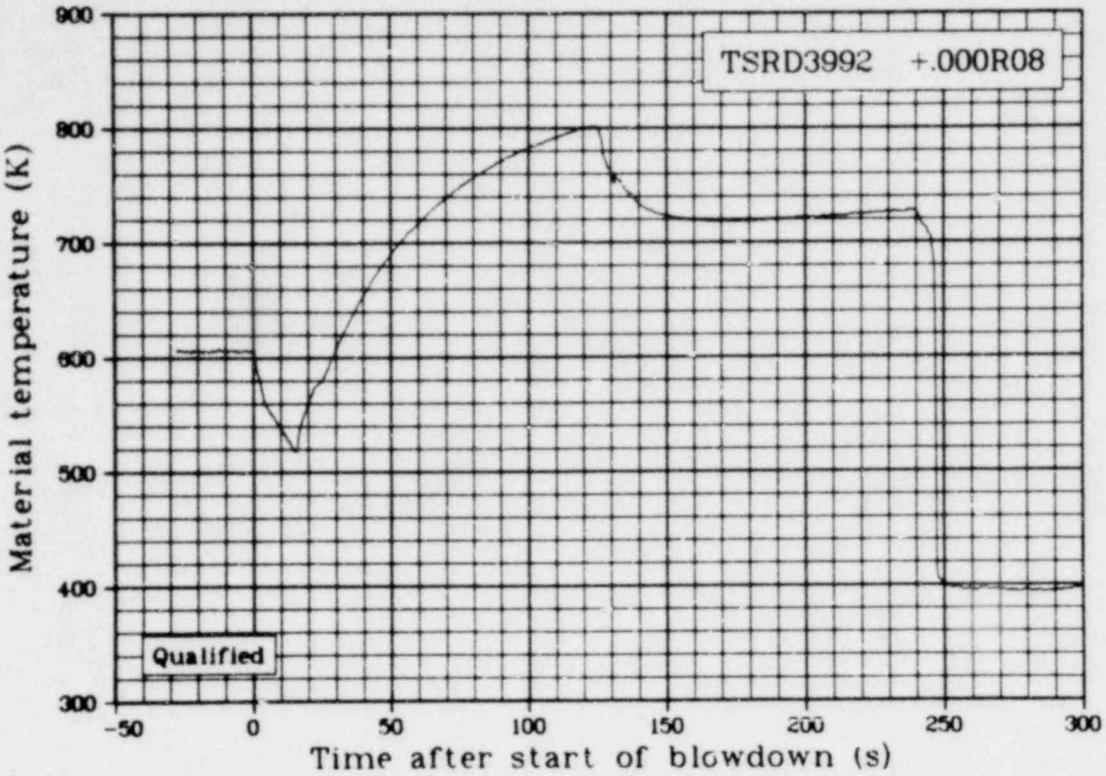

Fig. 483 Material temperature, Rod 399-2 shroud, at fuel stack midplane (TSRD3992 + .000R08), from -50 to 300 s.

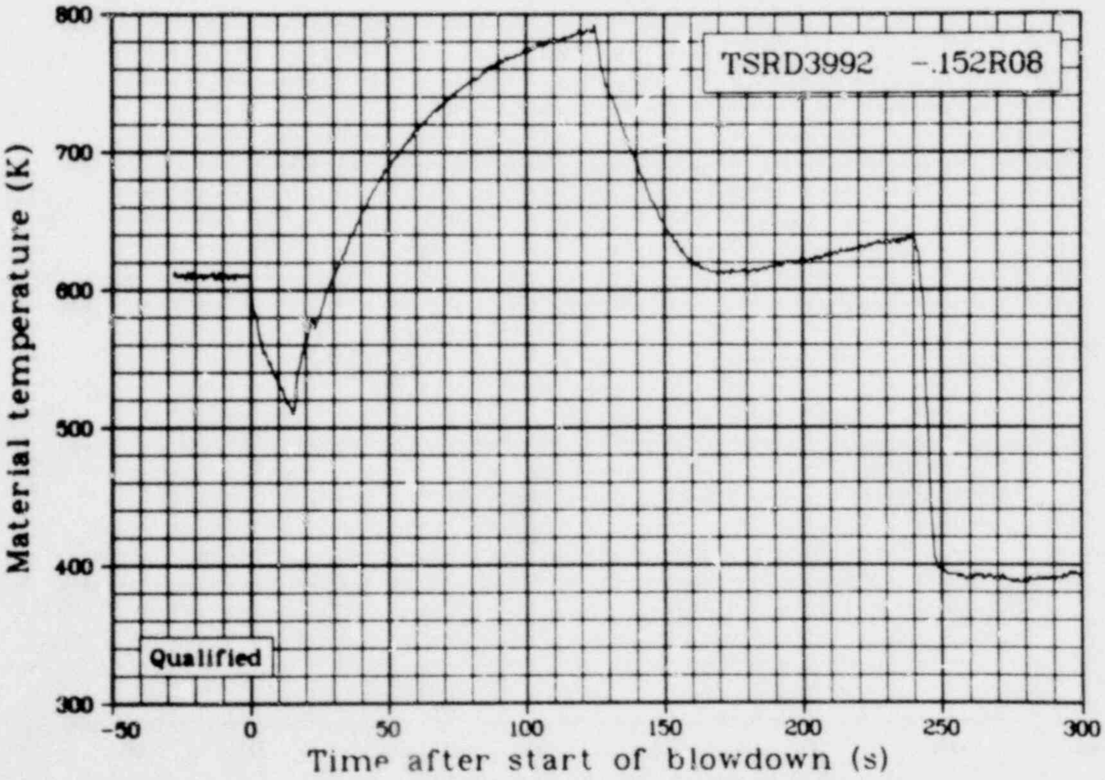

Fig. 484 Material temperature, Rod 399-2 shroud, 0.152 m below fuel stack midplane (TSRD3992 -.152R08), from -50 to 300 s.

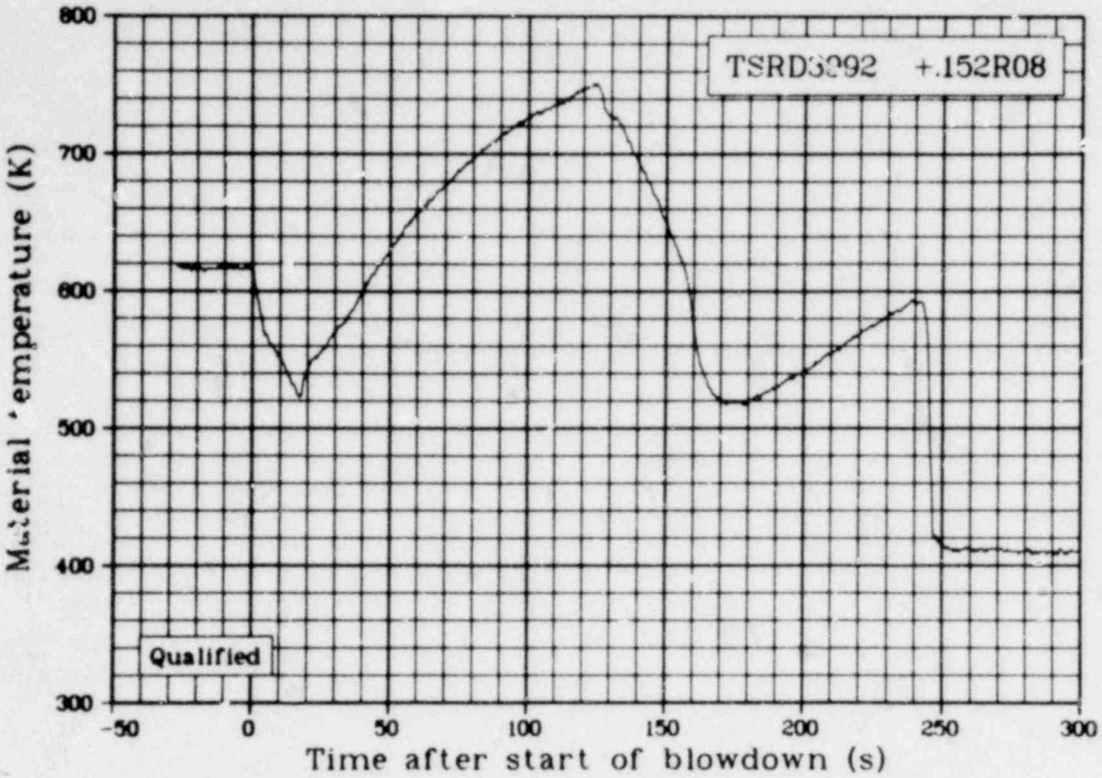

Fig. 485 Material temperature, Rod 399-2 shroud, 0.152 m above fuel stack midplane (TSRD3992 + .152R08), from -50 to 300 s.

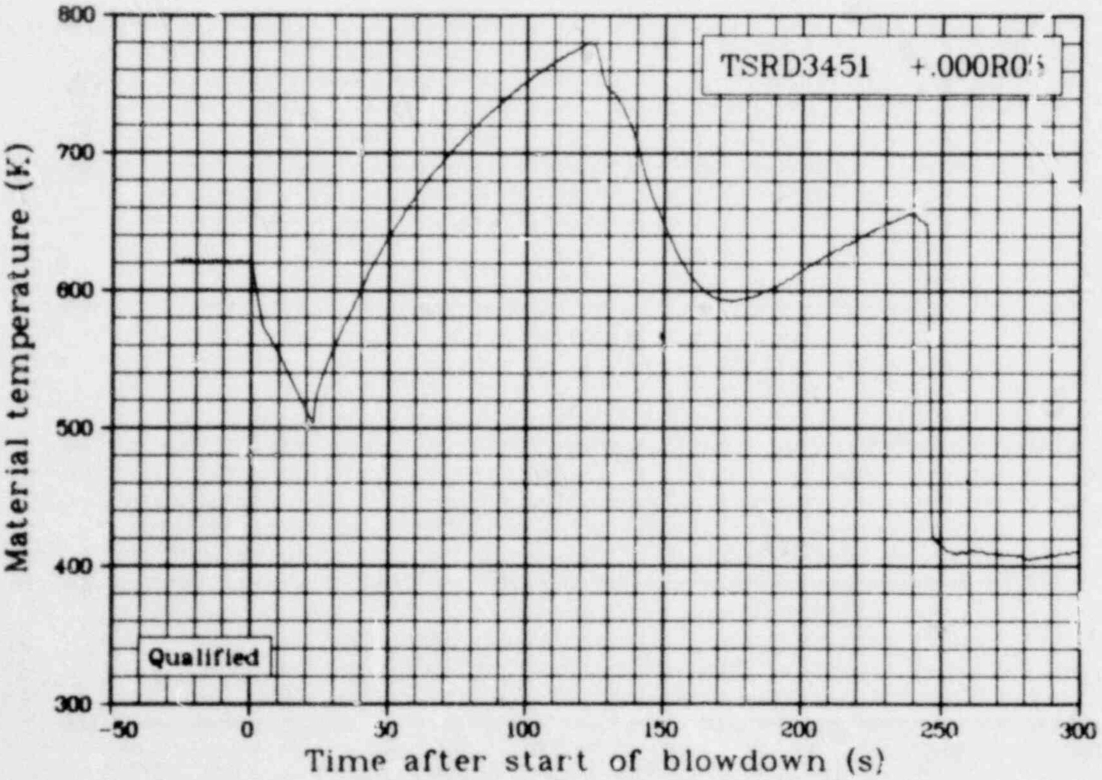

Fig. 486 Material temperature, Rod 345-1 shroud at fuel stack midplane (TSRD3451 + .000R05), from -50 to 300 s.

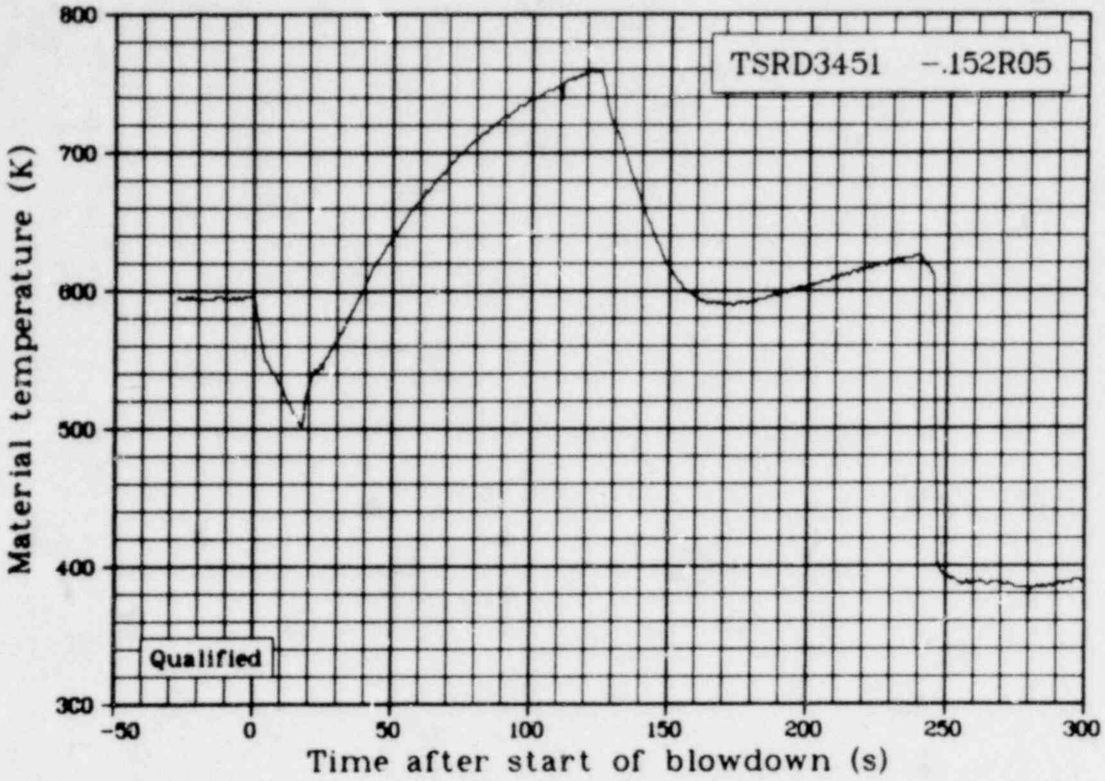

Fig. 487 Material temperature, Rod 345-1 shroud. 0.152 m below fuel stack midplane (TSRD3451 -.152R05), from -50 to 300 s.

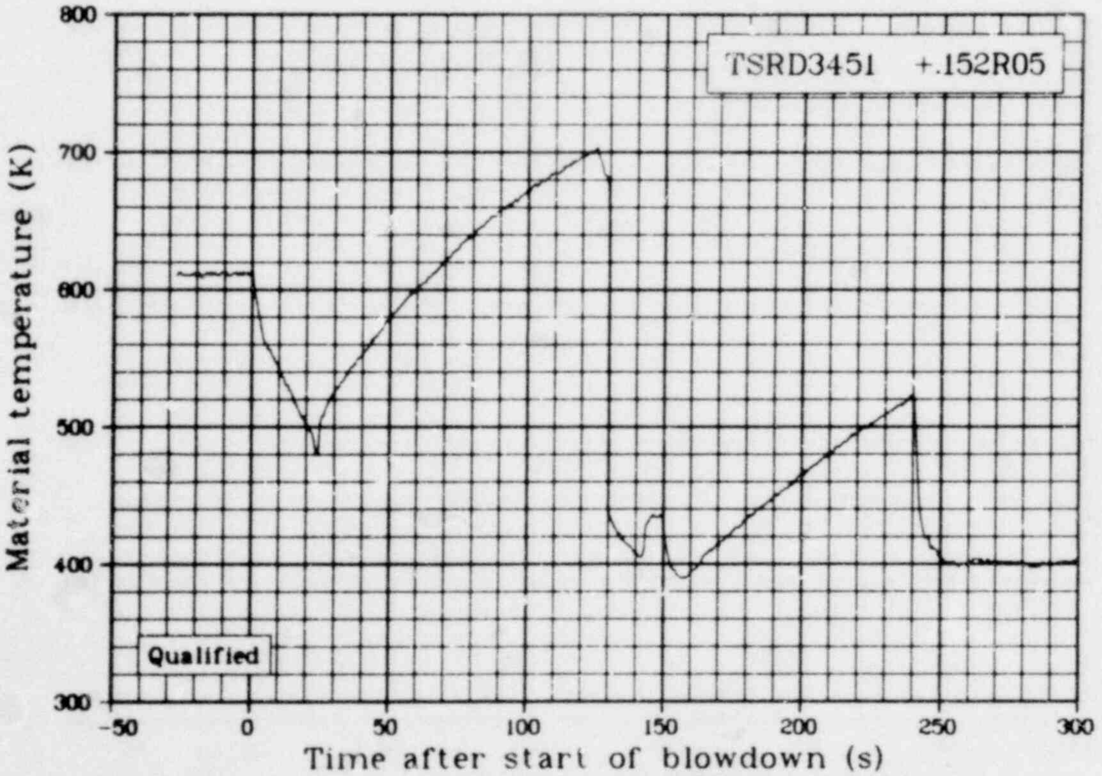

Fig. 488 Material temperature, Rod 345-1 shroud, 0.152 m above fuel stack midplane (TSRD3451 + .152R05), from -50 to 300 s.

1405 339

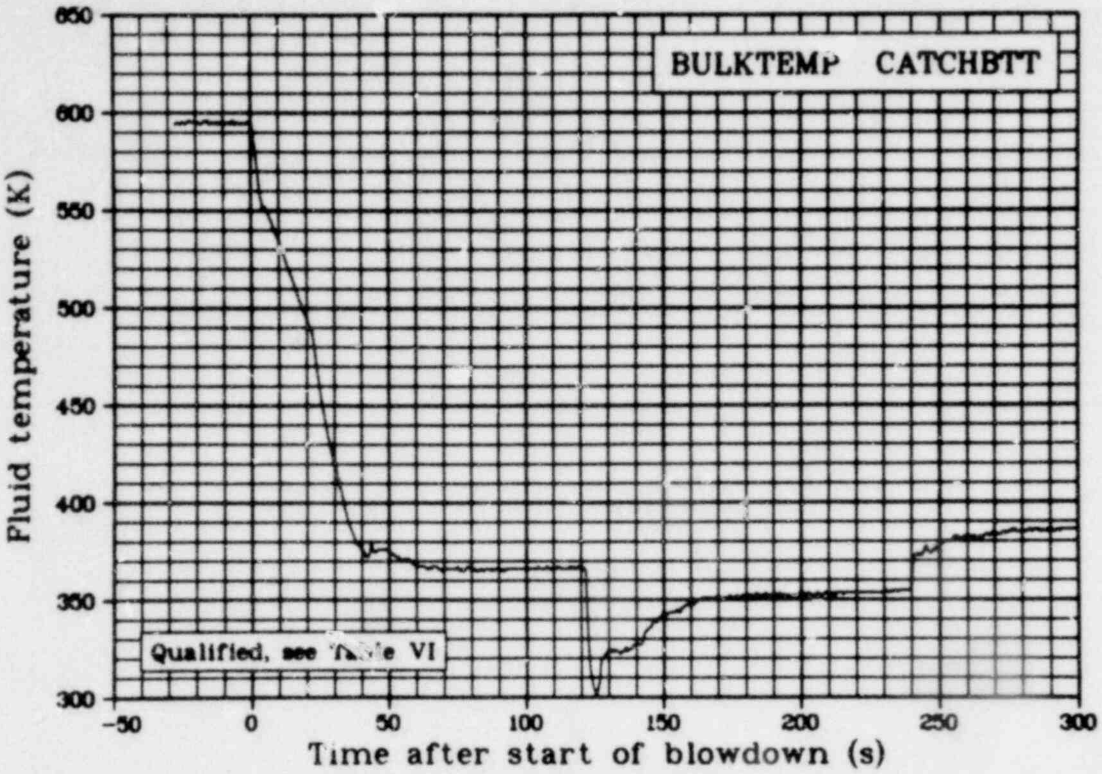

Fig. 489 Fluid temperature in test train catch basket (BULKTEMP CATCHBTT), from -50 to 300 s.

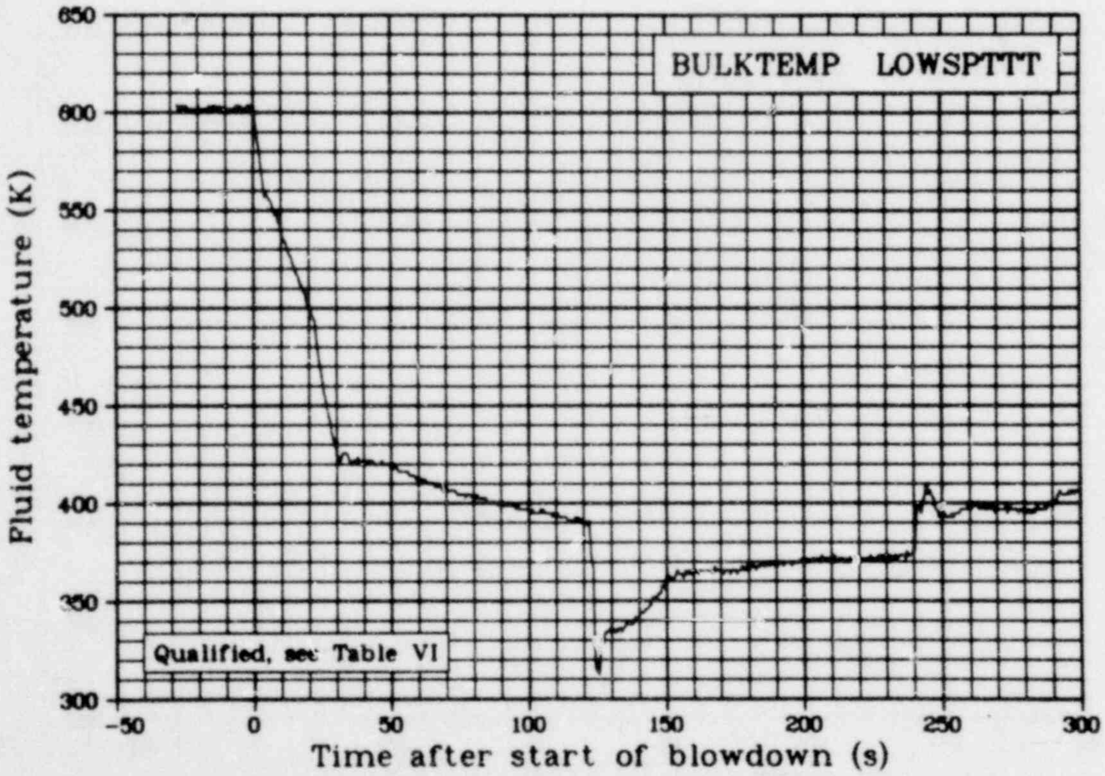

Fig. 490 Fluid temperature below test train lower support plate (BULKTEMP LOWSPTTT), from -50 to 300 s.

1405 340

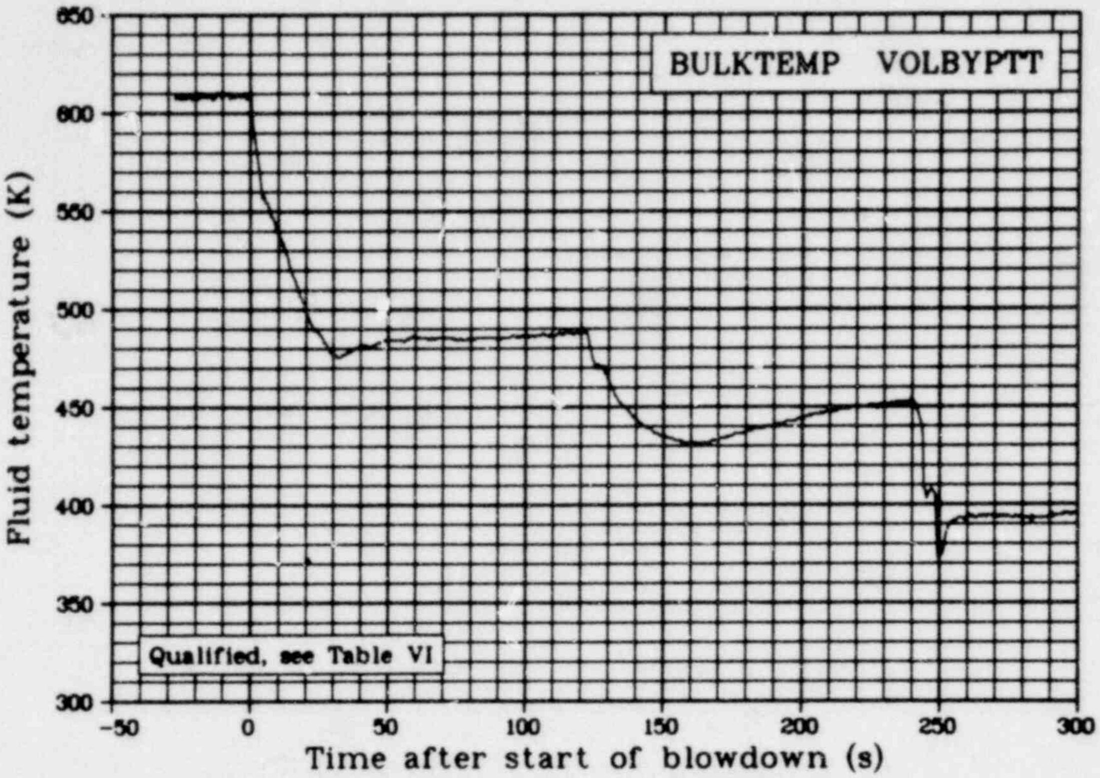

Fig. 491 Fluid temperature in bypass volume at fuel stack midplane (BULKTEMP VOLBYPTT), from -50 to 300 s.

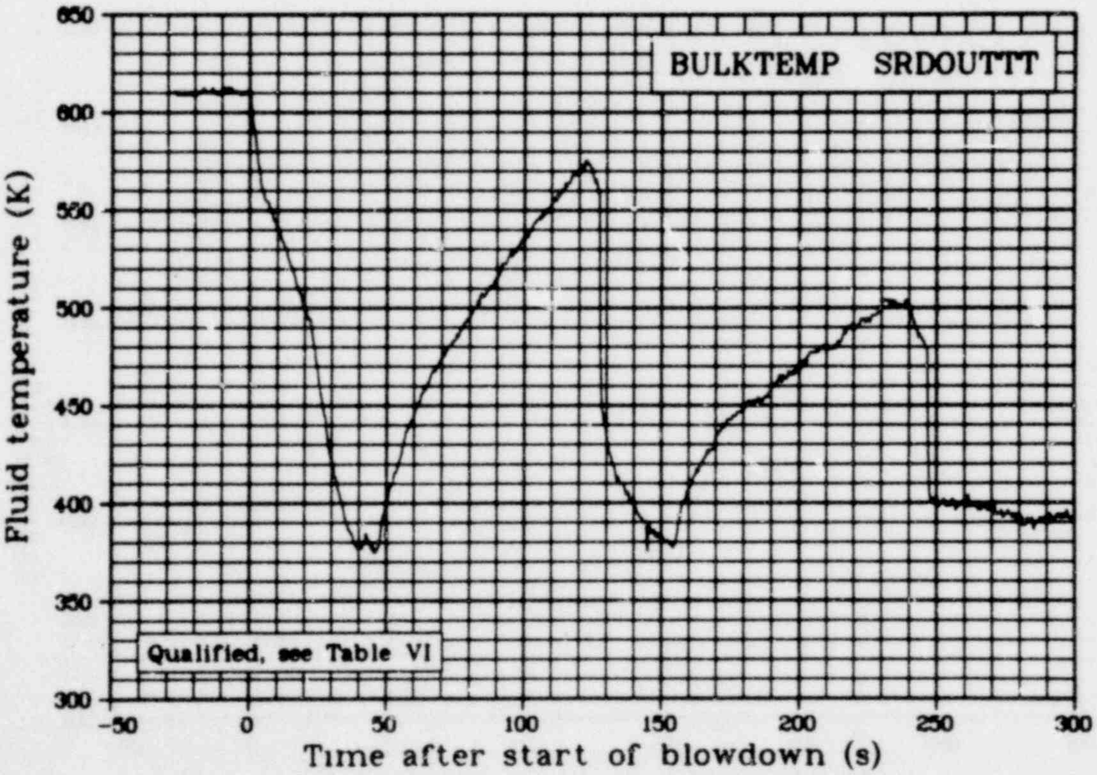

Fig. 492 Fluid temperature 0.05 m above flow shroud outlets (BULKTEMP SRDOUTTT), from -50 to 300 s.

1405 341

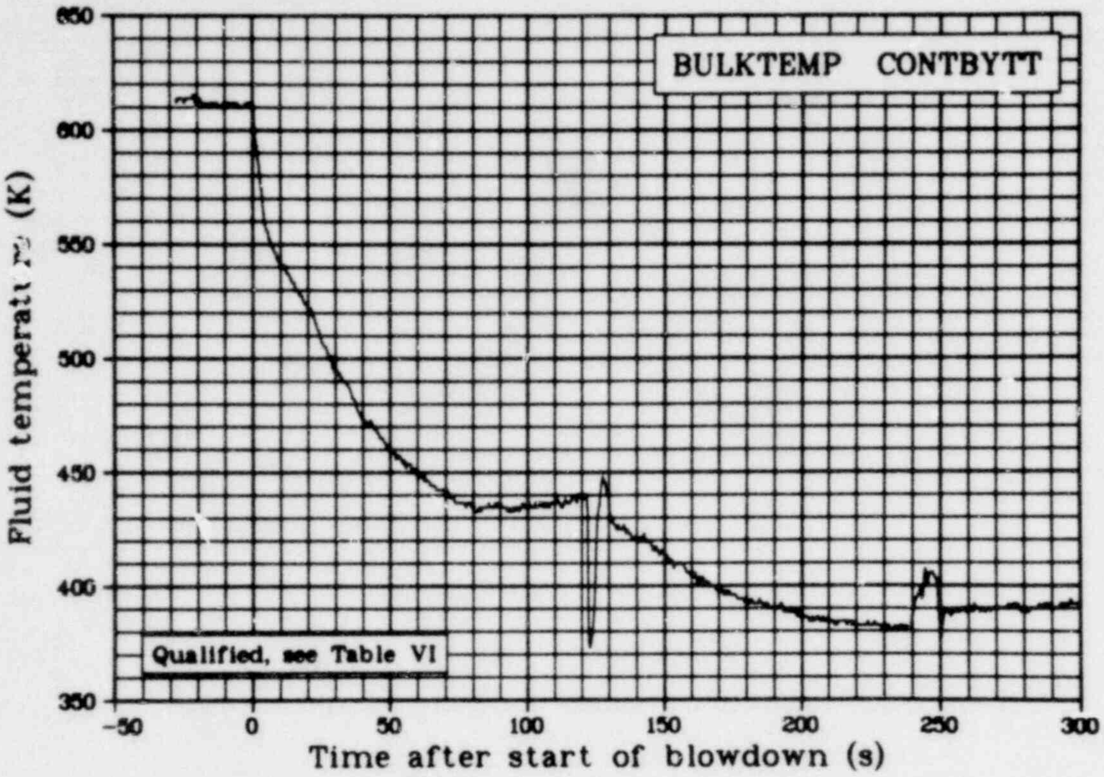

Fig. 493 Fluid temperature at test train controlled bypass inlet (BULKTEMP CONTBYTT), from -50 to 300 s.

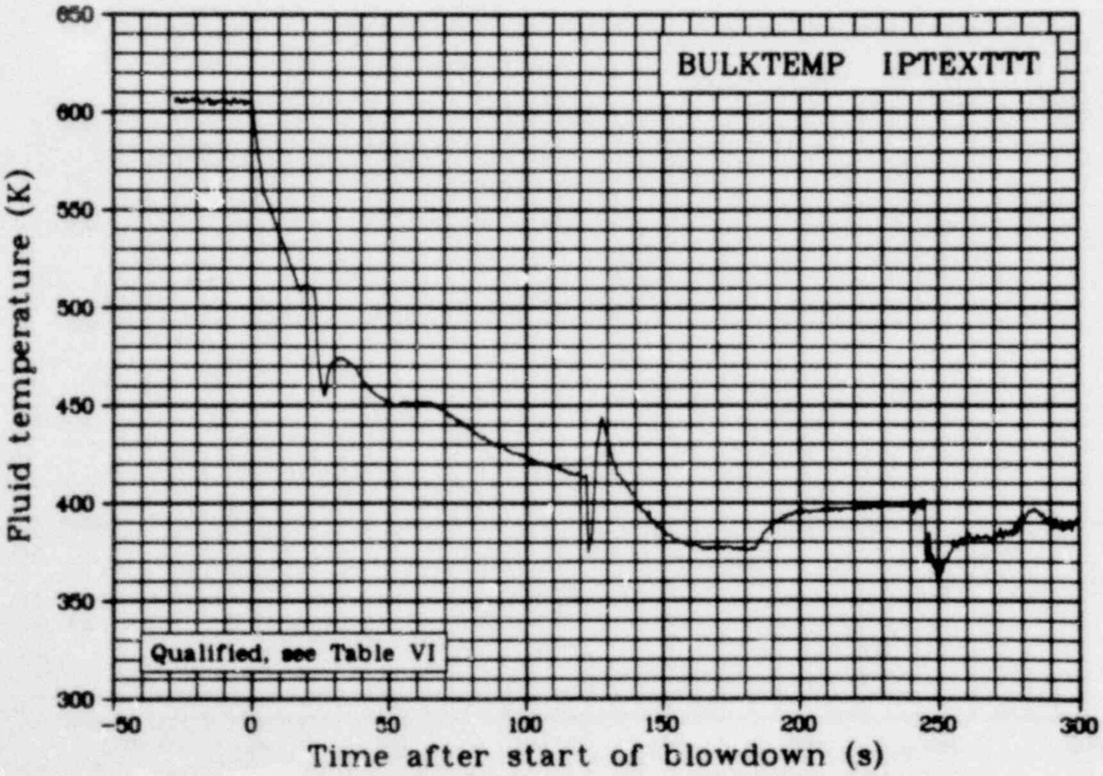

Fig. 494 Fluid temperature at IPT exit (BULKTEMP IPTEXTTT), from -50 to 300 s.

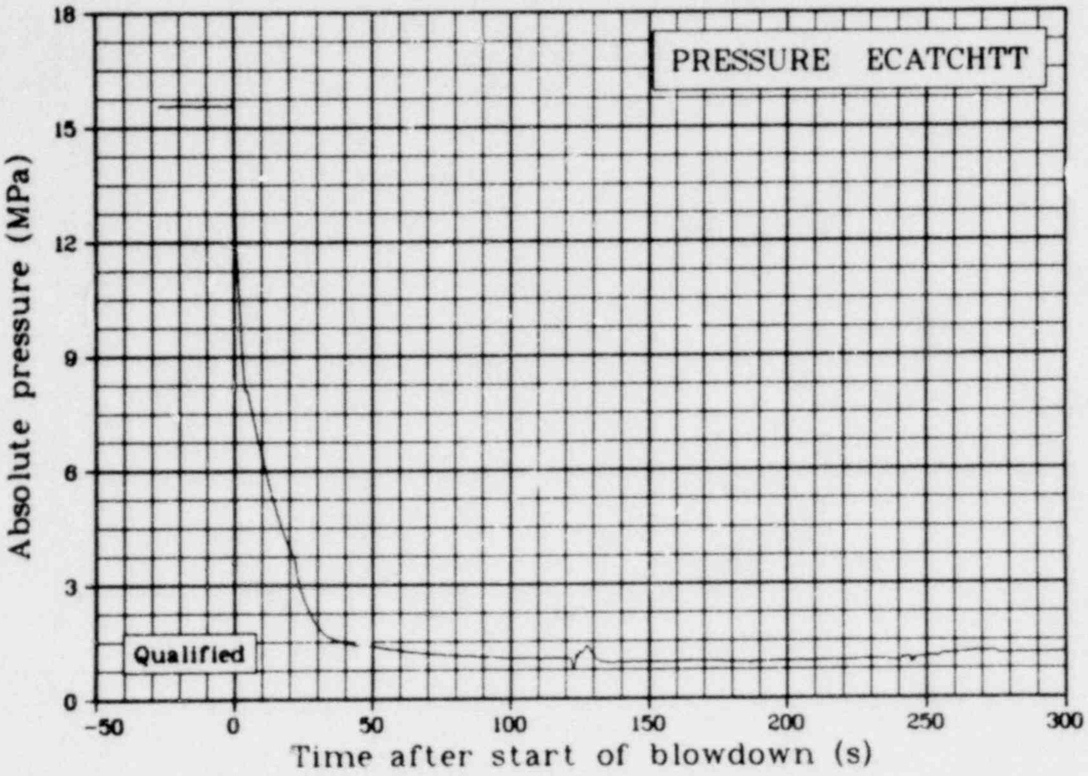

Fig. 495 Absolute pressure in test train catch basket (PRESSURE ECATCHTT), from -50 to 300 s.

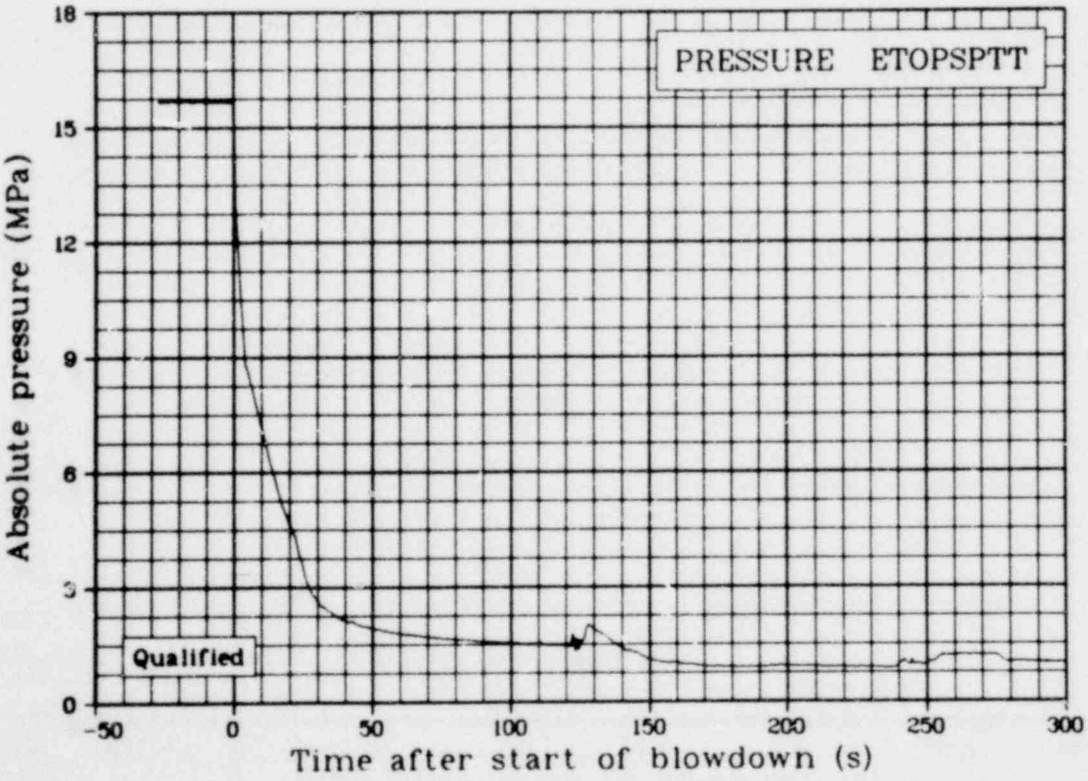

Fig. 496 Absolute pressure above test train top support plate (PRESSURE ETOPSPTT), from -50 to 300 s.

1405 343

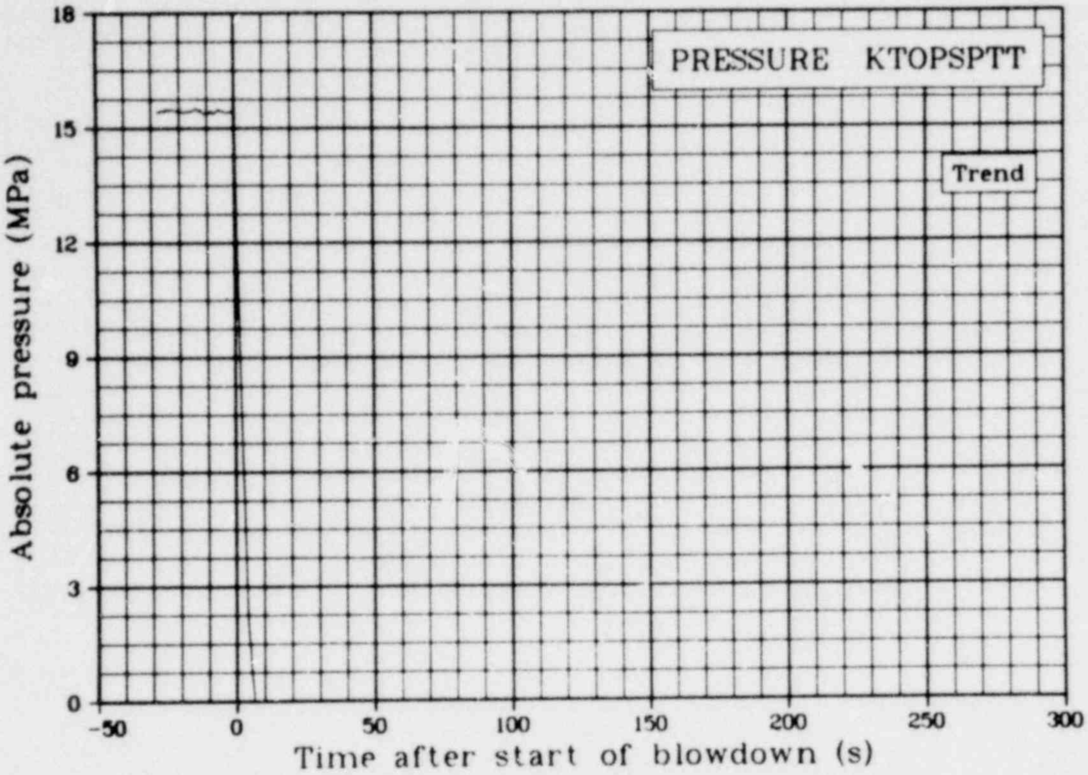

Fig. 497 Absolute pressure above the test train top support plate (PRESSURE KTOPSPTT), from -50 to 300 s.

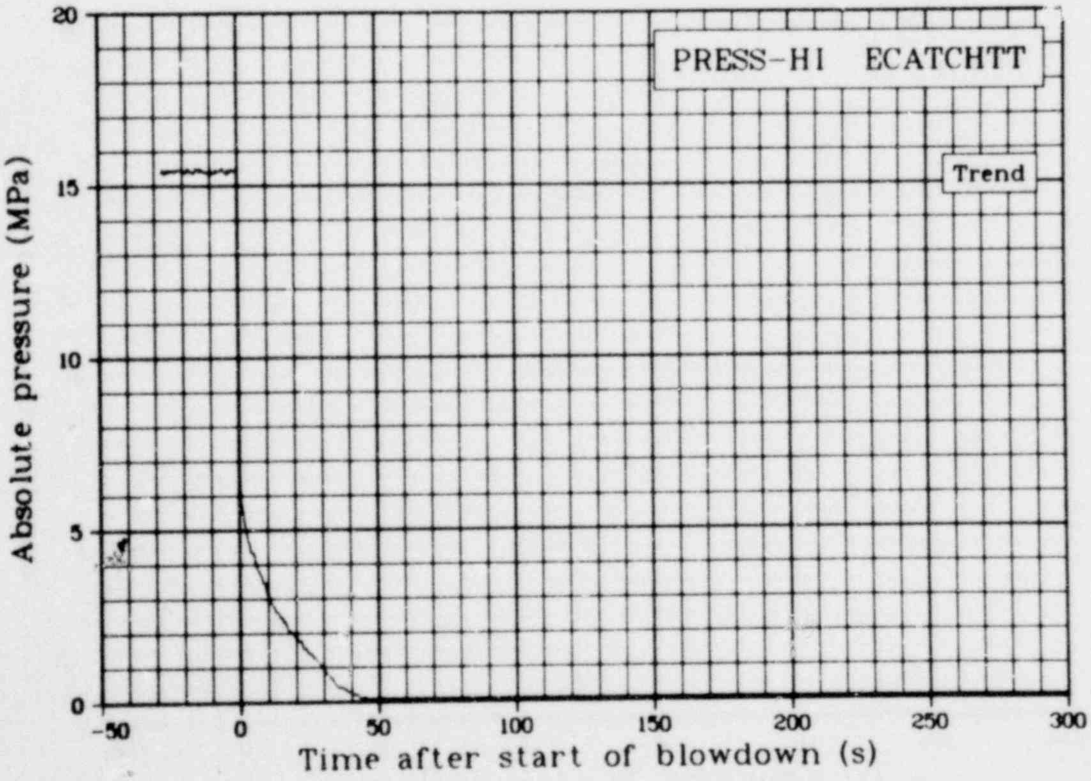

Fig. 498 Absolute pressure in test train catch basket (PRESS-HI ECATCHTT), from -50 to 300 s.

1405 344

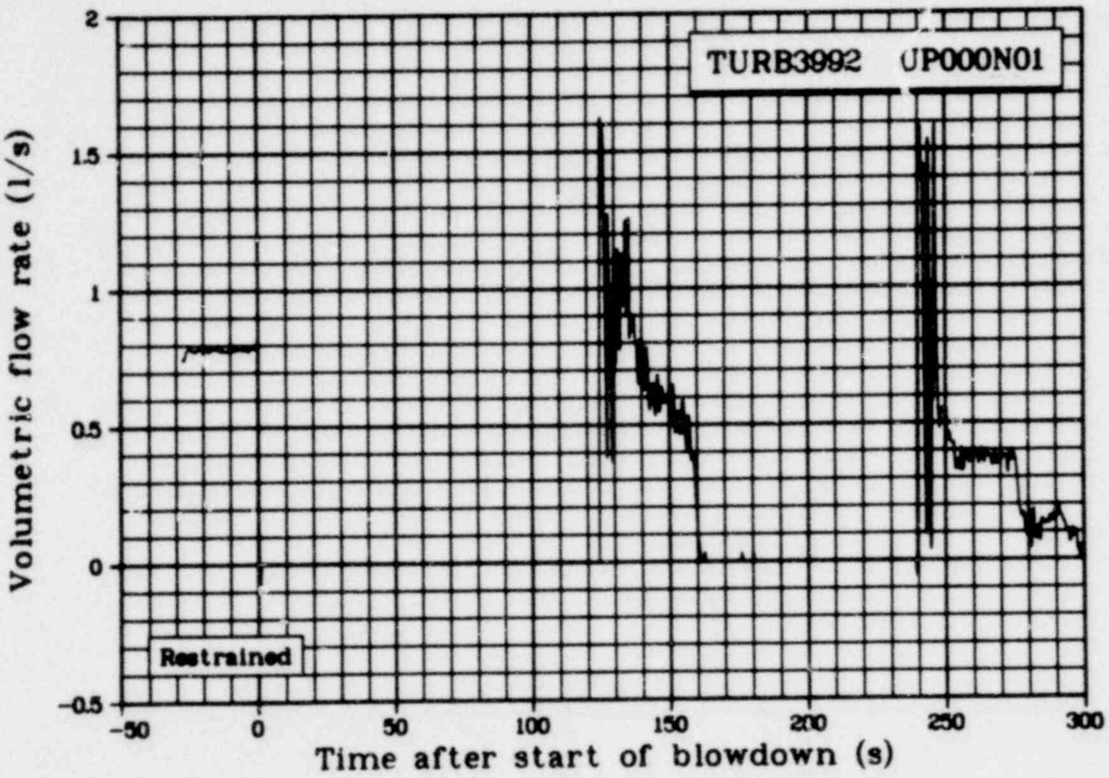

Fig. 499 Volumetric flow rate in Fuel Rod 399-2 upper shroud (TURB3992 UP000N01), from -50 to 300 s.

1405 345

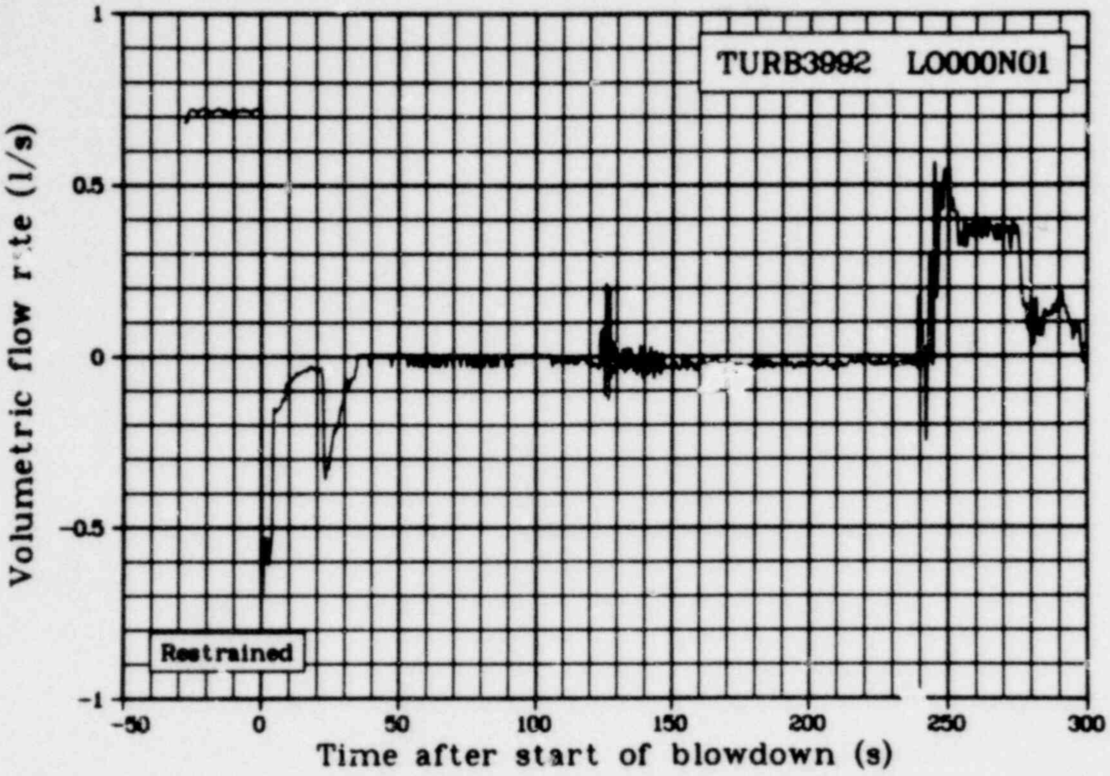

Fig. 500 Volumetric flow rate in Fuel Rod 399-2 lower shroud (TURB3992 L0000N01), from -50 to 300 s.

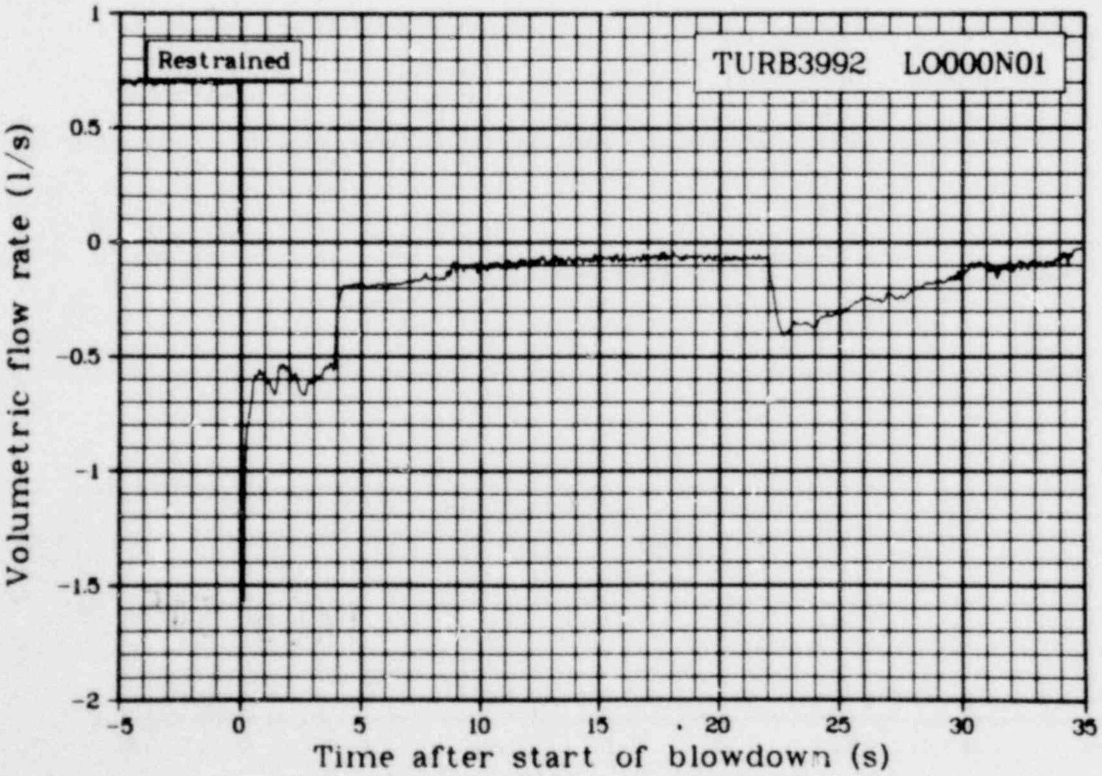

Fig. 501 Volumetric flow rate in Fuel Rod 399-2 lower shroud (TURB3992 L0000N01), from -5 to 35 s.

1405 346

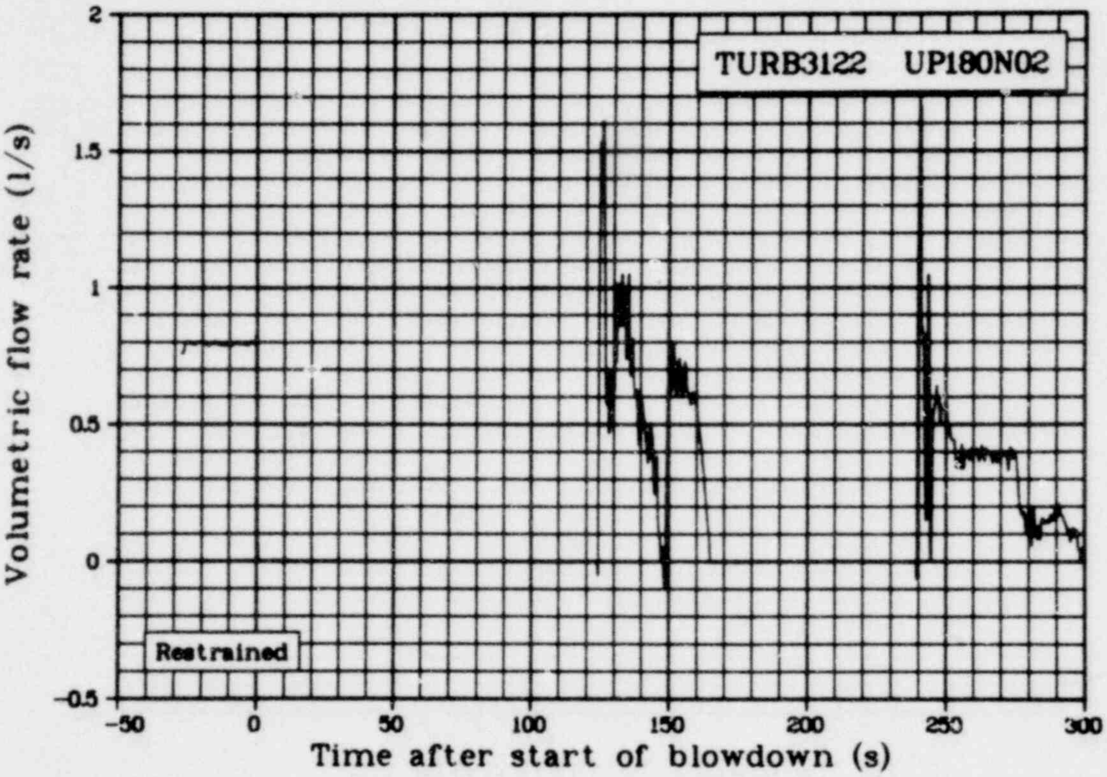

Fig. 502 Volumetric flow rate in Fuel Rod 312-2 upper shroud (TURB3122 UP180N02), from -50 to 300 s.

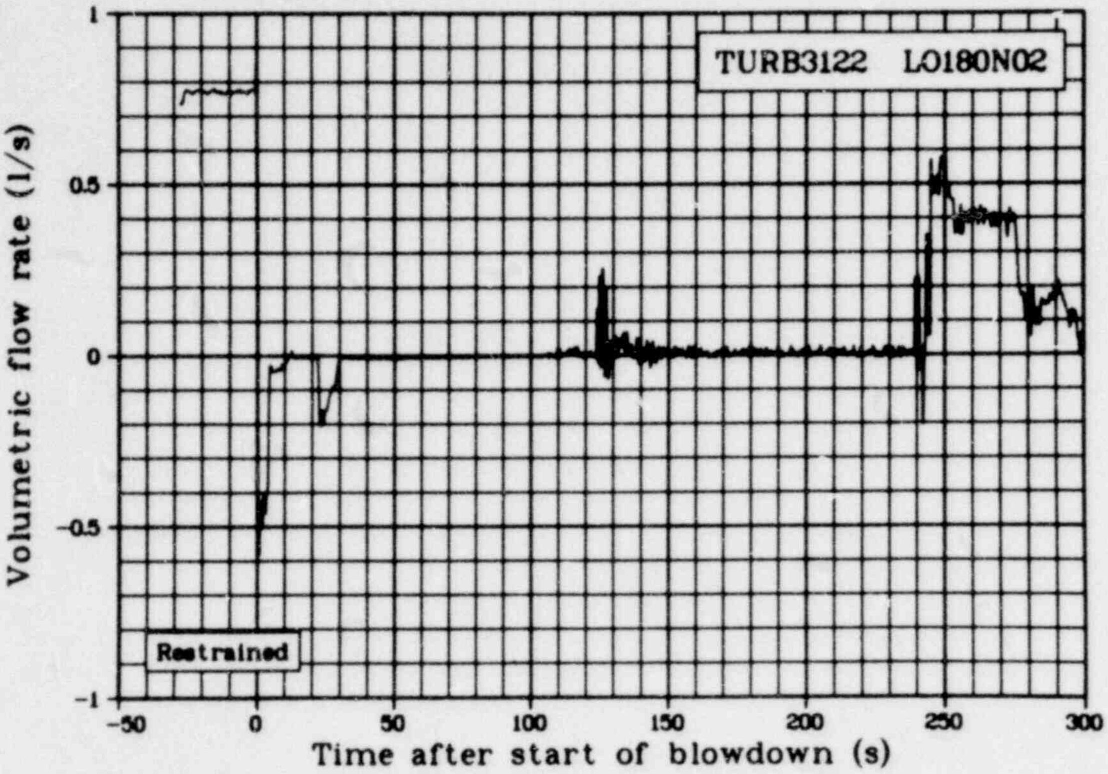

Fig. 503 Volumetric flow rate in Fuel Rod 312-2 lower shroud (TURB3122 L0180N02), from -50 to 300 s.

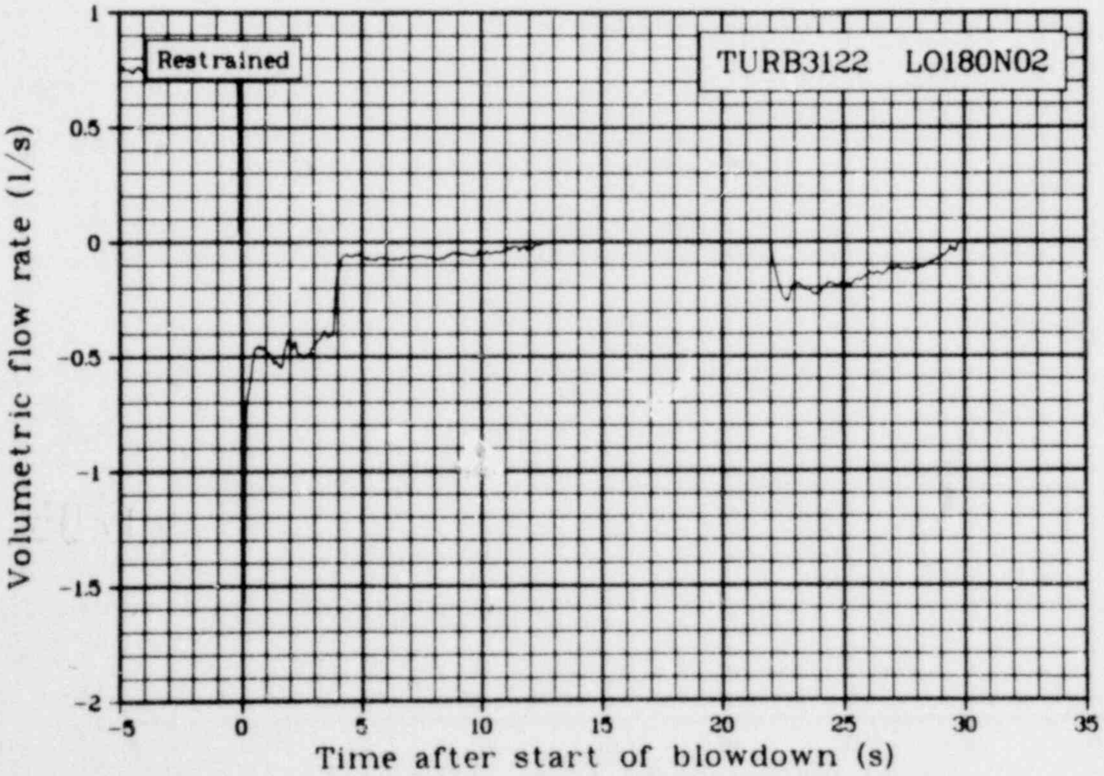

Fig. 504 Volumetric flow rate in Fuel Rod 312-2 lower shroud (TURB3122 L0180N02), from -5 to 35 s.

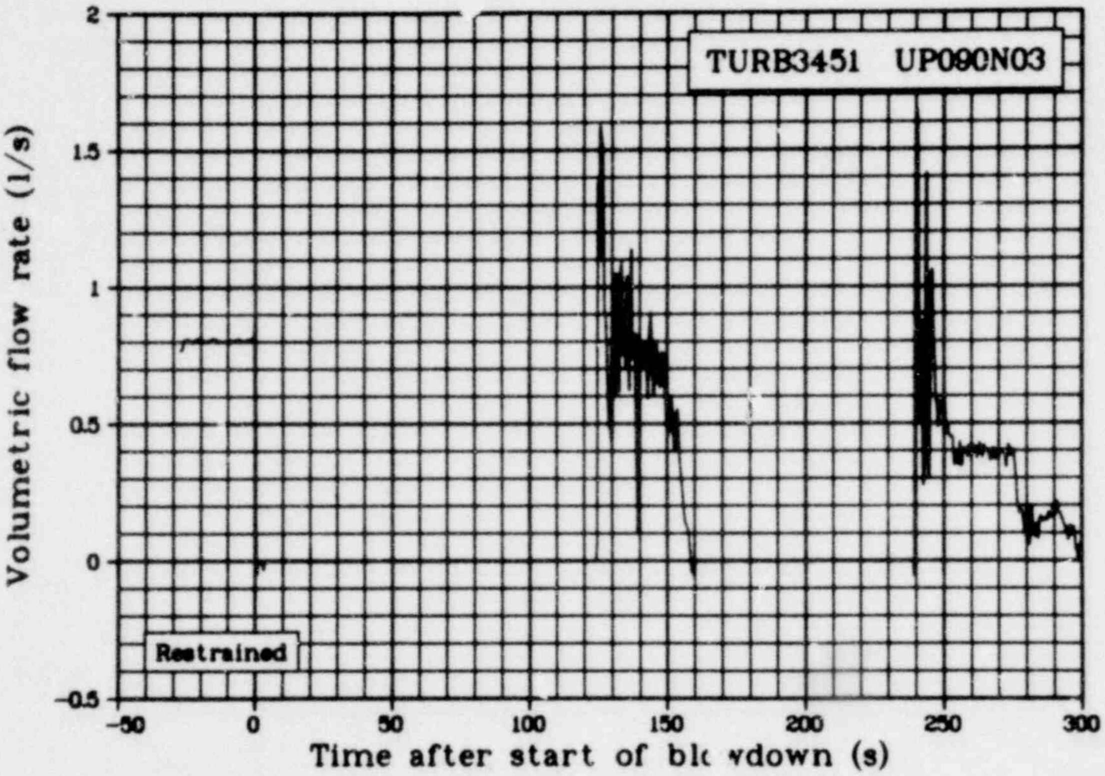

Fig. 505 Volumetric flow rate in Fuel Rod 345-1 upper shroud (TURB3451 UP090N03), from -50 to 300 s.

1405 349

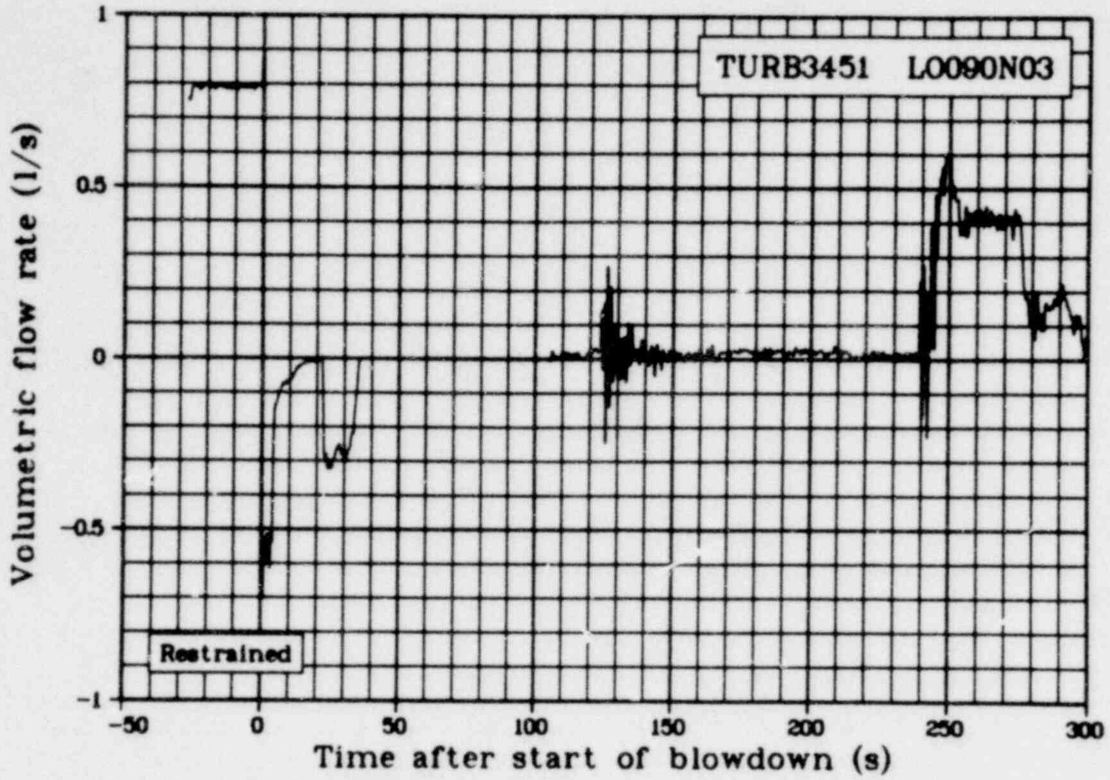

Fig. 506 Volumetric flow rate in Fuel Rod 345-1 lower shroud (TURB3451 L0090N03), from -50 to 300 s.

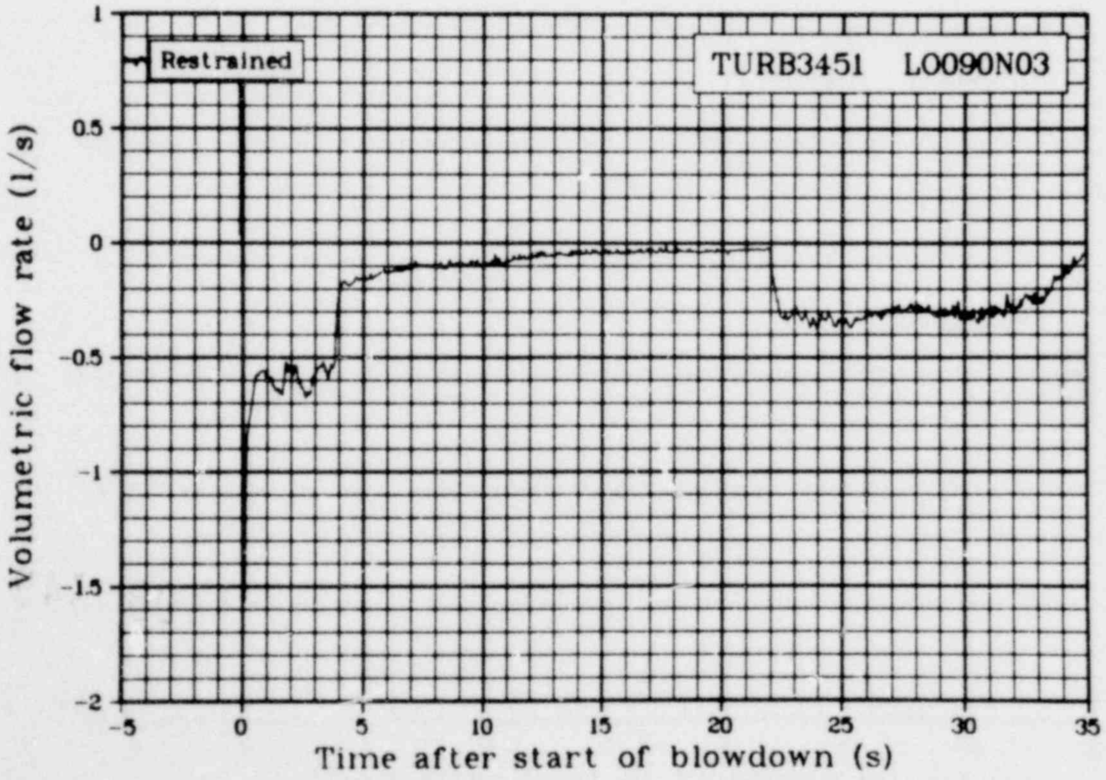

Fig. 507 Volumetric flow rate in Fuel Rod 345-1 lower shroud (TURB3451 L0090N03), from -5 to 35 s.

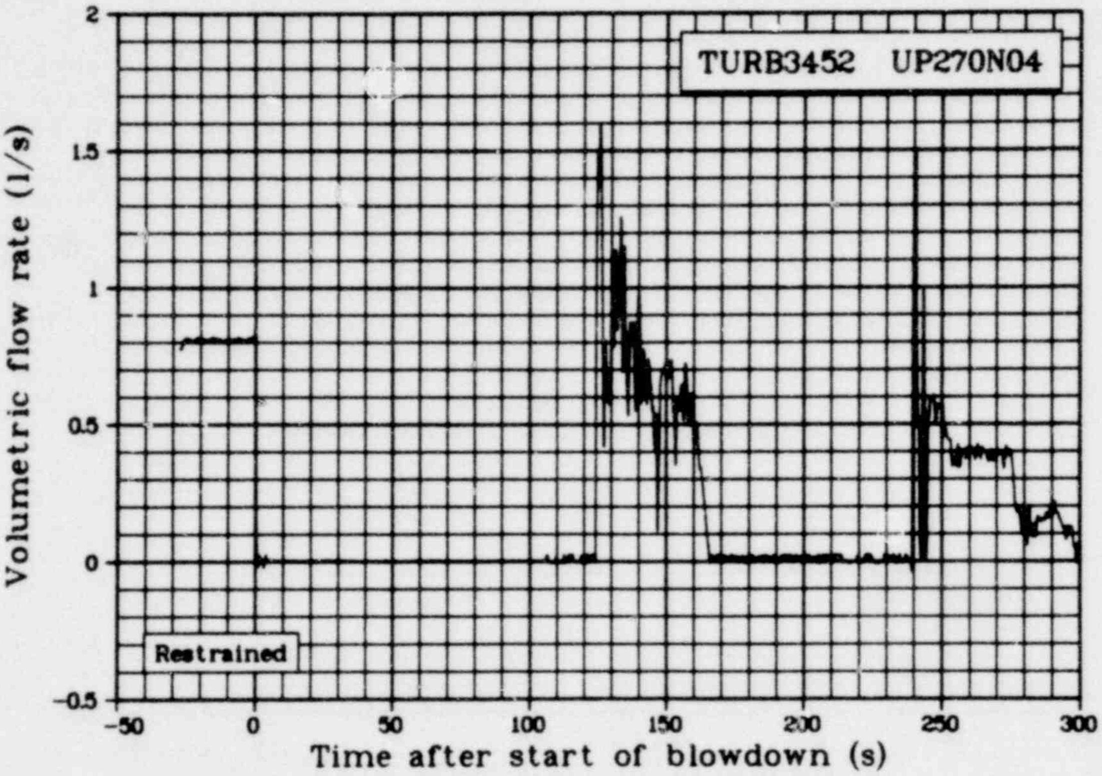

Fig. 508 Volumetric flow rate in Fuel Rod 345-2 upper shroud (TURB3452 UP270N04), from -50 to 300 s.

1405 351

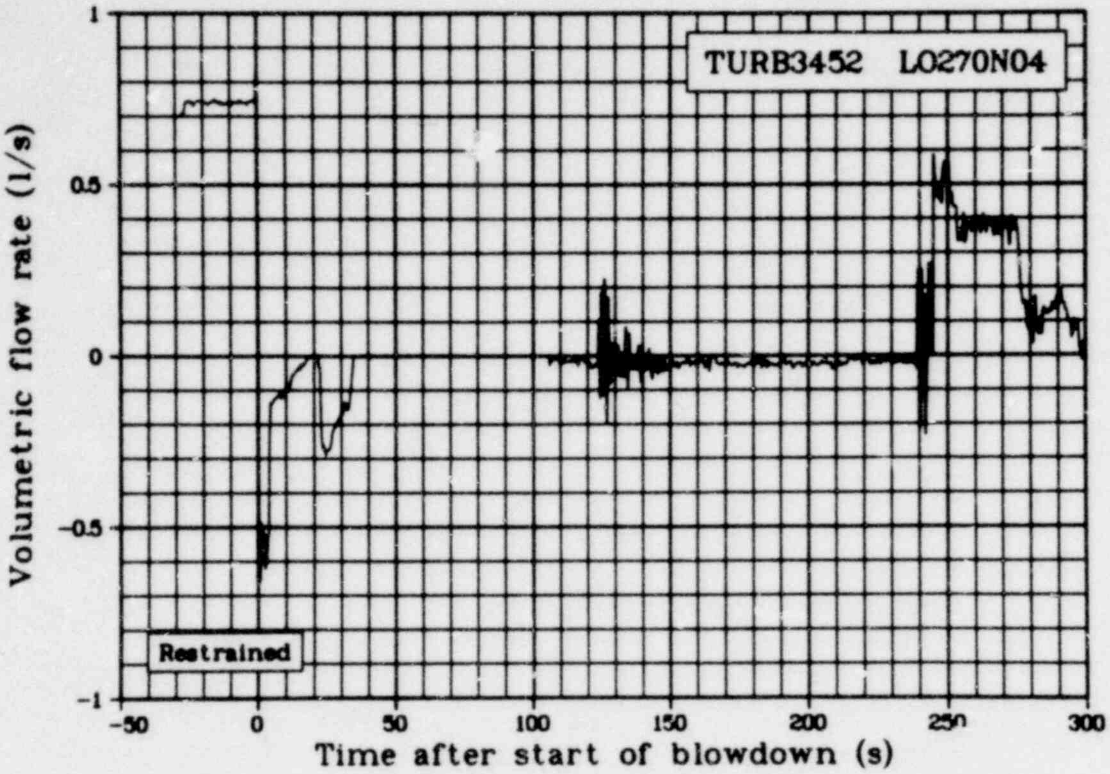

Fig. 509 Volumetric flow rate in Fuel Rod 345-2 lower shroud (TURB3452 LO270N04), from -50 to 300 s.

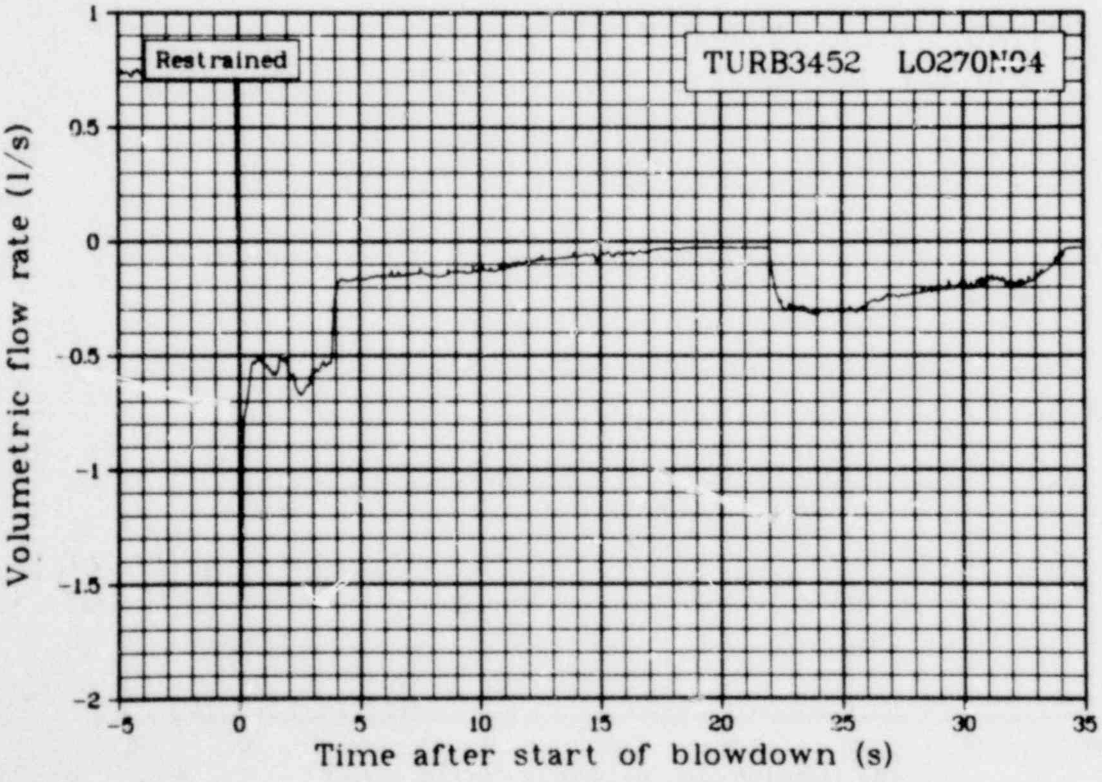

Fig. 510 Volumetric flow rate in Fuel Rod 345-2 lower shroud (TURB3452 LO270N04), from -5 to 35 s.

1405 352

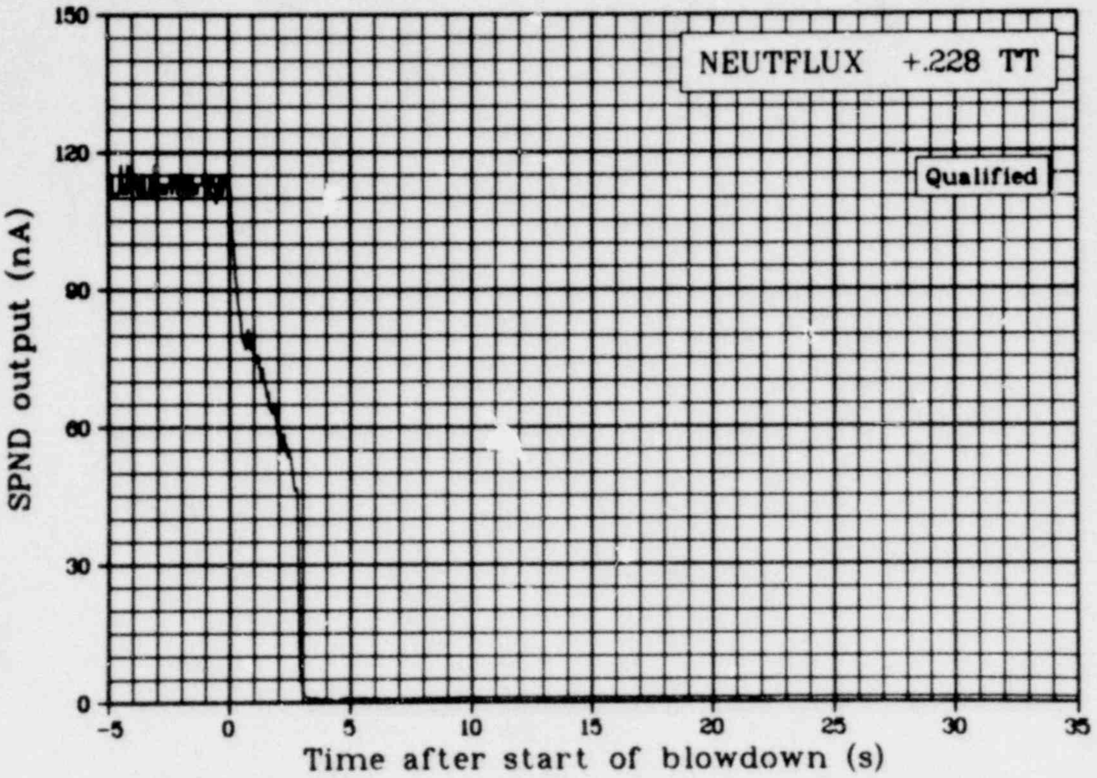

Fig. 511 Neutron flux 0.228 m above fuel stack midplane (NEUTFLUX +.228 TT), from -5 to 35 s.

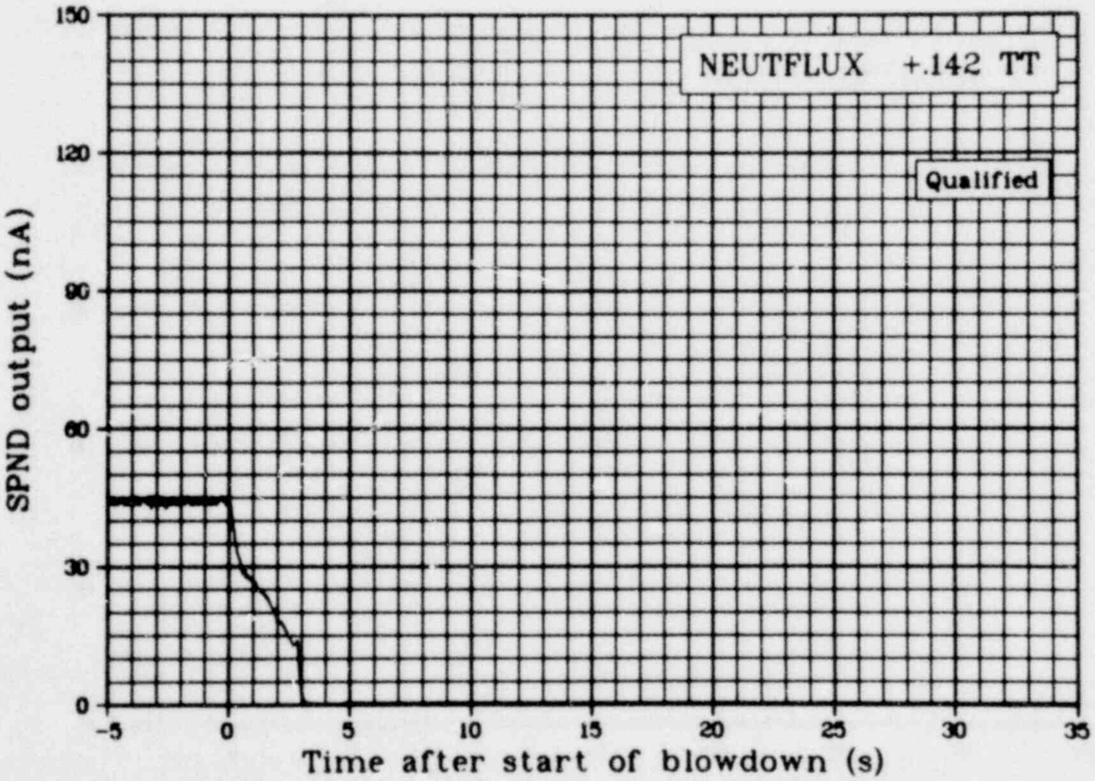

Fig. 512 Neutron flux 0.142 m above fuel stack midplane (NEUTFLUX +.142 TT), from -5 to 35 s.

1405 353

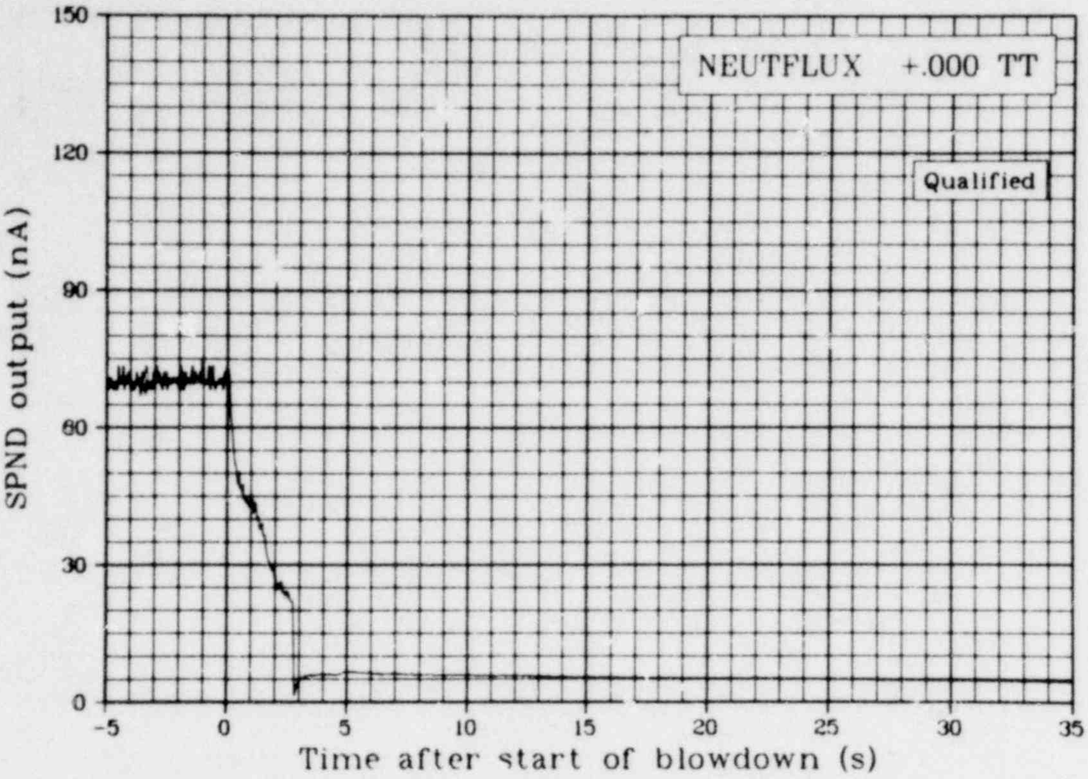

Fig. 513 Neutron flux at fuel stack midplane (NEUTFLUX +.000 TT), from -5 to 35 s.

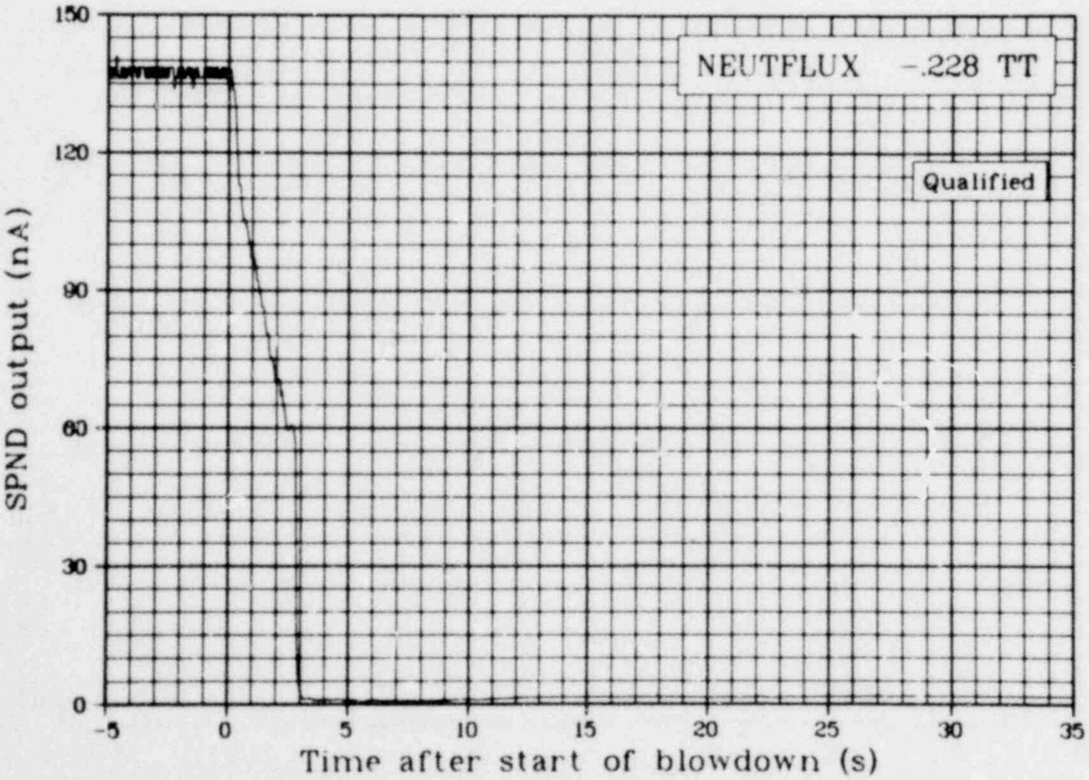

Fig. 514 Neutron flux 0.228 m below fuel stack midplane (NEUTFLUX -.228 TT), from -5 to 35 s.

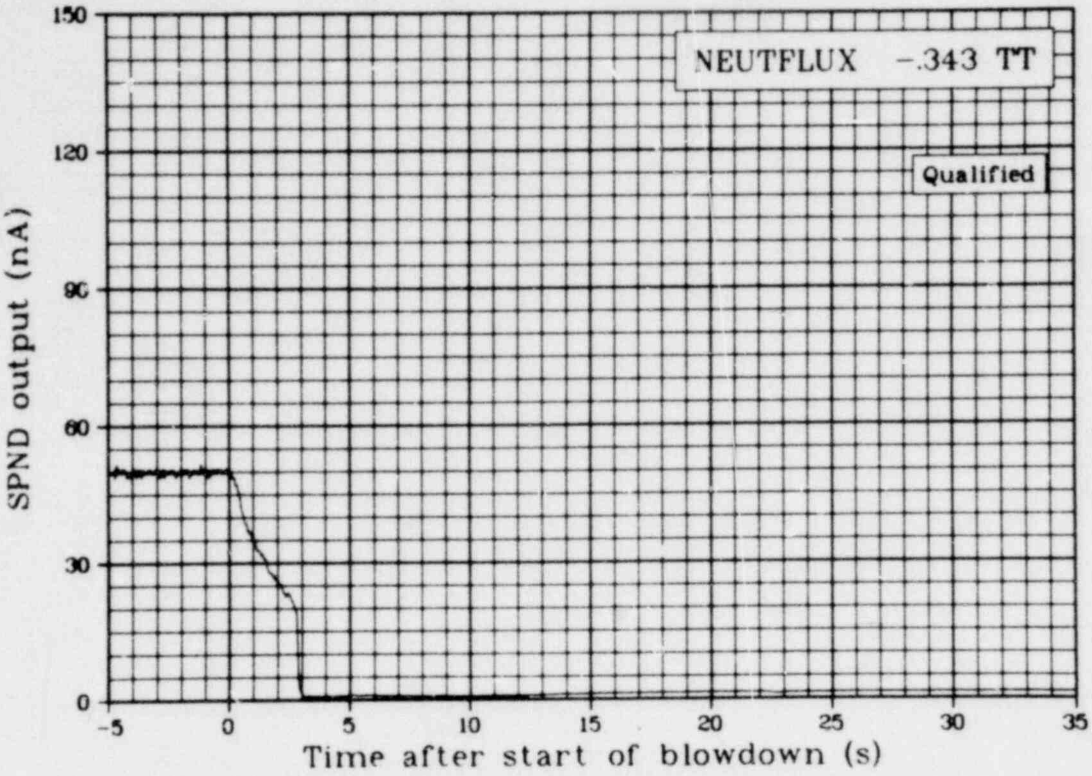

Fig. 515 Neutron flux 0.343 m below fuel stack midplane (NEUTFLUX -.343 TT), from -5 to 35 s.

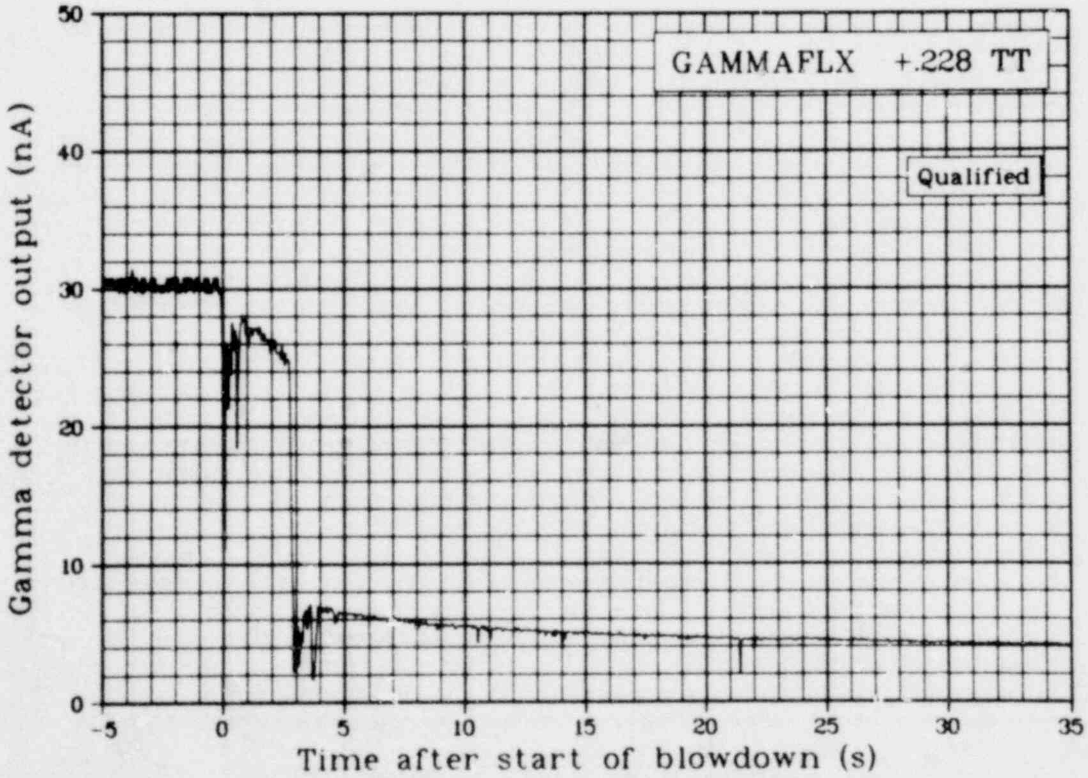

Fig. 516 Gamma flux 0.228 m above fuel stack midplane (GAMMAFLX +.228 TT), from -5 to 35 s.

1405 355

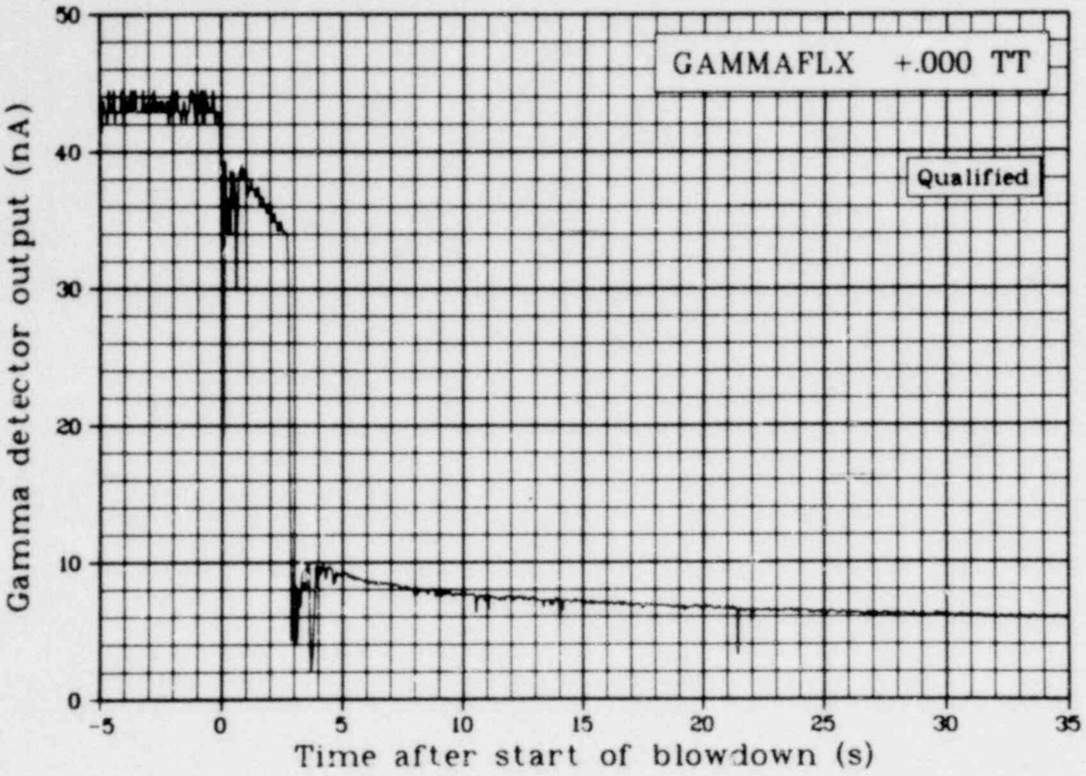

Fig. 517 Gamma flux at fuel stack midplane (GAMMAFLX +.000 TT), from -5 to 35 s.

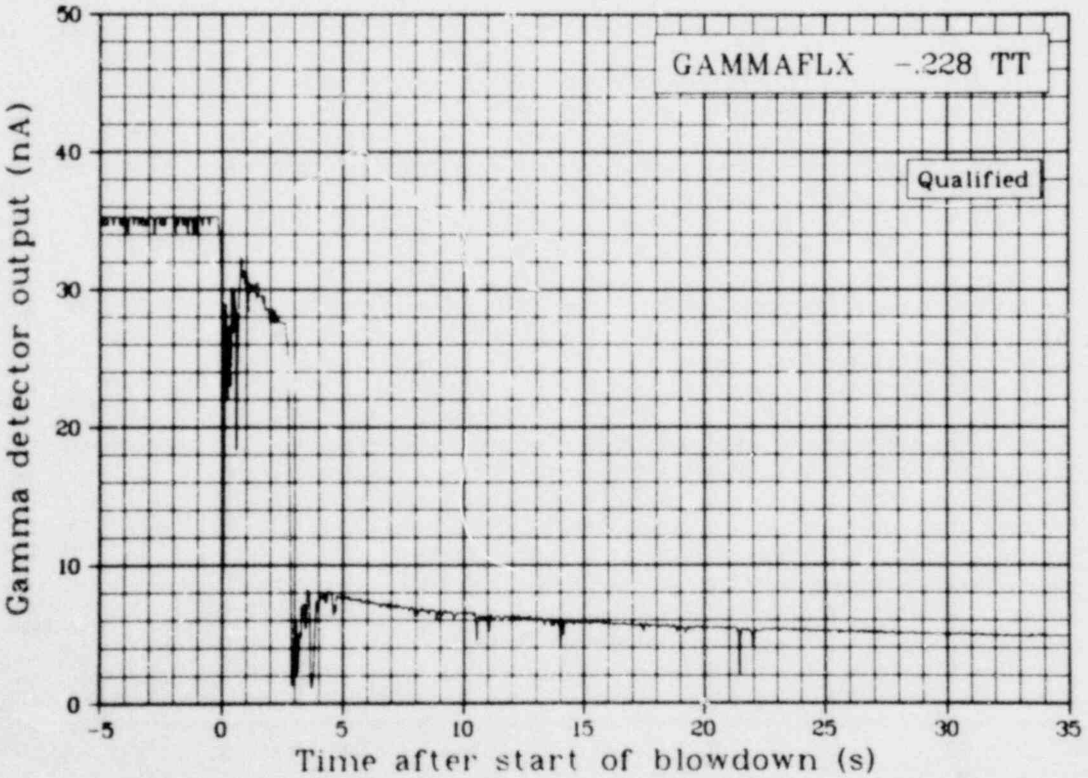

Fig. 518 Gamma flux 0.228 m below fuel stack midplane (GAMMAFLX -.228 TT), from -5 to 35 s.

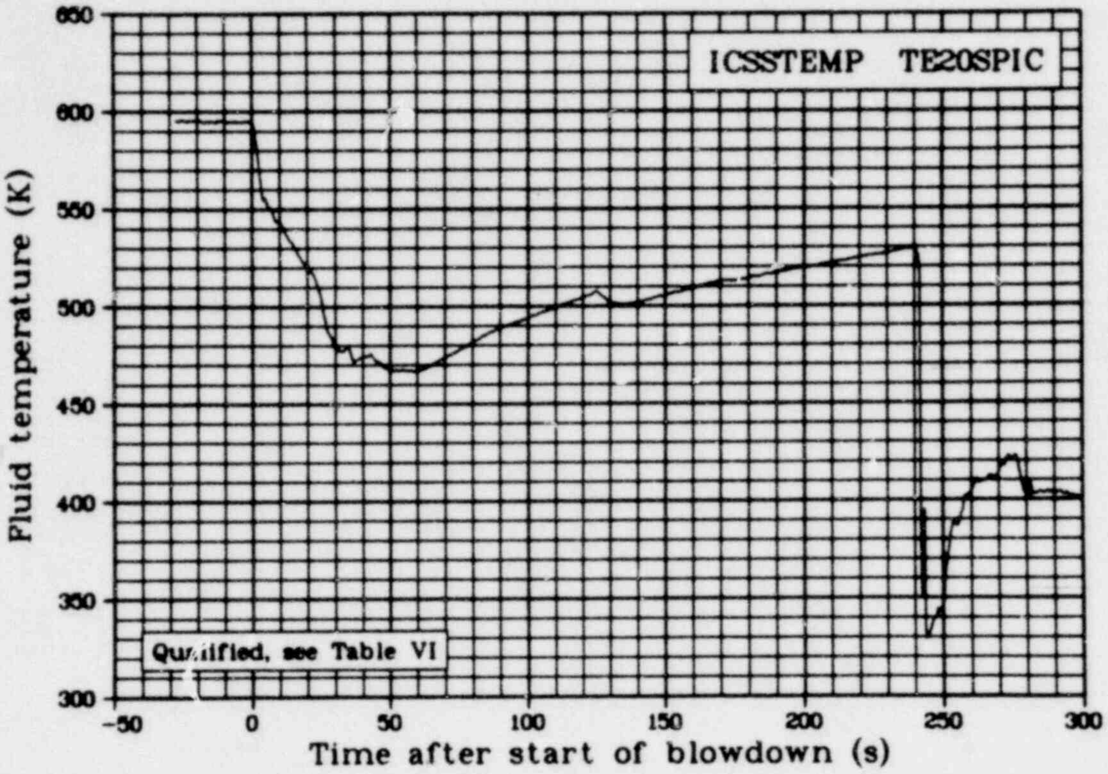

Fig. 519 Fluid temperature in initial condition spool (ICSSTEMP TE20SPIC), from -50 to 300 s.

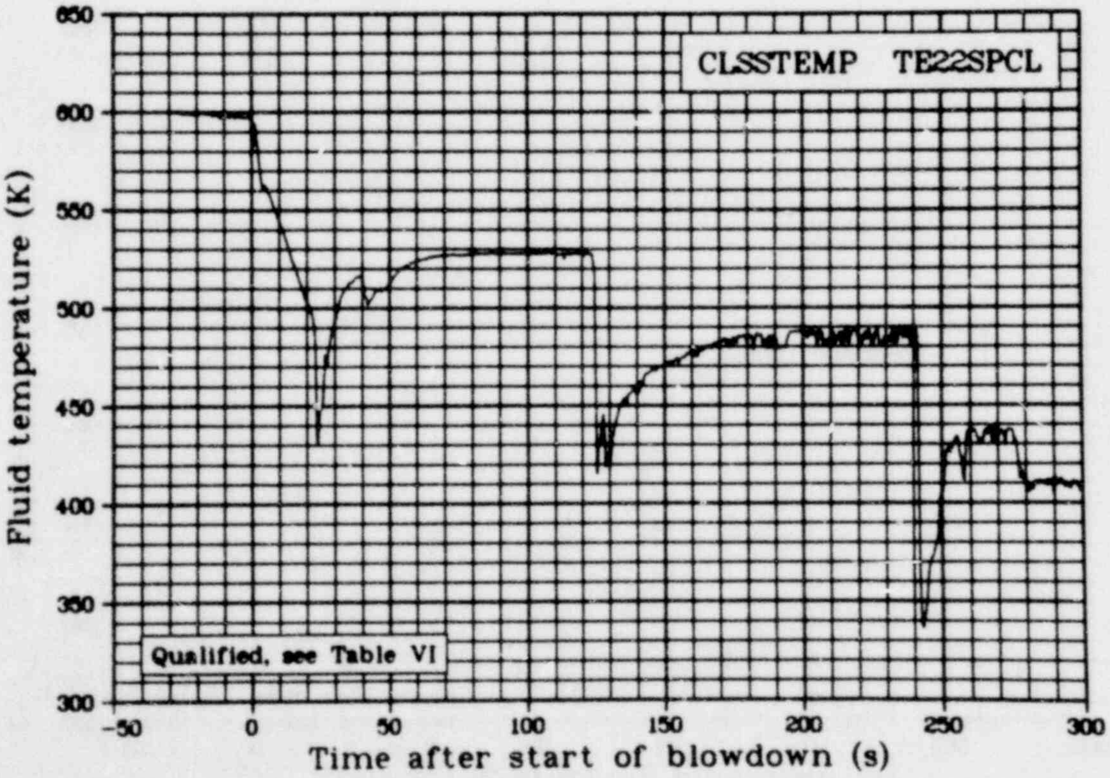

Fig. 520 Fluid temperature in cold leg blowdown spool (CLSSTEMP TE22SPCL), from -50 to 300 s.

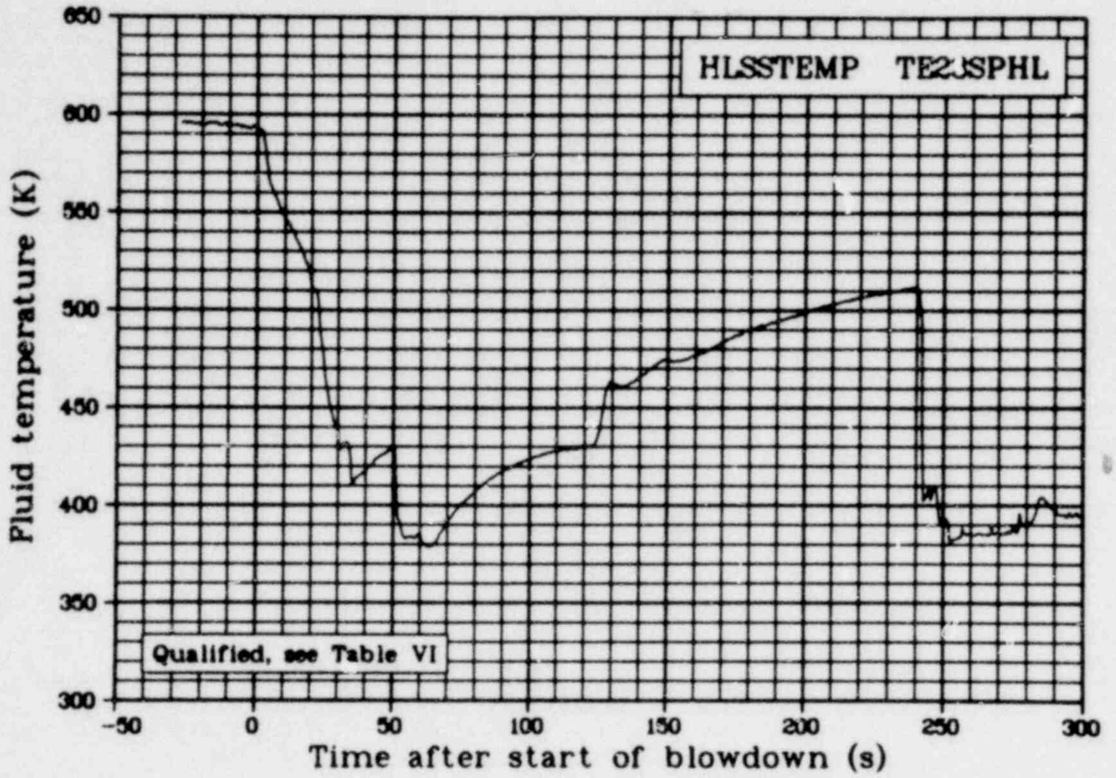

Fig. 521 Fluid temperature in hot leg blowdown spool (HLSSTEMP TE23SPHL), from -50 to 300 s.

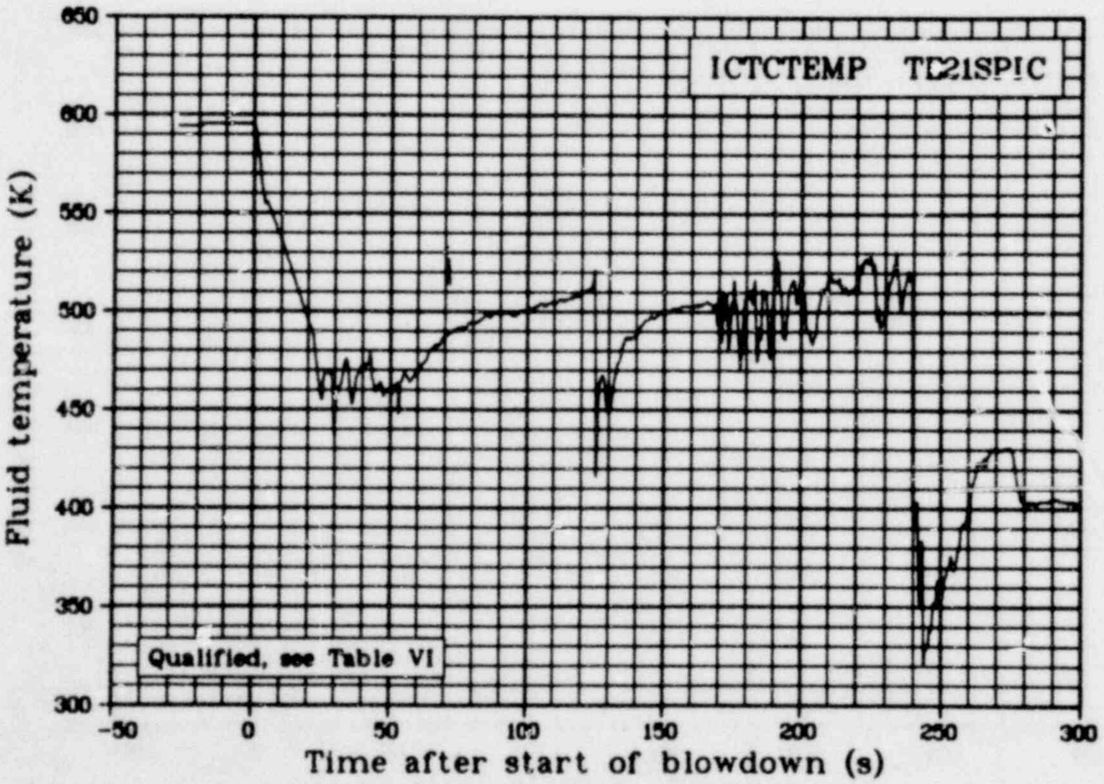

Fig. 522 Fluid temperature in initial condition spool (ICTCTEMP TE21SPIC), from -50 to 300 s.

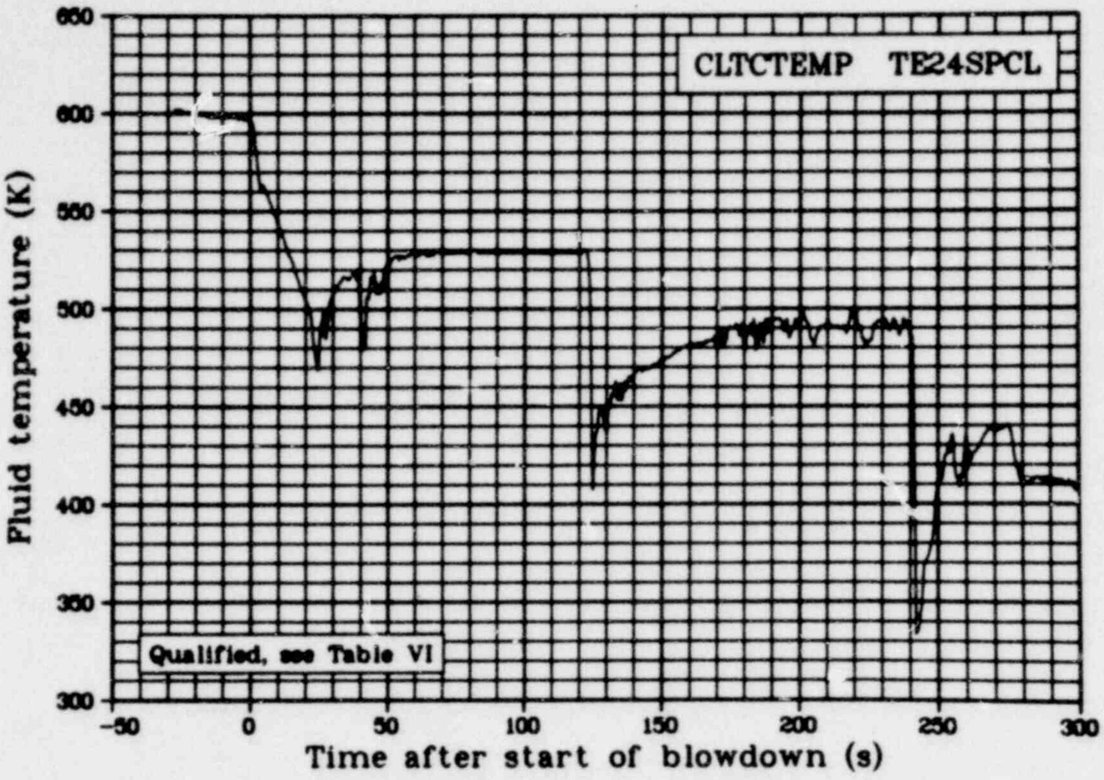

Fig. 523 Fluid temperature in cold leg blowdown spool (CLTCTEMP TE24SPCL), from -50 to 300 s.

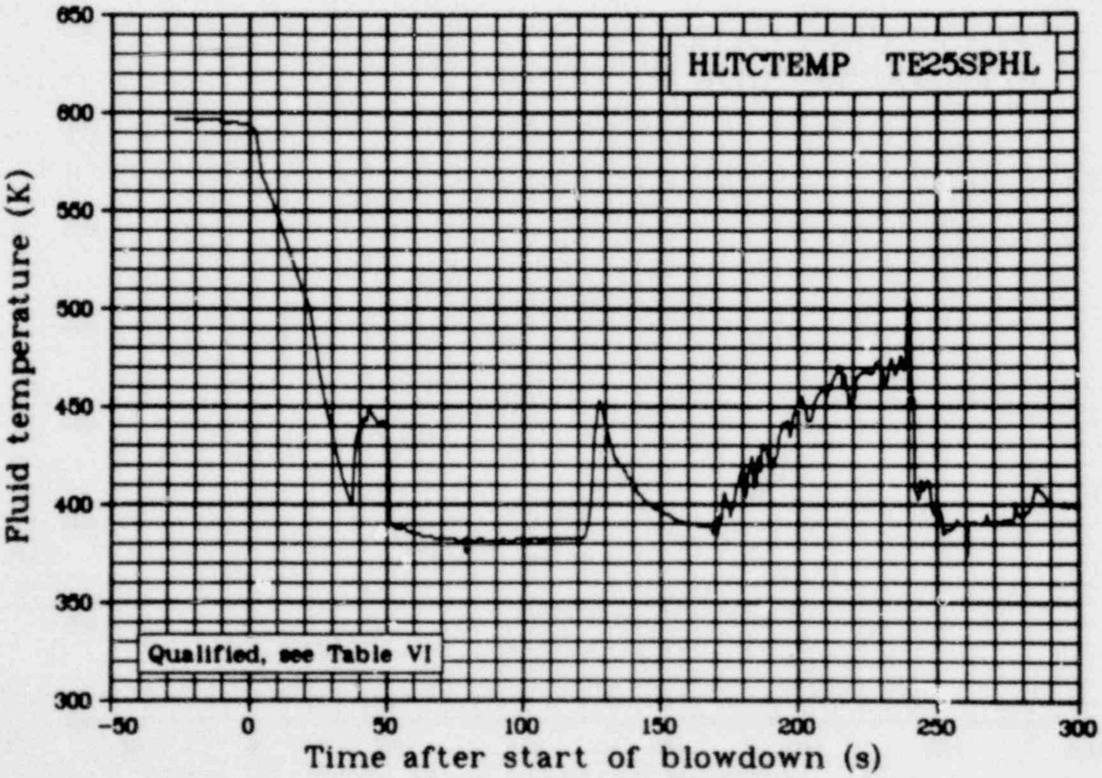

Fig. 524 Fluid temperature in hot leg blowdown spool (HLTCTEMP TE25SPHL), from -50 to 300 s.

1405 359

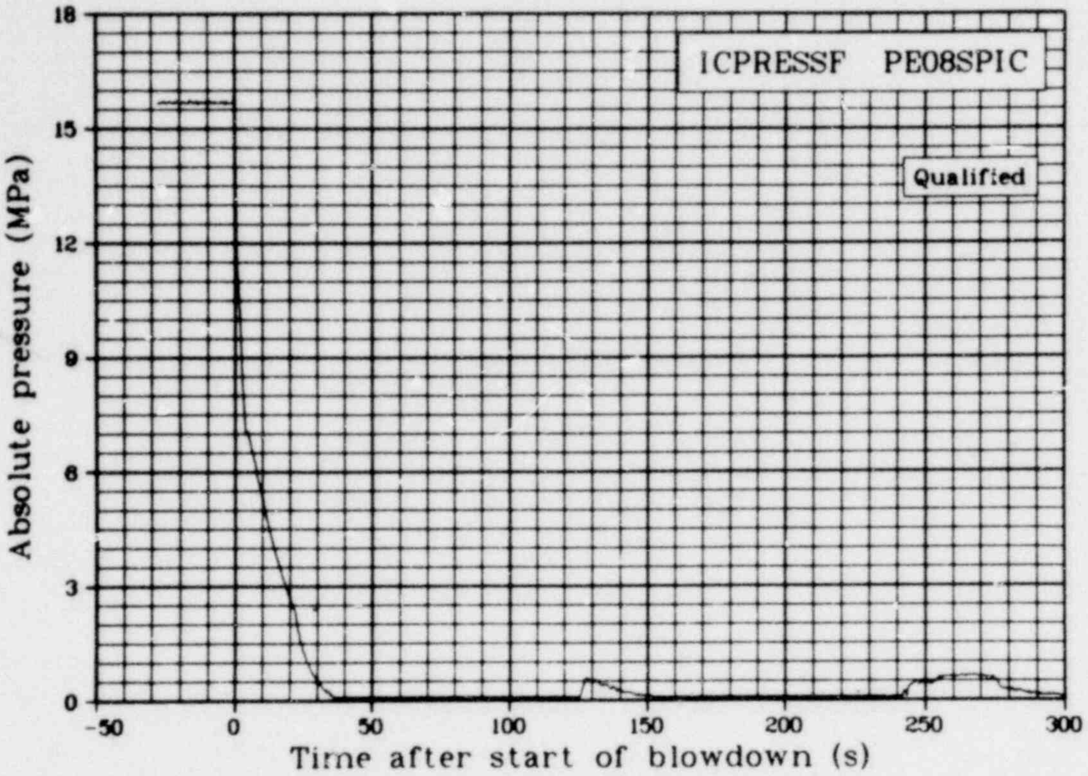

Fig. 525 Absolute pressure in initial condition spool (ICPRESSF PE08SPIC), from -50 to 300 s.

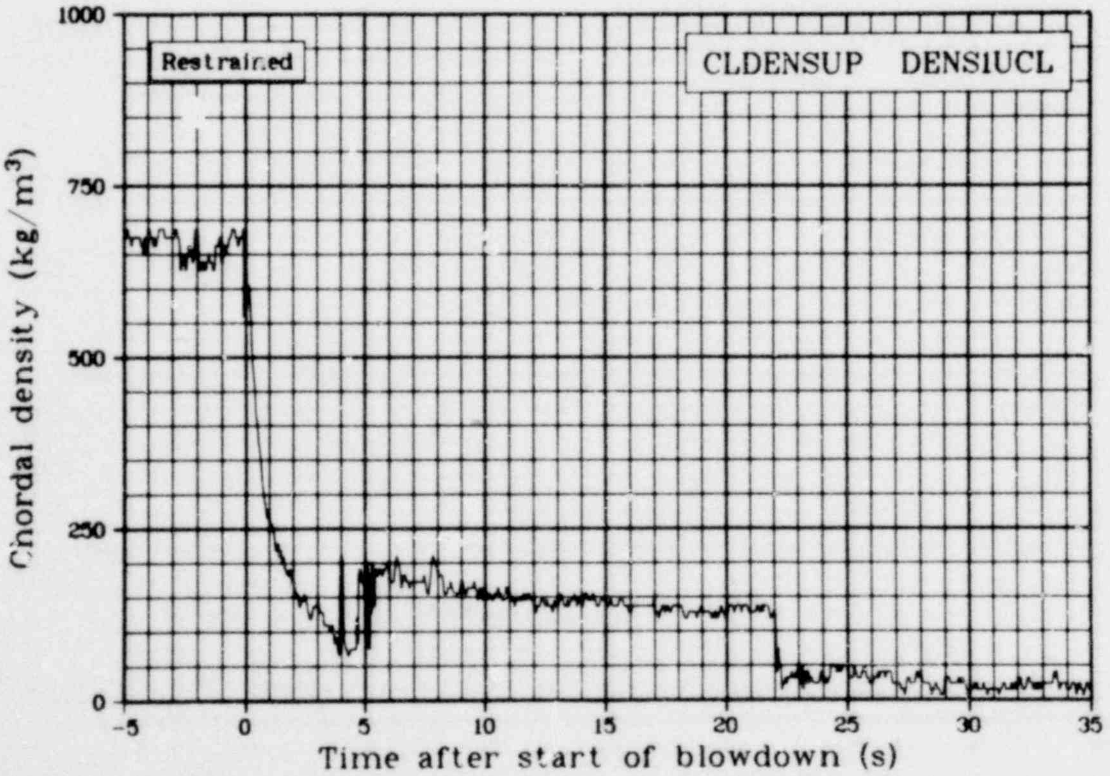

Fig. 526 Chordal density of upper beam in cold leg blowdown spool (CLDENSUP DENS1UCL), from -5 to 35 s.

1405 360

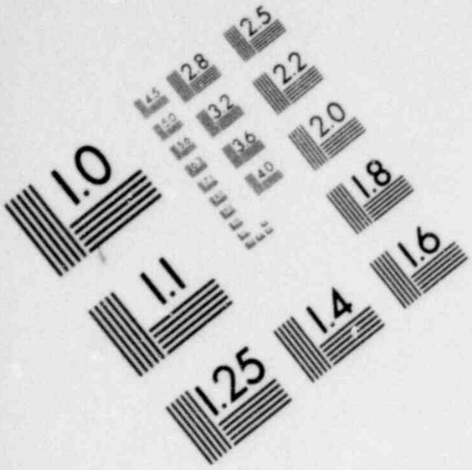

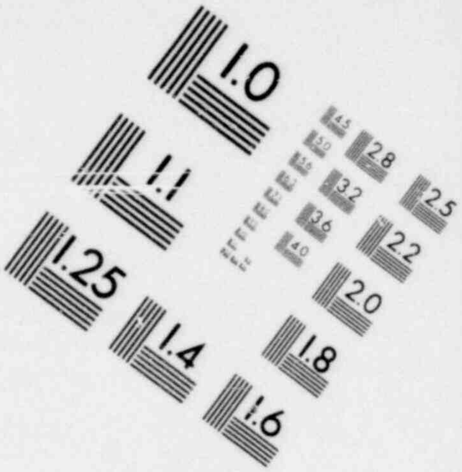

IMAGE EVALUATION TEST TARGET (MT-3)

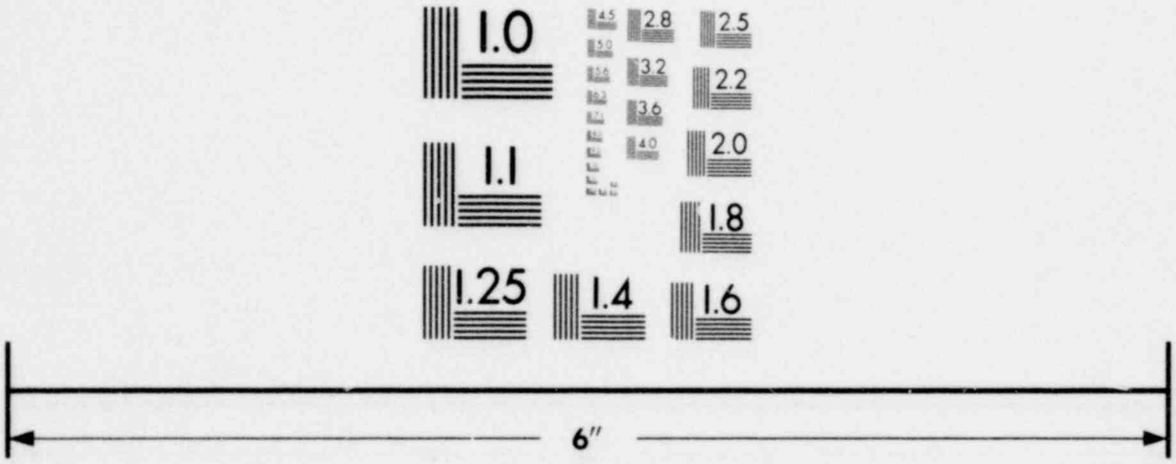

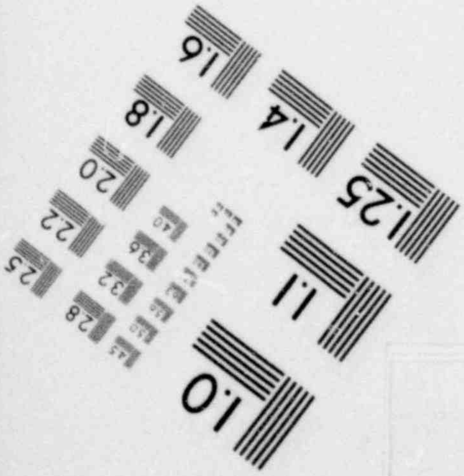

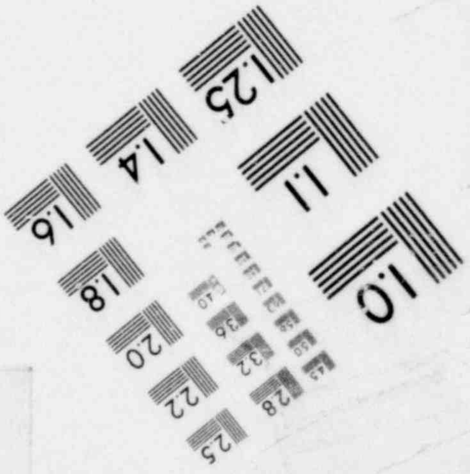

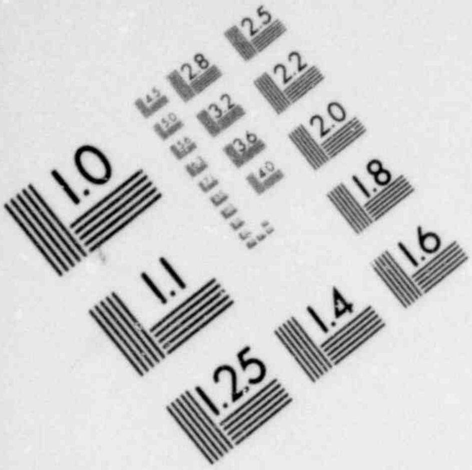
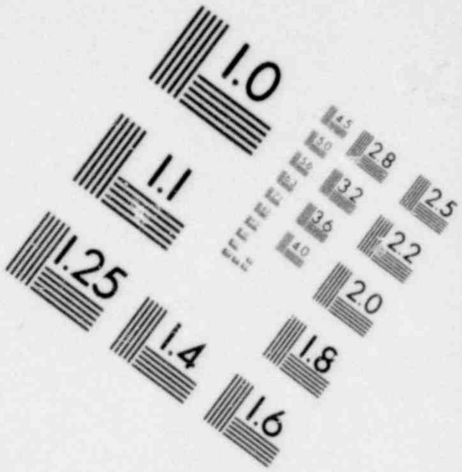

IMAGE EVALUATION TEST TARGET (MT-3)

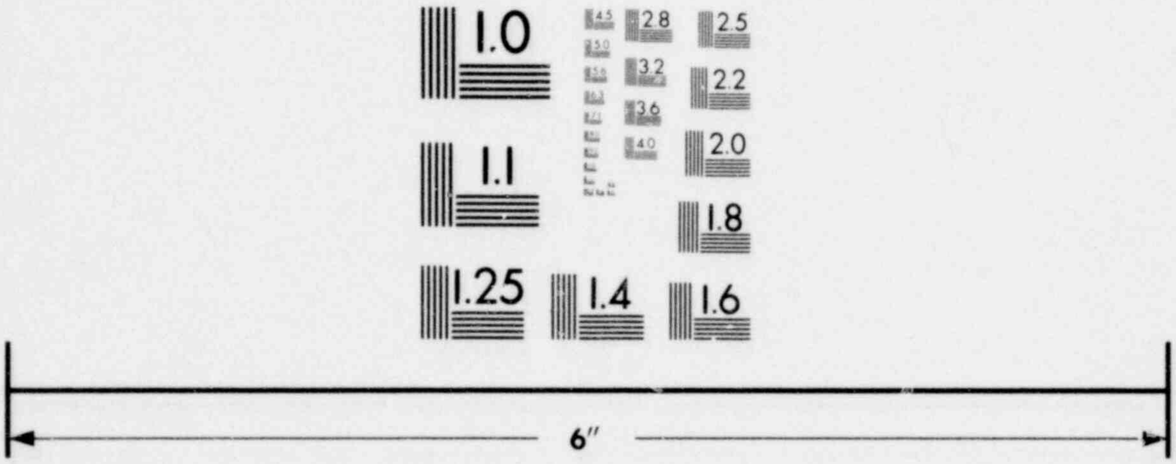

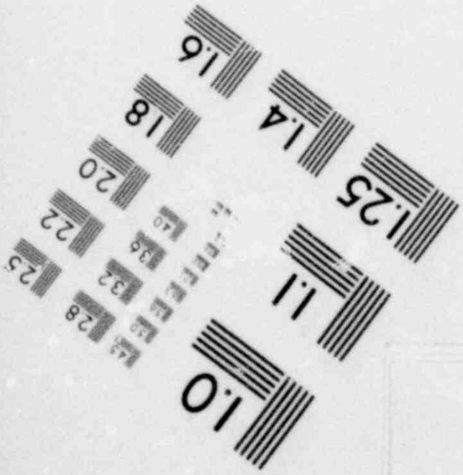
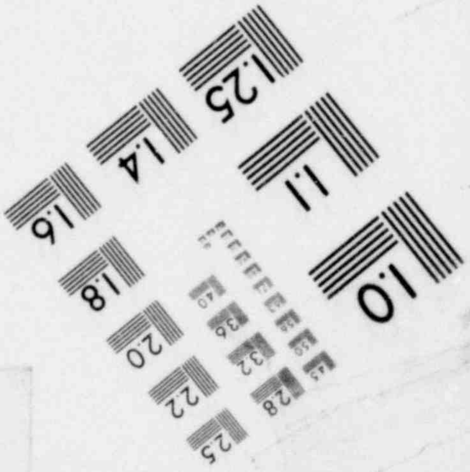

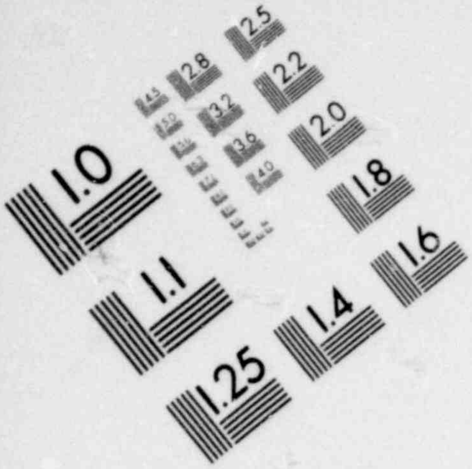

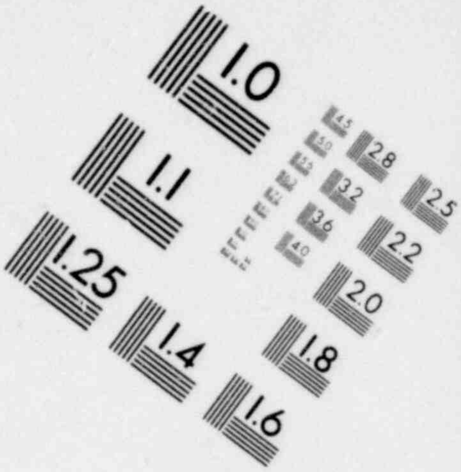

IMAGE EVALUATION TEST TARGET (MT-3)

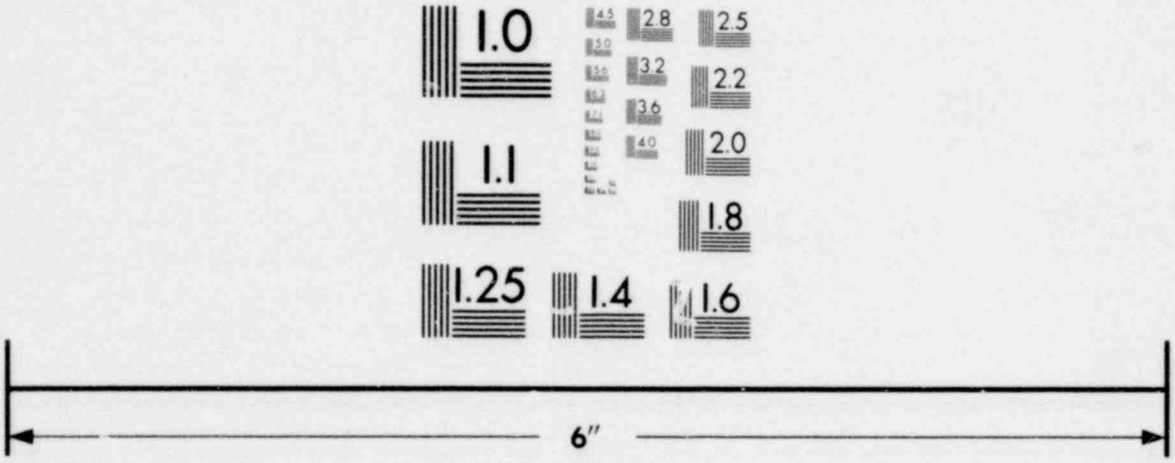

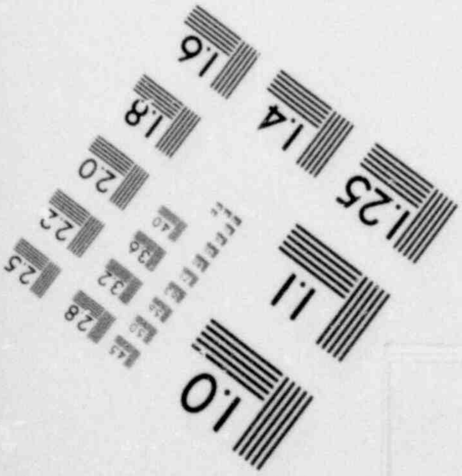

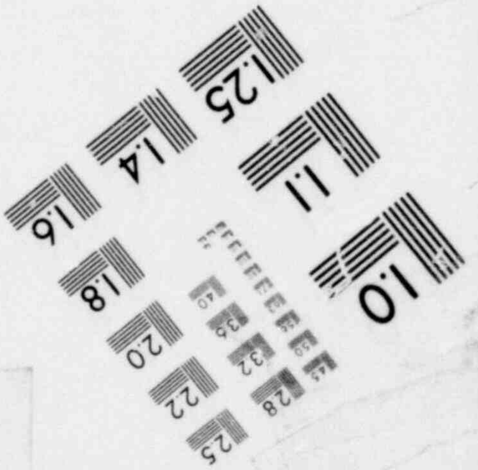

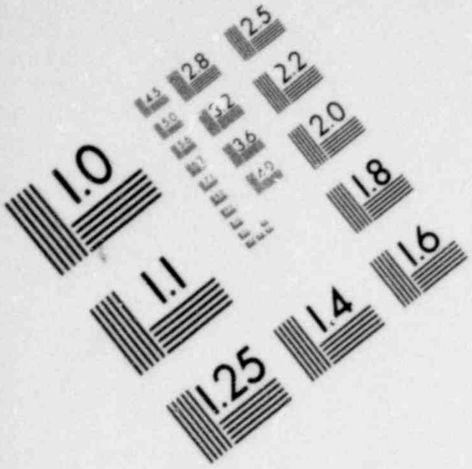

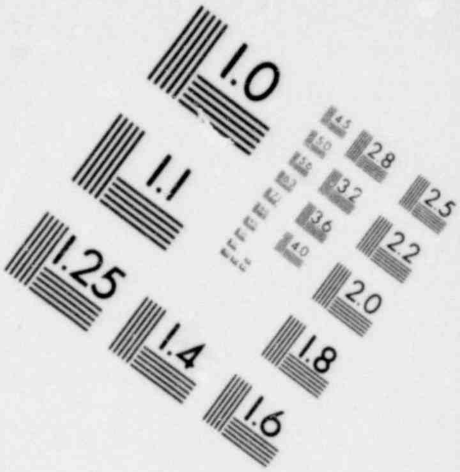

IMAGE EVALUATION
TEST TARGET (MT-3)

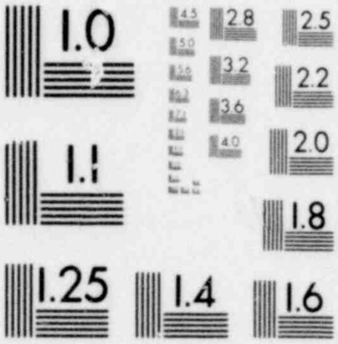

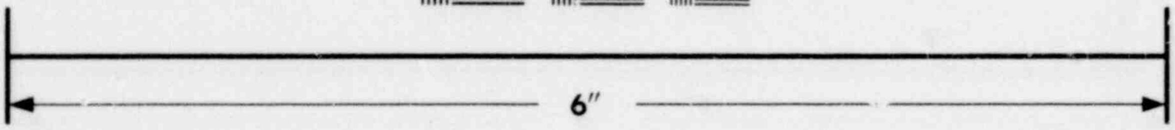

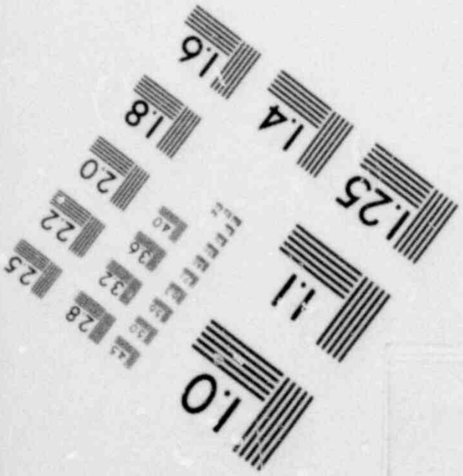

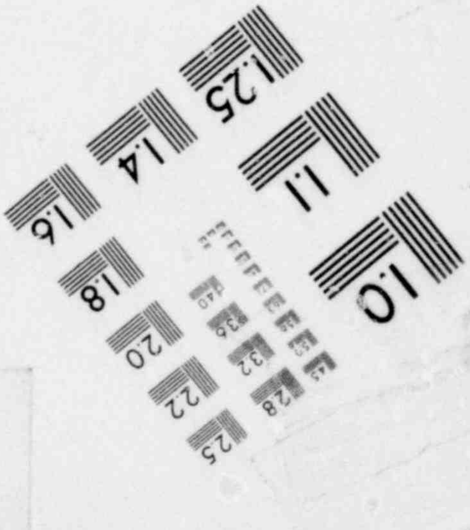

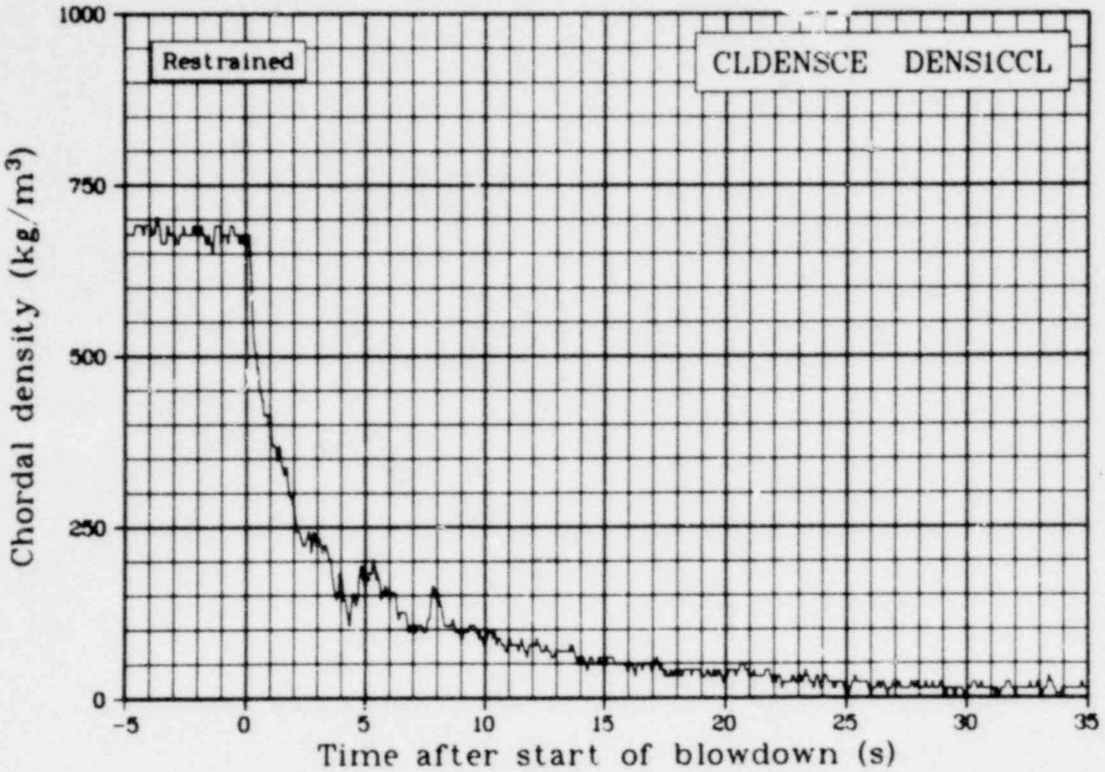

Fig. 527 Chordal density of center beam in cold leg blowdown spool (CLDENSCE DENS1CCL), from -5 to 35 s.

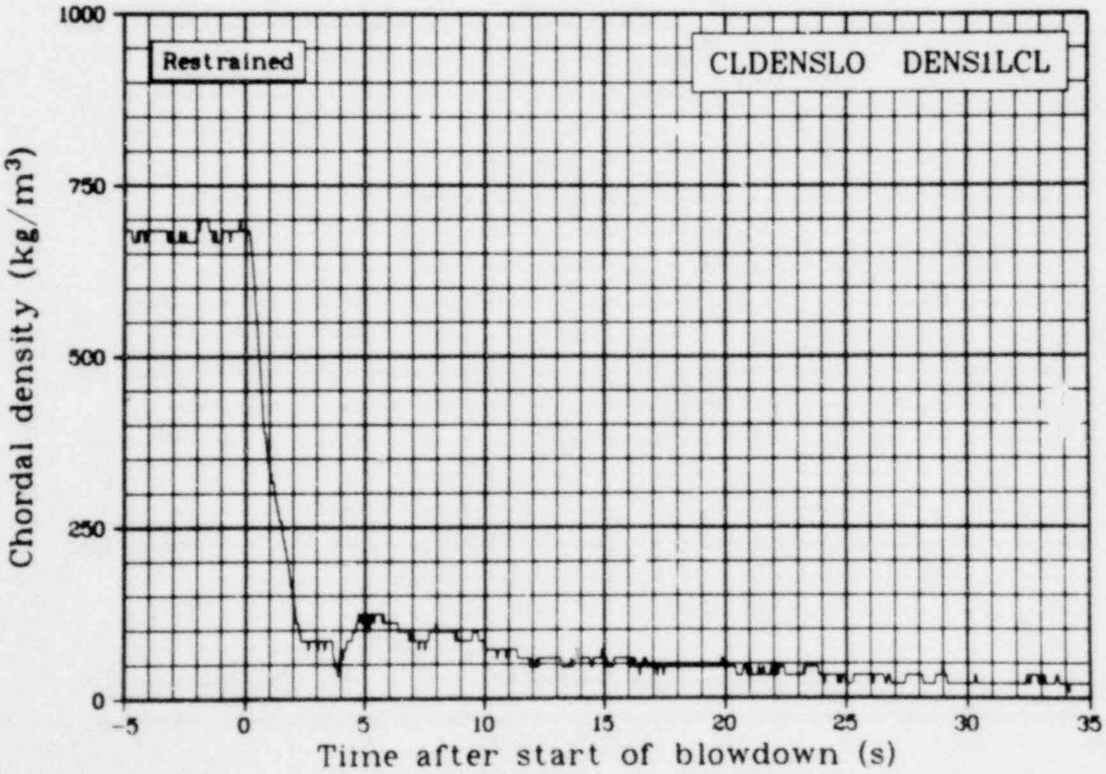

Fig. 528 Chordal density of lower beam in cold leg blowdown spool (CLDENSLO DENS1LCL), from -5 to 35 s.

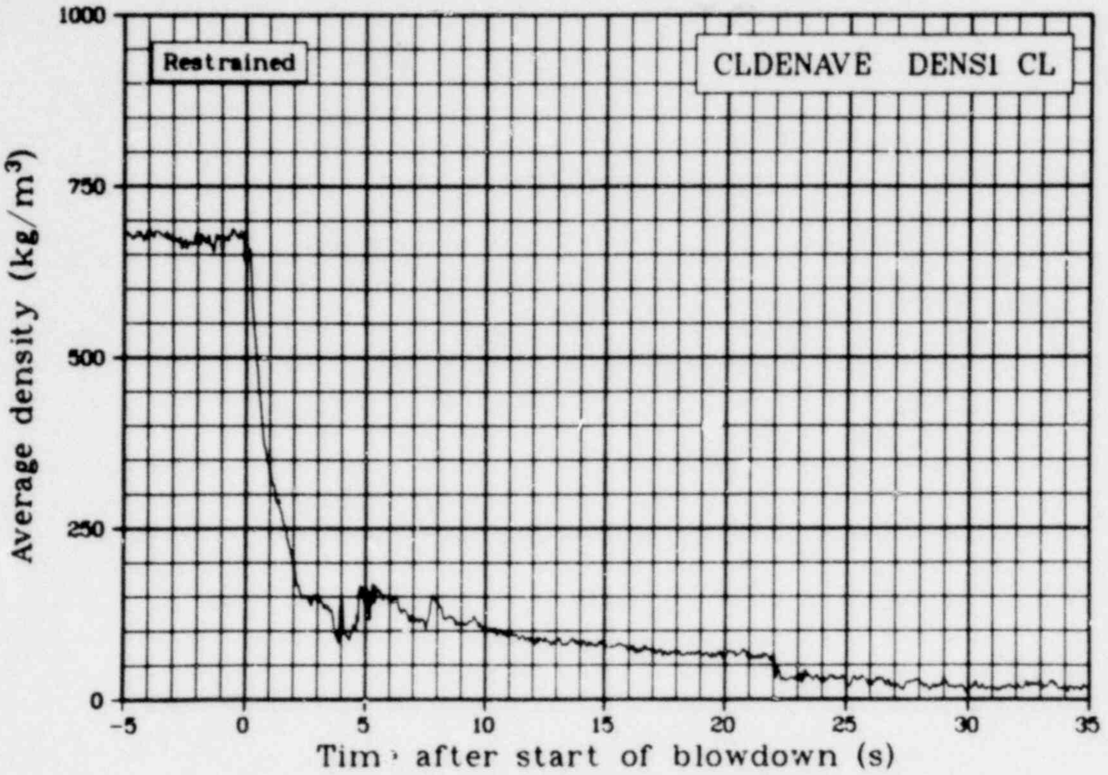

Fig. 529 Average density of cold leg blowdown spool (CLDENAVE DENS1 CL), from -5 to 35 s.

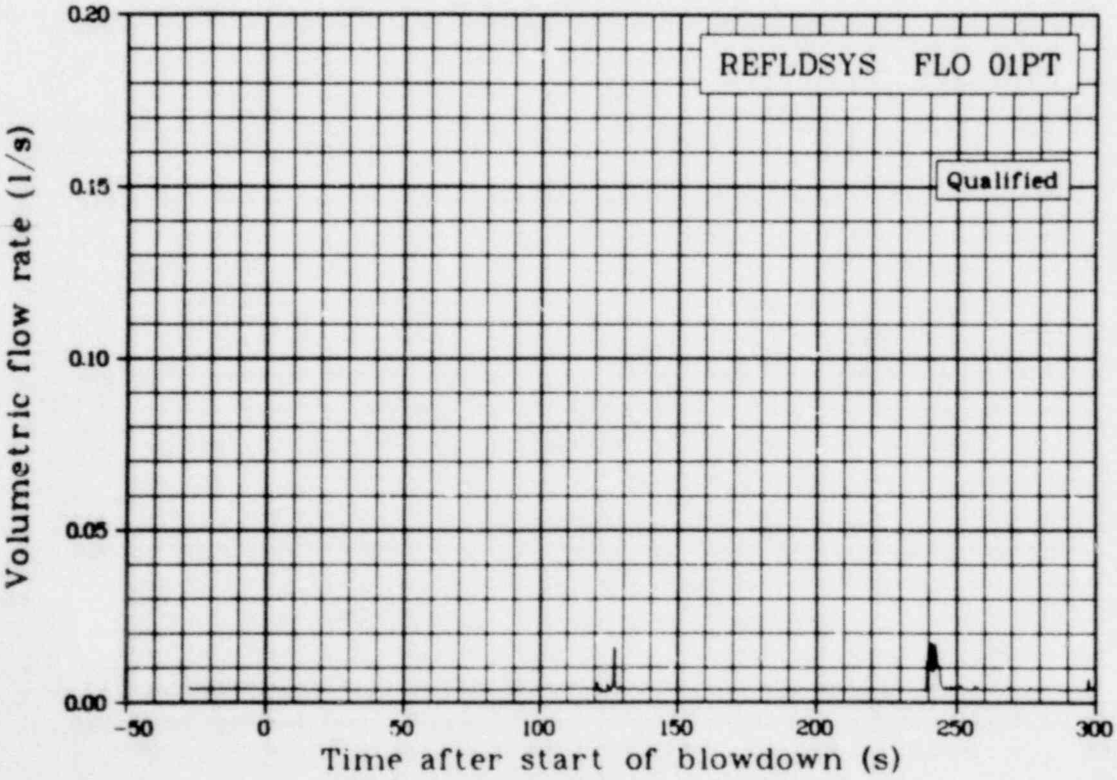

Fig. 530 Volumetric flow rate in reflood line No. 1 (REFLDSYS FLO 01PT), from -50 to 300 s.

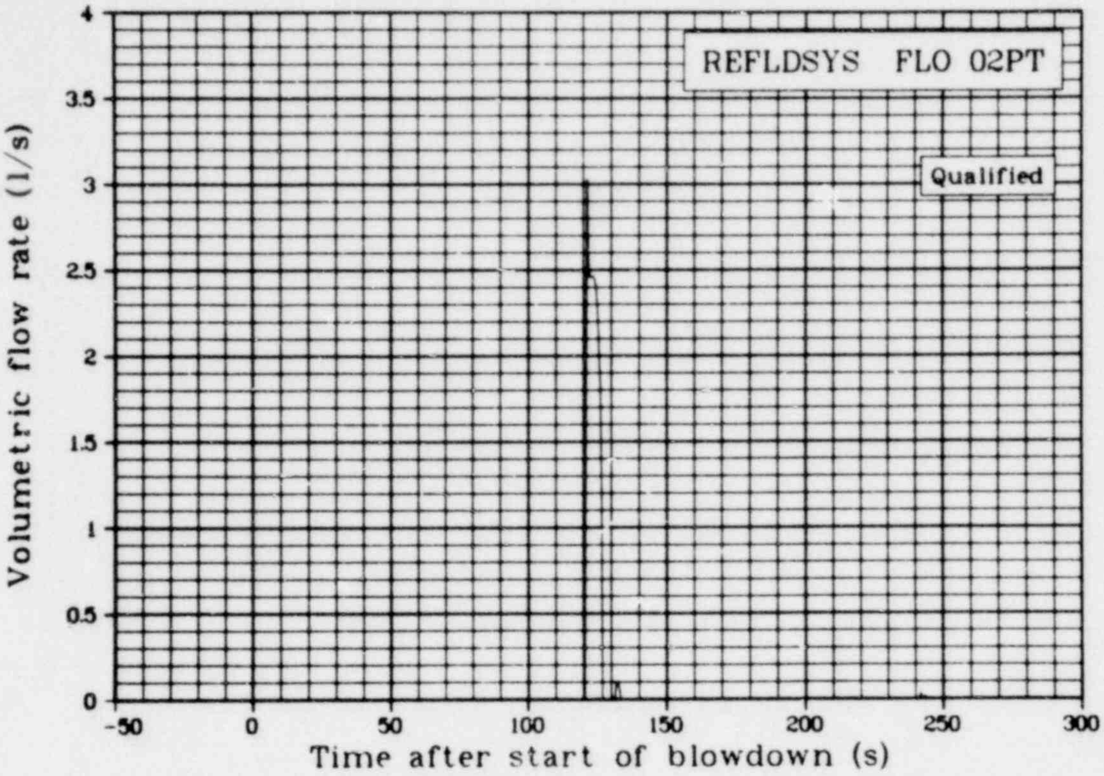

Fig. 531 Volumetric flow rate in reflood line No. 2 (REFLDSYS FLO 02PT), from -50 to 300 s.

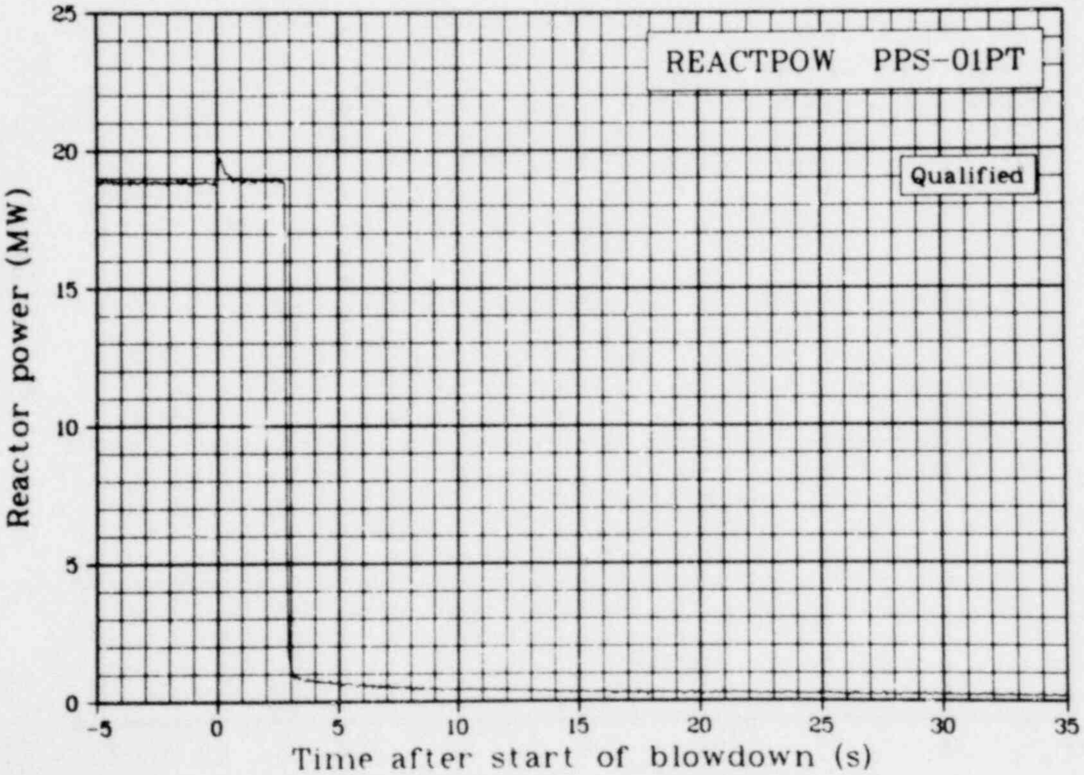

Fig. 532 Reactor power from Core Ionization Chamber PPS 1 (REACTPOW PPS-01PT), from -5 to 35 s.

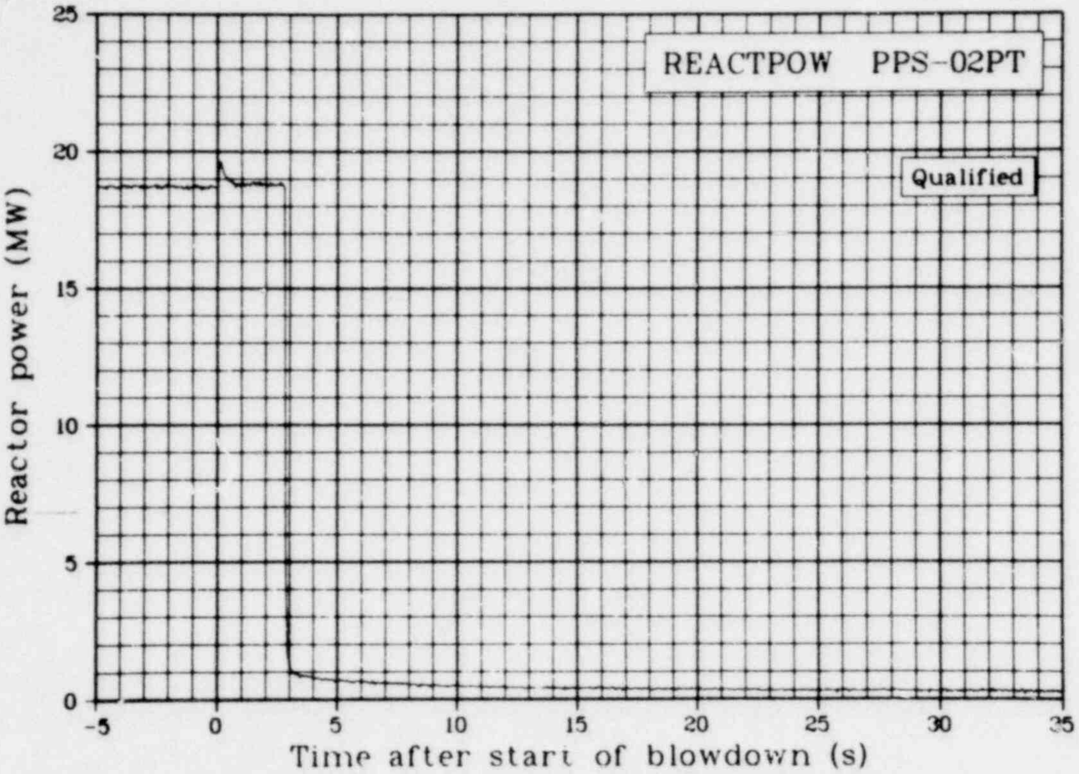

Fig. 533 Reactor power from Core Ionization Chamber PPS 2 (REACTPOW PPS-02PT), from -5 to 35 s.

1406 004

V. REFERENCES

1. D. L. Reeder, *LOFT System and Test Description (5.5-ft Nuclear Core 1 LOCEs)*, NUREG/CR-0247, TREE-1208 (July 1978).

2. P. G. Prassinos, B. M. Galusha, D. B. Engelman, *Experiment Data Report for LOFT Power Ascension Experiment L2-3*, NUREG/CR-0792, TREE-1326 (July 1979).

APPENDIX A

POSTTEST DATA ADJUSTMENTS AND QUALIFICATION

1406 006

APPENDIX A

POSTTEST DATA ADJUSTMENTS AND QUALIFICATION

Many of the instrumentation transducers used during the conduct of Test LLR are recognized to have the potential for responding erroneously, in varying degrees, to extraneous environmental stimuli such as pressure, temperature, neutron flux, gamma radiation, vibration, and mechanical strain. In addition, the data acquisition and recording system and the signal conditioning equipment may also have contributed unwanted or distorted signals to the measurement channel while the transducer output was being processed and recorded.

Although the errors introduced into the data by these spurious secondary inputs generally do not exceed the specified error ranges of the transducers, significant improvement in measurement accuracy can be achieved if the secondary sensitivity can be identified and removed. Since the exact values of the spurious inputs to which different transducers might be sensitive cannot be easily predicted and are sometimes inconvenient to measure, secondary effects have been accounted for by correcting the data after the test.

Data acquired at the PBF during the performance of the Thermal Fuels Behavior Program testing are appraised by a data integrity review committee for quality and validity. The appraisal process determines whether the measurement channel output represents the phenomenon being measured. The data review and examination process ascertains that verified calibration equations have been applied and that offsets and corrections have also been applied to remove any identifiable spurious secondary effects from the data. As a result of the review and examination by the review committee, each measurement is assigned one or more of the following classifications as a function of time.

(1) *Qualified engineering unit data (QEUD).* These data represent the phenomenon measured within the defined uncertainty limits. These data must meet the following criteria: (a) verified calibrations and all corrections have been applied, (b) independent data were used for comparison with this data and agreement was found between the data during the period of interest within specified uncertainty limits, (c) verified engineering unit conversion equations have been applied, and (d) uncertainty limits have been established and can be verified.

(2) *Restrained.* These data represent the phenomenon measured with one or more of the following constraints: (a) verified calibrations have been applied but not all corrections have been made, (b) offsets and corrections cannot be adequately determined, and (c) uncertainty limits have been established but cannot be adequately verified.

(3) *Trend.* These data have been verified to represent the relative changes in the phenomenon but do not necessarily represent the absolute level in the measured phenomenon due to: (a) instrument calibrations do not adequately represent the environment measured by the transducer, (b) the calibration and performance of the DARS are questionable but known errors have been eliminated, (c) uncertainty limits cannot be adequately quantified, (d) transducer performance is questionable but relatively correct, or (e) no corrections can be made to adequately compensate for environmental effects. The data have met the following criteria: (a) instrument and DARS calibrations have been applied, (b) wild points have been removed, (c) data have been appropriately filtered, and (d) relative uncertainty limits have been defined.

(4) *Failed.* Data are irretrievable due to a transducer, signal conditioning, or data channel failure or inadequate rejection of extraneous noise, transient, or frequencies.

1406 007

APPENDIX B

UNCERTAINTY ANALYSIS

1406 008

APPENDIX B

UNCERTAINTY ANALYSIS

Analyses have been performed on Test LLR data to provide a guide to the uncertainty associated with data measurements in the Power Burst Facility (PBF) system. The possible sources of data measurement error have been termed (1) random uncertainties and (2) systematic or bias uncertainties.

(1) *Random Uncertainties*. An overall random uncertainty value has been derived for each PBF measurement by combining all known uncertainty sources of the detector device, signal transmission, data acquisition, and engineering unit conversion. This value is listed in Table B-I and may be interpreted as an approximate 95% confidence interval or 1.96 times the standard deviation.

(2) *Bias Uncertainties*. All data in this report were reviewed to determine the quality and validity of the data. Each measurement was compared with redundant or similar measurements, calculated values, and preblowdown initial conditions to determine the required offsets or adjustments. The bias uncertainties are the expected errors in the offsets that were applied to the data. These 2-σ deviations are listed in the second column of Table B-I.

Other random and systematic uncertainties exist in the data but they could not be adequately analyzed for this report. These uncertainties include measurement dependent and independent uncertainties. A detailed and comprehensive measurement independent uncertainty analysis of the PBF measurement system is currently in progress.

1406 009

TABLE B-I

MEASUREMENT UNCERTAINTIES FOR LLR TESTS

Measurement		Random Uncertainties[a]	Bias Uncertainties				
			Test LLR-S0	Test LLR-3	Test LLR-5	Test LLR-4	Test LLR-4A
Fuel Rod							
TFCL3121	+.08TC01	b	c	c	c	±200 K	--
TFCL3122	+.00TC02	b	c	c	c	±200 K	c
TFCL3123	+.08TC03	b	--	--	--	--	--
TFCL3124	+.00TC04	b	c	±50% Reading	--	--	--
TFCL3451	+.08TC05	b	--	--	±21 K	±50 K	±20 K
TFCL3452	+.00TC06	b	--	--	±20 K	±50 K	±20 K
TFCL3992	+.08TC08	b	--	--	--	--	±50 K
PLNMTEMP	312-1R01	±3% Reading	±7 K	±10 K	±10 K	±5 K	--
PLNMTEMP	312-2R02	±3% Reading	±5 K	±10 K	±10 K	±5 K	±5 K
PLNMTEMP	312-3R03	±3% Reading	±15 K	±5 K	--	--	--
PLNMTEMP	312-4R04	±3% Reading	±5 K	±5 K	--	--	--
PLNMTEMP	345-1R05	±3% Reading	--	--	±10 K	±5 K	±5 K
PLNMTEMP	345-2R06	±3% Reading	--	--	±10 K	±5 K	±5 K
PLNMTEMP	399-2R08	±3% Reading	--	--	--	--	±6 K
CLAD3121	+0818001	±3% Reading	±5 K	±5 K	±10 K	±5 K	--
CLAD3121	+0800001	±3% Reading	±5 K	±8 K	±10 K	±5 K	--
CLAD3122	+0818002	±3% Reading	±6 K	±10 K	±14 K	±14 K	±5 K
CLAD3122	+0000002	±3% Reading	±5 K	±10 K	±10 K	±5 K	±15 K
CLAD3123	+0818003	±3% Reading	±5 K	±10 K	--	--	--
CLAD3123	+0800003	±3% Reading	±5 K	±5 K	--	--	--
CLAD3124	+0818004	±3% Reading	±5 K	±5 K	--	--	--
CLAD3124	+0800004	±3% Reading	±5 K	±5 K	--	--	--
CLAD3451	+0818005	±3% Reading	--	--	±10 K	±5 K	±5 K
CLAD3451	+0800005	±3% Reading	--	--	±11 K	±5 K	±5 K
CLAD3992	+0018008	±3% Reading	--	--	--	--	±5 K
CLAD3992	-1400008	±3% Reading	--	--	--	--	±5 K

TABLE B-I (continued)

Measurement		Random Uncertainties[a]	Bias Uncertainties				
			Test LLR-SO	Test LLR-3	Test LLR-5	Test LLR-4	Test LLR-4A
RODPRESS	312-1R01	±0.65 MPa	±100% Reading	±300% Reading	±300% Reading	±300% Reading	--
RODPRESS	312-2R02	±0.65 MPa	±100% Reading	±300% Reading	±300% Reading	±300% Reading	±300% Reading
RODPRESS	312-3R03	±0.65 MPa	--	±300% Reading	--	--	--
RODPRESS	312-4R04	±0.65 MPa	±100% Reading	±300% Reading	--	--	--
RODPRESS	345-1R05	±0.65 MPa	--	--	±300% Reading	±300% Reading	±300% Reading
RODPRESS	345-2R06	±0.65 MPa	--	--	±300% Reading	±300% Reading	±300% Reading
RODPRESS	399-2R08	±0.65 MPa	--	--	--	--	±300% Reading
LVDT ROD	312-1 01	±50% Reading	c	c	±5 mm	±1 mm	--
LVDT ROD	312-2 02	±50% Reading	c	c	±5 mm	--	c
LVDT ROD	312-3 03	±50% Reading	c	c	--	--	--
LVDT ROD	312-4 04	±50% Reading	c	c	--	--	--
LVDT ROD	345-1 03	±50% Reading	--	--	±5 mm	±1 mm	c
LVDT ROD	345-2 04	±50% Reading	--	--	±5 mm	±1 mm	--
LVDT ROD	399-2 01	±50% Reading	--	--	--	--	c
Test Train							
INLTTEMP	312-1R01	±3% Reading	±9 K	±9 K	--	--	--
INLTTEMP	312-2R02	±3% Reading	±5 K	±22 K	±15 K	±5 K	±5 K
INLTTEMP	312-3R03	±3% Reading	±5 K	±15 K	--	--	--
INLTTEMP	312-4R04	±3% Reading	±20 K	±5 K	--	--	--
INLTTEMP	345-1R05	±3% Reading	--	--	±10 K	±5 K	±5 K
INLTTEMP	345-2R06	±3% Reading	--	--	±27 K	±5 K	±5 K
INLTTEMP	399-2R08	±3% Reading	--	--	--	--	±5 K
OUT TEMP	312-1R01	±3% Reading	±5 K	±13 K	--	--	--
OUT TEMP	312-2R02	±3% Reading	±12 K	±20 K	±10 K	±5 K	±19 K
OUT TEMP	312-3R03	±3% Reading	±5 K	±17 K	--	--	--
OUT TEMP	312-4R04	±3% Reading	±6 K	±5 K	--	--	--
OUT TEMP	345-1R05	±3% Reading	--	--	±44 K	±5 K	±27 K
OUT TEMP	345-2R06	±3% Reading	--	--	±10 K	±5 K	±8 K
OUT TEMP	399-2R08	±3% Reading	--	--	--	--	±5 K
MIDT3121	+.000R01	±3% Reading	±7 K	±9 K	--	--	--
MIDT3121	-.152R01	±3% Reading	±6 K	±7 K	--	--	--

TABLE B-I (continued)

		Bias Uncertainties				
Measurement	Random Uncertainties[a]	Test LLR-S0	Test LLR-3	Test LLR-5	Test LLR-4	Test LLR
MIDT3121 +.152R01	±3% Reading	±10 K	±5 K	--	--	--
MIDT3123 +.000R03	±3% Reading	±9 K	±5 K	--	--	--
MIDT3123 -.152R03	±3% Reading	±17 K	±5 K	--	--	--
MIDT3123 +.152R03	±3% Reading	±33 K	±22 K	--	--	--
MIDT3451 +.000R05	±3% Reading	--	--	±18 K	±8 K	±5 K
MIDT3451 -.152R05	±3% Reading	--	--	±10 K	±18 K	±27 K
MIDT3451 +.152R05	±3% Reading	--	--	±48 K	±5 K	±50 K
MIDT3992 +.000R08	±3% Reading	--	--	--	--	±5 K
MIDT3992 -.152R08	±3% Reading	--	--	--	--	±16 K
MIDT3992 +.152R08	±3% Reading	--	--	--	--	±7 K
DELT3121 225 R01	±3% Reading	±0.1 K	±1 K	--	--	--
DELT3122 225 R02	±3% Reading	±1 K	±1 K	±1 K	±1 K	±5 K
DELT3123 225 R03	±3% Reading	±1 K	±1 K	--	--	--
DELT3124 225 R04	±3% Reading	±0.2 K	±1 K	--	--	--
DELT3124 135 R04	±3% Reading	±0.1 K	±1 K	--	--	--
DELT3451 225 R05	±3% Reading	--	--	±1.5 K	±1 K	±5 K
DELT3452 225 R06	±3% Reading	--	--	±1.5 K	±1 K	--
DELT3992 225 R08	±3% Reading	--	--	--	--	±5 K
DELT3121 CVSP R01	±3% Reading	--	--	±5 K	±2 K	--
DELT3122 CVSP R02	±3% Reading	--	--	±7 K	±2 K	--
TSRD3121 +.000R01	±3% Reading	±6 K	±17 K	±10 K	±5 K	--
TSRD3121 -.152R01	±3% Reading	±5 K	±22 K	±16 K	±12 K	--
TSRD3121 +.152R01	±3% Reading	±44 K	±48 K	±17 K	±36 K	--
TSRD3123 +.000R03	±3% Reading	±5 K	±8 K	--	--	--
TSRD3123 -.152R03	±3% Reading	±29 K	±5 K	--	--	--
TSRD3123 +.152R03	±3% Reading	±26 K	±40 K	--	--	--
TSRD3451 +.000R05	±3% Reading	--	--	±45 K	±14 K	±5 K
TSRD3451 -.152R05	±3% Reading	--	--	±38 K	±7 K	±44 K
TSRD3451 +.152R05	±3% Reading	--	--	±34 K	±4 K	±49 K
TSRD3992 +.000R08	±3% Reading	--	--	--	--	±5 K
TSRD3992 -.152R08	±3% Reading	--	--	--	--	±29 K
TSRD3992 +.152R08	±3% Reading	--	--	--	--	±30 K

TABLE B-I (continued)

Measurement		Random Uncertainties[a]	Bias Uncertainties				
			Test LLR-SO	Test LLR-3	Test LLR-5	Test LLR-4	Test LLR-4A
BULKTEMP	CATCHBTT	±3% Reading	±5 K	±10 K	±10 K	±6 K	±5 K
BULKTEMP	LOWSPTTT	±3% Reading	±7 K	±5 K	--	--	±5 K
BULKTEMP	VOLBYPTT	±3% Reading	±5 K	±5 K	±10 K	±5 K	±5 K
BULKTEMP	SRDOUTTT	±3% Reading	±8 K	±13 K	±10 K	±5 K	±9 K
BULKTEMP	CONTBYTT	±3% Reading	±10 K	±10 K	±10 K	±5 K	±5 K
BULKTEMP	1PTEXTTT	±3% Reading	±5 K	±6 K	±10 K	±5 K	±5 K
PRESSURE	ECATCHTT	±0.65 MPa	±2.4 MPa	±2.5 MPa	c	±3 MPa	±0.2 MPa
PRESSURE	ETOPSPTT	±0.65 MPa	±2.4 MPa	±2.5 MPa	c	±2.6 MPa	±0.3 MPa
PRESSURE	KTOPSPTT	±0.65 MPa	±8.5 MPa	±1.25 MPa	±0.2 MPa	±8 MPa	±3.1 MPa
PRESS-HI	ECATCHTT	±0.65 MPa	±14 MPa	±7 MPa	c	--	±1.1 MPa
TURB3121	UP000N01	d	±1% Reading	±0.03 1/s	±0.05 1/s	±0.1 1/s	--
TURB3121	L0000N01	d	±1% Reading	±0.03 1/s	±0.05 1/s	±0.1 1/s	--
TURB3122	UP180N02	d	±1% Reading	±0.07 1/s	±0.05 1/s	±0.1 1/s	±0.03 1/s
TURB3122	L0180N02	d	±1% Reading	±0.03 1/s	±0.05 1/s	±0.2 1/s	±0.03 1/s
TURB3123	UP090N03	d	±1% Reading	±0.03 1/s	--	--	--
TURB3123	L0090N03	d	±1% Reading	±0.03 1/s	--	--	--
TURB3124	UP270N04	d	±1% Reading	±0.03 1/s	--	--	--
TURB3124	L0270N04	d	±19% Reading	±0.07 1/s	--	--	--
TURB3451	UP090N03	d	--	--	±0.05 1/s	±0.1 1/s	±0.03 1/s
TURB3451	L0090N03	d	--	--	±0.05 1/s	±0.1 1/s	±0.03 1/s
TURB3452	UP270N04	d	--	--	±0.05 1/s	±0.1 1/s	±0.03 1/s
TURB3452	L0270N04	d	--	--	±0.05 1/s	--	±0.03 1/s
TURB3992	UP000N01	d	--	--	--	--	±0.03 1/s
TURB3992	L0000N01	d	--	--	--	--	±0.03 1/s
TURBINEM	CONTBYTT	d	±1% Reading	±0.03 1/s	±0.05 1/s	±0.2 1/s	--
NEUTFLUX	+.343 TT	±8% Reading	--	--	--	--	--
NEUTFLUX	+.228 TT	±8% Reading	±50% Reading	±50% Reading	±30% Reading	±50% Reading	±50% Reading
NEUTFLUX	+.142 TT	±8% Reading	±50% Reading	±50% Reading	±30% Reading	±50% Reading	±50% Reading
NEUTFLUX	+.000 TT	±8% Reading	±50% Reading	±50% Reading	±30% Reading	±50% Reading	±50% Reading
NEUTFLUX	-.114 TT	±8% Reading	±50% Reading	±50% Reading	±30% Reading	±50% Reading	--
NEUTFLUX	-.228 TT	±8% Reading	±50% Reading	±50% Reading	±30% Reading	--	±50% Reading
NEUTFLUX	-.343 TT	±8% Reading	±50% Reading	±50% Reading	±30% Reading	±50% Reading	±50% Reading

TABLE B-I (continued)

Measurement		Random Uncertainties[a]	Bias Uncertainties Test LLR-S0	Test LLR-3	Test LLR-5	Test LLR-4	Test LLR-4A
GAMMAFLX	+.228 TT	±17% Reading	±50% Reading	±50% Reading	±30% Reading	±50% Reading	±50% Reading
GAMMAFLX	+.000 TT	±17% Reading	±50% Reading	±50% Reading	±30% Reading	±50% Reading	±50% Reading
GAMMAFLX	-.228 TT	±17% Reading	±50% Reading	±50% Reading	±30% Reading	±50% Reading	±50% Reading
Measurement Spool							
ICSSTEMP	TE20SPIC	±1% Reading	±5 K	±4 K	±2 K	±5 K	±5 K
CLSSTEMP	TE22SPCL	±3% Reading	±5 K	±6 K	±5 K	±5 K	±5 K
HLSSTEMP	TE23SPHL	±3% Reading	±6 K	±5 K	±10 K	±5 K	±5 K
ICTCTEMP	TE21SPIC	±3% Reading	--	--	--	--	±5 K
CLTCTEMP	TE24SPCL	±3% Reading	±10 K	±5 K	±84 K	±5 K	±5 K
HLTCTEMP	TE25SPHL	±3% Reading	±7 K	±92 K	±80 K	±5 K	±5 K
ICPRESSF	PE08SPIC	±0.65 MPa ±2% Reading	--	±2.2 MPa	0	±0.8 MPa	±0.2 MPa
CLPRESSF	PE10SPCL	±0.65 MPa ±2% Reading	±1.4 MPa	±0.4 MPa	±2.4 MPa	±2.2 MPa	--
HLPRESSF	PE12SPHL	±0.65 MPa ±2% Reading	±0.7 MPa	±0.5 MPa	±1.0 MPa	--	--
ICPRESSW	PE09SPIC	±0.65 MPa ±2% Reading	±0.7 MPa	±0.1 MPa	±0.5 MPa	±0.8 MPa	--
CLPRESSW	PE11SPCL	±0.65 MPa ±2% Reading	±1.9 MPa	±2.0 MPa	±2.0 MPa	±0.6 MPa	--
HLPRESSW	PE13SPHL	±0.65 MPa ±2% Reading	±0.8 MPa	±0.8 MPa	±1.0 MPa	±0.2 MPa	--
DELPCLHL	DPE-05HL	±10% Reading	±10% Reading	±10% Reading	±10% Reading	--	--
ICSVFLOW	FE05SPIC	c	±1% Reading	±1% Reading	±20% Reading	--	--
CLSVFLOW	FE06SPCL	c	±1% Reading	±1% Reading	±20% Reading	±20% Reading	--
HLSVFLOW	FE09SPHL	c	±1% Reading	±1% Reading	±20% Reading	--	--
CLDENSUP	DENS1UCL	0	--	--	0	--	0
CLDENSCE	DENS1CCL	0	--	0	0	--	0
CLDENSLO	DENS1LCL	0	--	--	0	--	0
CLDENAVE	DENS1 CL	0	--	--	0	--	0

1406 014

TABLE B-I (continued)

Measurement		Random Uncertainties[a]	Bias Uncertainties				
			Test LLR-S0	Test LLR-3	Test LLR-5	Test LLR-4	Test LLR-4A
HLDENSUP	DENS2UHL	0	--	--	0	0	--
HLDENSCE	DENS2CHL	0	--	--	0	0	--
HLDENSLO	DENS2LHL	0	--	--	0	0	--
HLDENAVE	DENS2 HL	0	--	--	0	0	--
Plant							
REFLDSYS	FLO 01PT	±0.1 l/s	±0.1 l/s	--	±0.1 l/s	--	±0.1 l/s
REFLDSYS	FLO 02PT	±0.1 l/s	±0.1 l/s	±0.1 l/s	±0.1 l/s	--	±0.1 l/s
REACTPOW	PPS-01PT	±10% Reading	±1% Reading	±0.1 MW	±0.3% Reading ±0.03 MW	±0.17 MW	±1% Reading
REACTPOW	PPS-02PT	±10% Reading	±1% Reading	±0.1 MW	±0.3% Reading ±0.4 MW	±0.23 MW	±1% Reading

---

a. These uncertainties remain the same for each of the LLR tests unless otherwise noted.

b. For temperatures <1000 K, ±5% Reading and for temperatures >1000 K, ±10 Reading.

c. Magnitude of uncertainty could not be quantified.

d. The random uncertainty varied for each test as follows:

Test LLR-S0	±0.1 l/s prior to blowdown, ±0.7 l/s after blowdown initiation.
Test LLR-3	±0.2 l/s prior to blowdown, ±0.4 l/s after blowdown initiation.
Test LLR-5	±0.2 l/s prior to blowdown, ±0.5 l/s after blowdown initiation.
Test LLR-4	±0.2 l/s prior to blowdown, ±0.5 l/s after blowdown initiation.
Test LLR-4A	±0.2 l/s prior to blowdown, ±1.7 l/s after blowdown initiation.

DISTRIBUTION RECORD FOR NUREG/CR-0927

(TREE-1272)

Internal Distribution

1 - R. J. Beers, ID

2 - P. E. Litteneker, ID

3-5 - INEL Technical Library

6-50 - Special Internal

External Distribution

51-52 - Saul Levine, Director
Office of Nuclear Regulatory Research, NRC
Washington, D.C. 20555

53-393 - Distribution under R3, Water Reactor Safety Research - Fuel Behavior

1406 016

DOCUMENT/ PAGE PULLED

ANO. 7911280414

NO. OF PAGES 1 MICROFICHE

REASON:

☒ PAGE ILLEGIBLE:

☐ HARD COPY FILED AT: PDR [✓ CF]
OTHER ____________

☐ BETTER COPY REQUESTED ON ____/____/____

☒ PAGE TOO LARGE TO FILM:

☐ HARD COPY FILED AT: PDR [✓ CF]
OTHER ____________

☐ FILMED ON APERTURE CARD NO. ____________

1406 017